The sleeping brain at work : perceptual processing and learning in human sleep Thomas Andrillon

Thomas Andrillon

THÈSE DE DOCTORAT
de l'Université de recherche
Paris Sciences et Lettres –
PSL Research University

préparée à
l'École normale supérieure

LE CERVEAU DORMANT AU TRAVAIL: traitement et apprentissage perceptifs durant le sommeil chez l'Homme

par Thomas Andrillon

Ecole doctorale n°158
Spécialité : Neurosciences
Soutenue le 14 Avril 2016

Composition du Jury :

M. Shihab SHAMMA
Ecole Normale Supérieure
Président du jury

M. Jan BORN
Université de Tübingen
Rapporteur

M. Marcello MASSIMINI
Université de Milan
Rapporteur

Mme. Hélène BASTUJI
Université de Lyon
Membre du jury

M. Karim BENCHENANE
ESPCI
Membre du jury

M. Sid KOUIDER
Ecole Normale Supérieure
Directeur de thèse

ENS ÉCOLE NORMALE SUPÉRIEURE
PSL RESEARCH UNIVERSITY PARIS

École Normale Supérieure

École Doctorale Cerveau Cognition Comportement

Laboratoire de Sciences Cognitives et Psycholinguistique

Équipe Cerveau et Conscience

Le cerveau dormant au travail : traitement et apprentissage perceptifs durant le sommeil chez l'Homme

Thomas Andrillon

Thèse de doctorat en Neurosciences

Sous la direction de Sid Kouider

Présentée et soutenue publiquement le 14 Avril 2016

Devant un jury composé de :

Marcello MASSIMINI	Université de Milan	Rapporteur
Jan BORN	Université de Tübingen	Rapporteur
Hélène BASTUJI	Université de Lyon	Examinatrice
Karim BENCHENANE	ESPCI	Examinateur
Shihab SHAMMA	ENS	Examinateur
Sid KOUIDER	ENS	Directeur

École Normale Supérieure

École Doctorale Cerveau Cognition Comportement

Laboratory of Cognitive Sciences and Psycholinguistics

Brain and Consciousness Team

The sleeping brain at work: perceptual processing and learning in human sleep

Thomas Andrillon

Dissertation for the degree of Doctor in Philosophy

Under the supervision of Sid Kouider

Publicly defended on April 14th, 2016

Before the Doctoral Committee composed of:

Marcello MASSIMINI	University of Milan	Referee
Jan BORN	University of Tubingen	Referee
Hélène BASTUJI	University of Lyon	Examiner
Karim BENCHENANE	ESPCI	Examiner
Shihab SHAMMA	ENS	Examiner
Sid KOUIDER	ENS	Supervisor

À Sophie, à Julien,
à ces êtres aimés
dont les voix se sont tues.

« Je ne cesserai jamais de m'émerveiller que cette chair soutenue par ses vertèbres, ce tronc joint à la tête par l'isthme du coup et disposant autour de lui symétriquement ses membres, contiennent, et peut-être produisent un esprit qui tire parti de mes yeux pour voir et de mes mouvements pour palper… J'en sais les limites, et que le temps lui manquera pour aller plus loin, et la force, si par hasard lui était accordé le temps. Mais il est, et, en ce moment, il est Celui qui Est. Je sais qu'il se trompe, erre, interprète souvent à tort les leçons que lui dispense le monde, mais je sais aussi qu'il a en lui de quoi connaître et parfois rectifier ses propres erreurs. J'ai parcouru au moins une partie de cette boule où nous sommes ; j'ai étudié le point de fusion des métaux et la génération des plantes ; j'ai observé les astres et examiné l'intérieur des corps. Je suis capable d'extraire de ce tison que je soulève la notion de poids et de ces flammes la notion de chaleur. Je sais que je ne sais pas ce que je ne sais pas ; j'envie ceux qui sauront d'avantage, mais je sais qu'ils auront tout comme moi à mesurer, peser, déduire et se méfier des déductions produites, faire dans le faux la part du vrai et tenir compte dans le vrai de l'éternelle admixtion du faux. Je ne me suis jamais entêté à une idée par crainte du désarroi où je tomberais sans elle. Je n'ai jamais assaisonnée un fait vrai à la sauce du mensonge, pour m'en rendre à moi-même la digestion plus facile. Je n'ai jamais déformé les vues de l'adversaire pour en avoir plus aisément raison (…). Ou plutôt si : je me suis surpris à le faire, et me suis chaque fois réprimandé (…). J'ai rêvé mes songes ; je ne les tiens pas pour autre chose que des songes. Je me suis gardé de faire de la vérité une idole, préférant lui laisser son nom plus humble d'exactitude. Mes triomphes et mes dangers ne sont pas ceux qu'on pense ; il y a d'autres gloires que la gloire et d'autres bûchers que le bûcher. J'ai presque réussi à me défier des mots. Je mourrai un peu moins sot que je ne suis né. »

Marguerite Yourcenar, *L'Œuvre au Noir* (1968)

Table of Contents

Résumé

Tous les soirs, nous nous endormons; tous les matins, nous nous réveillons. De ce qui advient entre temps nous gardons peu de souvenirs. Les personnes qui nous entourent pourraient nous dire que nous avons bougé, parlé, ri ou crié, que les émotions les plus vives ont pris le contrôle de notre corps sans pour autant avoir laissé le moindre souvenir. Ou encore, les personnes qui nous entourent ont pu bouger, parler, rire ou crier sans que nous nous en rendîmes compte le moins du monde. Ou au contraire, nous pouvons émerger de la plus fantastique des aventures dans un lit pourtant bien calme, bercé par le calme tic-tac de l'horloge. Il semble que le sommeil opère une dissociation complète entre ce qui arrive dans notre environnement immédiat et dans notre esprit, sans pour autant que la chose éveille en nous la moindre alarme. À tout moment qui plus est, nous pouvons nous réveiller et reprendre conscience de notre environnement de façon quasi instantanée. Curieusement, il semble que certains sons aient une plus grande facilité à nous réveiller que d'autres.

Sommes-nous donc complètement déconnectés de notre environnement quand nous dormons ? Dans les années 60, David Formby et col. montrèrent que la pertinence d'un son importe en effet, en observant que les jeunes mères se réveillent plus aisément en entendant le cri de leur propre enfant plutôt que celui d'un autre. Plus tard, Hélène Bastuji et col. démontrèrent que les traitements sensoriels peuvent être préservés pendant le sommeil sans pour autant nécessairement conduire à un réveil. Cette capacité à analyser les informations venant du monde extérieur pendant le sommeil pourrait s'appuyer sur un phénomène appelé 'sommeil local' : le fait que certaines régions cérébrales puissent être réveillées dans un cerveau globalement endormi. Dans le Chapitre 1, je présenterai quelques études explorant la physiologie du sommeil et montrant que le sommeil est un phénomène plus local que la description qui est en classiquement faite. À la lumière de ces travaux, je soulignerai la nécessité de considérer le sommeil à des échelles spatiales (Études 1 et 2) et temporelles (Étude 3) plus précises.

Au cours de cette thèse, j'ai également exploré les conséquences fonctionnelles de ce sommeil local en étudiant notamment jusqu'à quel point les processus cognitifs sont préservés pendant le sommeil naturel chez l'homme. Notre approche est plutôt simple : les personnes participant à nos expériences devaient catégoriser des sons (des mots, des phrases, des bruits) pendant qu'elles étaient éveillées. Une fois que l'exercice était devenu automatique, ces participants étaient invités à le poursuivre confortablement allongés dans l'obscurité. La plupart du temps, ceux-ci se sont endormis en écoutant les sons. Nous enregistrions en parallèle l'activité cérébrale au moyen d'un électroencéphalogramme et avons utilisé ces enregistrements afin de déterminer d'une part si les individus dormaient et d'autre part s'ils continuaient à catégoriser les stimuli.

En faisant varier les instructions données ou la nature des sons, nous avons pu déterminer si ces dormeurs pouvaient extraire des informations complexes à partir des entrées auditives et si ces informations pouvaient être utilisées pour prendre des décisions ou pour être apprises.

Dans le chapitre 2, je détaillerai nos efforts consistant à examiner quels traitements sont possibles pendant le sommeil. En utilisant l'approche évoquée ci-dessus, nous avons pu montrer que les dormeurs peuvent traiter une information auditive à un haut niveau de représentation (niveau sémantique ou lexical, Études 4 et 5). En outre, nos données suggèrent que cette information peut être envoyée vers d'autres régions cérébrales et permettre des prises de décision. Je décrierai également les mécanismes permettant au cerveau de traiter ces informations extérieures ou au contraire de s'en isoler (Étude 5). Enfin, je monterai comment les dormeurs peuvent non seulement traiter de façon complexe une information pendant le sommeil mais aussi sélectionner une source d'information en particulier quand deux sont présentées en compétition (Étude 6).

Le cerveau éveillé apprend sans cesse et le simple fait d'user de ses sens peut conduire à la formation de nouveaux souvenirs, qu'ils soient implicites ou explicites, grossiers ou élaborés. De semblables traces mnésiques apparaissent-elles quand le cerveau dormant traite les informations extérieures ? Le Chapitre 3 se concentrera sur cette question. Dans une première étude (Étude 7) nous avons obtenu d'encourageant résultats : traiter une information même endormi peut conduire à l'établissement d'un souvenir implicite. Afin d'approfondir ce premier résultat ainsi que les mécanismes sous-jacents, nous avons étudié la capacité du cerveau dormant à former de nouvelles représentations (Études 8 et 9). Je présenterai ici des données expérimentales montrant que le cerveau endormi peut à la fois créer et supprimer de nouvelles traces mnésiques en fonction du stade de sommeil. Ce travail nous a en outre permis de formuler une synthèse du rôle du sommeil dans la mémoire, notamment quant à la fonction bien établie du sommeil dans la consolidation des souvenirs.

En résumé, au cours de mon doctorat j'ai essayé de rendre compte de la richesse du sommeil. Bien loin de l'inactivité, le sommeil est un équilibre dynamique dans lequel les informations extérieures peuvent être traitées, permettant au cerveau de décider s'il vaut mieux continuer à dormir ou se réveiller. L'aphorisme d'Héraclite, vieux de plus de 2000 ans, trouve ici une modeste confirmation:

"Même une âme plongée dans le sommeil
s'attèle au travail et aide
à donner un sens au monde".

Summary

Every night we fall asleep and every morning we wake up. From what happens in the meantime, little is remembered. Others may say that we have moved, talked, laughed or cried, that the strongest and most vivid emotions took control of our body without leaving the faintest memory behind. Or others may have moved, talked, laughed or cried without our slightest notice. On the contrary, we can emerge from the most fantastic adventure in a quiet bed, cradled by a peaceable ticking clock. Without causing us much alarm, it seems that sleep entails a dissociation between what happens in our environment and within our mind. Yet, at any moment, we can wake up and immediately regain consciousness of the surrounding world. Interestingly, it seems that certain sounds are more likely to awake us than others.

Thus, are we completely disconnected from our environment when we sleep? Indeed, loudness is not the only criterion that determines whether a sound will wake up a sleeper. In the 60s, David Formby and colleagues showed that relevance matters when observing that young mothers wake up more easily to the cry of their own child. Later, Hélène Bastuji and colleagues demonstrated that sensory processing can be preserved in sleep without necessarily leading to an awakening. The maintenance of some ability to monitor the external world while being sleep could rely on a phenomenon called local sleep, i.e. the fact that some brain regions could be awake in a globally sleeping brain. In Chapter 1, I will present several studies exploring sleep physiology and showing that sleep is a more local phenomenon than usually described. In the light of such evidence, I will stress the need to consider sleep at refined spatial (Studies 1 and 2) and temporal (Study 3) scales.

During my doctoral work, I also explored the functional consequence of local sleep and the extent to which cognitive processes are preserved during natural human sleep. Our approach was rather simple: participants to our experiments were asked to discriminate acoustic stimuli (e.g. words, sentences, sounds…) while awake. Once the task at hand had been automated, participants were invited to continue it while comfortably laying in a dark room. Most of the time, they fell asleep while listening to our stimuli. We recorded neural activity with scalp electroencephalograpy and used it to assess both the vigilance of participants and their ability to discriminate the stimuli. By varying the task instructions and the nature of stimuli, we could probe whether sleepers can extract

complex information from the acoustic signal and, whether this information can be used to make decisions or for learning.

In Chapter 2, I will detail our efforts to examine to which extent external information can be processed during sleep. Using the approach detailed above, we showed that sleepers can access acoustic information at a rather high level of representation (i.e. semantic or lexical level; Studies 4 and 5). Importantly, we showed that this information can be routed to other brain areas up to the decision level. I will also describe the mechanisms allowing the sleeping brain to process or on the contrary inhibit sensory information (Study 5). Finally, I will show that sleepers can not only process complex information but also that sleepers can select and lean toward one source of information when two sources are presented in competition (Study 6).

The awake brain is constantly learning and the fact of experiencing almost inevitably leads to the establishment of memory traces, being it explicit or implicit, strong or fine. Are similar memories formed when the sleeping brain processes external information? This question will be the focus of Chapter 3. Our initial effort (Study 7) led to encouraging observations: processing information while asleep may allow the formation of implicit mnesic traces. To better explore this question and the underlying mechanisms, we investigated whether a new representation can be created during sleep (Studies 8 and 9). I report here evidence that the sleeping brain can both establish and suppress novel mnesic traces depending on sleep stages. This work allowed us to formulate an integrative view of the role of sleep in memory and especially the well-established function of sleep regarding memory consolidation.

In summary, in the course of my Ph.D., I tried to better depict the richness of sleep. Far from being an idle state, sleep is a dynamic equilibrium in which the environment can be monitored, allowing the brain to decide whether to stay asleep or to wake up. Heraclitus' aphorism stated more than 2000 years ago finds here a modest corroboration:

"Even a soul submerged in sleep
is hard at work and helps
make something of the world".

List of publications

Peer-Reviewd Publications:

Sleep Spindles in Humans: Insights from Intracranial EEG and Unit Recordings
Andrillon* T., Nir* Y., Staba RJ., Ferrarelli F., Cirelli C., Tononi G., Fried I.
The Journal of Neuroscience (2011)

Regional Slow Waves and Spindles in Human Sleep
Nir Y., Staba RJ., Andrillon T., Vyazovskiy VV., Cirelli C., Fried I., Tononi G.
Neuron (2011)

Inducing Task-Relevant Responses to Speech in the Sleeping Brain
Kouider S., Andrillon T., Barbosa L., Goupil L. & Bekinschtein T.
Current Biology (2014)

Single-Neuron Activity and Eye Movements during Human REM Sleep and Awake Vision
Andrillon* T., Nir* Y., Cirelli C., Tononi G. & Fried I.
Nature Communications (2015)

Perceptual Learning of Acoustic Noise Generates Memory-Evoked Potentials
Andrillon T., Kouider S., Agus T. & Pressnitzer D.
Current Biology (2015)

Submitted or Under-Review:

Formation and Suppression of Acoustic Memories in Human Sleep
Andrillon T., Pressnitzer D., Léger D. & Kouider S.

Implicit Memory for Words Heard during Sleep
Andrillon T. & Kouider, S.

Neural Markers of Responsiveness to the Environment in Human Sleep
Andrillon T., Poulsen AT.; Hansen LK., Léger D. & Kouider S.

Napping: a Public Health Issue
Faraut B., Andrillon T., Vecchierini MF. & Léger D.

Selective Neuronal Fatigue Precedes Human Cognitive Lapses
Nir Y., Andrillon T., Suthana N., Cirelli C., Tononi* G., and Fried* I.

In preparation:

Attentional Tracking of Relevant Signals during Human Sleep
Legendre* G., Andrillon* T. & Kouider S.

*: Equal contribution

Keywords and acronyms

NREM	Non-Rapid Eye-Movement
REM	Rapid Eye-Movement
SW	Slow-Wave
SWS	Slow-Wave Sleep
SWA	Slow-Wave Activity
ACh	Acetylcholine
STDP	Spike-Timing Dependent Plasticity
EEG	Electroencephalogramphy
EOG	Electroocculography
EMG	Electromyography
MEG	Magnetoencephalography
LFP	Local Field Potentials
MUA	Multi-Unit Activity
SUA	Single-Unit Activity
TMS	Transcranial Magnetic Stimulation
fMRI	Functional Magnetic Resonance Imaging
ERP	Event-Related Potential
AEP	Auditory-Evoked Potential
LRP	Lateralized Readiness Potential
ITPC	Inter-Trial Phase Coherence
FFT	Fast Fourier Transform
SEM	Standard Error of the Mean
FDR	False Discovery Rate

Figures and Tables

Main figures:

Main tables:

Acknowledgements

On the first day of the entrance examination at the Ecole Normale Supérieure (ENS), I remember walking the (for some) mythical *rue d'Ulm*. On the pavement, footprints painted in a vivid orange headed to the ENS. I saw a sign in them. And indeed, during the 7 past years, I have found there the guidance I needed to become a scientist, and benefited from the counsel of many brilliant researchers and professors.

First and foremost, I want to thank my PhD supervisor: Sid Kouider. Not only Sid taught me what I needed to learn in order to perfect my training in research, but he also did so with the right method: he always took care that I developed a form of independence while always being there to rescue me when I was stuck and despaired. I am profoundly thankful for his care in giving me the impression I was climbing ahead while safeguarding me the whole way. I also had the chance to have a supervisor who always tried to highlight my research through various collaborations with other researchers and the participation to many conferences. Thanks to Sid, I have traveled a lot and met people whom I am sure will be part of my future. But most importantly, Sid set me on fantastic research tracks. I owe him the seeds of this doctoral work. Seeds that I remember considering quite crazy or even impossible at first. Nonetheless, I learnt to trust his instinct and (French) flair and the craziness happened not to be so crazy. After all those years however, I have not penetrated the mystery of Sid's intuitions. I hope though that Sid and I will continue our work together, even from afar, and that, one day, I would have finally learnt how he manages to shoot for the moon without missing it.

I want also to thank the other mentors who accompanied me during this doctorate. At the ENS, I had the chance to benefit from the expertise of Daniel Pressnitzer, Alain de Cheveigné and Catherine Tallon-Baudry. Daniel, notably, was always there to check how our projects were progressing, with humor and good mood, and I am thankful for the efforts he made to put my work and myself under the spotlight. Within the *Laboratoire de Sciences Cognitives et Psycholinguistique* (LSCP), I had the chance to be able to reach researches who, even if we did not always share the same academic field, always brought their advises and experience when I needed it. In particular, I wish to thank Jérôme Sackur for his ever-pertinent insights and depth of thoughts. In the first months of my doctorate, I had the chance to meet and start collaborating with Damien Léger at the *Hôtel-Dieu* Hospital. I am deeply thankful for his genuine interest, solid counsel and unfailing trust. Over the three past years, I also had the opportunity to experience teaching for the first time and it has been a true revelation. I thank the professors who supervised me at the *Université Pierre et Marie Curie* (Mathilde Grassi) and at the Cogmaster (Sid, Jérôme Sackur and Claire Sergent). Lastly, during my doctoral studies and before, I had the chance to be mentored by dedicated professors (Laurent Bourdieu, Matthias Pessiglione and Anne Christophe) who always toke great care to orientate me in academia's maze.

Intertwined with the research I conducted in Paris, I had the opportunity to collaborate with researchers abroad and particularly with Chiara Cirelli and Giulio Tononi in Wisconsin, and with Yuval Nir and Itzhak Fried in Tel-Aviv. The time I spent at the University of Wisconsin represents a key moment in my still-young academic career and I will always be in debt with Chiara Cirelli and Giulio Tononi for such opportunity. I will always be admiring their vision of science and I do hope that I will have the chance and honor to interact with them in the future. As for Yuval, I cannot tell how much he taught me about research and life in general, and I am proud to consider him (and be considered) more as a friend than anything else.

I focused so far on the tree of professors who help me, each in their own way, to grow up as a scientist. But I also benefited, beyond all possible expectations, from my comrades in research: the post-doctorate fellows, students or research assistants I had the opportunity to work with. At the LSCP, I had the chance to meet Leonardo Barbosa, who was always there to help me, to teach me and to cheer me up. His knowledge is hard to surpass and my doctorate would have been much harder without him. Next to me, as two horses on the same harness, Alexandre Cremers was a true brother-in-arms and his endless curiosity is one of the things that make me realize the chance I have to spend my time with such colleagues. Yue Sun shared with Alexandre,

Leonardo and I the same room of PhD candidates (and much more) for these past years. Thanks to his capacity of adaptation and of always asking the right questions. I am sure he will progress smoothly in his academic dreams. I wish also to thank Louise Goupil, in a very special way. She is the one who started the sleep projects with Sid and she paved the way for my own work. Her humility and tenacity will always serve me as an example. I cannot describe all the reasons why I cherish my present and past colleagues at the LSCP but I hope they will know why they all have a special place in my mind: Nathan Faivre, Gabriel Reyes, Hernan Anllo, Jan Balaguer, Hielke Prins, Guillaume Legendre, Matthieu Koroma, Alya Vlassova, Sofie Gelskov, Hao Zhang, Andreas Poulsen, Lorna Le Stanc, Romain Trachel, Romain Grandchamp, Margaux Romand-Monnier... I want also to thank Michel Dutat, Vireak Ul and Cécile Girard for their assistance regarding my experimental work. Still at the ENS but some floors upstairs, I learnt from Trevor Agus the hidden beauty of white noise. At the *Hôtel-Dieu* hospital, I was saved many times by Maxime Elbaz and Stéphane Rio. I picked up a lot from their stories of veterans from the electroencephalography. Brice Faraut, Caroline Gauriau and Virginie Bayon have also been important figures during my doctoral work. I am much in debt with the people who helped me there when I was running my sleepless experiments (Livio de Sanctis and Audrey Dalbin) and especially with the ones who sometimes stayed with me the whole night (Hernan Anllo, Chiara Varazzani and Marlène). In Wisconsin, I had the opportunity to share my days with fantastic minds and, by now, great friends: Simone Sarasso and Ugo Faraguna (whose encyclopedic knowledge about Italian *bestemie* is of great use for me now), Michele Bellesi, Mélanie Boly, Bessie Hung, Stéphanie Maret, Aaron Nelson, Luisa de Vivo and Vlad Vyazovskiy. Back in France, I had the chance to interact with the members of the sleep research community through the VIFASOM group, whose members (and in particular the members of the *Institut de Recherche Biomédicale des Armées* such as Mounir Chenaoui) have been a second scientific family for me. I thank them for their precious inputs. The *Société Française de Recherche et Médecine du Sommeil* was also very supportive and I thank them for their interest in my work.

I know that this list is already long and yet not exhaustive. The success of this doctoral work is due to the people who helped me more than anything else. I wish to thank the examiners (Hélène Bastuji, Karim Benchenane, Jan Born, Marcello Massimini and Shihab Shamma) who agreed to evaluate this work and in particular my referees (Jan Born and Marcello Massinimi). Hélène Bastuji together with Lionel Naccache was instrumental in the progress of this work since they saw it building up and counseled me on the way. I wish to thank as well Isabelle Arnulf and Satoru Miyauchi, who shared with me their expertise on REM sleep and helped me in my endeavor in this new territory.

On a more personal level, I am surrounded by great friends, who are sometimes far from the research world but who have been always patient and curious of what I have been doing all these years. Some of them even participated to my experiments, for which I am very grateful. My numerous family (Dominique and Béatrice, my parents; Nicolas, Xavier, Vincent et Laure, my brothers and sister; Anne-Gaëlle, Veridiana, Anne-Laure et Jaime, their consorts; Élise, Louis, Martin, Philippe and Clotilde, my more than fantastic nieces and nephews) was also there for me in the good as in the bad times and I am proud to have grown up in such constellation. Il peut paraître étrange de remercier ses parents pour une modeste these, étant donné que je leur dois tant et plus, néanmoins je le fais avec joie. Une pensée spéciale pour ma grand-mère, qui garde malgré les ans toute sa jeunesse d'esprit. Sono adesso molto fortunato perché ho anche una seconda famiglia (Chiara, Carolina, Erminia e Massimo) che sta molto attenta a me. Spero che sappiano quanto la loro gentilezza sia preziosa per me. E poi, c'è questo topolino che si nasconde nelle pieghe della mia mente, e chi mi accompagna in ogni pensiero.

Finally, I would like to express the honor I had to meet so many bright minds and good friends. Sadly, not all of them are still alive to read these lines. Each in their own way, Julien Fussler and Sophie Thomain, to whom this doctorate is dedicated, are models I hope I will never fail.

I have walked past and forth the still-mythical *rue d'Ulm* more than I can count. Enough to know it, in all its details; enough to have seen it changed, in its own immutable way. On the pavement, the footprints have disappeared. Maybe another sign that now, it is time for me to find my own way and make it through.

General Introduction

The Sleeping Gypsy
Henri Rousseau (1897)

What is sleep?

Sleep is ubiquitous

From our very first cry to our last breath, sleep marks the passage of days. Whatever its potential costs and whatever we think we could achieve in the meantime[1], humans organize their lives and societies around sleep. This centrality of sleep in existence may have inspired Shakespeare when he wrote these immortal verses[2]:

'*We are such stuff*
As dreams are made on, and our little life
Is rounded with a sleep.'

In Humans, sleep is characterized by the disappearance of the surrounding world. Aristotle in his rich essay on sleep (Aristotle, 350BC) describes it as a "privation of waking" that is to say the inability to "exercis[e] sense-perception". Indeed, every night our minds dissolve at times into nothingness at times into a phantasmagoric inner world. Personal experience suggests that we cease to experience our environment while we sleep, since we cannot really tell what happened over these many hours. The direct consequence is that sleepers remain quite unresponsive to external stimulations, just as Gulliver when tied up by the Lilliputs. Such unresponsiveness can be objectively measured, providing a defining criterion for sleep that can be applied to both Humans and animals (Cirelli and Tononi, 2008).

Using the absence of responsiveness to probe sleep, it has been shown that sleep expands much further than the humankind (see Figure 0-1) and phenomena resembling human sleep have been described in all animal species studied so far, from fruit flies to platypuses (Cirelli and Tononi, 2008). Even animals for which sleep represents an ecological disadvantage do sleep. For example, migratory birds must fly for extended periods without landing. In this context, sleeping becomes both difficult to achieve and dangerous to maintain. Down the sea, dolphins need to periodically reach the surface in order to breathe, which implies that they cannot stop swimming in order to sleep. Hence, the ecological niches of these species put a huge pressure on sleep. But sleep remains, in an adapted way. In these species can be found what is called unihemispheric sleep (Rattenborg et al., 2000). Its principle is simple: one cerebral hemisphere only sleeps at a time, letting the other hemisphere deal with the environment and its potential dangers. Thus, even in the most constrained and unfavorable environments, animals do sleep. But how then can sleep be defined so as to take into account all its implementations?

[1] Plato for example considered sleeping too much as 'shameful and unworthy': 'A sleeping man does not worth anything, just as a dead man' (Plato, Laws, 370-345 BC).
[2] Shakespeare, The Tempest (1611) Act IV Scene I

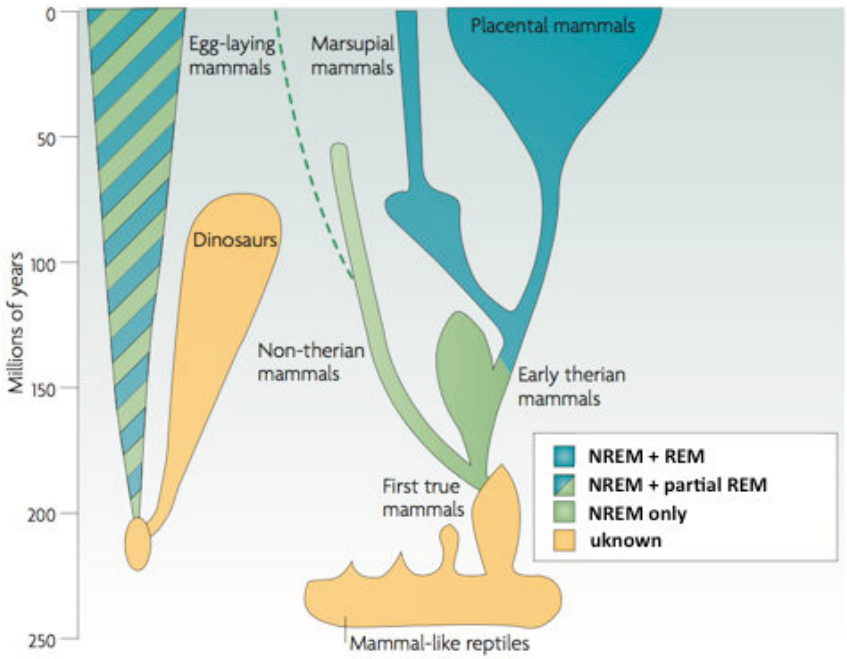

Figure 0-1 Presence of NREM and REM sleep across Vertebrates

All studied animals so far have been shown to sleep (even if some particular cases are still a matter of debate (Cirelli and Tononi, 2008)). But there are important differences across species. While placental mammals like primates or rodents show two types of sleep alternating within a night (NREM and REM sleep, see below), non-therian mammals do not show signs of REM-sleep. Other species show REM-sleep only during the early stage of life. Crucially, NREM sleep is present in all these species. Adapted from (Hobson, 2009).

Sleep as a state

Amongst human beings, the best way to know whether a person is asleep is simply to have a look. A still and curled posture, deep breathing, closed eyelids are well-known signs of sleep. If some doubt persists, asking is enough. An absence of response would probably mean that the person is asleep. Of course, such a definition lacks both specificity and sensitivity and can be hardly transferred to non-human species. But the core idea can be reprieved: sleep is a state in which the responsiveness to external stimuli is greatly diminished.

In 1862, Ernst Kohlschütter made the first detailed description of how sleepers get disconnected from their environment (Kohlschütter, 1862) by measuring the intensity a sound needed to awake a sleeper. This 'perturbational' approach that consists in determining the arousal threshold was later used to operationally characterize sleep in humans (Rechtschaffen et al., 1966). A similar approach is recommended to assess sleep in animals (Cirelli and Tononi, 2008). Such measure has the advantage to probe the most striking consequence of sleep at the subjective level in an objective manner. However, it supposes the ability to stimulate an organism in an appropriate way so as to record a behavioral response when the arousal threshold is exceeded. This is not always possible.

Let's take the example of patients with disorders of consciousness (in a vegetative, minimally conscious or locked-in state). These patients cannot always interact with their surrounding environment. How can we possibly assess whether they sleep or not? It is obviously not possible to rely on behavioral markers. Instead, sleep (and wakefulness) can be defined at the neural level. Indeed, with the invention of the EEG in 1924 by Hans Berger (Berger, 1929) came quickly the discovery that the waking and sleeping brain had a very different electrical activity (Loomis et al., 1935). I will detail later the changes occurring during sleep, but the most striking is the replacement of low-amplitude desynchronized rhythms by high-amplitude synchronized oscillations (see Figure 0-3). Similar changes in neo-cortical activity can be observed in other mammals and birds. Nowadays, the EEG is routinely used in hospitals (and soon at home) to accurately monitor sleep without perturbing it.

EEG is also one of the key tools to investigate sleep, its mechanisms and functions. Accordingly, it is the technique I relied on for most of the work presented here. Using EEG, two different types of sleep have been clearly identified in mammals: Rapid Eye-Movement (REM) sleep (also called Paradoxical Sleep) and Non-Rapid Eye-Movement (NREM) sleep (often referred as Slow-Waves Sleep, SWS). They both occur while individuals are lying in a horizontal position, with eyelids closed, a reduced or absent muscle tone and increased arousal thresholds. However, NREM and REM sleep have also many different properties, stressing the variety of states that the term sleep encompasses.

Sleep as a process

Defining sleep as a state, surely, has an undeniable operational efficiency. But from a closer perspective, sleep seems much more than a mere condition. We sleep not necessarily for the enjoyment of it, but for a purpose and this purpose is to be found in our waking life. Indeed sleep has a restorative effect on the mind and body that will persist even after awaking. These long-term effects of sleep are things we look for when, for example, one takes a nap after a short night or because she got tired driving (Figure 0-2). Sleep can be therefore seen as a process: we sleep to realize a specific end. I will review in more details the many benefits of sleeping.

Figure 0-2 Road sign in Australia

Sleep is a process also in the sense that it is not a monolithic condition: sleep is a series of states that are laid out in a precise order. Indeed, our nights are structured in cycles, which vary in

numbers and durations across nights and individuals but share the same core properties (Figure 0-4). Each of these cycles starts with a gradual increase in the intensity and EEG markers of NREM sleep. Sleepers then stabilize in deep NREM sleep during which the brain activity is dominated by sleep slow-waves. Next, NREM sleep suddenly dampens and sleepers transit to a brain activity closer to wakefulness (REM sleep) although they do not wake up. After an episode of REM sleep, a new descent to NREM sleep starts again marking the beginning of a new cycle.

Another reason to conceptualize sleep as a process rather than a state is that sleep does not appear randomly but is built upon the preceding wakefulness period. Scientific articles dealing with sleep often mention the term 'sleep pressure': the more one stays awake, the more she will get tired and the easier it will be to fall asleep (Borbely and Achermann, 1999). Thus, sleep can sometimes irrepressibly appear at the worst moment possible. Sleep also depends on the time of the day: it is easier to fall asleep right after lunch time (even if we don't eat) than later in the afternoon even if the time spent awake has increased. These views have been succinctly summed up by Alexander Borbély in his "two process model of sleep" (Borbély, 1982). According to this model, sleep is regulated by two processes: (i) a circadian process which determines for example that we, humans, usually sleep at night while rodents sleep during the day, (ii) an homeostatic process which gradually builds up with time spent awake. These two processes interact in shaping sleep. For example, the proportion of Slow-Waves Sleep (SWS) increases with time spent awake prior to sleep illustrating the built up of the homeostatic pressure (Dijk et al., 1987; Friedman et al., 1979). Reversely, this pressure is dissipated during the night and the proportion of SWS within sleep cycles declines within a night (Riedner et al., 2007). This link between wake activity and sleep intensity is use-dependant and the circuits that have been solicited the most during the wake period get 'tired' first and sleep more soundly (Huber et al., 2004; Hung et al., 2013). Sleep can be therefore seen as a process reflecting and compensating our waking life, i.e. the price we pay for being awake (Tononi and Cirelli, 2014).

The function(s) of sleep

Seeing sleep as process comes down to attribute to sleep one or several functions. However, despite the elements briefly presented below, the search for the function of sleep is still one of the biggest challenges of sleep research (Tononi and Cirelli, 2014). Scientists have reach a quite good understanding of what is sleep, how it works and how it is regulated but less regarding its purpose. The problem is not really the lack of candidates but rather the multiplicity of functions that sleep seems to subserve and the difficulty to prove the specificity of sleep in their accomplishment[3].

To gather clues about the potential function of sleep, one strategy consists in examining the effect of its absence, i.e. the effects of sleep deprivation. Acute sleep deprivation leads to death after few days, as evidenced in animals (Orzeł-Gryglewska, 2010). Sleep loss affects cognitive performance but also the immune system, triggers hormonal changes, obesity, alters cardio-vascular function. Sleep seems therefore very important to the correct functioning of the

[3] Concerning this search for a function of sleep, Chiara Cirelli and Giulio Tononi reminded appropriately the words of the mythical phoenix: *"Che vi sia ciascun lo dice, dove sia nessun lo sa" ("that there is one they all say, where it may be no one knows"* Wolfgang Amadeus Mozart and Lorenzo da Ponte, Cosi fan tutte (1790)).

organism, not only the nervous system. Accordingly, the immune systems has been shown to benefit from SWS (Westermann et al., 2015). Sleep seems also very important for the conservation of energy (Benington and Heller, 1995), the cleansing of metabolic waste in the central nervous system (Xie et al., 2013), and the maintenance of the nervous system at the circuit or neuronal level (Maquet, 1995; Tononi and Cirelli, 2014).

Acute sleep deprivation impairs also a variety of cognitive abilities (Alhola and Polo-Kantola, 2007; Durmer and Dinges, 2005). The spectrum of cognitive processes affected goes from the simple reactivity to unpredicted stimuli to more complex processes such as attention allocation, memory, cognitive control, emotional balance, reasoning, creativity (De Gennaro et al., 2001; Doran et al., 2001; Gevers et al., 2015; Gujar et al., 2011; Harrison and Horne, 2000, 1999; Wimmer et al., 1992). At the neural level, sleep deprivation translates into the intrusion of sleep-like activity within the awake brain (Hung et al., 2013; Vyazovskiy et al., 2011). This has been interpreted as the fact that neurons cannot maintain their level of waking activity for an indeterminate amount of time and when neurons get 'tired', they 'fall' into sleep (Tononi and Cirelli, 2014; Vyazovskiy and Harris, 2013).

Sleep would thus be a process allowing the brain to recover its optimal functioning in the safest way, i.e., at a given time when the consequences of getting disconnected and unresponsive minimally impair survival. An extensive literature has also assessed the function of sleep in memory (Diekelmann and Born, 2010; P Peigneux et al., 2001; Rasch and Born, 2013; Tononi and Cirelli, 2014) (see also p20-21 and Discussion). Although the exact mechanisms are still unclear (see Chapter 3 and Discussion), sleep has an important role (i) in the consolidation of existing memories, (ii) in the ability to create novel associations between existing memories and (iii) in the ability to form new memories in ensuing wakefulness. The fact that the brain goes offline during sleep could be crucial to fulfill this memory function by suppressing potential external interferences during the consolidation and transfer of memories (Diekelmann and Born, 2010).

Can one or any of these functions be coined as 'the function of sleep'? To conclude on this issue, scientists must firstly control for the circadian confound: sleep occurring at a certain phase of the circadian cycle, it is therefore easy to confound something co-occurring with sleep for something caused by sleep (Frank and Cantera, 2014). Functions of sleep should be specific to sleep. Among the functions listed above, which ones necessitate to be asleep, e.g. in a state of disconnection from the environment? Metabolic recovery or the consolidation of the immune memory does not need, a priori, such disconnected state. However, it has been argued that the neural homeostasis and memory consolidation functions would match this criterion since they benefit from the brain going offline (Diekelmann and Born, 2010; Tononi and Cirelli, 2014). Thus, according to Allan Hobson, "sleep is of the brain, by the brain and for the brain" (Hobson, 2005).

Another view, championed by Jeremy Siegel advances that there is no real function of sleep (Siegel, 2009). On the contrary sleep can be regarded as an adaptive phenomenon and a simple variant of the dormant state that spans both animal and vegetal kingdoms. In this view, sleep is the mere extreme of a continuum including rest. This argument is based on the failure to find (i) a function that necessitates being asleep and (ii) a function that would be common for all the species known to sleep. This argument also reckons on the variety of sleep properties across species and the absence of obvious boundary between resting and sleeping. While thought provoking, this approach falls short at explaining certain key features of sleep (e.g. a sensory

disconnection far more pronounced than during rest, the existence of REM sleep) and their striking preservation across species and biotopes.

The fact that NREM and REM sleep subserve different functions may account for the difficulty to identify 'the function of sleep'. Indeed NREM sleep is the part of sleep that is most vital to animals since (i) not all animals experience REM sleep or an equivalent of it (see Figure 0-1), (ii) in Humans, REM sleep can be suppressed for long period of times, using for example anti-depressors (Mayers and Baldwin, 2005), without causing noticeable issues. On the other hand, acute sleep deprivation triggers REM sleep intrusion (animals falling into REM sleep directly from wake) stressing the importance of this state (Orzeł-Gryglewska, 2010).

In conclusion, sleep affects our brain but also our behavior and mind *through* the brain. As a 'neuro-apprentice', I am especially interested in the causal link between changes in brain activity and changes at the behavioral and phenomenological levels. Countless studies have confirmed the interest of such reductionist approach and the tight correlation between the transformation of brain dynamics at sleep onset and the loss of awareness or, on the contrary, its recovery during dreams (Nir and Tononi, 2010; Tononi and Massimini, 2008).

The physiology of sleep

As we have seen, sleep is a rich, complex and ubiquitous phenomenon that is hardly reduced to a unique definition due to the variety of its implementations in the animal kingdom. However, sleep has been mostly studied in vertebrates and especially mammals such as cats, rodents and humans. These species present a highly organized central nervous system whose activity follows the same common characteristics (Buzsáki, 2006). Among these shared properties is the impact of sleep on brain activity. I will give here few elements on sleep physiology, which will be recurrently mentioned throughout this manuscript.

NREM and REM sleep

When examining EEG recordings across an entire night, brain activity clearly fluctuates between 3 drastically different states: (i) wakefulness, (ii) NREM sleep and (iii) REM sleep. Figure 0-3 shows representative snapshots of these 3 stages as well as their associated spectral profiles.

During wakefulness, the EEG signal is dominated by low-amplitude fast rhythms such as alpha oscillations ([8, 12] Hz). The alpha rhythm is a resting oscillation, increasing when the eyelids are closed, potentially due to the disengagement of the visual cortex (Cantero et al., 2002). Interestingly, alpha oscillations slowly fade with drowsiness and mark the transition with light NREM sleep (NREM sleep stage 1, NREM1). Quickly after the disappearance of alpha oscillations, other rhythms appear, which are specific to NREM sleep. K-complexes for example are the biggest non-pathological brain response that can be recorded from the Human EEG. It consists in an isolated high-amplitude slow-wave ([0.5, 4] Hz) that can be either spontaneous or evoked by an external stimulation (Halasz, 2005). Another hallmark of NREM sleep are sleep spindles, a waxing-and-waving [10, 16] Hz oscillation, which is the central topic of Study 2 (Andrillon et al., 2011). The apparition of the first slow-waves and spindles mark the transition toward consolidated sleep and the NREM sleep stage 2 (NREM2). Then, slow oscillations tend to become more and more frequent, and to occur in trains rather than in isolation. The transition to an EEG signal dominated by slow-waves mark the onset of NREM sleep stage 3 (NREM3).

Usually after an episode of continuous NREM3, sleep lightens again announcing the transition to REM sleep. REM sleep could be easily mistaken with wakefulness at first sight since the brain activity recovers in REM sleep properties similar to wakefulness (EEG activity is dominated again by low-amplitude desynchronized fast rhythms as in wakefulness). In REM sleep, NREM sleep attributes, such as slow-waves and sleep spindles, are no longer seen. Surprisingly, alpha oscillations are also absent despite the closed eyelids. More surprising is the apparition of rapid eye-movements in the electrooculogram (EOG) (Aserinsky and Kleitman, 1953), as if the recorded individual was awake in its bed, looking around. The contrast between a wake-like brain activity and the fact that the sleeper is profoundly asleep with a highly reduced if not absent muscle tone (as recorded through and electromyogram, EMG) inspired Michel Jouvet in calling it ‘paradoxical sleep’ (Jouvet, 1992), although the term of Rapid Eye-Movement (REM) sleep is now more widely used.

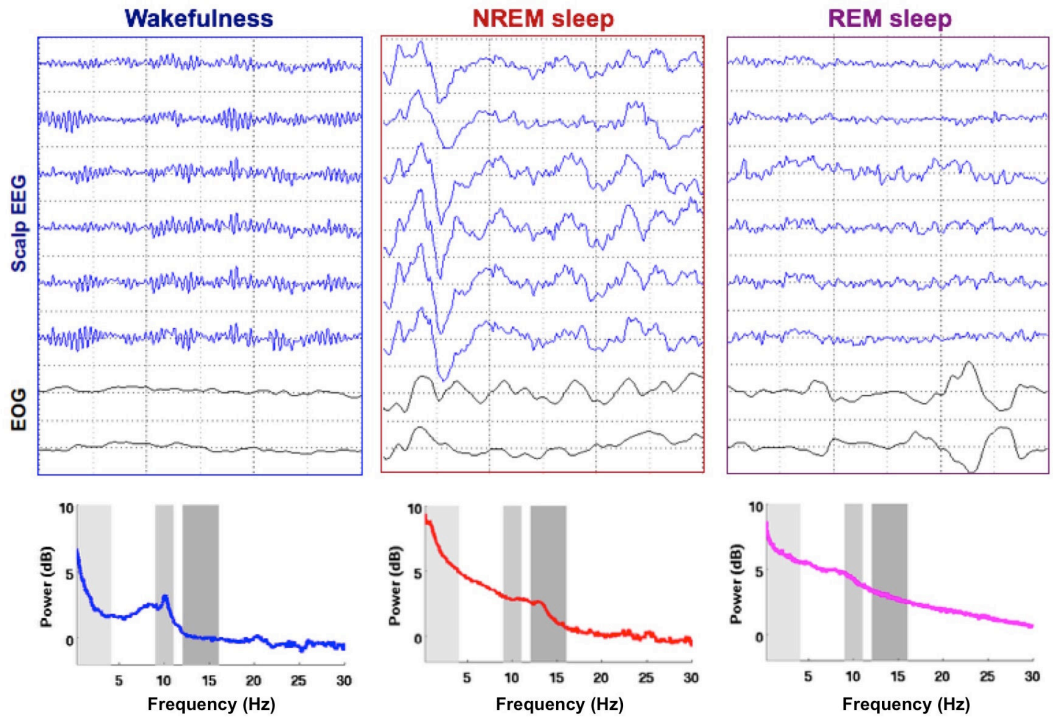

Figure 0-3 Electrical activity of the brain across wake and sleep

Top: Scalp electroencephalographic (EEG, blue curves) and electrooculographic (EOG, black curves) recordings performed in a healthy young adult during wakefulness with closed eyelids (left), NREM sleep (middle) and REM sleep (right). Note the drastic changes occurring in the different states. From wakefulness to NREM sleep, fast oscillations are replaced by slow-waves. REM sleep is characterized by a partial recovery of wake-like rhythms as well as the presence of saccades in the EOG (opposite deflections). Bottom: Power spectra corresponding to the different states obtained through a Fast Fourier Transform on the EEG signal displayed atop. Wakefulness is characterized by a peak in the alpha band (~10 Hz), NREM sleep by an increase in the delta (< 4 Hz) and spindle (11-16 Hz) bands.

The American Society of Sleep Medicine set a series of guidelines defining precisely these different stages and their neural signature (Iber et al., 2007). Here are some key points summing up sleep physiology:

			Wake	light NREM	deep NREM	REM
EEG	**delta**	<4Hz		K-complexes	slow-waves trains	
	theta	[5-8]Hz				predominant
	alpha	[8-12]Hz	if eyes closed			
	sigma	[12-16]Hz		spindles	spindles	
	fast	>20Hz	high			
EOG			saccades	slow (at sleep onset)	none	saccade-like
EMG			high	low	low	absent

The hypnogram and the structure of sleep

As already mentioned above, NREM and REM sleep are not randomly distributed within a night but follow a precise structure. The hypnogram depicts this structure by showing the succession of sleep stages across times. Figure 0-4 shows a typical example of hypnogram. The first sleep cycle has been highlighted in yellow.

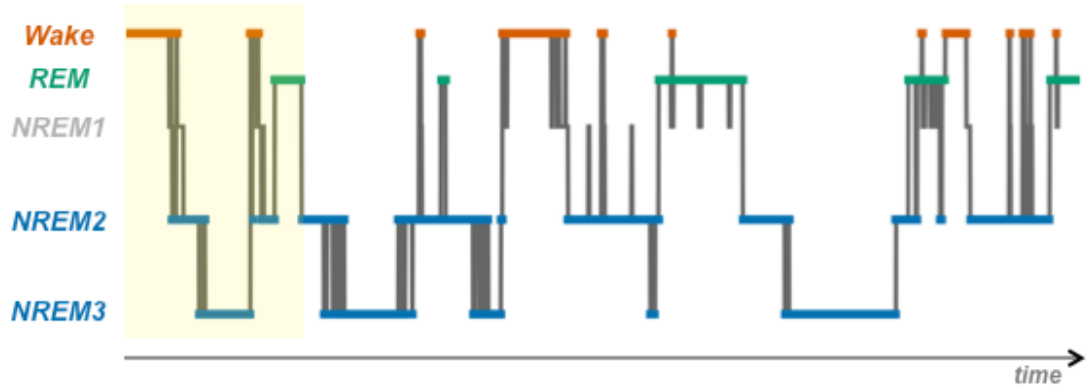

Figure 0-4 Hypnogram of a healthy young individual

The hypnogram shows the succession of sleep stages across a night. A pattern can be quickly recognized: the succession of NREM and REM episodes. The first sleep cycle is highlighted in yellow. It is characterized by an initial descent from wakefulness to NREM3 via NREM1 and 2. Then NREM sleep dampens and a transition toward REM sleep appears. One typical night contains several cycles. The proportion of REM sleep within a cycle increases during the night and the proportion of NREM3 decreases. Awakenings are more frequent at the end of recordings. Note that here the large number of recordings may be due to the fact that sleepers were presented with auditory stimuli during the entire night (see Studies 4-7 and 9).

Each cycle starts first with NREM sleep, followed by REM sleep. Transitions may be accompanied by periods of wakefulness. It is worth noting that the proportion of REM sleep and awakenings tend to increase with the time spent asleep. For example the last cycle contains many awakenings from NREM2, and the individual did not enter the NREM3 stage. This illustrates the dissipation of the aforementioned homeostatic pressure (sleep gets lighter and more fragile toward the end of the night). On Figure 0-4, NREM1 was put in gray color to emphasize the specificity of this stage. Neither wake nor consolidated sleep, NREM1 usually spans the hypnagogic (i.e. sleep onset) period. It is a very rich ever-changing state (Hori et al., 1994; Ogilvie, 2001). However, such heterogeneity makes hypnagogia quite hard to study and its twilight nature places it out of scope of the present manuscript.

Macro and micro dynamics of NREM sleep

I have described so far sleep physiology as a series of snapshots rather than as a dynamic process. And indeed, sleep physiologists have mainly focused on stable states such as deep NREM sleep (usually called in rodents Slow-Waves Sleep, SWS) and REM sleep. Nonetheless, transitional states such as light NREM sleep, which marks the passage between wake and SWS

or SWS and REM sleep, are preponderant in Humans and amount for 50 % of the total amount of sleep in healthy young adults (25-35 years old, (Carskadon and Dement, 2011)). Thus, periods of continuous slow-wave trains are preceded by rather long episodes of light NREM sleep during which NREM hallmarks (slow-waves and spindles) appear only occasionally. It is therefore important not only to distinguish the different NREM stages but also to consider the broader context in which they occur, especially when considering sleepers' ability to process external information. Light NREM is present at transition between states of deep stable sleep and represents a state in which the sleeping brain is more responsive to external stimuli (see Studies 4-6).

Light NREM sleep has also been seen as a forerunner which prepares the brain for deep NREM sleep (De Gennaro et al., 2000). Indeed, transiting from wakefulness to deep NREM sleep is not instantaneous since the apparition of slow-waves is the result of a profound change in the functioning of the brain. The larger the brain, the more complex such process is (Buzsáki et al., 2013), which could explain why Humans spend more time in transitional states than rodents. These changes are controlled by cholinergic neurons in the brainstem, which implies a rather slow dynamics (Mircea Steriade, 2003).

A recent study (Siclari et al., 2014a) has shown how NREM sleep hallmarks change through sleep onset. Siclari and colleagues propose to sort slow-waves into two types reflecting drastically different processes. Type-I slow-waves, that are predominant in light NREM sleep, could be approximated to K-complexes (i.e. isolated, usually evoked slow-waves occurring in light NREM sleep (Colrain, 2005; Loomis et al., 1938)). Rather global subcortico-cortical events, these type-I slow-waves affect a broad fronto-medial network and are associated to the activation of wake-promoting structures. Such properties may favor the processing of external information, as some of the data presented in Study 9 suggest. Through the nesting of other sleep rhythms such as sleep spindles and hippocampal ripples (Staresina et al., 2015), these type-I slow-waves could also organize the replay and consolidation of existing memories (Diekelmann and Born, 2010). On the other hand, type-II slow-waves (which can be approximated to NREM3 slow-waves) reflect local synchronization processes. The local nature of slow-waves will be presented in Study 1. By putting the brain into a state in which cortical regions become functionally independent (Massimini et al., 2005), the impact of type-II slow-waves on sensory processing could be diametrically different than for type-I slow-waves (see Discussion). Finally, Siclari et al. proposed that these type-II slow-waves are associated to the homeostatic recovery of neuronal networks (synaptic homeostatsis). They could therefore have an opposite effect on memory formation compared to type-I slow waves as well (see Study 9).

The micro-dynamics of sleep is very relevant when exploring how the brain processes information. As we have seen, slow-wave sleep is populated by slow-waves, which correspond to periods of neuronal silencing (OFF state or down-state) followed by a rebound activity (up-state) (Nir et al., 2011; Mircea Steriade, 2003) (see also Figure 0-5). This succession of down and up-states has been proposed to explain the lack of responsiveness and the loss of awareness during sleep (Tononi and Massimini, 2008). Indeed, off-states would cut any neural computation and break the temporal integration of information (Pigorini et al., 2015), which is necessary for the brain to perform complex processes. In study 5, I will present evidence showing that indeed down-states occurring right after stimuli are detrimental for integrated processes such as the preparation of a motor response.

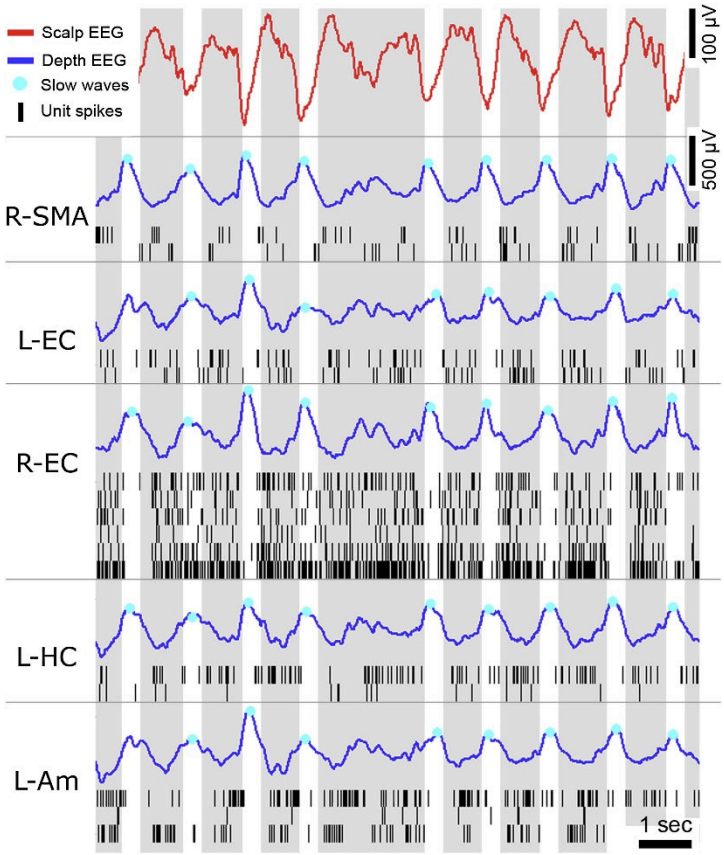

Figure 0-5 Slow-waves and neuronal silencing

Slow-waves recorded during NREM3 in an epileptic patient implanted with depth electrodes (Nir et al., 2011). The top red curves show the scalp EEG with its characteristic trains of slow-waves. Blue curves show the corresponding depth EEG across different brain regions (SMA: supplementary motor area, EC: entorhinal cortex, HC: hippocampus, Am: amygdala, R: right, L: left). Slow-waves span here very distant regions, which is quite rare. Slow-waves' down-states are marked with a blue dot (negative peak on scalp EEG, positive peak in depth EEG). These down-states are accompanied by a silencing of neurons (black vertical ticks: each line shows a different neuron recorded in the same region as the depth EEG, each ticks correspond to a spike). Down-states are followed by an up-state (positive peak at the scalp level, negative in depth EEG), a rebound in units' activity. Reproduced from (Nir et al., 2011) (see Study 1).

NREM sleep spatial dynamics

Sleep is not only a dynamic process in time but also in space, a dimension that had been rather overseen until recently (Nobili et al., 2012). This could be due to the focus on sleep stages that are stable across time, as mentioned above. It might also be due to the favored animal model for sleep physiology: rodents. Rodents indeed have a rather small brain (and are usually recorded with few electrodes), which makes the observation of regional differences more difficult than in larger brains such as in Humans. In the first chapter of this manuscript, I will present studies I have contributed to (Studies 1 and 2) that are part of a larger re-description of sleep as a more local phenomenon than previously thought (Andrillon et al., 2011; Nir et al., 2011).

Indeed, textbooks usually depict sleep as a rather global phenomenon (Mircea Steriade, 2003). In particular slow-waves have been described as a global synchronization process during which large portions of the neocortical neurons go silent (OFF state), followed by an identically synchronous up-state. However, this view has been recently challenged. Giulio Tononi and Chiara Cirelli's group showed that slow-waves could be locally modulated depending on wake activity, portraying sleep as a use-dependent process (Huber et al., 2006, 2004). It has been later shown that, in human scalp EEG, these slow-waves were not perfectly synchronous across brain regions but traveled within the cortex along a fronto-parietal axis (Massimini et al., 2004). This fronto-parietal axis is more an average trend than a rigid path and slow-waves seem to emerge in various brain locations (Mak-McCully et al., 2015; Siclari et al., 2014a). With Yuval Nir, Chiara Cirelli and Giulio Tononi, I had the chance, as a Master student, to dive into the brain of epileptic patients[4] and to have a closer look on these slow-waves (Nir et al., 2011). Indeed, scalp recordings reflect only partially the underlying cortical activity. Deep structures or regions in which neurons are not well aligned will be less (or not at all) reflected in the scalp EEG signal. One of the reason sleep and slow-waves were seen as a truly global phenomenon could have stemmed from these limitations: local phenomena are less likely to show up at the scalp level. What we found is that, when recording many different brain regions, slow-waves are rarely global (Nir et al., 2011). A similar analysis of sleep spindles reach the same conclusions (Andrillon et al., 2011).

The spatial aspect of sleep has also been emphasized during the sleep onset period. In a important study performed again thanks to the participation of epileptic implanted patients, Michel Magnin and colleagues showed that sleep onset is not synchronous across brain regions (Magnin et al., 2010). On the contrary, some regions fall into NREM sleep minutes before others. Interestingly, the Hippocampus is one of the first to fall asleep, a fact corroborated by another study showing the early appearance of sleep spindle before neocortical and scalp sleep onset (Sarasso et al., 2014). Such phenomenon could explain the so-called sleep-related amnesia: it is quite common to fall asleep while reading a book or watching a movie. The last lines of the book or the last scene of the movie read or seen before falling asleep are usually not remembered. This could be explained by the fact that, before falling asleep, we may spend a few minutes with an awake neocortex but an asleep hippocampus (Magnin et al., 2010; Sarasso et al., 2014). Under these conditions, the formation of the long-term memories necessary to remember the elements perceived during this period of time would be greatly impaired.

Another highly interesting development of the study of regional differences during sleep concerns our waking life. Indeed, local sleep has been found in wakefulness too. In a seminal study, Vlad Vyazovksiy and colleagues showed the OFF periods can be recorded in awake behaving animals after sleep deprivation (Vyazovskiy et al., 2011). Not only can neurons locally fall asleep in a context of global wakefulness, but this local OFF periods can affect behavior. Thus, lapses of attention could be reinterpreted as a phenomenon of local sleep, establishing a continuum between wake and sleep. Other studies in human scalp recordings showed evidence for intrusion of sleep-like pattern during wakefulness after sleep deprivation (Bernardi et al., 2015; Hung et al., 2013). Wake and sleep can be therefore seen as a dynamic continuum. And the

[4] Studies 1 to 3 are based on data from implanted epileptic patients. It is important to remember that these patients are not implanted with intracranial electrodes, a very intrusive procedure, for research but as part of their treatment. The data collected is used primarily to plan the resection of the epileptic focus. These patients can also participate to research protocol if they wish. We are, of course, immensely grateful for their help in advancing scientific knowledge and trust.

intrusion of sleep in wake (or wake in sleep) could potentially impair (or restore) the processing of sensory information.

The REM sleep paradox

As we said earlier, REM sleep offers a drastic contrast with NREM sleep in terms of brain activity. In only few seconds, the trains of slow-waves, characteristic of deep NREM sleep, are replaced by low-amplitude high-frequency rhythms (Jouvet, 1965). At first sight, the sleepers seem to have awakened. EOG traces show the occurrence of bursts of rapid eye-movements (Aserinsky and Kleitman, 1953), the heartbeat and the respiration frequency increase. Yet, the sleeper is still in bed, profoundly asleep. The absent muscle tone visible on the EMG indicate a paralysis of the skeletal muscles, preventing any movement to be made. An awake brain in a sleeping body, such is the paradox of REM sleep (Jouvet, 1992).

Thus, instead of the bi-stability observes in deep NREM sleep (Steriade et al., 2001), during which OFF and ON periods alternate, neurons in REM sleep show a tonic regime of activity (Nir and Tononi, 2010). At the systemic level, the cortico-cortical connectivity is restored (Massimini et al., 2010) compared to NREM sleep. And the complexity of the neural activity increases back, almost up to the wake level (see Study 5 for example), which is in line with the frequent occurrence of dreams in REM sleep. Interestingly, this complexity has been shown to precisely track the level of consciousness in anesthesia or in patients with disorders of consciousness (Abásolo et al., 2015; Casali et al., 2013; Schartner et al., 2015). All of these changes could be mediated by a modification of the neuromodulation compared to NREM sleep. Indeed REM sleep is characterized by levels of Acetylcholine that are quite similar to wakefulness (Jones, 2005; Siegel, 2004), which could explain the recovery of wake-like activity.

Yet, from a functional point of view, REM sleep is very different from wakefulness and despite a brain activity resembling the awake state, sleepers are quite isolated from their environment in REM sleep (Rechtschaffen et al., 1966). Even if dreams frequently occur and consciousness is regained (Yuval Nir et al., 2013), external stimuli are rarely integrated to the dream scenery. Why? Until recently, the mechanisms gating sensory information during REM sleep remained a complete mystery. But a very recent study from Chiara Cirelli and Giulio Tononi's group may bring the beginning of an answer (Funk et al., 2016). Despite decades of detailed investigation of sleep physiology, they discovered something that had gone unnoticed: the presence of NREM-like slow-waves in the superficial layers of primary sensory cortices during REM sleep. The locality of these slow-waves may explain why they had not been observed before. By disrupting the activity of the superficial layers within primary cortices, which receive most of the sensory thalamic inputs, such slow-waves may isolate the cortex from the surrounding environment. In addition, since these slow-waves are circumcised to primary cortices, the remaining cortical regions could still perform computations close to wake activity, leading to the generation of dreams. I will discuss these gating mechanisms in the Discussion.

The sleeping brain is not dormant

As we have seen in the preceding section, sleep physiology is very rich and reflects a highly structured and dynamic phenomenon. What are the consequences on the sleeping brain ability to respond to external stimulations? Is the brain truly isolated from its environment during sleep as subjective introspection and behavioral observations suggest? Can the sleeping brain process sensory information without waking up? Up to which level?

Sleep and phenomenology

One of the most classical arguments brought to stress how active can the sleeping brain be concerns dreams. Every night indeed, we create new worlds. Most of the time we do not notice and do not remember, some will eventually never or rarely do, but if someone wakes you up at the correct moment of the night, there is a very high probability that you will be able to report glimpses of these worlds (Nir and Tononi, 2010). Nonetheless, if dreams occur every night, they do not occur at any moment during the night. Parts of sleep will be truly blank even when forcing the awakening. What causes the brain to enter, at times such void, and at times universes as rich as the real world? This question had been laid out more than 2,000 years ago by Aristotle (Aristotle, 350BC):

> *"Further, in addition to these questions, we must also inquire what the dream is, and from what cause sleepers sometimes dream, and sometimes do not; or whether the truth is that sleepers always dream but do not always remember (their dream); and if this occurs, what its explanation is."*

Awakening sleepers during their night showed a strong relationship between REM sleep and oneiric imagery (Nir and Tononi, 2010). While dreams are not completely absent in NREM, they are rare and usually rather simple (e.g. static images). In REM sleep however, dreams can last for extended periods of time and deploy complex plots and scenes.

The core questions regarding dreams are still unanswered. Why do we dream? How are dreams generated? What do we dream of certain contents? Some even put the very existence of dreams into questions such as the philosopher Daniel Dennett (Dennett, 1976). According to him, dreams could be a mere construction (or reconstruction) performed upon awakening. Several arguments can be brought against this view. The strongest may be found in RSBD patients (REM sleep Behavior Disorders (Schenck et al., 1986)). These patients are deprived of skeletal muscle paralysis during REM sleep (which explains the near absent muscle tone observed in the EMG). The consequence is highly turbulent nights. As said above, the REM sleeping brain has an activity closed to wakefulness, which implies activations within the motor cortices. In RSBD patients such activations are enacted resulting in complex motor patterns. These patients move, talk, sing, fight, dance, and copulate while sleeping. Interestingly, these movements correspond to their dream reports (Leclair-Visonneau et al., 2010) making it clear that dreams are generated during REM sleep.

But if movements in RSBD patients open a window on the dream scenery, does it mean that eye-movements, which are preserved even in healthy individuals, share the same property? This issue has been debated for decades and is still debated nowadays (Arnulf, 2011). Rapid eye-

movements (REMs) in REM sleep are triggered by the so-called PGO (Ponto-Geniculo-Occipital) waves (Jouvet and Michel, 1959). Through PGO waves, the brainstem sends to the neo-cortex a volley of activation that generates, among other activations, the eye-movements. What happens during and after this volley? Are PGO waves pulling the strings of the cortex and generate dreams in a stochastic way (Hobson, 1990)? Does each eye-movement in REM sleep correspond to a change in the visual scene as in wakefulness? In Study 3 we explored the neural activity around eye-movements within the medio-temporal lobe, a structure heavily involved in conscious vision and memory. We found similarities with wake activity associated to the processing of visual images (Andrillon et al., 2015b). This result suggests that sensory processes are performed around eye-movements. Investigating how sensory information flows during REM sleep in comparison with wake vision or mental imagery (i.e. top-down vs. bottom-up flow) could help disentangling these opposite views on dream generation. But what happens when we do not dream? Is the brain truly inactive at that time?

Sleep and its reversibility

Sleep, unlike coma, anesthesia or other disorders of consciousness leading to a state of unresponsiveness, is quickly and spontaneously reversible. This reversibility is both a potential advantage (allowing sleepers to wake up when endangered) and a challenge (to prevent the brain to wake up when not necessary). This reversibility fluctuates within a night as shown by the evolution of arousal thresholds (Rechtschaffen et al., 1966). Thresholds are maximal at the beginning of the night when deep NREM sleep and slow-waves train are predominant, which suggests that these sleep oscillations may participate to sensory gating. These thresholds vary also across individuals, which has an obvious impact on sleep quality. Interestingly, the density of sleep spindles is predictive of the arousal thresholds (the more an individual shows sleep spindles, the higher her threshold (Dang-Vu et al., 2010)), suggesting also a role of sleep spindles in sleep protection.

Interestingly, stimulus intensity is not the only parameter determining whether a stimulus will wake up a sleeper or not. The relevance or familiarity of the stimulus also matters. In the 60s, Formby and colleagues showed that mothers, right after their child's birth, wake up more easily for their own baby's cry compared to another baby (Formby, 1967). Similarly, Oswald and colleagues showed that sleepers are more sensitive to their own name during their sleep than someone else's name (Oswald et al., 1960). These simple experiments show that equally loud stimuli do not necessarily impact sleep the same way. Is it because these stimuli are processed as more relevant during sleep, or does their familiarity modify the 'subjective intensity' of these stimuli? In other words, does this differential processing of information originate in sleep, or is it a consequence of an increase sensitivity acquired during wakefulness? In the following section I will detail studies that have investigated this question by examining sleepers' ability to process information while remaining asleep (see (Atienza et al., 2001; Bastuji, 1999; Hennevin et al., 2007) for reviews). This has been done by examining the covert responses of the brain to external stimuli, and by checking that equivalent processes occur during sleep compared to wakefulness (see Box p19).

Are sleepers isolated from their environment?

It was initially thought that sleepers were quite isolated from their environment and that, unless the stimulation was strong enough to lead to an awakening, sensory information would not reach the neo-cortex during sleep. Bal and McCormick proposed that the changes in the dynamics of the thalamo-cortical loops occurring during NREM sleep (such as during sleep spindles) would prevent the thalamus from relaying sensory information from the peripheral senses to the neocortex ('thalamic gating hypothesis', (McCormick and Bal, 1994)). Indeed, except for olfaction, all sensory information passes by the thalamus before reaching the neo-cortex (Jones, 2007). If the thalamus does not relay sensory information anymore, the resultant would be a neo-cortex isolated from its peripheral senses. In accordance with this view, fMRI recordings showed that sensory information provided during sleep spindles or slow-waves down-state are effectively blocked at the thalamic level (Schabus et al., 2012).

However, ligtht NREM sleep is dominated by K-complexes and sleep spindles, which are phasic events, i.e. they do not occur continuously. Can information pass to the cortex in between these events? Recent studies have largely tempered the thalamic gating hypothesis by showing a remarkably faithful encoding of acoustic information in primary sensory cortices during NREM and REM sleep (Issa and Wang, 2008; Y. Nir et al., 2013). But does this reflect a purely passive encoding of information at a low-level of representation or can more complex computation be performed?

This question has been the object of a series of studies in the 00's (see (Atienza et al., 2001; Bastuji, 1999; Hennevin et al., 2007) for reviews). These studies relied on the comparison of brain responses to different stimuli categories (e.g. contrasting participants' brain responses to their own name vs. another name as in (Perrin et al., 1999)) to unravel the preservation of specific processes during sleep. During wakefulness, the occurrence of a given process (i.e. differentiating one's own name from another name) is associated to differences in the brain responses triggered by the two types of stimuli. These differences can be measured using fMRI and EEG recordings. EEG has been more extensively used to study sleep for a number of reasons: its good temporal resolution compared to fMRI which allows to track the rapid changes occurring during sleep, the difficulty to sleep in an fMRI scanner, the cost, etc. So far, most studies relied on the Event-Related Potentials (EPRs) approach (see Box below). They have shown for example that, even when sleep is preserved, sleepers' own name elicited a different brain response that someone else's name (Perrin et al., 1999). Non-familiar stimuli can also be processed in their context. This has been shown using the so-called 'oddball paradigm', in which a series of identical tone is played, intermixed with, from time to time, a different sound (the oddball). The repetition of the same standard sound can be seen as a rule and the occurrence of the oddball as a violation of this rule. The awake brain reacts to the oddball sound in a specific manner, which corresponds the detection of the rule violation. Such detection is conserved during sleep (Nordby et al., 1996; Ruby et al., 2008), stressing the fact that, as in wakefulness, the sleeping brain processes external sounds in their context.

Even higher levels of representation can be accessed in light NREM sleep. Studies using linguistic material (pairs of words, sentences…) demonstrated that the sleeping brain preserves its ability to detect semantic violations (Bastuji et al., 2002; Brualla et al., 1998; Ibanez et al., 2006), and thus, can have access to high-level contents. One of the daunting questions that these

studies ask is whether the processes evidenced here in sleep are passive processes, or whether the sleeping brain remains, to a certain extent, proactive.

In Chapter 2, I will present studies that I conducted under the supervision of Sid Kouider to tackle this issue. We relied on a paradigm developed with Louise Goupil and Tristan Bekinschtein (Kouider et al., 2014) . In these experiments sleepers were asked to classify words while falling asleep (see Studies 4-5 and 7). Participants were asked to indicate stimuli category through hand responses. When participants fell asleep, they stopped overtly responding to stimuli. However, we observed that during sleep participants continued to prepare for the appropriate response. Such covert motor preparation was assessed through the analysis of brain responses to sounds with the EEG (Kouider et al., 2014) (see also Study 4). The presence of such task-induced motor preparation indicates that, not only can sleepers process the stimuli correctly in order to perform the task, but also, that the information about the stimuli can be routed to other non-sensory areas dealing with motor preparation. We therefore revealed the maintenance of goal-directed and distributed processes, performing computations that are very close to what happens during wakefulness. Hélène Bastuji and colleagues went even further in a case study involving an implanted epileptic patient: they showed an overt response to a nociceptive stimuli during NREM sleep without any global arousal (Mazza et al., 2014). The sleeping brain, thus, does not seem to be a dormant brain but is capable of complex sensory and cognitive processing.

What could be the mechanisms underlying the processing of external information during sleep? Local aspects of sleep provide a very interesting framework to understand the experimental results cited above. Indeed, if sleep depth can be regionally modulated, one could think that some regions can even wake up in a context of a globally sleeping brain (Nobili et al., 2012). Bastuji and colleagues showed that indeed arousal can be local during sleep (Peter-Derex et al., 2015). This local arousal could allow for the recovery of wake-like processing. In Studies 5 and 9, I will show that the processing of information is indeed associated with a local modulation of sleep depth and the recovery of wake-like auditory responses. But only the use of intracranial recordings could confirm this hypothesis.

The Event-Related Potentials (ERPs) technique and its application to sleep

The Event-Related Potentials (ERPs) technique[1] has been extensively used to investigate sensory and cognitive processes in the sleeping brain. This technique relies on the averaging of the EEG signal in dozens if not hundred of repetitions of the same experimental condition (e.g. presentation of stimulus A). By doing so, activity that is unrelated to the stimulus is averaged out. Indeed, the EEG signal can be seen as a combination of oscillations. Averaging oscillations that are not in phase (across a sufficient amount of trials) leads to a null average. However, if the stimulus evokes a stereotypical pattern of activity phase-locked to stimulus onset, such pattern will not be cancelled out and will be visible in the average EEG response (the ERP). Thus, the ERP technique can be seen as a simple de-noising tool.

Averaging the EEG signal in response to sounds reveals a series of negative and positive peaks (or components), each of them marking the occurrence of a given processing stage. While components close to stimulus onset are usually related to the processing of sensory information (and can be used to assess whether a given stimulus was encoded), later components can reflect higher-order processes (e.g. semantic processes, expectations…)[2]. For example, the N1 potential (a negative deflection occurring about 100ms after stimulus onset) has been related to the encoding of auditory information within the primary and secondary auditory cortices[3] and is weakly affected by the nature of the stimulus (a word and a sound will produce very similar N1 although they are quite different types of information). Later potentials such as the N400 (a negativity at 400ms after stimulus onset) or the P3 (a positivity around 600ms) are, on the contrary, greatly affected by the cognitive processes following sensory encoding. When hearing a series of sounds, a rare tone embedded in a stream of recurrent tones will elicit a strong P300. Here the potential is not elicited by the information contained within the stimulus but reveals brain's ability to process a sound in its context.

ERPs can be also computed in relation to internally generated events such as hand (see Studies 4-5) or eye movements (see Study 3). Similarly, in sleep, since behavioral responses are usually abolished, ERPs can be used to probe cognition by comparing ERPs in response to sounds across wake and sleep[4,5]. For example, when playing semantically congruous (dog-leash) and incongruous (cat-coin) word-pairs to an awake individual, a larger N400 is observed for the incongruous pair[6]. The observance of this N400 is usually interpreted as the ability to access and integrate the meaning of these two words as well as to react when the pair seems odd. The preservation of a similarly larger N400 for incongruous pairs than for congruous pairs in sleep would mean that this ability is conserved and that sensory information can be accessed at the semantic level during sleep[7,8].

Yet, such approach relies on the assumption that responses to sounds or ERP components associated to given cognitive processes are similarly observed in brain states whose dynamics are drastically different. And indeed, sleep slow oscillations largely affect ERPs[2,9]. Since ERP components are usually equated to precise brain processes, a modification of the ERP between wake and sleep would make its interpretation difficult. Sleep-related activity (that are typically high in amplitude) can also mask smaller differences in the EPRs: the absence of a given difference in the ERP in sleep does not mean a disappearance of the process observed in wakefulness. Another disadvantage of the ERPs is the need for large amount of data to average out the non-phase locked activity and evidence the ERPs. Sleep being a dynamic process, different states are potentially confounded within a single ERP trace.

One alternative is to use multi-variate analyses. In such analyses, instead of analyzing the average brain response in a given electrode, all the data available from all sensors, time-points and trials are taken into account (see 10 for an application to sleep). In Study 6 we applied such approach. This allowed us to investigate precisely the influence of sleep micro-structure on sensory processing.

1. Luck, S. J. An introduction to the event-related potential technique. (MIT Press, 2005).
2. Picton, T. W. Human auditory evoked potentials. (Plural Pub, 2010).
3. Näätänen, R. & Picton, T. The N1 Wave of the Human Electric and Magnetic Response to Sound: A Review and an Analysis of the Component Structure. Psychophysiology 24, 375–425 (1987).
4. Bastuji, H. Evoked potentials as a tool for the investigation of human sleep. Sleep Med. Rev. 3, 23–45 (1999).
5. Atienza, M., Cantero, J. L. & Escera, C. Auditory information processing during human sleep as revealed by event-related brain potentials. Clin. Neurophysiol. 112, 2031–2045 (2001).
6. Kutas, M. & Federmeier, K. D. Thirty years and counting: finding meaning in the N400 component of the event-related brain potential (ERP). Annu Rev Psychol 62, 621–47 (2011).
7. Bastuji, H., Perrin, F. & Garcia-Larrea, L. Semantic analysis of auditory input during sleep: studies with event related potentials. Int J Psychophysiol 46, 243–55 (2002).
8. Brualla, J., Romero, M. F., Serrano, M. & Valdizan, J. R. Auditory event-related potentials to semantic priming during sleep. Electroenc Clin Neurophysiol 108, 283–90 (1998).
9. Colrain, I. M. & Campbell, K. B. The use of evoked potentials in sleep research. Sleep Med Rev 11, 277–93 (2007).
10. Strauss, M. et al. Disruption of hierarchical predictive coding during sleep. Proc. Natl. Acad. Sci. 112, E1353–E1362 (2015).

Can sleepers learn while they sleep?

When we are awake, interaction with our environment continuously imprints on our brain (Kolb and Whishaw, 1998). As I will show in Study 8, even pure noise can leave mnesic traces as soon as it recurs (Andrillon et al., 2015a). If sleepers can process external information, can they also learn from it? In Chapter 3, I will focus on this exciting question.

There is an extensive literature on the role of sleep in memory consolidation (see (Diekelmann and Born, 2010; P Peigneux et al., 2001; Rasch and Born, 2013; Tononi and Cirelli, 2014; Walker and Stickgold, 2006) for reviews) but only a handful of studies on the formation of new memories during sleep. This is not due to a lack on interest since the ability to learn while we sleep would have huge implications in our daily lives. The topic was accordingly an intense topic of investigation and triggered a scientific race between the American and Soviet blocks during the Cold War. However, the learning of novel information during sleep has proven difficult to establish, even when such information would be easily learnt during wakefulness (Bruce et al., 1970; Emmons and Simon, 1956; Wood et al., 1992). Due to methodological issues, many claims, made at that time for the occurrence of learning during sleep, had to be discarded. The few methodologically sound studies that convincingly evidence learning effects during sleep focus on fear or delay conditioning, which are forms of memory that do not rely on the hippocampal structure (Beh and Barratt, 1965; Fifer et al., 2010; Ikeda and Morotomi, 1996; Maho and Hennevin, 2002). This distinction is of importance since declarative memories (i.e. memories than can be consciously recalled and manipulated in a goal-directed fashion) rely on the hippocampus (Eichenbaum, 2008). On the other hand, fear and delay conditioning are forms of learning rudimentary enough to be implemented by basic neural networks (Carew and Sahley, 1986). Attempts to probe hippocampus-dependent learning during sleep have often led to negative results (Hennevin et al., 2007; Wood et al., 1992).

Why would the sleeping brain be unable to learn as during wakefulness? It had been initially proposed that the blockade of sensory information at the thalamic level (McCormick and Bal, 1994) would prevent learning. Indeed, under such circumstances, the information to be learnt would be inaccessible to the neo-cortical and hippocampal regions, impairing any ability to learn (as information that is not processed cannot be learnt). And indeed, the few notable exceptions having demonstrated hippocampus-dependent learning in sleep have bypassed thalamic relays by relying on olfactive stimuli (olfactive information that does not transit through the thalamus (Jones, 2007)) (Arzi et al., 2014, 2012), on endogenously generated activations (de Lavilléon et al., 2015) or on direct stimulations of hippocampal cells (Maho and Bloch, 1992). Yet, we have seen earlier that sensory information can reach the cortex under certain conditions. Sensory information can be even accessed at high levels of representation during sleep, which is known to favor learning when we are awake (Craik and Tulving, 1975).

To account for the lack of learning despite the fact that information appears to be processed, several hypotheses can be brought out. It has been proposed that during sleep, memory systems are involved in the offline consolidation of existing memories (Diekelmann and Born, 2010) which could imply a disconnection for the sensory systems and the outside world or between sensory systems themselves (Fischer et al., 2006; Robertson, 2009) in order to prevent any interference while memories are strengthened or displaced. Alternatively, it has been proposed that the core mechanism of learning (i.e. synaptic plasticity) is modified in sleep, preventing the

formation of new memories (Synaptic Homeostasis Hypothesis (Tononi and Cirelli, 2014)). Indeed, modifications of synapses are thought to be the basis of any form of learning (Eichenbaum, 2008; Klampfl and Maass, 2013). These mechanisms are under the control of neuromodulators such as Acetylcholine (ACh) and Noradrenaline (NA) (Pawlak, 2010). Importantly, these neuromodulators happen to be down-modulated during sleep (Jones, 2005; Siegel, 2004). ACh for example is at a low-level of secretion in NREM sleep and NA is suppressed in both NREM and REM sleep. According to the Synaptic Homeostasis Hypothesis, learning would be impaired in NREM sleep due to the impairment of its associated synaptic mechanisms. In Study 9, I will present evidence that could integrate these different views (Genzel et al., 2014).

One last hypothesis that could explain the absence of sleep-learning relates to memories' strength. When we learn a set of words while awake, the memory for the words is often paired with a memory of the context in which the words had been learned (episodic memory). Knowing the origin of a memory can increase our confidence in its reliability, which is crucial to optimally use such memories. In sleep, it can be hypothesized that memories, when formed, are weaker (just as sensory processing seem weaker). Therefore, memory traces might not be strong enough to be explicitly recalled or behaviorally measurable. Yet, detailed analyses of behavioral and brain responses could unravel the existence of a mnesic trace. This will be the focus of Study 7.

Sleep as a tool

So far, I have focused on sleep, its nature, its mechanisms and its functions. Along the different chapters of this manuscript, I will expand on these various themes with the firm conviction that the approach I have developed throughout my Ph.D. can help exploring these questions. However, this work could also provide novel insights in the study of other cognitive functions. Here, I will present how sleep can be seen, not as an end, but as a tool to investigate different aspects of consciousness, perception and memory.

The study of consciousness and the contrastive approach

Consciousness, as sleep, is an obvious phenomenon: the world would not exist without the faculty of representing it to ourselves. For a long time considered a non-scientific or meta-physic question, cognitivists have found ways to explore this daunting question.

First, consciousness can be considered in its intransitive sense, as a state. What does it mean to be conscious? How can I know whether other human beings, animals or machines are conscious (Tononi and Koch, 2015)? Sleep is a very interesting tool to understand how can a brain be at a time conscious and how can the same brain be, only minutes later, unconscious. Indeed, every night we undergo what may be the closest approximation to death, the disappearance of ourselves as a conscious mind. Perhaps these transitions can tell us much and more about the neural basis of consciousness (Tononi, 2012). Along these lines, Giulio Tononi and Marcello Massimini showed that sleep onset is accompanied by the breakdown of brain's functional connectivity (Massimini et al., 2005). They hypothesized that the associated loss in the ability to integrate information was at the foundation of consciousness (Tononi and Massimini, 2008).

From a more practical point of view, sleep can be used to benchmark the so-called consciousness-meters. In the recent years, several approaches have been designed in order to acurately determine whether an individual (a patient in coma or under anesthesia, an healthy subject, a sleeper) is conscious or not (Casali et al., 2013; Chennu et al., 2014; King et al., 2013). Sleep could help assessing the precision of these metrics. Indeed, within a night, the same individual can undergo many different conscious states and report them. This would allow the alignment of the 'consciousness-meter' with the subjective report, the gold standard of consciousness research[5].

Second, consciousness can be considered in its transitive sense. Being conscious of something means that we represent a specific content to ourselves. This apparently simple operation opens an infinity of potential computations (Dehaene, 2014) and explains the richness of consciousness (Kouider et al., 2010). Cognitivists have studied in details the mechanisms and functions of transitive consciousness (see (Dehaene, 2014) for a thorough review). To do so, they mostly relied on the so-called contrastive approach. The idea is to present to participants two versions of the same sensory information: for example an image and a degraded version of this image. If the experimental paradigm is well tuned, the degraded image can still be processed by the brain, although it is not consciously accessed (Dehaene et al., 2006). A contrast can therefore be

[5] Reversely, these metrics can also be used to explore sleep, as we will see in Study 5.

established between the properties of the two conscious and unconscious processes (Kouider and Dehaene, 2007). The degradation can take different forms: brief presentation (subliminal stimulation and masking), presentation of two images on each eye (binocular rivalry and continuous flash suppression) (see (Landry et al., 2014) for an overview). Of course, these techniques are not limited to the domain of vision (e.g. in audition: (Kouider and Dupoux, 2005)).

The contrastive approach has notably been used for two purposes: (i) identifying the processes that can be performed unconsciously and (ii) identifying the signature of consciousness. But the contrastive approach has some limitations for both these purposes. Identifying processes that can be performed unconsciously by using the contrastive approach can seem a bit odd. Indeed, if the participant may indeed be unconscious of the specific content presented, the participant remains fully conscious (in the intransitive sense), fully conscious of performing a task, fully conscious of task instructions and sometimes fully conscious of making decisions on unconscious information. As for the second purpose, the contrastive approach also has its limits. Indeed identifying the signature of consciousness (also called NCCs: neural correlates of consciousness (Crick, 2000)) is difficult given the fact that the two stimulations cannot be equally compared. To be processed unconsciously, the information was indeed degraded (especially when using the masking technique). The differences observed can de therefore due to the stimulus strength rather than the fact of being conscious of it. Even when the stimulation is equated in both conscious and unconscious conditions, the difference in brain activity can be due to the consequences rather than the causes of being conscious.

Stimulating sleepers can bring a partial solution to these purposes: the identification of processes that can be performed unconsciously and the identification of their neural correlates. Sid Kouider and I developed an approach in which we "degraded" the participant rather than the information to perceive. Indeed, sleep (and especially NREM sleep) can be seen as a natural modulation of consciousness (Figure 0-6). Under these circumstances, it is possible to study how the very same information (stimulations were kept constant across wake and sleep in our studies) is processed by a conscious and awake brain, by a sleeping and unconscious brain (NREM sleep) or even by a sleeping, conscious but disconnected brain (REM sleep). In other words, sleep allows to manipulate conscious levels rather than conscious contents in order to study whether a process can be performed unconsciously in the transitive and intransitive senses of consciousness.

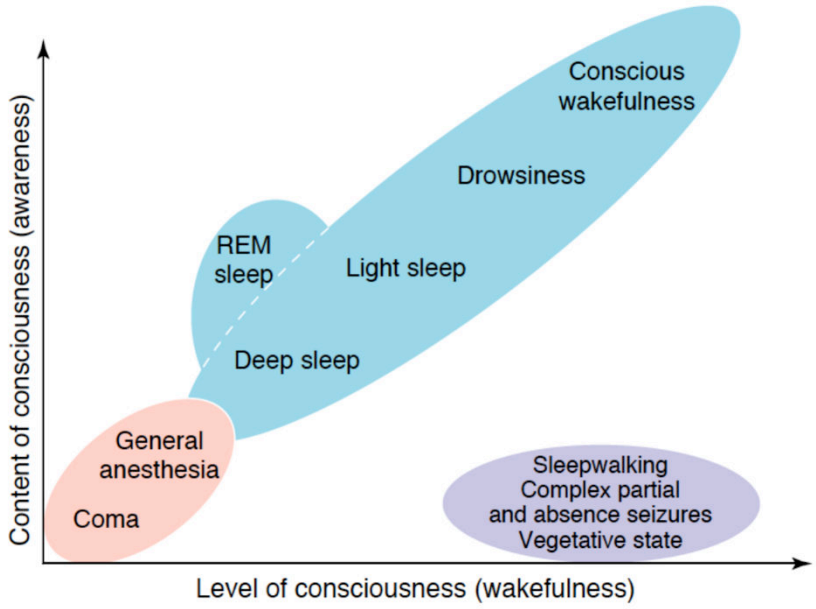

Figure 0-6 Sleep as a modulation of conscious contents and levels

Consciousness is greatly affected by individuals' state: from states in which conscious levels and contents are minimal such as in comatose patients to wakefulness where both levels and contents are maximal. The different sleep stages can allow an exploration of these two axes. By targeting the appropriate states, it is possible for example to study the impact of the modifications of either conscious levels or contents on sensory processing. From (Laureys, 2005).

Studying a brain in a vat?

In his book, *Consciousness explained* (Dennett, 1991), the philosopher Daniel Dennett invites its reader to the following thought experiment: imagine that you are just a brain in a vat and that all you know about the surrounding world is provided to you by a sophisticated machine. Dreams are perhaps (with ketamine-induced anesthesia (Sarasso et al., 2015)) the best approximation to such a brain in a vat. Even more interesting: the machine providing you with all the sensory inputs making up your dream is your brain itself. Dreams represent therefore a unique case of conscious perception without actual sensory input. When we see something in our dreams, are the mechanisms involved similar as when we see something in our environment?

In Study 3, I will present the work I have conducted with Yuval Nir, Chiara Cirelli, Giulio Tononi and Itshak Fried on ocular movement during REM sleep (Andrillon et al., 2015b). Our question was rather simple: do eye-movements in REM sleep share the same function as in wakefulness, that is to say exploring the visual environment (Wurtz, 2008). We discovered that neurons in the visuo-mnemonic pathway (medio-temporal lobe: amygdala, hippocampus, entorhinal cortex, parahippocampal gyrus) react similarly after an eye-movement performed in REM sleep, after an eye-movement performed in wakefulness and when an image is directly presented to participants' eyes. This result suggests that, not only do eye-movements subserve the same function in REM sleep as in wakefulness, but also suggests that seeing during our dreams involve the same mechanisms as when seeing the real world. In other words that dreams are made with the same 'stuff' as reality. However, the question of how these dreams are

generated is still open. Are dreams akin to perception or to imagination? Are dreamers active in the making of their dreams or are dreams the resultant of random volley of activations from the brainstem (Nir and Tononi, 2010)?

Using another approach (Siclari et al., 2013), Francesca Siclari and Giulio Tononi investigated the neural basis of dream contents. The principle is simple: sleepers are awaken in the middle of REM sleep and asked to report what they had in mind (i.e. the content of their dream) when they were woken up. The EEG of participants was recorded in parallel and using the source reconstruction approach, Siclari and colleagues mapped the various contents reported with the corresponding neural sources. These maps are strikingly similar with what could be obtained with awake participants experiencing similar contents (Siclari et al., 2014b), corroborating the perceptual nature of dreams. Besides, dreams also provide situations that are quite difficult to imagine when awake. Some dreams for example are purely abstract: participants report dreaming of concepts without any perceptual implementations. Recordings such dreams could thus provide neural correlates of conscious thoughts purified from any perceptual representation.

Among the obstacles in using dreams to study consciousness and conscious contents it should be noted the fact that (i) dreams are not controlled by sleepers, and that (ii) dreams' content is accessible only when the dream is interrupted, through post-hoc and necessarily imperfect reports. However, there is a third state, between dreams and wakefulness, which could solve these issues: lucid dreaming (LaBerge, 2000). During a lucid dream, sleepers are aware that they dream and regain their sense of agency. They can therefore communicate with the outside world through eye-movements to manifest their awareness and they can dictate the content of their dreams. Lucid dreams are quite rare events but, aside from the methodological difficulties, they could provide scientists a way to study purely endogenous contents in a systematic and robust manner.

Exploring memory through sleep

I will finish this section with some words on the interest of sleep in studying memory, which will be the topic of Chapter 3.

Memory is a very complex and polymorph phenomenon (Eichenbaum, 2008). Crucially sleep could help understanding the mechanisms underlying memory formation. In Study 8, we show a form of perceptual learning that is supposed to occur automatically and independently from attention (Andrillon et al., 2015a; Luo et al., 2013). However controlling for the influence of attention is always difficult. With Study 9, we strengthened the argument of automaticity by showing that such learning can occur even during sleep.

While memory can be simply defined as the storage of information within the brain, its implementations are multiple. However, a clear line can be drawn between explicit and implicit memory. Let's say that I just presented to you a series of words with the instruction to memorize as much items as you can. When meeting the day after, I will present you again with the same words, alongside novel items. Your task is now to determine which words had been presented the day before and which are the new ones (a paradigm called Old New recognition task). For some items, you may be pretty sure of your answer since you explicitly and precisely remember hearing or seeing the corresponding words the day before. But for other items, you may be less

sure and rely on fainter cues such as a sense of familiarity (Tulving, 1985). Nevertheless, you may be right in saying that you recognize the world. Such form of memory is called implicit memory.

In the case mentioned above, explicit and implicit memory positively and jointly contribute to your answers. What would happen if they were in conflict? Arzi and colleagues designed experiments in which human participants were conditioned during their sleep (Arzi et al., 2012). In a recent study (Arzi et al., 2014), they conditioned smokers: the cigarette smell was associated to a very unpleasant one (rotten fish). During the week after the conditioning night, cigarette consumption of the test group significantly diminished. Importantly, similar conditioning in wake does not lead to a decrease in cigarette consumption. Associating tobacco to repulsive stimuli can work, but the conscious brain knows better!

In Study 7, I similarly investigated the difference between explicit and implicit memory. In this study, participants performed an Old New recognition test on items previously heard. However and unknown to participants, some of the old items were presented when they were awake and some while they were asleep (Kouider et al., 2014). These words were processed and accessed at a high level of representation during sleep. Such access would automatically lead to the formation of a mnesic trace in wakefulness. What about sleep? I will show that the processing of this information lead to an implicit form of memory. Brain and behavioral responses to the words heard during sleep indicate that they are differentially processed compared to novel items. Yet, participants consistently declared them as novel and could not differentiate them for new words. Such results could be interpreted as a conflict between the presence of an implicit trace and the absence of explicit memory. In such conflicting situation, the implicit trace may be overlooked because it is not linked to any explicit recollection. Thus, these results could helps us understanding whether implicit and explicit memories are truly independent processes (Squire et al., 2007) and how they are implemented in the brain (Study 7).

Key points:

- **Sleep is an ubiquitous and vital phenomenon but some core questions concerning its function remain unsettled;**
- **Sleepers are usually unresponsive, yet it does not mean that the sleeping brain is a dormant brain;**
- **Sleep is a complexly structured phenomenon, its spatial and temporal dynamics may influence greatly brain's ability to process external information;**
- **Sleep can be used as a tool to investigate cognitive functions such as consciousness, perception or memory.**

Chapter 1: The Richness of sleep

Le Miroir
Pablo Picasso (1932)

Note on contributions:

In this Chapter's studies (Studies 1-3), intracranial recordings from epileptic patients were analyzed. Itzhak Fried performed all surgeries and Yuval Nir collected data. I was not directly involved in data collection. In Study 1, I contributed to the sleep spindles analyses and some of the analyses demonstrating the existence of local slow-waves (paragraphs 3 to 5 in the Results section). I completed all the analyses of Studies 2 and 3 in close collaboration with Yuval Nir. Studies 1 and 2 were published during my Master degree. However, the results detailed in these studies motivated the direction I undertook in my doctoral research and I decided to include these studies in the present manuscript.

Study 1:
Regional slow waves and spindles in human sleep

Published in **Neuron**
April 14, 2011

Yuval Nir[1], Richard J. Staba[2], **Thomas Andrillon**[1,3], Vladyslav V. Vyazovskiy[1], Chiara Cirelli[1], Itzhak Fried[4,5], and Giulio Tononi[1]

[1] *Department of Psychiatry, University of Wisconsin-Madison*
Madison, WI, USA

[2] *Department of Neurology, David Geffen School of Medicine, University of California-Los Angeles*
Los Angeles, CA, USA

[3] *Department of Cognitive Studies, École Normale Supérieure*
Paris, France

[4] *Department of Neurosurgery and Semel Institute for Behavioral Neuroscience, David Geffen School of Medicine, University of California-Los Angeles*
Los Angeles, CA, USA

[5] *Functional Neurosurgery Unit, Tel Aviv Medical Center and Sackler School of Medicine, Tel Aviv University*
Tel Aviv, Israel.

Summary

The most prominent EEG events in sleep are slow waves, reflecting a slow (< 1Hz), oscillation between up and down states in cortical neurons. It is unknown whether slow oscillations are synchronous across the majority or the minority of brain regions - are they a global or local phenomenon? To examine this, we recorded simultaneously scalp EEG, intracerebral EEG, and unit firing in multiple brain regions of neurosurgical patients. We find that most sleep slow waves and the underlying active and inactive neuronal states occur locally. Thus, especially in late sleep, some regions can be active while others are silent. We also find that slow waves can propagate, usually from medial prefrontal cortex to the medial temporal lobe and hippocampus. Sleep spindles, the other hallmark of NREM sleep EEG, are likewise predominantly local. Thus, intracerebral communication during sleep is constrained because slow and spindle oscillations often occur out-of-phase in different brain regions.

Introduction

Sleep is defined by behavioral unresponsiveness, and is usually regarded as a global phenomenon. Indeed, sleep is accompanied by global changes in neuromodulation (Jones, 2005), and the transition from waking to sleep is accompanied by clearcut changes in the electroencephalograph (EEG): from low-amplitude high-frequency activity to high-amplitude low-frequency slow waves (below 4Hz) and sleep spindles (Steriade, 2000).

Intracellular recordings indicate that sleep slow waves reflect a bistability of cortical neurons undergoing a slow oscillation (< 1Hz) between two distinct states, each lasting hundreds of milliseconds. Up states are associated with depolarization and vigorous firing, whereas in down states the membrane potential is hyperpolarized and neuronal firing fades (Contreras and Steriade, 1995; Crunelli and Hughes; Destexhe and Contreras, 2006; Destexhe et al., 2007; Steriade et al., 1993c; Steriade et al., 2001; Timofeev et al., 2001). Although a role has been suggested for thalamic oscillators (Crunelli and Hughes, 2010), the slow oscillation can be generated and sustained in cerebral cortex alone (Amzica and Steriade, 1995a; Shu et al., 2003; Steriade et al., 1993a; Timofeev et al., 2000; Timofeev and Steriade, 1996). The slow oscillation affects virtually all neocortical neurons (Amzica and Steriade, 1995b; Chauvette et al., 2010; Sejnowski and Destexhe, 2000), is remarkably synchronous when examined in brain slices (Sanchez-Vives and McCormick, 2000), in animals under anesthesia (Steriade et al., 1993b, c), and in natural sleep as shown by intracellular recordings of up to four neurons simultaneously (Chauvette et al., 2010; Volgushev et al., 2006). But are slow oscillations truly global events, i.e. occurring in phase across most brain regions, or can the slow oscillation occur locally, i.e. in a minority of regions independently of other brain areas?

Recent observations have shown that slow waves can be locally regulated so that their intensity varies among cortical regions. Prolonged waking induces an increase in slow wave activity (SWA, EEG power below 4Hz) which is largest over frontal cortex (Finelli et al., 2001; Werth et al., 1997). High-density EEG (hd-EEG) demonstrates that sleep slow waves can be locally regulated as a function of prior use and plastic processes (Esser et al., 2006; Huber et al., 2006; Huber et al., 2004). Slow waves propagate along major anatomical pathways (Massimini et al., 2004; Murphy et al., 2009) so that individual waves may be driven by distinct cortical origins (Riedner et al., 2007). Additional evidence for local sleep goes beyond local regulation of slow waves in non-rapid Eye-Movement (NREM) sleep. For example, when falling asleep cortical activity is highly variable across brain regions (Magnin et al., 2010). Moreover, in natural sleep of some animals (e.g. dolphins) one hemisphere can be awake while the other asleep (Mukhametov et al., 1977). Finally, in humans, some sleep disorders (e.g. sleep walking) suggest the existence of "dissociated states" (Mahowald and Schenck, 2005), where some brain regions are "asleep" when others are simultaneously "awake".

Given the recent evidence supporting local regulation of SWA, we hypothesized that sleep slow waves may occur locally such that neurons alternate between active and inactive states at different times in different brain regions. To evaluate this possibility, simultaneous recordings of intracranial depth EEG and spiking activities of isolated units were obtained in 8-12 brain regions in the cortex and hippocampus of thirteen individuals undergoing presurgical clinical testing. The results provide direct evidence for local slow waves, revealing a continuum of global-local waves with the majority of events being confined to specific regions. At one extreme, typical of early NREM sleep, high-

amplitude slow waves were usually global, detectable with scalp EEG. At the other extreme, more typical of late NREM sleep, slow waves could be entirely local, where any region could be active or inactive. In addition, we find that sleep spindles – the other EEG hallmark of NREM sleep - also occur mostly locally, establishing that the two fundamental sleep oscillations are mostly confined to local circuits. We also reveal a robust tendency of sleep slow waves to propagate from medial prefrontal cortex to the medial temporal lobe (MTL) and hippocampus. Both local occurrence and propagation of slow wave events reflect the underlying connectivity such that transitions into activity in a given region can be predicted by the activity of its afferent regions.

Results

Polysomnographic sleep studies and sleep slow waves

We obtained full night continuous polysomnographic sleep recordings in thirteen neurosurgical patients, lasting 421 ± 20 minutes (mean ± SEM). Figure 1-1 illustrates the experimental setup and provides an overview of the data. Polysomnography included electrooculogram (EOG), electromyogram (EMG), scalp EEG, and video monitoring. Sleep-wake stages were scored as waking, NREM sleep stages N1 through N3 and REM sleep according to established guidelines (Iber et al., 2007). Depth intracranial electrodes recorded activity in 129 medial brain regions in frontal and parietal cortices, parahippocampal gyrus, entorhinal cortex, hippocampus and amygdala (Figure 1-1E and Table S 1-1).

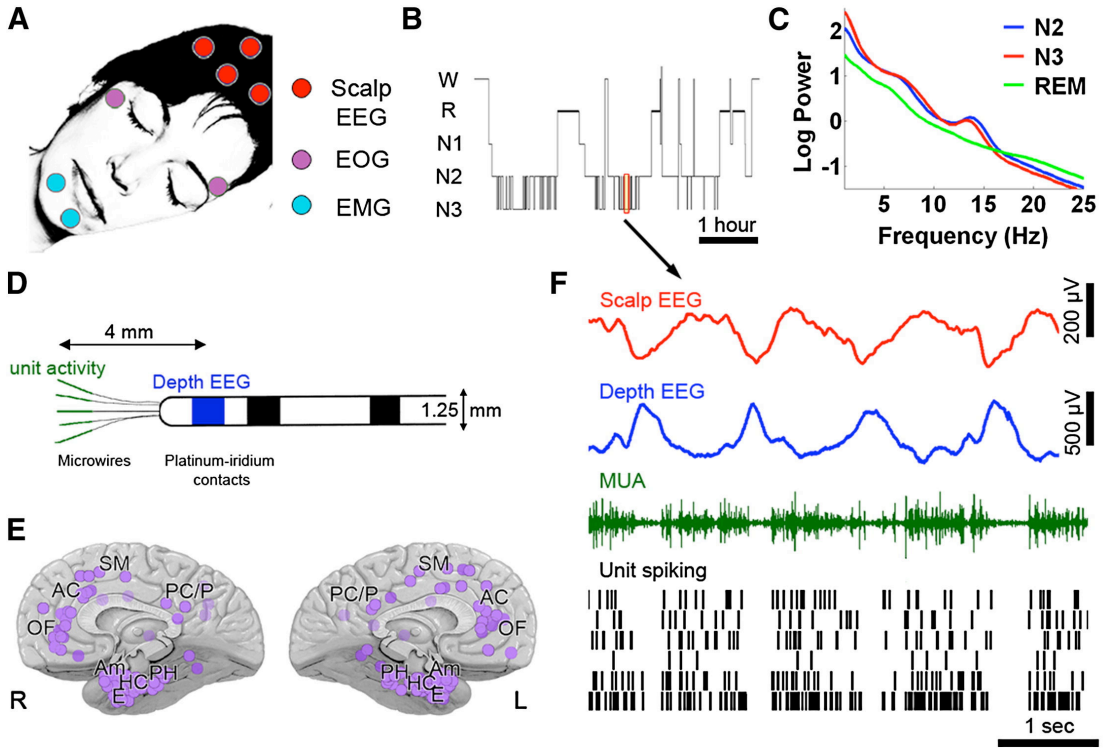

Figure 1-1 Sleep studies and data overview

(A) Setup for polysomnographic sleep recordings. (B) Hypnogram: time-course of sleep-wake stages in one representative individual. W, wake; R, REM sleep; N1-N3, NREM sleep, stages 1-3. (C) Average power spectra of scalp EEG in the same individual computed separately in stages N2 (blue), N3 (red) and REM sleep (green). Note high power in slow wave (<4Hz) and spindle (10-16Hz) range in NREM sleep. (D) Diagram of flexible probes used for concomitant recording of depth EEG (platinum contacts, blue) and unit activity (microwires, green). (E) Overview of 129 depth electrode locations in 13 individuals encompassing multiple brain regions seen from medial view. Abbreviations: OF, orbitofrontal cortex; AC, anterior cingulate; SM, supplementary motor; PC/P, posterior cingulate / parietal cortex; PH, parahippocampal gyrus; HC, hippocampus; E, entorhinal cortex; Am, amygdala; L, left hemisphere; R, right hemisphere. (F) Example of data acquired during 6 sec of NREM sleep. Rows (top to bottom) show activity in scalp EEG (Cz, red), depth EEG (entorhinal cortex, blue), multi-unit activity (MUA) in one microwire (green) and spiking activity in six isolated single-unit (black bars).

We simultaneously recorded scalp EEG, depth EEG, multi-unit activity (MUA), and neuronal spiking activity (Figure 1-1D) from a total of 600 units (355 single units, 245 multiunit clusters).

Measures of overnight sleep in patients resembled normal sleep in individuals without epilepsy (Figure 1-1). Average (± SEM) sleep efficiency (sleep time per time in bed) was 82 ± 2 % . NREM sleep, REM sleep, and wake after sleep onset (WASO) constituted 75 ± 2 %, 13 ± 2 %, and 12 ± 2 % of sleep time, respectively. Moreover, power spectra of scalp EEG data in individual subjects (Figure 1-1) revealed robust SWA and spindle (10-16Hz) power throughout NREM sleep, while REM sleep was characterized by power in the theta (4-8Hz) range and in high frequencies (above 20Hz), in accordance with previous studies (Campbell, 2009). All patients showed typical NREM-REM sleep cycles, and some showed homeostatic decline of SWA throughout sleep. These results indicate that sleep measures were in general agreement with typical findings in healthy young adults (e.g. (Riedner et al., 2007)).

Having characterized sleep using standard non-invasive polysomnography, individual slow waves in NREM sleep were identified in the depth EEG of each brain region separately. Although sleep profiles were within the normal range, we further verified that detected waves reflected physiological sleep slow waves rather than epileptic events (Experimental Procedures). Putative slow waves were separated to those preceded (within 1s) by an interictal spike ("paroxysmal" discharges) versus those unrelated to epilepsy ("physiological" sleep slow waves). The shape of physiological sleep slow waves was symmetrical and significantly different than that of asymmetrical paroxysmal discharges (Figure S 1-3A). Specifically, in paroxysmal slow waves following interictal spikes the rise slope was 44% ± 0.07 steeper than the fall slope (n=129 depth electrodes, $p < 7.4E-5$, paired t-test on rise and fall slopes). In addition, paroxysmal discharges were limited to specific sites in comparison to physiological slow waves, which were detected in all brain structures in all patients. Thus, in many channels virtually no interictal spikes were observed before slow waves (and nearly all putative slow waves were physiological), while in a few channels many events were pathological (mean = 14%, range - 0.06% - 46%). By contrast, the number of physiological slow waves was consistent between electrodes, with numbers matching those found in healthy individuals (37.3 ± 0.5 slow waves per minute of NREM sleep), as in (Riedner et al., 2007).

Neuronal activity underlying sleep slow waves

Next, isolated unit discharges underlying physiological sleep slow waves were examined. Figure 1-2 provides an example of EEG and unit activities during global slow waves occurring in unison across multiple brain regions during deep NREM sleep in one individual. Negative peaks in the scalp EEG tightly corresponded to positive peaks of depth EEG in cortical and subcortical structures across different lobes and hemispheres. Locally, extracellular recordings revealed an OFF period where unit spiking activity ceased almost entirely, likely corresponding to the down state of the slow oscillations as recorded intracellularly. As in previous work (Vyazovskiy et al., 2009), we use the terms "ON" and "OFF" periods, instead of "up" and "down" or "depolarized" and "hyperpolarized" states (Steriade et al., 2001), because activity and silence periods were defined here based on extracellular activity rather than membrane potential fluctuations measured intracellularly. In contrast, positive peaks in scalp EEG tightly corresponded to

negative peaks of depth EEG and to ON periods with rigorous spiking, in accordance with a depolarized up state.

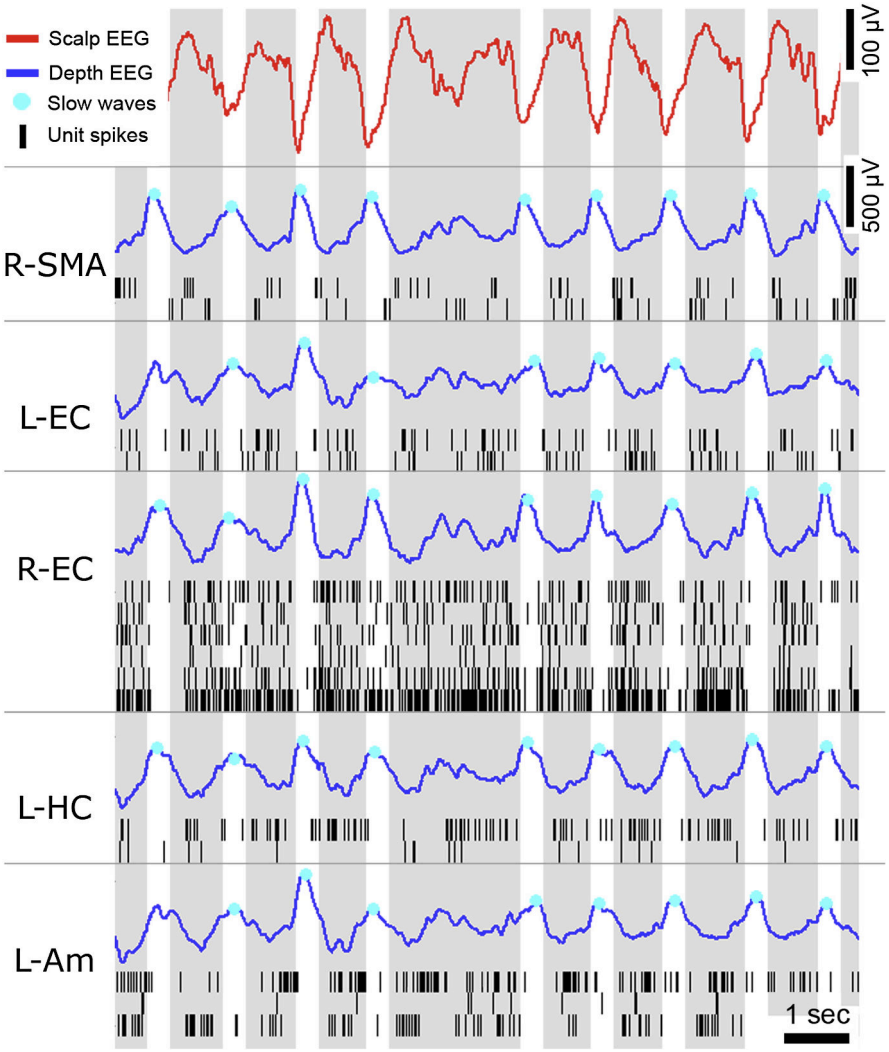

Figure 1-2 Example of EEG and single-unit activity during global sleep slow waves

Example of EEG and unit activities in multiple brain regions during 11.5sec of deep NREM sleep in one individual. Rows (top to bottom) depict activity in scalp EEG (Cz), right supplementary motor area (R-SMA), left entorhinal cortex (L-EC), right entorhinal cortex (R-EC), left hippocampus (L-HC), and left amygdala (L-Am). Red, scalp EEG; blue, depth EEG; black lines, unit spikes. Cyan dots show individual slow waves detected automatically in each channel separately. Gray and white vertical bars mark ON and OFF periods occurring in unison across multiple brain regions.

We set out to examine quantitatively the relation between sleep slow waves and the underlying spiking activity across all brain regions where units were detected (Figure 1-3). Individual slow waves were detected automatically in the depth EEG of each brain region separately (e.g. cyan dots in Figure 1-2), and unit spiking activity surrounding slow waves was averaged. When focusing on the highest amplitude waves in each channel (top 20%), positive and negative peaks in depth EEG were associated with marked decreases and increases in unit discharges, respectively (Figure 1-3A, B, n=600). This result should be viewed as a lower limit on the modulation strength since timing variability across individual neurons introduced a temporal jitter, thereby smearing the average result. Therefore, the wave-triggered average of spiking activity was computed in each unit

separately, searching for the minimal (maximal) rate while allowing for different time offsets around EEG peaks (n=600, average of 10,595 waves per neuron). The minimal firing rate around EEG positivity was 39% ± 1 compared with the mean firing rate in NREM (N2+N3) sleep, and the mean latency of such OFF periods was 72ms ± 9 before the positive EEG peak. Around EEG negativity, a maximal firing rate of 198% ± 11 was found across individual units, at 46ms ± 10 before the negative EEG peak.

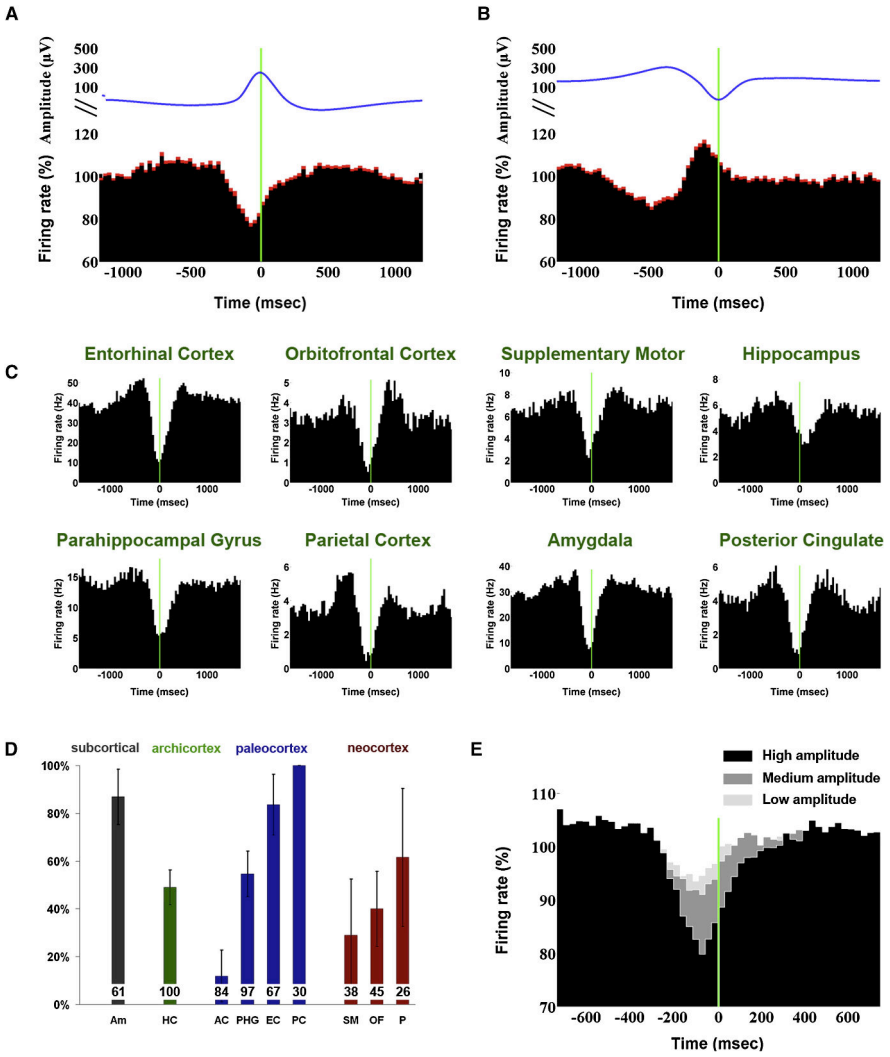

Figure 1-3 Spiking activity underlying EEG slow waves

(A) Wave-triggered averaging of unit spiking activity, time locked to the positive peak of depth EEG slow waves (OFF periods). Red shades denote SEM across neurons (n=600 in all brain structures) (B) Same as (A) time locked to the negative peak of depth EEG slow waves (ON periods). (C) Examples of neurons in different individuals and brain structures with spiking activity highly linked to EEG slow waves. (D) Percentage of units linked to sleep slow waves in different brain structures Numbers at base of bars mark the number of units in each brain structure, and error bars denote SEM across electrodes. (E) Wave-triggered averaging of units in all brain structures (n=600) as a function of amplitude of the positive EEG peaks. Slow waves were divided into three amplitude percentiles so that black, dark gray, and light gray depict high, medium, and low-amplitude slow waves, respectively.

In each subject and in each brain region, individual neurons whose activity was highly modulated by slow waves were identified (Figure 1-3C). Such neurons were found not only in neocortex, but also in limbic structures such as hippocampus and amygdala.

Given the variability across individual neurons, we examined the percent of neurons showing significant phase locking to sleep slow waves separately in each brain structure (Figure S 1-4 and Experimental Procedures). The results revealed considerable variability (Figure 1-3D): the lowest percentages of phase locked neurons were found in anterior cingulate (12% ± 11, n=84 units in 11 regions, mean and SEM across electrodes). Neocortical regions (41% ± 11, n=109 units in 16 regions), hippocampus (49% ± 7, n=100 units in 17 regions), and parahippocampal gyrus (55% ± 10, n=97 units in 13 regions) showed intermediate effects, while the highest percentages of phase locked neurons were found in amygdala (87% ± 11, n=61 units in 9 Amygdala regions), entorhinal cortex (84% ± 13, n=67 units in 10 regions), and posterior cingulate cortex (100% ± 0, n=30 units in 3 regions). Since slow waves were detected in the depth EEG recorded ~4mm away from unit activity, the percentages of modulated neurons should be regarded as a lower bound. Given that slow wave amplitudes change throughout sleep with the dissipation of sleep pressure (Riedner et al., 2007), it was of interest to check whether slow wave amplitudes were indicative of the level of unit activity modulation. To this end, unit activities were averaged around slow waves depending on the peak amplitude of the depth EEG (Figure 1-3E). The amplitude of EEG waves was parametrically related to the degree of modulation in underlying unit activity. Thus, our results demonstrate that within specific brain structures, sleep slow waves in depth EEG reliably reflect synchronous transitions between ON and OFF periods among many neurons.

Importantly, unit discharges associated with pathological waves were markedly different in that firing rate was significantly different before and after the EEG positivity, in accord with the asymmetry observed in depth EEG (Figure S 1-3B). The clear distinction found in spiking activity underlying physiological vs. pathological waves supports the notion that sleep slow waves and epileptic events could be reliably separated.

Extent of local sleep slow waves

Next we examined if, to what extent, and under what circumstances slow waves occur locally, i.e. out of phase between brain regions. We operationally define a local (global) slow wave as an event detected in less (more) than 50% of recording locations. Numerous incidences of regional slow waves were found (Figure 1-4A, see Figure S 1-5 for additional examples). In such incidences, diverse measurements (depth EEG, MUA, spiking of individual neurons) jointly indicated that one brain region was in an OFF period while another region was active.

To explore this phenomenon quantitatively we examined to what extent slow waves occurred near-simultaneously (±400ms) across multiple brain structures and in scalp EEG. For each wave, the underlying unit activity at concordant sites (i.e. where the same EEG wave was observed) was compared with that found in non-concordant sites (i.e. where the "seed" wave was not observed in the "target" region). The results (Figure 1-4B) revealed a clear difference in underlying spiking activity ($p < 6.8E-07$, paired t-test between concordant and non-concordant conditions across neurons).

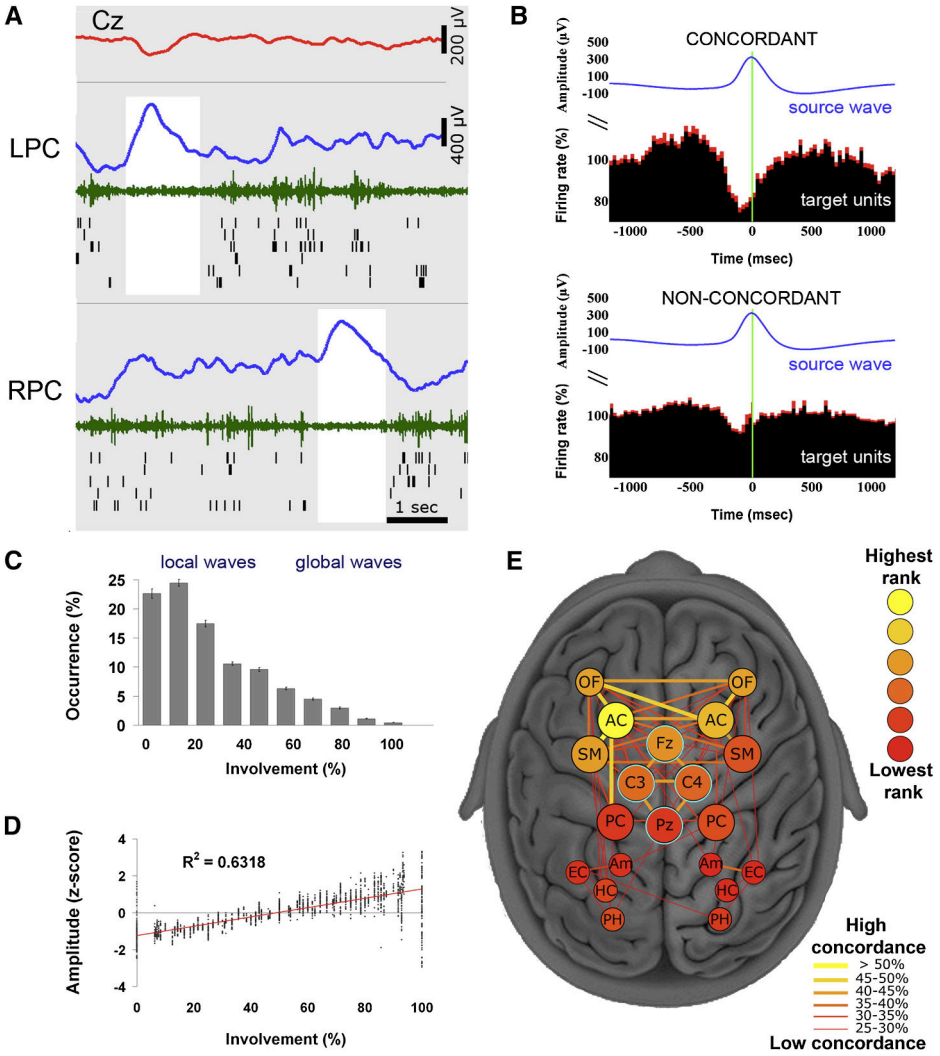

Figure 1-4 Local sleep slow waves

(A) An example of local sleep slow waves occurring at different times in left and right posterior cingulate cortices, where 100% of units are locked to slow waves. Rows (top to bottom) depict activity in scalp EEG (Cz, red), left posterior cingulate, and right posterior cingulate. Blue, depth EEG; green, MUA; black lines, single-unit spikes. White shadings mark local OFF periods. (B) Units in concordant "target" regions (expressing the same EEG slow wave, upper panel) exhibit a clear OFF period, while units in non-concordant "target" regions do not exhibit a clear OFF period. Wave-triggered averaging of "target" units is time locked to the positive peak of depth EEG in the "seed" region (blue trace). Red shades denote SEM across neurons (n=410 in all brain structures). (C) Most slow waves are local. Distribution of slow wave involvement (percent of monitored brain structures expressing each wave). (D) Global slow waves are of high amplitude. Scatter plot of slow wave amplitudes as a function of involvement (percent of brain structures expressing each wave). (E) A graph depicting the tendency of each pair of regions to express waves concordantly. Nodes (individual regions) are depicted schematically as seen from above, where deep regions away from scalp (MTL) are smaller and scalp electrodes are surrounded by cyan. Node color (legend) denotes the rank of each region - how often it is involved in slow waves seen in other regions. Edge width and color (legend) denotes the probability of each pair of regions to express slow waves concordantly, while node color expresses the region's rank (i.e. its average probability to be concordant with all neighbors). Note that regions in prefrontal cortex have higher ranks and show concordance across hemispheres relative to MTL.

We quantified the number of brain structures involved in each slow wave (i.e. the number of channels in which a particular wave was detected). The distribution of involvement was skewed towards fewer regions (Figure 1-4C) indicating that slow waves were typically spatially confined. Mean slow wave involvement was 27.1% ± 0.4 of monitored brain regions (n=129 electrodes). Moreover, 85% ± 0.7 of slow waves were detected in less than half of the recording sites indicating that most slow waves were local, given the definition above. There was a strong tendency ($r = 0.79$, $p << 1E-10$) of widespread waves to be of higher amplitude than spatially restricted lower-amplitude waves (Figure 1-4D). The high variability in amplitude and spatial extent of slow waves suggests a continuum rather than a categorical dichotomy between local and global waves. At one extreme, waves could be entirely local, where one region was ON and others were OFF and vice versa, and such local waves could be observed in any brain structure. At the other extreme, high-amplitude waves occurred in unison across the brain. Nearly all waves fell somewhere along this gradual continuum, with most waves being more local than global given our working definition. Finally, we examined whether specific pairs of brain structures had a strong tendency to express local slow waves concordantly, and whether particular brain regions had a strong degree of involvement in slow waves (Figure 1-4E). Medial prefrontal regions such as the anterior cingulate and orbitofrontal cortex were typically more involved than regions in MTL. In addition, homotopic cortical regions across hemispheres tended to be concordant in prefrontal cortex (but not MTL), and there was a slight bias of regions in the left hemisphere to be more involved in slow waves.

Extent of local sleep spindles

Our results thus far demonstrate that slow waves, the most prominent EEG event of NREM sleep, occur mostly locally. This suggests that sleep, usually associated with highly synchronized activity, has an important local component. We thus wondered whether sleep spindles, the other hallmark of NREM sleep EEG (Loomis et al., 1935), also occur locally. Spindles are generated in the highly interconnected thalamic reticular nucleus and the neocortex governs their synchronization through corticothalamic projections (McCormick and Bal, 1997; Mircea Steriade, 2003). Asynchronous spindles were reported in non-physiological conditions (Contreras et al., 1997a, 1996; Gottselig et al., 2002).

To examine this issue, spindles were detected automatically in each depth electrode separately (Experimental Procedures, Figure S 1-6) and we examined to what extent spindles occurred concurrently across frontal and parietal channels. Examination of local vs. coincident spindles was carried out only in cortical sites that had regular spindle occurrences, thereby excluding the possibility that local occurrence of spindles arises merely from their total absence in remote brain structures. As defined for slow waves, we operationally define a local (global) sleep spindle as an event detected in less (more) than 50% of recording locations. Numerous incidences of sleep spindles occurring in specific brain areas were found (Figure 1-5A). Regional spindles occurred without spindle activity in other regions, including homotopic regions across hemispheres and regions with equivalent signal-to-noise ratio (SNR) showing the same slow waves.

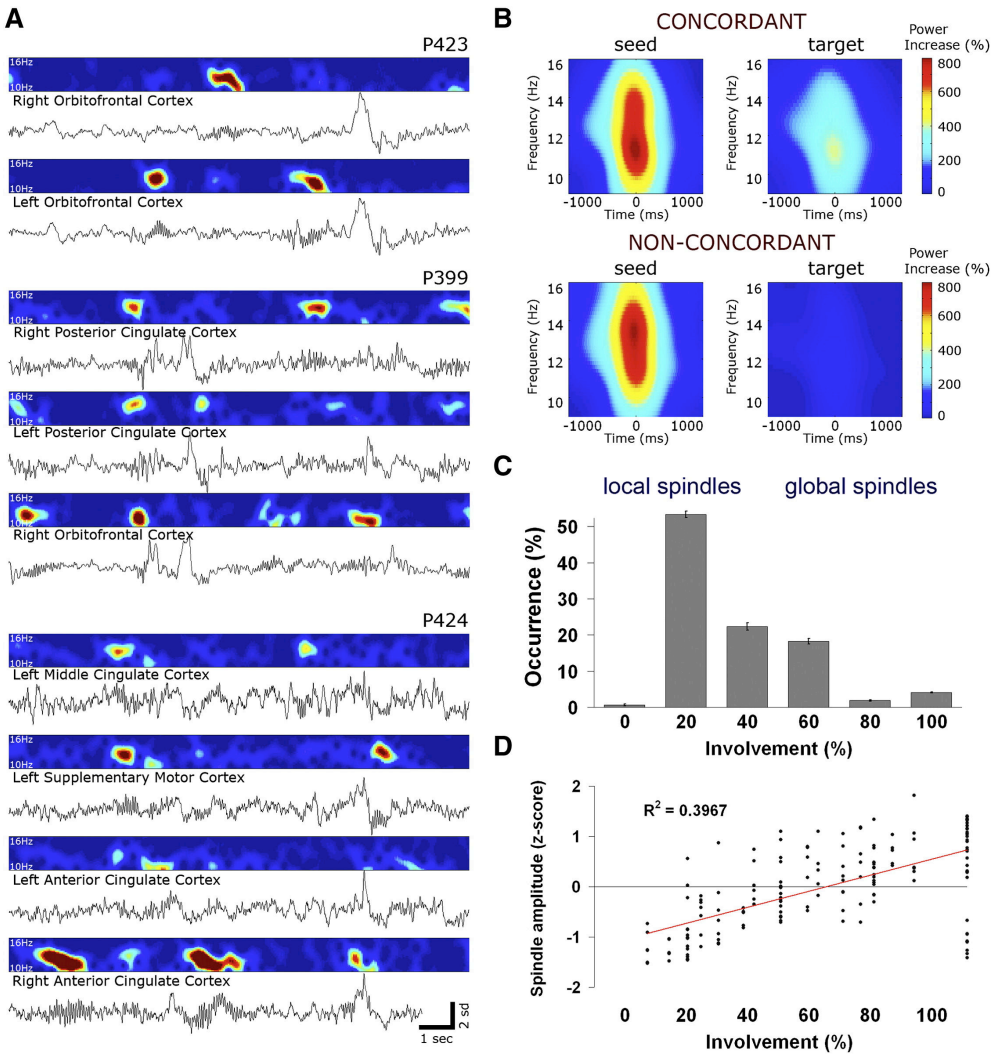

Figure 1-5 Local sleep spindles

(A) Three examples in three different patients of depth EEG along with corresponding spectrograms in the spindle frequency range (10-16Hz) during 15sec of NREM sleep. Note that regardless of slow waves, local spindles often occur without spindle activity in other regions, including homotopic regions across hemispheres and regions with equivalent SNR showing the same global slow waves. (B) Quantitative analysis of spindle occurrence across pairs of channels. Top row (concordant events, 34% of cases) shows spectrograms for events in which a spindle was detected in the "seed" channel but not in the "target" channel (N = 13,750 events in 156 pairs of regions in 12 individuals). Bottom row (non-concordant events, 66% of cases) shows spectrograms for events in which a spindle was detected in the seed channel but not detected in the target channel (N = 26,874 events in 156 pairs of regions in 12 individuals). Note that spindle power in non-concordant target channels is at near-chance levels, indicating that our detection can reliably separate between presence and absence of spindle activity (C) Distribution of involvement (percent of monitored brain structures expressing each spindle) across 22,914 spindles in 50 electrodes of 12 individuals. Note that the distribution is skewed to the left, indicating that most spindles are local. (D) Scatter plot of spindle amplitudes as a function of involvement (percent of brain structures expressing each spindle) shows that global spindles have some tendency to be of higher amplitude ($r = 0.63$, $p < 0.0001$, $n = 177$).

We set out to quantitatively establish to what extent local sleep spindles occur across the entire dataset. We determined for each spindle in a given region whether spindles were present or not in other brain structures (Experimental Procedures). The spectral power changes in concordant sites (34% of events where a spindle was detected in both "seed"

and "target" channels, Figure 1-5B top row) were compared with those at non-concordant sites (66% of events where a spindle was detected in the seed channel but not in the target, Figure 1-5B bottom row). A clear difference in spectral power was revealed ($p < 1E-41$, paired t-test), pointing to significant differences in underlying neuronal activity, and indicating that non-concordant events are indeed regional spindles. Furthermore, the analysis of those cases where target channels did not exhibit any increase in spindle spectral power above the noise level (Experimental Procedures) revealed that 32% of all non-concordant events were local in the strongest sense, i.e. a full-fledged spindle occurred in the seed channel while spectral power in the target channel was not different from chance. Importantly, the occurrence of local spindles was independent of local slow waves, since spindles occurring in isolation (i.e. not associated with a slow wave within ± 1.5s) constituted 53.7% ± 3.1 of all events and a separate analysis confirmed that such "isolated" spindles were likewise mostly local (Figure S 1-7). In addition, comparing homotopic regions revealed that 40.4% ± 1.7 of spindles were observed only in one hemisphere (mean ± SEM across 9 pairs), indicating that differences between anterior and posterior regions could not account for spindle locality.

Next, we quantified the involvement in spindle events by computing the number of brain structures in which each spindle was observed. The distribution of involvement in sleep spindles was skewed towards fewer regions (Figure 1-5C), indicating that spindles were typically spatially restricted. Mean involvement for sleep spindles was 45.5% ± 0.3 of brain regions (n=50 depth electrodes). Moreover, 75.8% ± 0.9 of spindles were detected in less than 50% of regions, indicating that most spindles were local given the definition above. Finally, as was the case for slow waves, the spatial extent of spindles was significantly correlated with spindle amplitude (Figure 1-5D, $r = 0.62$, $p < 0.0001$, $n = 177$).

Changes in spatial extent of slow waves and spindles between early and late sleep

Increasing evidence suggests that early and late NREM sleep differ substantially in underlying cortical activity (V. V. Vyazovskiy et al., 2009). Hence, it was of interest to determine whether the spatial extent of slow waves and spindles changes between early and late NREM sleep. To this end, we focused on episodes of early and late NREM sleep in five individuals exhibiting a clear homeostatic decline of SWA during sleep (). We identified separately slow waves, spindles, and K-complexes - isolated high-amplitude slow waves that are triggered by external or internal stimuli on a background of lighter sleep (Colrain, 2005). We examined for each type of sleep event separately how its spatial extent varied between early and late sleep (Figure 1-6). Slow waves became significantly more local in late sleep as compared to early sleep (Figure 1-6A, involvement of 30.4% ± 0.57 in early sleep vs. 25.0% ± 0.62 in late sleep, $p<2.6E-10$, unequal variance t-test). This result is in line with the finding that local waves were usually low-amplitude, and low-amplitude waves typically occur in late NREM sleep when homeostatic sleep pressure has largely dissipated (Riedner et al., 2007). By contrast, K-complexes were mostly global and stereotypical throughout the night, i.e. they did not show significant changes between early and late sleep (Figure 1-6B, involvement of 54.8% ± 4.4 in early sleep vs. 52.5% ± 1.9 in late sleep, $p = 0.98$). Interestingly, sleep spindles became slightly less local in late sleep, as sleep pressure dissipated (Figure 1-6C, involvement of 44.2% ± 0.6 in early sleep vs. 47.1% ± 0.5 in late sleep, $p < 0.00014$). This result once again

supports the notion that local sleep spindles cannot be simply explained by an association with local slow waves.

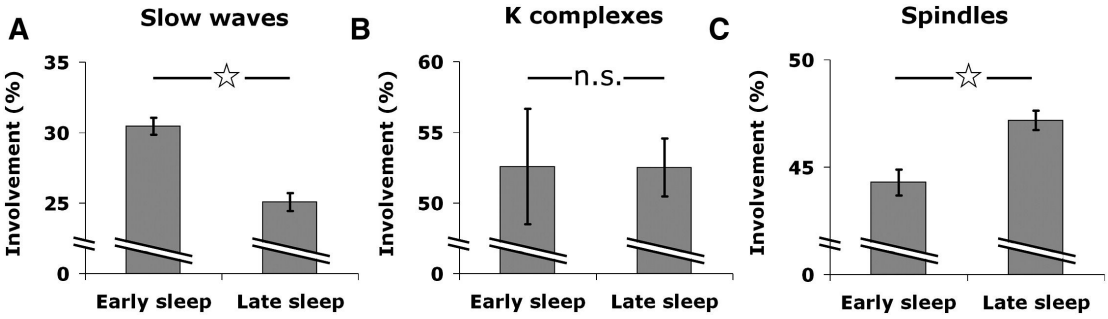

Figure 1-6 Changes in spatial extent of slow waves and spindles between early and late sleep

(A) Slow waves become more local in late sleep. Slow wave involvement (percent of monitored brain structures expressing each wave) in early NREM sleep vs. late NREM sleep in five individuals exhibiting a clear homeostatic decline of SWA during sleep (Figure S 1-1). Error bars denote SEM (n=1436 and 1698 events in early and late sleep). Asterisk denotes statistically significant difference ($p<2.6E-10$, unequal variance t-test). (B) K complexes are more global and similar in early and late sleep. Same sleep segments and analysis as (A). Error bars denote SEM (n=148 and 181 events in early and late sleep; $p=0.98$, unequal variance t-test). (C) Spindles become more global in late sleep. Same sleep segments and analysis as (A). Error bars denote SEM (n=1272 and 2554 events in early and late sleep, $p < 0.00014$, unequal variance t-test).

Sleep slow waves propagate along typical pathways

To examine whether slow waves propagate along typical pathways, we checked for consistent temporal delays between brain regions in which the same wave was observed. Figure 1-7A provides an example of mean slow waves in depth EEG of different brain structures in one individual, revealing a propagation trend from medial frontal cortex to the MTL and hippocampus. This propagation was evident also when examining the distribution of lags for individual waves (Figure 1-7A, right). Despite variability in the timings of individual waves, some regions consistently preceded scalp EEG whereas others followed it.

A systematic analysis of depth EEG established that slow waves had a strong propensity to propagate from medial frontal cortex to the MTL and hippocampus. Specifically, we identified all slow waves that were detected within ±400ms across several brain structures (Experimental Procedures). Sorting regions according to the order in which their slow waves were detected revealed a clear tendency of slow waves to propagate from medial frontal cortex to the MTL (Figure 1-7B), which was highly significant statistically (Figure 1-7C, $p < 2.3E-08$, unequal variance t-test). In addition, this propagation tendency was consistent across individual subjects (Figure S 1-8) and robust to different examinations (Figure S 1-7D).

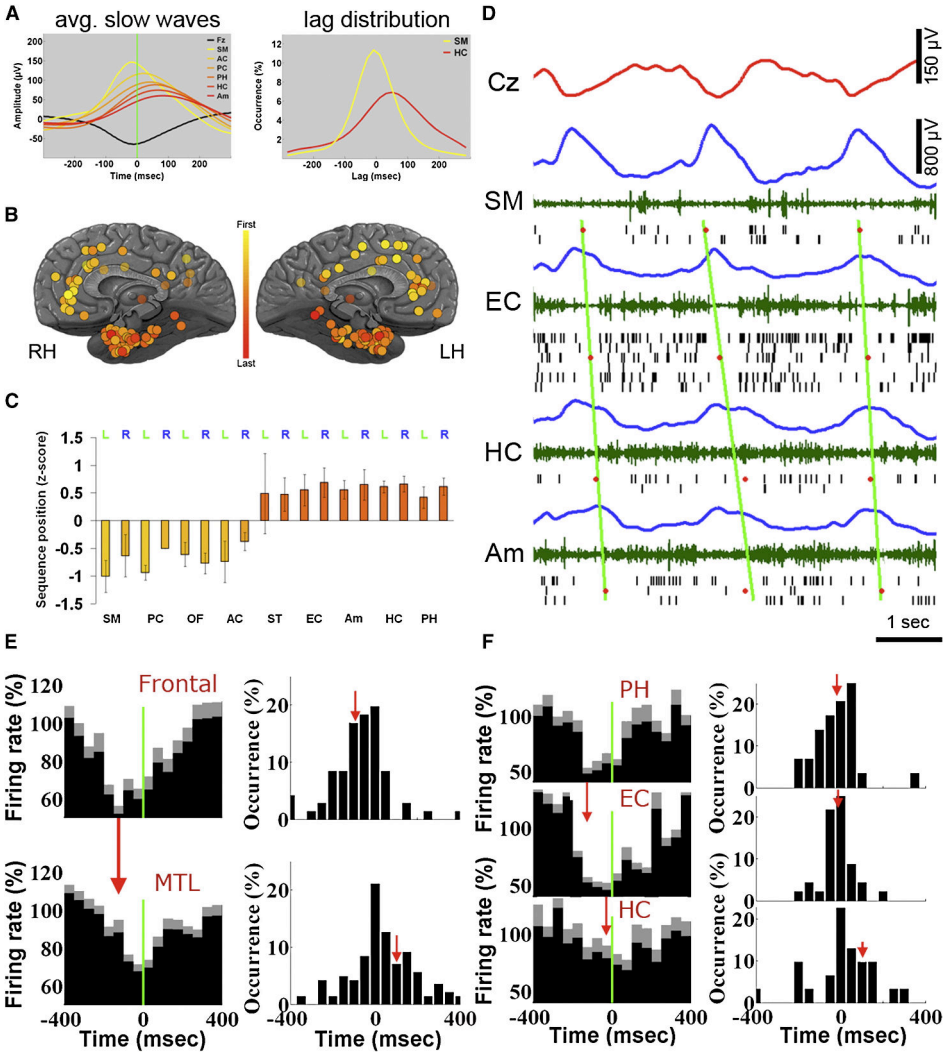

Figure 1-7 Sleep slow waves propagate across typical paths

(A) Left: average depth EEG slow waves in different brain structures of one individual illustrate propagation from frontal cortex (yellow) to MTL (red). All slow waves are triggered by scalp EEG negativity. Black, scalp mean waveform. Right: distributions of time lags for individual waves in supplementary motor area (SM, yellow) and hippocampus (HC, red) relative to scalp. (B) Mean position in sequences of propagating waves in all 129 electrodes across 13 individuals. Each circle denotes one depth electrode according to its precise anatomical location. Yellow-red colors denote waves observed sooner in frontal cortex compared with MTL (see legend). (C) Quantitative analysis: mean position in propagation sequences as a function of brain region. Abbreviations: SM, supplementary motor area; PC, posterior cingulate; OF, orbitofrontal cortex; AC, anterior cingulate; ST, superior temporal gyrus; EC, entorhinal cortex; Am, amygdala; HC, hippocampus; PH, parahippocampal gyrus. (D) An example of individual slow waves propagating from frontal cortex to MTL. Rows (top to bottom) depict activity in scalp EEG (Cz, red), supplementary motor area (SM) , entorhinal cortex (EC), hippocampus (HC), and amygdala (Am). blue, depth EEG; green, MUA; black lines, spikes of isolated units. Red dots mark center of OFF periods in each brain region based on the middle of silent intervals as defined by last and first spikes across the local population. Diagonal green lines are fitted to OFF period times via linear regression and illustrate propagation trend. (E) Left, the average unit activity in frontal cortex (top, n=76) and MTL (bottom, n=155), triggered by the same scalp slow waves reveals a robust time delay (illustrated by vertical red arrow). Right, distribution of time delays in individual frontal (top) and MTL (bottom) units reveals a time delay of 187ms. Red vertical arrows denote mean time offset relative to scalp EEG (F) Left, the average unit activity in parahippocampal gyrus (PH, n=32), entorhinal cortex (EC, n=49) and hippocampus (HC, n=35), triggered by the

same depth EEG slow waves reveals a cortico-hippocampal gradient of slow wave occurrence (illustrated by vertical red arrows). Right, distribution of time delays in individual PH, EC, and HC units reveals a time delay of 121ms between PH and HC. Red vertical arrows denote mean time offset relative to depth EEG.

Figure 1-7D shows an example of individual slow waves propagating across multiple brain structures. As can be seen, time offsets in OFF periods in different brain regions followed a propagation from frontal cortex to the MTL (diagonal green lines). Next, slow wave propagation was quantitatively examined in unit discharges in all 11 individuals in whom unit recordings were obtained simultaneously in frontal and MTL regions. Mean spiking activities underlying slow waves in medial frontal cortex vs. MTL revealed a robust time offset (Figure 1-7E, left). Across individual neurons, minimal firing in frontal neurons (n=76) was -85 ms ± 22 relative to scalp Fz negative peak, whereas minimal firing in MTL neurons (n=155) was +102ms ± 20 relative to the same time reference, indicating an average difference of 187ms (Figure 1-7E, right). The statistical significance of this time offset was confirmed via bootstrapping by computing time delays of individual neurons while randomly shuffling their anatomical labels ($p << 1E-10$, Figure S 1-7G). In fact, across 10,000 iterations, not even one instance was found in which a random time offset between the two groups of neurons was as high as (the real) 187ms. Next, we examined whether within the MTL, spiking activities could also reveal a preferred direction of signal propagation between cortex and hippocampus. In 11 individuals in whom unit recordings were obtained simultaneously from multiple MTL regions, slow wave-triggered averaging of spiking activity (Figure 1-7F, left) revealed that slow waves occurred first in the parahippocampal gyrus, next in entorhinal cortex, and lastly in the hippocampus, emulating the anatomical pathways (see also Discussion). Across individual neurons minimal firing in parahippocampal neurons occurred -19 ms ± 20 relative to positive peak of depth EEG slow waves in MTL, while minimal firing in hippocampal neurons occurred +103 ms ± 47 relative to the same time reference, indicating that slow waves exhibited an average time difference of 122ms between cortex and hippocampus (Figure 1-7F, right). The statistical significance of this time offset was confirmed via bootstrapping while randomly shuffling anatomical labels ($p < 0.0097$, Figure S 1-7H).

Finally, we examined whether hippocampal sharp-wave/ripple (SWR) bursts may precede and drive responses in medial prefrontal cortex (mPFC), a primary projection zone of hippocampal output in primates (Cavada et al., 2000). To this end, we focused on seven subjects in whom hippocampal ripples were recorded simultaneously along with spiking activities in hippocampus and mPFC. Hippocampal ripples were detected and their relation to sleep slow waves examined (Experimental Procedures and Figure S 1-7). In line with previous observations (Clemens et al., 2007; Molle et al., 2006; Sirota et al., 2003), hippocampal ripples were found to occur preferentially around ON periods (Figure S 1-8D). A fine time scale examination of spiking activities revealed that hippocampal neurons transiently elevated their firing rates around ripple occurrence (Figure S 1-8E). Across individual hippocampal neurons (n=72), time offsets of peak firing were -31 ms ± 7 from detected ripples (Figure S 1-8G). Adjacent entorhinal neurons also elevated their firing rates transiently albeit to a lesser degree (Figure S 1-8E), and time offsets were -2 ms ± 9, indicating that they followed hippocampal neurons by 29ms on average. By contrast, individual mPFC neurons did not show a consistent transient firing rate increase (Figure S 1-8G). Rather, mPFC neurons only exhibited a sustained increase in firing that was significantly higher than the mean rates in NREM sleep (Figure S 1-8E, $p < 0.05$, unequal variance t-test), most probably due to the fact that ripples occurred preferentially during ON periods. These results suggest that ripples

reflect hippocampal output that is largely confined spatially to the MTL. By contrast, slow wave-triggered averaging of spiking activity in mPFC and hippocampus once again revealed that slow waves in prefrontal cortex preceded those found in hippocampus (Figure S 1-8F). On the whole, our results suggest that signal propagation in slow wave sleep primarily follows a cortical-hippocampal direction.

Afferent synaptic input predicts occurrence and timing of activity onsets in individual slow waves

What determines whether and when a given region transitions into an active state? We hypothesized that this process is not entirely stochastic and is determined by what proportion of its afferents have just transitioned to an active state. To test this possibility, we focused on the amygdala and its afferents. This choice was guided by the fact that projections to the amygdala in primates are mostly ipsilateral and arrive from diverse sources, with a notable contribution from other limbic structures such as entorhinal cortex, cingulate cortex, hippocampus, as well as medial prefrontal and orbitofrontal cortices serving mainly as input sources (Amaral et al., 1992; McDonald, 1998).

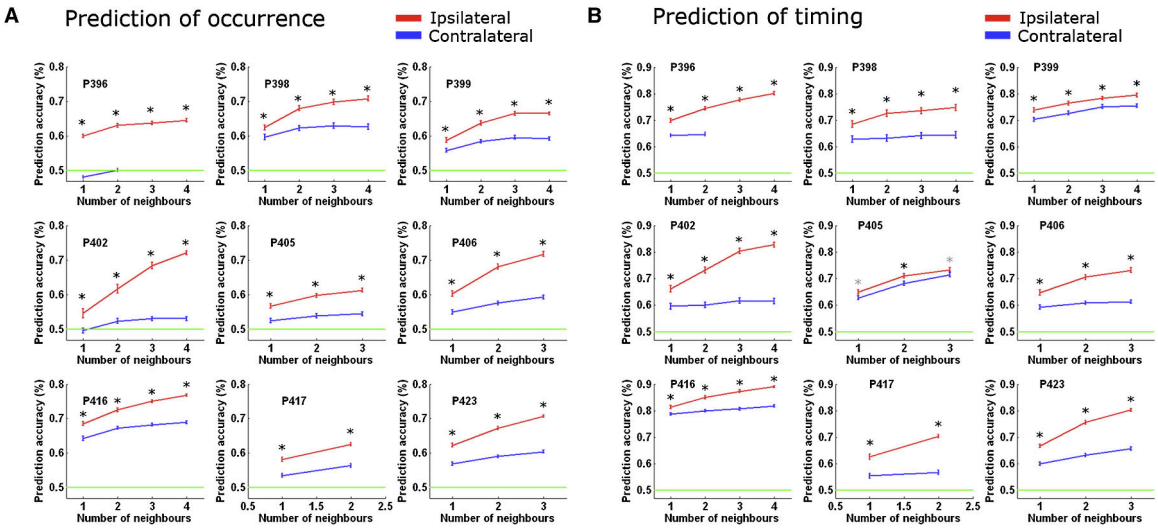

Figure 1-8 Afferent Information Predicts Occurrence and Timing of Activity Onsets in Individual Slow Waves

(A) Predicting occurrence of individual amygdala slow waves with information about slow waves in other limbic regions. Each sub-panel shows prediction accuracies for one individual using either ipsilateral (red) or contralateral (blue) information, as a function of the number of regions made available to the classifier. Green horizontal line shows chance prediction at 50%. Error bars denote SEM across 100 classifier iterations in which training and testing datasets (individual waves) as well as the identity of available neighbors were shuffled. Black and gray asterisks denote significant differences in prediction accuracy ($p<0.001$ and $p<0.05$ respectively, paired t-test). Note that in all 9 individuals, prediction was significantly more accurate using ipsilateral information, reflecting the fact that bulk anatomical projections to amygdala arrive from ipsilateral brain regions ($p < 1E-39$ in all 9 individuals, paired t-test, n=100 classifier iterations). (B) Same as above when predicting the timing of individual amygdala slow waves (before or after slow waves in parietal scalp electrode Pz). Timing prediction was likewise more accurate based on ipsilateral information ($p < 1.4$ E-7 in 8 individuals and $p = 0.02$ in ninth individual, paired t-test, n=100 classifier iterations).

We capitalized on this anatomical organization and examined whether we could predict the occurrence and timing of individual slow waves in the amygdala. Crucially, if transitions into ON periods indeed reflect cumulative drive of anatomical afferents, we expected that we could better predict the occurrence of events based on ipsilateral limbic afferents than based on equivalent contralateral information.

To examine this possibility, we inspected data in 17 hemispheres of 9 individuals in which signals from amygdala and several other limbic structures were recorded. A linear classifier was trained with a subset of slow waves to utilize information about the occurrence, amplitude, and timing of transitions into population ON periods (positive peaks in depth EEG) in ipsilateral (or contralateral) limbic regions to predict the occurrence and timing of individual slow waves in the amygdala (Experimental Procedures). Its performance was then tested with a separate subset of waves (Figure 1-8). In all 9 individuals, the information from ipsilateral afferent regions led to significantly greater accuracy in predicting the occurrence of slow waves in the amygdala ($p < 1E\text{-}39$ in all 9 individuals). Moreover, ipsilateral prediction accuracy monotonically increased as a function of the number of afferent regions that were made available for classifier training (Figure 1-8A, red, slope = 0.04 $\pm$ 0.005 percent correct per neighbor). By contrast, contralateral prediction was sometimes at near-chance levels and did not depend as strongly on the number of regions (Figure 1-8A, blue, significantly smaller slopes, $p < 5.4^{-4}$ via paired t-test). Along the same line, the timing of individual slow waves in the amygdala (whether they occurred before or after the parietal scalp electrode) could be more accurately predicted with information from ipsilateral afferent regions ($p < 1.4^{-7}$ in 8 individuals and $p = 0.02$ in ninth individual, Figure 1-8B). Thus, despite the probabilistic nature of activity onsets in slow waves, the underlying process is not entirely stochastic and reflects the cumulative drive of afferent synaptic input.

Discussion

By examining simultaneous depth EEG and single-unit recordings in multiple regions of the human brain we show that ON and OFF periods of spiking activity and corresponding EEG slow waves typically involve a limited number of brain regions. Similarly, sleep spindles are mostly local. In addition, slow waves have a tendency to propagate from prefrontal cortex to the MTL and hippocampus. We also found that activity onsets in individual waves reflect the afferent synaptic drive to a given region.

Local sleep slow waves

The main novel observation reported here is that most sleep slow waves are in fact confined to local regions, i.e. detected in a minority of brain areas. Specifically, in most cases we found that when some brain regions were in an ON state, neurons in other brain regions were completely silent. The unique dataset employed here was instrumental in unequivocally establishing this phenomenon, since (i) the large size of the human brain facilitated simultaneous recordings across multiple distant sites; (ii) the simultaneous recording of depth EEG, MUA, and spiking of individual neurons allowed us to establish that differences between depth EEGs in different regions reflect local activities rather than noise.

Typically, less than 30% of monitored brain regions were involved in each slow wave event. Although our sampling was mostly limited to medial brain areas, it represented activity in multiple (8-12) regions across lobes and hemispheres, so it is reasonable to infer that these results can be generalized to the entire brain. When global ON and OFF states were observed, they were associated with large slow waves in scalp recordings, usually during deep sleep early in the night, or with K-complexes throughout the night. Local slow waves tended to co-occur across homotopic prefrontal regions, but not across homotopic regions in the MTL (Figure 1-4E), supporting the role of callosal pathways in slow wave synchronization and propagation (Amzica and Steriade, 1995). Medial prefrontal regions including the anterior cingulate and orbitofrontal cortex were among the most involved in slow wave occurrence.

The demonstration that slow waves are mostly local shows that examples of isolated slow waves (Mohajerani et al., 2010; Sirota and Buzsaki, 2005) constitute the rule rather than the exception. It is also consistent with evidence that the intensity of sleep slow waves can vary across brain regions (Finelli et al., 2001), that sleep can be regulated locally (Huber et al., 2006, 2004), and that multiple local generators could contribute to EEG SWA (Murphy et al., 2009; Riedner et al., 2007).

Local sleep spindles

In physiological conditions spindles are believed to reflect global signal propagation between cortex and thalamus (Achermann and Borbely, 1998; Contreras et al., 1996; Mircea Steriade, 2003). Although spindles are generated in the thalamus, the neocortex governs spindle synchronization through corticothalamic projections (Mircea Steriade, 2003). Asynchronous spindles were observed during development (Khazipov et al., 2004) or in non-physiological conditions such as decortication, cortical depression, and acute

stroke, where a non-functional cortex is not able to exert its normal synchronizing influence (Contreras et al., 1997a, 1996; Gottselig et al., 2002)

By simultaneously examining spindle occurrence across multiple brain regions (Figure 1-5), the present results demonstrate that, like most slow waves, most sleep spindles occur locally in natural sleep. Thus, each spindle event was usually detected in only a minority of brain regions. Even when applying the most conservative criteria, treating any spindle spectral power above the noise level as a spindle event, approximately one third of events occurred independently across regions. As found for slow waves, the spatial extent of spindles was correlated with their amplitude. Although spindles are often associated with slow wave up-states (Molle et al., 2002; Steriade et al., 1993b), spindles occurred locally in a way that was independent of local slow waves. Also, the local occurrence of spindles cuts across the distinction between fast (13-15Hz) centroparietal spindles and slow (11-13Hz) frontal spindles (Anderer et al., 2001) since spindles of the same frequency can occur in isolation between homotopic regions across hemispheres. It is an open question whether local and global spindles may be mediated by different mechanisms such as corticothalamic projections from different layers (Jones, 2009) or thalamocortical projections via the core and matrix cells (Rubio-Garrido et al., 2009; Zikopoulos and Barbas, 2007).

Some previous data hinted at the possibility that sleep spindles may occur or be regulated locally. One study reported that during drowsiness spindles occurred in medial prefrontal cortex while posterior regions showed alpha activity (Caderas et al., 1982). Another study reported that spindle power can vary and correlate with motor learning (Nishida and Walker, 2007). A recent study using non-invasive magnetoencephalography found that the average coherence between pairs of sensors was significantly lower than that found between scalp EEG (Dehghani et al., 2010a), implying asynchronous generators. Indeed, the present findings demonstrate that local sleep spindles constitute the majority of events in natural human sleep.

Taken together, the finding that both slow waves and spindles are mainly confined to local regions adds to the evidence suggesting that sleep arises from activities of local circuits and is not exclusively a global phenomenon (Krueger et al., 2008). In isolated cortical slices long periods of silence are interrupted by short bursts of activity much like the EEG of preterm newborns (tracé alternant) (Kristiansen and Courtois, 1949). Prior use and induction of plastic changes lead to regional enhancements of SWA in human sleep (Esser et al., 2006; Huber et al., 2006, 2004) and rodent sleep (Vyazovskiy et al., 2000; Werth et al., 1997). In addition, local circuits may exhibit OFF periods even during wakefulness while the animal is performing a task (Vyazovskiy et al., 2009). Imaging studies demonstrate some local modulation of thalamocortical activity in slow wave sleep (Albouy et al., 2008; Braun et al., 1997; Dang-Vu et al., 2005; Maquet, 2000) Apart from local slow waves, clinical evidence suggests the existence of "dissociated states" (Mahowald and Schenck, 2005). For example, in sleepwalking and REM sleep behavior disorder some brain circuits may be asleep while others are awake (Bassetti et al., 2000; Mahowald and Schenck, 2005; Terzaghi et al., 2009). Naturally occurring sleep patterns in dolphins (Mukhametov et al., 1977), seals (Siegel, 2009), and birds (Rattenborg et al., 2001) also suggest that parts of the brain can be awake while others are asleep. Overall, such evidence implies that although sleep is often considered as a global phenomenon, it may be best understood in relation to activities of local circuits.

Unit discharges underlying sleep slow waves

A tight relation between EEG sleep slow waves and underlying unit activity was evident in all monitored brain structures (Figure 1-2 and Figure 1-3). Although there was considerable variability among individual neurons, in each brain region the activity of a substantial portion of neurons was phase locked with slow waves (Figure 1-3D). Moreover, the amplitude of EEG slow waves reflected the degree of modulation in neuronal firing (Figure 1-3E). A tight relation between EEG slow waves and underlying unit activity is a widely established phenomenon in natural sleep of mammals, as demonstrated by extracellular recordings (Amzica and Steriade, 1998; D. Ji and Wilson, 2007; Noda and Adey, 1970; Sirota et al., 2003; V. V. Vyazovskiy et al., 2009), owing to the fact that within each region, the activity of different neurons is highly synchronized (Destexhe et al., 1999). In neocortex, sleep slow waves reflect a slow oscillation of membrane potential fluctuations, as demonstrated by intracellular recordings (Isomura et al., 2006; Steriade et al., 2001; Volgushev et al., 2006). Recent studies in human cortex have similarly demonstrated that slow waves reflect alternations between neuronal firing and suppressed activity (Cash et al., 2009; Csercsa et al., 2010; Le Van Quyen et al., 2010, 2008). Our results extend these observations to multiple regions in the human brain (Figure 1-3C). Neurons phase-locked to slow waves were found not only in neocortex, but also in limbic paleocortex (e.g. cingulate cortex, parahippocampal gyrus, entorhinal cortex), archicortex (hippocampus), and in subcortical structures (amygdala). Although neurons in subcortical structures seem to lack the inherent bistability of cortical neurons (Isomura et al., 2006), their activity is nevertheless modulated by slow oscillations generated locally or imposed by the cortex (Pare et al., 2002; Wolansky et al., 2006) Indeed, our recordings demonstrate that neurons in entorhinal cortex, hippocampus, and amygdala modulate their spiking activities in concert with EEG slow waves.

Propagation of sleep slow waves and cortico-hippocampal dialogue

Previous studies suggested that slow waves may have a tendency to propagate along an anterior-posterior axis through the cingulate gyrus and neighboring structures (Murphy et al., 2009), which constitute an anatomical backbone of anatomical fibers (Hagmann et al., 2008). By simultaneously recording from 8-12 brain structures directly, the current results establish that slow waves indeed propagate in the human brain as previously suggested (Massimini et al., 2009b, 2004), and as observed in part in rodents (Vyazovskiy et al., 2009) and cats (Volgushev et al., 2006). The consistent tendency of slow waves to propagate along distinct anatomical pathways (e.g. cingulum) indicates that such waves can be used to investigate changes in neuronal excitability and connectivity.

By recording EEG and spiking activities from multiple adjacent MTL structures we demonstrate that cortical slow waves precede hippocampal waves in the human brain. As far as can be inferred from medial brain structures, the results reveal a sequential cortico-hippocampal propagation of slow waves along well-known anatomical paths, from the parahippocampal gyrus, through entorhinal cortex, to hippocampus (Figure 1-7F), as was observed in intracellular recordings in rodents (Isomura et al., 2006). A similar cortico-hippocampal succession was revealed when focusing exclusively on hippocampus and mPFC recorded simultaneously in seven patients (Figure S 1-8F). Our results are in line with previous animal studies (Hahn et al., 2007; Isomura et al., 2006, p. 200; D. Ji and Wilson, 2007; Molle et al., 2006; Sirota et al., 2003) and with a recent study of human depth EEG (Wagner et al., 2010). That cortical slow waves precede hippocampal waves

is also compatible with a cortical origin for sleep slow waves (Chauvette et al., 2010; Steriade et al., 1993c).

We also examined whether hippocampal SWR bursts may be driving responses in mPFC on a fine time scale as suggested recently (Wierzynski et al., 2009). Our results reveal a clear tendency of hippocampal ripples to occur around ON periods of slow waves (Figure S 1-8), as reported previously (Clemens et al., 2007; Molle et al., 2006; Sirota et al., 2003). Moreover, delayed and attenuated spike discharges were observed in entorhinal cortex compared with hippocampus (Figure S 1-8). Since the entorhinal cortex provides both the major input to and receives output from the hippocampus, our results support the notion that ripples reflect hippocampal output (Chrobak and Buzsaki, 1996). Local effects of hippocampal output within the MTL are in line with a recent human study reporting some incidences of delayed gamma bursts in parahippocampal cortex following hippocampal ripples (Le Van Quyen et al., 2010). However, transient firing in mPFC units was not found following ripple occurrence (Figure S 1-8). The apparent discrepancy with (Wierzynski et al., 2009) is most likely related to the fact that our data represent a different neuronal population in the mPFC where neuronal activity is highly modulated by slow waves (compare to their Figure 1-1), but differences in species and electrode locations may contribute as well.

More generally, the direction of the cortico-hippocampal dialogue in sleep has been a hotly debated issue. An influential suggestion has been that signals propagate from cortex to hippocampus during wakefulness, and from hippocampus to cortex during sleep (Buzsaki, 1998). Since declarative memories become progressively more resistant to hippocampal damage, it is thought that the hippocampus "transfers" such memories to the cortex by replaying activity patterns during SWRs in sleep (Lee and Wilson, 2002). The current results add to existing evidence showing that during NREM sleep neural activity propagates predominantly from the neocortex to the hippocampus (Hahn et al., 2007; Isomura et al., 2006; D. Ji and Wilson, 2007; Molle et al., 2006; Sirota et al., 2003). Future studies are needed to determine whether within this robust cortico-hippocampal broadcast there may be islands of functionally relevant hippocampo-cortical transmission (Tononi et al., 2006).

Cumulative synaptic input determines transitions to ON periods

While slow waves reflect spontaneous alternations of activity and silence in corticothalamic networks, what causes the transition from silence to activity in a given brain region remains unclear. Several scenarios could explain the source of transitions at the network level. One possibility is that whether and when a given region will transition into an ON period is determined by a global process such as subcortical common input, which could serve as a main "switch". However, since most slow waves occur locally and since slow oscillations are also observed in vitro (Sanchez-Vives and McCormick, 2000), such a global mechanism seems implausible. A second possibility is that transitions to activity are stochastic and driven by intrinsic processes within each region. For example, currents that are activated close to the resting membrane potential (such as the hyperpolarization-activated depolarizing current (McCormick and Pape, 1990)) could lead neurons to discharge during OFF periods and initiate activity that would then spread within a region, irrespective of other brain regions. A third possibility is that synaptic drive gradually builds up prior to the onset of ON periods, so that if and when a region becomes active reflects the cumulative input to that region (Chauvette et al., 2010).

By capitalizing on the amygdala, for which ipsilateral projections constitute the dominant input (Amaral et al., 1992; McDonald, 1998), we show that predicting individual ON periods is significantly more accurate when based on information from ipsilateral limbic regions compared with contralateral limbic regions. This suggests that the state of afferent regions provides particularly relevant information about the transition into an active state. Moreover, within ipsilateral regions, the prediction grew stronger depending on the number of inputs made available to the classifier, whereas this effect was much weaker for contralateral regions. Taken together, our results suggest that the cumulative synaptic input to a given region is a major determinant of whether and when it will enter an active state.

Potential confounding factors

Our data were recorded in medicated epilepsy patients in whom abnormal events during seizure-free periods may affect brain activity in slow wave sleep (Dinner and Lüders, 2001). Inter-ictal epileptiform activity, as well as anti-epileptic drugs (AED) and their adjustments could affect sleep in general, and the nature of slow waves in particular. Therefore, it was imperative to confirm that our results could indeed be generalized to the healthy population, and multiple observations strongly suggest that this is indeed the case. First, our overnight recordings were carried out prior to routine tapering of AEDs to ensure a less significant contribution of epileptiform activities. Second, sleep measures were within the expected normal range, including distribution of sleep stages, NREM-REM cycles, and EEG power spectra of each sleep stage (Figure 1-1). By specifically detecting pathological interictal spikes and paroxysmal discharges and separating them from physiological sleep slow waves, several additional features were revealed that clearly distinguish these phenomena (Figure S 1-3). Third, the occurrence rate of paroxysmal discharges was highly variable across channels, limited in its spatial extent, and entirely absent in some channels. By contrast, the number of physiological sleep slow waves was highly consistent across channels, and in line with that reported in healthy individuals. Fourth, all the results reported here, including a tight relation between EEG slow waves and unit activities, local slow waves and spindles, and slow wave propagation, could be observed in every individual despite drastically different clinical profiles (Table S2). This consistency argues against contributions of idiosyncratic epileptiform events, for which underlying unit activities are highly variable (Wyler et al., 1982). Fifth, comparing the morphology of sleep slow waves and interictal paroxysmal discharges revealed a significant difference in the waveform shape of pathological events. Sixth and most importantly, our analysis of spiking activities underlying physiological vs. pathological waves revealed significant differences, confirming our ability to separate sleep slow waves from epileptic events (Figure S 1-3). Specifically, elevated firing rates around interictal spikes, presumably reflecting a high degree of synchrony among neurons within the epileptogenic focus (Wyler et al., 1982)led to highly asymmetric patterns.

Functional significance

The observation that most slow waves are local has several implications. Although sleep slow waves are the most conspicuous electrical activity pattern observed during sleep, it is not yet clear whether they serve a specific function. However, since EEG SWA is tightly regulated (i.e. increases with time awake and decreases during sleep) and is a

reliable indicator of sleep need (Borbely and Achermann, 1999), it may serve some restorative function. Moreover, slow wave deprivation (Aeschbach et al., 2008; Landsness et al., 2009) and enhancement (Marshall et al., 2006) impair and improve learning, respectively, suggesting that slow waves, or perhaps spindle, gamma, and ripple oscillations that are grouped by the slow oscillation, may play a role in memory consolidation (Diekelmann and Born, 2010; Stickgold and Walker, 2007; Tononi and Cirelli, 2006). The present results offer some constraints on how slow waves may aid memory consolidation. The fact that the up-state in one brain region is usually out of phase with respect to other brain regions constrains the nature of such information transfer during up states. In addition, when slow waves do occur across several brain regions, they have a clear tendency to propagate across typical paths so that they occur with typical time delays across different regions. This trait imposes a directionality to plasticity-related processes, and such propagating waves may play a role in time-dependent synaptic plasticity (Ermentrout and Kleinfeld, 2001), such as spike timing-dependent plasticity (Caporale and Dan, 2008).

The results also refine our view of what happens in the brain in late sleep at the end of the night. Once sleep pressure has largely dissipated, NREM sleep is dominated at the EEG level by low-amplitude slow waves (Riedner et al., 2007). As shown here, low-amplitude scalp slow waves do not reflect small waves occurring simultaneously across the brain, but mostly represent local waves occurring out of phase across different brain regions. Therefore, whatever functional process is supported by slow waves, it occurs more and more locally towards the end of sleep. Moreover, the fact that in late sleep many brain regions remain in an ON state while only a minority of areas are in an OFF state may not be unrelated to the increased occurrence and intensity of dreaming in NREM sleep towards the end of the night (Nir and Tononi, 2010). Finally, local slow waves observed in wake are usually interpreted as reflecting pathology (e.g. lesions). Given that local slow waves are the norm in sleep, similar events in wake could be re-interpreted as reflecting 'piecemeal-sleep'.

The finding that most sleep spindles are local may also bear functional implications. That spindle oscillations in cortico-thalamic-cortical loops maintain regional specificity during sleep provides further evidence that spontaneous activity during resting states is locally organized. Thus, rather than just implementing a global "thalamic gate", sleep spindle oscillations may contribute to synaptic plasticity in a circuit-specific manner.

In summary, the current results further extend and refine our evolving view of neuronal activity in sleep by showing that the two fundamental brain oscillations of sleep - slow waves and spindles - occur mostly locally. It may be that a functional disconnection among different sectors of the corticothalamic system may represent a unique feature of sleep, with as yet unexplored functional consequences.

Experimental Procedures

Subjects and sleep studies

Thirteen patients with intractable epilepsy were implanted with intracranial depth electrodes to identify seizure foci for potential surgical treatment. Electrode location was based solely on clinical criteria. All patients provided written informed consent to participate in the research study, under the approval of the Medical Institutional Review Board at UCLA. Sleep studies were conducted on the hospital ward 48–72 hr after surgery, lasted 7 hours on average, and sleep-wake stages were scored according to established guidelines. The montage included two EOG electrodes, two EMG electrodes, scalp electrodes at C3, C4, Pz and Fz, two earlobe electrodes used for referencing, and continuous video monitoring.

Data acquisition and spike sorting

In each patient 8–12 depth electrodes were implanted targeting medial brain areas. Both scalp and depth EEG data were continuously recorded at a sampling rate of 2 kHz, bandpass-filtered between 0.1-500 Hz, and re-referenced offline to the mean signal recorded from the earlobes. Intracranial / depth EEG refers to data recorded from the most medial platinum-iridium contact along the shaft (Figure 1-1D, blue). Each electrode terminated in eight 40-μm microwires from which extracellular signals were continuously recorded (referenced locally to a ninth non-insulated microwire) at a sampling rate of 28/30 kHz and bandpass-filtered between 1-6000 Hz. Action potentials were detected by high-pass filtering the extracellular recordings above 300Hz and applying a threshold at 5 SD above the median noise level. Detected events were further categorized as noise, single- or multi-unit events using superparamagnetic clustering as in (Nir et al., 2008). Unit stability throughout sleep recordings was confirmed by verifying that spike waveforms and inter-spike-interval distributions were consistent and distinct throughout the night (Figure S 1-4). For visualizations purposes in Figure 1-1F, Figure 1-4A, Figure 1-7D, Figure S 1-5, multi-unit activity (MUA) traces were extracted from microwire recordings by filtering the signals offline between 300-3000Hz.

Analysis of slow waves, sleep spindles, and hippocampal ripples in depth EEG data

Detection details for all events are given in the Supplemental Data. Putative slow waves were subdivided into those preceded (within 1s) by an interictal spike ("paroxysmal" discharges) and those unrelated to paroxysmal events ("physiological" sleep slow waves). Physiological slow waves occurring near-simultaneously across channels (within ± 400 ms, Figure S 1-5) were considered 'concordant' events (Figure 1-4). For slow wave propagation (Figure 1-7) we focused on events identified in Fz and in intracranial recordings of at least three brain structures, although the results were highly robust to the exact detection parameters and to other examinations (Figure S 1-7). To compare timing of unit discharges within MTL (Figure 1-5F), we defined time zero based on the positive peak of EEG slow waves in parahippocampal gyrus (9/13 subjects), or entorhinal cortex (4/13 subjects). For analysis of local spindles, spectrograms were computed in ± 1sec intervals around peak spindle power, using a short-time Fourier transform with a

window of 744ms and 95% overlap, and normalizing power relative to random intervals as in (Sirota et al., 2003).

Relationship between neuronal spiking and sleep slow waves

Phased-locked spiking (Figure 1-3D) was assessed by extracting the instantaneous phase of the depth EEG filtered between 0.5-4Hz ±500ms surrounding slow wave positive peaks via the Hilbert transform, testing for nonuniformity of the phase distribution of spike occurrences using Rayleigh's test, and determining critical p-values using shuffled data to control for asymmetries in the EEG waveforms (Figure S 1-4). Slow-wave-triggered averaging was conducted for each unit separately using the highest amplitude slow waves in each channel (top 20%). The timing and magnitude of firing rate modulations were defined based on the maxima/minima using 20ms bins. Propagation in unit activities were evaluated across all significantly phase-locked units within a region (Figure 1-7E-F, Figure S 1-8, left), or for individual units separately using 20ms bins (Figure 1-7E-F, Figure S 1-8, right). Statistical significance of time differences between spiking activities of individual units in distinct brain structures (Figure 1-4E,F) was evaluated via bootstrapping by (a) assigning a random anatomical label to each neuron separately (either frontal or MTL for Figure S 1-7G, either PH or HC for 'within MTL' analysis in Figure S 1-7H), (b) creating surrogate groups with the same number of units as the real data, and (c) computing the random time offset between the two groups as was done for the real data (Figure S 1-7).

Dynamics throughout sleep

In five individuals exhibiting a clear homeostatic decline of SWA during sleep we analyzed slow waves, K-complexes and sleep spindle separately in early and late NREM sleep (Figure S 1-1). Putative K-complexes were detected in Fz recordings as isolated slow waves (within ±3s) with peak-to-peak amplitude > 75 μV.

Prediction of individual slow waves via linear classifier

Classification was performed with a support vector machine using a linear (dot product) kernel, using data from 17 hemispheres of 9 individuals in which signals from amygdala and other limbic structures were recorded. The occurrence, amplitude and timing of transitions into population ON periods (positive peaks in depth EEG) were used to train (80% of events) and test (20% of events) a linear classifier using either ipsilateral or contralateral limbic information. Differences between ipsilateral vs. contralateral prediction accuracy were evaluated using a paired t-test with df=100 (number of classifier iterations) for each number of neighbors separately.

Supplemental Data

Supplemental Experimental Procedures

Subjects

Thirteen neurosurgical patients with pharmacologically intractable epilepsy were implanted with intracranial depth electrodes to identify seizure foci for potential surgical treatment (Fried et al., 1999b) Electrode location was based solely on clinical criteria. Prior to implantation, patients provided written informed consent to participate in the research study, under the approval of the Medical Institutional Review Board at UCLA. All surgery was performed by I.F. For each subject, localization of the seizure onset zone was based on recordings during hospital monitoring, in combination with prior functional and anatomical neuroimaging (see Table S1B for details).

Polysomnographic sleep studies

Sleep studies were conducted on the hospital ward 48–72 hr after surgery (see Table S1B for details). All sleep recordings were obtained at a minimal interval of 12 hours from identifiable seizures. The montage included two electrooculogram (EOG) electrodes, two electromyogram (EMG) electrodes, scalp electrodes at C3, C4, Pz and Fz, two earlobe electrodes used for referencing, and continuous video monitoring. Sleep-wake stages were scored according to established guidelines (Iber et al., 2007), and power spectra for different sleep stages (Figure 1-1C, Figure S 1-1C) were calculated using Fast Fourier Transform with 0.1Hz bin resolution on 10sec data segments.

Data acquisition

Electrode location was based solely on clinical criteria and varied among patients. Coverage was obtained in the following regions: hippocampus, amygdala, entorhinal cortex, parahippocampal gyrus, temporal gyrus, fusiform gyrus, temporo-occipital junction; anterior, middle and posterior cingulate; supplementary motor area, inferior frontal gyrus, orbitofrontal cortex, and parietal cortex (Figure 1-1E & Table S 1-1A). Each patient was implanted with 8–12 flexible polyurethane depth electrodes (1.25 mm diameter) stereotactically targeted to specific medial brain areas. Each electrode tip was localized using post-implant computed tomography (CT) co-registered with pre-implant magnetic resonance imaging (MRI) (Brain Navigator Grass-Telefactor Corp., Philadelphia, PA). EEG data were continuously recorded, sampled at 2 kHz, and bandpass-filtered in hardware between 0.1 Hz and 500 Hz. Intracranial / depth EEG refers to data recorded from the most medial platinum-iridium contact along the shaft of the electrodes (Figure 1-1D, blue) . Both scalp and depth EEG were re-referenced offline to the mean signal recorded from the earlobes.

Extracellular microwire recordings were simultaneously obtained continuously (Cheetah Recording System; Neuralynx, Tucson, AZ for 10 patients; Neuroport Recording System; Blackrock, Salt Lake City, UT for 3 patients). Each electrode terminated in a set of nine 40- μm platinum-iridium microwires with impedances ranging from 200 to 500 kΩ (Fried et al., 1999b) Signals from eight microwires were referenced locally to the ninth non-insulated microwire, sampled at 28 kHz (10 patients) or 30 kHz (3 patients)

and bandpass-filtered in hardware between 1 Hz and 6 kHz. For further details regarding data acquisition, see (Nir et al., 2008; Staba et al., 2004).

Unit identification

Units were identified using the 'wave_clus' software package (Quian Quiroga et al., 2004) as described previously (Nir et al., 2008). Briefly, extracellular microwire recordings were high- pass filtered above 300Hz, a threshold was set at 5 SD above the median noise level, detected events were clustered using superparamagnetic clustering, and categorized as noise, single- or multi-unit clusters. Classification of single- and multi-unit clusters was based on the consistency of action potential waveforms, and by the presence of a refractory period for single units, i.e. less than 1% of inter-spike-intervals (ISIs) within 3ms (Figure S 1-4A). The stability of unit recordings throughout long (~7h) sleep recordings was confirmed by comparing action potential waveforms and ISI distributions of detected units separately in 1 hour intervals, and verifying that both waveforms and ISI distributions were indeed consistent and separable between different clusters throughout the night (Figure S 1-4B). Multi- unit activity (MUA) traces, used for visualizations purposes in Figure 1-1F, Figure 1-4A, Figure 1-7D, Figure S 1-5, were extracted from each microwire by filtering the recorded signal offline between 300Hz and 3000Hz.

Detection of sleep slow waves and their separation from paroxysmal events

Individual slow waves were detected as described previously (Riedner et al., 2007). In brief, for each scalp or depth channel separately, the EEG signal was band-pass filtered offline to the slow wave range (0.5-4.0 Hz) using a zero-phase 4th order Butterworth filter (MATLAB, The Math Works Inc, Natick, MA). Individual half-waves in scalp (and depth) EEG were detected as negative (positive) deflections between two zero crossings. Waves detected in sleep stages N2 or N3 whose consecutive zero crossings were separated by 0.25 to 1.0 seconds were considered slow waves and their positive and negative peak amplitudes were stored for further analysis. Similar results were obtained using peak-to-peak measures instead of zero-crossings (not shown).

To rule out false detections of pathological paroxysmal events, putative slow waves were further separated into those preceded (within 1s) by an interictal spike ("paroxysmal" discharges) and those unrelated to paroxysmal events ("physiological" sleep slow waves). To this end, epileptiform interictal spikes were identified by high-pass filtering offline above 100Hz and detecting events whose amplitude exceeded 5 SDs above the mean and whose duration was under 70ms (de Curtis and Avanzini, 2001). We verified visually that automatic detection was effective in identifying interictal spikes in each channel separately.

Dynamics throughout sleep. In five individuals exhibiting a clear homeostatic decline of SWA during sleep we analyzed separately early NREM sleep (Figure S 1-1D, cyan) and late NREM sleep (Figure S 1-1D, yellow). Putative K-complexes (Colrain, 2005) were distinguished from other slow waves by identifying in Fz data high-amplitude waves (peak-to-peak > 75 μV) that were isolated from other slow waves (no other high-amplitude waves occurring within +/- 3sec).

Locality and propagation of sleep slow waves in depth EEG data

Local waves. To investigate the possibility of slow waves occurring independently in various brain regions, for each physiological sleep slow wave we examined the signals in all other channels within ± 400 ms around the detected peak in the "seed" channel, using each channel as seed in turn. Channels in which the slow-wave-filtered EEG had a single peak in this time window were considered concordant with the seed channel (Figure S 1-5). A ± 400 ms window was chosen based on the average profile of slow waves as seen in Figure 1-3A and the results were highly robust to the exact parameters used (e.g. windows of ± 200 ms or ± 800 ms, not shown). We computed the probability of each pair of brain regions (e.g. A,B) to express slow waves concordantly, and created an undirected graph (Figure 1-4E) where the color and width of each edge depicts this probability for each pair of regions, while the color of each node expresses its rank (its average probability to be concordant with all neighbors).

Propagating waves. For the analysis of propagation of slow waves across the entire brain (Figure 1-7B,C) we focused on waves which could be identified in scalp EEG (Fz, seed), as well as in at least three brain structures intracranially. Concordant peaks (relative to seed channels) and their time offsets were used to evaluate delays and possible propagation across brain structures (Figure 1-7). For each wave, we extracted a propagation sequence by sorting time offsets of EEG positive peaks, for example A-C-D-B. We then computed the average position of each brain region in all propagation sequences and normalized for different sequence lengths (different number of monitored regions in different individuals) by applying a z-score transformation (Figure 1-7C). For each brain region, we color coded the precise anatomical location of its corresponding depth electrode according to its mean position in propagation sequences (Figure 1-7B). Importantly, the results were highly robust to other examinations, for example when defining waves based on different brain channels rather than by scalp detection (Figure S 1-7), when focusing on particular sleep stages or when using EEG negative peaks to define timing (Figure S 1-7). As was the case for concordance of local waves (above), propagation results were also highly robust to the exact parameters used for identifying the same wave across channels (not shown). For example, Fz-triggered-averaging of depth EEG with no detection parameters gave rise to similar propagation trends (Figure 1-7A). For examining propagation of unit discharges within MTL (Figure 1-5F), we defined time zero based on slow wave detection in parahippocampal gyrus EEG when possible (9/13 subjects), or based on detection in entorhinal cortex EEG otherwise (4/13 subjects).

Spiking activities during sleep slow waves

Phase locking. Phase locking to slow waves (procedure illustrated in Figure S 1-4 and result shown in Figure 1-3D) was assessed as follows. Depth EEG was filtered in the slow wave range (0.5-4.0 Hz) and individual slow waves were detected as above. For each slow wave, we extracted the instantaneous phase of the filtered EEG in a window of ±500ms surrounding the positive peak via the Hilbert transform. We computed the distribution of phase values at action potential times and computed a p-value using Rayleigh's test for nonuniformity. Since non-uniformity can be partially attributed to asymmetries in the EEG waveforms (Siapas et al., 2005), the critical p-values for significance were determined for each unit separately as the 95th percentile after

examining p-values across 1,000 iterations while shuffling action potential timings within each segment.

Wave-triggered averaging. Slow-wave-triggered averaging was performed separately for each unit. To this end, we focused on the 20% slow waves with the highest amplitude detected in each channel (Riedner et al., 2007). Focusing on high-amplitude waves helped visualize the effects but did not qualitatively affect the result, as seen in Figure 1-3E, where the result was computed separately after sorting all slow waves into three equally subdivided percentiles based on the amplitude of the positive peak. The timing and magnitude of firing rate modulations were defined based on the maxima/minima while using 20ms bins.

Propagation in unit activities. Propagation of slow waves in each region's spiking activities was evaluated on average and for individual units separately. On average, we computed the mean wave-triggered averaging result across phase locked units in each region (left panels in Figure 1-7E,F and Figure S 1-8E). In addition, the time of minimal firing was extracted for each phase- locked unit separately while using 20ms bins (distributions on right in Figure 1-7E,F and Figure S 1-8F).

Ripple detection

Hippocampal ripples were detected automatically using similar methodology as in our previous work (Le Van Quyen et al., 2008). First, microwires in which high-amplitude sinusoid-like 80-200 Hz oscillations could be visually discernable above background in the raw local field potential were selected. The instantaneous amplitude was extracted via the Hilbert transform and an amplitude threshold was set at 3 SDs calculated over the entire length of the band-pass filtered signal across sleep. Events whose amplitude in the ripple range exceeded the threshold for 20-50 ms (Figure S 1-8A) were identified. Our results are insensitive to the precise choice of threshold (2-5 SDs). For each channel, the average power spectra (> 80Hz) of detected events was examined (see Figure S 1-8B for mean spectrum). To avoid high-frequency oscillations in epileptogenic hippocampi, we discarded 2 channels exhibiting a bimodal distribution with significant power above 200Hz (Staba et al., 2004). Next, detection was collapsed across microwires situated within the same hippocampus by choosing events that were detected on at least two separate microwires within 15ms (Figure S 1-8C). We found 30 times more ripples in NREM sleep compared with REM sleep, a ratio of 3.1 : 0.43 (7 fold) in terms of ripples per minute when controlling for the duration of sleep stages. This provided further indication that our detection largely captured physiological ripples, known to rarely occur in REM sleep (Staba et al., 2004).

Sleep spindles detection

EEG spindles were detected automatically as described in previous reports (Clemens et al., 2007; Ferrarelli et al., 2010). In order to minimize false detections, the parameters of spindle detection were optimized for depth recordings based on extensive visual inspection of the data recorded in every individual. The procedure is illustrated in Figure S 1-6 and consists of a sequential three-step process implemented in Matlab (The Math Works Inc, Natick, MA). First, the channels with spindle activity in NREM sleep were chosen for further analysis (significant spectral power increases in spindle range as

compared with a 1/f model, $p < 0.001$, paired t-test across 10s segments, see Figure S 1-6A). Second, individual spindle events were selected based on their spectral content and duration (Figure S 1-6B) as follows. The EEG signal of each electrode was band-pass filtered between 10 and 16Hz (-3dB at 9.2Hz and 16.8Hz) using a zero-phase 4th order Butterworth filter. Next, the instantaneous amplitude in the spindle-frequency range was extracted via the Hilbert transform. To avoid excessive multiple crossings of thresholds within the same spindle event, instantaneous amplitude was temporally smoothed using a Gaussian kernel (σ=40ms). Events with amplitude greater than mean + 3SD (computed across all artifact-free NREM sleep epochs) were considered putative spindles and detections within 1s were merged. A threshold of mean + 1SD defined start and end times, and events with duration between 0.5s and 2s were selected for further analysis. Detected spindles within ± 1s of paroxysmal events (see above) were discarded. Third, those channels, in which an increase in spectral power within the detected events was restricted to the spindle-frequency range (10-16 Hz) rather than broadband (unpaired t-test (α=0.001) between maximal spectral power in detected vs. random events, Figure S 1-6C), and with at least 1 spindle per min of NREM sleep were chosen for further analysis. Finally, we focused on the frontal and parietal channels, where spindle-events could be reliably detected and successfully separated from paroxysmal events. This highly conservative procedure of including in the analysis only the channels with high spindle SNR, ensured that local occurrence of spindle events (below) does not arise merely as a result of the lack of spindles or poor spindle SNR in some channels.

Analysis of local spindles

For each detected sleep spindle, we examined whether other channels showed a detection whose time window overlapped with the detected event in the "seed" channel, using each channel as seed in turn. Channels which showed (or did not show) such spindle detections were labeled 'concordant', and 'non concordant', respectively (Figure 1-5B). In both seed and target regions we computed the spectral dynamics (spectrograms) in ± 1sec intervals aligned to the peak spindle power in the seed channel. Spectrograms were computed using a short- time Fourier transform with a window of 744ms and 95% overlap, and normalized in each channel separately relative to power modulations in random intervals with no detected spindles in the seed channel (Sirota et al., 2003). Statistical comparison of spindle power in concordant and non-concordant cases was carried out via a t-test based on peak power. To determine the percent of cases in which "entirely local" spindles occurred (i.e. seed channel showed detected spindle while nothing different from chance occurred in a target channel), we relaxed our spindle detection criteria (above) so that any events that exceed a confidence interval of 95% (rather than mean + 3SD) were considered as spindles.

Prediction of individual slow waves via linear classifier

Classification was performed with a support vector machine implemented in the Matlab function "svmclassify" with a default linear (dot product) kernel (MathWorks).

Data. Data in 17 hemispheres of 9 individuals in which the amygdala and other limbic structures were monitored were used. All slow waves were detected using the algorithm described above and the information on each slow wave (timing, amplitude) refers to the positive (negative) peaks in depth (scalp) EEG, which correspond to the transition into

ON state (Figure 1-3A). For each slow wave detected on the scalp (Pz), we first determined if there was also a slow wave occurring in the amygdala, and if so, we also determined whether it was preceded or followed by the scalp slow wave. We selected an equal number of scalp slow waves with and without detections in amygdala, and for waves expressed in both channels, we selected an equal number of waves occurring earlier and later in the amygdala, so that chance prediction for occurrence and timing will be at 50%. The labels present/absent and before/after served as the categories, and the classifier was trained to predict whether new individual waves fell into one category or the other. The number of individual slow waves varied between subjects (mean = 423; range = 182 - 748). Training of the classifier using either ipsilateral or contralateral limbic information was based on three parameters: the occurrence, amplitude and timing of slow waves. Thus, if, for example, four regions (medial prefrontal, anterior cingulate, posterior cingulate, and entorhinal cortex) were monitored in the same hemisphere as the left amygdala, in total 12 parameters were used as the training data for each slow wave, corresponding to the occurrence, amplitude, and timing of slow waves in each of these four structures. The entire process was performed separately for slow waves in left and right amygdala, and the results were averaged for each individual.

Classification. For each set consisting of the amygdala and the input structures (for example, left amygdala and three ipsilateral limbic regions) and for a given number of input regions whose information was made available (e.g. 2 neighbors), performance of the classifier was evaluated across 100 iterations. In each iteration, 80% of waves were chosen randomly as the "training" set (to optimize the linear combination of input information), whereas the remaining 20% of waves served as the "testing" set (to evaluate prediction accuracy). For a given number of input regions (e.g. 2) the specific structures that were used for training were chosen randomly in each iteration (e.g. [1 4]), so that the result for few neighbors will not reflect prediction based on specific brain structures. Replacing realistic labels for amygdala (presence/timing of actual slow waves) with noise yielded chance (~50%) performance as expected (not shown). The differences between ipsilateral vs. contralateral prediction accuracy were evaluated using a paired t-test with df=100 (number of classifier iterations) for each number of neighbors separately.

Statistical analyses: bootstrapping. The statistical significance of time differences between spiking activities of individual units in distinct brain structures (Figure 1-4E,F) was evaluated via bootstrapping as follows. We assigned a random anatomical label to each neuron separately (either frontal or MTL for Figure S 1-7G, either PH or HC for 'within MTL' analysis in Figure S 1-7H), created surrogate groups with the same number of units as the real data, and computed the random time offset between the two groups as was done for the real data. This procedure was repeated across 10,000 iterations to create the null distribution of time offsets. A final p- value was computed by examining the percent of random iterations that showed a time offset equal or greater than the one observed in real data (Figure S 1-7).

Supplemental Figures

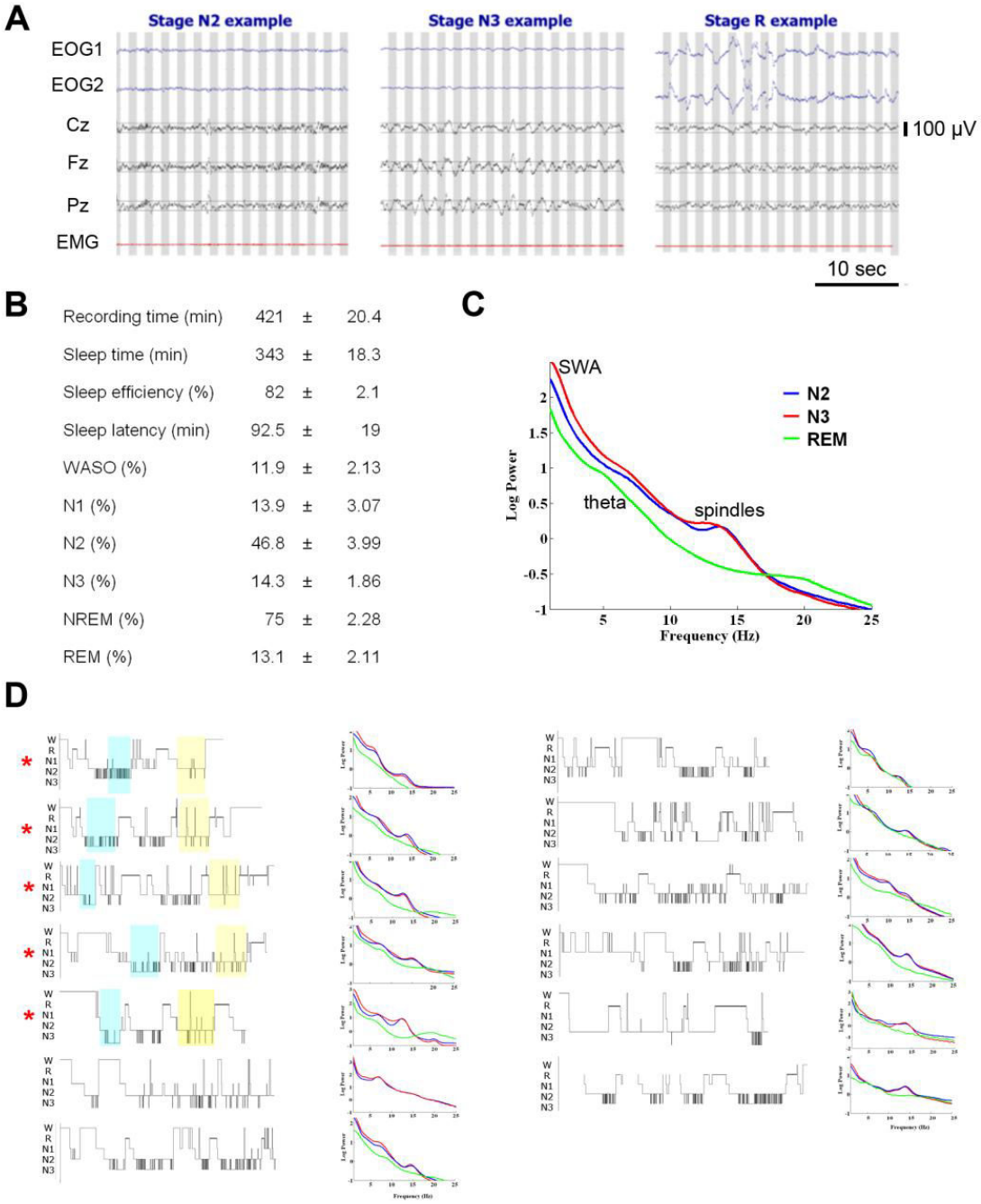

Figure S 1-2 Patient sleep resembles normal sleep in healthy individuals

(A) Representative examples of 30s polysomnographic data used for sleep scoring in stages N2 (left), N3 (middle) and REM sleep (right) in one individual. (B) Sleep measures for the entire night expressed as mean ± SEM (n=13). Sleep efficiency corresponds to total sleep time per time in bed. Sleep latency is to Stage 2. WASO refers to waking after sleep onset; NREM, non-rapid eye-movement; REM, rapid eye-movement. (C) Average power spectra of scalp EEG in all derivations as a function of different sleep stages. Blue, N2; Red, N3; Green, REM sleep. (D) Individual hypnograms (time course of sleep stages throughout sleep) and power spectra of scalp EEG in all 13 individuals. In hypnograms, rows (top to bottom) denote wake (W), REM sleep (R), N1, N2, and N3. Colors in power spectra as above. First five individuals (red asterisks) mark patients who showed the typical homeostatic dissipation of SWA throughout sleep and in whom

early NREM sleep (cyan shading) and late NREM sleep (yellow shading) were further analyzed separately.

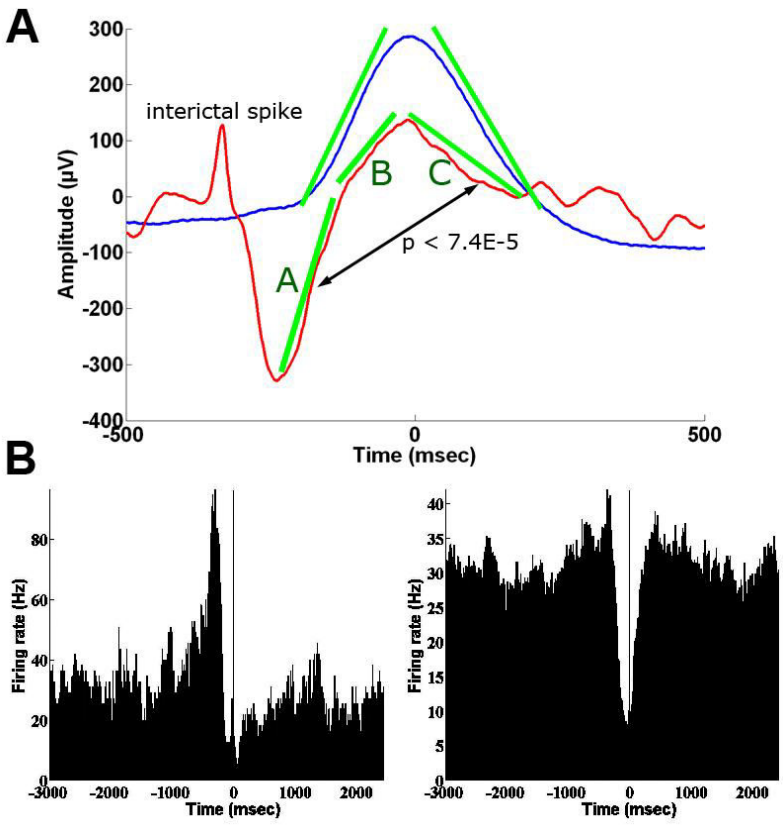

Figure S 1-3 Physiological sleep slow waves are different from pathological paroxysmal discharges

(A) Mean waveforms of physiological sleep slow waves (blue) and epileptogenic paroxysmal discharges (red) aligned by the positive peak of the slow waves. Note that physiological sleep slow waves are largely symmetrical. By contrast, in pathological events, a sharp interictal spike (at average time -334msec) is followed by an asymmetrical slow wave. Specifically, the rise slope of such waves had two components A,B and a fall component C. The slope of the initial rise slope A was steeper by 44% ± 0.07 (n=129 depth electrodes) than the fall slope of component C ($p < 7.4E-5$, paired t-test on rise and fall slopes). (B) A comparison of spiking activity of the same individual neuron triggered by pathological paroxysmal discharges (left) or by physiological sleep slow waves (right). Note the pronounced difference in activity underlying pathological vs. physiological conditions, in accordance with the difference in symmetry seen in the EEG.

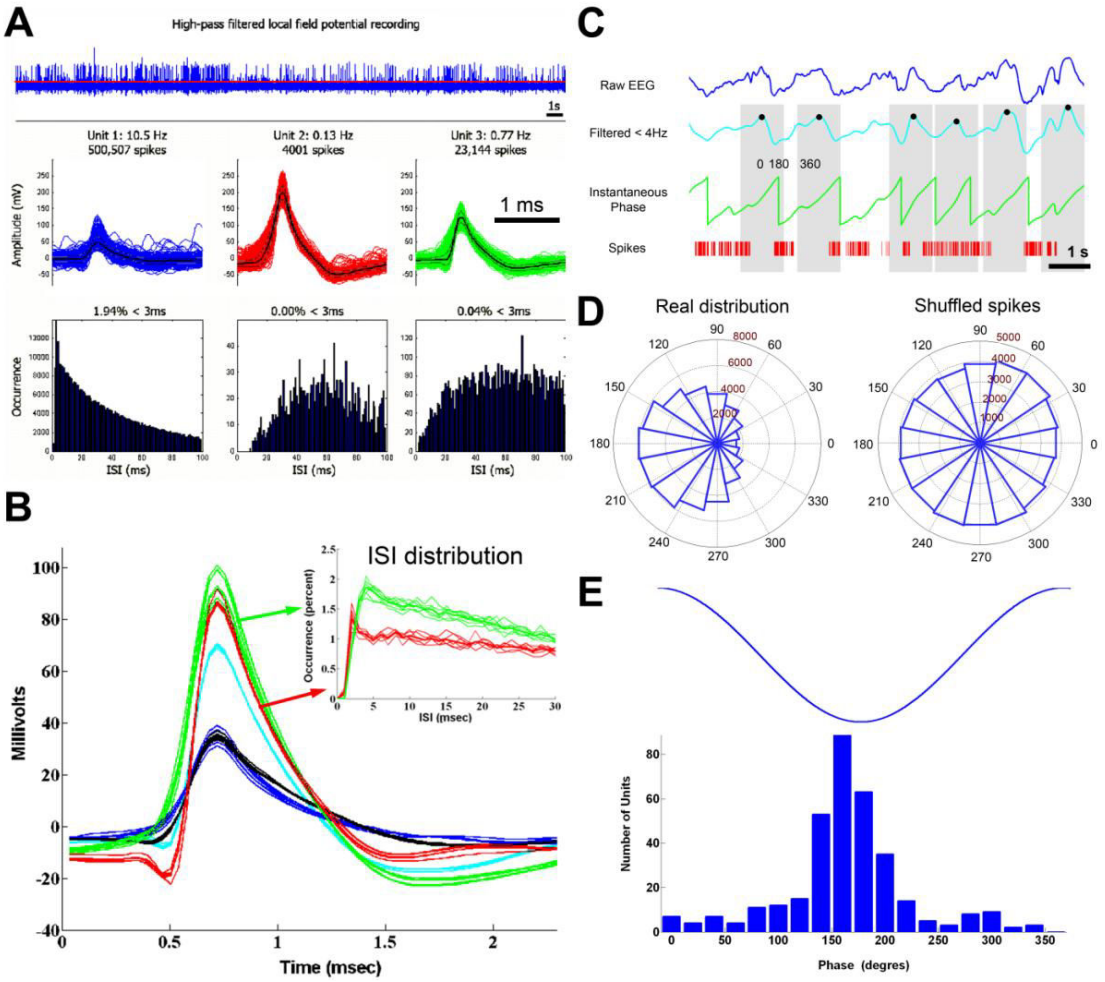

Figure S 1-4 Unit identification, stability and phase locking to EEG slow waves

(A) An illustration of unit identification scheme. Top row depicts the high-pass filtered LFP (>300Hz) along with the threshold for spike identification set at 5 SDs above the noise level (red line). Middle row shows action potential waveforms for three detected units. Bottom row shows the distribution of inter-spike-intervals (ISIs). Based on the consistency of waveforms and the occurrence of ISIs within the expected refractory period (<3ms), we categorized clusters as a multi-unit cluster (blue), two single-unit clusters (red and green), and a noise cluster (not shown). (B) Waveforms and ISI distributions are consistent and distinct throughout sleep. Mean action potential waveforms for 5 distinct units recorded in the same individual. Each color denotes a different unit and each trace denotes the mean waveform in separate 1h intervals throughout sleep. Note that waveforms were consistent and separable between different units throughout sleep, confirming the stability of our unit recordings throughout long (~7h) recordings. Inset depicts ISI distributions in separate 1h intervals for two units. (C) Illustration of phase locking analysis on a 10 sec data segment. Raw depth EEG (blue trace) is filtered in the slow wave range (0.5-4.0 Hz, cyan trace) and slow waves are detected using an automated algorithm (black dots). For each slow wave, we focus on a window of ±500ms surrounding the positive peak in depth EEG (gray zones). The instantaneous phase of the filtered depth EEG is extracted via the Hilbert transform (green trace). We then examine the spiking activity of each unit (red vertical lines) separately in relation to slow wave phase. (D) We compute the distribution of phase values at times of action potentials in intervals surrounding slow waves ("Real distribution") and a p-value is computed using Rayleigh's test for nonuniformity. The critical p-value for significance is determined for each unit separately as follows. Rayleigh p-values are computed across 1,000 iterations while shuffling the action potential timings within each segment ("Shuffled spikes" is

an example of one such iteration). A unit is considered to be phase locked to slow waves only if the Rayleigh p-value for its real distribution is smaller than the critical p-value defined as the 95th percentile across shuffled iterations for the same unit. (E) Phase distribution for all neurons significantly phase locked to depth EEG slow waves (n=307, 51%). Note the robust tendency of phase locked units to fire around the negative peak of depth EEG slow waves (ON periods).

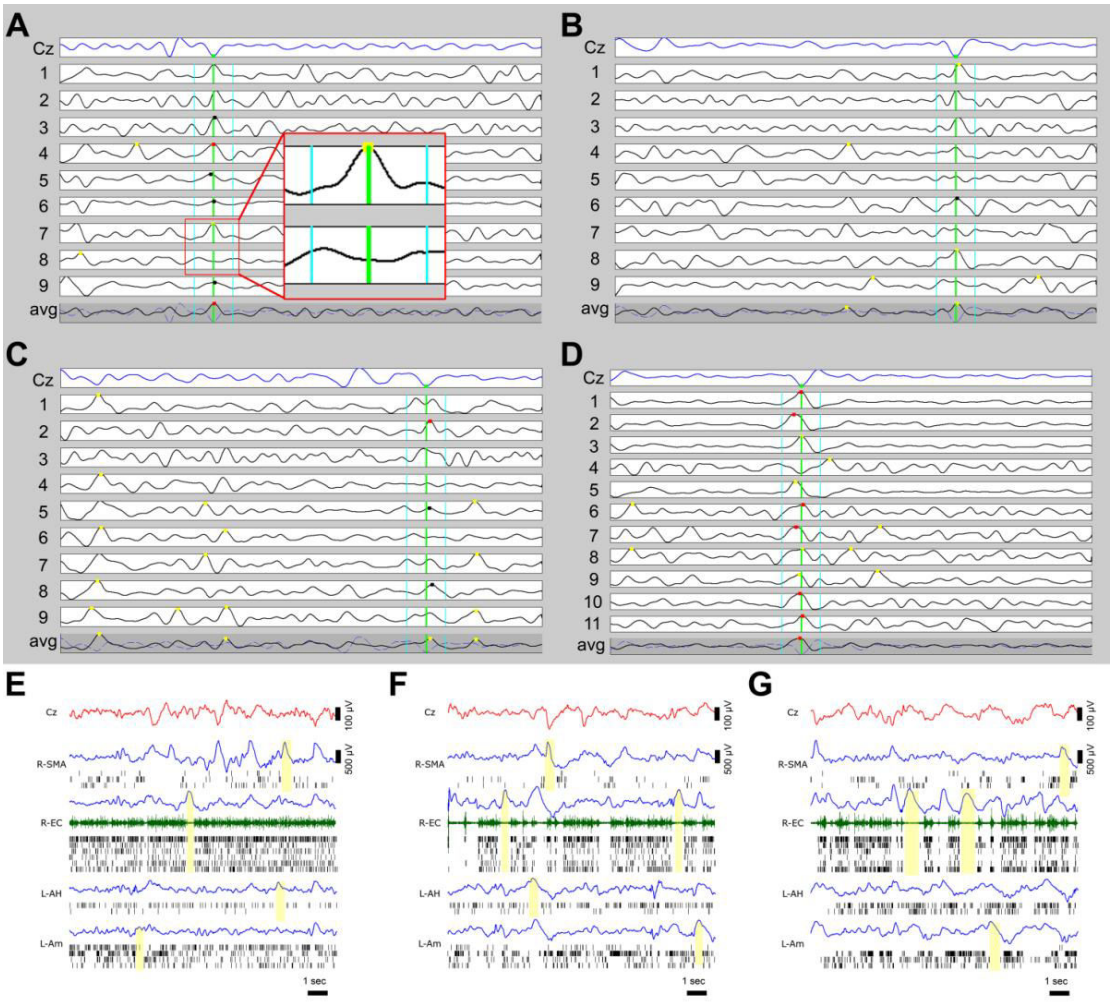

Figure S 1-5 Sleep slow waves across multiple brain regions

(A-D) Four 10s examples of slow wave identification across multiple channels in different individuals. In each panel, top row (blue trace) depicts scalp EEG (Cz); other numbered rows depict intracranial EEG from a different brain structure; bottom row (gray background) depicts the EEG averaged across all intracranial channels. Green and cyan vertical bars denote a slow wave detected on the scalp and corresponding activity in each brain region. Red/black dots mark slow waves concordant with scalp EEG, while yellow dots mark local slow waves, non-concordant with scalp EEG. Blown-up inset in panel (A) illustrates how a slow wave detected on the scalp can be concordant in one brain structure and non-concordant in another. (E-G) Three examples of local sleep slow waves in one individual (different from the one in Figure 1-4). In each example, rows (top to bottom) depict activity recorded in scalp EEG (Cz), right supplementary motor area (R-SMA), right entorhinal cortex (R-EC), left hippocampus (L-AH), and left amygdala (L-Am). Red, scalp EEG; blue, intracranial EEG; green, MUA; black lines, spikes of isolated units. Vertical yellow bars mark the occurrence of local OFF periods in distinct brain regions according to EEG positive peaks and cessation of unit firing.

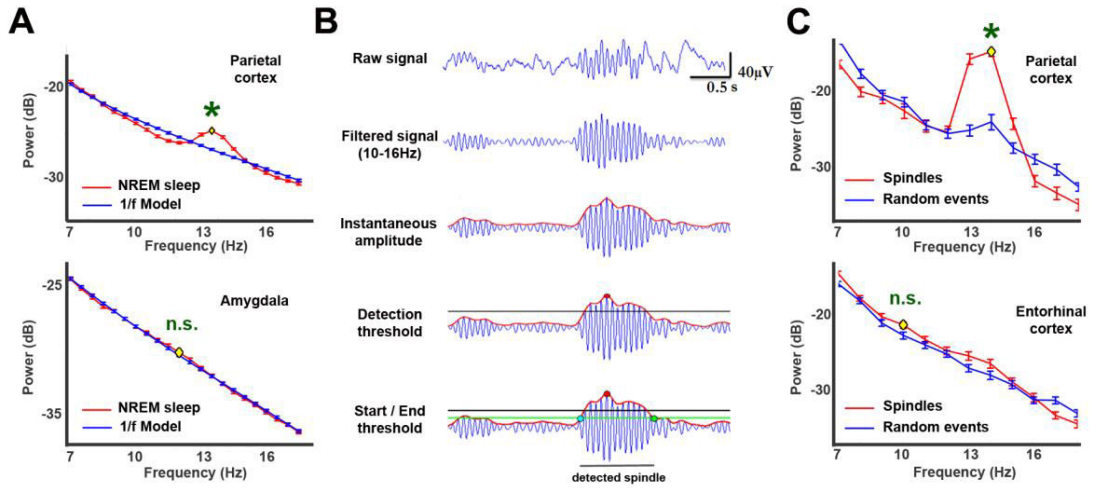

Figure S 1-6 Illustration of spindle detection scheme in scalp and depth EEG

Spindle detection was based on a sequential three-step process as follows: (A) Channels with spindle activity in NREM sleep were chosen for further analysis. Spectral profiles of a typical selected channel (parietal lobe, top) and a typical discarded channel (amygdala, bottom). For each channel, power in NREM sleep (red) was compared with a 1/f model (blue), and channels whose spectral profile shows a significant peak (asterisks) in the spindle range (10-16Hz) were considered for further analysis. Yellow dots denote frequency with maximal power difference and error bars denote SEM across 10s epochs of NREM sleep. (B) Individual spindle events were selected based on their power and duration. Raw EEG (top row) is filtered in the spindle range (10-16Hz, second row). The instantaneous amplitude is extracted via the Hilbert transform (red trace, third row). A detection threshold is set at mean + 3SD of spindle power across NREM sleep (horizontal black line, fourth row) and peaks exceeding this threshold (red dot) are considered putative spindles. A start/end threshold is set at mean + 1SD of spindle power across NREM sleep (horizontal green line, bottom row) thereby defining start and end times (cyan and green dots respectively) and determining spindle duration. Events whose duration is between 0.5s and 2s were considered for further analysis. (C) Channels in which power increases of detected events were specific to the spindle range rather than broadband were chosen for final analysis. Spectral profiles of detected events in a typical selected channel (parietal lobe, top) and a typical discarded channel (entorhinal cortex, bottom). For each channel, power of detected events (red) is compared with power of random 1s segments (blue), and channels with a significant peak which is specific to the spindle range (10-16Hz) are chosen for final analysis. Note that detected events in entorhinal cortex had a diffuse broadband power increase. Yellow dots denote frequency with maximal power difference and error bars denote SEM across detected events.

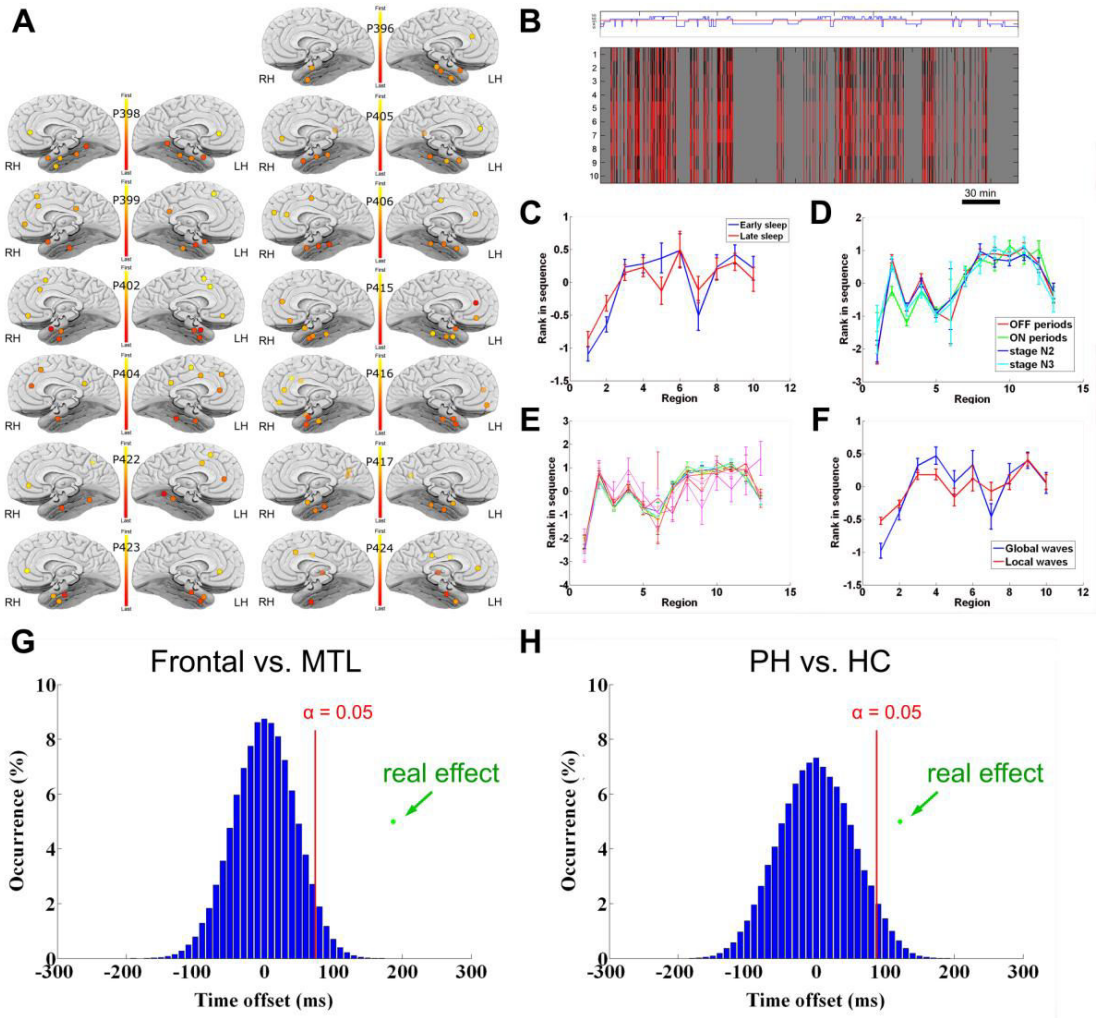

Figure S 1-7 Slow wave propagation is a robust phenomenon

(A) Slow wave propagation is consistent across individual subjects. Mean position in sequences of propagating waves is shown separately for each individual (n=13). Each circle denotes one depth electrode according to its precise anatomical location. Yellow-red colors denote a tendency to express propagating waves sooner-later (see legend). Note that the tendency of slow waves to propagate from prefrontal cortex to the medial temporal lobe can be observed in most individual data. (B-F) Slow wave propagation is robust to different examinations. (B) Propagation sequences are stable in individual slow waves. An example of propagation sequences for all slow waves in one individual. Top inset denotes hypnogram where periods above red threshold are NREM sleep episodes. Bottom inset shows a color-coded plot where each numbered row is a distinct brain region, each column is one slow wave, and colors (black to red) denote position within that wave's propagation sequence. Note that in the top two rows, slow waves tend to be observed earlier (black) in a consistent manner across individual waves. (C) Propagation sequences are stable throughout sleep. A comparison between typical position in propagation sequences (y-axis) and anatomical location (x-axis) separately for the first and second half of sleep in one individual. Regions are sorted from left to right on x-axis according to a anterior-to-posterior axis, with entorhinal cortex, hippocampus and amygdala as most right (last in propagation sequences). Error bars denote standard-error of the mean across individual waves. Note that propagation trends are similar between early and late sleep. (D) Propagation sequences are stable between ON and OFF periods and sleep stages. Similar results are obtained when considering separately positive peaks in intracranial EEG (OFF periods, blue), negative peaks in intracranial EEG (ON periods, red), positive peaks in stage N2 only (stage 2 OFF periods,

green), or positive peaks in stage N3 only (stage 3 OFF periods, cyan). Axes and error bars as above. (E) Propagation sequences are stable when using different regions to detect waves. When using each brain region in turn as the "central" channel in the slow wave detection process (multiple colors). Note that this demonstrates that frontal-MTL propagation can not be explained by easier detection of slow waves in frontal channels. Axes and error bars as above (F) Propagation sequences are stable when considering separately local and global waves. A similar propagation trend is observed when considering separately local slow waves (red, maximum of 4 brain regions involved) and global waves (blue, minimum of 5 brain regions involved). Axes and error bars as above. (G-H) Bootstrapping analysis of slow wave propagation in unit activities. (G) Distribution of random time delays between OFF periods in "frontal" units (n=76) and MTL units (n=155) after randomly shuffling the anatomical identity of individual units. Note that the real mean time offset between OFF periods of individual units is 187ms (green dot, $p << 1E-10$), while the confidence interval of $\alpha = 0.05$ is at 74ms (vertical red line). (H) Distribution of random time delays between OFF periods within the MTL: in parahippocampal (PH) units (n=32) and hippocampal (HC) units (n=35) after randomly shuffling the anatomical identity of individual units. Note that the real mean time offset between OFF periods of individual units is 122ms (green dot, $p < 0.0097$), while the confidence interval of $\alpha = 0.05$ is at 88ms (vertical red line).

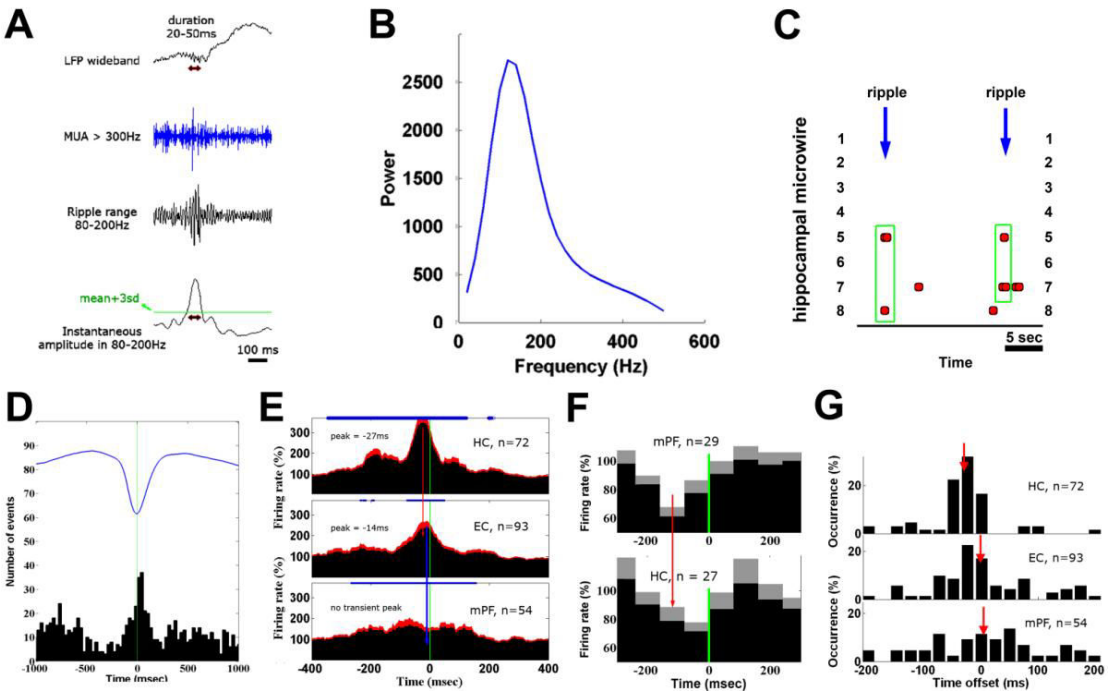

Figure S 1-8 Hippocampal ripples

(A-C) Ripple detection. (A) Example of automatic ripple detection in the LFP of an individual microwire. Rows (top to bottom) show the wideband LFP, MUA (in blue), the band-passed filtered LFP to the ripple range (80-200Hz), the instantaneous amplitude extracted via Hilbert transform along with the detection threshold (horizontal green line) set at mean + 3SDs of amplitude in ripple range. Note that the ripple event is clearly oscillatory and can not be entirely explained by leakage of high frequency components seen in the MUA of the same microwire (blue). (B) Mean power spectrum (band-passed > 80Hz) of detected ripples. Note that for the physiological ripples included in our analysis, spectral distribution is unimodal and lacks substantial epileptiform high frequency oscillations (HFOs) above 250Hz. (C) An example of the procedure employed for integrating ripple detections across 8 microwires spanning the same hippocampal formation. Red dots mark detection in individual microwires and blue arrows show the overall detection for that hippocampus, when events were detected in at least two separate microwires within 15ms (green boxes). (D) Ripples occur preferentially during ON periods. Black bars depict number of detected hippocampal ripples (y-axis) in 30ms bins around negative peak of intracranial EEG (x-axis), reflecting ON periods. Blue waveform shows the mean waveform of hippocampal slow waves used as triggers. Note that ripple occurrence is 5 times more likely around the ON period as compared to the OFF period (compare zero with a few hundred milliseconds away from zero). (E) Ripples represent spatially constrained hippocampal output. Ripple-triggered-averaging of spiking activities in multiple brain structures recorded simultaneously in 7 patients. Rows (top to bottom) show mean spiking activity in hippocampus (n=72), entorhinal cortex (n=93), and medial prefrontal cortex (mPFC, n=54). Blue dots on top show statistically significant deviations from mean firing rate in NREM sleep. Note that entorhinal cortex shows a delayed transient peak following the hippocampus whereas the increase in mPFC firing rate does not show a transient peak of spiking activity. (F) Slow wave OFF periods appear sooner in mPFC compared to hippocampus. Slow-wave triggered averaging of mPFC neurons (n=29, top) and hippocampal neurons (n=27, bottom) recorded simultaneously in 7 patients. Gray shades denote SEM across neurons. (G) Distribution of time delays in individual neurons around ripple occurrence in hippocampus, entorhinal cortex, and mPFC. Vertical red arrows denote delays of -31 ms ± 7 (mean ± SEM) in hippocampus, -2 ms ± 9 in entorhinal cortex, and +5 ms ± 13 in mPFC.

A

		LH													RH												
	Pt	H	A	EC	PH	TG	AC	MC	PC	OF	SM	P	TO	PT	H	A	EC	PH	TG	AC	PC	OF	SM	P	FG	TO	IFG	
1	396	5	4	2	8					1					2		2											24
2	398				6		9								5		11	2										33
3	399	14			7				1		12					13		15		14			12					88
4	402	3	9	5											2	6	10			1			6					42
5	404						9		6											10	11							36
6	405	3	4		11					2					5	1		3				7						36
7	406	6	8		13		3								8	8		6		4								56
8	415																											
9	416	3		1			3			10					16	8	7		12									60
10	417				4							8			9			8						7				36
11	422				8		1			11	8			2	5			6				7		10				58
12	423	5		8						7					1		11											32
13	424	8		10		12	13	13											12	17		3			11			99
		47	25	26	57	12	38	13	7	31	20	8		2	53	36	41	40	24	46	11	17	18	17	11			600

B

	P	Age	Gender	Handedness	Seizure onset	Resection / outcome	Imaging: PET & MRI	Recording length (h)	Recording start time
1	396	27	M	R	Left temporal	Left temporal, seizure free	metabolic and structural abnormalities left temporal	7.0	11:00 PM
2	398	41	F	R	Left temporal spreading to right entorhinal cortex	Left temporal, significant improvement	metabolic abnormalities bilateral temporal lobe, normal structural	5.1	12:41 PM
3	399	43	F	R	Right prefrontal cortex	Right prefrontal, seizure free	normal metabolism, right frontal dysplasia	6.3	11:45 PM
4	402	25	F	R	Bilateral medial temporal lobe	No surgery	Mild metabolic abnormality right temporal, normal structural	6.6	11:30 PM
5	404	25	M	L	Left prefrontal	Left prefrontal, significant improvement	Normal metabolism, periventricular structural abnormalities	10.9	6:29 PM
6	405	38	F	R	Right medial temporal lobe spreading to parahippocampal gyrus	Right MTL, seizure free	Mild metabolic abnormality bilateral temporal, possible dysplasia right temporal	6.6	10:29 PM
7	406	33	F	R	Left medial temporal lobe	No surgery	Mild metabolic abnormaility left temporal, structural abnormality right frontal lobe	6.6	10:40 PM
8	415	39	M	R	Left medial temporal lobe	Left temporal, seizure free	Normal	7.7	10:13 PM
9	416	26	M	R	Bilateral medial temporal lobe and right inferior frontal gyrus	No surgery	Mild metabolic abnormaility right temporal, mild structural abnormaility left temporal	7.7	10:43 PM
10	417	23	M	R	Right parietal	Right parietal, seizure free	Metabolic abnormality right parietal lobe, normal structural	8.7	9:51 PM
11	422	19	F	R	Bilateral multifocal	No surgery	Normal	7.9	10:01 PM
12	423	52	F	R	Left medial temporal lobe	To be determined	metabolic and structural abnormalities left temporal	8.3	10:09 PM
13	424	26	M	R	Left lateral temporal	Left lateral temporal to be resected	metabolic abnormalities right temoral, dysplasia left frontal	7.9	10:15 PM

Table S 1-1 Recording details and patient information

(A) A full description of the brain structures and number of units identified in our recordings. Rows correspond to individual patients and columns correspond to different brain regions. Green boxes mark implanted brain regions and numbers show detected units. Abbreviations: LH, left hemisphere; RH, right hemisphere; H, hippocampus; A, amygdala; EC, entorhinal cortex; PH, parahippocampal gyrus; TG, temporal gyrus; AC, anterior cingulate; MC, middle cingulate; PC, posterior cingulate; OF, orbitofrontal and medial prefrontal cortex; SM, supplementary motor area; P, parietal cortex; TO, temporo-occipital, PT, posterior temporal cortex; FG, fusiform gyrus; IFG, inferior frontal gyrus. (B) Clinical information and sleep study details for all patients.

Study 2:
Sleep spindles in humans:
Insights from intracranial EEG and unit recordings

Published in **the Journal of Neuroscience**
December 7, 2011

Thomas Andrillon [1, 2]*, Yuval Nir [1]*, Richard J. Staba [3], Fabio Ferrarelli [1], Chiara Cirelli[1], Giulio Tononi [1] and Itzhak Fried [3,4]

[1] *Department of Psychiatry,*
University of Wisconsin-Madison
Madison, WI, USA

[2] *Department of Cognitive Studies,*
École Normale Supérieure
Paris, France

[3] *David Geffen School of Medicine,*
University of California-Los Angeles
Los Angeles, CA, USA

[4] *Functional Neurosurgery Unit,*
Tel Aviv Medical Center and Sackler School of Medicine,
Tel Aviv University,
Tel Aviv, Israel.

** contributed equally to this work*

Summary

Sleep spindles are an electroencephalographic (EEG) hallmark of non-rapid eye-movement (NREM) sleep and are believed to mediate many sleep-related functions, from memory consolidation to cortical development. Spindles differ in location, frequency, and association with slow waves, but whether this heterogeneity may reflect different physiological processes and potentially serve different functional roles remains unclear. Here we exploited a unique opportunity to record intracranial depth EEG and single-unit activity in multiple brain regions of neurosurgical patients to better characterize spindle activity in human sleep. We find that spindles occur across multiple neocortical regions, and less frequently also in the parahippocampal gyrus and hippocampus. Most spindles are spatially restricted to specific brain regions. In addition, spindle frequency is topographically organized with a sharp transition around the supplementary motor area between fast (13-15Hz) centroparietal spindles often occurring with slow wave up-states, and slow (9-12Hz) frontal spindles occurring 200ms later on average. Spindle variability across regions may reflect the underlying thalamocortical projections. We also find that during individual spindles, frequency decreases within and between regions. In addition, deeper sleep is associated with a reduction in spindle occurrence and spindle frequency. Frequency changes between regions, during individual spindles, and across sleep may reflect the same phenomenon, the underlying level of thalamocortical hyperpolarization. Finally, during spindles neuronal firing rates are not consistently modulated, although some neurons exhibit phase-locked discharges. Overall, regional spindle diversity can be well accounted for by anatomical considerations while differences in spindle frequency could be indicative of variable hyperpolarization levels.

Introduction

Sleep spindles constitute an EEG hallmark of NREM sleep (Achermann and Borbely, 1998; Andersen and Andersson, 1968; De Gennaro and Ferrara, 2003; Destexhe and Sejnowski, 2001; Loomis et al., 1935; Mircea Steriade, 2003). In humans, spindles are classically defined as waxing-and-waning 10-16Hz oscillations lasting 0.5-2s (Gibbs, 1950). Comparable sleep spindles have been found in all tested mammalian species (Zepelin et al., 1994) and similar phenomena occur during barbiturate anesthesia (Contreras et al., 1997a) and in vitro (McCormick and Bal, 1997).

The neurophysiological mechanisms of spindle generation reflect the intrinsic properties and interactions between inhibitory cells in the thalamic reticular nucleus (RE) and bursting thalamocortical (TC) relay neurons (Mircea Steriade, 2003; Steriade, 2000). The GABAergic neurons in the highly interconnected thalamic RE act as pacemakers and are both necessary and sufficient for spindle generation (Bal et al., 1995; Destexhe et al., 1998; Destexhe and Sejnowski, 2001; Halassa et al., 2011; Marini et al., 1992; Morison and Bassett, 1945; Steriade et al., 1987; Steriade and Timofeev, 2003). Spindle waxing is attributed to gradual cell recruitment in RE-TC-RE loops (Steriade et al., 1993a; von Krosigk et al., 1993). The source of spindle waning and termination is less clear but possibly involves the depolarizing action of the thalamic I_H current and/or corticothalamic influence (Bal et al., 1995; Bonjean et al., 2011; Luthi and McCormick, 1998; Timofeev et al., 2001). Spindle synchronization is controlled by the neocortical feedback, as decortication or spreading depression lead to asynchronous spindles (Contreras et al., 1997a; Contreras and Steriade, 1996).

Increasing evidence suggests that sleep spindles in human sleep are a diverse rather than prototypical phenomenon. One distinction involves fast (13-15Hz) centroparietal versus slow (11-13Hz) frontal spindles (Anderer et al., 2001; Gibbs, 1950; Schabus et al., 2007). Another distinction is between spindles that occur on a background of low-amplitude EEG in stage 2 sleep and are easily identified visually (Iber et al., 2007), and spindles associated with slow waves (Molle et al., 2002; Steriade et al., 1993b). The functional role of spindles remains unclear, although they may play a role in memory consolidation (Schabus et al., 2004), cortical development (Khazipov et al., 2004), regulation of arousal (Destexhe and Sejnowski, 2002), and in maintaining a disconnection from the external environment through a "thalamic gate" (Mircea Steriade, 2003). In addition, spindles have been recently explored as a potential biomarker for psychiatric disorders such as schizophrenia (Ferrarelli et al., 2010). To be able to identify the role(s) spindles could play during normal states of vigilance and to exploit them as a biomarker for pathology, it is necessary to first better understand spindle properties through a comprehensive investigation of their characteristics when they occur most prominently, i.e. human sleep. To this aim, here we characterize in detail sleep spindles in human sleep using simultaneous recordings of intracranial depth EEG and unit spiking activities in multiple brain regions in the cortex and hippocampus of thirteen individuals undergoing presurgical clinical testing.

Materials and Methods

Subjects and polysomnographic sleep studies

Thirteen patients (6 males, 7 females) with pharmacologically intractable epilepsy (ages 19-52) underwent monitoring with depth electrodes (Figure 2-1A) for seizure foci identification and potential surgical treatment (Fried et al., 1999b). Patients provided written informed consent to participate in the research study, under the approval of the Medical Institutional Review Board at UCLA. Electrode location was based only on clinical criteria, and all surgery was performed by Itzhak Fried.

Sleep recordings were conducted 48-72 hr after surgery, at a minimal interval of 12 hours from identifiable seizures, and lasted for about 7 hours between 2300 and 0600. In addition to continuous video monitoring, the montage included two electrooculogram (EOG), two electromyogram (EMG), and four scalp electrodes (positioned at C3, C4, Pz, Fz) as well as two earlobe electrodes for referencing. Sleep-wake stages were scored according to established guidelines (Iber et al., 2007).

Data Acquisition

Electrode location varied between patients based on their clinical profiles. Electrodes were placed in frontal, parietal, and cingulate cortices, as well as temporal lobe regions such as hippocampus, amygdala, entorhinal cortex and parahippocampal gyrus (Figure 2-1B). For each patient, 8-12 flexible polyurethane depth electrodes (1.25 mm diameter) targeted specific regions, typically medial limbic brain areas. Each electrode position was identified using post-implant computed tomography (CT) co-registered with pre-implant magnetic resonance (MR) imaging (Brain Navigator, Grass-Telefactor Corp., Philadelphia, PA). Scalp and intracranial depth EEG data were continuously recorded, sampled at 2kHz, bandpass-filtered in hardware between 0.1Hz and 500Hz and re-referenced offline to the mean signal of the earlobes electrodes.

Each depth electrode terminated in a set of eight insulated 40-μm platinum-iridium microwires (impedances 200 to 500 kΩ) (Fried et al., 1999b) (Figure 2-1A). Microwire signals were simultaneously recorded continuously (Cheetah Recording System; Neuralynx, Tucson, AZ for 10 patients; Neuroport Recording System; Blackrock, Salt Lake City, UT for 3 patients), sampled at 28 kHz (10 patients) or 30 kHz (3 patients), band-pass filtered in hardware between 1Hz and 9kHz, and referenced locally to a ninth non-insulated microwire.

Detection of spindles and their separation from pathological events

Spindles were detected automatically following previously published algorithms (Clemens et al., 2007; Ferrarelli et al., 2010) based on a sequential three-step process (see Figure 2-1E-G) implemented in Matlab (MathWorks) as follows. First, to minimize false detections, only channels with robust spindle activity in NREM sleep were chosen for further analysis. In each individual channel, spindle (9-16Hz) power in NREM sleep was compared with a fitted $1/f^{\alpha}$ model (both were estimated across multiple 10s epochs) and

channels with a difference that was statistically significant at $p < 0.001$ (unpaired t-test for maximal peak) were further considered (Figure 2-1E). Second, putative spindles were selected based on their power and duration. EEG signals were band-pass filtered between 9 and 16Hz (-3dB at 8.8 and 17.3Hz) using a zero-phase 4th order Butterworth filter. The instantaneous amplitude was computed via the Hilbert transform and two thresholds were defined based on this amplitude time-course across artifact-free sleep epochs. A detection threshold was set at mean + 3SD and amplitudes exceeding this threshold were considered potential spindles. A start/end threshold was set at mean + 1SD and events whose duration was between 0.5s and 2s were further considered (Figure 2-1). Detections within 1s were merged as single events. Third, since transient events can introduce power increases across a wide range of frequencies including the spindle range (De Gennaro and Ferrara, 2003), only events in which power increases were *specific* to the spindle range rather than broadband were chosen for final analysis. For each channel, power of detected events was compared via an unpaired t-test with power of random 1s segments in NREM sleep (Figure 2-1G). Channels exhibiting weaker diffuse broadband power increases ($p >= 0.0001$ at maximal difference) were excluded. We further verified the spectral specificity of each spindle by excluding any detection that coincided with control events that were above mean+5SD in the 20-30Hz range.

Sleep spindles were separated from pathological interictal epileptiform events as follows. As was recently done for slow waves (Nir et al., 2011), epileptiform interictal spikes were separately detected automatically in depth EEG by high-pass filtering offline above 100Hz and by identifying events whose amplitude exceeded mean + 5SD and whose duration was under 70ms (de Curtis and Avanzini, 2001). We verified visually that such automatic detection was effective in identifying interictal spikes in each channel separately. Based on this detection we discarded *post-hoc* any putative spindles within ±1s of interictal spikes. In addition, the parameters of the spindle detection algorithm (e.g. frequency range, filter settings, thresholds) were optimized after extensive visual inspection to minimize false detections of epileptiform activities as spindles, although a wide range of parameters yielded similar detections (not shown). Naturally, the density and duration of spindles reported throughout the paper depend on the specific detection parameters employed.

In the hippocampus, we visually selected for further analysis a subset of the automatically detected events that also exhibited a clear waxing-and-waning spindle shape. We computed in each hippocampal electrode separately the probability of such spindles to co-occur with detected events in other locations as p = number of concomitant spindles for a given pair of structures / number of hippocampal spindles.

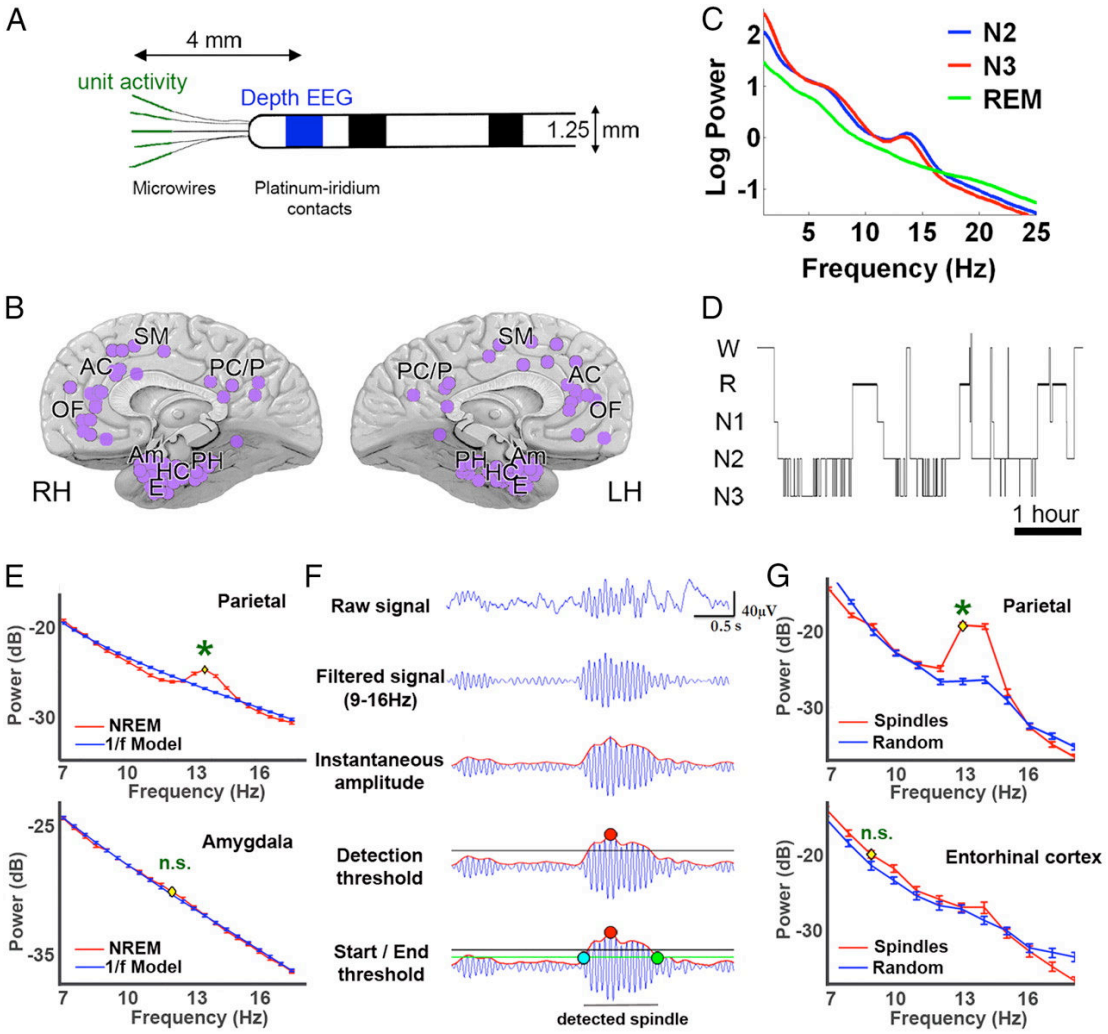

Figure 2-1 Data overview and spindle detection

(A) Illustration of flexible probes used for simultaneous recording of depth EEG (platinum contacts, blue) and unit activity (microwires, green). (B) Overview of 129 depth electrode locations in 13 individuals spanning multiple brain regions as seen from medial view. Abbreviations: OF, orbitofrontal cortex; AC, anterior cingulate; SM, supplementary motor; PC/P, posterior cingulate / parietal cortex; PH, parahippocampal gyrus; HC, hippocampus; E, entorhinal cortex; Am, amygdala; LH, left hemisphere; RH, right hemisphere. (C) Example power spectra of scalp EEG in one representative individual in stage N2 sleep (blue), N3 sleep (red) and REM sleep (green). Note high power in slow wave (<4Hz) and spindle (11-16Hz) range in NREM sleep. (D) Hypnogram: time-course of sleep-wake stages in the same individual. W, wake; R, REM sleep; N1-N3, NREM sleep, stages 1-3. (E) Spindle detection step 1: channels with spindle activity in NREM sleep are chosen for further analysis. Spectral profiles of a typical selected channel (parietal lobe, top) and a typical discarded channel (amygdala, bottom). For each channel, power in NREM sleep (red) was compared with a $1/f\alpha$ model (blue), and channels with a significant peak (asterisks) in the range of 9-16Hz are considered for further analysis. Yellow dots denote frequency with maximal power difference and error bars denote SEM across 10s epochs of NREM sleep. (F) Spindle detection step 2: individual spindles were selected based on their power and duration. Raw EEG (top row) is filtered in the spindle range (9-16Hz, second row). The instantaneous amplitude is extracted via the Hilbert transform (red trace, third row). A detection threshold is set at mean + 3SD of spindle power across NREM sleep (horizontal black line, fourth row) and peaks exceeding this threshold (red dot) are considered putative spindles. A start/end threshold is set at mean + 1SD of spindle power across NREM sleep (horizontal green line, bottom row) thereby defining start and end times (cyan and green dots respectively) and

determining spindle duration (between 0.5s and 2s). (G) Spindle detection step 3: channels in which power increases of detected events were specific to the spindle range rather than broadband were chosen for final analysis. Spectral profiles of detected events in a typical selected channel (parietal lobe, top) and a typical discarded channel (entorhinal cortex, bottom). For each channel, power of detected events (red) is compared with power of random 1s segments (blue), and channels with a significant peak which is specific to the spindle range (9-16Hz) are chosen for final analysis. Note that detected events in entorhinal cortex had a diffuse broadband power increase. Yellow dots and error bars as above.

Timing and frequency of spindles

For each detected spindle, several parameters were stored for further analysis including start and end times, frequency, and amplitude. The timing of individual spindles was determined as the mean of their start and end times (center), thereby avoiding influence by the choice of the start/end threshold.

The frequency of each detected spindle was estimated by computing the spectrogram in 10s intervals (short-time Fourier transform, 744ms window, 95% overlap) and identifying the maximal power for each event within the spindle frequency range with a resolution of 0.2Hz. Next, distribution of spindle frequencies were computed per channel and later averaged for each brain region (Figure 2-2B).

Spectral dynamics during individual spindles in specific regions (e.g. Figure 2-2C) were evaluated by computing spectrograms (as above) in 2s windows centered around the time of maximal amplitude. Differences in frequency between the beginning and end of spindles (e.g. Figure 2-2C) were evaluated in each event separately by comparing the instantaneous frequency (in spectrograms) between start and end times via a paired t-test (α=0.05).

Comparing timing and frequency across regions

For each pair of channels in the same individual, concomitant spindles were selected if there was temporal overlap in their occurrence. Both channels were considered as the "seed" and "target" alternatively and spectrograms (as above) were aligned to the time of maximal amplitude in the seed channel (e.g. Figure 2-3C). For each spindle event separately, the timing of maximal amplitude and the frequency at maximal amplitude were compared across the two channels and the mean difference in timing and frequency across spindles was computed for each pair (Figure 2-3). Next, electrode locations in frontal and parietal locations were grouped into ten regions: bilateral orbitofrontal cortices, anterior cingulate cortices, pre-supplementary motor areas, supplementary motor areas, and posterior cingulate cortices (Figure 2-3B). In twelve individuals in whom there was more than one such location, the typical delay between all pairs of spindles for any given pair of region (e.g. left orbitofrontal cortex vs. right posterior cingulate cortex) was averaged (edge color in Figure 2-3B). Furthermore, each region was ranked in each individual from 0 (earliest detection) to 1 (latest detection) and such ranks were similarly averaged across individuals (node colors in Figure 2-3B). We also examined whether the timing differences between regions (pooled in 50ms bins) were proportional to frequency differences via linear regression (Figure 2-3D).

Association of spindles with slow waves

Individual slow waves (positive and negative peaks in the EEG filtered below 4Hz that were separated by 0.25s to 1s) were automatically detected as described previously (Riedner et al., 2007) and separated from abnormal paroxysmal events (Nir et al., 2011). The highest amplitude waves in each channel (top 20%) were used to examine spindle occurrence ±2s around down-states (depth positive and surface negative peaks) or up-states (depth negative and surface positive peaks) in 100ms bins (Figure 2-4B). Confidence intervals (α=0.05) were estimated by computing the mean and SD of spindle occurrence across the 4s detection interval and significant deviations from chance were identified via a paired t-test for each electrode and each time bin separately.

Local sleep spindles

For each detected spindle, we examined whether other channels recorded a spindle that temporally overlapped with the spindle in the "seed" channel, using each channel as seed in turn. The presence or absence of coincident spindles between channels was labeled 'concordant' or 'non-concordant', respectively (Figure 2-5B). In both seed and target regions we computed the spectral dynamics (spectrograms as above) in ± 1sec intervals aligned to the peak spindle power in the seed channel. Spectrograms were normalized in each channel separately relative to power modulations in random intervals with no detected spindles in the seed channel (Sirota et al., 2003). Statistical comparison of spindle power in concordant and non-concordant cases was carried out via a t-test based on peak power. To determine the percent of cases in which "entirely local" spindles occurred (i.e. seed channel showed detected spindle while nothing different from chance occurred in a target channel), we reduced our detection criteria (above) to include spindles that exceeded a confidence interval of 95% (rather than mean + 3SD).

Dynamics of spindles throughout sleep

In a subset of five individuals exhibiting a clear homeostatic decline of slow wave activity (SWA) during sleep, early and late NREM sleep were analyzed separately. We compared the density, frequency, amplitude, and locality of spindles between early and late NREM sleep via non-parametric Mann-Whitney U-tests (α=0.01) separately for different spindle categories (e.g. all spindles, fast vs. slow, frontal and centroparietal, see Figure 2-6A). The dynamics of spindle frequency *within* NREM sleep cycles was further examined. To this end, NREM sleep cycles were identified visually as continuous time intervals in NREM sleep preceding REM episodes (N=16 cycles in 8 individuals). Figure 2-6B shows four of these NREM episodes (the third one being discarded since it is disrupted by a brief arousal). To compile results across individuals and cycles that varied in their duration, each cycle was divided into shorter epochs (n=10 bins per sleep cycle) and the mean SWA and spindle parameters were computed for each bin (Figure 2-6C). Bins were sorted based on their SWA and the frequency and density of spindles was compared across varying depths of sleep (as indicated by SWA levels).

Spiking activities during spindles

Units were identified using the 'wave_clus' software package (Quiroga et al., 2004) as described previously (Nir et al., 2008). Briefly, a threshold was set at 5SD above the median noise level of the high-pass filtered signal (above 300Hz), detected events were clustered using superparamagnetic clustering, and categorized as noise, single- or multi-unit clusters. Classification of putative single-units and multi-unit clusters was based on the consistency of action potential waveforms, and by the presence of a refractory period for putative single units, i.e. less than 1% of inter-spike-intervals (ISIs) within 3ms. The stability of unit recordings was confirmed throughout long (~7h) sleep recordings by comparing action potential waveforms and ISI distributions of detected units separately in 1 hour intervals, and verifying that both waveforms and ISI distributions were indeed consistent and separable between different clusters throughout the night.

Neuronal action potential discharges recorded on individual microwires were examined in relation to sleep spindles detected in the depth EEG (macro-electrode ~4mm away) in the same brain structure (see Figure 2-1A), as was recently done for slow waves (Nir et al., 2011). To quantify changes in firing rate during spindles, action potentials were binned in 100ms bins ±2s around the middle of each spindle. Confidence intervals (α=0.05) were estimated across the 4s interval and significant deviations from chance were identified via a paired t-test for each bin separately (Figure 2-7A).

Phase-locked unit discharges during spindles (Figure 2-7B) were examined as follows. Depth EEG was filtered in the spindle (9-16Hz) range and individual spindles were detected as above. For each spindle, we extracted the instantaneous phase of the filtered EEG via the Hilbert transform. We examined the distribution of phase values at action potential times ("real distribution" in Figure 2-7C) and computed a p-value using Rayleigh's test for nonuniformity ('circ_mean' function, Circular Statistics Toolbox for Matlab). Since non-uniformity can be partially attributed to asymmetries in the EEG waveforms (Siapas et al., 2005), the critical p-values for significance were determined using bootstrapping for each unit separately as the 95th percentile after examining p-values across 1,000 iterations while shuffling action potential timings within each segment ("shuffled spikes" in Figure 2-7C). Finally, the preferred phase was determined for each phase-locked unit.

Statistical Analysis

Error bars in figures denote standard error of the mean (SEM = SD/$\sqrt{}$(n-1). Student T-tests were performed after confirming normal distributions via Kolmogorov-Smirnov tests or the Mann-Whitney U-test rank sum test (non-parametric) when normality could not be established.

Results

Polysomnographic sleep studies

Polysomnographic sleep studies were conducted in 13 neurosurgical patients with intractable epilepsy. Continuous overnight recordings lasted 421 ± 20 minutes (mean ± SEM). Polysomnography included electrooculogram (EOG), electromyogram (EMG), scalp EEG, and video monitoring. Figure 2-1A-D summarizes the experimental recording setup during sleep. Sleep-wake stages were scored following established guidelines as waking, NREM sleep stages 1 through 3 and REM sleep (Iber et al., 2007). Intracranial depth EEG was recorded in 129 medial brain regions bilaterally in frontal and parietal cortices as well as multiple limbic structures in the medial temporal lobe (Figure 2-1B). While it should be noted that our sampling was mostly limited to medial brain areas, scalp topography suggests that human spindle activity is maximal at midline regions (Ferrarelli et al., 2007), thereby making our data particularly well suited to examine sleep spindles. We simultaneously recorded scalp EEG, depth EEG, and spiking activity from a total of 600 units (355 putative single units, 245 multiunit clusters).

Measures of overnight sleep in patients were in general agreements with typical findings in healthy young adults (Riedner et al., 2007). Sleep efficiency, time spent in different sleep stages, NREM-REM sleep cycles, and power spectra of scalp EEG resembled normal sleep characteristics. Moreover, in every subject, power spectra of scalp EEG data in NREM sleep (Figure 2-1C) revealed robust slow wave activity (<4Hz) and spindle (9-16Hz) power. These results indicate that sleep measures were similar to those of normal sleep in individuals without epilepsy.

Spindle occurrence across multiple regions in the human brain

Having characterized sleep using standard non-invasive polysomnography, we proceeded to identify individual spindles in NREM sleep in the scalp EEG and in the depth EEG of each brain region separately using an automatic algorithm (see Methods and Figure 2-1E-G). Channels with robust spindle activity in NREM sleep (Figure 2-1E) in which power increases of detected events were specific to the spindle range rather than broadband (Figure 2-1G) were identified. Table 2-1 provides the results of spindle detection across multiple brain regions. In the scalp EEG, spindles were robustly observed (90 ±4.7% of electrodes showed spindle detections; mean ± SEM across individuals) and their density (1.9 ±0.13 spindles/min) was consistent with densities reported in healthy individuals (Ferrarelli et al., 2010; Wei et al., 1999). Spindle density was significantly higher during sleep stage N2 than N3 (1.9 ±0.14 vs. 1.6 ±0.14 spindles/min respectively, $p < 10E-3$ via paired t-test, $n = 46$ channels). In the depth EEG, frontal and parietal cortices exhibited robust spindle detections (82% and 89% respectively) with densities comparable to those observed in scalp EEG (1.8 ±0.16 and 1.3 ±0.29 spindles/min, respectively).

Region	Number of channels with spindle detections		Density (spindles/min)	
Scalp				
Fz	12/13	(92%)	1.8	(±0.30)
C3–C4	22/26	(85%)	1.9	(±0.22)
Pz	12/12	(100%)	1.8	(±0.30)
	46/51	**(90%)**	**1.9**	**(±0.13)**
Frontal lobe				
Supplementary motor area	3/3	(100%)	1.2	(±0.49)
Orbitofrontal cortex	14/15	(93%)	2.2	(±0.24)
Anterior cingulate	14/16	(88%)	1.6	(±0.25)
Presupplementary motor area	4/7	(57%)	1.5	(±0.90)
Lateral frontal	2/4	(50%)	1.8	(±0.86)
	37/45	**(82%)**	**1.8**	**(±0.16)**
Parietal lobe				
Posterior cingulate	7/8	(88%)	1.1	(±0.29)
Posterior parietal	1/1	(100%)	2.2	(NA)
	8/9	**(89%)**	**1.3**	**(±0.29)**
Temporal lobe				
Temporal gyrus	4/6	(80%)	2.1	(±0.28)
Parahippocampal gyrus	11/16	(69%)	1.3	(±0.25)
Hippocampus	9/23	(44%)	1.1	(±0.13)
Entorhinal cortex	4/13	(31%)	0.74	(±0.11)
Amygdala	4/19	(21%)	0.89	(±0.18)
	32/79	**(41%)**	**1.2**	**(±0.12)**

Table 2-1 Spindle occurrence across multiple regions in the human brain

Columns (left to right) show the brain region, the number of channels with spindle detections (over the total number of electrodes in that region), and the mean density of spindles per minute (±SEM across electrodes, n=13 individuals). Note that while frontal and parietal regions showed robust spindle activity (comparable to scalp EEG channels), there was large variability in the occurrence and density of spindles in the medial temporal lobe.

Spindle occurrence was further examined in the medial temporal lobe (MTL), where the presence of physiological spindles is still debated (Malow et al., 1999; Nakabayashi et al., 2001; Pare et al., 2002). The current results indicate reliable spindle occurrence in the parahippocampal gyrus (PHG, 69% of channels with a density of 1.3 ±0.25 spindles/min) and hippocampus (44% of channels with a density of 1.1 ±0.13 spindles/min), while spindle occurrence was lower in entorhinal cortex and amygdala (31% and 21% of channels with a density of 0.74 ±0.11 and 0.89 ±0.18 spindles/min, respectively). Given the variability in spindle occurrence in the MTL that could be due in part to epileptogenicity, we analyzed spindles in MTL separately from spindles in frontal and parietal cortices, and present these data in the final section of the results.

Fast centroparietal spindles differ from slow frontal spindles

Since scalp EEG studies have long suspected a distinction between slow (11-13Hz) and fast (13-16Hz) spindles (Anderer et al., 2001; De Gennaro and Ferrara, 2003; Gibbs, 1950; Schabus et al., 2007), we computed the distribution of frequencies across all spindles in each channel separately across multiple brain regions (see Methods). In scalp EEG, centroparietal electrodes (C3, C4, Pz) showed a significant albeit diffuse

dominance of fast spindles, whereas slow spindles prevailed in frontal derivations (Fz). Average spindle frequencies in Pz and Fz were 12.6 ±0.23 Hz vs. 11.3 ±0.30 Hz, respectively (mean ± SEM across individuals) and these differences were statistically significant ($p < 0.01$, non-parametric Mann-Whitney U-test across 24 channels). Next, the mean frequency of spindles was mapped across individual depth electrodes (Figure 2-2A). In contrast to the small differences in frequency observed with scalp EEG, the intracranial results reveal a topographical organization with a clear difference between fast (>12.5Hz) centroparietal spindles and slow (<12.5Hz) frontal spindles. The distributions of spindle frequencies were averaged within and compared between the following five regions: orbitofrontal cortex (OF), anterior cingulate cortex (AC), pSMA, SMA, and posterior cingulate cortex (PC).

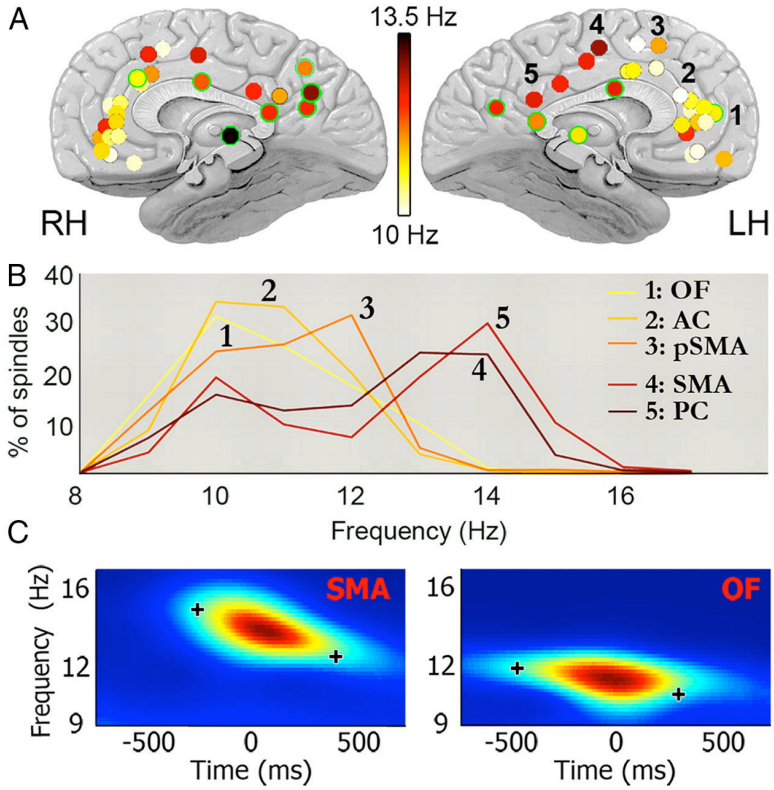

Figure 2-2 Fast centroparietal spindles differ from slow frontal spindles

(A) Average frequency of spindles across all depth electrodes (n=50 electrodes in 13 individuals). The color of each circle denotes the mean spindle frequency in an individual electrode according to its precise anatomical location. Green outlines marks electrodes placed more laterally than the midline. Note the contrast between slow (9-12Hz) frontal spindles and fast (13-16Hz) centroparietal spindles. The two outliers in the medial prefrontal cortex (red circles) were the only electrode placements in one atypical individual in whom parietal spindles may be even faster. Numbers as in legend of panel B. (B) Distribution of spindle frequencies grouped by region. Slow spindles are found in prefrontal regions (1-3) while fast spindles are found in centroparietal regions (4-5). Note the difference in spindle frequency between SMA and adjacent pSMA. Abbreviations: OF, orbitofrontal; AC, anterior cingulate; pSMA, pre-supplementary motor area; SMA, supplementary motor area; PC, posterior cingulate. (C) In each brain region, spectral frequency decreases during individual spindles. Spectrogram shows mean frequency dynamics in a representative centroparietal electrode in the SMA (left, n=159 spindles) and in frontal electrode in the OF (right, n=237spindles). Black crosses mark the mean instantaneous frequency around the beginning and end of spindles (13.8 and 12.5Hz for fast spindles, 11.5 and 10.3Hz for slow spindles). Note that frequency decreases during fast spindles and to a lesser degree during slow spindles.

The results (Figure 2-2B) confirm the distinction between slow and fast spindles hinted at by scalp EEG. Furthermore, a difference between adjacent pSMA and SMA was observed in the same patient, and it nearly reached statistical significance across patients despite the limited sample (10.9 ±0.72Hz vs. 12.6 ±0.19Hz respectively, $p = 0.057$, non-parametric Mann-Whitney U-test, $n=7$ channels) supporting the notion of two spindle groups rather than a continuous cortical gradient (see also Discussion). In addition, while frontal spindles were exclusively slow, centroparietal spindles had a bimodal distribution with a majority of fast spindles and fewer slow spindles, and this was also evident in the data of individual channels. By "centroparietal" we refer here to those fast spindles occurring from the SMA proper back to posterior cingulate and parietal cortex, although some of these locations are in the frontal lobe.

We also found that in the same brain region, frequency decreases during individual spindles. Figure 2-2C shows the average frequency dynamics in a representative SMA electrode (fast spindles, left) and an OF electrode (slow spindles, right). As can be seen, the instantaneous frequency of fast SMA spindles dropped on average from 13.8 to 12.4Hz, and slow OF spindles showed a similar deceleration (from 11.5 to 10.4Hz on average). A quantitative analysis across the entire dataset (2,851 fast and 10,607 slow spindles in 50 channels) revealed a significant decrease of -0.8Hz/s in instantaneous frequency between spindle start and end times (-0.8 ±0.04Hz/s and -0.8 ±0.02Hz/s for fast and slow spindles, respectively, $p < 10E-12$ between start and end times via two-tail t-test).

Fast centroparietal spindles precede slow frontal spindles

To further understand the distinction between fast centroparietal and slow frontal spindles, we examined whether these occurred independently or with consistent temporal relations. Figure 2-3A shows examples of individual spindles recorded simultaneously across several brain regions. As can be seen, fast centroparietal spindles occurred before slow frontal spindles, and the successive temporal occurrence across channels was accompanied by a decrease in spindle frequency. Next, a quantitative analysis of time offsets across all pairs of brain regions was conducted and the order in which spindles appeared was computed (Figure 2-3B). The results indicate that centroparietal spindles (in SMA and PC) occurred before slow frontal spindles (pSMA, AC, and OF) with a time difference of 203 ±16ms (mean ± SEM across 2,024 pairs of spindles, $p < 10E-12$ via one-tail t-test). Sorting regions according to the order in which their spindles were detected revealed that centroparietal regions typically preceded frontal locations (Figure 2-3B). In contrast, within centroparietal regions and within frontal regions no significant time differences were found, supporting the notion of a discontinuous transition in timing and frequency between fast centroparietal and slow frontal spindles (see Discussion). Figure 2-3C provides an example of the average timing relation between all spindle pairs (n=139) detected concomitantly in the PC and AC in one individual. As can be seen, timing and frequency differences appear closely linked. Indeed, a quantitative analysis of all pairs of regions across the entire dataset revealed that timing and frequency of spindles were tightly related ($r = 0.90$, $n = 9,741$ spindles). Overall, the reduction in spectral frequency with respect to time delay between spindles was -1.3 ±0.5Hz/s, and this negative rate was comparable to that found for fast spindles within the same regions (-0.8 ±0.02Hz/s, see previous section).

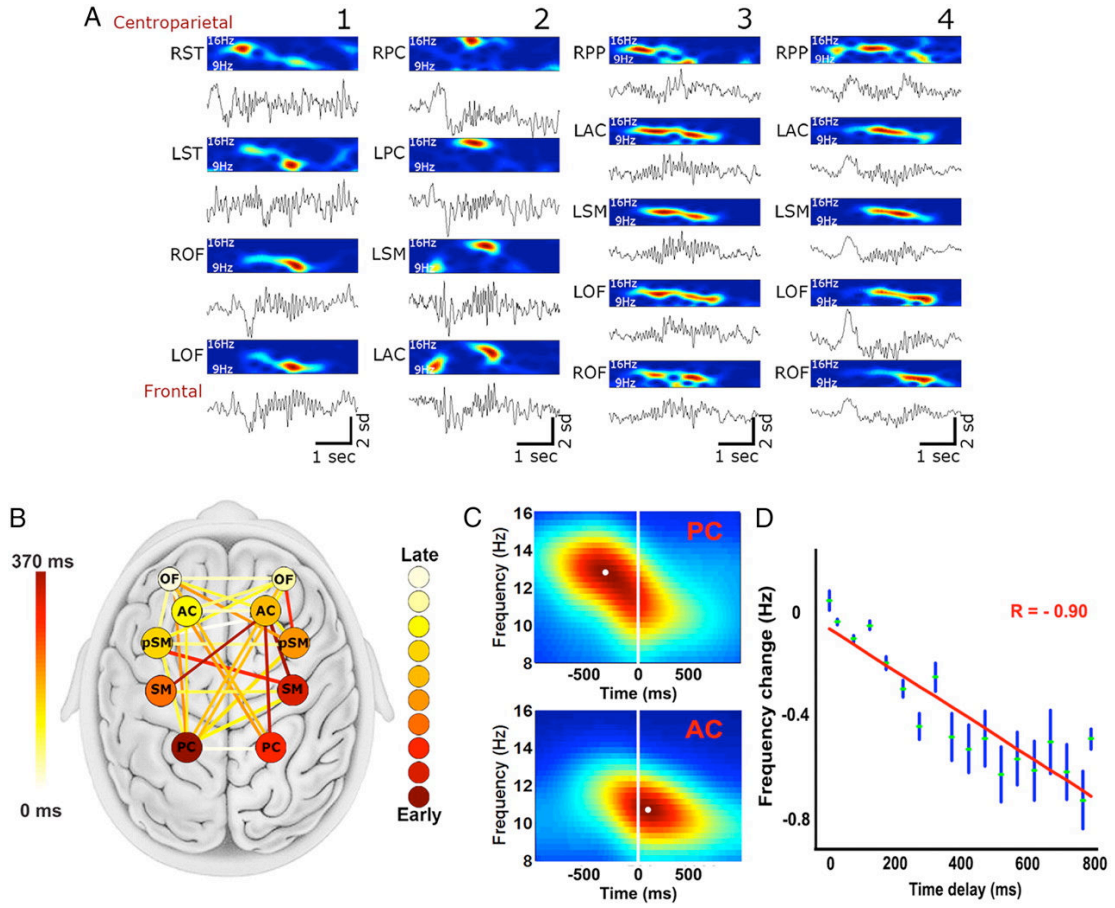

Figure 2-3 Fast centroparietal spindles precede slow frontal spindles

(A) Four examples of individual spindles in three individuals showing depth EEG along with corresponding spectrograms in the spindle range (9-16Hz) during 4sec of NREM sleep. When spindles occur in multiple brain regions, fast centroparietal spindles precede slow frontal spindles. (B) Quantitative analysis of time offsets in spindle occurrence. A graph showing the order in which spindles are detected across multiple regions (node color) and the mean temporal delays between each pair of regions (edge color). Mean order and timing across spindles for all individuals (n=12) indicate that centroparietal spindles precede frontal spindles. Abbreviations as in Figure 2. (C) An example of differences in timing and frequency between posterior cingulate (PC) and anterior cingulate (AC) in one individual. Spectrograms are aligned to peak power of PC spindles. Note that AC shows a hint of an early fast component aligned with peak power in PC while its peak is at lower frequencies and delayed by over 500ms. (D) Frequency decreases (y axis) and temporal delays (x axis) are closely related in individual spindles (R=0.90, n = 9,741 spindles in 50 electrode pairs).

Association of spindles with slow wave up-states

Since spindles are often associated with slow wave up-states (Amzica and Steriade, 1998; Molle et al., 2002; Steriade et al., 1993b), we examined how this association may vary for different spindles detected across different brain structures. We have recently characterized in detail slow waves and underlying unit activities in the same dataset (Nir et al., 2011). Here we used the same automatic detection of slow waves in each individual channel and examined the occurrence of spindles around positive and negative peaks in depth EEG, corresponding to down and up states, respectively. Figure 2-4A depicts an

example of an individual slow wave detected in the anterior cingulate followed by a spindle, whereas Figure 2-4B presents the quantitative analysis of spindle detections around slow waves across the entire dataset. Higher spindle occurrence (Figure 2-4B, *right*) was found in the 0-500ms interval following negative peaks in depth EEG (up states), in line with previous reports (Molle et al., 2002; Steriade et al., 1993b).

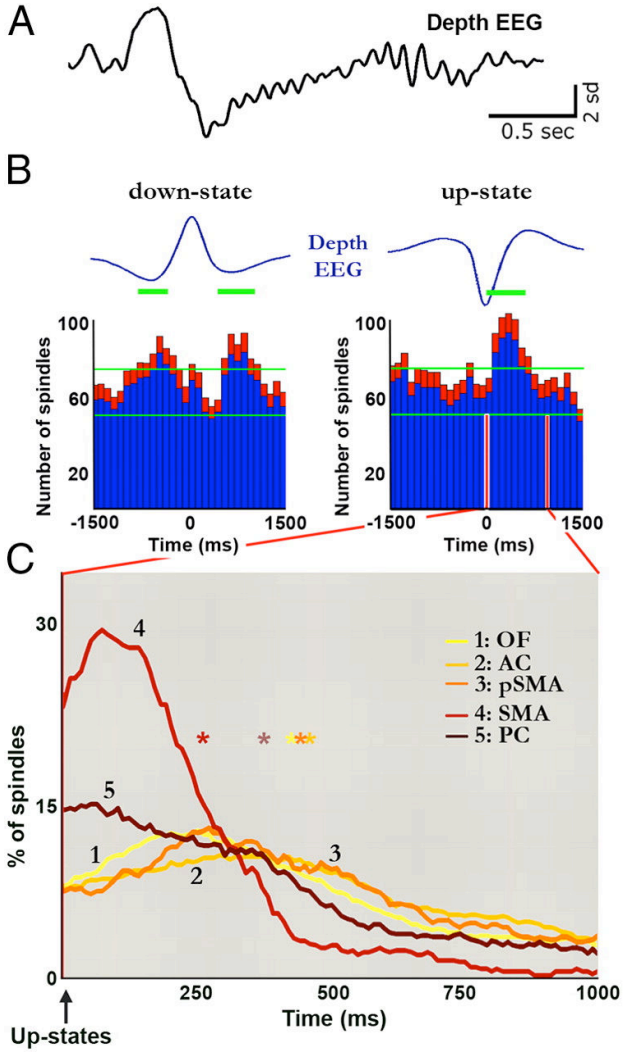

Figure 2-4 Association of spindles with slow wave up-states

(A) Example of a single spindle associated with a slow wave up-state as recorded in the depth EEG of the anterior cingulate cortex. (B) Number of detected spindles around slow wave down-states (left, positive peaks in depth EEG) and up-states (right, negative peaks in depth EEG). Blue traces show average slow waves (n=13 individuals). Red shading, SEM across channels. Green horizontal lines, confidence interval (α=0.05). Thicker green bars, significant deviations from chance. Note that around slow waves, spindles occur more often after transition to the up-state. (C) Regional differences in association of spindles with slow wave up-states. Note that fast centroparietal spindles (regions 4-5, red-brown colors) are more tightly associated with slow waves up-states. Asterisks mark the average time to up-states for each region.

Next, association of spindles with slow wave up states was compared between different brain regions in the second immediately following the transition to up states when spindle occurrence was maximal (Figure 2-4C). Fast centroparietal spindles were found to be more tightly associated with up states compared with slow frontal spindles. Specifically, the average delays from negative peaks in the depth EEG to maximal

spindle density in the SMA and PC were 267 ±11ms and 363 ±11ms, respectively, while frontal regions exhibited longer delays (AC, 460 ±8ms; OF, 425 ±6ms; pSMA, 449 ±14ms). The difference between centroparietal delays and frontal delays was statistically significant ($p < 10E-12$, unpaired two-tailed t-test). Spindles exhibited the shortest delay with up-states in the SMA, the region where spindles were also detected earliest. More generally, typical time differences between regions were maintained for spindles associated with slow wave up-states. Thus, the tighter association between centroparietal spindles and slow wave up states is consistent with their earlier occurrence compared with slow frontal spindles (see also Discussion).

Local sleep spindles

Although concomitant spindles were observed across multiple recording sites (above), we recently found that both sleep spindles and slow waves often occur independently in separate brain regions (Nir et al., 2011). We present these findings here as well to place them in the context of a comprehensive examination of sleep spindles in the human brain. Examination of local vs. simultaneous spindles was carried out only in cortical sites that had regular spindle occurrences, thereby excluding the possibility that local occurrence of spindles arises merely from their total absence in remote brain structures. Numerous examples of local sleep spindles occurring in specific brain regions were found (Figure 2-5A). Local spindles occur without spindle activity in other regions, including homotopic regions across hemispheres and regions with equivalent signal-to-noise ratio (SNR) showing global slow waves. We set out to quantitatively establish to what extent local sleep spindles occur across the entire dataset. We determined for each spindle in a given region whether spindles were present or not in other brain structures (Methods). The spectral power changes in concordant sites (45% of cases where a spindle was detected in both "seed" and "target" channels, Figure 2-5B top row) were compared with those at non-concordant sites (55% of cases where a spindle was detected in the seed channel but not in the target, Figure 2-5B bottom row). The results revealed a clear difference between peak spectral power values of concordant and non-concordant conditions across spindles in target channels ($p < 10E-48$, paired t-test), indicating significant differences in underlying neuronal activity, and that non-concordant cases are indeed local spindles. Furthermore, the analysis of those cases where target channels did not exhibit any increase in spindle spectral power above the noise level (Methods) revealed that 32% of all non-concordant cases were local in the strongest sense, i.e. a full-fledged spindle was detected in the seed channel while spectral power in the target channel was not different from chance. Importantly, the occurrence of local spindles was independent of local slow waves, since spindles occurring in isolation (i.e. not associated with a slow wave within ± 1.5s) constituted 37 ±2% of all cases and a separate analysis confirmed that such "isolated" spindles were likewise mostly local (Figure 2-5C). In addition, comparing homotopic regions revealed that 36 ±2% of spindles were observed only in one hemisphere (mean ± SEM across 12 pairs), indicating that differences between anterior and posterior regions could not account for spindle locality.

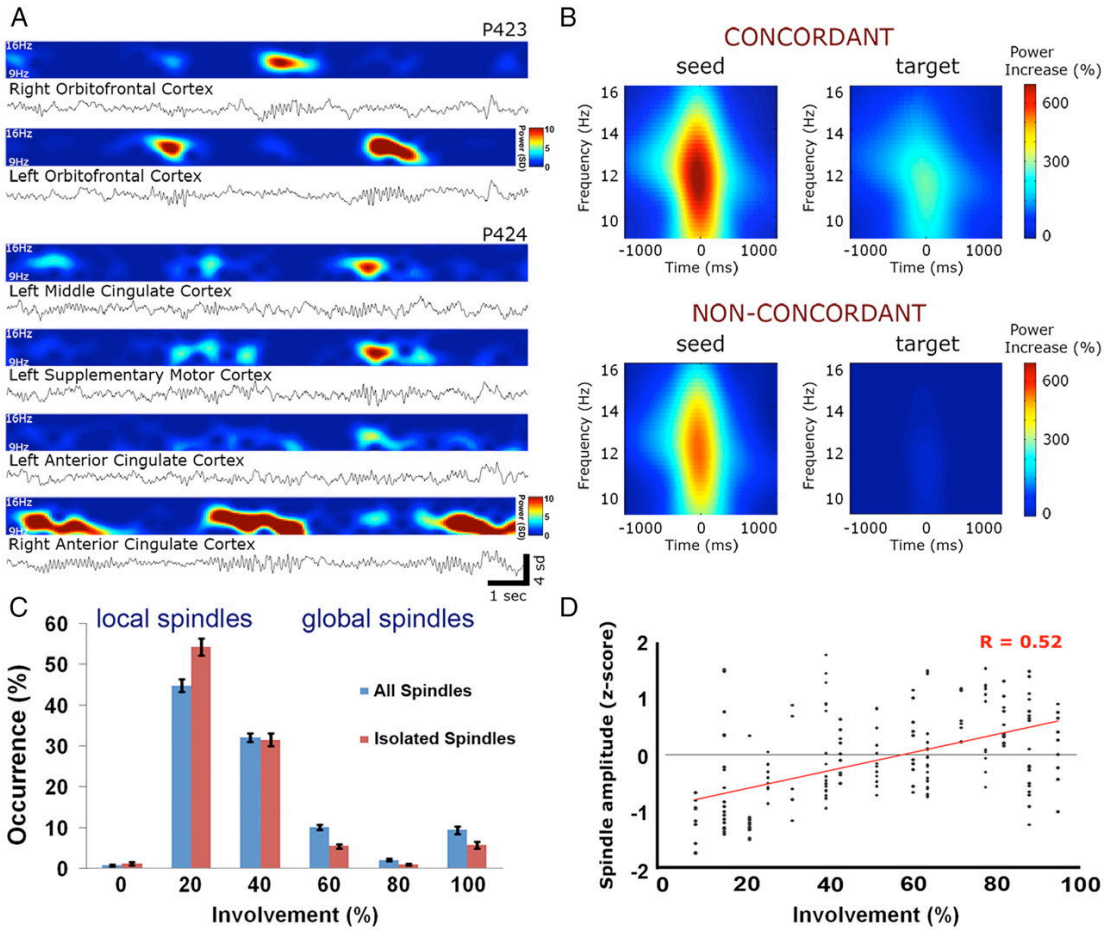

Figure 2-5 Local sleep spindles

(A) Two examples in two different individuals of depth EEG along with corresponding spectrograms in the spindle frequency range (9-16Hz) during 15sec of slow wave sleep. Note that regardless of slow waves, local spindles robustly occur without spindle activity in other regions, including homotopic regions across hemispheres and regions with equivalent SNR showing the same global slow waves. (B) Quantitative analysis of spindle occurrence across pairs of channels. Top row (concordant spindles, 45% of cases) shows spectrograms for cases in which a spindle was detected in the "seed" channel as well as in the "target" channel (N = 27,338 in 170 pairs of regions in 12 individuals). Bottom row (non-concordant spindles, 55% of cases) shows spectrograms for cases in which a spindle was detected in the seed channel but not in the target channel (N = 32,797 in 170 pairs of regions in 12 individuals). Note that spindle power in non-concordant target channels is at near chance levels, indicating that our detection can reliably separate between presence and absence of spindle activity. (C) Most sleep spindles are local. Distribution of involvement (percent of monitored brain structures expressing each spindle) for all spindles (blue bars, n = 21,240 spindles in 49 electrodes of 12 individuals) and for isolated spindles (red bars, spindles without a slow wave within ± 1.5s, 37% of events). Note that 73% of spindles are observed in less than 50% of electrodes indicating that most spindles are local (D) Scatter plot of spindle amplitudes as a function of involvement shows that global spindles have some tendency to be of higher amplitude ($r = 0.52$, $p < 0.0001$, $n = 170$).

Next, we quantified the involvement of multiple regions in spindles by computing the number of brain areas in which spindles were observed. The majority of sleep spindles involved a limited number of brain regions (Figure 2-5C), indicating that local spindles were more frequent than global spindles. Mean involvement in individual spindles was 48 ±0.7% of monitored brain regions (mean ± SEM across 49 depth electrodes), indicating that most spindles were predominantly local. Finally, the spatial extent of spindles was

significantly correlated with spindle amplitude (Figure 2-5D, $r = 0.52$, $p < 0.0001$, $n = 212$).

Deep sleep is associated with lower spindle frequencies

The variability in spindle spectral frequency between brain structures and during individual spindles described in the preceding paragraphs could be due to changes in levels of thalamocortical polarization. Since the degree of thalamic hyperpolarization dictates the period of spindle oscillations (McCormick and Bal, 1997; Mircea Steriade, 2003), we hypothesized that spindles during deep sleep (early in the night or in the middle of NREM cycles when SWA is highest), would contain lower spectral frequencies than spindles during lighter sleep (late in the night or closer to REM transitions when SWA is lower).

To examine this possibility, we first compared spindle frequencies in five individuals showing a typical homeostatic decline of SWA, i.e. a progression from deep early sleep with powerful slow waves to lighter sleep late in the night. Spindle frequency was significantly lower in early deep sleep when SWA was highest (Figure 2-6A, reduction of 0.63 ± 0.12Hz, mean $\pm$ SEM across 16 channels, $p = 0.0004$, non-parametric Mann-Whitney U-test). The modulation of spindle frequency in early vs. late sleep was specific to slow spindles ($p = 0.002$ for slow frontal spindles vs. $p = 0.62$ for fast spindles, Mann-Whitney U-test).

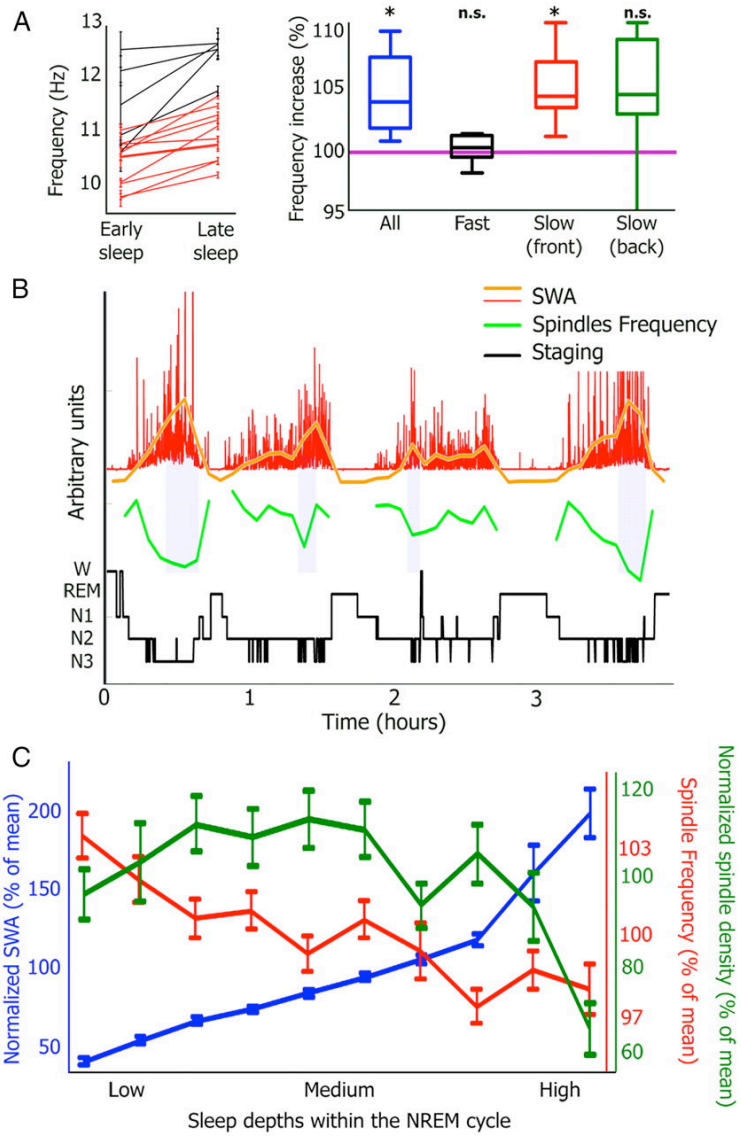

Figure 2-6 Deep sleep and high SWA are associated with lower spindle frequencies

(A) Frequency of slow spindles changes between early and late NREM sleep (n=5 individuals, see Methods). Left, frequency changes in centroparietal channels (black bars) and frontal channels (red bars). Right, frequency changes for all channels (blue), fast spindles in centroparietal channels (black), slow frontal spindles (red) and occasional slow spindles in centroparietal channels (green). (B) Example of time-course of SWA and spindle frequency dynamics throughout sleep in the anterior cingulate of one individual. Note that within NREM cycles, spindle frequency is lowest when SWA is highest (vertical purple bars) and increases towards transitions to REM sleep. (C) Quantitative analysis across the entire dataset (n=8 individuals) comparing sleep depth (as measured by SWA, blue) with spindle frequency (red) and density (green). Note that deep sleep (high SWA on the right) is accompanied by fewer spindles ($r = -0.73$, $p = 0.02$) with lower frequencies ($r = -0.81$, $p = 0.005$). Error bars denote SEM across NREM sleep intervals (n=16, see Methods).

Along the same line, spindle frequency changed within NREM cycles in accord with changes in SWA. Figure 2-6B shows an example of dynamics in spindle frequency and SWA across sleep in one individual, illustrating that in the middle of each NREM cycle when SWA was highest, spindle frequency was lowest. Next, this relation was examined in all NREM cycles followed by REM epochs (16 cycles in 29 depth EEG channels and 8 individuals, see Methods). Each NREM cycle was divided into 10 intervals with equal

duration and SWA, spindle frequency and spindle density were computed separately for each interval (Figure 2-6C). Both spindle frequency and spindle density were negatively correlated with SWA during NREM episodes (r= -0.81, p = 0.005 and r = -0.73 p = 0.02). These results indicate that deeper sleep and higher SWA are associated with lower spindle frequencies and fewer events.

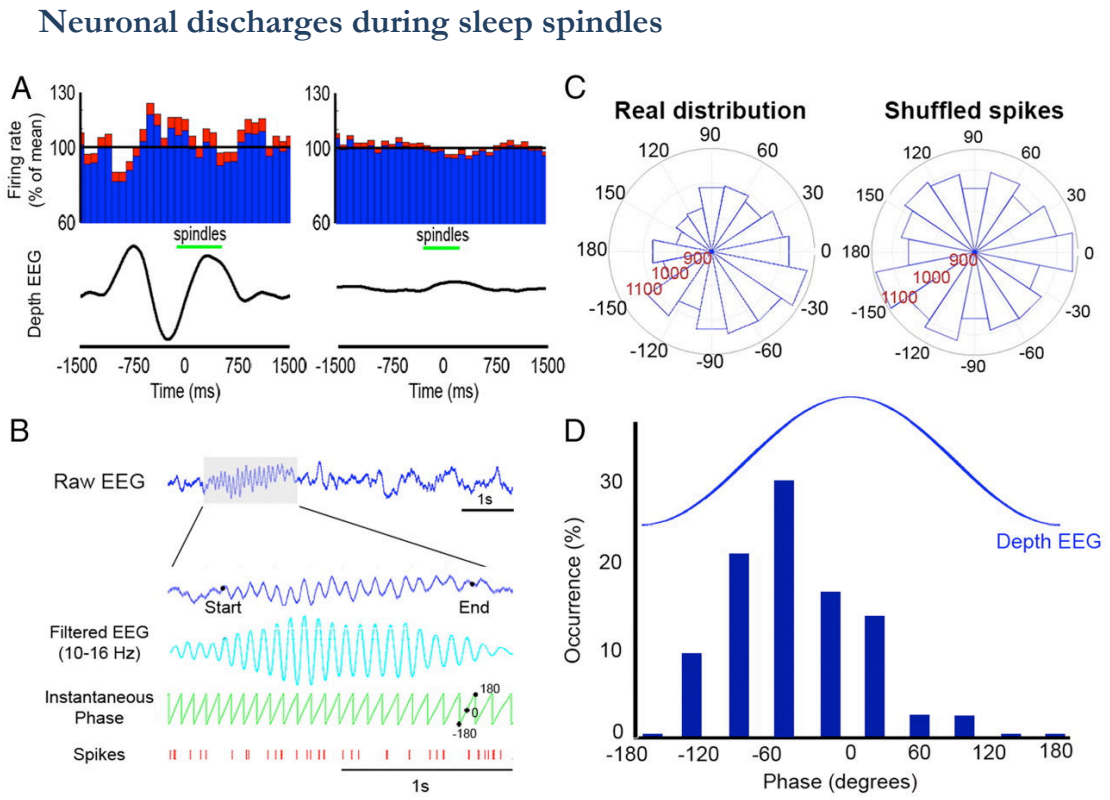

Figure 2-7 Unit discharges during sleep spindles

(A) Spindle-triggered averaging of unit spiking activity (n= 207 units), time locked to the positive peak closest to the middle of the spindles in depth EEG (n = 40 channels). Left, spindles associated with slow waves up-states (8.5% of events). Right, all spindles. Red shades denote SEM across neurons. Black traces below bar graphs show the average depth EEG at those times. In contrast to robust firing rate modulations around transitions to UP states, generally firing rates modulations are largely absent during spindles. (B) Example of phase-locking analysis for one neuron and one spindle. For each detected spindle, raw depth EEG (blue trace) is filtered in the spindle range (9-16Hz, cyan trace). The instantaneous phase is computed (green trace) and phase values are extracted for each action potential (red bars). (C) Phase-locking of spikes for the same unit displayed in A across all spindles ("real distribution") and for spikes randomly shuffled within each spindle ("shuffled spikes"). A unit is considered phase-locked only if the Rayleigh p-value for its real distribution is smaller than the critical p-value defined as the 95th percentile across shuffled iterations. (D) Cumulative histogram of preferred firing phase for all phase-locked neurons (n=41/212, 20% in 12 individuals). Note the tendency of phase-locked units to fire between the negative and positive peaks of spindles in the depth EEG.

Given that spiking activity across the human brain is tightly locked to EEG slow waves (Nir et al., 2011) we examined whether cortical neurons consistently modulated their firing rate during spindles. Examination of firing rates in putative single-units from individual subjects revealed little evidence for consistent modulations in relation to

spindles. On average across all 207 cortical units, we found that 8.5% of spindles - those occurring around transitions from inactive to active (UP) periods - were accompanied by robust firing rate modulations (Figure 2-7A, left), as expected (Nir et al., 2011). In contrast, when considering all spindles (n=63,724) firing rate modulations were largely absent (Figure 2-7A, right), although a small (~4%) yet significant reduction in neuronal discharges was observed 100-400 ms following the peak amplitude of spindles, likely reflecting a diffuse tendency for an inactive (DOWN) state to occur at that time.

Next, we evaluated the phase-locking of unit discharges during spindles to determine if units preferably fire at a specific phase of spindle oscillations (Figure 2-7B). Figure 2-7C presents an example unit in which spikes preferably occurred at a particular phase (-30 degrees) during spindles. Overall, 19.5% of neurons showed significant phase locking ($p < 0.05$, see Methods) with a tendency to fire more at the ascending phase of the spindle oscillation (preferred phase = -35 ±8.5 degrees, SEM across units) as measured with depth EEG (Figure 2-7D).

On average, phase-locked units had a higher firing rate than the average firing rate (5.9 ±1.2Hz vs. 3.1 ±0.3Hz, $p = 0.004$, Mann-Whitney U-test for putative single units). It could be argued that the firing of many neurons is phase-locked during spindles, but only high firing rate neurons allow enough statistical power to reveal this phenomenon. However, 46% of phase locked neurons had firing rates that were below the mean rate across the entire population. Alternatively, higher firing rates in phase-locked units may reflect a bias towards specific cell types such as interneurons (see also Discussion).

Spindles in the Medial Temporal Lobe (MTL)

Spindle occurrence in the MTL and its possible relation to pathology in epilepsy patients is a matter of continued debate (Malow et al., 1999; Nakabayashi et al., 2001; Pare et al., 2002). Our results (Table 2-1) revealed reliable spindle occurrence in the PHG, a dependable albeit lower occurrence in the hippocampus, and lower spindle occurrence in the entorhinal cortex and amygdala. Could such events reflect epileptiform activity? To address this, spindle detections in MTL were further analyzed in relation to the seizure onset zone (SOZ) based on the medical records of the patients. We examined whether inclusion in the epileptic focus (25 of 64 MTL channels) could predict spindle detection and spindle density in each region separately. If detected events in the MTL solely reflect epileptiform activities rather than physiological spindles, the number of channels with spindles and their density would be higher within the SOZ. However, we found that in PHG and hippocampus the majority of channels with spindles were outside the SOZ (64% and 63% respectively), and observed a trend for more hippocampal spindles outside the SOZ (1.1 vs. 0.8 spindles/min outside and inside the SOZ, respectively). In the entorhinal cortex and amygdala, spindle occurrence was comparable within and outside the SOZ. Finally, we examined to what extent spindles detected in PHG and hippocampus co-occurred with spindles in frontal and centroparietal cortices remote from the SOZ. We found that detected events in hippocampus (Methods) co-occur more often with frontal/parietal spindles than with events detected in amygdala or entorhinal cortex ($p < 0.05$, Mann-Whitney U-test). It should be noted that due to possible volume conduction and lack of clear firing rate modulations our results cannot resolve the long-lasting controversy of potential epileptiform nature of hippocampal spindles. Nevertheless, these results indicate that although MTL spindles are less frequent and

more variable, PHG and hippocampus may exhibit physiological spindles that may transcend possible links to pathology.

Sleep spindles and epilepsy

Our data were recorded in medicated epilepsy patients in whom abnormal events during seizure-free periods may affect sleep, and sleep spindles in particular (Dinner and Lüders, 2001; Steriade, 2005). Therefore, it was imperative to confirm that our results could be generalized to the healthy population, and multiple observations strongly suggest that this is the case. First, overnight recordings were carried out prior to routine tapering of anti-epileptic drugs to ensure a less significant contribution of epileptiform activities. Second, sleep measures were within the expected normal range, including distribution of sleep stages, NREM-REM cycles, and EEG power spectra of each sleep stage. Third, we specifically detected paroxysmal discharges and separated them from physiological sleep spindles, and we also confirmed that pathological events were not falsely detected as spindles through extensive visual inspection of each individual's data (Methods). Fourth, the occurrence rate of paroxysmal discharges was highly variable across channels, limited in its spatial extent, and entirely absent in some channels. By contrast, all the results reported here could be observed in every individual despite highly idiosyncratic clinical profiles. Fifth and most importantly, previous analysis revealed significant firing rate modulations in the same neurons during paroxysmal discharges (Nir et al., 2011), whereas unit discharges were not robustly modulated during sleep spindles, attesting to a good separation between pathological and physiological spindles. Since interictal spikes and sleep spindles may be confounded in a more complex manner in the MTL, we adopted a conservative approach and analyzed those spindles separately from data obtained in frontal and parietal cortices based on a visual detection. Overall, we are confident that the current results can be generalized to individuals without epilepsy.

Discussion

Spindle occurrence and thalamic projections

Spindles were observed most frequently in neocortical regions, less often in the hippocampus and parahippocampal gyrus, but were not robustly detected in amygdala and entorhinal cortex (Clemens et al., 2010; Malow et al., 1999; Nakabayashi et al., 2001; Pare et al., 2002; Sirota et al., 2003), likely reflecting the underlying thalamic projections. For example, the lack of spindles in amygdala is consistent with sparse thalamocortical projections that only target the lateral nucleus (Jones, 2007). Moreover, many thalamic nuclei that are reciprocally connected with the RE project robustly to frontal and parietal cortices where spindles are abundant. By contrast, dorsal thalamic nuclei projecting to the MTL are not reciprocally connected with the RE in cats where spindles are absent (Barr et al., 2007; Pare et al., 1987; Steriade et al., 1984). The difference in spindle occurrence between the hippocampus and entorhinal cortex is puzzling and may reflect variability of the recording layers in different structures.

Slow and fast spindles

Our intracranial results confirm and refine the proposed distinction between slow (9-12Hz) frontal and fast (13-16Hz) centroparietal spindles (Anderer et al., 2001; Clemens et al., 2010; De Gennaro and Ferrara, 2003; Jankel and Niedermeyer, 1985; Jobert et al., 1992; Loomis et al., 1935; Nakamura et al., 2003). We find that (a) this distinction is present in each individual (b) spindle frequency shows a sharp transition between SMA and pSMA, (c) centroparietal spindles show a bimodal distribution whereas frontal spindles are exclusively slow, (d) frontal spindles often have frequencies as low as 9-10Hz.

What gives rise to slow and fast spindles? Thalamocortical (TC) projections from different nuclei terminate in cortical regions that exhibit slow vs. fast spindles. Posterior and lateral dorsal nuclei project to centroparietal cortex, whereas ventral and anterior dorsal nuclei mainly project to prefrontal regions (Cappe et al., 2009; Jones, 2007; Zhang et al., 2009). Some anterior nuclei (e.g. ventral anterior (VA) and ventral anterior magnocellular (VAmc)) project diffusely along the cingulate cortex (Jones, 2002) and could explain occasional slow spindles in centroparietal regions. Since spindles arise from RE-TC-RE loops, this model implies a preserved topographical organization between thalamic nuclei and sub-regions in the RE sheet (Guillery and Harting, 2003; Jones, 2007, p. 200; Lam and Sherman, 2011; Steriade and Timofeev, 2003). Finally, the difference in spindle frequency between SMA and pSMA suggests that these adjacent cortical regions receive input from different thalamic nuclei (Akkal et al., 2007).

Faster spindle frequencies are associated with earlier time onsets

Fast centroparietal spindles precede slow frontal spindles with a significant difference between adjacent SMA and pSMA, as was the case for spindle frequency. Spindle timing is closely related to spindle frequency such that the regional delays are well correlated to frequency differences in individual spindles. Furthermore, frequency decreases during

spindles within each brain region such that frontal spindles show a hint of an early fast component aligned with centroparietal spindles and vice versa. Thus, individual spindles exhibit different frequencies and timings in distinct regions.

Timing and frequency differences in spindles have been noted but their close relation during individual spindles had yet to be established (Anderer et al., 2001; Clemens et al., 2010; Dehghani et al., 2010a; Nakamura et al., 2003; Zygierewicz et al., 1999). Earlier studies suggested that timing differences among cortical spindles reflect propagation along the RE rather than through intracortical pathways (Contreras et al., 1997a; Kim et al., 1995). Accordingly, spindles may propagate along the RE from its caudal section to its rostral section, progressively innervating different dorsal nuclei (posterior to anterior), which project topographically to the cortex generating spindles with different frequencies at different times in different locations.

Sleep spindles are mostly local

Spindles have been traditionally regarded as events reflecting global signal propagation between thalamus and cortex. While local spindles have been noted in previous studies (Andersen and Andersson, 1968; Contreras et al., 1997b, 1996) , asynchronous spindles were usually associated with non-physiological conditions. The current results further extend our recent demonstration that most sleep spindles occur locally in natural sleep, as do sleep slow waves (Nir et al., 2011). Most spindles occurred locally in a way that was independent of slow waves and of their frequency content: "isolated" spindles as well as both slow and fast spindles could occur independently between homotopic regions across hemispheres. These findings join other suggestions that spindles may occur or be regulated locally (Caderas et al., 1982; Dehghani et al., 2010a; Halassa et al., 2011; Nishida and Walker, 2007) and support the notion that sleep arises from activities of local circuits (Esser et al., 2006; Huber et al., 2004; Krueger et al., 2008; Nir et al., 2011; Vyazovskiy et al., 2000; Werth et al., 1997). It is an open question whether local and global spindles may be mediated by different mechanisms such as corticothalamic projections from different layers or different thalamocortical projections via the core and matrix cells (Jones, 2009; Rubio-Garrido et al., 2009; Zikopoulos and Barbas, 2007).

The relation of spindles with sleep slow waves

Around slow waves, spindles tend to occur preferentially at up states (Molle et al., 2002; Mircea Steriade, 2003). Such association between the depolarizing component of slow waves and subsequent spindles has also been termed K-complex but this terminology is still under debate (Amzica and Steriade, 1998; Cash et al., 2009). Centroparietal spindles tend to occur shortly after the transition to up states and since up states are believed to trigger spindles through corticothalamic projections, this suggests that centroparietal cortex may exert particularly powerful corticothalamic feedback. Given that slow waves propagate from prefrontal cortex towards posterior regions (Massimini et al., 2004; Nir et al., 2011), and spindles occur sooner in posterior regions (above), the net result is that frontal spindles occur later during slow wave up states.

Our results confirm and extend the notion of reciprocal relation between SWA and spindle frequency and density (De Gennaro and Ferrara, 2003; Himanen et al., 2002;

Steriade and Amzica, 1998; Wei et al., 1999). In stage N3 when SWA is maximal, spindle density is reduced. In early NREM sleep when SWA is highest, spindle frequency is significantly lower. Moreover, the level of SWA within NREM cycles is anti-correlated with spindle frequency and density. Thus, few spindles with lower frequency occur in the middle of NREM cycles when SWA is highest. Towards the transition to REM sleep when SWA tapers off, spindles increase in density and frequency.

Unit discharges during sleep spindles

We found that firing rate modulations of cortical neurons during spindles are weak and unreliable compared with those observed during slow waves (Nir et al., 2011), largely consistent with previous reports (Sirota et al., 2003). This seems at odds with suggestions that sleep spindles play an important role in disconnection from the external environment or in memory consolidation (Diekelmann and Born, 2010) but perhaps specific neuronal populations are more strongly modulated during spindles (Dehghani et al., 2010b). Another possibility is that inhibition in NREM sleep (Evarts, 1964; Steriade et al., 1974) may occur concomitantly with spindle-driven post-synaptic potentials in dendrites and often cancel out the excitation such that spindles may not reliably drive spike firing (Contreras et al., 1997b).

In addition, we found that spindles affected spike timing in cortical neurons. The discharges of 20% of neurons were significantly phase-locked, firing maximally in the ascending slope of spindles in the depth EEG as in animal studies (Contreras and Steriade, 1996; Sirota et al., 2003). The precise proportion of entrained neurons and their preferred phase should be interpreted cautiously, since unit discharges were recorded ~4mm away from depth EEG and their laminar profiles remain unknown, and these methodological limitations may possibly underlie minor differences with studies in other species (Dehghani et al., 2010b; Sirota et al., 2003). That spike timing is modulated by sleep spindles and is also implicated in plasticity processes (Caporale and Dan, 2008) supports the notion that spindles may have a role in synaptic plasticity (Khazipov et al., 2004). A trend for higher firing rates in phase-locked units could suggest that specific cell types (e.g. inhibitory interneurons) preferentially modulate their spike timing in concert with spindles, but our data could not resolve this intriguing possibility.

Spindle density and frequency as reflections of thalamic hyperpolarization

We suggest that the level of thalamic hyperpolarization may be a key factor governing multiple spindle properties such as their spectral frequency, density, regional variability, dynamics during individual events, and across sleep. In TC cells, the degree of hyperpolarization affects the duration of the hyperpolarized state and consequently dictates the period of thalamic spindle oscillations (McCormick and Bal, 1997; Mircea Steriade, 2003). Along this line, we find that deeper sleep (higher SWA and presumably stronger thalamic hyperpolarization) is associated with lower frequency spindles. In addition, spindles arise at membrane potentials around -60mV, while slow waves arise at more hyperpolarized levels (-68 to -90mV), and these two states are mutually exclusive at the level of individual thalamic neurons (Nunez et al., 1992). Indeed, we find that high SWA is associated with fewer spindles, presumably since strong hyperpolarization

reduces the recruitment of neurons that support spindle generation. As for regional differences, posterior thalamic nuclei receive stronger cholinergic innervations (Jones, 2007) and this may explain faster spindles in those nuclei projecting to centroparietal cortices. Alternatively, generation of slow and fast spindles may reflect intrinsic properties of cells in thalamic and RE neurons (e.g. distributions of neurotransmitter receptors or ionic channels) leading to differential hyperpolarization levels in specific thalamic sub-regions. Finally, frequency decreases during each spindle could also reflect increasing hyperpolarization. Cortical neurons are increasingly more involved in the waning and termination phases of spindles (Contreras et al., 1996; Mircea Steriade, 2003), and these corticothalamic projections are believed to exert an overall inhibitory influence through their strong influence on RE cells (Golshani et al., 2001). If this hypothesis is correct, a simple non-invasive EEG measure of spindle frequency could provide an important proxy for the level of thalamocortical polarization at any given time.

Supplemental Figures

		LH													RH													
	Pt	H	A	EC	PH	TG	AC	MC	PC	OF	SM	P	TO	PT	H	A	EC	PH	TG	AC	PC	OF	SM	P	FG	TO	IFG	
1	396	5	4	2	8					1					2		2											24
2	398				6		9								5		11	2										33
3	399	14			7				1		12					13		15		14			12					88
4	402	3	9	5											2	6	10			1			6					42
5	404						9		6											10	11							36
6	405	3	4		11					2					5	1		3				7						36
7	406	6	8		13		3								8	8		6		4								56
8	415																											
9	416	3		1			3			10					16	8	7		12									60
10	417				4							8			9			8						7				36
11	422				8		1			11	8			2	5			6				7		10				58
12	423	5		8						7					1		11											32
13	424	8		10		12	13	13											12	17		3			11			99
		47	25	26	57	12	38	13	7	31	20	8		2	53	36	41	40	24	46	11	17	18	17	11			600

Table S 2-1 Recording details

A full description of the brain structures and number of units identified in our recordings. Rows correspond to individual patients and columns correspond to different brain regions. Green boxes mark implanted brain regions and numbers show detected units. Abbreviations: LH, left hemisphere; RH, right hemisphere; H, hippocampus; A, amygdala; EC, entorhinal cortex; PH, parahippocampal gyrus; TG, temporal gyrus; AC, anterior cingulate; MC, middle cingulate; PC, posterior cingulate; OF, orbitofrontal and medial prefrontal cortex; SM, supplementary motor area; P, parietal cortex; TO, temporo-occipital, PT, posterior temporal cortex; FG, fusiform gyrus; IFG, inferior frontal gyrus.

	P	Age	Gender	Handedness	Seizure onset	Resection / outcome	Imaging: PET & MRI	Recording length (h)	Recording start time
1	396	27	M	R	Left temporal	Left temporal, seizure free	metabolic and structural abnormalities left temporal	7.0	11:00 PM
2	398	41	F	R	Left temporal spreading to REC	Left temporal, significant improvement	metabolic abnormalities bilateral temporal lobe, normal structural	5.1	12:41 PM
3	399	43	F	R	Right prefrontal cortex	Right prefrontal, seizure free	normal metabolism, right frontal dysplasia	6.3	11:45 PM
4	402	25	F	R	Bilateral MTL	No surgery	Mild metabolic abnormality right temporal, normal structural	6.6	11:30 PM
5	404	25	M	L	Left prefrontal	Left prefrontal, significant improvement	Normal metabolism, periventricular structural abnormalities	10.9	6:29 PM
6	405	38	F	R	Right MTL spreading to RPHG	Right MTL, seizure free	Mild metabolic abnormality bilateral temporal, possible dysplasia right temporal	6.6	10:29 PM
7	406	33	F	R	Left MTL	No surgery	Mild metabolic abnormaility left temporal, structural abnormality right frontal lobe	6.6	10:40 PM
8	415	39	M	R	Left MTL	Left temporal, seizure free	Normal	7.7	10:13 PM
9	416	26	M	R	Bilateral MTL and R IFG	No surgery	Mild metabolic abnormaility right temporal, mild structural abnormaility left temporal	7.7	10:43 PM
10	417	23	M	R	Right Parietal	Right parietal, seizure free	Metabolic abnormality right parietal lobe, normal structural	8.7	9:51 PM
11	422	19	F	R	Bilateral multifocal	No surgery	Normal	7.9	10:01 PM
12	423	52	F	R	Left MTL	To be determined	metabolic and structural abnormalities left temporal	8.3	10:09 PM
13	424	26	M	R	Left lateral temporal	Left lateral temporal to be resected	metabolic abnormalities R temoral, dysplasia L frontal	7.9	10:15 PM

Table S 2-2 Patient information and details of sleep studies

Clinical information and sleep study details for all patients.

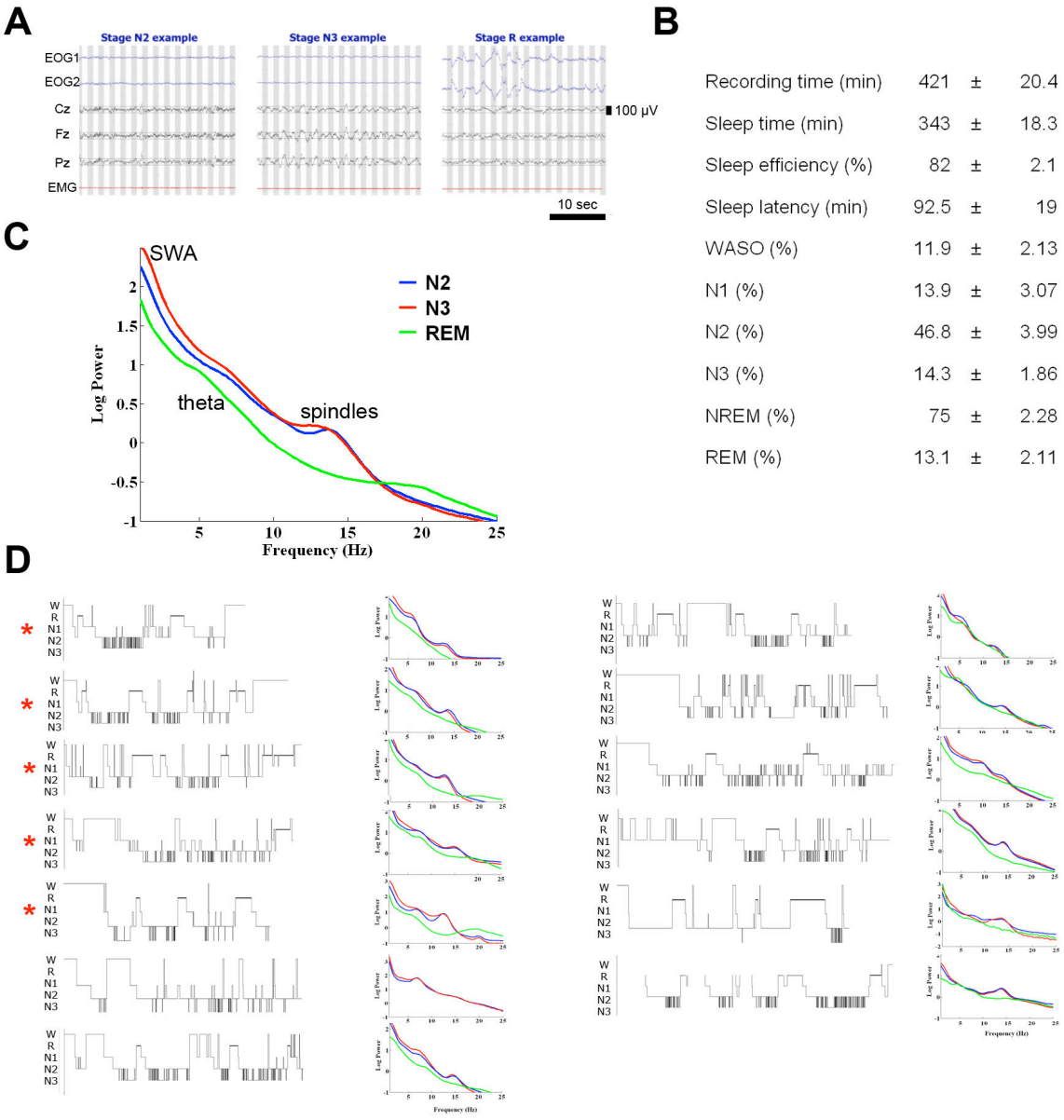

Figure S 2-1 Patient sleep resembles normal sleep in healthy individuals

(A) Representative examples of 30s polysomnographic data used for sleep scoring in stages N2 (left), N3 (middle) and REM sleep (right) in one individual. (B) Sleep measures for the entire night expressed as mean ± SEM (n=13). Sleep efficiency corresponds to total sleep time per time in bed. Sleep latency is to Stage 2. WASO refers to waking after sleep onset; SWS, slow-wave sleep (N2 + N3); NREM, non-rapid eye movement; REM, rapid eye-movement. (C) Average power spectra of scalp EEG in all derivations as a function of different sleep stages. Blue, N2; Red, N3; Green, REM sleep. (D) Individual hypnograms (time course of sleep stages throughout sleep) and power spectra of scalp EEG in all 13 individuals. In hypnograms, rows (top to bottom) denote wake (W), REM sleep (R), N1, N2, and N3. Colors in power spectra as above. First five individuals (red asterisks) mark patients who showed the typical dissipation of SWA throughout sleep (see Figure S2).

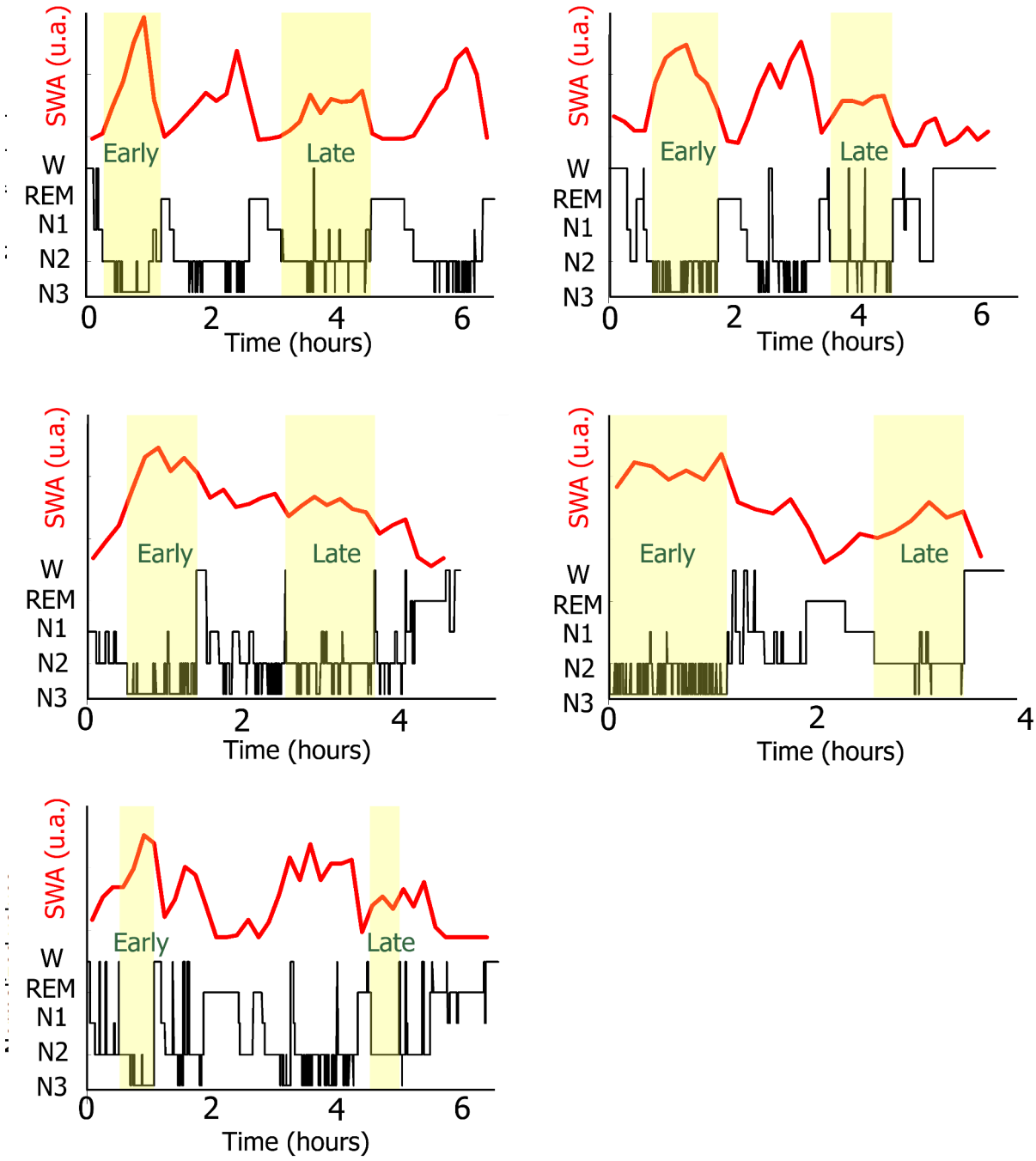

Figure S 2-2 Homeostatic decline of SWA throughout sleep

Individual hypnograms (black) and time-courses of SWA (red) in five individuals who showed a clear homeostatic decline of SWA throughout sleep. Sleep stages: W, wake; REM, rapid eye-movement sleep; N1, N2 and N3: non-rapid eye-movement sleep stages 1,2 and 3. Yellow highlights denote intervals of 'early' and 'late' sleep used for analysis presented in Figure 7.

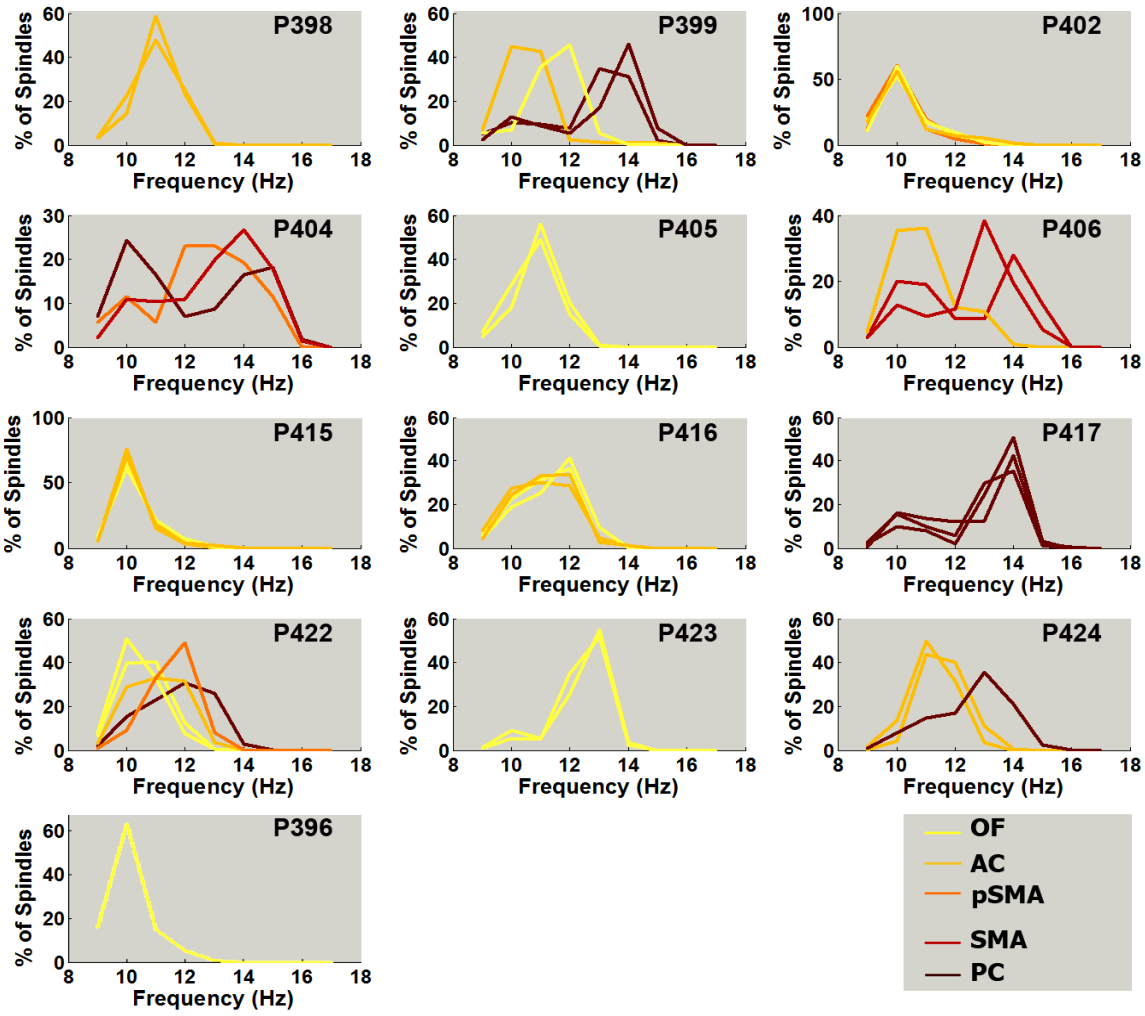

Figure S 2-3 Figure S3. Spindle frequencies across all individuals and electrodes.

Spindle frequency distributions in each individual and depth electrode separately. Note that in every individual, fast centroparietal spindles differ from slow frontal spindles despite individual variability in the exact spindle frequencies. While frontal spindles consist of one group of slow events, centroparietal spindles often have a bimodal distribution with most spindles being fast and some being slow.

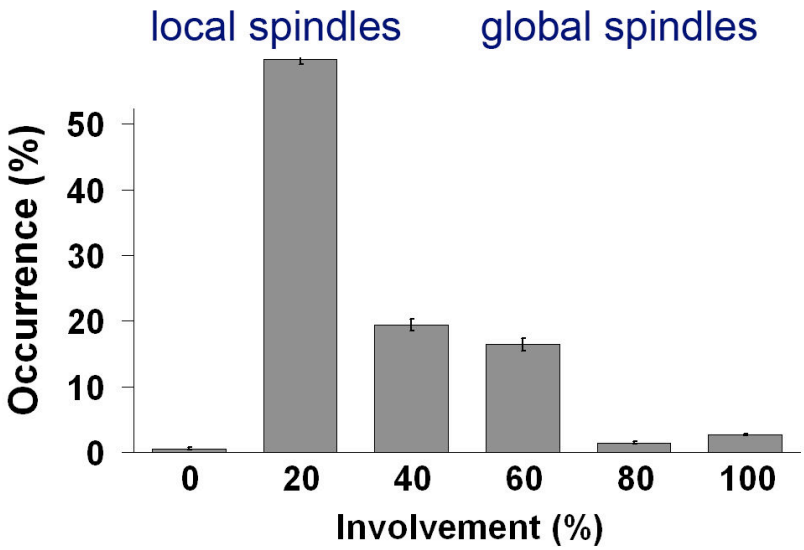

Figure S 2-4 Spindles that are isolated from slow waves are also mostly local

Distribution of involvement (percent of monitored brain structures expressing each spindle) across 22,914 events in 50 electrodes of 12 individuals. "Isolated" spindle events in this analysis (without a slow wave in ± 1.5s) constituted 53.7% ± 3.1 of events. Note that the distribution is skewed to the left, indicating that most "isolated" spindles are local and that the phenomenon of local spindles can not be explained by local slow waves.

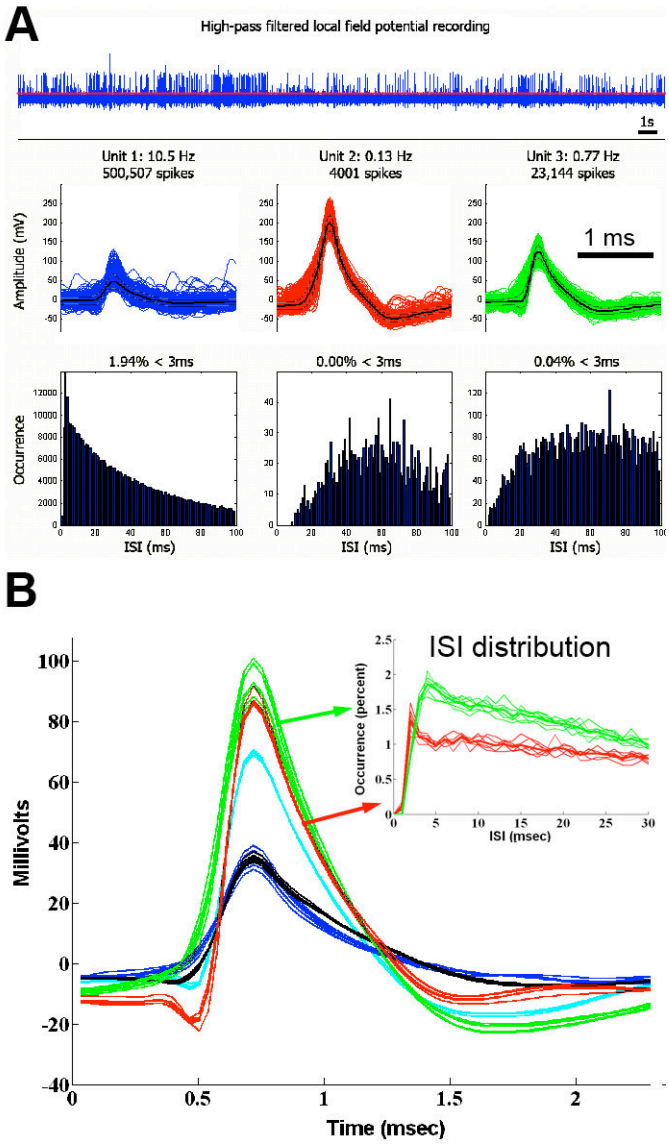

Figure S 2-5 Unit identification and stability throughout sleep recordings

(A) An illustration of unit identification scheme. Top row depicts the high-pass filtered LFP along with the threshold for spike identification set at 5 SDs above the noise level (red line). Middle row shows action potential waveforms for three detected units. Bottom row shows the distribution of inter-spike-intervals (ISIs). Based on the consistency of waveforms and the occurrence of ISIs within the expected refractory period (<3ms), we categorized clusters as a multi-unit cluster (blue), two single-unit clusters (red and green), and a noise cluster (not shown).

(B) Waveforms and ISI distributions are consistent and separable throughout sleep. Mean action potential waveforms for 5 distinct units recorded in the same individual. Each color denotes a different unit and each trace denotes the mean waveform in separate 1h intervals throughout sleep. Note that waveforms were consistent and separable between different units throughout sleep, confirming the stability of our unit recordings throughout long (~7h) recordings. Inset depicts ISI distributions in separate 1h intervals for two units.

Study 3:
Single-neuron activity and eye movements during human REM sleep and awake vision

Published in **Nature Communications**
August 11, 2015

Thomas Andrillon [1,2,3,*], Yuval Nir [4,*], Chiara Cirelli [3], Giulio Tononi [3], and Itzhak Fried [5,6]

[1] *Laboratoire de Sciences Cognitives et Psycholinguistique, Institut d'Études Cognitives, Ecole Normale Supérieure Paris, France*

[2] *Ecole Doctorale Cerveau Cognition Comportement, ENS – EHESS – Paris VI – Paris V Paris, France*

[3] *Department of Psychiatry, University of Wisconsin-Madison Madison, WI, USA*

[4] *Department of Physiology and Pharmacology, Sackler School of Medicine, and Sagol School of Neuroscience, Tel Aviv University Tel Aviv, Israel*

[5] *Department of Neurosurgery, David Geffen School of Medicine and Semel Institute For Neuroscience and Human Behavior, UCLA Los Angeles, CA, USA*

[6] *Functional Neurosurgery Unit, Tel Aviv Medical Center and Sackler School of Medicine, Tel Aviv University Tel Aviv, Israel*

* contributed equally to this work

Summary

Are rapid eye movements (REMs) in sleep associated with visual-like activity, as during wakefulness? Here we examine single-unit activities (n=2057) and intracranial EEG across the human medial temporal lobe (MTL) and neocortex during sleep, wakefulness, and during visual stimulation with fixation. During sleep and wakefulness, REM onsets are associated with distinct intracranial potentials, reminiscent of ponto-geniculate-occipital waves. Individual neurons, especially in the MTL, exhibit reduced firing rates prior to REMs as well as transient increases in firing rate immediately after, similar to activity patterns observed upon image presentation during fixation without eye movements. Moreover, the selectivity of individual units is correlated with their response latency, such that units activated after a small number of images or REMs exhibit delayed increases in firing rates. Finally, the phase of theta oscillations is similarly reset following REMs in sleep and wakefulness, and after controlled visual stimulation. Our results suggest that REMs during sleep rearrange discrete epochs of visual-like processing as during wakefulness.

Introduction

A seminal discovery in sleep research identified sleep periods with rapid eye movements (REMs), vivid dreams, electroencephalographic (EEG) activation and muscle atonia, known as REM sleep (Aserinsky and Kleitman, 1953; Dement and Kleitman, 1957; Jouvet and Michel, 1959). Since its discovery, a straightforward, fascinating question endures: are REMs non-specific signatures of arousability or do they represent specific times at which visual-like processing is updated?

The intuitive "scanning hypothesis", relating directional properties of REMs in sleep to shifts of gaze scanning the dream imagery, has proven difficult to assert. REMs have been shown to be highly similar to saccades during wakefulness in terms of their kinematic properties (Sprenger et al., 2010) and we use the terms interchangeably throughout. Retrospective comparisons of REM directions with dream recall yielded highly inconsistent results (Berger and Oswald, 1962; Dement and Kleitman, 1957; Dement and Wolpert, 1958; Jacobs et al., 1972; Roffwarg et al., 1962), reviewed in detail in (Arnulf, 2011). Several lines of evidence oppose the scanning hypothesis: for example, REMs in sleep ("s-REMs") persist in animals and humans without sight (e.g. fetuses, congenitally blind who do not report visual dreams). Visual dreams also occur in NREM sleep (Nir and Tononi, 2010) and during ~80% of REM sleep that is devoid of REMs ("tonic REM sleep"). Indeed, it could be that REMs reflect general arousal and are analogous to penile erections that occur throughout REM sleep but do not necessarily imply sexual contents in dreams (Schenck et al., 2007). On the other hand, recent studies with patients who enact their dreams due to absence of muscle paralysis (REM Sleep Bheavior Disorder, (Schenck et al., 1986)) suggest that, when present, REMs scan the dream scene (Arnulf, 2011). Overall, the evidence to date is limited to relating REMs in human sleep to either reports of dream content or to overt behavior, but the underlying changes in brain activity have remained relatively unexplored.

Thus, an important and tractable question is whether s-REMs co-occur with similar modulations in neuronal activity as during wakefulness, particularly in regions associated with visual-mnemonic processing (such as occipitotemporal cortex and the medial temporal lobe (MTL)). Indeed, during wakefulness each saccade ("w-REMs") gives rise to a discrete epoch of visual processing (VanRullen and Koch, 2003), associated with behavioral saccadic suppression and a subsequent visual response (Burr and Morrone, 2005; Henderson, 2003; Ibbotson and Krekelberg, 2011). In animals, s-REMs often coincide with stereotypical potentials termed ponto-geniculo-occipital (PGO) waves (Brooks and Bizzi, 1963; Farber et al., 1980; Gucer and Viernstein, 1979; Jouvet and Michel, 1959). However, the relation of s-REMs with neuronal activity in high-order visual and mnemonic circuits remains unknown.

The goal of this study was to establish the relation between s-REMs and underlying activity in visual-mnemonic regions, and to compare such modulations with those occurring during waking vision. To this end, we examined the underlying intracranial EEG (n=172 depth electrodes) and single-unit activities around REMs during sleep and wakefulness (n=600) and during controlled visual stimulation (n=1457) in neurosurgical epilepsy patients. The results demonstrate, for the first time, that MTL activity during s-REMs shares many properties with that observed during saccades and vision. A plausible interpretation is that s-REMs represent privileged time-points at which neuronal activity and associated visual-like processing is updated.

Results

Rapid eye movements in sleep and wakefulness

To compare neuronal activity underlying REMs in sleep and wakefulness, we conducted full-night (421 ± 20 min (mean ± SEM)) polysomnographic sleep studies with adjacent epochs of wakefulness (n=13 participants), as well as recordings during controlled visual stimulation (n=9 participants) and an eye-movement paradigm (one participant), in nineteen neurosurgical patients with intractable epilepsy. Participants were implanted with depth electrodes (Figure 3-1A-C) that recorded depth EEG and spiking activity during sleep and wake from 600 units (355 putative single units, 245 multi-unit clusters), as described in detail elsewhere (Nir et al., 2011).

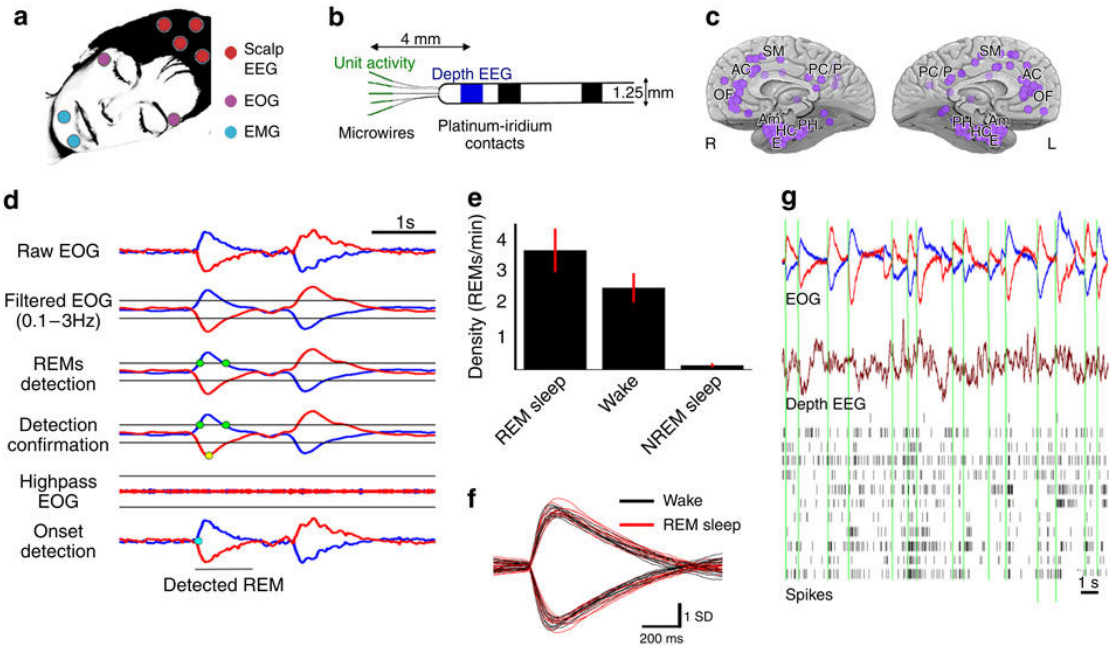

Figure 3-1 Data overview and eye movement detection

(A) Set-up for polysomnographic sleep and wake recordings. (B) Illustration of flexible probes used for recording depth EEG (blue: platinum contact) and unit activity (green: microwires). (C) Medial view of depth electrode locations (purple dots) spanning multiple brain regions. SM, Supplementary motor; PC/P, posterior cingulate/parietal cortex; PH, parahippocampal gyrus; HC, hippocampus; E, entorhinal cortex; Am, amygdala; LH, left hemisphere; RH, right hemisphere. (D) REM detection: 1st row, raw EOG showing 2 typical REMs in REM sleep. 2nd row, band-pass filtered (0.1-3Hz) EOG with thresholds set at mean+2SD (black lines). 3rd rows, detection of epochs crossing the threshold in one EOG channel (green dots). 4th row, detection is confirmed with opposite polarity in second EOG channel (yellow dot). 5th row, verification that epoch is free of epileptic spikes in high-pass filtered trace. 6th row, visual confirmation of REM onset. (E) Occurrence of REMs across vigilance states (mean ± SEM, n = 11/12/13 in REM sleep, wake, and NREM sleep, respectively). Note the near-absence of REMs in NREM sleep. (F) Average traces of REMs in each participant during wakefulness (black, n=12) and REM (red, n=11). (G) Example of EOGs (top, red/blue), depth EEG (brown) and unit spiking activities in the MTL (black lines) during 20s of wakefulness. Vertical green lines depict detections of REM onsets. Note that some REMs are associated with a tendency of neurons to show transient spike-train responses shortly after REM onset.

Stability of unit recordings across several hours was assessed in detail (Figure S 3-1). Recordings also included synchronized scalp EEG, electrooculogram (EOG), electromyogram (EMG) and continuous video monitoring. Sleep–wake stages were scored following established guidelines (Iber et al., 2007). Sleep architecture and power spectra of scalp EEG were in general agreement with typical findings in healthy young adults.

REMs were detected in EOG traces in a semi-automatic fashion (Methods, Figure 3-1D-F). REMs were selected for further analysis when at least 20 events were detected for a given subject and sleep stage (n=12 and 11 individuals for wakefulness and REM sleep, respectively). On average, 3.7 ± 0.8 and 2.6 ± 0.5 REMs per minute were detected in REM sleep and wakefulness, respectively, while detection in NREM sleep was not significantly different from zero (Figure 3-1E; p=0.17, Mann-Whitney U-test, n=13 patients), attesting to a low rate of false detections. The relatively low density of REMs in wakefulness likely reflects the experimental setup (overnight recordings in darkness) and EOG measurements that best capture saccades with a large horizontal component (see Supplemental Note for further details).

The morphology of REMs in sleep and wakefulness was highly similar (Figure 3-1F), in line with previous studies (Sprenger et al., 2010; Takahashi and Atsumi, 1997). For example, when subtracting the EOG traces of w-REMs and s-REMs, no statistical differences were found (paired t-test, n=11 pairs, α=0.05, FDR correction for multiple comparisons).

Modulation of neuronal activity during rapid eye movements

We set out to examine if neuronal activity, especially that occurring in MTL regions including the amygdala, hippocampus, entorhinal cortex and parahippocampal gyrus (Table 3-1), is robustly modulated in concert with REMs, and to what extent such activity is reminiscent of visually evoked activity in wakefulness. To this end, we compared neuronal activity during (a) REM sleep ("s-REMs"), (b) spontaneous REMs in wakefulness ("w-REMs"), and (c) during a controlled visual stimulation paradigm in which subjects maintained fixation during short (200ms) presentation of images. Figure 3-1G depicts representative traces of eye movements along with simultaneously recorded neuronal activity and depth EEG in the MTL. As can be seen, in some cases REMs were associated with modulations in spiking activity.

We proceeded to quantify the REM-related changes in neuronal activity across the entire dataset, and further compared such activities to visually evoked responses to pictures of faces and places (n=133 responsive neurons out of 1457 overall; 27 sessions in 8 individuals, see Methods). A triggered-averaging analysis was performed around REM onsets, as well as following controlled visual stimulation (Figure 3-2). We examined simultaneously recorded scalp EEG (n=12, 10, and 4 electrodes located at Pz in wake, sleep, and visual experiment, respectively), depth EEG (n=53 (13 patients), 51 (11 patients), and 13 (2 patients) recording sites in wake, sleep, and visual experiment, respectively) and spiking activity within the MTL (n=437, 349, and 1049 in wake, sleep, and visual experiment, respectively).

Regions	Number of recorded units		% of modulated units		% of biphasic units		% of REMs with spike-trains	
	w-REMs	s-REMs	w-REMs	s-REMs	w-REMs	s-REMs	w-REMs	s-REMs
MTL								
Am	61 (6)	45 (5)	34.4 (3)	17.8 (3)	34.4 (5)	20.0 (4)	23.7	19.5
PHG	97 (7)	78 (6)	25.8 (6)	30.8 (5)	23.7 (6)	20.5 (6)	20.7	19.3
HC	100 (11)	80 (9)	27.0 (10)	31.3 (9)	19.0 (9)	15.0 (4)	20.8	16.1
EC	78 (6)	59 (5)	28.2 (6)	30.8 (6)	20.5 (6)	18.6 (5)	28.7	23.2
Total	336	217	28.3 (**)	27.9 (**)	23.5 (**)	18.3 (**)	23.5	19.5
Frontal								
AC	69 (6)	32 (5)	30.4 (4)	27.4 (3)	15.9 (4)	8.1 (3)	23.5	15.7
SMA	37 (3)	37 (3)	18.9 (1)	21.6 (2)	8.1 (2)	10.8 (2)	32.0	26.7
OFC	54 (6)	47 (5)	18.5 (4)	31.9 (4)	13.0 (3)	17.0 (5)	27.4	23.5
Total	160	146	23.8 (*)	27.4 (*)	13.1 (ns)	11.6 (ns)	27.6	22.0

Table 3-1 Bi-phasic single-unit modulation around REMs is more prevalent in the MTL compared to frontal regions.

The number of recorded units by brain region and vigilance state is depicted (1st column) along with the proportion of neurons modulated in any direction (2nd column) and those presenting a bi-phasic pattern of activity (decreasing activity before REMs and showing transient increases after REM onsets, 3rd column). For each region and each column, we indicated in parenthesis the number or patients in which these units were recorded. Statistical significance was established by comparing these proportions to those obtained for random time-points (paired Mann-Whitney U-test between real and surrogate proportions, n=8 and n=6 pairs in the MTL and frontal lobe, respectively). Note that significantly higher proportions of bi-phasic firing patterns were found only in MTL regions (*: $p<0.05$, **: $p<0.01$). , ns: $p\geq0.05$). Fourth column: the proportion of REMs associated with transient spike-train responses (see Supplemental Methods). On average, such spike-train responses were detected only for a minority of REMs.

Scalp event-related potentials (ERPs) around REMs (Figure 3-2B) during both sleep and wakefulness revealed a waveform in line with previous studies (Jagla et al., 2007), consisting of an initial transient peak before saccade onset ([-25 0]ms, $p<0.001$, one-tailed t-test compared to a [-800 -400]ms baseline) followed by a second positive component ([50 200]ms $p<0.001$). Following controlled visual stimulation, the scalp ERP exhibited a more delayed positive component ([200-600]ms, $p<0.05$) (Figure 3-2B, right). In the depth EEG ("dERP"), robust evoked potentials were found across MTL regions in relation to REMs with a similar positivity around 150ms as found in the scalp EEG ($p<0.01$, Figure 3-2C). This component was absent during visual presentation without eye movements ($p>0.8$, Figure 3-2C, right). Notwithstanding, a late negativity ([300 400]ms, $p<0.05$) was observed within the MTL after REMs in sleep and wakefulness as well as after the presentation of images with fixation. Since depth EEG signals were referenced to ear lobes (thereby attenuating ocular artifacts (Kovach et al., 2011)), the presence of robust dERPs in the MTL (and especially components occurring hundreds of milliseconds after eye movement onsets) suggests an underlying modulation of neuronal activity upon REMs in both sleep and wakefulness, whose late component is reminiscent of visual-evoked activity.

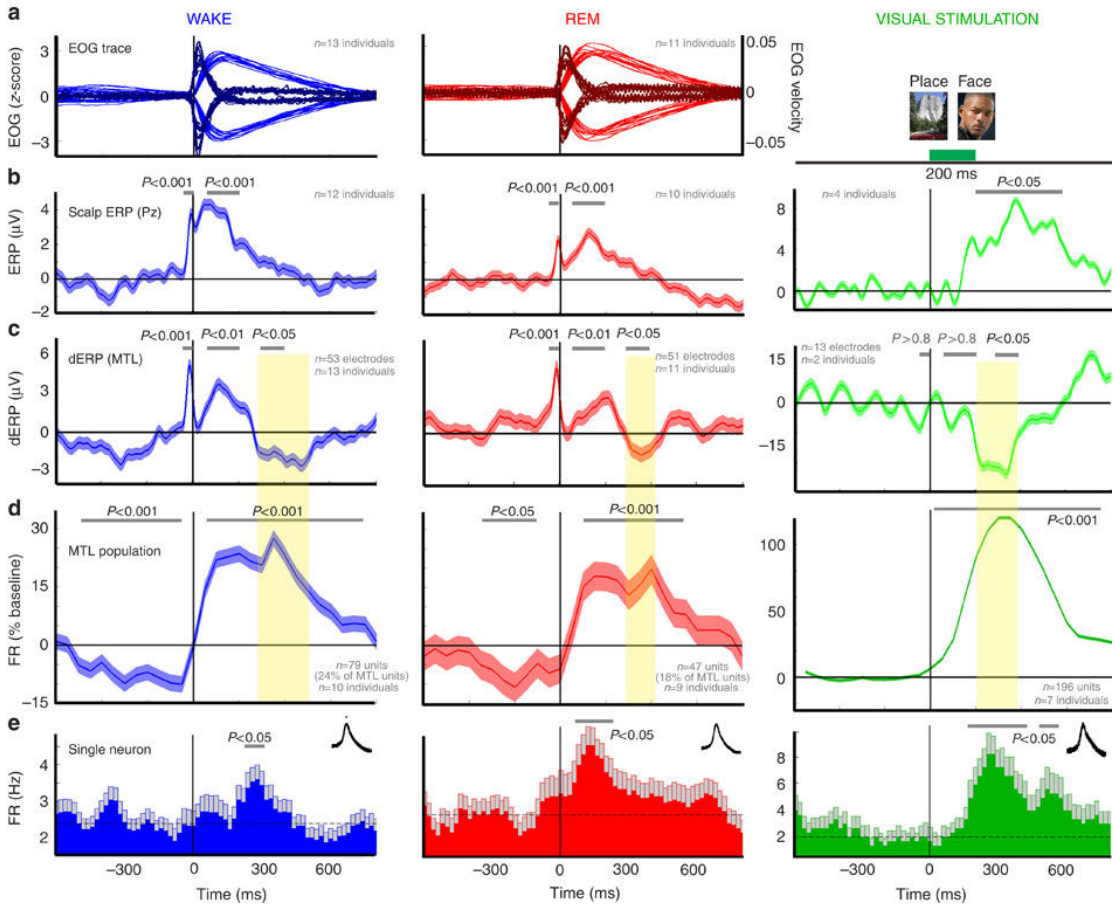

Figure 3-2 REM-triggered averaging of neuronal activity

REM-triggered averaging of multiple signals of interest in wakefulness (left) and REM sleep (middle), as well as during controlled visual stimulation (right). Intracranial recordings (panels C-E) focused on MTL regions. (A) Mean (± SEM) waveform of EOG traces (light colors: amplitude; dark colors, velocity). (B) Mean scalp ERPs computed at Pz. (C) Mean depth EEG potentials (dERP), (D) mean peri-REM time histogram for 'biphasic' MTL neurons in wakefulness (n=79 units, n=16,738 REMs), REM sleep (n=47 units, n=4,510 REMs), and visual stimulation (n=196 units, n=23,248 trials). Note the reduction in firing rate ([-400 0ms]) and increased activity ([150 550ms]) relative to REM onsets, and similar increased activity upon visual stimulation (right). Yellow shading highlights a time window in which negative components in the dERPs are associated with increase neuronal activity in all 3 conditions. Bars illustrate statistical deviances from baseline corrected for multiple comparisons (Methods). (E) Representative examples of activity in individual neurons (black inset: spike waveform) around REM onsets in wake and sleep (same neuron from parahippocampal gyrus), and visual stimulation (different neuron but from same brain region). Peri-REM-time histograms were computed on 120ms bins (100ms overlap). Mean firing rate of each neuron is marked with a dashed horizontal line, gray bars above illustrate statistically significant deviations from baseline (t-test, $p<0.05$). Error bars denote the SEM across patients (A,B), dEEG channels (C) or REMs (D,E).

Most importantly, single-unit spiking activity was robustly modulated around REMs, and this modulation was highly similar across wakefulness and REM sleep. A pattern consisting of a reduction in firing rate just before REM onsets, followed by subsequent increased spiking was observed in the average activity of all recorded units in wakefulness. A similar albeit weaker modulation was likewise observed in the average activity across all units during REM-sleep (Figure S 3-2A, n=412 and n=318 in wakefulness and sleep, respectively). We searched for neurons whose activity was

significantly modulated in any direction and at any time interval around REMs (see Methods and Figure S 3-2 for full details of selection process). From this unbiased approach, the stereotypical bi-phasic pattern of activity emerged in both sleep and wakefulness (Figure S 3-2B). We then focused on the units showing this bi-phasic pattern in MTL regions specifically for further analysis (Methods, see Figure 3-2D and E for MTL population average and representative neurons, respectively) since neurons that showed bi-phasic modulations around REMs were more readily observed in the MTL (Table 3-1, 24% of all MTL units in wake (n=79 in 10 patients) and 18% in REM sleep (n=47 in 9 patients)) compared with frontal lobe regions (13% in wake and 12% in REM sleep). In contrast, non bi-phasic modulation profiles were observed as frequently across regions (Table 3-1). Along the same line, when searching for bi-phasic activity profiles around random time-points (instead of real REMs) a significantly lower proportion of MTL neurons was found (one-tail paired Mann-Whitney U-Test, $p<0.01$, see Supplemental Material) but the proportion of frontal lobe neurons did not show such a difference ($p=0.9$). The higher proportion of bi-phasic modulations in the MTL argues against a global non-specific activity pattern.

Finally, the temporal dynamics of increased MTL firing following REMs was reminiscent of neuronal responses in the controlled visual experiment (Figure 3-2D,E, right), although these were of stronger amplitude ($p<0.001$) – a difference to be expected given that stimuli were specifically selected to drive strong responses in the recorded neurons (Methods). On average, around REMs, bi-phasic neurons reduced their firing by 11% in sleep and 7% in wake at -200ms ($p<0.005$, t-test) and increased their firing by 17% in sleep and 22% in wake at +250ms ($p<0.001$, t-test). The post-REM increase coincided in time with the negativity observed in the dERPs. The pre-REM reduction in firing was unrelated to effects of previous REMs, as it was similarly observed also when focusing on "isolated" REMs that did not occur in succession (not shown). In addition, visual responses were substantially later in time, peaking at 300ms after image onset, whereas post-REM activity peaked around 250ms after REM onset (equivalent roughly to 150ms after eventual fixation (Berchicci et al., 2012)). In summary, REMs in both sleep and wakefulness were associated with multiple signatures of transient neuronal activities in the MTL that were similar across vigilance states and reminiscent of visually evoked activity.

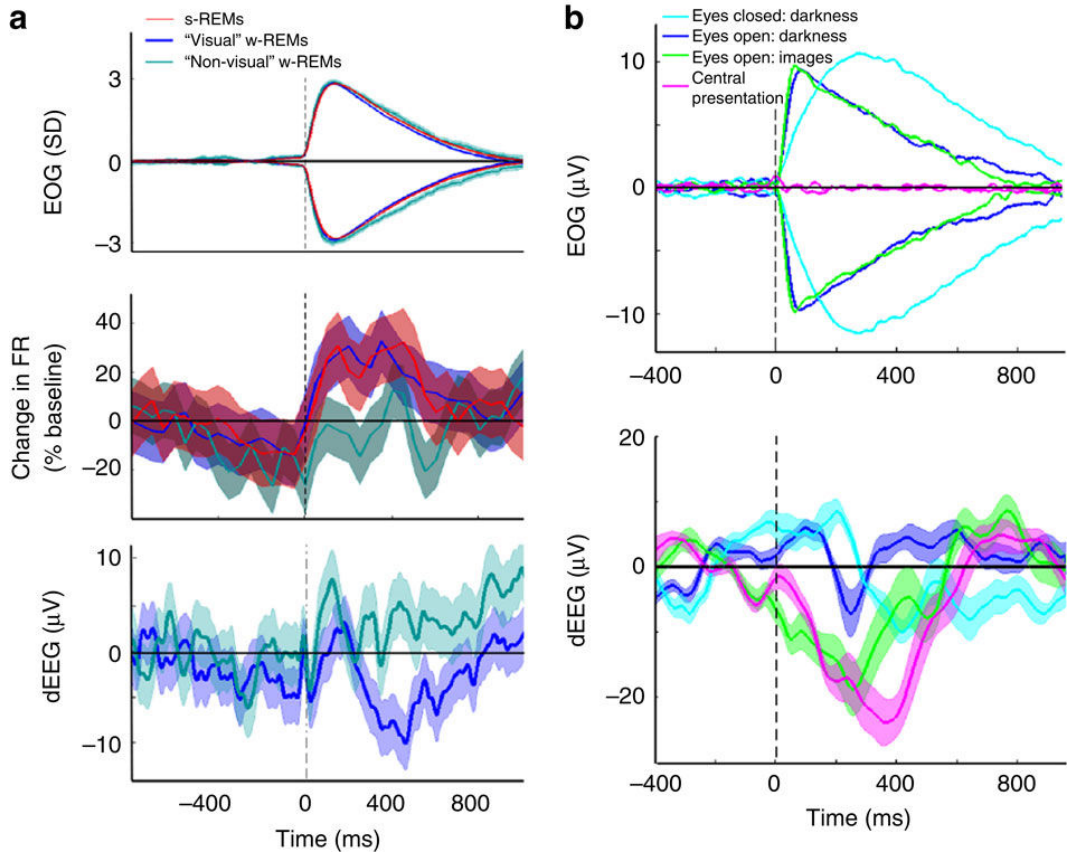

Figure 3-3 Comparison of neuronal activity underlying visual and non-visual REMs

(A) REM-triggered averaging of single-unit firing rate in wakefulness, separately for epochs tagged as 'non-visual' (open eyes in a dark room, green) or 'visual' (patient watching TV/DVD or interacting with people in a well-lit room, blue). s-REMs during REM sleep are superimposed for comparison (red). Top: Mean waveform of EOG traces for 'visual' w-REMs (blue), 'non-visual' w-REMs (green), and s-REMs (red) could not reveal differences between conditions. Middle: Average peri-REM-time-histogram ('visual': N=79 units and 1,250 REMs; 'non-visual': N=47 units and 140 REMs) expressed in percentage change of baseline. Statistical analysis matched for sample size (n=140 REMs in both conditions) revealed a significant decrease in firing rate prior to REM onsets for both 'visual' and 'non-visual' epochs, whereas a significant increase was observed following REM onsets only for 'visual' w-REMs ('visual': $p<0.05$, 'non-visual': $p=0.33$, Mann-Whitney U-test). Bottom: dERP time-locked to REMs onset ('visual': N=287 REMs in 70 channels, 'non-visual': N=287 REMs in 50 channels). Numbers of REMs were equated across conditions (n=287). Note the negative deflection between 200 and 500ms for 'visual' REMs only. Error-bars show standard-deviation across REMs. (B) Average EOG and intracranial dERPs in one participant when performing saccades in darkness with eyes-closed (cyan, N=42), eyes-open in darkness (dark blue, N=47), when performing saccades to pictures presented at the periphery (green, N=55) or when being presented with images directly at the center of fixation (magenta, N=59). Top: EOG traces corresponding to the 4 different experimental conditions. Note the major difference in shape between the eyes-closed and eyes-open conditions. Bottom: MTL dERPs time-locked to the onset of saccades/image presentation. Note that while evoked responses following image presentation and saccades appear similar, saccades in darkness reveal a much weaker or absent modulation.

To further investigate to what extent REM-related effects were driven by motor aspects of eye movements ('corollary discharge') vs. visual-like aspects, we further divided wakefulness into putatively 'visual' and 'non-visual' periods based on behavioral notes (e.g. watching television or meeting family in a well-lit room as 'visual' vs. lying with open

eyes in a dark room as 'non-visual', see Supplemental Methods). The rate of w-REMs in 'visual' periods was significantly greater than in 'non-visual' periods (14.7 ± 14.6 vs. 0.7 ± 2.8 REMs per minute, $p<0.05$, Mann-Whitney U-test). Analysis of evoked potentials (Figure 3-3) revealed that both 'visual' and 'non-visual' epochs were associated with a significant suppression of firing rates prior to REM onsets (difference from baseline: $p<0.01$, between 'visual' and 'non-visual': $p=0.09$, Mann-Whitney U-test, N=110 units and 140 REMs across 8 patients). However, only 'visual' epochs showed a robust increase in neuronal activity after REM onsets within the MTL (difference between 'visual' and baseline: $p<0.05$; 'non-visual' and baseline: $p=0.33$). Similarly, dERPs of 'visual' and 'non-visual' differed in their late negative potential (Figure 3-3A) which was present only for 'visual' REMs (significant difference observed 375-475ms after REM onset, t-test, $p<0.05$, FDR correction). Moreover, a controlled paradigm during wakefulness in one individual further compared neuronal modulations occurring around w-REMs with closed eyes or during darkness with saccades towards visual targets (or passive fixation). Interestingly, already at the level of EOG waveforms, eye movements with open eyes and those occurring during REM sleep were highly similar, whereas w-REMs with closed eyes during wakefulness had markedly slower kinematics (Figure 3-3B). Intracranial evoked potentials in the MTL revealed a negative deflection following image presentation that also resembled those found after REMs (in Figure 3-2C). This negative deflection was significantly attenuated during w-REMs without visual input (Figure 3-3B). Taken together, these results suggest that neuronal modulations within the MTL after REMs cannot be solely explained by a motor corollary discharge (see also Discussion).

Spike-train latency, selectivity, and theta phase reset

Given that the dominant pattern of neuronal activity around s-REMs included a transient increase in firing rate in the few hundred milliseconds following REM onsets, it was of interest to determine to what extent the detailed features of this activity resembled visual processing in wakefulness. In particular, a robust and recently described feature of human MTL responses to visual stimulation is the significant correlation between the latency and the selectivity of neuronal spike-trains, reflecting a hierarchical processing mode: a longer latency from image presentation is more readily found in neurons responding to fewer images (Mormann et al., 2008). We thus examined the presence and precise onset of spike-trains in individual trials following spontaneous REMs in sleep and wakefulness, as well as following controlled visual stimulation.

In MTL neurons, spike-trains were detected in 23.3 ± 1% (mean ± SEM) and 19.6 ± 1% of REMs in wakefulness and sleep respectively (N=209 and 152 units respectively). Despite the small subset of REMs associated with spike-trains, these events accounted well for the overall increase in firing rate (see Figure S 3-3). Moreover, the increase in firing rate for REMs associated with spike-trains was correlated across vigilance states even when regressing out the mean firing rate of each unit (Spearman's partial correlation: $r=0.28$, $p<0.01$, n=131 units in 8 patients). Furthermore, we found a significant correlation between the average latency of firing rate increase in each neuron (after REM onset) and its selectivity (tendency to increase firing rates only after a small subset of REMs, Methods). Figure 3-4A-C present this correlation for w-REMs (Spearman's rank correlation, $r = 0.26$, $p = 10^{-4}$, n=209 in 10 patients), s-REMs ($r = 0.33$, $p = 10^{-6}$, n=152 in 10 patients), and controlled visual stimulation ($r = 0.48$, $p = 10^{-8}$, n=142 in 9 patients). Crucially, when applying the same analysis on random time-points during REM sleep (not associated with eye movements), latency and selectivity were not significantly correlated ($p=0.3$ and $p=0.9$ for sleep and wake), indicating that this relation

occurred at specific moments, rather than reflecting basic properties of neuronal firing such as the average discharge rate. Moreover, in those cases where the same neurons were recorded in both wakefulness and REM sleep, the selectivity of neurons was highly correlated across vigilance states ($r = 0.71$, $p = 10^{-23}$, n=131 units in 8 patients, Figure 3-4D) such that neurons that were highly selective in their visual responses in wake also showed spike-trains following few s-REMs. This relation was conserved even when taking into account the average firing rate of these neurons (partial correlation: $r = 0.51$, $p = 10^{-11}$, n=131 units in 8 patients). The average latencies of neurons were also correlated across vigilance states (r=0.20, p=0.02, n=131 units in 8 patients) however this correlation was not significant when regressing out the average firing rate (partial correlation: r=0.09, p=0.3, n=131 units in 8 patients).

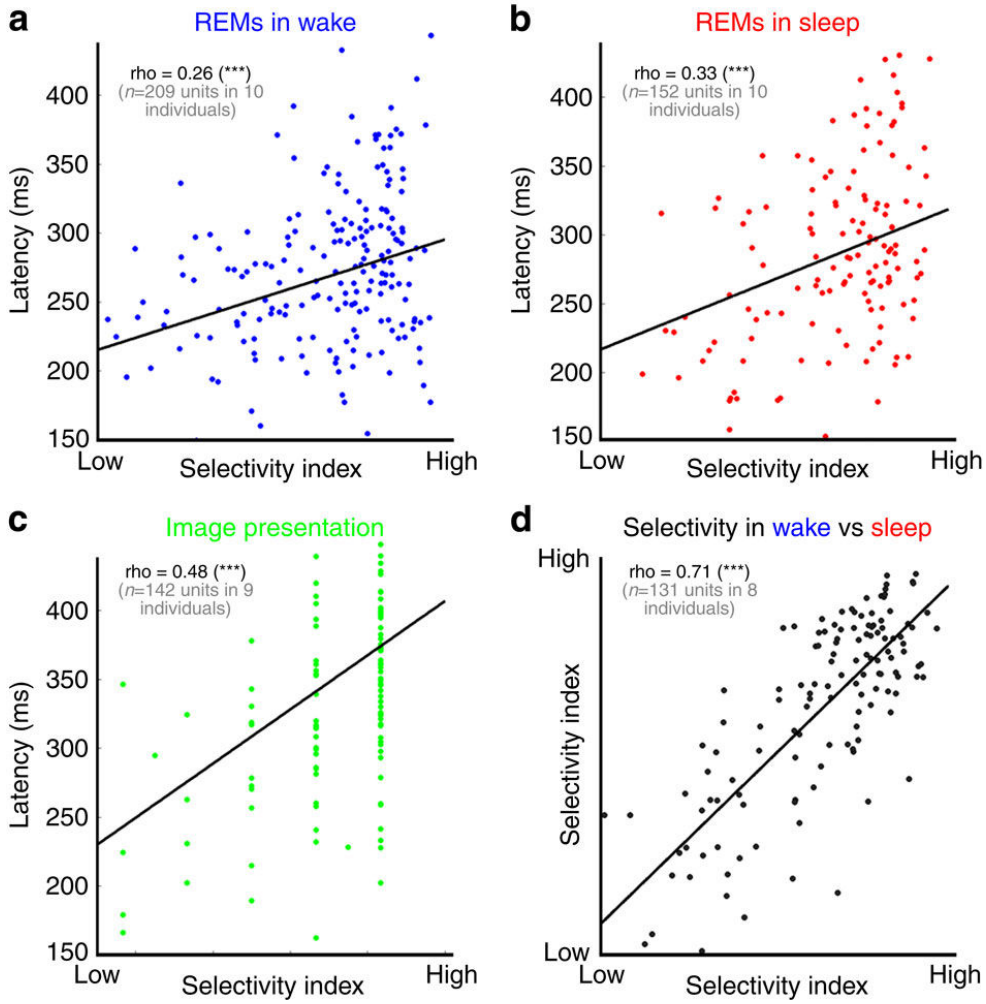

Figure 3-4 Comparison of transient spike-train properties in REM sleep and wakefulness

(A-C) Scatter plot of spike-train latency (ordinate) vs. selectivity (abscissa, percent of trials eliciting a spike-train after REMs or image presentations) in w-REMs (A), s-REMs (B), and in the visual stimulation experiment (C). Low selectivity: neurons responds to all REMs/pictures; high selectivity: neurons responds to few REMs/pictures. Selectivity in panel (C) is restricted to a limited number of discrete values due to the use of 6 images in the image presentation experiment. Note that in all three conditions a robust correlation was observed, indicating the existence of hierarchical processing along the visual-mnemonic axis. Such correlation could not be revealed in random time points during REM sleep and wake. (D) Selectivity following REMs is correlated in the same neurons across wakefulness and sleep (Spearman's rank correlation, $r = 0.71$, $p = 10^{-23}$; partial correlation taking average firing rate into account: $r = 0.51$, $p=10^{-11}$).

Finally, it is well established that theta (4-8Hz) oscillations prevail in the MTL during both wakefulness and REM sleep (Buzsáki, 2006) and that the phase of theta oscillations is reset upon engagement of visual-mnemonic mechanisms in humans (Rutishauser et al., 2010) and monkeys (Ito et al., 2011). We found comparable phase resets around 2-6Hz ('human theta', see (Watrous et al., 2011)) in s-REMs and w-REMs. A brief and broadband reset was visible at REM onsets (potentially reflecting a myogenic contamination) followed by a delayed, sustained, and frequency-specific increase in phase coherence around 2-6Hz (see Methods and Figure 3-5A,B). Such theta-band coherence was correlated across vigilance states (Pearson's r=0.27, p<0.05, see Supplemental Methods). Following controlled visual stimulation, stronger phase reset was observed in the MTL and the maximal effect occurred at similar time-frequency windows (Figure 3-5C).

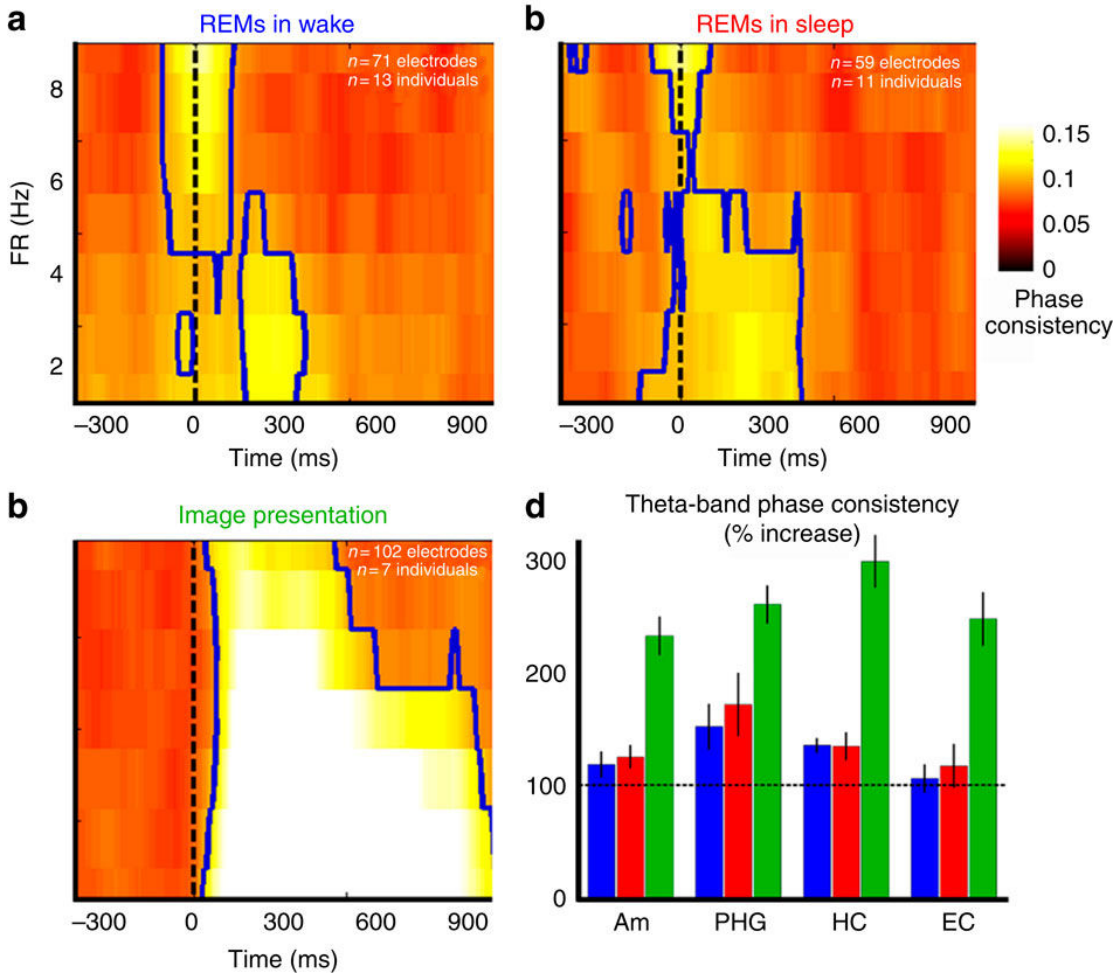

Figure 3-5 Reset of field oscillation phase following REMs and visual stimulation

(A-C) Phase consistency of intracranial dEEG within the MTL across time and frequency around w-REMs (A, N=71 channels), s-REMs (B, N=59 channels) and in the visual stimulation experiment (C, N=102 channels). Note that a significant increase within the lower theta-band (2-6Hz) can be seen in all conditions from 0 to ~400ms (blue lines: A,B: p<0.05; C: p<10-4, FDR correction). Following controlled image presentation a stronger phase reset is observed and the maximal effect occurs at similar time-frequency windows. (D) Phase coherence of dEEG by MTL region within the theta-band (2-6 Hz) following REMs in wakefulness (blue) and during REM-sleep (red) compared to controlled image presentation (green). Error-bars show SEM across channels. Phase coherence was averaged during the first 400ms following REMs or image onset.

When considering MTL regions separately (Figure 3-5D), hippocampus and parahippocampal gyrus showed strong phase resets while the entorhinal cortex did not show phase coherence above chance levels. These effects were consistant across vigilance states (ANOVA, effect of regions: $p<0.005$, $F=4.8$; effect of state: $p=0.4$, $F=0.6$). Similar differences between the theta phase coherence across MTL regions were observed during controlled imaged presentation. The stronger and delayed effects during controlled visual fixation (in comparison to REMs) mirrored those found in dERPs and single-unit firing rates (Figure 3-2 and Figure 3-3). Thus, the temporal dynamics of MTL activity were similar during REM sleep and during visual processing in wakefulness, possibly reflecting a partial conservation of the hierarchical processing in the visuo-mnemonic pathway.

Discussion

Despite decades of intense interest and debate, it has remained difficult to determine to what extent eye movements in REM sleep modulate brain activity. In this study, we show for the first time that in human REM sleep s-REMs were associated with transient bi-phasic modulations of spiking activity in the MTL associated with evoked potentials in depth EEG signals. A significant subset of MTL neurons exhibited a transient spike-train immediately following some s-REMs, as is the case during wakefulness. Indeed, multiple properties of this activity - including spike-train latency, selectivity, and the phase of simultaneous theta oscillations - were comparable during sleep and wakefulness and reminiscent of visual-mnemonic responses.

It is likely that dERPs co-occurring with modulations of neuronal activity are closely related to PGO waves, a hallmark of REM sleep (Amzica and Steriade, 1996; Gucer and Viernstein, 1979; Jouvet, 1992). PGO waves are sharp field potentials occurring concomitantly with s-REMs and were first observed in the pons, lateral geniculate nucleus and occipital cortex of cats. Recent studies described similar phenomena in humans (Ioannides, 2004; Lim et al., 2007; Miyauchi et al., 2009; P. Peigneux et al., 2001). Originally, PGO waves were believed to occur exclusively during sleep and only in the aforementioned brain structures (Brooks and Bizzi, 1963; Jouvet and Michel, 1959), but subsequent evidence suggested they are akin to visually evoked potentials (Brooks, 1968a; Mccarley et al., 1983) and that PGO potentials similar to the current dERPs occur across wide cortical territories (Brooks, 1968b). Although our electrode locations cannot unequivocally confirm the relation with PGO waves, it seems likely that the evoked potentials time-locked to s-REMs are closely related to PGO potentials.

The transient reduction in MTL neuronal activity immediately before REM onsets could be related to saccadic suppression (Uematsu et al., 2013), a behavioral phenomenon reflecting a transient increase in visual perception thresholds during saccades (Dodge, 1905; Wurtz et al., 2011). Saccadic suppression was initially attributed to degraded retinal input, but later studies pointed to a more complex process (Ibbotson and Krekelberg, 2011). However, the decreases in activity observed here may be somewhat earlier and longer in duration than to be expected, and future studies are needed to establish this connection.

Despite the resemblance between neuronal activity around REMs and following controlled visual presentation, post-REM modulation in both sleep and wake occurred earlier than that occurring during visual processing with fixation. In the ventral visual stream of awake macaques (V4, IT), visual responses during fixation are typically observed after 100-200ms (Thorpe and Fabre-Thorpe, 2001). In contrast, REMs in monkeys are associated with earlier modulations shortly after eventual fixation (Chelazzi et al., 2001; Jagadeesh et al., 2001; Rajkai et al., 2008), in line with the difference observed here. Why is activity around REMs earlier than during passive vision? One possibility is that the observed neuronal modulations reflect some form of 'attentional priming' (see below), rather than visual processing. Alternatively, during REMs some predictive expectation already exists and drives earlier visual activity in the neurons that will participate in representing the new image.

It is important to explicitly acknowledge several limitations of the present study. First, recordings were obtained in patients with refractory epilepsy. However, great care was taken to discard data recorded in close proximity to seizures, from epileptogenic regions, and to avoid REMs temporally close to interictal epileptic spikes (see Methods). In addition, it is well established that paroxysmal activities are far less prevalent during REM sleep (Nir et al., 2014). Finally, sleep architectures and grapho-elements were quantitatively and qualitatively within the range of those observed in healthy individuals(Andrillon et al., 2011; Nir et al., 2011). Second, dream reports were not collected. Nevertheless, given that the vast majority of awakenings from REM sleep yield vivid dream recalls (Nir and Tononi, 2010), it seems reasonable to assume that REM episodes analyzed here were likewise associated with dreaming. It is, however, important to note that dreams also occur during NREM sleep (Nir and Tononi, 2010), hence REMs may not be necessary for dream imagery. In addition, we were only able to acquire data in one individual during negative-control paradigms in wakefulness (i.e. REMs during eye closure or darkness), however the available data as well as retrospective analysis based on behavioral notes yielded significant differences. Finally, electrode locations were determined exclusively by clinical criteria and therefore it was not possible to examine activity in regions where PGO waves occur, or in brain regions implicated in saccade preparation. Indeed, neuronal dynamics in motor preparation centers giving rise to REMs may differ in sleep and wakefulness (Abe et al., 2004).

What is the functional significance of the current results? One possible explanation is that such modulation reflects a motor corollary discharge driven by oculo-motor networks, but several arguments suggest that this is an insufficient explanation: (a) The post-REM increase in spiking activity during sleep exhibits several detailed characteristics observed also during wakefulness (and upon visual processing), and therefore cannot be dismissed as a non-specific effect. Accordingly, individual neurons with longer spike-train latencies after s-REMs also exhibited greater selectivity, as in vision (Mormann et al., 2008). Both the magnitude and the selectivity of the response in individual units were stable across sleep and wakefulness. Moreover, such spike-train responses were associated with a phase reset of MTL theta oscillations; (b) we found different neuronal modulations after w-REMs associated with vision in comparison to non-visual contexts such as darkness (Figure 3-3). Along this line, the late ('lambda') component following saccades in human scalp ERPs is abolished in total darkness (Miyauchi et al., 1987). Although in monkeys w-REMs during darkness are also accompanied by a bi-phasic modulation of firing rates in occipitotemporal cortex and MTL, such modulation is weaker than that found during vision, as we observe here (Gallant et al., 1998; Jeannerod and Sakai, 1970; Kayama et al., 1979; Nakamura and Colby, 2000; Rajkai et al., 2008; Reppas et al., 2002; Ringo et al., 1994; Sobotka et al., 1997); (c) the fact that effects were strongest in the MTL (where retinotopic (re)mapping plays a minor role and where activity is tightly correlated with visual-mnemonic representations in humans) seems incompatible with a motor-only interpretation; (d) the timing of human MTL activity following REMs is still later than that following REMs in homologous macaque cortex as observed during visual processing. It seems more reasonable to expect such timing differences across species for visual-like, rather than motor, phenomena.

A second possibility is that REMs transiently increase cortical excitability and represent attentional shifts that 'reset' processing frames (Duhamel et al., 1992; Hamker et al., 2011; Kleiser et al., 2004). Brief pre-REM decreases in neuronal activity may prepare the ground for subsequent processing by increasing sensitivity to inputs and amplifying responses, thereby enhancing the signal-to-noise ratio. In addition, the observed

neuronal modulations co-occurred with a theta phase reset in the MTL, as in monkeys (Purpura et al., 2003). Modulations of hippocampal oscillatory activity in primates was found to be predictive of subsequent recognition in wakefulness (Ito et al., 2011; Jutras et al., 2013; Rutishauser et al., 2010). In this context, our findings support the notion that theta in primate MTL may play an important role in exploration of the visual (or mental) space (Killian et al., 2012). While the underlying mechanisms remain unclear, cholinergic modulations associated with PGO waves and theta oscillations may play an important role (Kramis et al., 1975; Steriade et al., 1990). The fact that peri-saccadic modulations in both sleep and wakefulness are earlier than those found during vision may further support the 'attentional reset' interpretation.

Finally, given that activity in the human MTL is tightly correlated with visual awareness (Rees et al., 2002), the current results may imply that REMs during sleep reflect a change of the visual imagery in dreams, but future studies are needed to unequivocally establish this possibility. In summary, the results establish that eye movements in REM sleep are associated with successive "micro-states" of cortical activity(Jones et al., 2007; Lehmann, 1971) and represent transitions between discrete epochs of visual-like processing. These findings open new paths for exploring in more detail the prospective roles of eye movements and intrinsic brain activity during sleep.

Methods

Subjects, data acquisition, and experimental paradigms

General procedures related to data acquisition have been described in detail elsewhere (Nir et al., 2011). Here, we examined 19 neurosurgical epilepsy patients (ages 19-52, 11 females). Patients provided written informed consent prior to participation in the research study, under the approval of the Medical IRB at UCLA. 13 patients participated in full-night sleep studies that also included epochs of wakefulness. Sleep-wake stages were scored off-line according to established guidelines (Iber et al., 2007). In each participant, 8-12 depth electrodes recorded intracranial depth EEG and single-unit activities, along with continuous video, EOG, EMG and scalp EEG from four scalp derivations, as in (Nir et al., 2011). Eight participants (four participated in the sleep studies) also performed a visual object recognition paradigm (n=27 sessions) that included 2 blocks * 12 minutes, when 24 trials * 12 pictures of famous people and landmarks were presented for 200ms on a laptop while participants performed a categorization task. One individual participated in a paradigm during wakefulness directly comparing activity during w-REMs in darkness, with closed eyes, towards visual targets and during visual stimulation with fixation. Spike sorting was performed offline separately for spontaneous sleep/wake data (n=600) and for visual stimulation sessions (n=1334) using 'wave_clus' (Nir et al., 2011; Quiroga et al., 2004).

Eye movement detection

Eye movements were detected through EOG recordings. Although indirect, this measure can be used to reliably infer about saccadic eye movements in both open eyes and closed eyes conditions (see Supplemental Note). EOG traces were obtained using two electrodes pasted below the left and above the right canthi, referenced to contralateral ear lobe signals. REMs were detected in a semi-automatic manner (Figure 3-1D) by applying a bandpass filter (0.1-3 Hz), setting a detection threshold (mean + 2 SD) and verifying: (a) duration < 1.5s, (b) opposite polarity across the two leads (corresponding to horizontal movements), (c) maximal slope > 1μV/ms, and (d) no interictal spikes within 0.5s. These parameters were chosen after careful visual examination of detected REMs. REM onsets were defined automatically as the first crossing of the 2 raw EOGs traces before the crossing of the detection threshold. All REM detections were verified visually. In addition, random time-points were selected from the same 10s segments but at least 4s away from any EOG deflections, serving as control epochs devoid of any ocular activity but matched in terms of occurrence rate and position within the ultradian cycle. Latency and selectivity were computed from these random time-points as a control and then compared to real REMs onsets (see Results section).

REM-triggered averaging

Evoked potentials were obtained by averaging scalp EEG (ERP) and depth EEG (dERP) signals around REM onsets, after preprocessing (notch filter at 60Hz and harmonics, band-passed between 0.1 and 30Hz), mean subtraction (using a [-800 -400]ms interval), selecting epochs devoid of interictal spikes, and smoothing with a Gaussian kernel of 5ms (80ms in Figure 3-3B). In addition, for each unit separately, an average peri-REM time histogram (PRTH) was computed using 100ms bins (50ms overlap, see Supplemental Methods). A mean PRTH across all neurons (Figure S 3-2A), all modulated neurons (Figure S 3-2B), and all bi-phasic units (Figure S 3-2C) was computed after

normalizing each neuron's PRTH (% of baseline activity at [-800 -400]ms). Due to the predominance of bi-phasic units within the MTL, subsequent analysis (as shown in Figure 3-2D and Figure 3-3A) were only performed for neurons within the MTL exhibiting significant bi-phasic modulations around REMs (see also Supplemental Methods).

Analysis of spike-train properties

Occurrence and latencies of spike-trains in individual trials (REMs or images) were determined by a Poisson spike train analysis as in (Hanes et al., 1995), separately for s-REMs, w-REMs, and following controlled visual stimulation. Selectivity was defined as: 100% - the percent of trials (either REMs or visual stimuli) for which a spike-train was detected. Comparison between individual neurons in wake and sleep (n=131, Figure 3-4D) focused on those neurons that were recorded in both vigilance states.

Theta Phase Consistency

Consistency of the phase in the time-frequency domain was determined by extracting the phase of EEG oscillations for each REM/image. Then, for each frequency-bin and time-interval, we estimated the consistency of the phase across REMs/images for a given dEEG channel. Statistical differences were evaluated by comparing each time and frequency point to baseline values and correcting for multiple comparisons (Supplemental Methods).

Supplemental Methods

Subjects

Nineteen patients with pharmacologically intractable epilepsy (ages 19-52, 11 females) underwent monitoring with depth electrodes for seizure foci identification and potential surgical treatment (Fried et al., 1999a). Patients provided written informed consent prior to participation in the research study, under the approval of the Medical Institutional Review Board at the University of California, Los Angeles, USA. Electrode location was based only on clinical criteria, and Itzhak Fried performed all surgery. For each subject, localization of the seizure onset zone was based on recordings during hospital monitoring, in combination with prior functional and anatomical neuroimaging (Nir et al., 2011). Thirteen patients participated in a full overnight sleep study that also included epochs of wakefulness, nine patients participated in a visual object recognition paradigm (four of these individuals participated in both experiments), and one individual participated in a paradigm directly comparing activity around eye movements in darkness, with closed eyes, towards visual targets and during visual stimulation with fixation during wakefulness.

Data Acquisition

For each patient, 8 to 12 flexible polyurethane depth electrodes (1.25 mm diameter, see Figure 3-1B) were placed in some of the following regions: hippocampus, amygdala, entorhinal cortex, parahippocampal gyrus, temporal gyrus, fusiform gyrus, temporo-occipital junction; anterior, middle and posterior cingulate; supplementary motor area, inferior frontal gyrus, orbitofrontal cortex, and parietal cortex. Electrode location varied between patients based on their clinical profiles (see Figure 3-1C for an overview). Electrode positions were verified using post-implant computed tomography (CT) co-registered with pre-implant magnetic resonance (MR) imaging (Brain Navigator, Grass-Telefactor Corp., Philadelphia, PA). Scalp and intracranial depth EEG data were continuously recorded, sampled at 2 kHz, bandpass-filtered in hardware between 0.1Hz and 500Hz and re-referenced offline to the mean signal of the earlobes electrodes. Scalp EEG (C3, C4, Pz and Fz), EOG, EMG, video, and behavioral observations were collected and preprocessed according to established guidelines for sleep study ploysomnography (Iber et al., 2007) (see Figure 3-1A). The two EOG electrodes (used for REM detection) were pasted below the left and above the right canthi and referenced to the contralateral ear lobe.

In addition, each depth electrode terminated in a set of eight insulated 40-μm platinum-iridium microwires (impedances 200 to 500 kΩ, see Figure 3-1B) (Fried et al., 1999a). Microwire signals were simultaneously recorded continuously (Cheetah Recording System; Neuralynx, Tucson, AZ for 10 patients; Neuroport Recording System; Blackrock, Salt Lake City, UT for 9 patients), sampled at 28 kHz (10 patients) or 30 kHz (9 patients), band-pass filtered in hardware between 1Hz and 9kHz, and referenced locally to a ninth non-insulated microwire.

Unit identification and spike sorting

Units were identified using the 'wave_clus' software package (Quiroga et al., 2004) as follows: (i) extracellular microwire recordings were highpass filtered above 300Hz, (ii) a 5 SD threshold above the median noise level was computed, (iii) detected events were categorized into either real clusters or noise based on the reliability of action potential waveforms and by the presence of a refractory period for single units, as in 23 (see Figure S 3-1A). The enduring nature of unit recordings throughout hours of continuous recordings (sleep studies: ~7h) was assessed by ensuring that action potential waveforms, and inter-spike-interval distributions were conserved in 1-hour intervals and that clusters remained separable throughout the recording session (see Figure S 3-1B). Overall, 600 units were identified for full-night sleep/wake recordings (355 putative single units, 245 multi-unit clusters) and 1,334 units for the visual stimulation sessions (541 putative single units, 916 multi-unit clusters).

Polysomnographic sleep studies

Sleep recordings were conducted at a minimal interval of 12 hours from identifiable seizures, 48-72 hr after surgery, and lasted for about 7 hours between 23:00 and 06:00. Sleep-wake stages (wakefulness, NREM sleep stages N1-N3 and REM sleep) were scored according to established guidelines (Iber et al., 2007). Additional information about sleep properties, hypnograms and power spectra of scalp EEG were can be found in previous publications (Andrillon et al., 2011; Nir et al., 2011). Wakefulness data relate here to periods preceding or following sleep as well as awakenings during sleep. On average, during these night recordings, patients had 4.5 (SD=2.2) continuous epochs of, at least, 1 minute of data scored as wakefulness (mean duration: 17.8 min, SD=15.2).

Behavioral notes during sleep studies were carefully examined to putatively distinguish between 'visual' and 'non-visual' epochs of wakefulness. Accordingly, in eight participants we were able to identify epochs which were either mostly 'non visual' (participant had open eyes while seated or lying in bed in a dark room; a total of 140 w-REMs in 304 minutes, 10% of REMs), or mostly 'visual' (participant actively watching TV/DVD or interacting with other people in a well-lit room; a total of 1250 w-REMs in 355 minutes). In order to compare neuronal firing rates around these 'visual' and 'non-visual' events (Figure 3-3A middle), we randomly selected 140 'visual' w-REMs (among 1,250) to yield an equal number of 'visual' and 'non-visual' REMs (287 REMs for the dEEG analysis, Figure 3-3A bottom). Firing rates ±500ms around REM onsets were compared to the baseline activity ([-800, -500]ms) across bi-phasic units and REMs (see Methods and below for a definition of bi-phasic units).

Visual stimulation studies

Eight patients participated in 22 sessions of a visual object recognition paradigm (2 sets of 6 pictures each). When possible, pictures were chosen based on their effectiveness in eliciting responses in the recorded neurons by means of a 'visual screening' experiment performed earlier that day (Quiroga et al., 2005). Each session included two blocks, lasting 12 minutes each. During each block, 4 face and 2 place images were presented on a laptop computer for 200ms while subjects performed a face/place task. Each picture

was presented 24 times in a pseudo-randomized order, with pseudo-random inter-stimulus intervals of 2-8s (uniform distribution).

Wakefulness eye movement paradigm

One individual participated in an eye-movement paradigm including four different experimental conditions examined in separate blocks: (a) saccades in darkness with open eyes, (b) saccades in darkness with closed eyes, (c) saccades to pictures presented at the periphery, (d) image presentation at the center of fixation. In the first two blocks (saccades in darkness), each trial started with a central fixation (white cross displayed on a portable computer screen superimposed on a dark background for [300 to 600]ms). A tone was then played (3,000 or 1,000 Hz, duration: 400ms), such that the low/high pitch tones instructed the patient to perform a horizontal saccade towards the left/right sides of the screen. The participant was instructed to maintain peripheral fixation for [1400 to 1700]ms until the appearance of a double beep (2,000 Hz, duration: 300ms) after which participant had to fixate at the central cross again, in preparation for the next trial. The next trials started after a [1600 to 1900]ms period and the central fixation cross was not visible while gaze was directed at the periphery. In each block (see above) a total of 30 saccades were made to each direction. In the 3rd block (saccades to pictures), trials likewise began with central fixation for [300 to 600]ms, after which a beep was played (2,000 Hz, duration: 400ms) and an image appeared at the periphery either to the left or right side of the screen. The subject was instructed to make a saccade toward the picture and to maintain the fixation for [1400 to 1700]ms until it disappeared. Then, the patient had to make a saccade back to the center where the central fixation cross re-appeared. Ten pictures were displayed 6 times each, randomly in either the left or right visual field. The next trial started after a [1600 to 1900]ms period. Finally, in the 4th block (vision with fixation), the participant was instructed to maintain fixation on a central cross while pictures appeared at random intervals. The participant followed a face/place categorization task by pressing two keyboard buttons; ten images (5 places, 5 faces) were presented 6 times each.

Detection of Rapid-Eye Movements (REMs)

We used EOG recordings as a proxy to track saccadic eye movements in wakefulness and sleep. EOG constitutes a reliable indirect measure of eye position even through closed eye-lids (see Supplemental Note). REMs were detected in a semi-automatic manner as illustrated in Figure 3-1D. The two EOG signals (Figure 3-1D, 1st row, blue and red curves) were first band-pass filtered between 0.1 and 3 Hz using a zero-phase 2nd-order Butterworth filter, to attenuate fast background activity (Figure 3-1D, 2nd row). A detection threshold was then set at mean + 2 SD of the EOG signals across the whole night (epochs with absolute amplitude over 1,000μV were discarded from this computation so that such abnormal voltage would not influence our estimation) (Figure 3-1D, 2nd row). Events crossing this threshold were considered REMs candidates (Figure 3-1D, 3rd row) and further inspected so that (1) the segments above threshold had a duration of less than 1.5s; (2) they corresponded to an amplitude exceeding an equivalent threshold in the other EOG trace and of *opposite* sign; (3) their maximal slope (temporal 1st derivative) was above a threshold of 1μV/ms (Figure 3-1D, 4th row). We discarded REMs too close to each other (<0.5s) as well as REMs in close vicinity (within 0.5s) with

detected epileptiform interictal spikes (rare). However, REMs tended to cluster in close succession, as illustrated in Figure 3-1G. Accordingly, 30±3% and 30±4% of REM onsets appeared within 1s from another REM onset in wakefulness and REM-sleep, respectively, Consequently, in both wakefulness and REM-sleep, the typical inter-REM interval was shorter than the expected value when considering uniform REM density across time (around 2.0s on average in wakefulness, see Supplemental Note and Figure 3-1). Possible residues of epileptiform interictal spikes were identified in the EOG signal by searching for abnormal increase (absolute amplitude superior to mean + 10 SD) in the 100-150 Hz band (Figure 3-1D, 5th row). We converged on these parameters after careful visual examination of the detected REMs and rejected candidates. We selected only the EOGs deflections with opposite phases since they correspond, in our EOG montage, to horizontal eye movements. Signal deflections that were in-phase across the two EOG traces were not analyzed since these may reflect either vertical eye movements or cortical potentials such as slow waves "leaking" to EOG measurements. REM onsets were defined automatically as the first crossing of the 2 raw EOGs traces before detected REMs (Figure 3-1D, 6th row). To ensure the quality of this detection scheme, *all* the automatically detected REMs and respective onset times were visually inspected. REM onsets were used as reference time points throughout our analysis, but considering other time (peaks of REMs, times of maximal slope) did not significantly alter the main results reported. In order to minimize the influence of outliers on inter-subjects or inter-units averaging, epochs of REM sleep and wakefulness with less than 20 REMs were discarded for each patient from subsequent analysis (except for the 'visual' vs. 'non-visual' comparison). In addition to this detection, random epochs were selected to be used as a control data set. For each identified REM, we detected nearby 2s epochs (within 10s of real REMs) during which there was no significant increase in either EOG channel and no traces of epileptiform interictal spikes. These "random" events matched REMs detection in terms of frequency of occurrence, sleep stages and presence within the ultradian cycle (i.e. time within sleep) for each patient.

Evoked potentials in scalp and depth EEG

Evoked potentials for depth EEG channels (dERP) in the MTL were computed as follows. Depth EEG channels were segmented in 10s segments, notch-filtered (2nd-order IIR notch filter at 60 Hz and harmonics) to eliminate electrical noise, bandpass-filtered (4th-order Butterworth filter between 0.1 and 30Hz) and corrected for baseline activity by subtracting the mean amplitude across 10s segments. Epochs around REMs onsets were selected ([-800 1000] ms) and averaged by channel and vigilance state. Statistical deviance between dERPs (around REMs) and baseline ([-800, -400]ms) was assessed using a paired t-test (alpha=0.05, n=11 patients) on fixed windows (pre-REMs: [-50 0]ms, post-REMs: [50 200]ms and late-component: [300 400]ms in the sleep study, [200 600]ms for image presentation) in order to match common components across conditions.

Analysis of spiking activities during REMs

A triggered-averaging analysis computing peri-REM-time histograms (PRTH) was performed for each unit separately as follows. Spike data were time-locked to REM onsets and averaged across REMs (Figure 3-2D,E) or units (Figure S 3-2) on a [-800, 1000]ms window with 100ms bins (50ms overlap). Only REMs showing at least one spike in the [-800, 1000]ms window were included in PRTHs (for MTL units: n=16,738

events in wakefulness and 4,510 in REM-sleep). Individual neuronal activity was normalized on a [-800, -400]ms window and expressed as a percentage of baseline activity. In Figure S 3-2, MTL and non-MTL units were averaged together. Only units with at least 10 remaining REMs were included in the PRTH for Figure S 3-2.

When considering all units from all recorded brain regions (Figure S 3-2, top), a clear bi-phasic pattern appeared in wakefulness with a reduction in neuronal activity just before REM onset akin to saccadic suppression evidenced in monkeys (Bremmer et al., 2009) ([-100, -50]ms) followed by an increase in neural activity. This increase lasted for about 500ms after REM onsets, which is in accordance with latencies observed in MTL units in response to visual stimuli (Mormann et al., 2008). Interestingly, a similar (albeit smaller) increase was observed in REM-sleep between unit discharges after REM onsets ([50, 400]ms) and either (i) pre-onset activity ([-100, -50]ms): one-tailed t-test $p<0.01$) or (ii) baseline ($p<0.05$). Significant modulations were then detected unit-by-unit by comparing each bin separately to PRTHs of the same unit computed around random epochs via bootstrapping: for each time-interval, the real firing rate around REMs was compared to surrogate values computed around random epochs across 500 iterations and compared via a paired Mann-Whitney U-test ($\alpha=0.005$, uncorrected). To facilitate averaging between low- and high-firing rate neurons, the mean PRTH across all modulated neurons was computed after normalization of each neuron's PRTH by the average firing rate over the entire window ([-800, 1000ms]). Figure S 3-2 (middle row) shows the emergence of a bi-phasic modulation pattern around REMs (activity over [50, 400]ms > [-100, 50]ms or baseline activity, one-tailed t-tests, $p<0.05$) despite the fact that our selection criterion did not impose a particular directionality.

Subsequently, in order to focus on units showing a significant bi-phasic modulations resembling the pattern emerging from the neuronal population, we specifically selected units showing a significant increase in neuronal activity by comparing the average firing rate across REMs per unit and per sleep stage before ([-500, 0]ms) and after ([100, 600]ms) REM onsets (one-tailed sign-test, $\alpha=0.1$). Figure S 3-2 (bottom row) shows the equivalent PRTHs for all units from all recorded brain regions and Table 3-1 summarizes the proportion of modulated and bi-phasic units in the MTL and frontal regions (496 out of 600 units, the remaining units recorded in other temporal/parietal regions). Since bi-phasic units were more observed within the MTL, we restricted our subsequent analysis (Figure 3-2, Figure 3-3, Figure 3-4, Figure 3-5 in main text) to these "bi-phasic" units recorded in MTL regions. Figure 3-2D shows the PRTHs for all bi-phasic MTL units. To ensure the robustness of the bi-phasic pattern obtained in Figure 3-2D, statistical tests across bins were controlled for multiple comparisons using a cluster-permutation approach (Maris and Oostenveld, 2007). Figure 3-2D show the presence of significant positive clusters after REMs onset in wakefulness and REM-sleep (Monte-Carlo p-value<0.0001, cluster threshold: $p<0.05$) preceded by a decrease in firing rate prior to REMs onset (Monte-Carlo p-value<0.0001 in wakefulness, $p<0.05$ in REM sleep, cluster threshold: $p<0.1$). In the visual stimulation task, we observed only a positive cluster after image onset (Monte-Carlo p-value<0.0001, cluster threshold: $p<0.05$).

Analysis of spike-train latency and selectivity

Existence and latencies of spike-trains in individual trials (picture presentations or eye movements) were determined by Poisson spike train analysis as in(Mormann et al., 2008). In this procedure, the inter-spike intervals (ISIs) of a given unit are processed

continuously over a [-800, 1000]ms window and the onset of a spike-train is detected based on its deviation from a baseline Poisson, i.e., exponential, distribution of ISIs. Only units with mean firing rate above 2 Hz were included in this analysis (i.e. units behaving as a Poisson-process). For each trial (either picture presentation in controlled visual experiment or REM in wakefulness or REM in sleep) we determined the presence of spike-trains in this trial and the latency as the time between REM/image onset and the onset of the first spike in the spike-train. Only latencies within the first 1000ms were considered and the overall latency of that neuron was taken as the mean across all trials. Selectivity was defined as 100% minus the percentage of trials (either REMs or visual stimuli) for which a spike-train was detected. In the visual presentation paradigm, this value was restricted to limited set of fixed values due to the fact that a set of 6 images was presented to each patient. In Figure 3-4 and Figure S 3-3, all units within the MTL were analyzed and not only bi-phasic units. Comparison between individual neurons in wake and sleep focused on those neurons that were recorded in both vigilance states (n=131, Figure 3-4D).

Analysis of phase consistency of intracranial EEG

Phase consistency across REMs was estimated as follows. First, we performed a time-frequency decomposition of the intracranial dEEG signal (EEGlab toolbox (Delorme and Makeig, 2004)) using a standard Fast-Fourier Transform on a 384ms window and a padding ratio of 2. Then the phase of the signal was extracted for all REMs/images and for each time and frequency. Phase coherence across REMs/image presentation was then computed using Euler's formula by time and frequency:

$$ITCP_{t,f} = \sqrt{\left(\frac{1}{n}\left(\sum^{n} \cos(\varphi_{t,f})\right)^2 + \frac{1}{n}\left(\sum^{n} \sin(\varphi_{t,f})\right)^2\right)}$$

(ITCP: inter-trial phase coherence; n: number of REMs/images; $\varphi_{t,f}$: phase of the dEEG signal at time t and frequency f)

Due to the circularity of phase, a uniform distribution of phases across trials leads to a null phase coherence value. However, the repeated occurrence of a particular phase across trials (REMs or images), regardless of its exact value, leads to a non-null phase coherence value (with a maximum at 1 when the exact same phase recurs from trial to trial). Therefore, this procedure provides a measure of the re-occurrence across all trials of a specific phase at the same time relative to trial onset. Each time and frequency point was then compared to the phase coherence within a [-507, -151]ms baseline window (paired t-test, False-Discovery Rate (FDR) correction for multiple comparison) in wakefulness (N=71 dEEG channels), REM sleep (N=59) and image presentation (N=102, see Figure 3-5). Correlation across vigilances states was assessed by means of Pearson's correlation method by averaging phase coherence over a [2, 6]Hz window and [0, 400]ms window after REMs onset in wake and sleep. Given that ITCP depends on the number of events used to estimate it (see equation above), the number of REMs was equated across wake and sleep for each dEEG channel (N=50 REMs per channel, N=57 channels).

Statistics

Error bars in all figures denote standard error of the mean (SEM = SD/√(n-1), where n is the number of data points) unless otherwise stated. Student T-tests were performed after confirming normal distributions via Kolmogorov-Smirnov tests. Mann-Whitney U-tests (non-parametric) were used when the normality was not confirmed. Correlations were examined using the non-parametric Spearman's rank correlation coefficient or Pearson's method for normally distributed pairs of variables. When necessary, corrections for multiple comparisons were performed using the False Discovery Rate (FDR) method (Benjamini and Yekutieli, 2011) or using a non-parametric cluster-permutation approach (Maris and Oostenveld, 2007).

Supplemental Note

Relation between electro-oculography (EOG) and saccadic eye-movements

Recording saccades with EOG

Since its discovery, the EOG has been extensively used to monitor ocular movements and saccades in particular. EOG is a reliable non-invasive measurement of eye-movements and numerous studies established its relation with gold-standard techniques such as high-end video monitoring. Saccades are classically defined as "a rapid conjugate eye movement that shifts the line of sight (center of gaze) rapidly from one part of the visual field to another, mainly used for orienting towards an object of interest. It is characterized by stereotyped relationships between amplitude, duration, and peak velocity. In human subjects, peak velocity typically rises along with saccade amplitude up to a saturation level of 400–500° per second, which is reached when the amplitude exceeds 10–30°, whereas duration rises linearly at a rate of 1.5–3 ms per degree starting from a minimum of 20–30 ms" (Squire, 2009).

There are various methods to reliably record saccades made by an individual. The most accurate methods are the magnetic search coil (Robinson, 1963) and video eye-tracking techniques (Carpenter, 1988; Marg, 1951; Straube and Büttner, 2007; Young and Sheena, 1975). However, these methods do not allow recording eye-movements with closed eyes or may cause major discomfort that render them unsuitable for prolonged sleep studies. To date, EOG is the most widely used technique to record saccadic eye movements with closed eyes (Iwasaki et al., 2005; Straube and Büttner, 2007). EOG is a non-invasive indirect proxy that records movements of the eyes through the perturbation of electric currents generated by the eyes (corneo-retinal potentials, (Abe et al., 2004; Young and Sheena, 1975)). Importantly, many studies have already compared in detail EOG with direct measurement of eye-movements to assess the reliability and limitations of this technique.

With electrode placement (montage) and referencing as employed in our study, EOG reliably captures horizontal saccadic movements from 5° up to 70-80° of angle deviation (Boulanger et al., 2012; Joyce et al., 2002; Marg, 1951; Straube and Büttner, 2007; Young and Sheena, 1975). In this approximate angle range, there exists a linear relationship between EOG and saccade amplitude (Baloh et al., 1975; Becker and Fuchs, 1969; Leigh, 2003; Straube and Büttner, 2007; Young and Sheena, 1975). However, the EOG is limited in the case of vertical eye-movements due to movements of the eye-lid(Ford et al., 1959; Iwasaki et al., 2005; Yee et al., 1985), therefore our study focuses on horizontal eye-movements.

Thus, EOG captures horizontal saccades with medium angle deviations (that encompass the bulk of naturally occurring saccades (Becker and Fuchs, 1969)) and, within this range, the amplitude of the EOG signal can be used to infer about saccade amplitude. Ideally, the EOG is frequently calibrated against eye tracking so that the amplitude of each saccade can be estimated accurately from EOG signals (with a precision of about 0.5° (Straube and Büttner, 2007)). Despite good inter-subject reliability (Baloh et al., 1975), calibration requires the participant to periodically follow tasks with open eyes, and was

therefore not feasible in the current sleep study. However, saccade duration and amplitude are tightly correlated with good inter-subject reliability (Bahill et al., 1975; Baloh et al., 1975). Duration represents a more robust estimate since it does not depend on the absolute EOG voltage and can thus be used to indirectly assess saccades amplitude.

Given the linear relationship between EOG duration and saccade amplitude in degrees, we estimated the amplitude of detected REMs by computing the duration of each REM (defined as the time interval between REM onset and REM peak in the EOG signal). Figure S 3-4 shows the distribution of REM durations, and the estimated saccade amplitude based on the established linear relationship. As can be seen, 90% of saccades were with durations within the 69-223ms range, corresponding to saccades between ~10° and ~70° of angle deviation. In line with the literature and the details of our algorithm, none of our detected REMs had durations shorter than 50ms (corresponding to saccades below 10° of angle deviation). All in all, the events detected in our study represent a broad range of saccades with angles mostly in the range of 10°-70°.

Detected REMs and their relation to saccades

In our study we recorded EOG signals using a standard montage that is recommended by the American Academy of Sleep Medicine (AASM) to record horizontal eye-movements during sleep studies (Iber et al., 2007), as well as for recordings of horizontal saccades (Straube and Büttner, 2007). We placed 2 electrodes on the right and left canthi referenced to earlobe electrodes, and the signals were band-pass filtered between 0.1 and 35Hz. Our own analysis supports the conclusion of previous studies that the specific filter settings do not significantly influence the detection outcome (Boulanger et al., 2012). Using a semi-automatic algorithm, we detected rapid eye movements in wake and sleep from EOG recordings (see Figure 3-1D, Methods section and Supplemental Material). The shape of detected events (see single events in Figure 3-1G, average in Figure 3-1F) is in very good agreement with EOG traces as described in those studies that directly compared EOG signals to saccadic eye movements with eye tracking (Boulanger et al., 2012; Plöchl et al., 2012). Therefore, the specific parameters used here to detect REM events are ideal to maximize the correspondence with horizontal saccadic eye-movements as detected with other techniques.

Saccades are typically considered to occur a few times every second during wakefulness, and this may seem at odds with our detected REMs - occurring 2.6 times per minute (0.04 per second) on average during wakefulness (Figure 3-1E). However, several factors can account for this apparent discrepancy:

> (1) Our recordings took place during overnight sleep studies, therefore some epochs during wakefulness correspond to time intervals in which patients were awake but with closed eyes in bed, not gazing around. Indeed, when focusing on 10s epochs in which *any* REMs were detected, the rate of REMs was found to be 0.2 ± 0.01 REMs *per second*, representing a 5-fold increase compared to all wakefulness epochs. As a comparison, a recent study using infrared (IR) eye-tracking to record saccades during free-viewing conditions reported an average inter-saccade interval of 0.73sec (Wang et al., 2012) (vs. 2.0s ± 0.1 in our study).

(2) Even when our participants were in fact awake with open eyes, they were looking around in a static hospital room with no specific instructions to explore a visual scene that could remain constant at moments,

(3) Our conservative detection was optimized to avoid false-positives and therefore probably underestimates the occurrence of REMs (entails false-negatives)

(4) As explained in the previous section, vertical eye-movements as well as small (<5°) and micro-saccades (<2°) are not reliably captured with EOG recordings, therefore our detected events constitute a subset of all saccades as recorded with video tracking.

Temporal dynamics of detected REMs and relation to saccades' dynamics

In the saccade research field, it is often customary to focus on saccade velocity (rather than amplitude/duration) i.e. to extract the 1st derivative (Straube and Büttner, 2007), whereas in the sleep polysomnography field it is customary to treat the EOG signal "as-is"[19-21]. The advantage of velocity is to clearly isolate the moment during which eyes are moving (non-null velocity). To better compare the temporal dynamics of REM reported here vs. saccades as classically described, we superimposed the EOG traces along with their 1st derivatives (as customary in saccade research). As illustrated in Figure S 3-5 (and in Figure 3-2 in the main manuscript) a saccade starts with a sharp increase in EOG velocity (Figure S 3-5, red arrow). The velocity reaches a peak (green arrow, after ~25ms) and decreases back to zero (pink arrow, end of saccadic movement). Thus, in terms of the *EOG* (light blue traces), the peak in the signal corresponds to the end of the saccade and the new fixation (Boulanger et al., 2012; Plöchl et al., 2012). EOG velocity highlights the transient nature of saccades (about 100ms) and verifies that in EOG traces, saccade duration can be approximated as the time between the onset and the peak in EOG amplitude (as defined in our Methods section).

It seems that the late slow component of the EOG trace returning to baseline (after the peak in amplitude, around 100-600ms) occurs after the new fixation and is not part of the saccadic main sequence. This slow drift could either reflect after-saccade physiological processes (such as up-shooting (Leigh, 2003; Straube and Büttner, 2007), correction for head-movements (Boulanger et al., 2012) or subsequent saccades) or, alternatively, could reflect in part our high-pass filter settings (0.1Hz, see ure S 3-7).

Supplemental Figures

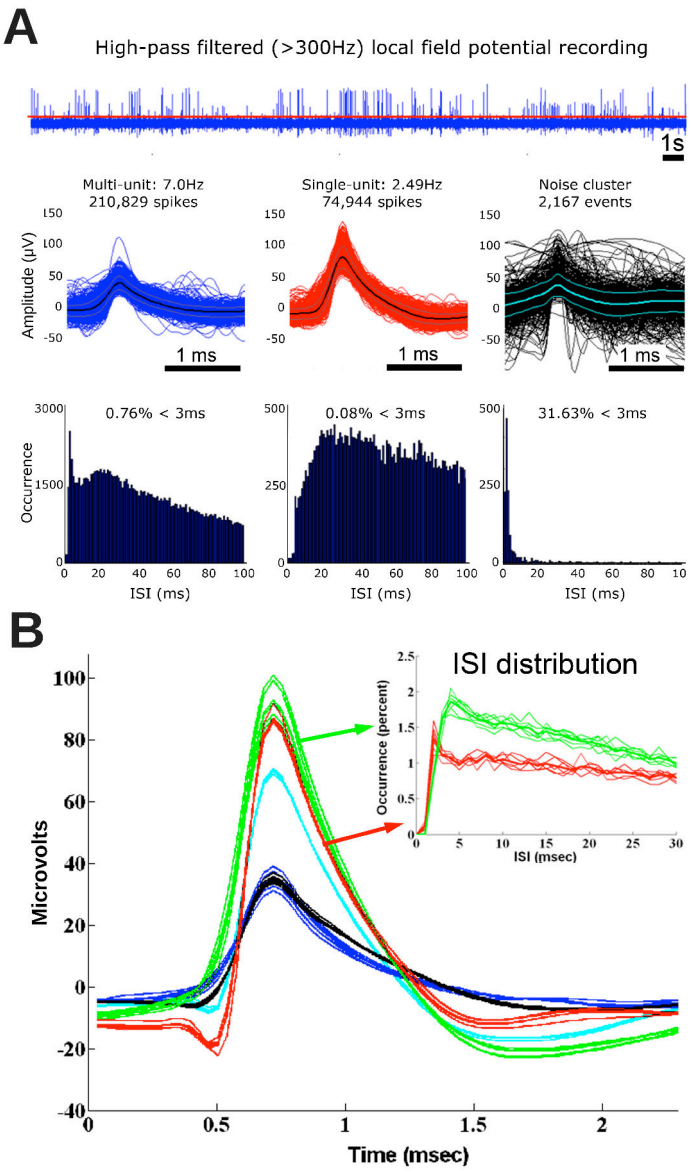

Figure S 3-1 Stability of unit recordings and identification

(A) Illustration of the unit identification scheme. Top row shows the high-pass filtered LFP along with the threshold for spike identification (5 SDs above the noise level (red line)). Middle row depicts action potential waveforms for three identified clusters. Bottom row shows the distribution of inter-spike-intervals (ISIs). Identification was based on the consistency of waveforms and the occurrence of ISIs within the expected refractory period (<3ms). Units were categorized either as multi-unit (blue), single-unit (red) or noise clusters (black). (B) Across long-duration recordings (~7h), waveforms and ISI distributions were consistent and separable as illustrated here by the mean action potential waveforms for 5 distinct units recorded in the same individual. Each color denotes a different unit and each trace denotes the mean waveform in separate 1h intervals throughout sleep. Inset depicts ISI distributions in separate 1h intervals for two units.

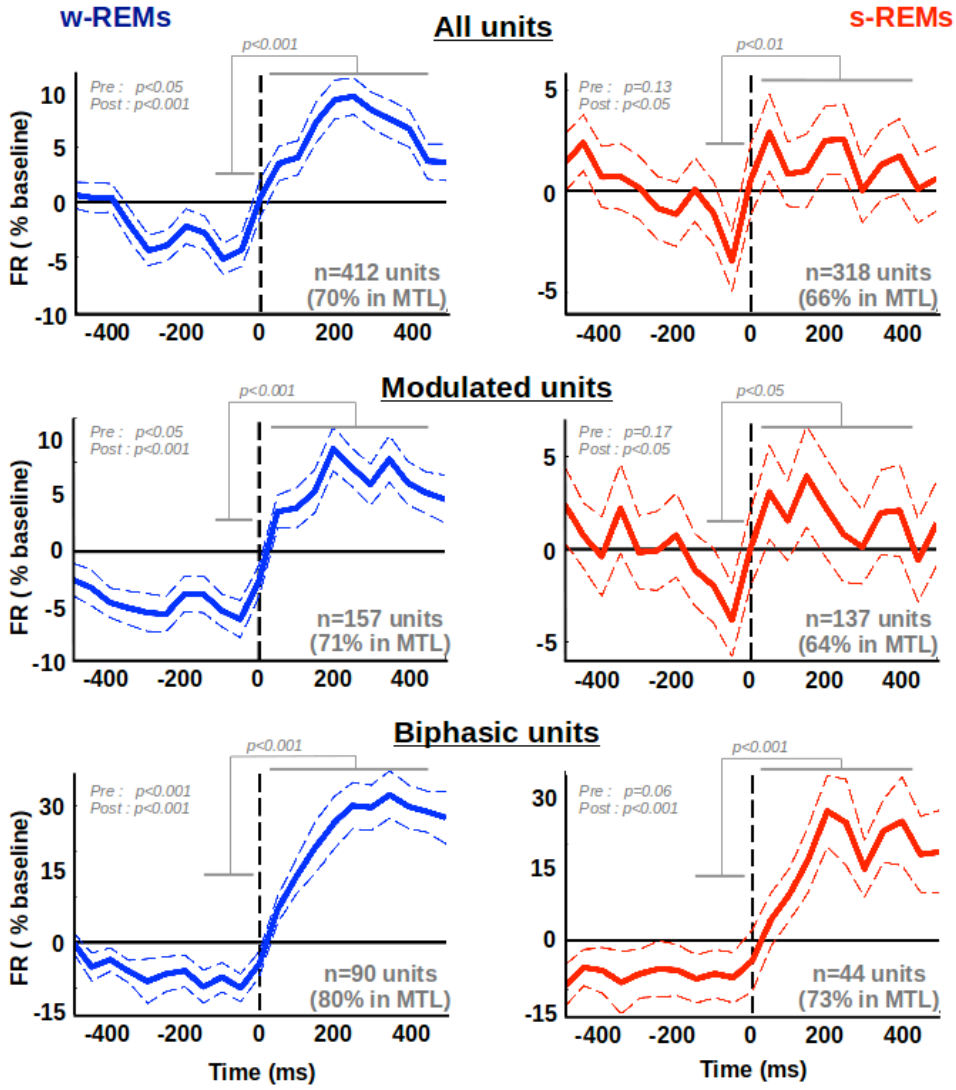

Figure S 3-2 Population neuronal activity shows a bi-phasic modulation around REMs in wakefulness and REM sleep

Bi-phasic neuronal responses to REM in wakefulness (w-REMs, blue, left panels) and REM-sleep (s-REMs, red, right panels) for all recorded units (A, top row), units showing significant modulations of their firing rate around REMs at any time and in any direction (B, middle row, see Methods) and units showing the specific bi-phasic pattern (C, bottom row). Units from all recorded brain regions were analyzed (see Figure 3-2 for an analysis focusing only on MTL neurons). Note that in both wake and sleep, a bi-phasic pattern emerges with a reduction in firing rate prior to REMs onset ([-100, -50]ms) and an increase immediately after REMs onset ([50, 400]ms). The significance of the modulation was assessed by comparing across units (one-tail paired t-tests) the activity after REM onsets to (i) the activity prior to REM onsets (see gray bars) or to (ii) baseline activity ("pre": [-100, -50]ms<baseline, "post": [50, 400]ms>baseline, see p-values reported on each panel). The number of units from all brain regions in each group (all, modulated and bi-phasic) is indicated as well as the proportion of these units located within the MTL (for an analysis focusing on MTL units, see Figure 3-2). Note the increase in MTL proportion for bi-phasic units. Error-bars show the SEM across units.

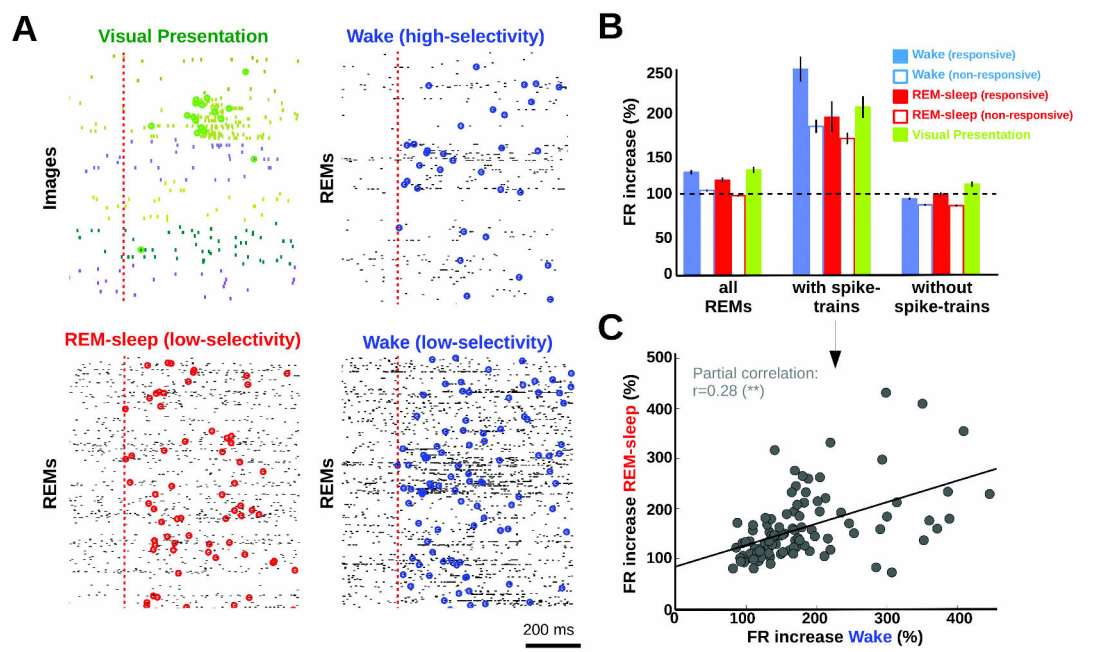

Figure S 3-3 Selective responses of units to images and REMs

(A) Raster plots of representative single-unit responses following image presentation (top left) or REMs in wakefulness (top right, bottom right) and REMs during REM-sleep (bottom left). Dotted vertical red line denotes the time of image presentation or detected REM onset. Each spike is marked by a vertical tick. For the visual presentation, 6 different images were presented and the responses are grouped by image where the color of each spike corresponds to a different image. In other subpanels, trials are ordered chronologically from first (bottom) to last (top) REM. Circles show the onset of the detected spike-trains after time zero. Note the selectivity of the unit in the visual presentation paradigm (spike-trains detected almost exclusively for one image in green). Similar high 'selectivity' could be observed for REMs in wakefulness (top right). Other units exhibited low 'selectivity' during REMs, showing spike-trains for a larger percent of REMs in the few hundred milliseconds following REM onset (bottom). (B) Increase in firing rates for responsive MTL neurons (filled bars, N=50 in wakefulness, N=19 in REM-sleep) or non-responsive neurons (unfilled, N=132 units in wakefulness, N=113 units in REM-sleep) for all REMs (left), REMs with detected spike-trains (middle) or without (right). Green bars show the equivalent for MTL units in response to images (N=70). Note that REMs associated with spike-trains accounted well for the average post-REM increase in neuronal activity (as seen in Figure 3-2D). Error bars denote SEM across units. (C) Correlation of post-REM responses across vigilance states for those MTL neurons recorded in both wakefulness and REM-sleep (N=131 units) and for REMs with spike-trains. A partial correlation coefficient was estimated (Spearman's correlation) to establish the effect above and beyond differences in the mean firing rate of individual units ($r=0.28$, $p<0.01$ (**)). Thus, the magnitude of neuronal modulations was correlated across REM-sleep and wakefulness

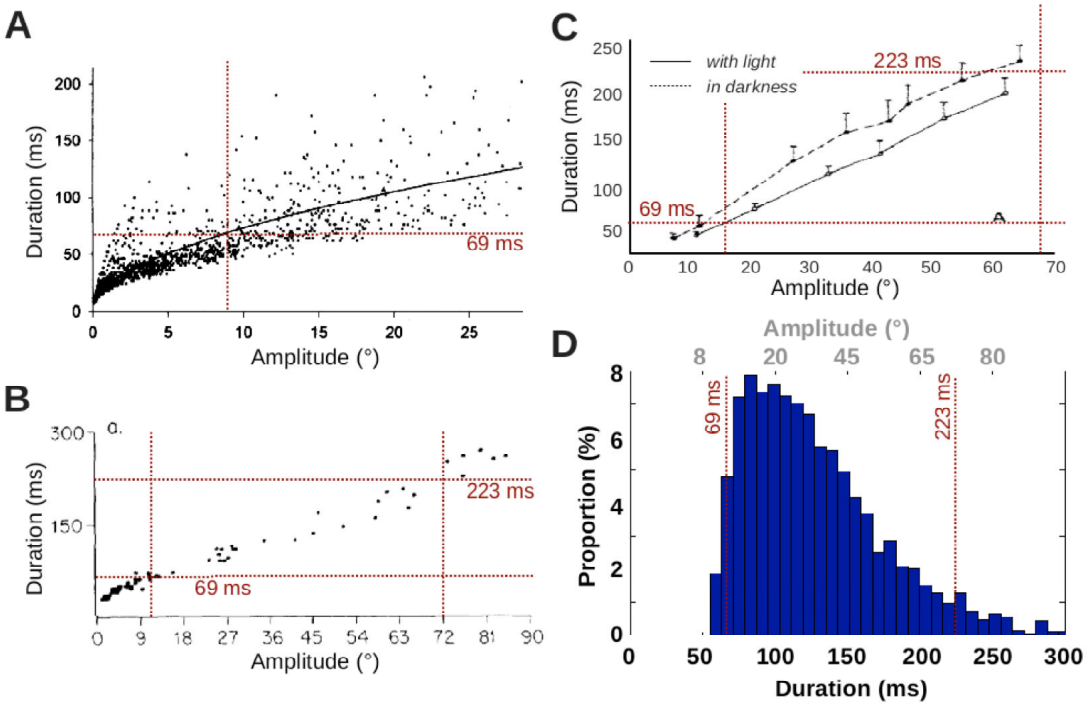

Figure S 3-4 Amplitude and duration of detected REMs

(A-C) For saccades larger than 5°, there is a linear relationship between saccades amplitude and duration (Panel A adapted from (Leigh, 2003), Panel B from (Baloh et al., 1975), Panel C from (Becker and Fuchs, 1969)). Red lines show the 5th and 95th percentile of REMs duration as detected in our dataset during wakefulness (n=2679 REMs). (D) Distribution of REMs duration: 90% of REMs lasted between 69 and 223ms. On top, an approximate scale gives the equivalence in deviation amplitude computed from panel A and B.

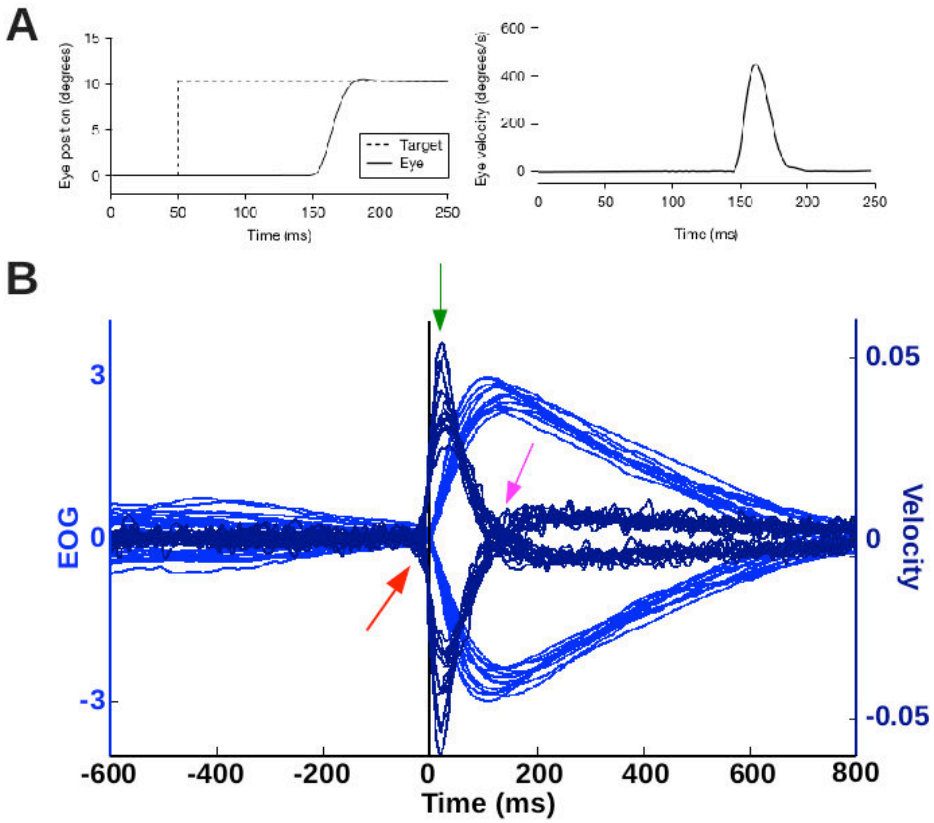

Figure S 3-5 Temporal dynamics of saccades and detected REMs

(A) Adapted from (Straube and Büttner, 2007), schematic representation of the saccadic dynamics. At 150ms after target presentation, a 10° saccade is made, lasting for ~30ms. This corresponds to a sudden increase in velocity. Velocity goes back to 0 by the time the eye position is stabilized to the new target. (B) EOG amplitude and EOG 1st derivative triggered-average for REMs detected in wakefulness and averaged by subject (N=13, time-locked to REMs onset). The amplitude and 1st derivative were computed on the EOG signal z-scored on the [-600, 800]ms time-window for each REM. The red arrows show saccade onset and velocity initial increase. The green arrow shows the velocity peak. The pink arrows show the saccade offset and new fixation, which corresponds to a null velocity and peak in EOG amplitude.

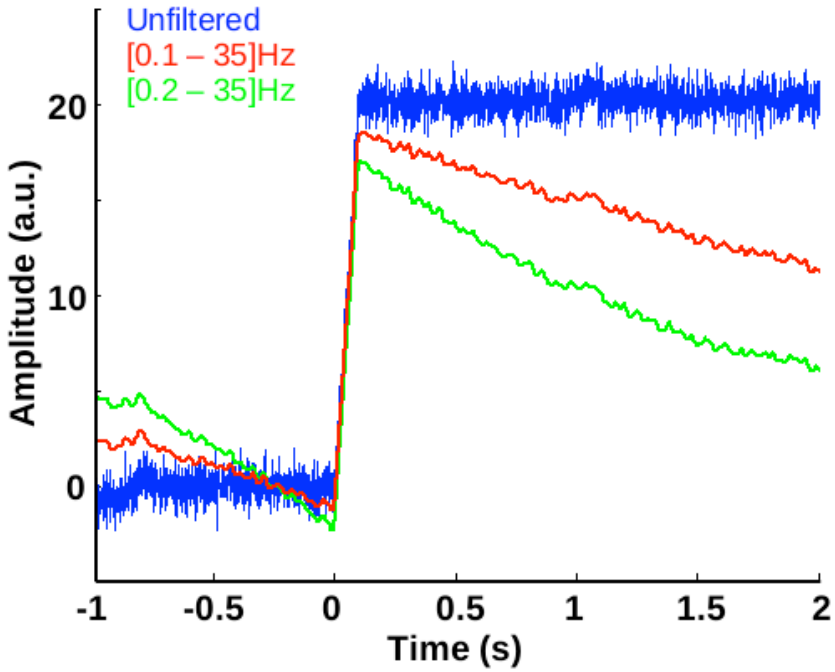

Figure S 3-6ure S 3-7 Effect of band-pass filtering on REMs average traces

Triggered-average of simulated data (Gaussian noise with step function modeling EOG data with saccades) with or without band-pass filtering. Note that with band-pass filtering, the post-saccadic potential is not constant as in the unfiltered case (step function) but drifts toward 0.

Chapter 2: Processing sensory information during sleep

Dawnbreakers
Herbert McClintock (1939)

Note on contributions:

Study 4: Louise Goupil, Tristan Bekinschtein and Sid Kouider designed Experiment 1. Louise Goupil collected the data. Leonardo Barbosa, Louise Goupil and myself analysed the data. Sid Kouider and myself designed Experiment 2. I analyzed the data in collaboration with Leonardo Barbosa.

Study 5: Sid Kouider and I designed the experiment. I collected and analyzed the data with the help of Andreas Tier Poulsen for the computation of the Lempel-Ziv complexity.

Study 6: Sid Kouider, Guillaume Legendre and I designed the experiment. Guillaume Legendre collected the data. Guillaume Legendre and I analyzed the data.

Study 4:
Inducing task-relevant responses to speech in the sleeping brain

Published in **Current Biology**
September 1, 2014

Sid Kouider[1], **Thomas Andrillon**[1-2], Leonardo S. Barbosa[1-2], Louise Goupil[1-2] & Tristan A. Bekinschtein[3,4]

[1] *Laboratoire de Sciences Cognitives et Psycholinguistique, CNRS/EHESS/DEC-ENS*
Paris, France

[2] *Ecole Doctorale Cerveau Cognition Comportement, ENS – EHESS – Paris VI – Paris V*
Paris, France

[3] *Cognition and Brain Sciences Unit, Medical Research Council, Cambridge, England, UK*

[4] *Department of Psychology, University of Cambridge*
Cambridge, England, UK

Summary

Falling asleep leads to a loss of sensory awareness and to the inability to interact with the environment (Ogilvie, 2001). While this was traditionally thought as a consequence of the brain shutting down to external inputs, it is now acknowledged that incoming stimuli can still be processed, at least to some extent, during sleep (Hennevin et al., 2007). For instance, sleeping participants can create novel sensory associations between tones and odours (Arzi et al., 2012) or reactivate existing semantic associations, as evidenced by event-related potentials (Bastuji et al., 2002; Brualla et al., 1998; Goupil and Bekinschtein, 2012; Ibanez et al., 2006). Yet, the extent to which the brain continues to process external stimuli remains largely unknown. In particular, it remains unclear whether sensory information can be processed in a flexible and task-dependent manner by the sleeping brain, all the way up to the preparation of relevant actions. Here, using semantic categorization and lexical decision tasks, we studied task-relevant responses triggered by spoken stimuli in the sleeping brain. Awake participants classified words as either animals or objects (Experiment 1) or as either words vs. pseudo-words (Experiment 2) by pressing a button with their right or left hand, while transitioning towards sleep. The lateralized readiness potential (LRP), an electrophysiological index of response preparation, revealed that task-specific preparatory responses are preserved during sleep. These findings demonstrate that despite the absence of awareness and behavioural responsiveness, sleepers can still extract task-relevant information from external stimuli and covertly prepare for appropriate motor responses.

Results

We studied whether the categorisation of spoken words can still trigger task-relevant motor plans during early sleep stages. One main difficulty in addressing this issue consists in instructing a new task to sleeping subjects, arguably because prefrontal regions dealing with executive functions are then particularly suppressed in comparison to other cortical regions (Maquet, 2000; Muzur et al., 2002). One potential solution is to rely on the induction approach commonly used by studies on implicit perception in awake participants. This research reveals that the processing stream involved in making a semantic classification can, through explicit practice, be automatized and bypass prefrontal regions. Under those conditions, the categorisation of visual words and numbers can lead to the covert activation of motor cortex even when those stimuli are masked and presented below the threshold of consciousness (Dehaene et al., 1998; Kouider and Dehaene, 2007). In the current study, we extend this task induction strategy to track the ability of sleepers in extracting task-relevant information from speech and prepare for the appropriate motor plan.

LRPs reveal semantic classification and response preparation before and after falling asleep

We recorded the EEG of human participants while they were awake and instructed to classify spoken words as animals or objects (Figure 4-1). This procedure allowed us to compute LRPs – a neural marker of response selection and preparation (Masaki et al., 2004) – by mapping each specific semantic category to a specific motor plan (e.g., animals with right hand, objects with left hand, counterbalanced across participants). This design allows for the assessment of lateralized response preparation towards the side associated with the appropriate semantic category. Thus, it allows testing whether sensory signals are processed beyond semantic levels, by probing how the meaning extracted from external words can lead to the covert selection and preparation of context-dependent actions. Testing conditions encouraged the transition towards sleep while remaining engaged with the same task-set: subjects received explicit allowance to fall asleep and were sitting in a dark room, eyes closed, in a reclining chair, listening to several repetitions of the same list of stimuli with a long inter-trial interval of 6-9 seconds. Crucially, participants received an entirely new list of words (N=48) during sleep to ensure that their responses were based on the extraction of word meaning rather than a mere reactivation of stimulus-response associations established during the wake stage.

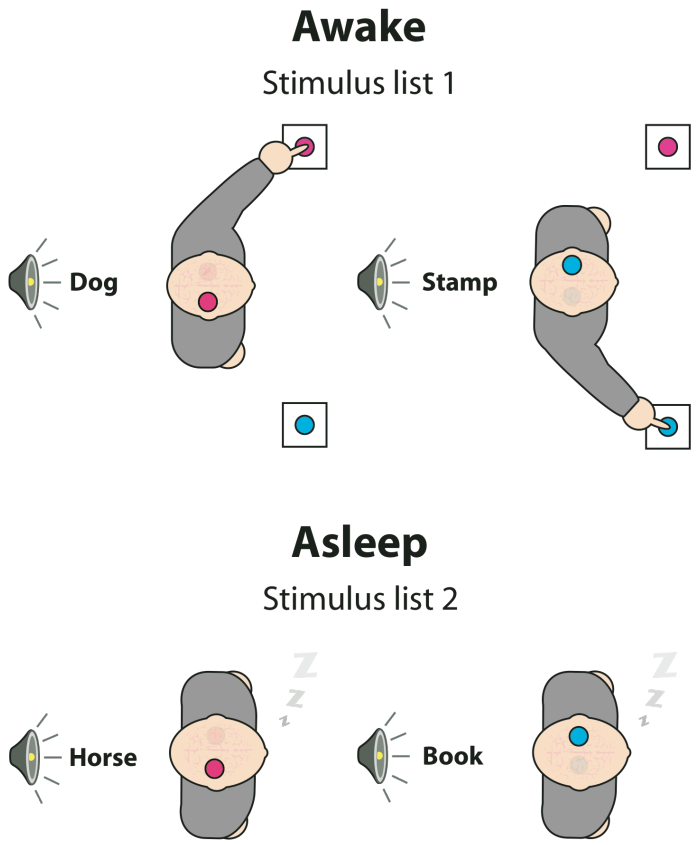

Figure 4-1 Experimental paradigm

A. Participants (N=18 in each experiment) first made overt manual responses either to animal vs. object names presented every 6 to 9 seconds (semantic decision task; Experiment 1), or to words vs. pseudowords (lexical decision task; Experiment 2), while wearing an EEG cap. B. After either falling asleep (Experiment 1) or entering the N2 stage (Experiment 2), as assessed both by the absence of behavioural responses and by electrophysiological markers of sleep, a second list of stimuli was presented and EEG indices of response preparation were used to evaluate covert classification.

Sleep onset was assessed online both behaviourally, by ensuring the absence of overt responses for at least two minutes of stimulation, and electrophysiologically, through sleep markers (i.e., disappearance of low-amplitude alpha/beta rhythms and development of high-amplitude delta/theta rhythms, see Figure S 4-1, presence of slow eye movements and other sleep graphoelements such as vertex sharp waves, regular spontaneous and evoked K-complexes or sleep spindles) before and after the presentation of each word. Participants underwent the transition from full wakefulness to light sleep and then oscillated primarily between stages NREM1 and NREM2. Note that trials were only considered as NREM1 when there was a complete lack of alpha rhythm accompanied by sleep markers. In order to discard epochs comprising brief awakenings and micro-arousals (i.e., re-appearance of a wake-like EEG activity for less than 3 seconds; mean = 11.6%, SD = 8%), and to ensure that each trial included in the sleep conditions genuinely reflected a sleep state, we performed an offline and conservative evaluation of sleep stages relying on strict criteria. Scoring was performed here by two trained neurophysiologists blind to experimental conditions who additionally verified that participants remained asleep after stimuli onset, by tracking any electrophysiological signs

of arousals (re-appearance of a wake-like EEG activity for more than 3 seconds (Iber et al., 2007), whether the trial was associated or not with a button press), or any micro-arousals. Details and statistics about sleep scoring are provided in the Supplemental Experimental Procedures (see also Figure S 4-1 for individual sleep architectures).

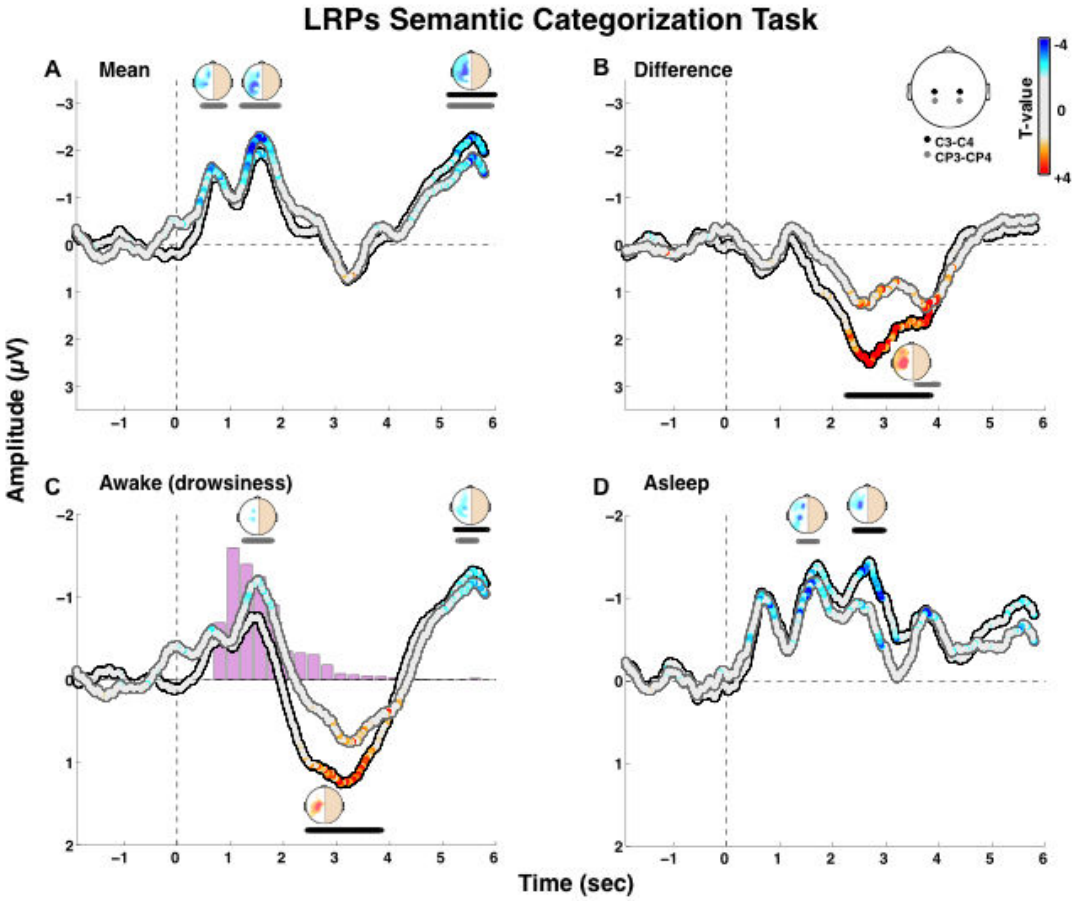

Figure 4-2 Motor preparation to semantic categories

Semantic categorization LRPs, computed by subtracting contralateral from ipsilateral activations (see Supplemental Experimental Procedures), revealed covert response preparation towards the target side (i.e., contralateral to the appropriate hand movement) in the vicinity of motor areas, both during wake and sleep trials. Time-series show the LRP curves from stimulus onset on central (C3/C4) and central posterior (CP3/CP4) electrodes for (A) the main effect, (B) the difference between sleep and wake conditions, and (C-D) the LRPs restricted to each condition. Bars above the time-series show significant clusters with a monte carlo p-value < 0.05. 2D topographies show the LRP over the whole scalp obtained for each couple of electrodes (i.e., left/right couples), during the peak of activation of each cluster (when both electrodes pairs reached significance at the same time, the topographies were identical in both peaks, and only one is shown for brevity). The color code shows significance at the sample level (time-series) and electrode level (topographies), with white color on all non-significant data points ($p > 0.05$). Histograms in the wake LRP show the RTs distribution.

Lateralized Readiness Potentials constitute a direct and sensitive measure of response selection and preparation towards the target side, which is maximal in amplitude at scalp sites over the motor/premotor cortices contralateral to the responding hand (Coles, 1989; Kutas and Donchin, 1980). LRPs, traditionally computed by reference to response onset, can also be measured by reference to stimulus onset (Leuthold, 2003a; Tollner et al., 2012a), making them suitable to measure cortical responses in the absence of overt

motor responses (i.e. during sleep). We first characterised the main (i.e., state-independent) effect of response preparation, by collapsing sleep and wake trials and computing stimulus-locked LRPs using cluster-based permutation analysis (see Supplemental Experimental Procedures). This analysis revealed a first negative deflection corresponding to the LRP with two significant peaks at 660 and 1620ms, primarily over central (C3/C4) and central posterior (CP3/CP4) electrodes (Figure 4-2a). Interestingly, after 2000ms the LRP returned to baseline for several seconds until the emergence of a second negative deflection peaking around 5570ms. Secondly, to test the difference between wake and sleep states we subtracted the wake condition from the sleep condition (Figure 4-2b). Remarkably, we found no significant difference for the first LRP deflection but a clear significant effect afterwards, during the opposite deflection around 2920ms for C3/C4 and 3800ms for CP3/CP4. Restricted analysis for each vigilance state confirmed the significant early LRP deflection for wake trials and, crucially, also for sleep trials separately (Figure 4-2c-d). However, the opposite and later positive deflection was present only during wake trials. As shown in Figure 4-2c, the distribution of response times during wake trials suggests that the initial LRP reflects the preparation of the motor plan, while the inversion of potential appears to follow manual responses. This interpretation was confirmed by performing a similar analysis on readiness potentials now time locked to the actual response showing the classical LRP deflection at response onset, followed immediately by the opposite deflection following the manual response (Figure S 4-2). As discussed below, this opposite deflection in the wake condition is likely to reflect a post-response checking mechanism that is exacerbated under conditions of drowsiness.

These results suggest that task-relevant motor preparation can be triggered during sleep. Yet, several potential issues should be addressed before drawing this conclusion. First, one might question whether participants in our study were truly asleep. Although our procedure for assessing sleep involved both online scoring and waiting for at least 2 minutes of absent responses before shifting to the new list of words, subjects sometimes pressed buttons either spontaneously or in response to auditory stimulation during the sleep list (14% of trials, not included in the analyses). Those button presses could be regarded as temporary arousals whereby the subjects might wake up for one or two trials, or even micro-arousals (i.e., less than 3 seconds). However, they might also reflect a nonconscious triggering of motor actions in responses to a sensory stimulation, as it is well-known in the literatures on visual masking (e.g., subliminal action priming; (Vorberg et al., 2003)) and blindsight patients (Cowey and Stoerig, 2004; Weiskrantz, 1990). In addition, past studies have shown that motor reflexes can be triggered during sleep (Dagnino et al., 1969). Finally, these button presses, might reflect, more simply, the fact that subjects during early sleep stages are prone to perform small movements considered in the literature as peripheral motor activations (i.e., unrelated to task or environmental contexts) such as muscle twitches (Chase and Morales, 2005). Inspection of the data revealed that in most cases button presses were associated with micro-arousals, although there were cases where button presses were not accompanied by any signs of arousal. Importantly, our results were computed not only by excluding any trial with button presses, but also after performing a conservative evaluation of their vigilance state. Indeed, in order to be fully confident that the trials we included in our analysis genuinely reflect a state of sleep, micro-arousals and arousals (associated or not with button presses) were detected and trials in the direct vicinity of these events were discarded, although they may be considered as sleep trials according to established guidelines. A related issue concerns the fact that our participants received the sleep list from the onset of NREM1, and thus our sleep condition reflects a mixture of NREM1 and NREM2

stages. Yet, contrary to NREM2, the NREM1 stage is sometimes regarded as an ambiguous transition state in which awareness and responsiveness might be partially preserved (Bareham et al., 2014; Goupil and Bekinschtein, 2012; Ogilvie, 2001). Our data set did not allow us to reliably separate the two sleep stages due to a lack of power, as the 48 items were distributed across both stages. It thus remains possible that, even controlling for electrophysiological and behavioural markers of arousal, participants may have somehow remained conscious aware during NREM1 late stages, To account for this potential issue and ensure that task-relevant responses can genuinely be triggered during sleep, a more stringent control of vigilance was implemented in the second experiment, where only NREM2 brain activity was considered in the sleep condition.

Another potential issue concerns the use in our study of a specific scoring method developed by Hori and collaborators for protocols with short epochs and focusing on hypnagogia (Hori et al., 1994; Tanaka et al., 1997). One might argue that this method, which is less commonly used, might underestimate the level of sleepiness and/or miss potential contaminations by micro-arousals in comparison to the standard scoring approach. We thus re-scored our semantic decision data using the widely used guidelines of the American Academy of Sleep Medicine (AASM) (Iber et al., 2007). We observed that the two scoring methods largely matched in terms of classifying trials in the wake or sleep state (93.1% overlap across participants; SD = 4.1%). Crucially, re-analyses of our data using the AASM scoring revealed a very similar pattern with a significant LRP deflection for sleep trials (see Supplemental Experimental Procedures and results in Figure S 4-3), confirming the presence of task-relevant responses during sleep even when using a more conventional method for scoring sleep. Finally, regarding the comparison with the wake state, a potential issue might be that the strong positive deflection we observed with a reversal of the LRP response after an overt motor response, might reflect specific conditions of drowsiness. Indeed, participants were tested while falling asleep and reaching a certain level of drowsiness, which might increase the reliance on post-response checking mechanisms, leading to the reconfiguration and amplification/reduction of ipsi/contra-lateral motor areas (Haggard, 2005; Praamstra et al., 2005). Hence, a more direct comparison between wake and sleep states would thus, not only exclude NREM1 trials as described above, but also compare sleep with conditions of full wakefulness (i.e., avoiding the drowsiness period where subjects are in the process of falling asleep).

LRPs for lexical decisions in full wakefulness and NREM2 sleep

We performed a second experiment in which we instructed participants to perform a lexical decision on spoken material. Participants classified auditory stimuli as words vs. pseudowords (i.e., items that don't exist in the lexicon, but share the same phonological properties as real words) with their left vs. right hand (counterbalanced across subjects). This second experiment, in addition to dealing with the potential issues mentioned above regarding the wake-sleep transition, allowed us to verify whether the induction approach can be generalized to other classification tasks on external stimuli. Here, the nap was preceded by a session where participants received the first list of stimuli under full wakefulness, while siting upright and not allowed to fall asleep. Participants were then presented repeatedly with the same list while now being reclined and allowed to fall asleep under similar testing conditions as in the semantic decision group. In addition, participants in this second experiment received the second list of stimuli (N=72) only after the onset of the NREM2 stage (i.e.,following the first appearance of a spontaneous

K-complex or sleep spindle). This design allowed contrasting LRPs during consolidated sleep vs. full wakefulness rather than during the transition where subjects are either drowsy or in a labile (NREM1) sleep stage. Since the Hori scoring is optimized for evaluating the hypnagogic period (primarily NREM1), we decided to apply AASM scoring for this second experiment, while also controlling for micro-arousals (see Supplemental Experimental Procedures and Figure S 4-4 for individual hypnograms). Trials associated with a button press and micro-arousals dropped to 2.3% (SD=1,7%) and 0.3% (SD=0.6), respectively, and were excluded from further analysis.

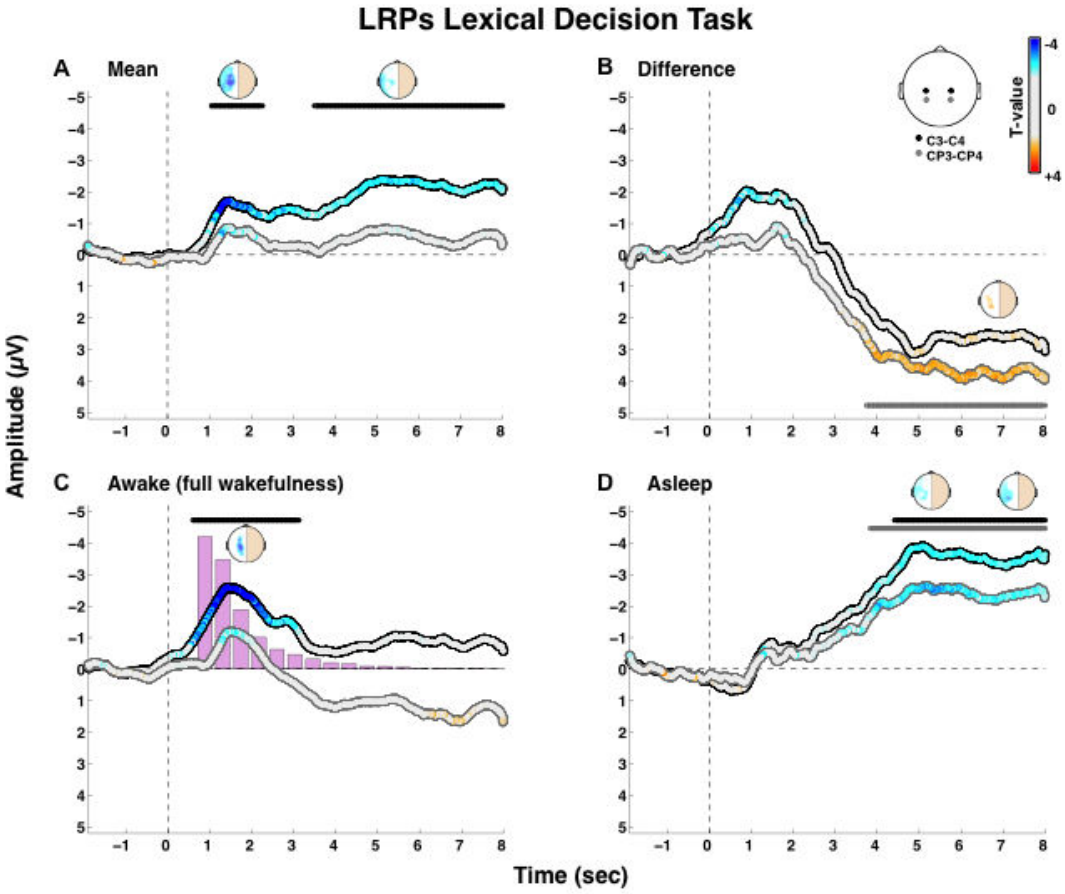

Figure 4-3 Motor preparation to lexical categories

Lexical decision LRPs (see Figure 4-2 for a description).

Analysis of the main (i.e., state-independent) effect of response preparation revealed two LRP clusters, with an early effect peaking at 1276ms and a later and more sustained effect peaking at 5016ms and extending from 3508ms until the end of the epoch at 8000ms (Figure 4-2a). Separate analyses for each vigilance state showed that the early LRP component was mostly driven by the wake condition, while the later and more sustained cluster was primarily driven by the sleep condition (Figure 4-2c-d). Indeed, while the LRP in the wake condition was rather transient and overlapped with the reaction times distribution, the LRP during sleep corresponded to a large and sustained response developing slowly over time. As a consequence, the contrast of wakefulness (i.e., the difference between wake and sleep trials, Figure 4-2b) revealed a trend for an early negativity, suggesting a stronger early LRP under wake conditions, and a significant and sustained positivity for the late component, reflecting a delayed LRP during sleep. These results confirm the presence of covert task-relevant responses to speech during sleep, and extend the finding in the semantic decision from experiment 1 to the

classification of lexical properties during the NREM2 state. Notably, the opposite deflection found in Experiment 1 under drowsy conditions was not observed here under conditions of full wakefulness. It is also interesting to observe that the LRP during sleep was further delayed in time compared to Experiment 1. We interpreted this finding as the involvement of slower mechanisms of evidence accumulation during the N2 stages in Experiment 2, compared to the mixture of N1 and N2 responses in Experiment 1 (Ogilvie, 2001).

One might still argue that participants in our study were somewhat aware of the spoken stimuli, with fleeting micro-arousals that are difficult to detect in the EEG, resulting in a state of transient arousal/drowsiness not allowing them to perform an overt behavioural response. In order to directly address this issue, through an operational measure of stimulus awareness, we instructed participants to performed an explicit recognition task right after the lexical decision experiment, after regaining full consciousness. They were presented with the stimuli either from the wake list, from the sleep list or from a new list of completely novel items (counterbalanced across participants), and were instructed to classify each stimulus as either old or new, and then rate their confidence about their decision on a scale ranging from 1 (completely guessing) to 7 (completely sure).

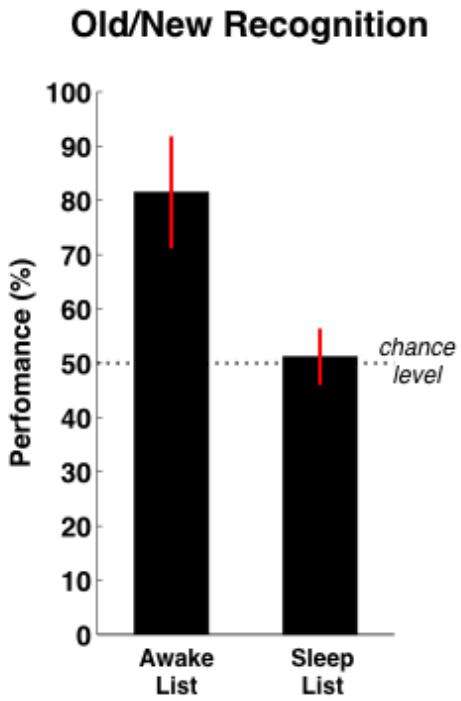

Figure 4-4 Memory test upon awakening

Results of the old/new explicit recognition test performed immediately after the nap. Participants received stimuli from the wake list, sleep list and an entirely new list, and were instructed to indicated which items has been played previously or was entirely new. Performance, computed by comparing responses of the wake and sleep lists to the new list, revealed high-accuracy performance for the wake list, but chance-level performance for stimuli presented during sleep. Error bars denote 1 SD.

The post-test revealed that participants could distinguish new words from words presented during the wake period (performance=81,5%; *d'*=2.16; both $p<0.0001$), but crucially not from words presented during sleep (performance=51,2%; *d'*=0.13; both n.s). Consistently, the post-decision confidence estimates also did not differ between the

new and sleep lists (mean confidence: 4.79 vs 4.80, respectively, n.s), while they were significantly higher for the list presented during the preceding period of wakefulness (5.80; both ps <0.001). Overall, these results add strong evidence supporting the fact that participants did not have explicit access to the stimuli presented during sleep, and confirm that the LRP obtained during sleep most likely reflects a nonconscious form of speech processing.

Discussion

There is now converging evidence that environmental stimuli can still be processed during sleep, at least to a certain degree (Hennevin et al., 2007). For instance, meaningful stimuli (e.g. own names, own baby's cry, fire alarm) are more likely to lead to awakening (Bruck et al., 2009; Formby, 1967; Oswald et al., 1960; Portas et al., 2000). Furthermore, sleeping participants, while in REM or non-REM stages, can create novel sensory associations between tones and odours (Arzi et al., 2012) or reactivate existing semantic associations as evidenced by the presence of an N400 component in EEG (Bastuji et al., 2002; Brualla et al., 1998; Goupil and Bekinschtein, 2012; Ibanez et al., 2006). Besides, sleepwalkers are able to re-enact recently learned sequences of movements (Oudiette et al., 2011). Thus, there is evidence, albeit scarce, that sleep does not preclude meaning extraction or the activation of learned associations and sensorimotor links. However to date, no study has directly tested the possibility that environmental stimuli are processed in a flexible manner, all the way up to the preparation of task-relevant responses. Here, using LRPs, we show that sleeping participants are still able to prepare for the appropriate response on semantic and lexical decision tasks practiced before falling asleep. The current design, using single word presentations, does not directly test for meaning extraction (unlike classical N400 paradigms using word pairs or sentences). However, our study reveals speech processing through semantic and lexical categorization by demonstrating the preparation of motor plans conditional on the meaning of spoken words. These results not only confirm previous findings showing that semantic information can still be extracted during sleep, but further show that this nonconscious meaning extraction can be routed by the task context and reach higher processing levels, up to motor preparation stages. This suggests that when processing environmental information during sleep, at least during early non-REM stages, only the final stages related to action execution might be suppressed.

An important remaining question, therefore, is where in the neural stream ranging from motor preparation to action execution lays the bottleneck responsible for the lack of behavioural response. Previous studies revealed that sleep is associated with both the inhibition of dorso-lateral prefrontal cortex, a crucial area for executive functions (Maquet, 2000; Muzur et al., 2002), and the functional breakdown in thalamo-cortical connectivity, associated with the loss of wakefulness and sensory awareness (Massimini et al., 2005). On the contrary, neural activity in other cortical regions, including sensorimotor areas, do not importantly differ from the wake stage (Issa and Wang, 2008; Maquet, 2000; Y. Nir et al., 2013). The preserved functionality of these regions may support elaborate -albeit automatized- cognitive processes such as those observed in the present study. One might even expect that, as long as a given task has been induced during the wake stage, almost any processing stream could potentially remain activated during sleep. Future studies will be necessary to address this issue, and in particular whether even higher-order regions dealing with executive functions such as cognitive control or task-switching can be triggered using a task-induction strategy.

It remains to elucidate whether this finding would generalize to other sleep stages, and in particular to REM sleep, where there is an almost complete muscular paralysis but electrophysiological activity is closer to that of wakefulness. On the one side, because the strong inhibition of motor neurons during REM sleep involves only sub-cortical structures (such as the locus coeruleus which targets motor neurons in the spinal cord) and given the relatively preserved information processing capabilities during this stage (Chennu and Bekinschtein, 2012), one might still expect similar covert responses as

found here. On the other side, these findings might be restricted to the initial stages of sleep during which the thalamus is mostly deactivated while large parts of the cortex remain active (Magnin et al., 2010). Future studies relying on full night protocols will be necessary to address whether the integration of semantic and decision processes can bypass early sleep stages.

Beyond revealing unsuspected processing capabilities in the sleeping brain, this study uncovers a promising avenue to study nonconscious influences. Research investigating the distinction between conscious and nonconscious mechanisms (the so-called 'contrastive approach' (Baars, 1988)) generally focuses on the notion of contents of consciousness. In this framework, the participant can be nonconscious 'of' a specific content as in a typical situation of visual masking, but she remains fully conscious in the intransitive sense of being aroused and vigilant. For instance, while previous studies using subliminal priming have shown that invisible primes can trigger lateralized readiness potentials (Dehaene et al., 1998; Eimer and Schlaghecken, 1998), participants in these studies were still having conscious access to their goal-directed behaviors in order to perform a specific task on target stimuli. Here, although sleeping participants may continue to process information in a goal-oriented manner, this task-set is presumably maintained without the participant being conscious of it. Moreover, our experimental approach relying on levels rather than contents of consciousness allows not only to examine the neural consequences of perceptual processes when the subject is nonconscious in any possible respects, but also offers the opportunity to use sensory stimuli that are not degraded in any manner. Indeed, the strong degradation of sensory signals typically used to achieve robust unawareness in masking studies, either in the visual (Kouider and Dehaene, 2007) or the auditory modality (Kouider and Dupoux, 2005), unavoidably decreases the strength of neural responses, especially in brain regions dealing with high-level information (Kouider and Dehaene, 2007). Hence, studying sleep in this context allows pushing further the limits and extents of nonconscious processes and establishing the properties of a broader and more natural type of cognitive unconscious.

Supplemental Information

Participants

Eighteen native English speakers (6 women and 12 men, age range: 18-30 years) took part in Experiment 1. An additional 29 participants were tested but not included in the final analysis because of a failure to fall asleep (N=27) or due to excessive artefacts in the EEG signal (N=2). For Experiment 2, 18 native French speakers (12 women and 4 men, age range: 20-28 years) were included out of 22 subjects. Four subjects were thus excluded either due to not falling asleep (N=1) or note reaching the N2 stages (N=3). All subjects were right-handed, and reported no auditory, neurological or psychiatric alterations. To increase the probability that participants would fall asleep in our experimental setup, only easy sleepers, as assessed by the Epworth Sleepiness Scale, were selected for this study. This scale evaluates whether participants are used to easily falling asleep, for instance when watching TV or during train trips. Recruited participants were considered healthy with relatively high ESS scores but not corresponding to a condition of pathological sleep such as hypersomnia: the average ESS scores were 10.4 with (range 7-14) for Experiment 1, and 11.6 (range 7-16) for Experiment 2, while the maximum possible score is 24. Participants were also asked to avoid exciting substances as coffee, and to sleep 1-2 hours (20%) less than usual the night preceding experiment 1 and 2-3 hours (30%) less than usual for Experiment 2. They signed a written consent and were paid for their participation. Both experiments were approved by the relevant local ethical committees (Cambridge psychology research ethics committee for Experiment 1, Conseil d'évaluation éthique pour les recherches en santé for Experiment 2).

Stimuli

For Experiment 1, stimuli were spoken words selected from the CELEX lexical database (Linguistic Data Consortium, University of Pennsylvania). There were 48 names of objects and 48 names of animals. Half were monosyllabic and the other half disyllabic, with animal and object names matched as closely as possible in terms of combined (spoken and written) log lemma frequencies, as confirmed by an independent t-test ($p > 0.10$). Additionally, words within the two categories were matched in a pair-wise fashion regarding their phonological properties: each object name was matched with a similar animal name (for example "quilt" was matched with "quail"), ensuring that animal and objects names could not be differentiated in terms of sub-semantic (i.e., phonological) properties. The words were tape-recorded by a female voice and digitized. Two lists of 48 stimuli each were produced, one for the wake period and the other for the sleeping period (counterbalanced across participants). For Experiment 2, the material consisted of 216 auditory stimuli corresponding to 108 pairs of words and pseudowords (half CVC monosyllabic and half CV-CV disyllabic) recorded by a male native French speaker and digitized. Within each pair, words and pseudowords were matched in length and phonological (consonant-vowel) structure. The words were selected from the Lexique database (New et al., 2004) and the pseudowords were all legal and pronounceable combinations of sounds in French. Three lists of 72 stimuli matched for frequency and phonological structure were constructed such as to be counterbalanced across participants for the wake period, the sleep period and the new list in the old/new recognition task following the main experiment.

Procedure

Participants were lying down with their eyes closed in a comfortable reclining chair in a dark and electrically and acoustically shielded EEG cabin. Stimuli were presented binaurally through headphones (Experiment 1) or through loud speakers (Experiment 2). Participants were instructed to perform a semantic categorization on whether each spoken word referred to an animal or to an object (Experiment 1) or to perform a lexical decision on whether each spoken stimulus existed or not in French (Experiment 2), by pressing a button with either their left or right hand (with response hand counterbalanced between participants). For Experiment 1, they were told that they could fall asleep at any time during the task, but were asked not to stop responding deliberately before falling asleep (i.e. not to stop responding in order to fall asleep). For Experiment 2, participants first performed a full session with the wake list items (about 10 minutes) under conditions were they were fully wake and not allowed to fall asleep, before hearing the wake list again while being reclined and allowed to fall asleep under similar testing conditions as in Experiment 1. Testing conditions encouraged the transition towards sleep while remaining engaged with the same task-set (explicit allowance to fall asleep, dark room, eyes closed, reclining chair, several repetitions of the first stimulus list, long inter stimulus interval). The continuous, uninterrupted flow within and across the two lists of stimuli was aimed at reducing the probability of awakening.

While being awake, participants could hear up to 4 repetitions of the first list. In Experiment 1, they were presented with the second list of 48 items only once during sleep while in Experiment 2, they could receive the second list of 72 items up to 3 times to increase the number of sleep trials. Stimuli were presented in a random order with an inter-stimulus interval varying between 6 and 9 seconds in Experiment 1 and a fixed duration of 9 seconds for Experiment 2. The presentation of spoken items would switch to the second list without interrupting the pace of the experiment whenever the participant was assessed by the experimenter as being asleep (Experiment 1) or as entering the NREM2 stage (Experiment 2, see details below), For Experiment 2, stimulation was switched back to the wake list in cases of return to NREM1, (micro)-awakenings and/or button presses. Stimulus delivery and response collection was controlled by the E-Prime software (Psychology Software Tools, Pittsburgh, PA) for Experiment 1 and by the Matlab (MathWorks Inc. Natick, MA, USA) using the Psychophysics Toolbox (Brainard, 1997) for Experiment 2.

EEG recordings and analysis

The electroencephalogram was continuously recorded from 64 Ag/AgCl electrodes (NeuroScan Labs system for Experiment 1; Electrical Geodesic Inc system for Experiment 2), with Cz as a reference. The impedance for electrodes was kept following constructor recommendations. Data were acquired with a sampling rate of 500 Hz (Experiment 1) or 250 Hz (Experiment 2). For the wake trials, only the first list occurrence was analysed (Experiment 1: N=48, Experiment 2: N=72). Continuous data were epoched from -2000 to 6000ms (Experiment 1) or to 8000ms (Experiment 2) in relation to stimulus onset, low-pass filtered at 30Hz and baseline corrected in respect to the pre-stimulus window of 2000ms. Trials with any electrode passing an absolute threshold (Experiment 1 with the NeuroScan system: 1000 μV, Experiment 2 with the

Electrical Geodesic Inc system: 250 μV) were rejected from the analysis (this concerned only non-physiological events). We used a very liberal threshold because sleep trials may contain large-magnitude K-complexes.

Separate averages were computed for left (L) and right (R) hand trials, resulting in two average waveforms for each electrode and participant. Stimulus locked LRP were then computed according to the procedure by Coles (1989, (Coles, 1989)), using the ERP waveforms recorded from corresponding electrode pairs in each hemisphere as follow:

$$\begin{aligned} LRP = [&(R\ hand - L\ hand\ trials)\ on\ L\ electrode \\ &+ \\ &(L\ hand - R\ hand\ trials)\ on\ R\ electrode] * 0.5 \end{aligned}$$

Statistical significance was assessed through cluster/permutation statistics calculated within participants, allowing us to deal with the potential issue of multiple comparisons in a principled manner. Each cluster was constituted by the samples that consecutively passed a specified threshold (in this case sample p-value of 0.1). As demonstrated by Maris & Oostenveld (Maris and Oostenveld, 2007), this threshold doesn't change the type-1 error, and the method controls for false alarms independent of this value. The cluster statistics was chosen as the sum of the t-values of all the samples in the cluster. Then, we compared the cluster statistics of each cluster with the maximum cluster statistics of 1000 random permutations. The significance of LRPs was assessed during both for the wake and sleep conditions by using a threshold monte-carlo p-value of 0.05.

Sleep assessment for Experiment 1

Sleep onset was determined *online* by relying on both behavioural and electrophysiological criteria. Participants were assumed to be asleep if they were not responding for at least 2 minutes, and if they were presenting EEG and EOG patterns characteristic of NREM sleep: reduction of fast rhythms (alpha – beta) in favour of slower rhythms (theta waves), slow-eye movements, vertex sharp waves and possibly evoked and/or spontaneous K-complexes and sleep spindles. Once sleep onset was confirmed, the first list was switched to a second one, never heard by the participant. For Experiment 1, after switching list, participants could occasionally press a button (14% of the trials in the sleep list). An offline sleep assessment was therefore conducted to confirm the sleeping state and to remove arousals or ambiguous trials (i.e., with potential micro-arousals), as well as trials with a button press. For Experiment 1, in which we concentrated on wake-to-sleep transition, we used an extension of standard sleep staging adapted and validated by Hori and collaborators (Hori et al., 1994; Tanaka et al., 1997). This method allows for a more refined sleep scoring since it uses smaller epochs prior to the stimulus onset (4 seconds) and allows for a more detailed characterisation of the hypnagogic period at the time of the auditory stimulation. Wakefulness was characterized by regular responses to stimuli, presence of fast low-amplitude rhythms such as alpha rhythms (8-13 Hz) especially on occipital electrodes, eye-blinks or saccades. Participants were declared asleep after the disappearance of alpha rhythm, replaced by slower oscillations (vertex sharp waves, theta rhythms). On the EOG, presence of slow eye movements was also indicative of the wake to NREM1 transition. Finally, when spontaneous K-complexes or spindles occurred in the 4s epoch prior to stimulus onset, the trial was scored as NREM2.

Importantly, in our protocol, it was crucial to assess not only the context in which stimuli were played (determined through the careful examination of the pre-stimulus activity) but

also how these stimuli affected brain activity by potentially triggering micro-arousals. In order to retain as sleep trials only those for which participants were genuinely asleep and remained in this state, we visually detected and marked every sign of arousal (increase in low-amplitude fast rhythms such as alpha oscillations or oscillations above 16Hz for more than 3 seconds and stable for at least 10 seconds) or micro-arousal (increase in low-amplitude fast rhythms such as alpha oscillations or oscillations above 16Hz for less than 3 seconds) following the stimulus onset (see (Iber et al., 2007)). Although micro-arousals were accompanied with behavioural responses in only a few cases, such trials were discarded from our analysis to ensure a conservative sleep scoring. This resulted in a total average of 70.8 trials per participant in this experiment, corresponding to 42.6 and 28.2 trials per participants in the wake and sleep conditions, respectively. Remaining trials were discarded (e.g. trials from the sleep list that were potentially associated with micro-arousals and/or with a button press). Among the trials included in the sleep condition, 79.4% were scored as NREM1 and 19.7% as NREM2. However, in order to satisfy standard definitions, NREM2 was scored only after the first occurrence of a *spontaneous* spindle or K-complex. As a consequence, evoked K-complexes or sleep spindles were still observed in 27.2% of NREM1, which reflects a deeper sleep stage than the standard NREM1. None of the participants reached the NREM3 stage or showed a REM episode. When considering a -2 to 4s window around stimuli onset, K-complexes were observed in 24.5% of sleep trials (23.2% of NREM1 trials) and sleep spindles in 8.5% of sleep trials (4.9% of NREM1 trials).

Note that no consensus exists for a simple (e.g. scalar) criterion that can be used automatically to separate sleep from wake trials, arguably because of the individual differences in terms of amplitude/frequency range used to score vigilance states (see for instance (Klimesch et al., 1999) for alpha and theta rhythms). For these reasons, the sleep assessment was performed by visual inspection, ensuring an evaluation that is both conservative (i.e., eliminating any sign of micro-arousal) and adaptative (i.e., taking into account individual variability). Nevertheless, to verify the validity of our sleep scoring methodology, we developed a scalar criterion that would constitute a quantitative evaluation of the difference between trials in the sleep and wake conditions. This scalar Vigilance Index (VI) was defined as the ratio of the mean power in specific frequency ranges computed on C3-C4 electrodes over each epoch (i.e., -2 to 6 seconds around stimulus onset), using a fast Fourier transform:

$$VI = [\text{delta power} + \text{theta power} + \text{spindle power}] / [\text{alpha power} + \text{high-beta power}]$$

With delta corresponding to 0.1 – 4 Hz, theta to 4 – 7 Hz, spindle frequency to 11 – 16 Hz, alpha to 8 – 13 Hz, and high-beta to 20 – 40 Hz). Low-Beta was not included as it overlaps with the frequency of spindles. For each epoch, power was normalized by the power in high frequency range (215 – 245 Hz). Delta, theta and spindle power being classically associated with sleep while alpha and high-beta are associated with wakefulness (see Figure S 4-1 for an illustration), "sleep" trials should show higher VI values than "wake" trials. VI was computed for every trial in the sleep and wake conditions. The distribution of VI values across all trials was bi-modal ($p<0.01$, Hardigan Dip Test). Importantly, when considering VI values for "sleep" and "wake" trials separately, we checked that their respective distributions were statistically different ($p<0.001$, unpaired t-test). This was also true when considering subjects individually ($p<0.001$, unpaired t-test, Bonferroni correction). This demonstrates that we are genuinely dealing with two distinct brain states in our study.

Supplemental sleep scoring of Experiment 1 using standard guidelines

To ensure that our results did not reflect an underestimation of the level of sleepiness due to the sleep scoring method we used, and thus the possibility of missing potential contaminations by micro-arousals, we performed a re-scoring of our data using standard guidelines of the AASM (Iber et al., 2007). Data were first continuously scored as wake, NREM1 and NREM2 using 20s epochs. Regular correct responses to stimuli, presence of alpha rhythms on occipital regions, eye-blinks or saccades were indicative of wakefulness. NREM1 was defined by the replacement of alpha rhythms with theta rhythms. Presence of slow eye movements, vertex sharp waves, evoked K-complexes or sleep spindles were also indicative of NREM1 onset. Finally, epochs showing spontaneous K-complexes or spindles were scored as NREM2. In order to retain as sleep trials only trials for which participants were and remained asleep, NREM1 and NREM2 trials associated with motor responses or micro-arousal (increase in low-amplitude fast rhythms lasting less than 3s) and arousals (e.g. associated or not with button presses) were discarded from further analysis. The corresponding LRP results are presented in Figure S 4-3.

Sleep assessment for Experiment 2

For Experiment 2, in which we directly compared a state of full alertness with NREM2, we relied exclusively on the standard sleep scoring method of the ASSM relying on 20-30 seconds epochs [S8], which is more adapted to the evaluation of deeper sleep states. In order to focus on NREM2, participants were assumed to be fully asleep if they were unresponsive and after the occurrence of the first spontaneous K-complex or sleep spindle (i.e. not appearing within at least 1 second following stimulus onset). There were also trials scored as NREM3 but those were not included in the final analysis as it concerned fewer trials and only a restricted set of participants (N=11). There was a total average of 147.7 trials per participant, corresponding to 68.7 and 79 trials in the wake and sleep conditions, respectively. The same procedure as for Experiment 1 was used here to discard trials micro-arousals and button presses.

Old/new recognition post-test

Experiment 2 was followed, after awakening, by an explicit recognition test in which they were presented, in random order, with spoken words that were previously presented during the wake or sleep period, or new words that were not presented before. They were instructed to report, using one of two keys on a keyboard, whether the word was old (i.e., presented in the wake or sleep list) or new, without time pressure. Following their answer, they indicated their level of confidence on a scale ranging from 1 (completely guessing) to 7 (completely sure), again without time pressure. Each participant was presented with 108 words (36 words per condition). The old items from the sleep conditions that were subsequently scored as reflecting N1, (micro)-awakenings and/or button presses were discarded from the analysis, to match items used in the LRP analysis.

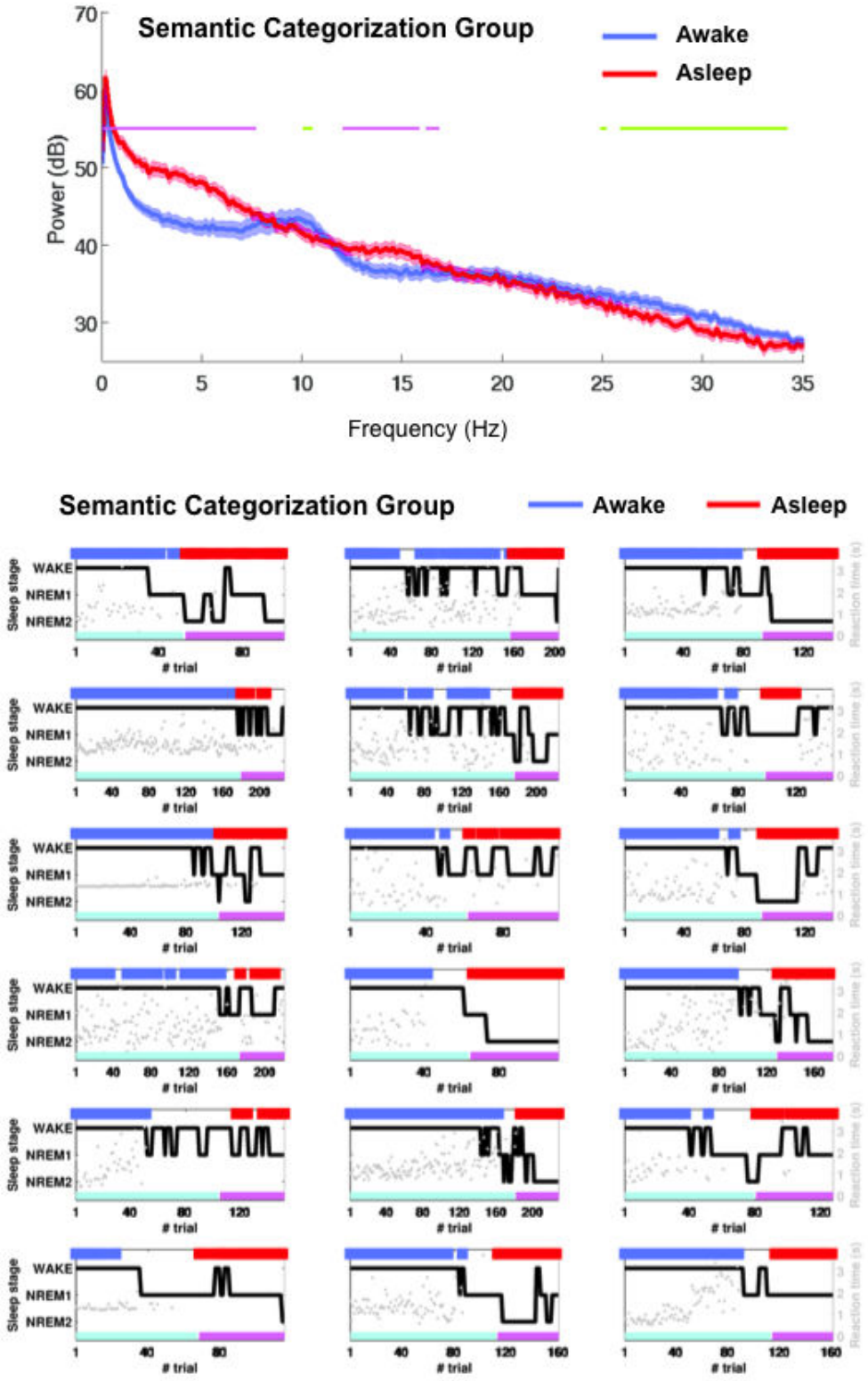

Figure S 4-1 Sleep assessment (Experiment 1)

Top. Average power spectra across participants for wake trials (blue) and sleep trials (red) in Experiment 1. Note the turnaround between alpha (8-13 Hz) and beta (20-40 Hz) rhythms predominant in wakefulness and sleep-related oscillations (delta (0.1-4 Hz), theta (4-7 Hz), spindle range (11-16 Hz)). Power spectra were computed on C3/C4 referenced to the mastoids with a fast Fourier transform and averaged across subjects. Purple bars mark frequencies for

which power was significantly higher in sleep compared to wake (paired t-test, 0.05, false detection rate correction). Light green bars mark frequencies for which power was significantly higher in wake compared to sleep (paired t-test, 0.05, false detection rate correction). Red and blue shadings denote standard-error to the mean. Bottom. Individual hypnograms. Black lines show the vigilance state per trial visually scored using AASM guidelines. Grey dots show recorded response times (RTs). Note the large variability in RTs typical of drowsiness. The line below each hypnogram contains information about the stimulus list (cyan: wake list; magenta: sleep list) and the line above each hypnogram depicts the final scoring taking into account behavioral and electrophysiological criteria (blue: "wake" trials; red: "sleep" trials).

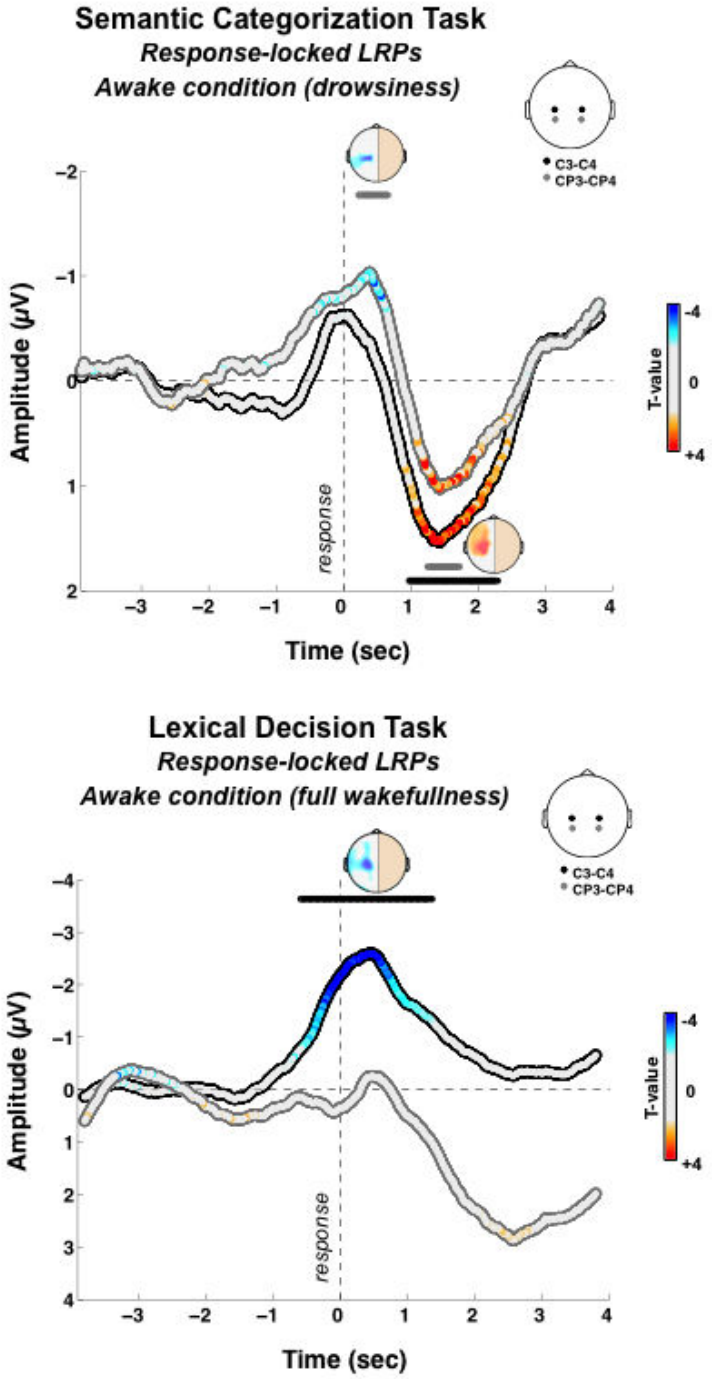

Figure S 4-2 Electrophysiological markers of motor preparation

Response-locked LRPs for Experiment 1 (top panel) and Experiment 2 (bottom panel). LRPs were here averaged with respect to the participant response on each trial (i.e. 0 ms corresponds to the response time). Baseline correction was performed with respect to a -4000 to -2000ms period before stimulus onset. Time-series show the LRP curves on central (C3/C4) and central posterior (CP3/CP4) electrodes (See Figure 4-2 for more details).

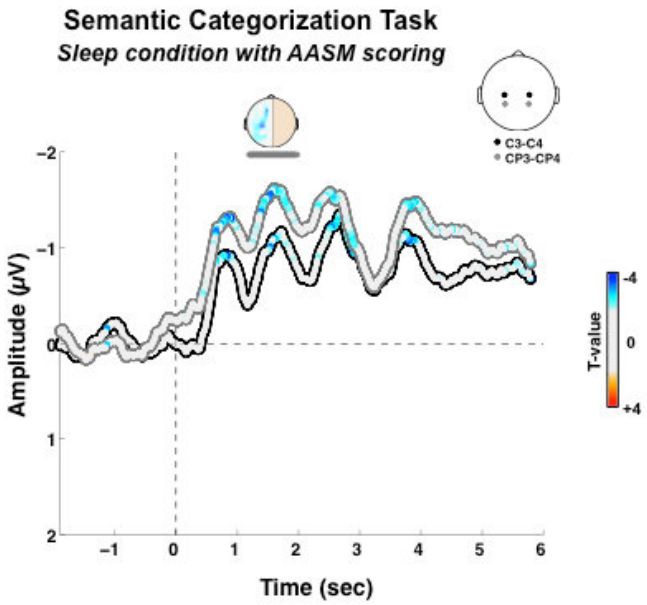

Figure S 4-3 Motor preparation to semantic categories

Stimulus-locked LRPs in Experiment 1 with standard sleep scoring. LRPs for the sleep condition in which trials were scored according to standard guidelines (see section on "Supplemental sleep scoring using standard guidelines" and Figure 4-2 for more details).

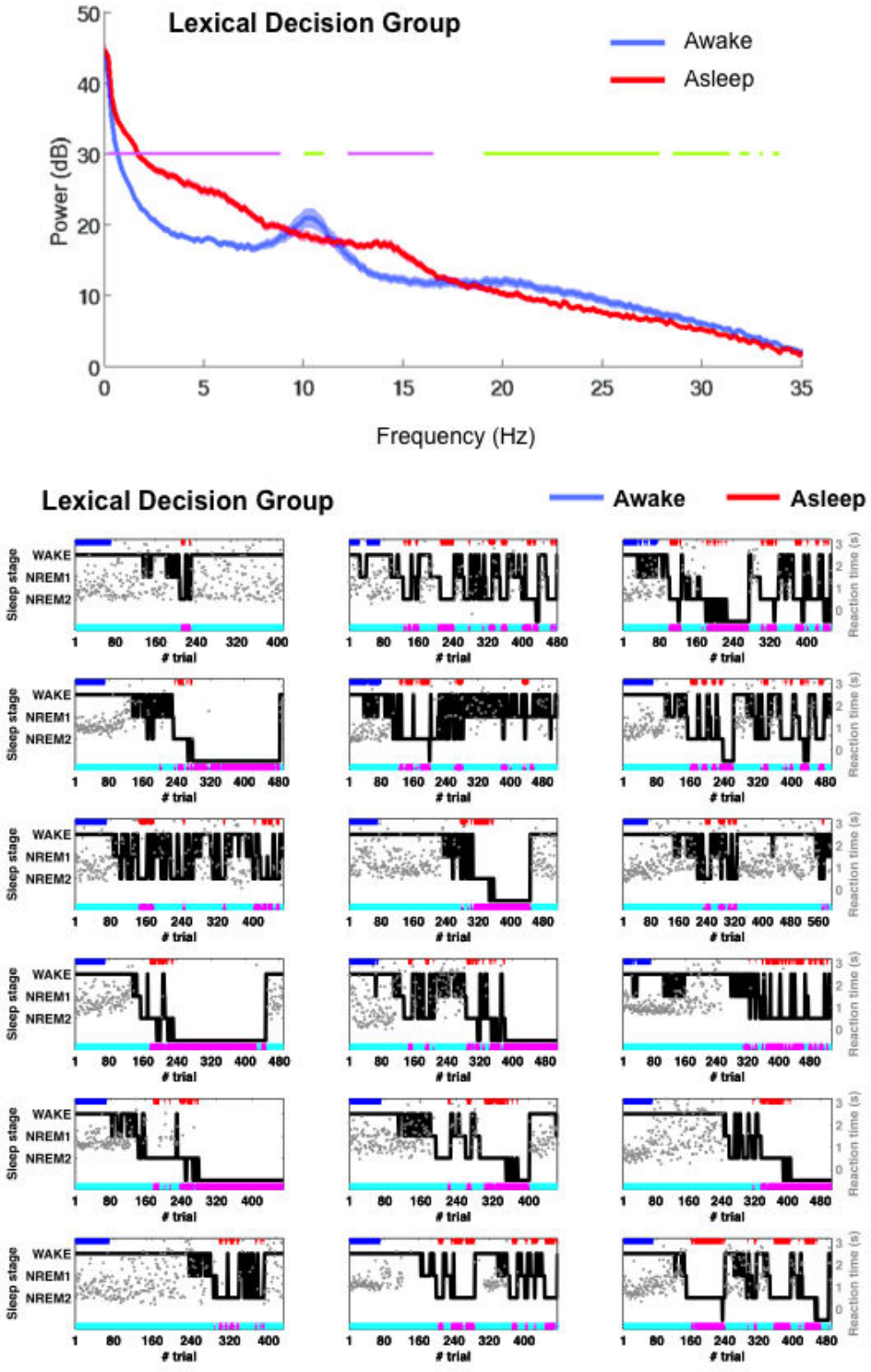

Figure S 4-4 Sleep assessment (Experiment 2)

Top. Average power spectra across participants for wake trials (blue) and sleep trials (red) in Experiment 2. Bottom. Individual hypnograms See Figure S 4-1 for details.

Study 5:
Neural markers of responsiveness to the environment in human sleep

Thomas Andrillon[1-2], Andreas Trier Poulsen[3], Lars Kai Hansen[3],

Damien Léger[4] & Sid Kouider[1]

[1] *Brain and Consciousness Group,*
École Normale Supérieure
Paris, France

[2] *Ecole Doctorale Cerveau Cognition Comportement,*
ENS – EHESS – Paris VI – Paris V
Paris, France

[3] *DTU Compute,*
Technical University of Denmark
Lyngby, Denmark

[4] *Centre du Sommeil et de la Vigilance,*
Université Paris Descartes, Hôtel Dieu,
Paris, France

Summary

Sleep is characterized by a loss of behavioral responsiveness. However, recent research has shown that the sleeping brain is not completely disconnected from its environment. How neural activity constrains the ability to process sensory information while asleep is yet unclear. Here, we instructed human volunteers to classify words with lateralized hand responses while falling asleep. Using an electroencephalographic (EEG) marker of covert motor preparation, we show the conservation of complex task-dependent sensory processes in light Non-Rapid Eye-Movement (NREM) sleep. However, these processes were abolished in deep NREM sleep and, importantly, in REM sleep despite the recovery of wake-like brain activity in this latter sleep stage. A detailed examination of the brain ongoing activity and its responses to sounds further specified the mechanisms gating the processing of external information. Acoustic stimulations were associated with a decrease of sleep depth and sensory processing could be related to a form of local awakening in NREM sleep. Indeed, sensory processing positively correlated with the Lempel-Ziv complexity, a measure that has been shown to track arousal in sleep and anesthesia. In REM sleep however, the relationship between complexity and external information processing was reversed. We propose that endogenously generated processes compete with the processing of external input in REM sleep. In NREM sleep, sensory activations were counter-balanced by evoked down-states, which blocked, when present, further processing of external information. Sleep can therefore be seen as a self-regulated process in which external information can be processed in lighter stages but suppressed in deeper stages. However, gating mechanisms drastically differ between NREM and REM sleep.

Introduction

Sleep can be operationally defined as a state of behavioral unresponsiveness (P Peigneux et al., 2001). Such disconnection from the external world may play a crucial role in memory consolidation, allowing the organisms to turn inward and protect endogenous mechanisms of neural plasticity from external interferences (Diekelmann and Born, 2010; Tononi and Cirelli, 2014)). Yet, this disconnection potentially comes at the expense of survival, as a sleeping organism becomes highly vulnerable to menaces from the environment. It thus remains unclear why and how this disconnection occurs. In particular, whether the brain is fully shut down from the environment, or whether it remains partially responsive to external events, remains an active topic of research. The influential thalamic gating hypothesis proposed that behavioral unresponsiveness was achieved very early on through the blockade of sensory information at the thalamic level, leading to the abolition of sensory cortical responses (McCormick and Bal, 1994). However, there is accumulating evidence showing that the brain is far from being isolated during sleep (Hennevin et al., 2007; Issa and Wang, 2008; Y. Nir et al., 2013). The very fact that sleep is quickly reversible argues against a complete disconnection. In fact, not only can sleepers awake at any moment but they can do so more easily for familiar and salient stimuli such as their own baby's cry (Formby, 1967) or their own name (Oswald et al., 1960). Even when sleep is preserved, stimulus familiarity impacts brain responses (Perrin et al., 1999), suggesting that the sleeping brain maintain some ability to track incoming information while staying asleep. In recent years, several studies have shown that the sleeping brain's ability to process external information extends far beyond such automatic processes. From the detection of semantic incongruity (Bastuji, 1999; Brualla et al., 1998; Ibanez et al., 2006) or the violation of simple rules (Ruby et al., 2008; Strauss et al., 2015) to the formation of new associations (Arzi et al., 2012; de Lavilléon et al., 2015), the cognitive processes involved during sleep appear far more elaborated than previously thought.

However, although these studies have demonstrated the preservation of cognitive abilities during sleep, the neural mechanisms allowing sleepers to process or isolate from external stimulations remain unsettled. The role of evoked slow oscillations such as K-complexes, a hallmark of NREM sleep, is particularly unclear (Halasz, 2005). K-complexes have been related to arousal systems (Halász, 2016; Siclari et al., 2014a) providing windows of wakefulness (Destexhe et al., 2007). Conversely, they have been described as local down-states (Cash et al., 2009) entailing large-scale neuronal silencing (Vyazovskiy and Harris, 2013) and protecting sleep against external stimulations (Bastien et al., 2000; Wauquier et al., 1995). Sleep spindles are also thought to enable sleeper's isolation by blocking incoming input at the thalamic level (McCormick and Bal, 1994). However, evidence supporting this function is scarce (Schabus et al., 2012) while cellular recordings showed remarkably preserved responses to sounds during spindles (Sela et al., 2016). REM sleep on the other hand has been far less studied. Paradoxically, even if brain activity in REM sleep resembles wakefulness and consciousness is regained (Hobson and Pace-Schott, 2002), sleepers remain largely unresponsive (Ermis et al., 2010). What are the mechanisms enabling such sensory disconnection? It has been proposed that dreams themselves would compete and block the processing of external inputs (Nir and Tononi, 2010) but direct evidence is still missing.

Here, we attempted to bridge the gap between functional and physiological explorations of sleep in humans. We relied on a paradigm that aimed at inducing task-dependent responses in the sleeping brain (Kouider et al., 2014). In practice participants felt asleep

while categorizing spoken words with lateralized responses. Using EEG recordings, we explored whether stimuli elicited brain activations corresponding to the motor preparation of the correct response (i.e. Lateralized Readiness Potential, (Masaki et al., 2004; Smulders et al., 2012)). The presence of such LRP implies that stimuli were not only encoded at the sensory level but also processed at a high-level of semantic representation and that such high-level information is used up to the preparation of a motor response (see Kouider et al., 2014). Thus, the presence of an LRP highlights the maintenance of complex distributed processes during sleep. While our previous study was limited to light daytime sleep (nap study), we investigated here all sleep stages in a full-night protocol. Furthermore, the presence or magnitude of the LRP was further evaluated in light of brain activity before and after the stimulus so as to provide novel insights about how the brain manages to both track its environment and preserve sleep.

Material and Methods

Participants

22 right-handed French native speakers (14 females, age 21-31) with no history of neurological or sleep disorders participated to this study. Participants underwent an interview with a sleep specialist and filled in questionnaires determining their sleep habits and their propensity to fall asleep in noisy environments. Participants did not differ from the general population. They were monitored for 7-10 days prior to the recording session through actigraphy and sleep diaries to ensure stable sleep/wake rhythms. Among these 22 participants, 4 participants were discarded from our analysis either for technical issues affecting the recordings (N = 1) or because the experiment was aborted (N = 3, participants experiencing difficulties to fall asleep with auditory stimulation). The protocol had been approved by the local ethics committee (Comité de Protection des Personnes, Ile-de-France I, Paris, France).

Experimental Procedure

Task. We adapted a procedure previously used during daytime naps (Kouider et al., 2014) to a full-night protocol in order to explore all sleep stages. The night of the recordings, participants were equipped for polysomnographic recordings. They were put to bed and spoken words in French were then played in isolation one after the other. These words referred either to an animal or to an object. Participants were instructed to perform a semantic-decision task by indicating the category of each word through right and left-hand responses. They were asked to categorize words as long as they were awake and to resume responding in case of an awakening. Subjects were reminded to do so whenever they awoke during the night without resuming to respond. However, participants were explicitly authorized to fall asleep while performing the task. Crucially, three different lists of words were played to participants according to their vigilance state, as assessed though an online assessment of sleep stages (see below). A list was played whenever participants were in NREM sleep, another list was played during REM sleep and a wake list was played otherwise, i.e. mainly during wakefulness. Thus, unpracticed words (i.e. novel words not previously categorized during wakefulness) were played in sleep to ensure that participants had to access the meaning of the word in order to prepare for the appropriate response without relying on stimulus-response associations formed while awake.

Stimuli.. Stimuli were French spoken words uttered by a female voice. Four lists of 72 words were created each containing 36 words referring to animals and 36 words referring to objects. Animals and objects words were matched in frequency and number of syllables using the Lexique database (New et al., 2004). Three of the 4 lists were used for the semantic-categorization task. The 4th list was used in the memory-test (see below). The attribution of the different lists to a given vigilance state or to the memory-test was counter-balanced across participants.

Apparatus. Response-handles were attached to participants' hands. The mapping between semantic categories and response-hands was counter-balanced across participants. Stimuli were played through loud speakers around 55dB (depending on participants' preferences) using the Psychtoolbox extension (Brainard, 1997) for Matlab

(Mathworks Inc., Natick, MA, USA). Stimuli were played every 6 to 9 s (random uniform jitter).

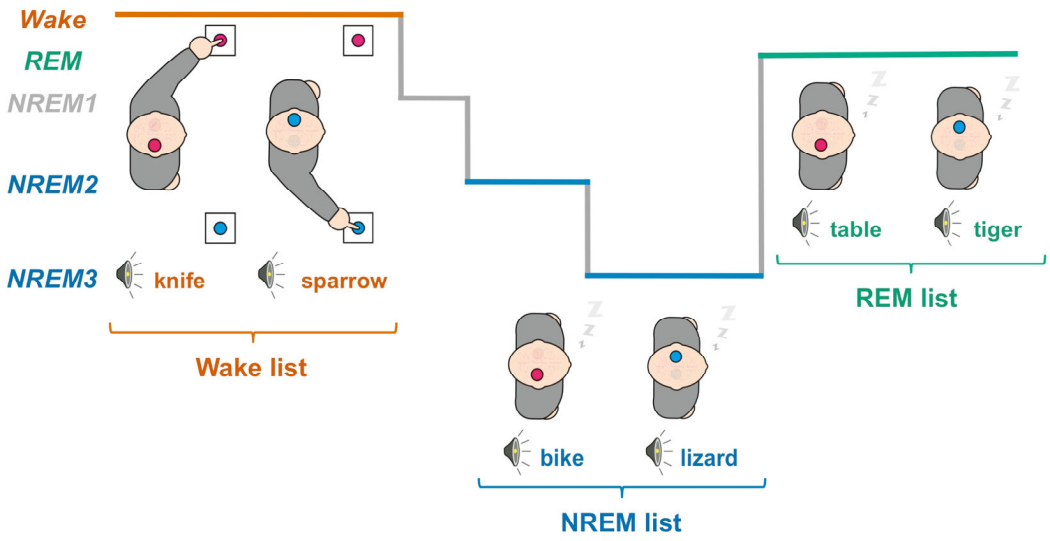

Figure 5-1 Semantic categorization task during full-night sleep

Illustration of the protocol. Different lists of animal and objects word were played to participants. Participants were instructed to classify these words through left and right hand responses according to their semantic category (here right-hand response for animals). Lateralized hand-response preparation involves the contra-lateral motor cortices, a task-dependent lateralization of brain activity that can be tracked with the EEG (Figure 5-2). Different lists of words were presented to participants. A list was restricted to NREM-sleep (NREM2 and NREM3, blue) and REM-sleep (green) while the wake list (red) was played otherwise. Changing list between wake and sleep prevents sleepers from using stimulus-response association learnt in wake to classify words in sleep. Words being novel, participants must have had access to the semantic level of each word representation to prepare for the correct response.

Data analysis

Electrophysiological recordings. Electroencephalographic (EEG, N = 19 derivations, 10-20 montage), electrooculographic (EOG, N = 2 derivations, positioned above the right canthus and under the left canthus), electromyograhpic (EMG, 1 derivation placed on the chin measuring muscle tone and 2 derivations on the right and left abductor pollicis brevis (thumb flexor muscle) recording muscle activity accompanying participants' responses) and electrocardiographic (ECG, N = 1 derivation) data were continuously recorded. Video monitoring was also available. EEG, EOG, ECG and EMG data were recorded with AgCl electrodes attached to participants' skin and hair with an adhesive paste (EC2, Natus Neurology Inc., Middleton, WI, USA). Signal were amplified through a B1IP or B2IP MEDATEC amplifier (Medical Data Technology SPRL, Bruxelles, Belgique) and recorded at a 200Hz sampling-rate. Impedances of scalp electrodes were generally below 5kΩ. EEG and EOG electrodes were referenced online to the opposite mastoids. An additional channel was used to synchronize EEG data with stimulus presentation.

Online sleep assessment. The presentation of stimuli was continuous but the words presented to participants were selected from lists that differed depending on participant's vigilance state (Figure 5-1). Vigilance states were scored online following standard guidelines (Iber et al., 2007). In practice, the experimenter waited for the apparition of NREM hallmarks (first spontaneous K-complex or sleep spindle, absence of signs of arousal) before switching to the NREM list. Similarly, the REM list was presented to participants when they entered the REM stage (absence of slow oscillations or sleep spindles, absence of alpha oscillations, presence of saw-tooth waves, rapid-eye movements, increase in theta oscillations, reduced or absent muscle tone). The experimenter typically waited for few minutes after the transition to the new sleep stage before switching the list to ensure its stability. The wake list was presented to participants whenever they showed signs of arousals (body movements, increase in low-amplitude desynchronized rhythms, EMG activation…). This online scoring was confirmed and refined offline (see below).

Offline sleep scoring. Wakefulness and sleep stages were scored following established guidelines (Iber et al., 2007). Only Fz, C3, C4 and Pz EEG derivations (within the 10-20 montage) were used along ECG and EMG derivations. EEG channels were first re-referenced to the average mastoids. The EEG and EOG signals were high-pass filtered above 0.1 Hz and then low-pass filtered below 30 Hz (two-pass Butterworth filters at the 5^{th} order). Using the same filter types, EMG data were band-pass filtered between 60 and 80 Hz. A notch-filter (2^{nd} order Infinite Impulse Response filter) around 50Hz was used on all channels to reduce line-noise. Vigilance states were continuously scored on 20-s-long windows as wakefulness, NREM sleep stage 1, 2 and 3 (NREM1, NREM2 and NREM3 stages resp.) and REM sleep. Importantly, epochs showing signs of arousal (increase in alpha oscillations or oscillations above 16Hz lasting more than 3 seconds) or micro-arousal (less than 3 seconds) in association with trial onsets were marked. The corresponding trials were not included in further analyses to avoid potential confounds.

Slow-waves detection. Slow-waves were detected in NREM sleep using algorithms that have been presented in details elsewhere (Nir et al., 2011; Riedner et al., 2007). Briefly, slow-waves were detected for each EEG channel by band-pass filtering the EEG signal between 0.2 and 3 Hz (two-pass Butterworth filter at the 3^{rd} order). The first order derivative was used to detect local extrema and identify single waves. Only slow-oscillations with a peak-to-peak amplitude exceeding 75 μV and a period of more than 0.5 s and less than 2 s were considered as slow-waves. These slow-oscillations were used to define light and deep NREM trials (see below).

EEG preprocessing. EEG data were analyzed using a combination of SPM (Functional Imaging Laboratory, Univ. College London, London, UK), FieldTrip (Oostenveld et al., 2011) and EEGlab (Delorme and Makeig, 2004) toolboxes running on Matlab (Mathworks Inc., Natick, MA, USA). We examined the brain activity in response to sounds by computing Event-Related Potentials (ERPs) and Lateralized Readiness Potentials (LRPs). To do so, the continuous EEG signal referenced to the average mastoids was high-pass filtered above 0.1 Hz (two-pass Butterworth filter at the 5th order) and then segmented on large temporal windows around stimulus onsets ([-14, 14] s). The EEG signal was then low-pass filtered below 40 Hz and notch-filtered around 50 Hz (same filter types as for the sleep scoring) to reduce line noise. Epochs were re-sized to focus on the activity around stimulus onsets ([-2, 7] s). Trials with absolute amplitude over central electrodes (Cz, C3, C4) exceeding a given threshold were discarded (a 150

μV threshold in wake and REM sleep, and larger 200 μV threshold in NREM sleep since NREM sleep contains high-amplitude physiological slow-waves).

Conditions of interest. NREM sleep being a quite heterogeneous state, ranging from NREM1 - a state in which participants may conserve some awareness of the surrounding world and are able to overtly respond to external stimuli - to NREM3 - in which brain dynamics is profoundly transformed - we divided NREM trials between light and deep NREM sleep. We thus divided trials in 4 different conditions of interest: (i) ***wake:*** correct trials during which participants were scored as awake and the wake list was played; (ii) ***light NREM sleep:*** trials scored as NREM2 or NREM3, during which participants were unresponsive and in which the NREM list was played but no slow-wave were detected (on a [-2, 3] s window time-locked to stimulus onset); (iii) ***deep NREM sleep:*** trials scored as NREM2 or NREM3, during which participants were unresponsive and in which the NREM list was played and slow-waves were detected (on a [-2, 3] s window time-locked to stimulus onset); (iv) ***REM sleep:*** trials scored as REM sleep, during which participants were unresponsive and in which the REM list was played. Importantly, we did not analyze the twilight NREM1 stage as well as trials in which any sign of arousal could be observed in the EEG signal to ensure that observed sensory processes are not due to (partial) awakenings. For each condition, only participants with at least 70 trials were included. On average, there were 174 ± 20 trials in the wake condition (mean ± standard error of the mean (SEM) across N=17 participants), 232 ± 28 in light NREM sleep (N=15), 400 ± 25 in deep NREM sleep (N=18) and 186 ± 9 in REM sleep (N=18). We also examined trials corresponding to the definition of light NREM and REM sleep with the exception that the wake list was presented to participants (i.e. trials already categorized during wakefulness). Indeed, participants were switched to the wake list whenever the experimenter was unsure of the state of the sleeper (later verified off-line), at transitions between states or when the experimenter had to attend to another participant (two participants participated in the experiment on each recording night). Although these trials containing practiced words were not randomly intermixed with the unpracticed words, they were scored offline as either REM or NREM sleep by two scorers blind to the list used and revealed ERPs and power spectra identical to the ones obtained in trials in which the sleep lists were played (Figure 5-3). Thus, these trials allowed us investigating how practiced (i.e., overtly categorized) words were processed during sleep, although precautions must be taken when interpreting such results (see Discussion).

Event-Related Potentials. ERPs were computed by averaging the EEG signal across trials for a given experimental condition after baseline correction ([-0.2, 0] s).

Lateralized Readiness Potentials. Lateralized Readiness Potentials (LRPs) allow the monitoring of action selection and preparation (Smulders et al., 2012). LRPs are usually computed with EEG data time-locked to motor responses but can also be computed time-locked to stimuli (Leuthold, 2003b; Tollner et al., 2012b). In our case, due to the absence of responses during sleep, we computed LRPs on stimulus-locked data. LRPs were computed using ERPs computed on the right (C4) and left (C3) electrodes placed over motor cortices:

$$LRP = \frac{(C3_{right-hand} - C3_{left-hand}) + (C4_{left-hand} - C4_{right-hand})}{2}$$

ERPs over C3 and C4 electrodes were computed similarly as described above except for the baseline correction ([-2, 0] s). Using this formula, LRP are characterized by a negative deflection starting before participants' response. In subsequent analyses, we extracted the amplitude of the LRP (LRP magnitude) over the temporal windows in which significant negative clusters were observed (Figure 5-2 and Figure 5-3). To examine how this LRP magnitude was dynamically related to others markers of responsiveness, we computed LRPs on windows of 60 consecutive left-response and right-response trials slid every trial (see Figure 5-4, Figure 5-5, Figure 5-6 and Figure 5-7). The LRP negative potential was extracted as a positive value (LRP magnitude) by adding a negative sign to the LRP formula. Other variables of the EEG signal were estimated on the same windows such as the Lempel-Ziv complexity (LZc, see below, Figure 5-4) or ERP components (see Figure 5-6 and Figure 5-7). These variables were z-scored across trials for each participant and then aggregated across participants to examine their correlation.

Time-Frequency analyses. To better understand how sleep rhythms impact sensory processing, we computed the time-frequency decomposition of the EEG signal in response to stimuli. To do so, we applied a Fast-Fourier Transform (FFT) on 1.28-s-long windows (padding ration of 2) on the preprocessed EEG signal (see above). The resulting power for each frequency and time was expressed as the log-ratio of the power at the corresponding frequency and time over the baseline activity ([-1.5, 0] s) at the same frequency. LRP magnitude and the activity within the slow-waves ([1, 6] Hz) and spindle ([11, 16] Hz) bands were extracted on windows of 60 consecutive right-hand and left-hand responses.

Lempel-Ziv complexity. The Lempel-Ziv complexity (LZc) measures the compressibility of a given signal (Ziv and Lempel, 1977). The higher the LZc value, the less compressible is the signal. A temporally predictable signal will have a low LZc value while an unpredictable signal will have a high LZc value. Previous studies have shown that LZc accurately tracks the level of consciousness in patients, healthy subjects under anesthesia and during sleep (Abásolo et al., 2015; Casali et al., 2013; Schartner et al., 2015). To calculate the LZc on the EEG signal, we implemented the approach developed by Schartner and colleagues (Schartner et al., 2015). Here, the complexity was computed at the sensor level and not in the source-space as originally done by Casali and colleagues (Casali et al., 2013). The raw EEG signal was first lowpass filtered below 85Hz (111^{th} order, Finite Impulse Response (FIR) filter) and then notch-filtered around 50Hz to reduce line noise (296^{th} order FIR filter). Matlab FDAtool was used to create equiripple FIR filters with linear phase to avoid phase distortion in the EEG. A surface Laplacian was then applied to the EEG data (BCILAB plug-in for the EEGLAB toolbox ((Delorme and Makeig, 2004; Kothe and Makeig, 2013) with a neighbor count of four) to minimize the influence of volume conduction. The data was then epoched around stimuli onset ([-2, 6]s), and the LZc was extracted for each trial by integrating the EEG data over all the sensors on 500-ms-long windows slid every 50 ms. Details of the LZc algorithm can be found elsewhere (Schartner et al., 2015). Briefly, for each window, the mean of the EEG signal was subtracted for each sensor and linear trends over the entire epoch were removed. A Hilbert transform was then applied to the signal in order to extract the envelope of the signal. Each channel was then binarised: values above the mean value of the envelope for the corresponding epoch and sensors were coded as 1, and 0 otherwise. The resulting binary matrix was then reshaped sensor-wise into a vector containing the time-points for all channels. The complexity was computed on such vector and normalized by the complexity calculated on the same vector, but with its elements randomly shuffled. After normalization, LZc is comprised between 0 (fully

compressible, i.e. predictable signal) and 1 (minimally compressible, i.e. as predictable as the shuffle data). The normalized complexity was thus computed for each trial and averaged across vigilance states (as scored offline) over the pre-stimulus baseline ([-1.5, 0]s) to compare the overall level of complexity between these different states (Figure 5-4a). We also examined how the complexity was affected by stimulations by averaging the LZc on a [-1.5, 6]s windows for each vigilance state separately (Figure 5-4b). To better compare the dynamics, LZc was normalized (ratio) by the level of complexity in the pre-stimulus window ([-1.5, 0]s). To relate the level of complexity with the index of motor preparation (LRP magnitude), the baseline LZc was extracted in wakefulness, NREM2 and REM-sleep on windows of 60 consecutive left and right hand-response trials slid every trial along the entire recordings. The values obtained were then z-scored across trials for each participant before examining their correlation (Figure 5-4c).

Sleep cycles identification. To examine how markers of responsiveness are modulated across NREM-sleep, we identified the sleep cycles based on each participant's hypnograms. A total of 100 cycles were individualized in 18 participants (5.6 ± 0.2 cycle per participant). Values of interest (LRP magnitude, LZc and delta (<4Hz) power) were computed on 60 right-hand and left-hand consecutive NREM trials (NREM2 and 3) slid every trial within each cycle. Delta power was extracted by applying a Fast-Fourrier Transform of the signal time-locked to stimulus onsets ([-2, 6]s) and normalizing the delta range (<4Hz) with higher frequencies ([20, 40]Hz, log ratio). Later on, each sleep cycle was normalized in duration in order to average variables of interests across sleep cycles. To do so, each cycle was divided in 30 equal bins and the mean value of the variables of interests was computed for each bin. Eighty-three cycles were eventually included in this analysis. The other cycles did not have enough NREM2 and NREM3 trials so as to be similarly normalized in duration.

Statistics. To correct for the multiple comparison problem when examining statistical differences between two time series (see Figure 5-2, Figure 5-3, Figure 5-4 and Figure 5-5), we used a cluster-permutation approach (Maris and Oostenveld, 2007). Each cluster was constituted by the samples that consecutively passed a specific threshold (here, $p < 0.1$ for LRPs and 0,05 otherwise). For each cluster, we computed the sum of the t-values of all the samples within the cluster. Then, we compared the cluster statistics of each cluster with the maximum cluster statistics of 1000 random permutations and obtained a non-parametric p-value (Monte-Carlo p-value: $p_{cluster}$). Significant clusters are displayed as horizontal bars on plots, and $p_{cluster}$ are reported in the main text and figures' legends. For scalp topographies of correlation analyses (Figure 5-6, Figure 5-7), the False Detection Rate (FDR) method was used to correct individual p-values (Benjamini and Yekutieli, 2011).

Results

Sleepers can classify words in during sleep

A classical LRP was observed when participants were awake and responsive (Figure 5-2a, significant cluster: [0.490, 2.025] s, $p_{cluster}$=0.002, N=17 participants), characterized by a large negative deflection starting before the average response time (RTs, black arrow) over motor electrodes (Figure 5-2a inset). When focusing on light NREM sleep, we observed a significant negative deflection for the LRP (Figure 5-2c, significant cluster: [3.035, 3.775] s, $p_{cluster}$=0.01, N=15 participants). As in wakefulness, this negative deflection was maximal over motor cortices (central electrodes, see inset Figure 5-2b) but was delayed compared to wake trials. This LRP is strikingly similar to our previous nap studies (Kouider et al., 2014).

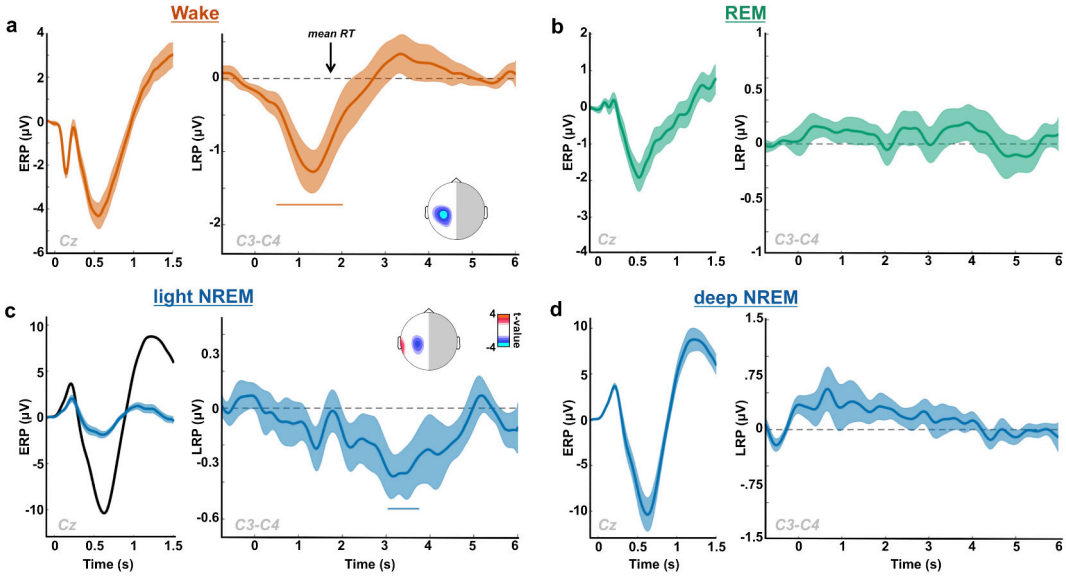

Figure 5-2 Lateralized Readiness Potentials (LRPs) across sleep stages

The Lateralized Readiness Potential (LRP) allows monitoring the lateralization of brain activity associated with motor selection and preparation. We used it here as an index of participants' ability to process sensory information up to the semantic level and to use this information in a flexible task-dependent fashion (see Material and Methods and (Kouider et al., 2014)). Each subpanel shows, on the right, the stimulus-locked ERP computed on Cz (a: in wakefulness, b: in REM sleep c: in light NREM sleep (blue, black curves show deep NREM sleep for comparison) and d: in deep NREM sleep). On the left, the corresponding stimulus-locked LRP computed on C3/C4 electrodes are plotted. Shaded areas represent the standard error of the mean (SEM) computed across participants. Colored horizontal bars show significant clusters for LRP ($p_{cluster}$<0.05). Insets show the scalp topographies of LRP averaged over the red and blue clusters. Curves were smoothed using a Gaussian kernel (width: 50ms for ERPs, 200ms for LRPs) for display only (statistics were performed prior to smoothing). Note that an LRP peaking over motor cortices is visible in light NREM, but is absent in deeper sleep stages (deep NREM and REM sleep).

However, no significant deviation in the LRP was observed in deep NREM sleep or REM sleep (Figure 5-2b,d), suggesting, at first glance, that processing of sensory information up to the decision level is abolished in deeper stages of sleep. Interestingly, light and deep NREM sleep also differed regarding the evoked responses to stimuli

(ERPs). Light NREM sleep was characterized by a reduction of the large negativity evoked by stimuli in NREM sleep (N550, (Picton, 2010)). This N550 is often attributed to evoked slow-waves (such as K-complexes) (Bastien et al., 2000) and entails large-scale neuronal silencing (Vyazovskiy and Harris, 2013), which could explain the absence of an LRP when the N550 is larger.

In REM sleep, only words previously heard in wake are classified

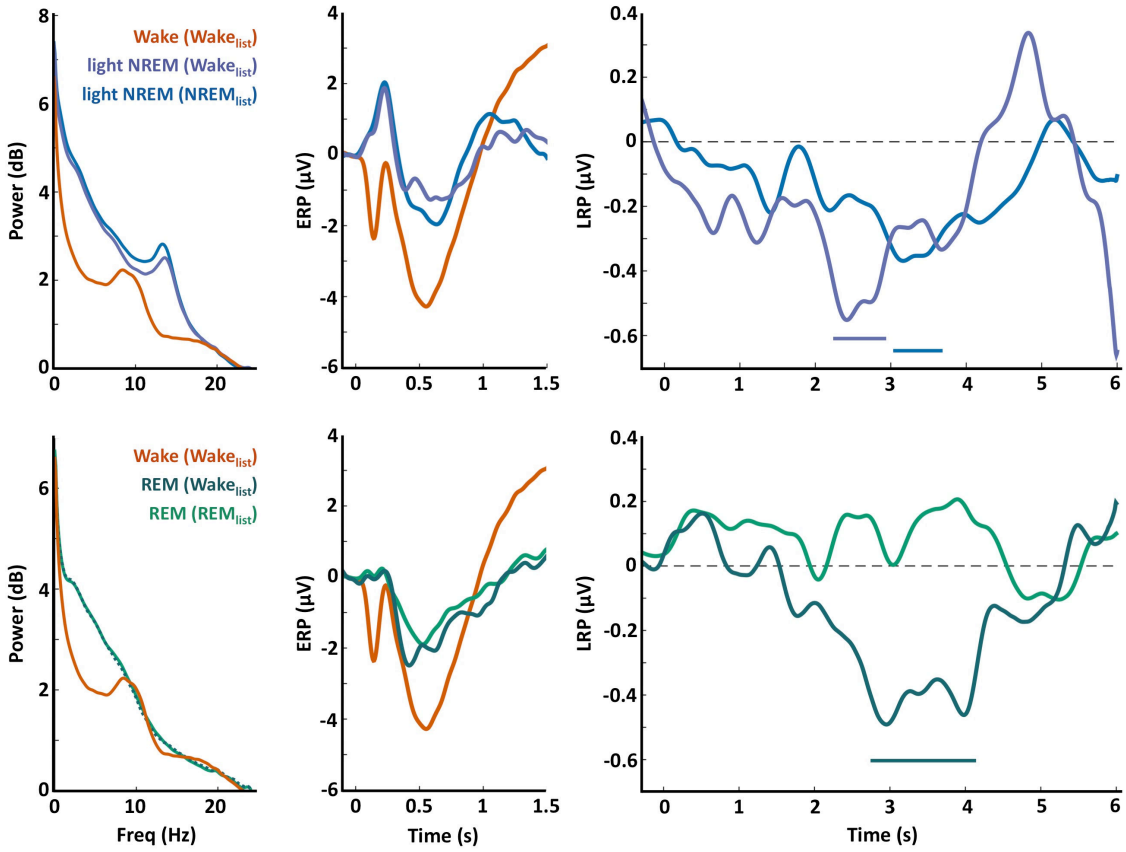

Figure 5-3 Lateralized Readiness Potentials (LRPs) in light NREM and REM sleep for words categorized during wakefulness

Top: Power spectra (left), stimulus-locked Event-Related Potentials (EPRs; middle) and stimulus-locked Lateralized Readiness Potentials (LRPs; right) computed in light NREM sleep for trials in which either the NREM list (blue) or the wake (purple) list was played. The wake ERPs and power spectrum (red curves) are displayed for comparison. Horizontal bars show the significant clusters for LRPs ($p_{cluster}<0.05$). Note the presence of a similar (and slightly earlier) LRP when words categorized during wakefulness were played. Bottom: Power spectra (left), ERPs (middle) and LRPs (right) computed in REM sleep for trials in which either the REM list (light green) or the wake (dark green) list was played. Interestingly, for words previously categorized in wakefulness, a clear LRP was observed ($p_{cluster}<0.05$) but not for novel words (as shown in Figure 5-2). Yet, the power spectrum and ERPs corresponding to the REM trials in which the wake list was played are typical of REM sleep and different from wake trials (red curves).

Does the absence of an LRP in REM sleep mean that stimuli were not processed at all, or is this absence due to the complexity of the task at hand? To investigate this issue, we took advantage of the fact that words from the wake list were sometimes presented in REM-sleep (see Material and Methods), albeit not intermixed with unpracticed words, which would have allowed a stronger comparison (see Discussion).

Importantly, the ERPs and power spectra were similar for both lists and differed from wake ERP and power spectrum (Figure 5-3). Strikingly, a clear LRP was also observed for the wake list only ([2.750, 3.200] s, $p_{cluster}$=0.036 and [3.230, 3.900] s, $p_{cluster}$=0.014, N=14 participants). This LRP suggests that sleepers can still map stimuli with the correct response side in REM sleep when stimuli are familiar, suggesting that part of the processing chain was conserved in this particular case. However it is possible that REM sleep was qualitatively different when the two lists were presented despite the overlap of the ERPs and power spectra (see Discussion). When repeating this procedure in light NREM sleep, an LRP was also observed for the words practiced in wake ([2.23, 2.9] s, $p_{cluster}$=0.011, N=15 participants).

The processing of information depends on the degree of neural complexity

We then set out to examine whether the overall complexity of the EEG signal was predictive of sleepers' ability to process information up to the decision level. To do so, we used a recently developed approach (Casali et al., 2013) consisting in measuring the temporal predictability of the EEG signal by reducing it to a single value: the Lempel-Ziv complexity (LZc, (Ziv and Lempel, 1977)). Applying this methodology to our data (Figure 5-3a) revealed a strong modulation of LZc according to the vigilance state ($F(3)=9.67$, $p=2.10^{-5}$). We could separate sleep and wake stages along a gradient matching the phenomenology associated to these states (Yuval Nir et al., 2013), confirming initial results in humans (Casali et al., 2013) and animals (Abásolo et al., 2015). Precisely, LZc was maximal in wakefulness (paired t-tests across participants with other sleep stages: all $p<0.005$) and minimal in deep NREM sleep. Light NREM and REM sleep had intermediary values with REM sleep being the closest to wakefulness (REM vs. wake: $t(17)=-3.3$, $p=0.004$; REM vs. light NREM: $t(17)=5.4$, p=5.10-5; light vs. deep nREM: $t(17)=-9$, p=7.10-8), in accordance with the fact that dreams are more frequent and complex in REM compared to light NREM sleep and quasi absent in deep NREM sleep (Nir and Tononi, 2010).

We then investigated whether this baseline LZc was predictive of LRP magnitude. LRP magnitude was extracted on the windows in which a LRP was observed in wakefulness (Figure 5-2a), light NREM sleep (Figure 5-2c) and REM sleep when the wake list was played (Figure 5-3). To facilitate the interpretation of the figures, the LRP formula was reversed so that the presence of an LRP would translate into a positive LRP magnitude (see Material and Methods). Importantly, the baseline LZc was positively correlated with LRP magnitude in wakefulness and NREM sleep (Pearons's coefficient: r=0.08 and 0.13, p=0.001 and 1.10^{-13}, across N=2035 and 3111 samples in 17 and 15 participants resp.) but this correlation was reversed in REM sleep (r=-0.23, $p=5.10^{-24}$, N=1937 samples in 18 participants). Comparing LZc in REM seep when practiced words were presented (LRP present) and when unpracticed words were presented (LRP absent) revealed again

that the presence of the LRP was associated to a lower amount of complexity (paired t-test: t(17)=3.5, p=0.004).

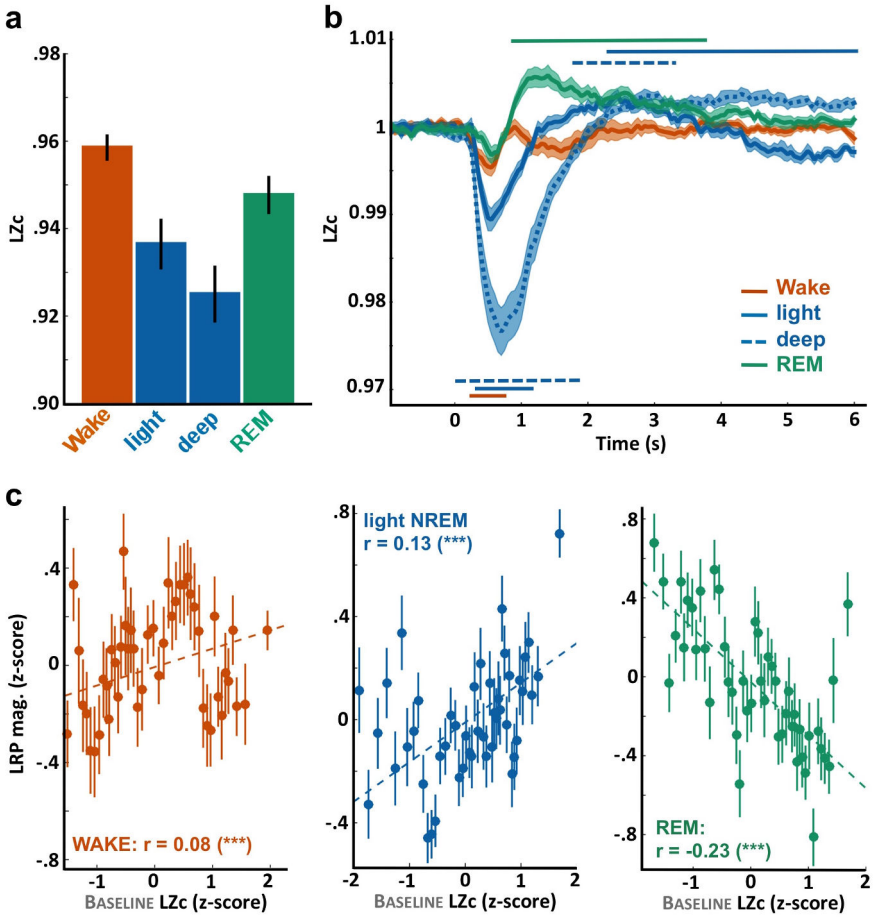

Figure 5-4 Lempel-Ziv complexity across sleep stages and in relation to motor preparation indexes

(a) The Lempel-Ziv complexity (LZc) extracted over the pre-stimulus activity ([-1.5, 0]s) was averaged across trials scored as wakefulness, light NREM, deep NREM and REM sleep. Error-bars depict the standard error of the mean computed across participants. LZc allowed to unambiguously separate the different vigilance states (one-way ANOVA: F(3)=9.67, p=2.10-5, N=18 participants). Post-hoc comparisons show high significant differences with a gradual decrease in complexity: wake>REM>light NREM>deep NREM (all paired t-tests, p<0.005). (b) LZc time-course locked on stimulus onsets and expressed as a ratio of the baseline level ([-1.5, 0]s). Stimuli strongly modulate the overall complexity of the EEG signal with an initial decrease ($p_{cluster}$<0.05, except for REM sleep). The initial decrease was followed by an increase in complexity in light NREM, deep NREM and REM sleep ($p_{cluster}$<0.05). (c) Correlation between the baseline LZc (see panel a) and the LRP magnitude computed across the entire night for wake (left), light NREM (middle) and REM sleep (right) trials. Correlations between the pairs of variables were assessed using the Pearson's method, which coefficient is displayed on each subplot along its significance level (***: p<0.005). Dotted line shows the linear fit between the pairs of variables. Values were z-scored across trials for each participant before being aggregated across participants. Values were binned for visual purpose (N=50 bins on the sorted LZc values). Error-bars depict the standard error of the mean of the LRP magnitude for the corresponding bin.

This paradoxical pattern contrasts with the correlation observed in NREM sleep and wakefulness, suggesting a diametrically opposed relationship between levels of consciousness and the degree of connectedness to the environment in NREM and REM sleep (Sanders et al., 2012).

We also examined how the LZc was modulated in responses to stimuli above and beyond its baseline level (Figure 5-4b). Stimulus onset was followed by a decrease in LZc (i.e. increase in signal predictability), potentially due to highly stereotypical EPRs. And indeed this decrease in LZc was more pronounced for the states in which high-amplitude ERPs were observed such as in NREM sleep (Figure 5-3). This decrease in LZc did not reach our significance threshold in REM sleep, a state in which auditory stimulation has less impact on brain activity (Bastuji, 1999; Picton, 2010). Interestingly, in NREM and REM sleep, this initial decrease was followed by an increase in LZc ($p_{cluster}<0.05$), which could be interpreted as a stimulus-induced modulation of sleep depth.

Sensory processing locally disrupt sleep rhythms

So, are the LRP observed in sleep and the associated increase in LZc reflecting the consequence of a partial awakening? To answer these questions we examined the consequences of auditory stimulation on sleep itself. Figure 5-5a shows the time-frequency decomposition of the EEG signal in response to sounds in NREM sleep (light and deep NREM) for electrode Cz. Stimulus onset was accompanied by an increase within the slow-wave (<6 Hz: $p_{cluster}=0.001$, N=18 participants) and spindle ([11, 16] Hz: $p_{cluster}=0.002$) ranges (Figure 5-5b). This increase was followed by a decrease within these two ranges (<6 Hz: [2.1, 6.3] s; [11, 16] Hz: [2.4, 5.0] s, both $p_{cluster}<0.001$), interestingly at a time corresponding to the apparition of an LRP in light NREM sleep. This results suggests that the preparation of task-related responses translates into a local-in-time modulation of sleep-rhythms and hence of sleep depth. Such modulation was also local-in-space. Indeed while the increase within the slow-wave and spindle range after stimulus onset showed a typical frontal topography (Figure 5-5b), the following decrease had a different topography and was prominent over central electrodes, i.e. over the sensors showing the LRP. It is important to note that this decrease within the slow-wave and sleep spindle ranges was not accompanied by an increase in frequency bands associated with wakefulness (alpha: [9, 11] Hz, beta: >16 Hz). Thus, in NREM sleep, the processing of auditory information resulted in a local (in time and space) modulation of NREM oscillations but this disruption did not lead to any observable trace of awakening on the scalp.

In REM sleep, brain responses were qualitatively different (Figure 5-5c-d): auditory input clearly disturbed REM sleep with an initial increase in higher frequencies (>12Hz, $p_{cluster}=0.01$) and a sustained decrease within the theta range ([4, 8]Hz, $p_{cluster}<0.001$). Interestingly, these increases were both maximal over central electrodes where auditory and motor components are observed in wakefulness (Picton, 2010; Smulders et al., 2012). However, these transient markers of arousal did not lead to the apparition of a clear LRP (Figure 5-2) unless when practiced words were presented (Figure 5-3).

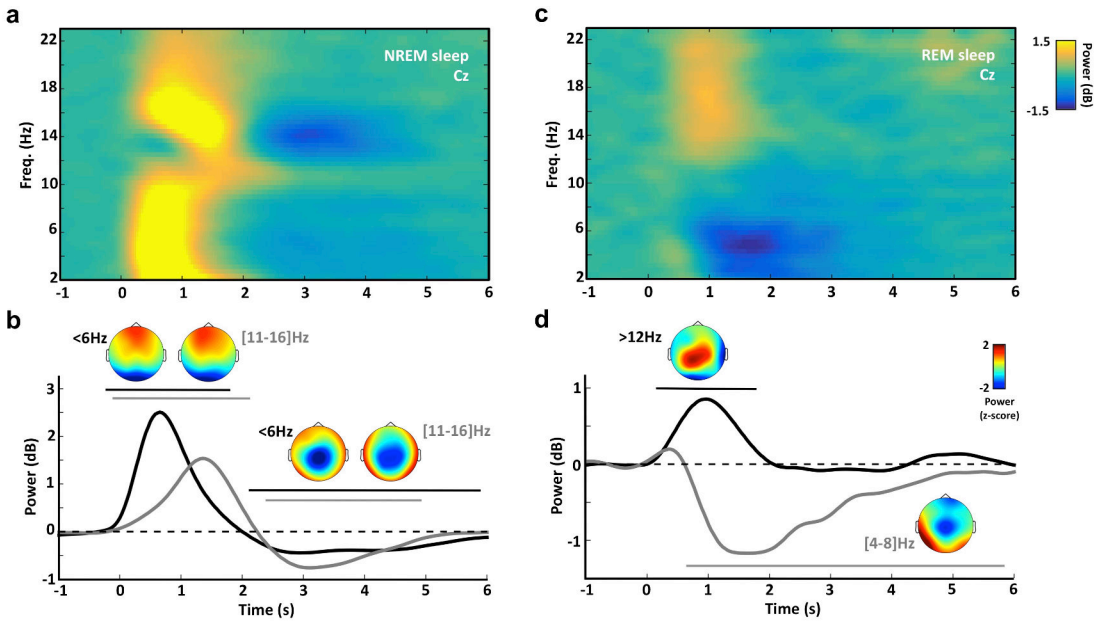

Figure 5-5 Local modulations of NREM sleep slow-waves and spindles in association to stimuli

(a) Time-frequency decomposition of the EEG signal at Cz in response to stimuli. The time-frequency decomposition was extracted for each trial in NREM sleep (light and deep) and averaged, first across trials then across participants (N=18) (see Material and Methods). Right after stimulus onset, a large increase in the low-frequency range (<6Hz) and spindle range ([11, 16] Hz) can be observed, which correspond to the slow-waves and spindles evoked by stimuli. Interestingly, these rhythms decreased later on, around the temporal window in which a LRP was observed in light NREM sleep (Figure 5-2). This decrease was confirmed in panel b by examining the modulation of the power (at Cz) in these 2 frequency bands (<6 Hz: slow-wave range, black curve; [11, 16] Hz: spindle range, gray curve). Horizontal bars show the significant clusters determined across participants ($p_{cluster}$<0.05). Insets show the scalp topographies of the power within the slow-wave and spindle ranges at trial onset ([0 2]s) and during the LRP window ([2.9, 3.8]s). Power was z-scored across sensors to emphasize regional differences. Note that the decrease associated to the LRP is centrally distributed for slow-waves and sleep spindles despite their originally frontal distribution, suggesting a local modulation of sleep rhythms. (c-d) Same as panel a but for REM sleep. Note the initial broadband increase in the higher frequency range (>12Hz) and the decrease within the theta range ([4, 8] Hz). Scalp topographies were computed by averaging power over the significant clusters ($p_{cluster}$<0.05).

Neuronal bi-stability gates sensory processing in NREM sleep

In NREM sleep, brain responses to stimuli were characterized by strong evoked potentials such as the P200 and the N550 (Figure 5-6a). These two potentials are of high interest since the P200 is thought to reflect an activation within the primary sensory cortices corresponding to the eliciting event (i.e. dependent of the sensory modality) while the N550 is thought to reflect a broad modality-independent neuronal silencing maximal at frontal cortices (Halász, 2016; Laurino et al., 2014). The respective scalp topographies of these potentials corroborated such view (Figure 5-6a, right). According to this interpretation, the P200 is a marker of brain responsiveness to external events while the N550 is associated to sleep protection against external perturbation.

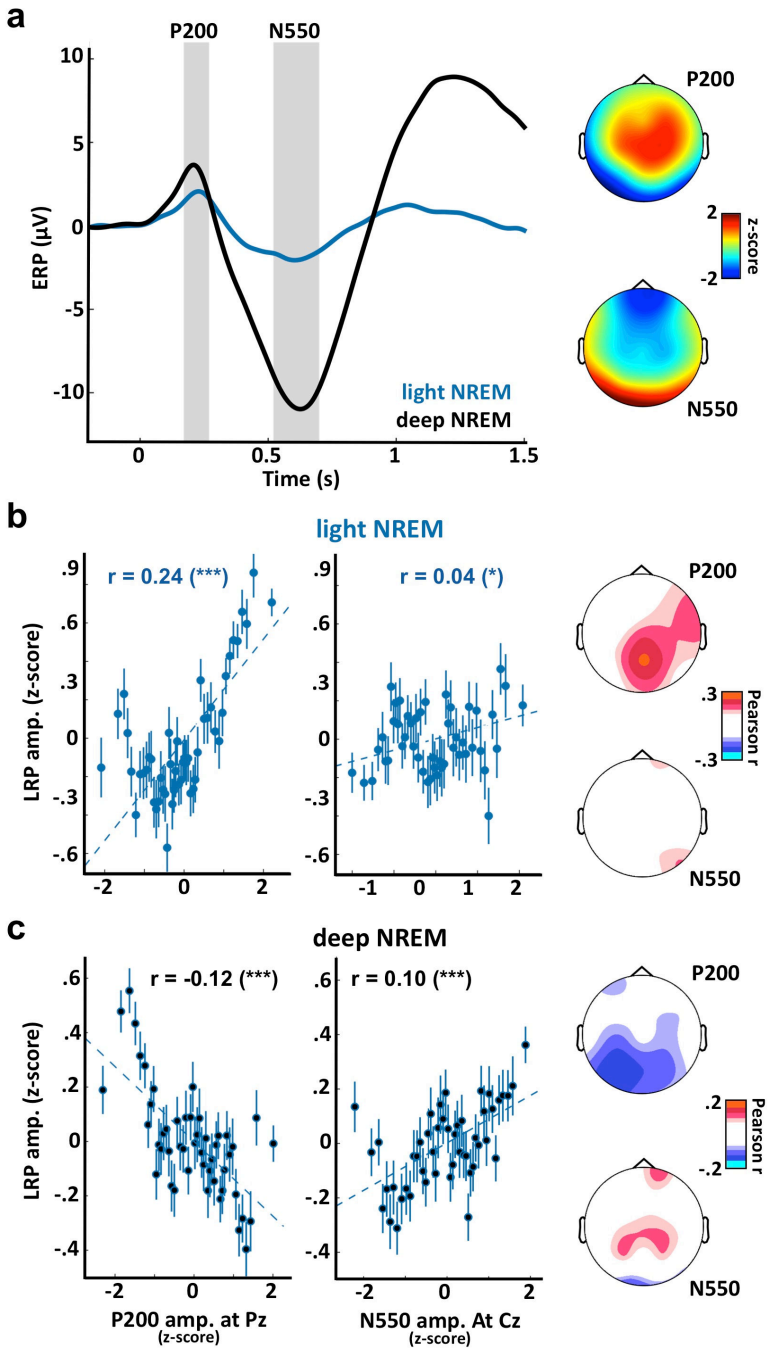

Figure 5-6 Bi-stability of neuronal responses in NREM-sleep gates sensory processing

(a) Event-Related Potentials computed at Cz for trials in light NREM (blue curve) and deep NREM sleep (black). Two distinct potentials are clearly visible: a positivity around 200ms (P200) maximal at centro-parietal electrodes (see scalp topography on the top right), a negativity around 550ms (N550) maximal for deep NREM sleep (trials associated with slow-waves) predominant at frontal electrodes (see scalp topography on the bottom right). The later P900 potentials correspond the up-state of evoked slow-waves. Scalp topographies were established by averaging the voltage over windows around the two potentials of interest (see gray areas on ERP plot). These values were average across participants and z-scored across channels to emphasize regional differences. (b) Correlations between the LRP magnitude and the P200 amplitude (left) or the N550 amplitude (right) for trials in light NREM sleep. P200 and N550 amplitudes were computed on Pz and Cz respectively. Correlations between the pairs of variables were assessed

using the Pearson's method, which coefficient is displayed on each subplot along its significance level (***: $p<0.005$; ns: $p>0.05$). Dotted line shows the linear fit between the two pairs of variables. Values were z-scored across trials for each participant before being aggregated across participants. Values were binned for visual purpose (N=50 bins on the sorted x-axis variable). Error-bars depict the standard error of the mean of the LRP magnitude for the corresponding bin. Scalp topographies on the right show the Pearson coefficients computed for each sensor (non significant coefficients were set to 0, $p>0.05$, FDR correction for multiple comparisons). (c) Same as in panel b for trials in deep NREM sleep. Note the reversal of the relationship between the LRP and the P200 from light to deep NREM, paralleled with the apparition of a large N550, showing a suppressive effect on LRP magnitude.

We thus examined whether the auditory responses (evoked-potentials associated to stimulus onset) were predictive of the apparition of an LRP. Interestingly, in light NREM sleep, the N550 was largely reduced which is in line with the fact that only trials without slow-waves were included. The P200 was also reduced. When examining the relationship between these events and the LRP magnitude in light NREM sleep (Figure 5-6b), a positive relationship was found between LRP magnitude and the P200 (Pearson coefficient at Pz: $r=0.24$, $p=6.10^{-42}$, N=3111 samples in 15 participants). This correlation was maximal over centro-parietal electrodes. Thus, the larger the P200, the larger the LRP in light NREM sleep. No clear correlation was observed with the amplitude of the N550 ($r=0.04$, $p=0.02$), which could be explained by the fact that, in light NREM, the N550 was more or less abolished. On the other hand, in deep NREM sleep, there was a clear positive correlation between the N550 amplitude and the LRP magnitude (Pearson coefficient at Cz: $r=0.10$, $p=10^{-4}$, N=6037 samples in 18 participants). Thus, the smaller the N550, the larger the LRP in deep NREM sleep. Interestingly, in deep NREM sleep, the relationship between LRP magnitude and the P200 was reversed (Pearson coefficient at Cz: $r=-0.12$, $p=10^{-20}$) compared to light NREM sleep. Such reversal could be due to the fact that the P200 activation can trigger a down-state (N550) in deeper stages of NREM sleep, which would ultimately inhibit information processing and reverse the relationship between the P200 and the LRP (see Discussion).

Auditory evoked potentials are predictive of motor preparation in REM sleep

We applied the same approach to REM sleep. Auditory stimuli in REM sleep also evoked archetypal potentials: a positivity around 200 ms followed by a negativity around 500 ms (Figure 5-7a). However, the topography and temporal profile of these potentials are quite different from NREM potentials. In REM sleep, the P200 is usually associated to the wake auditory P200, generated over the primary and secondary cortices (Picton, 2010). The scalp topography of the P200 with a maximum over central electrodes is concordant with this view. Contrary to light NREM sleep, the P200 was negatively correlated with the LRP magnitude in REM sleep (Pearson coefficient at Pz: $r=-0.13$, $p=4.10^{-11}$, N=2622 samples in 18 participants; Figure 5-7b).

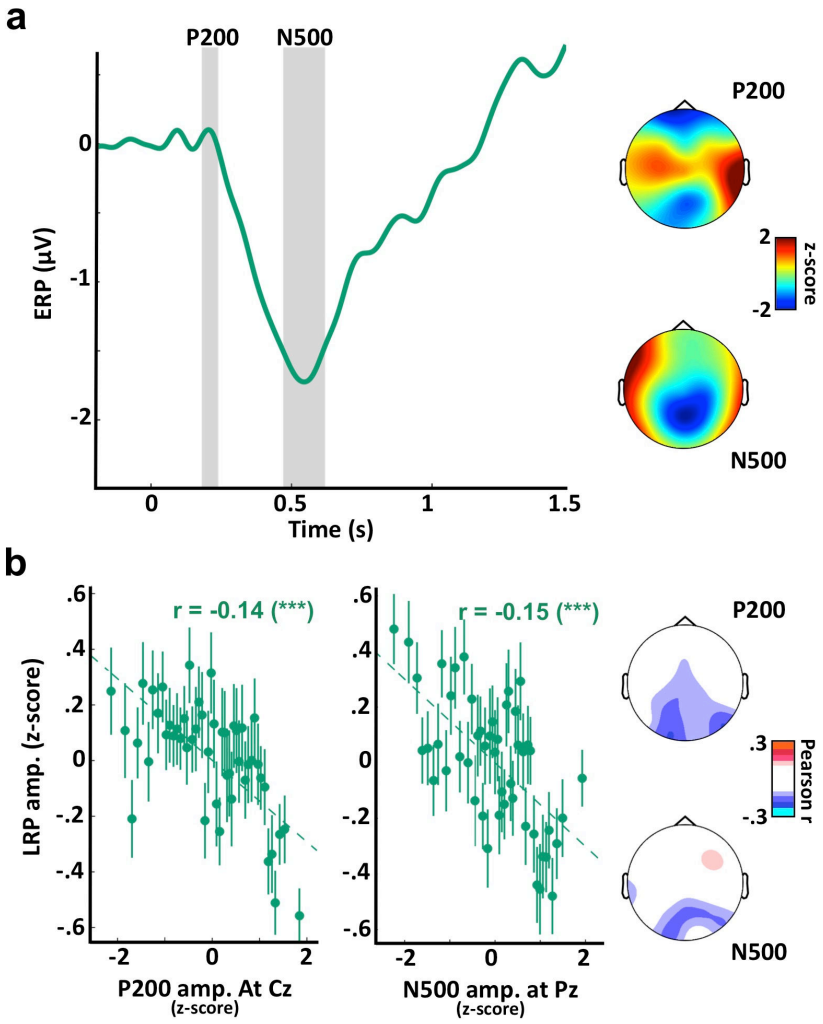

Figure 5-7 Evoked responses to sounds correlate with LRP magnitude in REM sleep

(a) Event-Related Potentials computed at Cz for trials in REM sleep. Two distinct potentials are again visible: a positivity around 200ms (P200) maximal at central electrodes (see scalp topography on the top right), a negativity around 500ms (N500) maximal at parietal electrodes (see scalp topography on the bottom right). Scalp topographies were established by averaging the voltage over windows around the two potentials of interest (see gray bar on ERP plot). These values were average across participants and z-scored across channels to emphasize regional differences. Note that these two potentials are quite different form the potentials described in NREM (Figure 5-6) in terms of temporal profile, amplitude and topography. (b) Correlations between the LRP magnitude and the P200 amplitude (left) or the N500 amplitude (right) for trials in REM sleep. P200 and N550 amplitudes were computed on Cz and Pz respectively. Correlation between the pairs of variables was assessed using the Pearson's method, which coefficient is displayed on each subplot along its significance level (***: $p<0.005$; ns: $p>0.05$). Dotted line shows the linear fit between the two pairs of variables. Values were z-scored across trials for each participant before being aggregated across participants. Values were binned for visual purpose (N=50 bins on the sorted x-axis variable). Error-bars depict the standard error of the mean of the LRP magnitude for the corresponding bin. Scalp topographies on the right show the Pearson coefficients computed for each sensor (non significant coefficients were set to 0, $p>0.05$, FDR correction for multiple comparisons). Similar correlations were obtained when focusing on REM trials during which wake items were played (not shown).

These negative correlations were maximal over occipital electrodes. Similarly, the N500, a potential that is prominent over occipital electrodes in REM sleep, was also negatively correlated with LRP magnitude (Pearson coefficient at Pz: $r=-0.15$, $p=3.10^{-14}$; Figure 5-7c), an opposite relationship than the one found in NREM sleep with the N550 potential. Similar correlations were observed when considering the REM trials in which words practiced in wake were played (P200: $r=-0.12$, $p=8.10^{-4}$; N500: $r=-0.15$, $p=7.10^{-15}$). These results indicate that the evoked potentials associated to auditory stimuli are predictive of later and more complex stages of processing (here motor preparation) and suggest that these auditory potentials are not an unspecific reaction to external stimuli.

Markers of responsiveness are modulated within sleep cycles

The presence of LRP in light NREM but not deep NREM sleep or REM sleep (when unpracticed words are presented) could be due to the fact that light NREM sleep is more pervasive to external information. Another interpretation would be that the ability to prepare for the adequate motor response slowly decays with the time spent asleep. Light NREM sleep occurring first, the LRP would be prominent in this state. To test this possibility we examined how the LRP magnitude was modulated within sleep cycles. Sleep cycles were detected using participant's hypnograms (see Material and Methods). For each cycle, we retrieved the dynamics of the LZc (Figure 5-4), the slow-wave power (a proxy for slow-wave density) and the LRP magnitude in the NREM part of the cycle (see Figure 5-8). In accordance with the archetypal profile of sleep cycles, slow-wave power density gradually increased at the beginning of the sleep cycle (descending slope) but decreased toward the end (ascending slope and transition to REM sleep, (Halász, 2016)). The LZc mirrored this pattern with a gradual decrease in overall complexity followed by a steep increase. Interestingly, the LRP magnitude followed the LZc dynamic and increased again toward the end of the cycle and during the ascending slope (u-shape). This result suggests that the capacity to process information is dynamically related to signal complexity and neural bistability rather than sleep stages. Indeed, toward the end of the cycles, dark colors indicate that trials were scored mostly as NREM3 but showed an increase in LRP magnitude. Thus, the beginning and end of NREM episodes might represent temporal windows in which monitoring of the surrounding environment is possible.

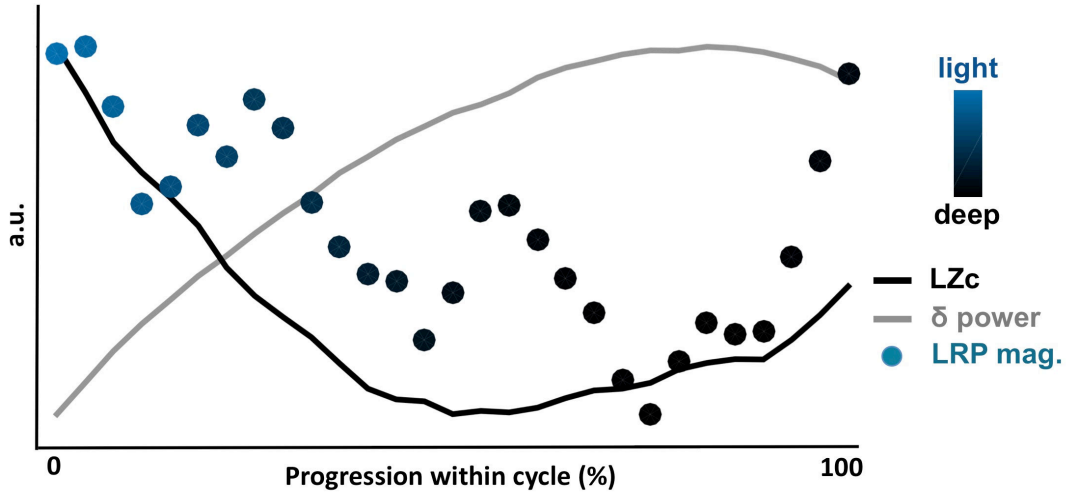

Figure 5-8 The ability to process information is dynamically modulated within sleep cycles

Modulation of the LRP magnitude (colored dots), the Lempel-Ziv complexity (LZc, black curve) and the delta power (gray curve) within the NREM sleep part of sleep cycles. Colors of dots (LRP magnitude) show the proportion of light and deep NREM trials included in the corresponding bin. A classical increase in delta power (a proxy for slow-wave density) is observed corresponding to the transition from light to deep NREM sleep. This increase in delta power is accompanied by a decrease in LZc and LRP magnitude. Note that both LZc and LRP have the tendency to increase again at the end of the NREM cycle, paralleling the transition from deep NREM sleep to REM sleep. LRP, LZc and delta values were estimated within each sleep cycle on fixed windows (see Material and Methods). Sleep cycles were then binned (N=30) so as to average cycles with different durations and values were normalized across the entire cycle to better visualize the dynamics of each variable of interest (expressed here in arbitrary units: a.u.).

Discussion

Several studies have shown that the sleeping brain is far from being disconnected (Issa and Wang, 2008; Nir et al., 2011; Portas et al., 2000; Sela et al., 2016). Not only can sleepers encode external information but they can also process this information at different levels of representation and analyze it in its context (Bastuji, 1999; Hennevin et al., 2007; Ruby et al., 2008; Strauss et al., 2015). Here, we provide compelling evidence that sleepers can even flexibly use sensory information to make decisions in accordance with our previous findings during daytime naps (Kouider et al., 2014).

Complex and distributed processes in the sleeping brain

Participants had to categorize spoken words based on their semantic category (animals vs. objects) while falling asleep. Responses were given through lateralized hand responses (right vs. left) when participants were awake. The rule matching one semantic category with a given response-side was arbitrary. To assess participants' responsiveness, we computed an LRP (Smulders et al., 2012). The LRP indicates whether brain activity is lateralized according to the expected response side. When computed on response-locked EEG data and during wakefulness, the LRP cluster started before the overt behavioral response itself (significant cluster: [-1.1 0.8]s, $p_{cluster}$=0.001, N=17 participants), confirming a functional link with the preparation of the response (Masaki et al., 2004). A similar negative deflection was also observed on the stimulus-locked LRP (Figure 5-2a). This negativity was conserved in light NREM sleep when unpracticed words were played (Figure 5-2c), with a similar timing and scalp topography as previously found in naps (Kouider et al., 2014).

Since the assignment of a stimulus category to a given response hand was counterbalanced across participants, the presence of an LRP can solely be explained by response-related activity. Thus, the presence of such LRP in sleep reflects the maintenance of complex and distributed processes during light NREM going from the encoding of the auditory information to the preparation of the appropriate motor response. The maintenance of such complex processing chain could seem at odd with the breakdown of functional connectivity reported at NREM sleep onset (Massimini et al., 2005) but could be explained by the automation of the task-set prior to sleep onset (Kouider et al., 2014). Since consciousness fades at NREM sleep onset (Tononi and Massimini, 2008), our results suggest that participants continued classifying the words without being aware of it (Dehaene et al., 1998; Kouider and Dehaene, 2007).

No LRP were observed in deep NREM sleep or REM sleep (for unpracticed words), suggesting that part of this chain is disrupted. However, when considering practiced words (wake list, Figure 5-1) played during sleep, an LRP was observed in both light NREM and REM sleep (Figure 5-3). Both auditory evoked potentials (AEPs) and power spectra were in accordance with either NREM or REM sleep staging, confirming that these trials genuinely corresponded to these stages. The presence of an LRP in REM sleep for practiced but not for novel words could be interpreted as a failure of the sleeping brain to access the meaning of words during the REM period. Under such circumstances, the sleeping brain would fail to categorize novel words, but could still rely on stimulus-responses contingencies previously learnt during wakefulness in order to prepare for the appropriate response. Alternatively, the presence of an LRP for practiced

words only could stem from a difference in sleep rather than stimulus type. Since the wake and REM lists were not randomly intermixed, we cannot rule out this interpretation. And indeed, despite equivalent power spectra and ERPs (Figure 5-3), trials during which the wake list was played showed smaller LZc values than trials of the REM list (paired t-test: $t(17)=3.5$, $p=0.004$). This smaller complexity for practiced compared to unpracticed words argue against the hypothesis that an LRP would be visible for practiced words because participants had been more awake.

The complexity of brain dynamics interacts with the processing of the environment

Certain periods of sleep proved more propitious for the induction of task-dependent responses. What dictates the brain to keep monitoring, at least partially, its environment during sleep? To investigate this question, we first relied on the Lempel-Ziv complexity (Ziv and Lempel, 1977). The LZc determines the temporal predictability of the EEG signal. Coupled to TMS stimulations, it has been used to determine the level of consciousness during anesthesia, sleep or in brain-damaged patients (Casali et al., 2013; Sarasso et al., 2015). LZc has also been applied to spontaneous neural data in humans (Schartner et al., 2015) and rodents (Abásolo et al., 2015), evidencing a remarkable link between complexity and consciousness levels. We confirmed these previous findings here in natural sleep and using scalp EEG (Figure 5-4). LZc decreased from wakefulness to deep NREM sleep. REM sleep showed intermediate complexity values, between wakefulness and light NREM sleep. Such pattern perfectly matches the phenomenology of these sleep stages (Laureys, 2005; Yuval Nir et al., 2013): consciousness is not absent from sleep since we dream, but dreams are usually more frequent and complex in REM sleep than NREM sleep and are quite rare in deep NREM sleep.

LZc did not only track participants' vigilance state but also predicted the magnitude of the LRP. In light NREM sleep, we observed a positive correlation between LZc and LRP (Figure 5-4b, middle), suggesting that sensory processing is associated with some sort of partial awakening. In REM sleep however this relationship was reversed (Figure 5-4b, left). The higher the LZc, the weaker the LRP. Interestingly, as said above, trials for which the wake list was played and an LRP observed (Figure 5-3) showed smaller LZc values than trials during which unpracticed words were used (no LRP). This opposite relationship between complexity and responsiveness in REM sleep could be related to the peculiarity of REM sleep, a state of consciousness disconnected from the environment, and emphasizes the difference between consciousness and responsiveness often observed in anesthesia (Sanders et al., 2012; Sarasso et al., 2015).

Neuronal bistability and the gating of sensory processing

By contrast to light sleep, no LRP was observed in deep NREM sleep. What could explain such a drastic difference? Light and deep NREM sleep were defined based on the presence of slow-oscillations. Light NREM sleep was notably characterized by a near-absence of the frontally distributed N550 potential (Figure 5-2 and Figure 5-6), which is usually linked to the down-states of stimuli-evoked K-complexes (Bastien et al., 2002; Halász, 2016). We therefore explored whether evoked responses (i.e. early stages of sensory processing) were predictive of the apparition of an LRP. We found that in light

NREM sleep, the P200 is positively correlated with LRP magnitude (Figure 5-6b). The P200 potential has been interpreted has a local stimulus-dependent excitation (Laurino et al., 2014) and could be related to the encoding of the stimulus. A pronounced P200 could evidence the sleeping brain's responsiveness to the external world.

However, in deep NREM sleep, this relationship was reversed (Figure 5-6c). In addition, in deep NREM sleep, large-amplitude evoked K-complexes (N550/P900 potentials) are visible and maximal over frontal electrodes. The more pronounced these potentials, the smaller the LRP. Indeed the N550 is associated to K-complexes' down-state, i.e. an episode of neuronal silencing (Mircea Steriade, 2003) perturbing the encoding and integration of information (Dang-Vu et al., 2010; Pigorini et al., 2015; Schabus et al., 2012). The N550 could therefore prevent the further processing of information by stopping the continuity of neural operations.

But how could be explained the reversal of the relationship between LRP magnitude and the P200? From light to deep NREM sleep, cortical neurons become more and more bi-stable and exhibit successions of neuronal silencing (down-states) and activations (up-states) (Mircea Steriade, 2003). Importantly, a local excitation can trigger a down-state (Halász, 2016; Menicucci et al., 2013; Sanchez-Vives et al., 2010). The P200 could therefore ignite a down-state that would shut down in turn any further processing. Thus, whenever the P200 would trigger a down-state, its relationship with sensory processing would reverse: from a potentiating activation to a suppressive mechanism. Increasing sleep depth could increase the probability that a local excitation transforms into a global silencing (Halász, 2016), by facilitating the apparition of down-states. It is also possible that a larger P200 would have a greater probability to trigger a down-state, sleep depth being kept equal. Indeed, the P200 was larger when down-states were observed (Figure 5-6a). Brain responses to sound could therefore follow a self-regulated process in NREM sleep whereby sensory activations are suppressed as a consequence of cortical bi-stability.

Could dreams gate sensory processing in REM sleep?

How the brain gets disconnected from its environment in REM sleep is still a mystery (Nir and Tononi, 2010). Indeed, the recovery of a wake-like brain activity and consciousness should favor the processing of external information and yet sleepers remain largely unresponsive in REM sleep. Accordingly, we did not observe an LRP for novel words during REM sleep (Figure 5-2) despite increased levels of neural complexity (Figure 5-4). A recent study described the presence of slow-waves in REM sleep restricted to the superficial layers of primary sensory cortices (Funk et al., 2016). These slow-waves could act as a gating mechanism since these layers are the main targets of thalamic relays (Jones, 2007) We showed here however that stimuli had a clear impact on cortical activity: signs of arousals could be observed after stimulus onset (Figure 5-5c-d, broadband increase in higher frequencies, decrease in theta oscillations) as well as strong auditory potentials (Figure 5-7). These activations indicate that sensory information did reach the cortex during REM sleep in accordance with previous studies (Bastuji, 1999; Y. Nir et al., 2013; Sallinen et al., 1996). However, no LRP was observed when novel words were played. It is therefore possible that the stimulus-evoked perturbations were confined in sensory areas and not further processed.

But what could be the mechanisms limiting the further processing of information at the cortical level? Indeed, REM sleep is characterized by a recovery of cortico-cortical

connectivity compared to NREM sleep (Massimini et al., 2010), which should allow the recovery of complex cortical processes when sensory information reaches the cortex. We propose that sensory information may compete with endogenous processes (i.e. dream contents) preventing the correct processing of the former. Indeed, brain activity sharing properties with wake sensory processing can be observed in REM sleep around eye-movements (Andrillon et al., 2015b), as well as the replay of previously learned information (Louie and Wilson, 2001). These endogenous contents could in turn interfere with the processing of external inputs. Accordingly, the overall degree of complexity had a negative impact on LRP magnitude (Figure 5-4). This 'informational gating' could also explain the surprisingly rare integration of external stimuli during REM sleep (Nir and Tononi, 2010). This gating mechanism could be mediated by a change in the balance between top-down and bottom-up signaling in favor of top-down processes (Funk et al., 2016; Nir and Tononi, 2010). Further investigations are needed to specifically investigate this question.

Consequences of external stimulations on sleep

How did stimulation affect sleep? Were participants able to covertly respond to stimuli in light NREM because they marginally awoke? To explore this question we examined the time-frequency decomposition of the EEG signal in response to sounds (Figure 5-5). In NREM sleep, we observed a two-step response to sounds (Figure 5-5a-b). Right after stimulus onset, power increased within the slow-waves and spindle range in accordance with the fact that sleep rhythms can be evoked by external stimulations (Halász, 2016). These increases were maximal over frontal electrodes and could correspond to a protective mechanisms ensuring that sleep is preserved (Halász et al., 2014; Laurino et al., 2014). After this initial increase, these oscillations decreased in power. Interestingly, the spatial and temporal distributions of this decrease overlap with the time and location of LRP in light NREM sleep (Figure 5-2c) and is concomitant with the increase in LZc following stimulus presentation (Figure 5-4b).

The initial protective response is therefore followed by a local modulation of sleep depth accompanying the processing of information. No sign of arousal was observed (alpha or high-frequency increase). However the absence of arousal at the scalp level does not preclude local awakening in motor or sensory areas of example (Nobili et al., 2011; Peter-Derex et al., 2015), a phenomenon called local sleep (Nir et al., 2011; Nobili et al., 2012). The local modulation of sleep depth associated here to sensory processing could reflect, at the scalp level, the occurrence of local wake within the sleeping brain.

In REM sleep, auditory stimulations also perturbed the theta rhythm (Figure 5-5c-d) and signs of arousals could be observed after stimulus onset (broadband increase in higher frequencies). Once again, these perturbations were maximal over central electrodes, potentially revealing the recruitment of auditory and motor regions by the acoustic perturbation.

Responsiveness is dynamically modulated during sleep cycles

We finally explored the dynamics of neural complexity (LZc), motor preparation (LRP magnitude) and delta power (a proxy for slow-waves density) across sleep cycles. Both

LZc and delta power followed a dynamic that precisely reflected the structure of sleep cycles with an initial descent toward deep NREM sleep characterized by a clear increase in delta power and decrease in neural complexity. The peak in delta power was followed by a steep decrease corresponding to the dampening of NREM sleep and the transition to REM sleep. This delta decrease was mirrored by an increase in complexity. The LRP magnitude was also robustly modulated within sleep cycles and paralleled complexity's dynamics, with notably an increase in LRP magnitude toward the end of sleep cycles. The disappearance of the LRP is therefore not due to a slow decay from the cycle onset but is tightly linked to sleep depth. A similar increase of brain responsiveness in the sleep cycles' ascending slope has been evidenced through the Cycling Alternating Patterns (Terzano et al., 1985). This fragility of sleep at the transition with REM sleep could be instrumental in allowing the brain to monitor its environment and decide whether to stay asleep or to wake up (Halász et al., 2004).

Overall, our data suggests that sleepers can complexly and flexibly process information during sleep. However this ability is finely regulated by the neural dynamics of the sleeping brain. Cortical bi-stability seems to play a suppressive role in NREM sleep, moving the sensory gating from the thalamus (McCormick and Bal, 1994) to the cortex (Tononi and Massimini, 2008). In REM sleep, we propose a completely different gating mechanisms by which endogenously generated information compete with and limits the processing of external information (informational gating).

Study 6:
Attentional tracking of relevant signals during human sleep

Guillaume Legendre[1*], **Thomas Andrillon**[1, 2*] and Sid Kouider[1]

[1] *Brain and Consciousness Group,*
École Normale Supérieure
Paris, France

[2] *École Doctorale Cerveau Cognition Comportement,*
Université Pierre et Marie Curie
Paris, France

* contributed equally to this work

Summary

Although sleep is characterized by a loss of behavioral responsiveness, the sleeping brain is far from being disconnected. Processing of external inputs has been evidenced in sleep, ranging from sensory encoding all the way up to complex processes of semantic integration and motor preparation. However, it remains unclear whether the sleeping brain can select which information to process. During wakefulness, we can effortlessly focus on and track a specific speaker and ignore other competing auditory sources in the environment, as illustrated by the cocktail party situation. Here, we investigated whether the sleeping brain could similarly resolve the cocktail party problem. We asked participants to listen carefully to stories while falling asleep. The stories were simultaneously presented with pseudo-speech that participants were instructed to ignore. By reconstructing both stimuli envelopes from the EEG signal, we could assess whether participants paid attention to the real or to the pseudo speech. Attention to the relevant stream was conserved in sleep. However attentional processes were transient and vanished in deep sleep. NREM sleep being characterized by the presence of particular sleep rhythms (K-complexes, slow-waves and sleep spindles), we examined their respective influence on sensory encoding and attention allocation. K-complexes were found to promote attention allocation while slow-waves seemed to specifically shut down the processing of the relevant stream in deep sleep. Sleep spindles however had only a moderate impact on attention orientation. Thus, our results provide a novel approach to the study of sensory coupling during sleep and emphasize important differences between light and deep NREM sleep in terms of sensory processing.

Introduction

Sleep is both a ubiquitous phenomenon and a vital need (Cirelli and Tononi, 2008). But the loss of responsiveness to the surrounding world places sleepers in a state of great vulnerability. Reversibility (i.e. sleepers' ability to wake up at any moment) is therefore one of the most crucial features of sleep (Halász et al., 2004). But for sleep to be efficient, sleepers must be able to wake up only when necessary. Thus, sleepers should maintain some ability to monitor their environment while being asleep in order to detect relevant stimuli. Accordingly, previous research has shown that despite the absence of behavioral responsiveness, the sleeping brain continues encoding incoming stimuli (Issa and Wang, 2008; Y. Nir et al., 2013). Furthermore, the analyses of EEG evoked responses to external inputs showed the preservation of a range of cognitive processes: the detection of familiar stimuli (Perrin et al., 1999) and semantic violations (Bastuji et al., 2002; Brualla et al., 1998; Ibanez et al., 2006), the integration of simple acoustic rules (Ruby et al., 2008; Strauss et al., 2015) and even the learning of novel associations (Arzi et al., 2012; de Lavilléon et al., 2015). Sensory information can not only be processed at a high level of representation but this information can also be used by non-sensory regions involved in the preparation of task-dependent motor plans (Kouider et al., 2014). Such preservation of complex and distributed processes during sleep is all the more striking since these studies have been performed mostly during Non-Rapid Eye-Movement (NREM) sleep, a state in which cortico-cortical connectivity is impaired (Massimini et al., 2005) and consciousness greatly diminished if not absent (Yuval Nir et al., 2013). However, most of these studies relied on the analysis of brain responses to isolated words, sentences or sounds. It is yet unclear whether the sleeping brain can select one source of information when several are presented concomitantly.

Allocating attentional resources, i.e. favoring the processing of one source of information compared to others, is indeed essential to efficiently face the crowded acoustic scenes that constantly surround us. When awake, this feat is achieved either through top-down attention, by selecting a given auditory source among others, or through bottom-up attention, when being attracted towards one source which is particularly relevant (Fritz et al., 2007). Although the underlying mechanisms are distinct, these two processes will work in a complementary and cooperative way. As a result, the neural representation of the attended information is enhanced (Ding and Simon, 2012a; Mesgarani and Chang, 2012; O'Sullivan et al., 2014; Xiang et al., 2010). Here, we investigated whether the sleeping brain could favor one source of information versus another based on a high-level criterion: its semantic relevance.

We used a dichotic cocktail party paradigm, a classical approach to explore auditory attention (Cherry, 1953). Human participants wearing an electroencephalographic (EEG) cap listened to two different speech streams at the same time, each one played at a different ear. One of the two streams presented was made of real speech (short stories, news, monologues) and the other of pseudo-speech (also called Jabberwocky). Pseudo-speech shares with real speech the same syntactic and phonologic properties (Hahne and Jescheniak, 2001) and therefore sounds much like real speech. However it is devoid of any meaning, contents words being replaced by pseudo-words, which are phonologically legal but absent from the lexicon. Participants were asked to pay attention to the real speech and to ignore the pseudo-speech. Focusing on the real speech is far from a trivial task since it implies (i) encoding both streams, (ii) separating the two streams, (iii) recognizing which one is the real speech, (iv) focusing and maintaining attention on the real speech. Here we investigated whether such processes could be successfully

completed during NREM sleep. Participants were first recorded while being fully awake. They were then authorized to fall asleep while performing the task and their neural responses to the acoustic stimuli were recorded during NREM sleep. Auditory stimulation was continuous and the task-set remained constant throughout the entire experiment.

Sensory encoding and attention allocation were assessed using a novel approach called stimulus reconstruction (Pasley et al., 2012). We built a model mapping the EEG signal to the syllabic rate of auditory streams (modulations of the acoustic envelope within the low-frequency range). The model was then used to reconstruct stimuli envelope using the EEG signal. By reconstructing what participants heard, this technique allows to dynamically track sensory encoding and attention. Indeed, previous research has stressed the importance of tracking the syllabic rate for speech comprehension (Doelling et al., 2014; Giraud and Poeppel, 2012a). The inability to reconstruct acoustic envelope from the EEG could therefore be interpreted as a loss in the capacity to track speech. In addition, when two sources are presented in competition, the attended stream is better reconstructed than the ignored one (Ding and Simon, 2012a; O'Sullivan et al., 2014). Comparing the quality of the two reconstructions could provide an insight on participants' attentional focus.

Stimulus reconstruction being performed during continuous acoustic stimulation, it constitutes a methodological advance compared to the standard event-related potentials (ERPs) approach, allowing us to study the dynamic nature of attentional engagement towards the environment. Furthermore, this approach allows exploring the influence of NREM sleep hallmarks (slow-waves, K-complexes and sleep spindles) on sensory encoding and attention. Indeed, these thalamo-cortical rhythms were thought to play a central role in the gating of sensory information to the cortex (McCormick and Bal, 1994). Yet, their exact impact on sensory processing remains unclear. Slow-oscillations such as K-complexes are either seen as a protective mechanism, suppressing sensory information to preserve sleep (Bastien et al., 2000; Wauquier et al., 1995) or, conversely, as windows of wakefulness (Destexhe et al., 2007; Halasz, 2005) allowing the sleeping brain to monitor its environment. Similarly, sleep spindles have been proposed as enabling sensory disconnection (Schabus et al., 2012). But cellular recordings show little impact of sleep spindles on cortical firing (Andrillon et al., 2011; Peyrache et al., 2011) and sensory encoding (Sela et al., 2016).

By reconstructing competing acoustic streams with EEG, we show here that sensitivity to auditory information is preserved throughout NREM sleep. Importantly, we also found an enhancement of the meaningful stream in NREM sleep. However, this enhancement was predominant in light NREM sleep and, contrary to wakefulness, attention allocation was transient. The enhancement of the meaningful stream disappeared in deep NREM sleep. This difference between light and deep NREM sleep could be traced back to sleep micro-structure and sleep rhythms. K-complexes allowed the recovery of attention allocation and seemed to play a central role in opening sleepers to their environment since they. On the contrary NREM3 slow-waves specifically suppressed the relevant stream, which can be seen as a protective mechanism. Sleep spindles on the other hand had a limited impact on stimulus reconstruction and attention allocation. These results show that the mechanisms of attentional monitoring are maintained during some periods of sleep, and reveal the role played by sleep rhythms in coupling and decoupling sleepers from their environment.

Methods

Audio material

Eighty texts (N = 80) in French were selected from Wikipedia articles (*www.wikipedia.org*), news reports, tales and monologues' transcripts from movies. They were first adapted to a length of about 180 words. Then, the syntax and vocabulary were simplified to produce easily tractable texts. Using the Lexique database (New et al., 2004), a pseudo-lexicon was created matching all the content words present in the French texts with a given pseudo-word. These pseudo-words were selected to ensure their similarity with the words of the French lexicon. French texts were then transformed in syntactically correct but meaningless texts (pseudo-texts) by replacing each content word with its pseudo-word counterpart (Fries, 1952). We therefore obtained eighty pairs of texts matched in total duration, syntax, word-frequency and prosody but that differed at the semantic level.

Real (meaningful) and pseudo (meaningless) texts were then converted into speech using IRCAMTTS, a text-to-speech Matlab-based software (Obin, 2011). Pauses of 150ms were imposed between sentences to maintain a constant auditory flow. The corresponding audio files were digitalized at a sampling rate of 44.1kHz (total duration: 73.63s +/- 0.04, mean +/- Standard Error of the Mean (SEM) across files). Then, the acoustical properties of the voice uttering the texts were manipulated using the IRCAMTRAX module (Roebel, 2010) for the Logic Pro software (Apple Inc., Cupertino, CA, USA). Two easily distinguishable voices were produced from the original neutral speaker by modulating the pitch and the size of the voice's vocal tract. Importantly, these transformations were performed after the text-to-speech procedure. Therefore, the same 80 pairs of real (meaningful) and pseudo (meaningless) texts could be pronounced either by a high-pitch or low-pitch voice without other parameters such as total duration or prosody being altered.

Novel pairs of texts were created for the dichotic stimulation. Each pair contained a real steam and a pseudo stream (created from a different real text). Pairs of real and pseudo streams were matched in terms of total duration and silence-to-signal ratio by increasing silences (portions of signal between 0.001 and -0.001 dB and longer than 50 milliseconds) with the adequate time constant. Length corrections were then applied by changing sound tempo with a Matlab (Mathworks Inc., Natick, MA, USA) implementation of the VSOLA algorithm (Dorran and Lawlor, 2003). Lastly, acoustic energy was normalized across all texts by setting the root-mean-square value of the acoustic signal to a standard value. Thus, pair of real and pseudo-stories had indentical durations and equivalent acoustic energy.

Frequency tags were also added to each sound stream by multiplying the auditory signal with a sine wave at a given frequency (41 or 44 Hz) with a 50% modulation depth. Training stimuli were not tagged. The pair of auditory streams presented in test trials contained each a different tag (41 or 44 Hz). These frequency tags did not prevent the understanding of the stories. The aim was to check whether attention could amplify the frequency tag present in the attended stream. However, and in accordance with a recent review (Varghese et al., 2015), we did not find, in wakefulness, a consistent modulation of these tags depending on attention allocation. This angle was therefore not further investigated.

The texts transformed into speech were used in our experiment as auditory stimuli. A trial refers to the full presentation of a story (diotic trials, training phase, see below) or pair of stories (dichotic trial, test phases) and therefore had rather long durations (1.29 +/- 0.00 minutes). During the dichotic trials, each auditory stream (real or pseudo) was assigned a side (left vs. right), voice (high vs. low) and frequency tag (41 vs. 44 Hz) that differed from its counterpart. These parameters were randomly selected for each trial.

Experimental procedure

Participants: Twenty-nine (N = 29) French native speakers (13 females, age: 18-33) with self-declared normal hearing and no history of sleep disorders participated to the sleep-study. Three participants were discarded from our analyses due to few (<1 minute of consolidated NREM-sleep, i.e. NREM2 or NREM3) or no sleep and two for technical issues. Participants were selected through questionnaires assessing their sleep habits and daytime sleepiness (Epworth scale: 10.97 +/- 0.14 on a scale of 24). In addition, they were required to sleep 30% less than usual the night before the experiment and deprived from stimulants the day of the recordings to increase the probability that they would fall sleep while hearing the acoustic stimuli. Participants were equipped with an actimeter the day prior to the recording session to check their compliance with sleep restriction. Recording sessions always occurred in the early or late afternoon to increase sleepiness and favor Non-Rapid Eye-Movement (NREM) sleep. The present protocol had been approved by the local ethical committee (Conseil d'Evaluation Ethique pour les Recherches en Santé, University Paris Descartes, Paris, France).

Protocol: The day of the recording sessions, participants were equipped with high-density electroencephalographic (EEG) nets (see below) and seated on a reclining chair in a dark, soundproof and magnetically shielded booth. Figure 6-1 illustrates the timeline of recording sessions. Participants started with a training phase during which they were exposed to 6 real and 6 pseudo texts played in a diotic fashion (i.e., the same text was presented to both ears at the same time). The training phase was self-paced.

Following the training phase, the first part of the test phase ("wake test") was initiated and the participants were presented with 8 dichotic trials: a real text was presented to one ear and a pseudo text to the other. Participants were asked to stay awake with eyes-closed during the training phase and wake test phases and were reminded to do so whenever drowsiness makers appeared in the EEG. Trials followed each other separated by a 4 to 6 s jitter (random uniform distribution). After this wake phase, the sleep test phase was initiated: participants were put in a reclined position and were allowed to fall asleep. Participants were presented with dichotic auditory streams similar to the initial test phase but composed of novel pairs of real and pseudo stories. Stimulations went on, trial after trial for about 40 minutes (30 trials) with a jitter of 4 to 6 s between trials (random uniform distribution).

Task instructions were rather simple. During the training phase, participants were asked to attentively listen to the diotic training stories. During the wake test phase (dichotic-trials), subjects were instructed to focus on the meaningful stream and to ignore the pseudo-text. In the sleep test phase, participants were asked to maintain their attention toward the meaningful stream as long as they remained awake and to resume the task in case of an awakening. Participants were explicitly allowed to fall asleep in the sleep test phase.

At the end of the recording session, participants answered a multiple-choice questionnaire on the texts heard during the experiment as well as texts that were not played (one question for each text, 4 options per question, N = 80 questions). Participants were asked to answer to every single question even if they did not hear or remember the corresponding story. In addition, following each question, participants had to indicate whether (1) they remembered hearing the text during the experiment and (2) they knew the answer to the question beforehand.

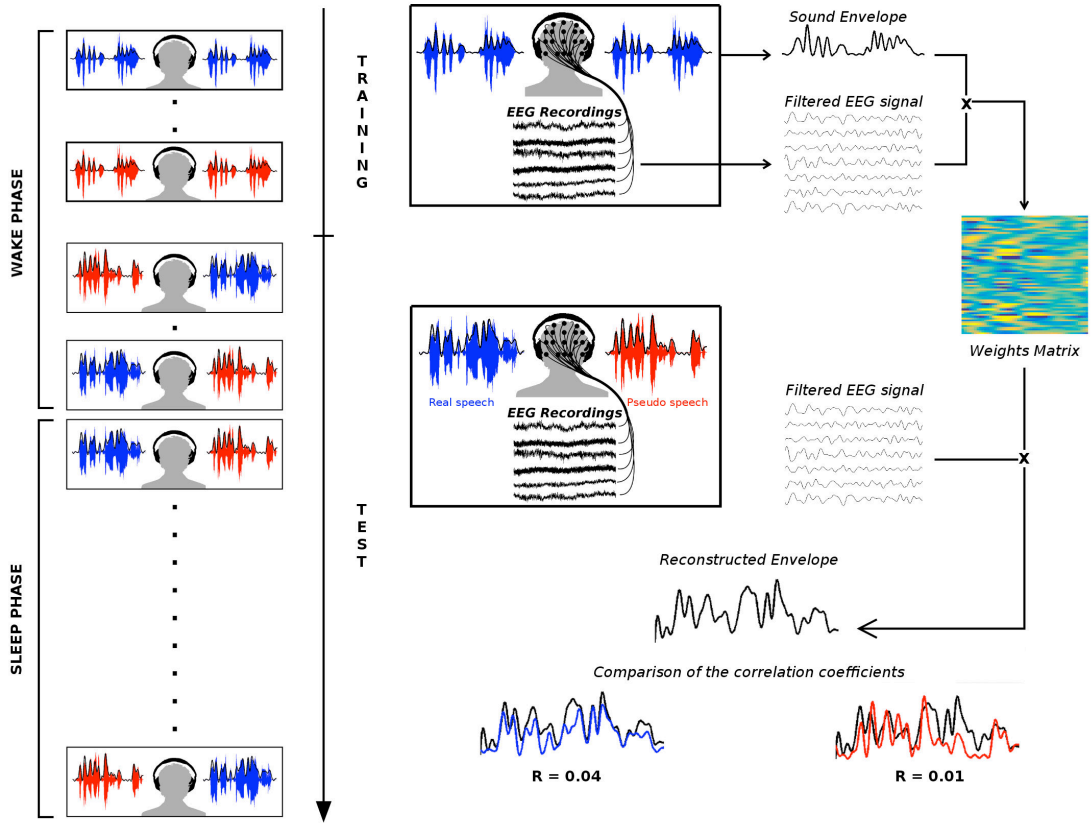

Figure 6-1 Experimental procedure

Left: Each recording session was composed of two parts: the training and test phases. During the training and at the beginning of the test phase, participants were instructed to stay awake and were authorized to fall asleep during the later part of the test phase. Right: During the first part of the experiment (training), participants listened to either real (red) or pseudo (blue) speech presented diotically (same information in both ears). The envelope of the sound and the filtered EEG signal (see Material and Methods) were extracted to train a linear filter (i.e. matrix of weights for each electrode and time-lag) mapping the EEG signal to the sound envelope. Then, participants went through a test phase during which two different streams (one real, one pseudo speech) were played (dichotic trials, different auditory information in the two ears). During the test phase, the linear filter was applied to the filtered EEG envelope and one reconstructed envelope was obtained for each trial (black curve). This envelope can be seen as a mixture of both auditory inputs. The reconstructed envelope was then compared to the original envelope of each input using Pearson's correlation method (reconstruction scores = Pearson's coefficient).

Behavioral data analyses

Responses to the questionnaire filled in by participants after the nap session were analyzed as follows. The mean performance scores on the questionnaire were computed for each participant. Questions for which participants declared that they knew the correct answer beforehand were discarded from further analysis (9.18 +/- 1.54 %, mean +/- SEM across 29 participants). The average score for each question was first computed on texts that participants did not hear during the experiment. All participants (including participants that did not sleep, N = 29) were included to estimate the chance level. Texts with a chance level above 50% (twice the theoretical chance level) were excluded from further analysis. For each participant included in the EEG analyses (N = 24), the average correctness was computed for the questionnaires heard in the different sleep stages (21.63 +/- 1.53 questions in Wakefulness, 11.65 +/- 1.71 questions in NREM sleep). Since participants might go through different sleep stages during a given trial, the sleep stage of the trial was determined as the lightest sleep stage encountered. Scores were compared to the theoretical chance level across participants (u-test, see also Table S 6-1). The scores obtained in NREM sleep suggest that participants did not remember the stories played during sleep contrary to stories heard while awake.

EEG recordings and acoustic stimulations

Brain responses to monaural and dichotic auditory stimuli were recorded with EEG using 65-electrodes gel-nets (EGI system, Electrical Geodesic Inc.). EEG signals were referenced online to Cz and sampled at 500Hz. Chin electromyograms (EMG) and electrooculograms (EOG) were extracted from sensors placed around the eyes and on the chin. Subjects were asked to close their eyes while listening to the auditory streams.

Acoustic stimuli were played at about 50 dB via an Echo Fire 12 (Echo Digital Audio Corp., Santa Barbara, CA, USA) soundcard. To check that a precise synchronization between auditory stimulations and EEG recordings was preserved throughout the recordings, a third audio channel was associated to the real and pseudo auditory streams. In this additional channel, a tone was played every second and sent to the EEG amplifier. We later on checked that this 1s pace had been conserved (maximal observed lag: 2 ms, i.e. 1 sample at 500Hz). To avoid any electromagnetic contamination from earplugs onto EEG recordings, a non-electrical auditory system was used (RLINK Ear Tone 3A, 10 Ohms, Interacoustic Inc., Middelfart, Denmark).

EEG and sound preprocessing

Sleep scoring: The continuous EEG and EOG signals were re-referenced to the mastoid electrodes (opposite mastoid for the EOG) and bandpass filtered between 0.1 and 30 Hz (two-pass Butterworth filter, 5th order). The EMG signal was obtained with a local derivation and bandpassed between 80 and 160 Hz (two-pass Butterworth filter, 5th order). Data was then segmented and scored on 20-s-long windows by an experienced scorer (TA) and following established guidelines (Iber et al., 2007). Only a subset of channels (C3, C4, Fz and Pz) were used to score vigilance states along two EOG channels and the chin EMG. Recordings were scored as wakefulness (49.00 +/- 2.59 minutes, mean duration +/- SEM across participants), NREM1 (9.24 +/- 0.97 minutes),

NREM2 (14.36 +/- 1.58 minutes) and NREM3 (5.69 +/- 1.42 minutes). None of the participant entered the Rapid Eye-Movements (REM) stage.

Stimulus Reconstruction: The EEG signal was here re-referenced to the signal averaged across all electrodes ('average referencing'). The EEG signal was then filtered between 2 and 8 Hz with a two-pass Butterworth filter (5th order) and then down-sampled at 100Hz to reduce data's dimensionality. The filtered EEG signal was segmented according to trials onset and offset. The amplitude of the filtered EEG envelope was subsequently extracted by applying the Hilbert transform. In addition, for each trial, the auditory streams played during this trial (1 stream for the training phase, 2 streams for the test phases) were filtered below 8Hz with a two-pass Butterworth filter (5th order) and down-sampled at 100Hz. The sound's envelope was obtained again by applying the Hilbert transform.

Stimulus Reconstruction

Rationale: The stimulus reconstruction is an approach that allows the reconstruction of an acoustic stimulus based on the neural data recorded while the stimulus was played (Mesgarani and Chang, 2012; O'Sullivan et al., 2014; Pasley et al., 2012; Zion Golumbic et al., 2013). Depending on the type of data recorded, different characteristics of the acoustic stimuli can be reconstructed. It has been shown recently that the scalp EEG signal could be used to reconstruct the envelope of an acoustic stream played concomitantly (O'Sullivan et al., 2014). Such reconstruction of the envelope is performed by building a linear model between the EEG signal and the sound signal. Interestingly, when two auditory streams are played concomitantly, both envelopes can be reconstructed. When a stream is attended and the other ignored, the attended stream's envelope is on average better reconstructed, allowing to track participants' attention with a high degree of accuracy (O'Sullivan et al., 2014). We deployed here a similar methodology.

Training: A first step in the stimulus reconstruction approach is to compute the linear model between the auditory stream and the EEG signal. The model here was trained on the diotic trials (1 stream played to both ears, 6 real and 6 pseudo texts for a total duration of 14.6 minutes). By using diotic trials, we ensured that the model was trained to decode sound's envelope in the absence of attentional bias. In addition, by using both real and pseudo texts in the training, we increase the probability that the decoders would be insensitive to the stimulus condition in the absence of attentional bias (see also control below). The linear model was optimized to map the EEG signal from each electrode to the sound envelope. EEG data was shifted compared to the auditory envelope from 0 ms to 500 ms (here referred as time-lags), which allows the integration of a broad range of EEG data to reconstruct each stimulus time-point (Mesgarani et al., 2009). In practice, this means that each sample in the auditory envelope was correlated with the bandpass EEG envelope from all sensors and all samples between 0 and 500ms relatively to the auditory signal. The obtained filter (matrix of weights: sensor per time-lags) was then used in the testing phase to reconstruct the stimuli (Figure 6-1).

Test: In the test phase, for each trial, two stimuli were played in competition. Using the model, one envelope can be reconstructed from the EEG signal recorded at that time.

The reconstructed envelope is assumed to correspond to a noisy mixture of both streams' envelope. In order to determine which stream was predominantly reconstructed (if any), the reconstructed envelope was compared to both original envelopes using the Pearson correlation method. For each trial, we therefore obtained two Pearson correlation coefficients, one for the real text (r_{text}) and one for the pseudo (r_{pseudo}) text. These correlation coefficients were used as an index of the quality of the stimulus reconstruction of the two streams. When r_{text} was higher than r_{pseudo}, that is to say when the reconstructed envelope was more similar to the real-text envelope than the pseudo-text one, attention was declared as being orientated to the real-text. Therefore, trials with $r_{text} > r_{pseudo}$ were scored as correct (1, attention oriented to the real text) and trials in which $r_{text} < r_{pseudo}$ were scored as incorrect (0). The decoding accuracy (Figure 6-2) is the average of these scores across participants.

The reconstruction was either performed on the entire trials (see Control below) or on smaller windows (Figure 6-2, Figure 6-3 and Figure 6-4). Indeed, during the sleep test phase, participants were not necessarily in the same sleep state for the entire trial duration. To get a better picture of the allocation of attention during the different sleep stages, trials were epoched in 10-s-long windows either locked on the sleep scoring (Figure 6-2a-b) or on the beginning of the trial (Figure 6-2c-d). The former epoching was used to get reliable scores of decoding across sleep stages (Figure 6-2a-b) whereas the latter was used to get the dynamics of decoding during trials (Figure 6-2c-d). In the later epoching, 10-s-long epochs might include sleep stage transitions. In such cases, the epoch was attributed the lightest sleep stage present in the epoch.

Control: In dichotic trials, the real and pseudo texts differed at the semantic level. We assumed that such semantic difference would not affect the ability to decode the envelope and that the differences observed in the dichotic trials are due to an attentional bias. To confirm this assumption, we verified that the model could reconstruct the real and pseudo texts similarly when presented in isolation (diotic trials). This was done by implementing a leave-one-out approach on the training data: for each participant, 5 out of 6 real and pseudo trials were randomly selected and used to train a model. The remaining real and pseudo trial (test set) were reconstructed using this model. The operation was iterated until all trials have been used as the test set. The corresponding Pearson coefficients were averaged across iterations and participants for real and pseudo texts. Both streams were reconstructed with highly significant correlation coefficients ($p < 0.001$, Figure S 6-1). Crucially, there was no observable difference between the real and pseudo texts ($p = 0.41$), indicating that the stimulus reconstruction approach is blind to the intrinsic difference between real and pseudo texts.

Individual Lags, Weights and Patterns

As said above, each time-point of the sound envelope was reconstructed by using 500ms of the EEG signal (time-lags). However, these different time-lags do not equally contribute to the stimulus reconstruction (O'Sullivan et al., 2014). To better understand the contribution of each lag, filters were trained on the EEG for each single time-lags. An envelope was then reconstructed for each trial and compared to the real and pseudo envelopes. A correlation coefficient was therefore obtained for each stimulus (real and pseudo) and individual lag. The corresponding values averaged across participants are shown in Figure 6-3. In all stages, three peaks of reconstruction were observed around 100, 200 and 300 ms. The positions of the peaks were determined by searching for the

maximum reconstruction coefficients for each stimulus (real and pseudo) between +0ms and+150ms, +150ms and +250ms and +250ms and +400ms in each vigilance state. The position of the peaks were averaged across participants and approximated to the closest time-lag. The Pearson coefficients for each peak and stream were extracted on a [-30, 30] ms window around the peak position (Figure 6-3, bars). For each peak, the weights of the individual filter were extracted from the model and displayed on a topographical map (Figure 6-3a). According to (Haufe et al., 2014), the patterns (i.e. the spatial profile of the EEG activity used by the model) were extracted for each peak using the following formula:

$$A = \Sigma_x W \Sigma_{\hat{s}}^{-1}$$

where A denote the pattern, $\sum_x$ the covariance of the EEG signal, W the weight matrix at the individual time-lag and $\sum_{\hat{s}}$ the covariance of the reconstruction.

Spindles and Slow-waves detection

We investigated the influence of NREM-sleep graphoelements (slow-oscillations and sleep spindles) on stimulus reconstruction (Figure 6-4). To do so, we relied on automated detection algorithms developed detailed elsewhere (Andrillon et al., 2011; Nir et al., 2011; Riedner et al., 2007).

To detect slow-oscillations, the raw EEG signal was re-referenced to the average mastoids. For each sensor, the EEG signal was first filtered between 0.2 and 3 Hz using a two-pass 3rd order Butterworth filter and down-sampled at 100Hz. Peaks and troughs of the filtered signal were detected as zero-crossings of the first order derivative. Portions of signal were determined as slow-oscillations when a peak and a trough were separated by more than 0.25 seconds and less than 2 seconds and the through-to-peak amplitude was greater than 75µV. Slow-oscillations comprised here both K-complexes and slow-waves. However, slow-oscillations detected in NREM2 had an asymmetrical profile characteristic of K-complexes and were often detected in isolation while slow-oscillations detected in NREM3 had a symmetrical profile and occurred in trains (Figure S 6-3). NREM2 slow-oscillations were therefore approximated to K-complexes and NREM3 slow-oscillation to standard sleep slow-waves.

Spindles were detected using an automated algorithm as well. The raw EEG signal was re-referenced to the mastoids. The EEG signal was then band-pass filtered between 11 and 16 Hz with a two-pass Butterworth filter at the 4th order. The envelope of the signal within the spindle band was extracted using the Hilbert transform applied on the filtered signal. Spindle candidates were detected as epochs during which a given threshold was overcome. The threshold used to identify these candidate spindles was set for each sensor and participant separately as the mean plus two standard deviations of the envelope amplitude recorded during all NREM2 and NREM3 epochs. Spindles candidates longer than 2.5 seconds or shorter than 0.5 seconds were discarded as well as spindles during which the envelope exceeded a maximal threshold (mean + 10 SD). See (Andrillon et al., 2011) for a complete description of this algorithm.

Decoding around sleep grapho-elements

For each detected grapho-element (slow-oscillations or sleep spindles), we applied the stimulus reconstruction approach with a maximum lag of 250 ms. We extracted the Pearson coefficients corresponding to the real and pseudo texts on sliding windows (4-s-long, positioned every 100ms) around each events onset ([-10, 10]s, see Figure 6-4). The central window (t=0) was locked on the negative peak of slow-oscillations (Figure 6-4a,c) and on the middle of spindles (Figure 6-4b). K-complexes and spindles were detected in NREM2 and slow-waves in NREM3. The slow-waves and spindles were detected on the Cz electrode. Time-courses were smoothed using a 500-ms-wide Gaussian kernel (Figure 6-4) for display only. Statistical tests were performed on the data prior to smoothing.

Statistics

Stimulus reconstruction scores were computed by correlating the auditory signal with the EEG signal. Pearson's method, a parametric assessment of the correlation between two signals, was used. Parametric statistics were used whenever possible (Student's t-tests for the comparison of two variables). Non-parametric statistics were used otherwise (Mann-Whitney u-tests for the comparison of two variables).

Given that participants did not have the same number of trials in each vigilance state, we used mixed-models to estimate the effect of different predictors (effect of the stream type, of sleep stages, of K-complexes or sleep spindles, …) on reconstruction scores and decoding accuracy (see Figure 6-2). Mixed-models analyses were performed in R (R Development Core Team) with the 'lme4' and 'lmerTest' R packages. Linear mixed-models were used to examine the effect of predictors on the reconstruction scores of the real or pseudo-stream and general linear mixed-models to examine the effects of these predictors on the decoding of attention (binomial variable). The corresponding p-values are reported in the main text, figure legends and supplementary material.

Time-plots typically include numerous data-points. To correct for the multiple-comparisons problem, we used cluster-permutation statistics (Maris and Oostenveld, 2007). In this principled approach, each cluster was defined as the time-points that consecutively passed a specified threshold (cluster p-value: $p<0.1$). The sum of the t-values of all the time-points within the cluster constituted the cluster statistics. This cluster statistics was compared for each cluster with the maximum cluster statistics obtained after the random permutations of the conditions examined (N = 2000). From these permutations, we computed a Monte-Carlo p-value that corresponds to the $p_{cluster}$ reported in the main text and figures' legend.

Results

Building an unbiased model for stimulus reconstruction

Here, we reconstructed the stimuli presented to participants using the continuous scalp EEG signal. More precisely, we focused on the low-frequency ([2-8] Hz) modulations of the acoustic envelope and we trained a model mapping the EEG envelope with the envelope of an acoustic stream presented in isolation (Figure 6-1, training). The auditory material used to train the model was made of real-speech trials (N=6, ~1 minute per trial) and of pseudo-speech trials (N=6, ~1 minute per trial). In the test trials, the model was used to reconstruct the envelope of two streams (one made of real-speech, the other of pseudo-speech) presented concomitantly. The model was thus trained on a distinct dataset (diotic stimuli, training phase) and then applied to a situation in which two streams were presented in competition (dichotic listening).

We first investigated whether the model was efficient enough to reconstruct the envelope of stimuli in wakefulness, and whether it was biased by the nature of stimuli (i.e. real vs. false-speech). We used a leave-one-out approach in which the model was successively trained on all but one of the training trials of each condition (i.e. *n-1* real-speech trials and *n-1* pseudo-speech trials). The model was then applied to the remaining training trials (1 real and 1 pseudo-speech trial). We computed the reconstruction scores (correlation between the original and reconstructed envelope, see Methods) for both types of trials (Figure S 6-1). Highly significant reconstruction scores were obtained for both trial types across participants (Pearson correlation coefficient: $R_{REAL} = 0.077$, $R_{PSEUDO} = 0.080$, two-tailed t-tests compared to 0: $t(23)=11.95$ and 10.20 resp., both $p<0.001$, N=24 participants), demonstrating the efficacy of the model in reconstructing the envelope of an hitherto novel auditory stream. Crucially, there was no difference between the reconstruction scores of the real and pseudo-speech (two-tailed paired t-test: $t(23)= -0.84$, $p=0.41$), demonstrating that our model was not biased towards one stimulus category.

We then verified that the model trained on diotic trials could reconstruct the envelope of streams presented in dichotic trials. In this situation, a reconstruction score (correlation coefficient) is obtained for each envelope (see Methods). In wakefulness (Figure 6-2b), both streams (real and pseudo-speech) led to correlation coefficients significantly higher than 0 (Pearson correlation coefficients: $R_{REAL} = 0.045$, $R_{PSEUDO} = 0.016$, one-tailed t-tests compared to 0: $t(23)=8.91$ and 4.67 resp., both $p<0.001$), indicating that the diotic model can successfully reconstruct stimuli envelope even when two streams are presented concomitantly.

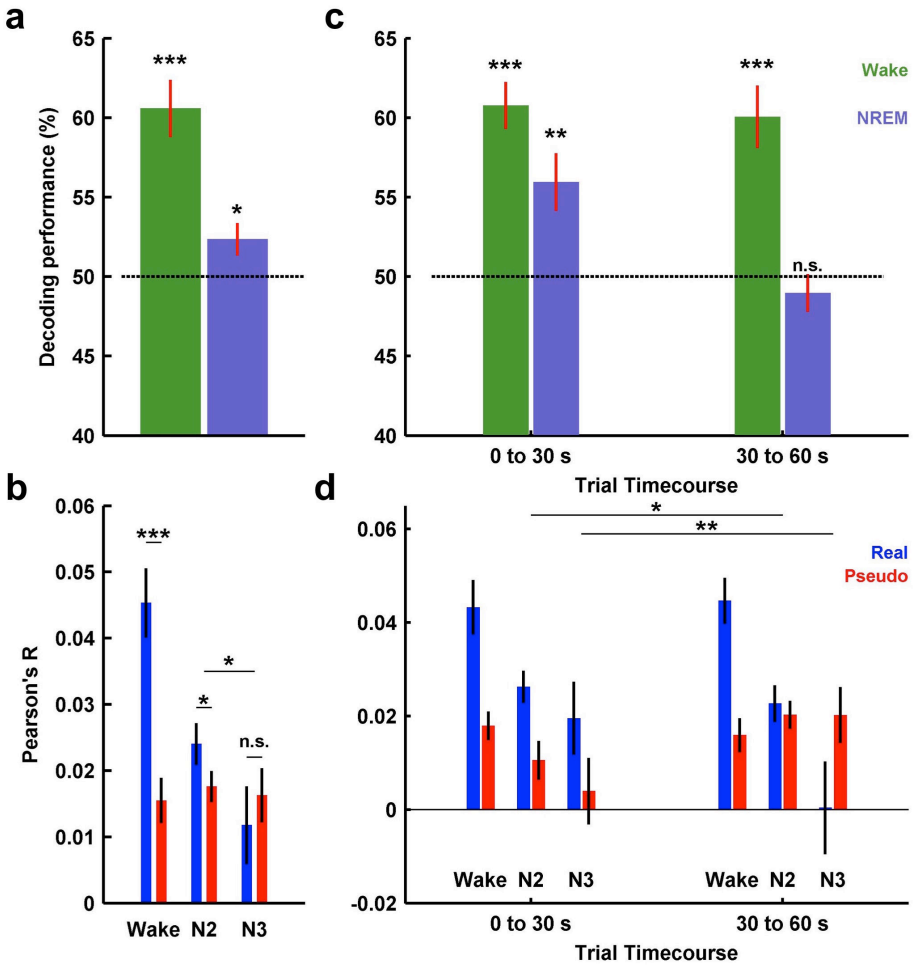

Figure 6-2 Reconstruction accuracy and decoding performance across wake and NREM sleep

(a) Decoding of attention allocation during wakefulness (green), and NREM sleep (NREM2 and NREM3 stages, purple) across participants (N=24). Error-bars denote the standard error of the mean computed across participants in all subpanels. Stars show the significance level of the t-tests comparing performance against the 50% chance level (***: p<0.005, **: p<0.01, *: p<0.05, ns: p>0.05). Note that attention could be successfully decoded in both wake and NREM sleep. (b) Reconstruction scores (Pearson correlation between the reconstructed and original envelopes, see Methods) for the real and pseudo stream in wakefulness, NREM2 (N2, light NREM sleep) and NREM3 (N3, deep NREM sleep). Stars between bars show the significant level of paired t-tests comparing the real and pseudo streams' reconstruction (across 24, 24 and 16 participants in wake, N2 and N3 resp., ***: p<0.005, **: p<0.01, *: p<0.05, ns: p>0.05). The stars between NREM2 and NREM3 values denote a significant interaction between the effect observed in NREM2 and NREM3 (mixed-model: p<0.05, see Methods). (c) Same as in panel a but for the beginning ([0, 30]s) and end ([30, 60]s) of trials separately. (d) Same as in panel c but for the beginning and the end of trials separately. Horizontal bars denote the interaction between the beginning and end of trials in N2 and N3 (mixed-model, ***: p<0.005, **: p<0.01, *: p<0.05, ns: p>0.05).

Sensory encoding and attention allocation in wake and sleep

In dichotic trials, participants were instructed to focus on one stream (real-speech) and ignore the meaningless competitor (pseudo-speech). Although they could be equally reconstructed when presented in isolation, both real and pseudo streams had markedly different reconstruction scores when presented in competition (Figure 6-2b). During wakefulness, as previously shown (O'Sullivan et al., 2014), the attended stream (here, the real-speech) led to higher reconstruction scores than the unattended pseudo-speech (two-tailed paired t-test: $t(23)=6.50$, $p<0.001$). As a result, comparing the correlation coefficients for both stream on a single-trial basis (see Methods) allowed us to decode attention allocation with good accuracy (60.6%, two-tailed t-test comparison with 50% chance-level: $t(23)=6.01$, $p<0.001$).

When examining trials presented in NREM sleep (NREM2 and NREM3 stages), we also obtained a significant albeit smaller decoding accuracy (52.4%, $t(23)= 2.36$, $p<0.05$), indicating that sleepers continued to amplify the meaningful stream. Stage NREM1 was not included in this analysis to ensure that the results obtained here were not due to transient episodes of wakefulness. Examining the reconstruction scores for the real and pseudo-speech stimuli in light and deep NREM sleep (resp. NREM2 and NREM3 stages) revealed a better reconstruction of the real-speech compared to the pseudo-speech for light NREM sleep but not for deep NREM sleep ($t(23)=2.29$, $p <0.05$ and $t(15)=-0.74$, $p=0.47$ resp.). A mixed-model applied to the reconstruction scores in sleep indicated a main effect of the stream type ($p=0.003$), as well as an interaction between stream type and sleep stage ($p=0.02$) but no effect of the sleep stage itself ($p=0.80$). This pattern of results is due to a gradual decline of the reconstruction score for the real-speech from wakefulness to deep NREM sleep (paired t-test between N2 and wake: $t(23)=4.7$, $p=1.10^{-4}$; N3 and wake: $t(15)=4.8$, $p=3.10^{-4}$; Figure 6-2b). Interestingly, the reconstruction score of the pseudo-speech remained constant across sleep stages (paired t-tests between N2 or N3 and wake for pseudo-speech: all $p>0.2$), suggesting that sleep is characterized by a gradual decrease of attentional engagement rather than an overall decrease in sensory encoding.

Within-trial dynamics of attention allocation in wake and sleep

To better understand whether sleepers could maintain their attention over long-time windows (trial duration: ~1 minute), we compared the decoding of attention allocation between the beginning ([0, 30]s) and end ([30, 60]s) of the test trials (Figure 6-2c). In wakefulness, decoding accuracy was constant over the entire trial (mixed model, beginning/end effect: $p=0.82$) and above the chance-level (post-hoc t-tests: $t(23)=7.46$, $p<0.001$ and $t(23)=5.21$, $p<0.001$ for the beginning and end of trials resp.). In NREM sleep, however, attention was successfully decoded at the beginning but not at the end of the trials (beginning/end effect: $p<0.05$; post-hoc t-tests: $t(23)=3.37$, $p<0.01$ and $t(23)=-0.89$, $p=0.38$).

This pattern was confirmed when examining light and deep NREM sleep separately. The attended stream was better reconstructed at the beginning of the trials than the end (Figure 6-2d). Accordingly, mixed models fitted on light and deep NREM sleep individually showed an effect of the stream type (light: $p=0.006$; deep: $p=0.038$) and of the position within the trial (marginal in light NREM sleep: $p=0.076$; deep: $p=0.004$) as well as an interaction between these two predictors (light: $p=0.039$; deep: $p=0.004$).

Interestingly, although this effect did not reach significance, the real-speech tended to be worse reconstructed than the pseudo-speech in deep NREM sleep ($t(16)=-1.67$, $p= 0.11$), a reversal that suggests the involvement of suppressive mechanisms (see below for further evidence).

Overall, these results indicate that, contrary to wakefulness, attention could not be maintained throughout the entire trials during sleep and that real-speech was enhanced at the beginning of trials only. In addition, the pattern of results observed suggest a potential inhibition of the real-speech in deep NREM sleep toward the end of the trials, which could be interpreted as a mechanism protecting sleep against external inputs (see Discussion).

Decoding profiles are similar across wake and sleep

To reconstruct the stimuli envelope from the EEG signal, the model integrates EEG data over relatively large temporal windows (i.e. 500ms). We examined the participation to the stimulus reconstruction of these different time-points, by training and testing our model using EEG data at fixed time-lags rather (see Methods and Figure 6-3). Such approach allows a better understanding of how the brain dynamically integrates auditory information (O'Sullivan et al., 2014). When examining wake data (Figure 6-3a), we replicated previous findings showing that individual time-lags do not uniformly contribute to the stimulus reconstruction (O'Sullivan et al., 2014). Rather, three peaks could be individualized at around 100, 200 and 300 ms. The scalp topographies and patterns extracted from these peaks are concordant with the notion that auditory cortices play a preponderant role in reconstructing stimuli's envelope (Figure 6-3a). Indeed patterns' topographies resemble the scalp distribution of auditory evoked potentials such as the N1 or P2 potentials, whose neural sources have been found in primary and secondary auditory cortices (Näätänen and Picton, 1987; Picton, 2011).

In light NREM sleep, the temporal profile of the stimulus reconstruction along individual-lags was strikingly similar to wakefulness (Figure 6-3b), suggesting that the same processing stages are preserved in sleep. In addition, the real-stream was better reconstructed than the pseudo-stream in the 2nd and 3rd peaks (significant clusters: [170,220] and [270,350] ms, $p_{cluster}<0.05$), with a trend for the 1st peak ($t(23)=2.02$, $p=0.054$). In deep NREM sleep (NREM3 stage) however, the reconstruction for the real and pseudo streams largely overlap, illustrating the loss of attentional effect in deep NREM sleep. These results support the notion that auditory information is processed with the same dynamic from wake to sleep.

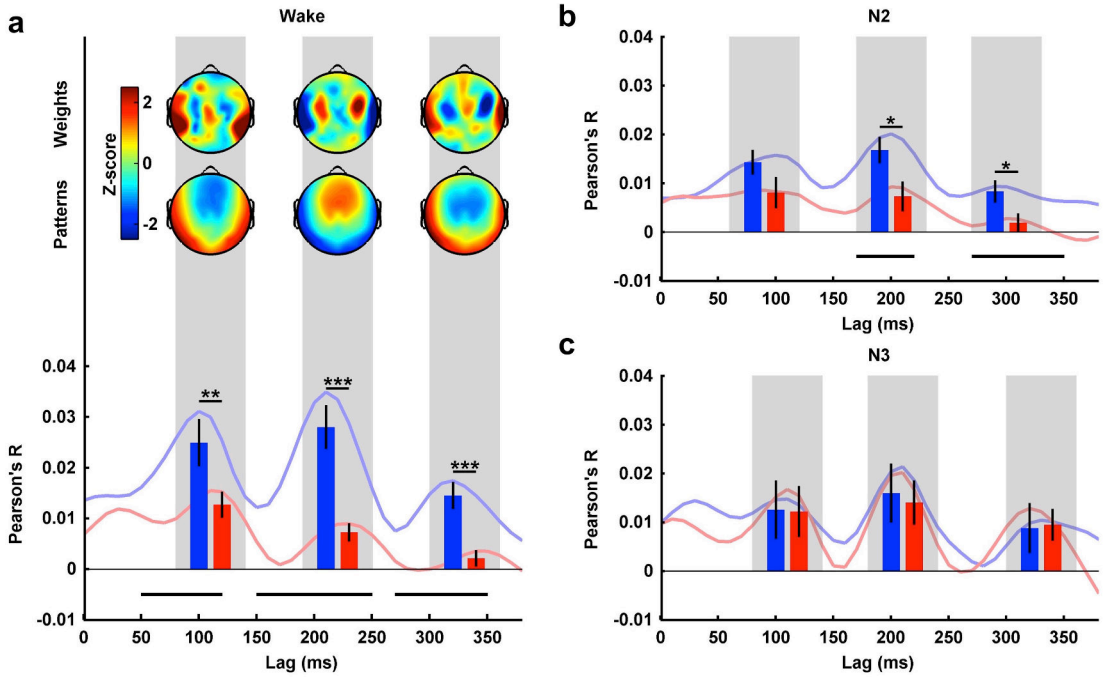

Figure 6-3 Spatio-temporal integration of acoustic information

(a) Bottom: Individual models were computed for each time-lag (see Material and Methods). Correlation coefficients for the real (blue) and pseudo (red) speech presented during wakefulness were extracted for each of these time-lags and averaged across participants (N=24 participants). Horizontal bars show significant clusters for the comparison between the blue and red curves (pcluster<0.05). Three main peaks can be observed at 110 ms, 230 ms and 330 ms respectively. Red and blue bars show the reconstruction scores extracted for these three peaks (see Methods). Error-bars denote the standard error of the mean computed across participants and stars between bars show the significant level of the t-tests comparing the real and pseudo streams' reconstruction (paired t-tests, ***: p<0.005, **: p<0.01, *: p<0.05, ns: p>0.05). Top: Scalp topographies of filter weights and patterns corresponding to the 3 different peaks (see Methods for details). Values were z-scored across electrodes to emphasize regional differences. Note that patterns' topographies are typical of auditory activity as recorded with EEG. (b) Same temporal profile as in panel a for NREM2 trials (N2, N=24 participants) when focusing on the beginning of trials (see Figure 6-2). Note the similarity of the profile with wakefulness. (c) Same temporal profile as in panel a for NREM3 trials (N3, N=16 participants) when focusing on the beginning of trials. Note the overlap between the real and pseudo speech in line with the absence of attention allocation as shown in Figure 6-2.

K-complexes, slow-waves and sleep spindles distinctively impact sensory encoding and attention

NREM2 and NREM3 stages are characterized by the presence of particular sleep rhythms: K-complexes, slow-waves and sleep spindles. We examined their respective influence on sensory encoding and attention allocation. To do so, we first detected these events through automated algorithms (see Methods). Slow-oscillations detected in NREM2 were approximated to K-complexes since they tended to be detected in isolation and had an asymmetric profile (Figure S 6-4). On the other hand, slow-oscillations detected in NREM3 were approximated to standard sleep slow-waves since they tended to appear in trains and had a more symmetrical profile. To examine the influence of these sleep rhythms, stimulus reconstruction was time-locked to the down-

states of slow-oscillations (K-complexes in NREM2 and slow-oscillations in NREM3) and to the middle of sleep spindles (Figure 6-4).

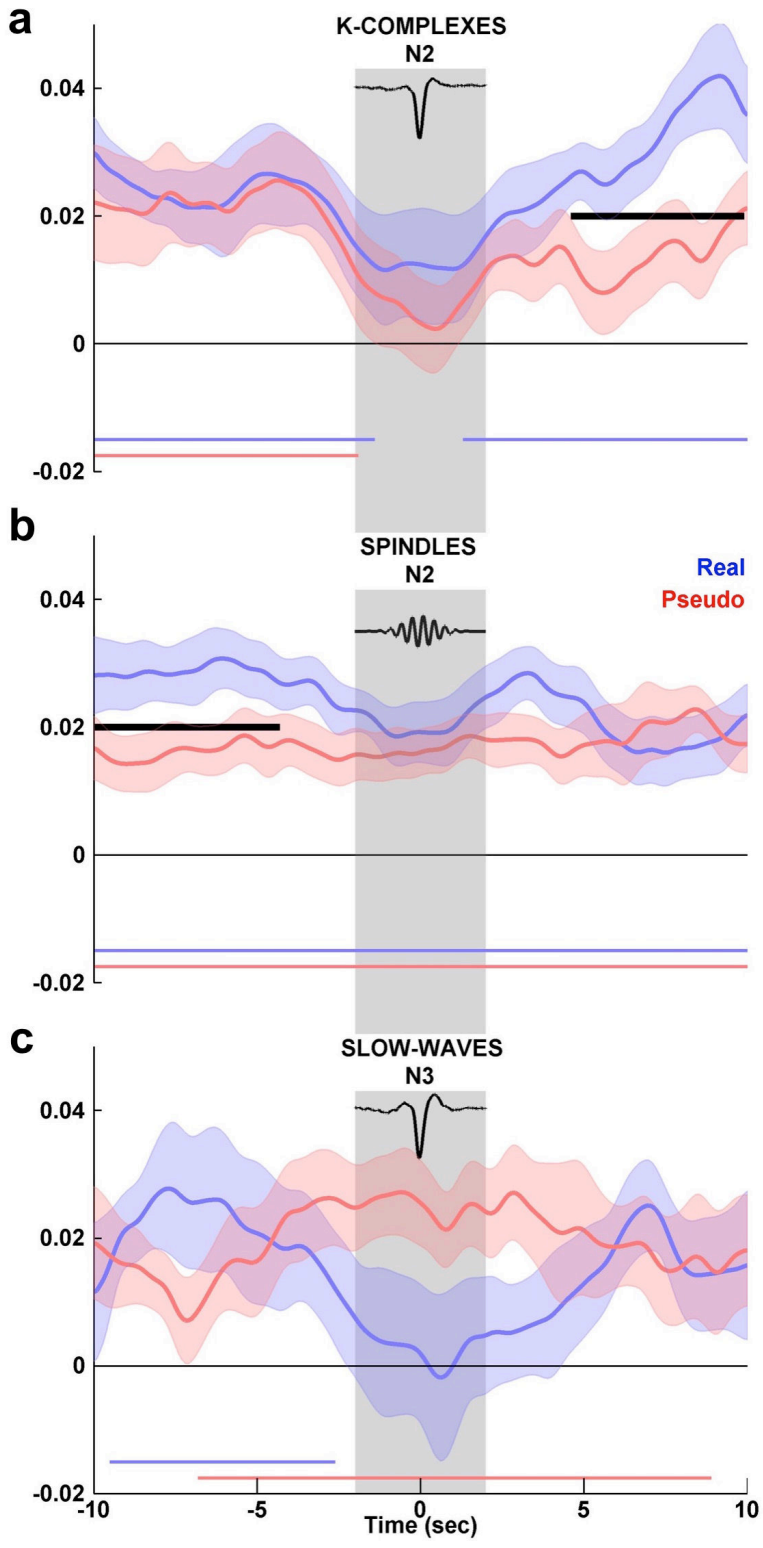

Figure 6-4 Impact of sleep spindles, K-complexes and slow-waves on stimulus reconstruction

In each panel, reconstruction scores (real-speech: blue; pseudo-speech: red) were time-locked to the graphoelements of interest (top: K-complexes in NREM2; middle: sleep spindles in NREM2; bottom: slow-waves in NREM3) and were averaged across participants (N=24, 24 and 16 resp.). The down-states of K-complexes and slow-waves and the middle of spindles were used as time=0. Shaded areas denote the standard error of the mean computed across participants. Curves were smoothed with a 500ms-wide Gaussian kernel for visual purposes only. Colored horizontal bars show the significant clusters when comparing reconstruction scores with 0 ($p_{cluster}<0.05$). Black horizontal bars show significant clusters when comparing the two reconstruction scores ($p_{cluster}<0.05$). The average traces of K-complex and slow-waves are displayed on top of the corresponding panel for comparison. An archetypal spindle is also shown. Note the differential impact of NREM2 K-complexes and NREM3 slow-waves on stimulus reconstruction.

Both streams were significantly reconstructed before K-complexes (cluster for R_{REAL}: [-10, -1.4] s, $p_{cluster}<0.01$; for R_{PSEUDO}: [-10, -1.9] s, $p_{cluster}<0.01$) with equivalent reconstruction scores (Figure 6-4a). During the occurrence of K-complexes, both streams were no longer reconstructed which is concordant with the fact that the K-complexes' down-states entail a period of neuronal silencing (M. Steriade, 2003) during which external information is no longer encoded at the cortical level (Schabus et al., 2012; Sela et al., 2016). Importantly, however, we found that after K-complexes, not only both streams were successfully reconstructed (significant clusters for R_{REAL}: [1.3, 10] s, $p_{cluster}<0.01$; for R_{PSEUDO} [6.4, 10]s, $p_{cluster}<0.05$) but the real-speech had even higher reconstruction scores than the pseudo-speech (difference: [4.6, 9.9]s, $p_{cluster}<0.05$). This result suggests that K-complexes trigger the recovery of wake-like attentional processes.

The temporal profile for slow-waves in NREM3 was markedly different (Figure 6-4c). The real-speech was successfully reconstructed before slow-waves ([-9.5, -2.6] s, $p_{cluster}<0.05$) whereas during slow-waves, this ability to reconstruct the real-speech was lost. Paradoxically, the reconstruction of the pseudo-speech stream was slightly improved during slow-waves and crossed our statistical threshold ([-6.8, 8.9] s, $p_{cluster}<0.01$). Therefore, contrary to K-complexes, the real and pseudo speech were differently affected by slow-waves. At no point around slow-waves though, was one stream significantly better reconstructed from the other in link with the observed loss of attention allocation in deep sleep (Figure 6-2). Thus, while K-complexes show a bi-phasic effect on stimulus reconstruction with a decrease in reconstruction scores for both streams followed by an increase in reconstruction scores for both streams (and more so for the real-speech), slow-waves in NREM3 negatively affected the real-speech only. This biased effect of slow-waves could explain the partial reversal of the relationship between the real and pseudo-speech from light to deep NREM sleep (Figure 6-2 and Figure 6-3; see also Discussion).

Sleep spindles in NREM2 had a rather moderate effect on stimulus reconstruction. Indeed, both streams were reconstructed during the entire [-10, 10]s window ($p_{cluster}<0.001$). However, while the real-speech was, on average, better reconstructed than the pseudo-speech before sleep spindles (difference: [-10 to -4.3]s , $p_{cluster}<0.05$), this difference disappeared during and after sleep spindles. Sleep spindles therefore seemed to affect moderately attention allocation but not sensory encoding. Furthermore, since sleep spindles and slow-oscillations often occur in association (De Gennaro and Ferrara, 2003), we estimated their respective effect on attention allocation: the difference of reconstruction scores between the real and pseudo speech was extracted on 10-s-long windows and the presence of K-complexes or sleep spindles were used as predictors in a

mixed model. While the presence of K-complexes had a positive impact on the index of attention ($p=5.10^{-6}$), there was no effect of sleep spindle on reconstruction scores ($p=0.86$; see Figure S 6-3).

Discussion

Attention is preserved during NREM sleep

Whether mechanisms of attention, leading to the amplification and monitoring of relevant signals in the environment, can be involved during sleep remains an unsettled issue. In addition, how sleep rhythms affect the coupling and decoupling (i.e. sensory isolation) from the environment is also unclear. Previous studies focused on the analyses of brain responses to single events (Atienza et al., 2001; Bastuji, 1999), making it difficult to address these questions. Here, investigating brain responses to multi-talker speech (a classical approach for testing attention allocation, (Cherry, 1953), we show that both attended and unattended streams are encoded in the brain and regardless of the vigilances state. Strikingly, attentional effects are also present during sleep, but attention allocation is wiped out by slow waves in deeper stages of sleep.

Our results provide clear evidence that sleepers can pay attention to a given source of information (Figure 6-2) even when the criterion participants had to use to select the correct stream (the presence of a meaning) imposed to parse streams at a high-level of representation. However, such attention allocation was transient and observed only in light NREM. This result contrasts with the sustained attention observed in wakefulness. Such a transient ability to attend is reminiscent of studies showing impairment of hierarchical information processing in NREM sleep (Strauss et al., 2015) as well as physiological investigations of NREM sleep showing a break-down of integrative processes (Pigorini et al., 2015). Importantly, the loss of attention allocation in deep NREM sleep was not due to the inability to reconstruct the streams but to a decline in the quality of the real-speech reconstruction. Indeed, the pseudo-speech reconstruction was surprisingly constant across sleep stages, suggesting that sleep onset mostly affects the amplification of relevant information rather than its encoding.

This interpretation is corroborated by the temporal profile of stimulus reconstruction (Figure 6-3). Stimulus reconstruction was maximal over 3 different temporal windows in wakefulness (Figure 6-3a). Interestingly, these peaks have been interpreted as reflecting different stage of sensory processing (O'Sullivan et al., 2014), with later peaks corresponding to higher levels of auditory processing. If such interpretation holds, our results would confirm previous findings showing an effect of attention at different levels of representations during wakefulness (Mesgarani and Chang, 2012; Zion Golumbic et al., 2013). Indeed the real-speech led to higher reconstruction score than the pseudo-stream within each peak (Figure 6-3a). Such broad attentional effect was conserved in light NREM sleep (Figure 6-3b), suggesting that, as in wakefulness, attention affects all stages of sensory processing during sleep. In deep NREM sleep however, the real and pseudo speech had overlapping temporal profiles indicating that wake processing stages were conserved but without any attentional amplification. Such results fit well with the preservation of sensory encoding in NREM sleep on the one hand (Y. Nir et al., 2013) and on the other hand with the impairment of top-down processes (Strauss et al., 2015) and executive functions (Maquet, 2000; Muzur et al., 2002), which are instrumental (even if not necessary) in the orientation of attention (Fritz et al., 2007).

The role of sleep rhythms in the processing of external inputs

While sleep is usually scored on large windows (Iber et al., 2007), an abundant literature suggests that its micro-structure is key to understand how sleep alters the processing of external inputs (Halasz, 2005; Massimini et al., 2012; McCormick and Bal, 1994). K-complexes have been associated to sensory processing since their discovery (Loomis et al., 1938) but their role is debated. Indeed, K-complexes can be elicited by external stimulations particularly when the stimulus is relevant or infrequent. They can be associated with signs of arousals, and their neural source depends on the nature of the eliciting stimulus (see (Colrain, 2005; Halasz, 2005; Halász, 2016) for exhaustive reviews on the topic). Along this line, it has been proposed that K-complexes are followed by up-states providing 'fragments of wakefulness' to the sleeping brain (Destexhe et al., 2007). However, K-complexes have also been depicted as isolated down-states (Cash et al., 2009) protecting sleep from external disturbances (Bastien et al., 2000; Wauquier et al., 1995).

Our results allow conciliating these views. By taking advantage of continuous stimulations, we show that K-complexes suppressed sensory encoding around the associated down-states while favoring, after the K-complex, both sensory processing and attention allocation (Figure 6-4a). Thus, depending on the time-scale considered, K-complexes can be seen as promoting or suppressing sensory processing. The use of isolated stimuli, frequent in ERP studies, could have dampened the manifestation of the 'Janus-faced' nature of K-complexes (Halasz, 2005).

In deep sleep, slow-oscillations occur in trains and have been shown to disrupt cortical processes (Pigorini et al., 2015) and the integration of information (Massimini et al., 2005). And indeed, the impact of K-complexes on sensory processing contrasted with the results obtained for slow-oscillations detected in deeper stages of sleep (Figure 6-4a,c). NREM3 slow-waves had a negative effect on the real-speech only (Figure 6-4c). This could be interpreted as an active suppression of meaningful stimuli in deep NREM mediated by slow-waves. What could be the mechanism underlying this suppression? Sleep slow-waves are thought to reflect the bi-stability of cortical neurons (Vyazovskiy and Harris, 2013) and the associated down-states have been associated to the suppression of sensory information (Schabus et al., 2012; Sela et al., 2016). Since slow-waves appear to be more local than previously described (Nir et al., 2011) and since competing stimuli are thought to be encoded by separate neural networks (Ding and Simon, 2012b; O'Sullivan et al., 2014), it is therefore possible that slow-waves may affect one stream (i.e. one network) and not the other. But how would the sleeping brain choose which stream to suppress? We argue here for a simple use-dependent mechanism. Indeed, slow-waves may be triggered by local activations within the cortex (Menicucci et al., 2013). Because the real-speech seemed to be better processed even in sleep, the network encoding real-speech could be more active than its pseudo-speech counterpart, which will increase the probability of triggering slow-waves within this network. This would explain the specific suppression of the real speech during slow-waves. Accordingly, the real-speech was slightly better reconstructed than the pseudo-speech before the slow-waves (Figure 6-4c).

Thus, despite common generative mechanisms (Halász, 2016), K-complexes and slow-waves could impact sensory processing differently. This difference could be explained by the fact that K-complexes and slow-waves entail fundamentally different synchronization processes, as recently proposed (Siclari et al., 2014a). According to this view, K-complexes reflect a global phenomenon that would jointly affect both real and pseudo streams. Accordingly, K-complexes' down-states appeared to transiently shut down

sensory processing as a whole (Figure 6-4a). In the case of a continuous stimulation however, the concomitant recruitment of the arousal system would favor the recovery of wake-like processing and attentional processes after K-complexes. On the other hand, slow-waves could represent local cortical synchronization processes disrupting information processing in a given network and in a use-dependent fashion. This interpretation fully accounts for our results and especially for the suppression of the meaningful stream in deep NREM sleep, without relying on any top-down processes determining which stream to suppress.

Sleep spindles seemed to have a much weaker effect on stimulus reconstruction as they suppressed the attentional effect but not the ability to reconstruct the stimuli. In addition and contrary to K-complexes, their presence or absence could not predict the decoding of attention on 10-s-long windows (mixed-model: $p=0.85$ compared to $p=7.10^{-6}$ for K-complexes). Such results could seem at odd with their putative role in sensory disconnection (McCormick and Bal, 1994; Schabus et al., 2012; Yamadori, 1971). However, intracranial studies suggest that sleep spindles moderately affect cortical units' activity (Andrillon et al., 2011; Peyrache et al., 2011) and that auditory encoding is preserved during sleep spindles (Sela et al., 2016). Our results further temper the view of spindles as a gating mechanism.

Overall, it seems that NREM sleep rhythms could well account for the pattern of results observed on average in light and deep NREM. Sleep rhythms observed in NREM2 promoted (K-complexes) or had a limited (sleep spindles) impact on sensory encoding and the orientation of attention, which could explain the preservation of attention allocation in light NREM sleep. On the contrary, slow-waves detected in NREM3 suppressed preferentially the meaningful stream, which could explain the partial reversal observed in deep NREM sleep between the real and pseudo speech in terms of reconstruction accuracy (Figure 6-2).

An example of unconscious attention

The results obtained here unambiguously demonstrate the preservation of attentional processes during sleep. Indeed, the meaningful stream was better reconstructed that the meaningless pseudo-speech in wakefulness and NREM sleep (Figure 6-2) although both streams were equally reconstructed when presented in isolation during wakefulness (Fig. S1). However the respective influence of top-down or bottom-up attentional processes (Fritz et al., 2007) cannot be here disentangled. Further investigations are needed to determine whether the real speech was enhanced because of task-instructions (active process) or due to a natural attraction to the real-speech (passive process).

Nevertheless and whatever the exact mechanisms at play, we show here for the first time that the brain can focus on a particular source of information during sleep, in a state of reduced if not absent consciousness (Yuval Nir et al., 2013). These results are concordant with the studies showing a dissociation between attention and consciousness (Koch and Tsuchiya, 2007). This work is also concordant with studies showing that information can be integrated unconsciously (Mudrik et al., 2014). Interestingly, we similarly show here that such unconscious integration of information is both possible but more short-lived than during wakefulness. This could be due to the de-activation of the pre-frontal cortex during sleep (Muzur et al., 2002). Indeed pre-frontal areas are instrumental in maintaining an integrative processing of information (Dehaene et al., 2006). In addition, the loss of

cortico-cortical connectivity associated to NREM sleep could explain the difficulty in maintaining attention over long periods of time (Tononi and Massimini, 2008). Overall, these results could provide a novel approach to the study of attention and its relationship with consciousness.

Supplemental Figures

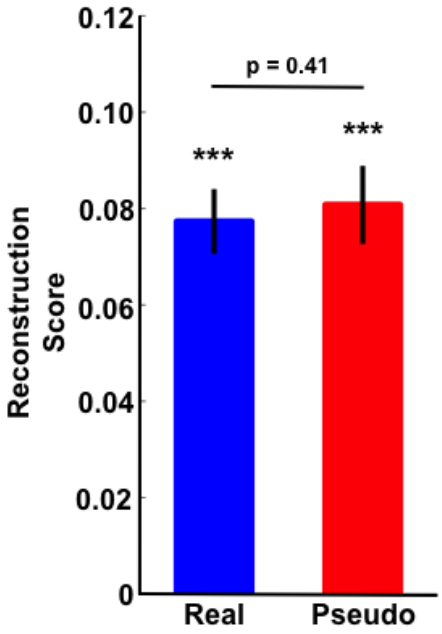

Figure S 6-1 Stimulus reconstruction is not biased by speech category

Using the training trials (real or pseudo speech presented in isolation), we reconstructed both real and pseudo streams using a leave-one-out approach (see Methods). Reconstruction scores averaged across participants are displayed here. Error-bars denote the standard error of the mean across participants (N=24). Both streams were successfully reconstructed (t-tests against 0: both $p<0.001$). Crucially, there was no difference in the reconstruction scores between the real and pseudo speech (paired t-test: $p=0.41$).

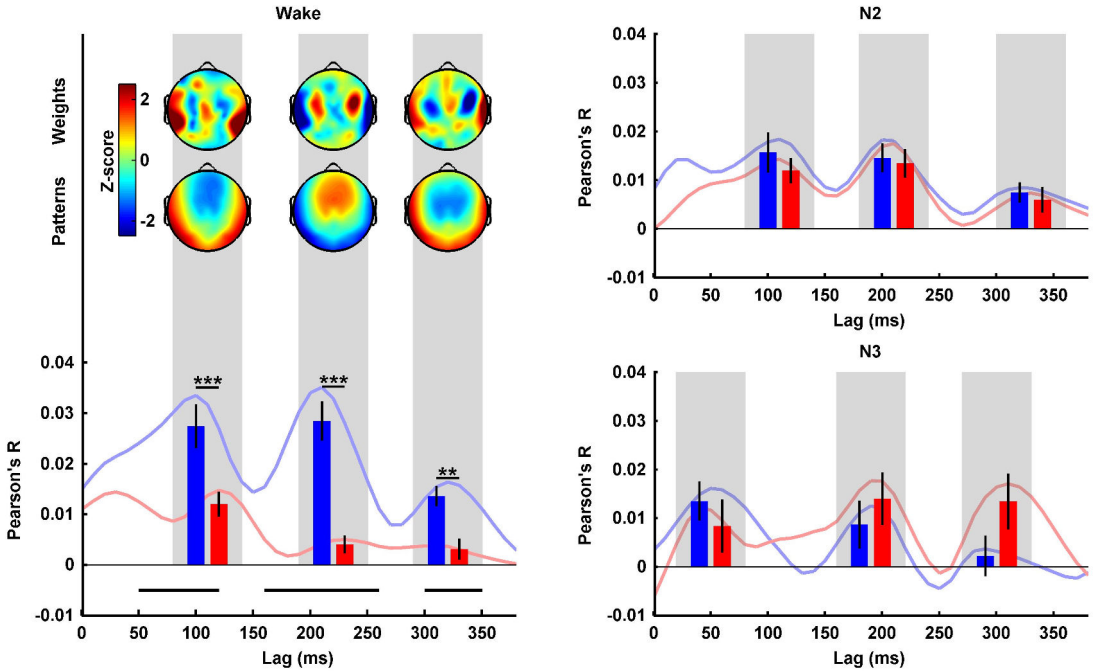

Figure S 6-2 Spatio-temporal integration of acoustic information (2nd half of trials)

Same information as displayed in Figure 6-3 (see legends for details) but for the second half of the trials. The scalp topographies of the patterns and weights are extracted on the training dataset and are therefore identical as in Figure 6-3.

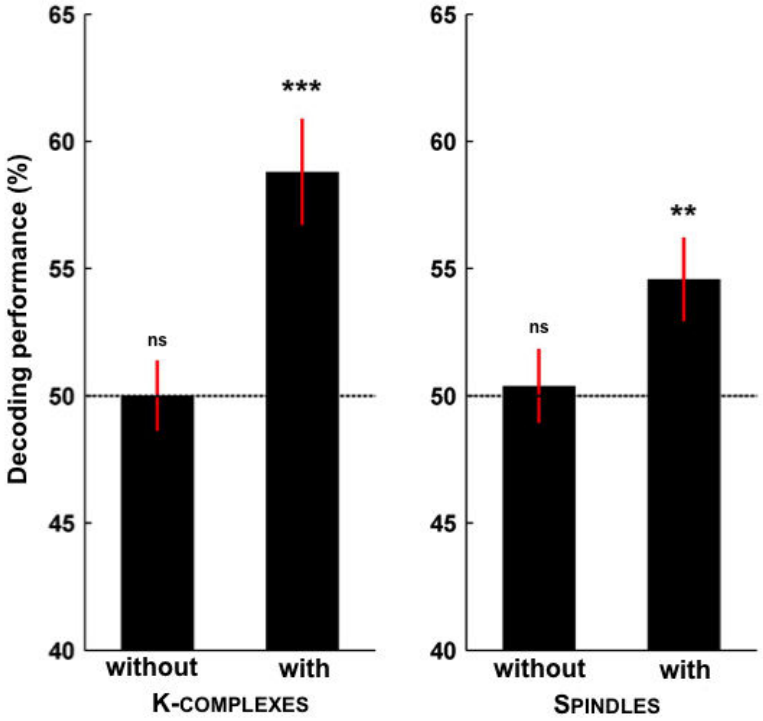

Figure S 6-3 Impact of K-complexes and sleep spindles on the decoding of attention

Right: Decoding accuracy averaged across participants for 10-s-long epochs showing (right) or not (left) a K-complex. Left: Decoding accuracy for epochs showing or not a sleep spindle. Error-bars denote the standard error of the mean computed across participants (N=24). Stars atop bars show the significance level of the t-test comparing decoding accuracy with the chance level (50%): ***, $p<0.005$; **, $p<0.01$; *, $p<0.05$; ns, $p>0.05$. Note that the presence of K-complexes and sleep spindles correlated with higher (and significant) decoding accuracies. However, since K-complexes and sleep-spindles are temporally associated (Molle et al., 2002), a mixed-model taking into account the presence of K-complexes and sleep spindles showed a significant effect of K-complexes on decoding performance ($p=7.10^{-6}$) but not of sleep spindles ($p=0.85$).

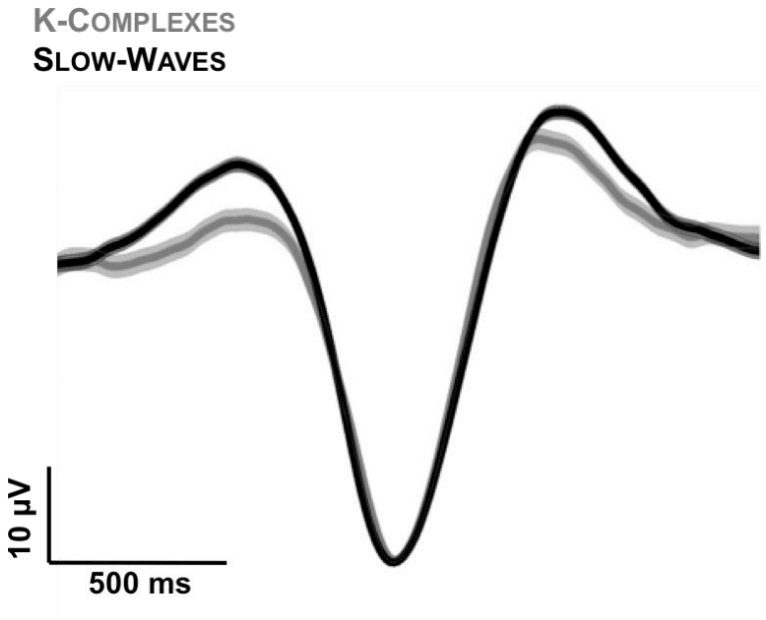

Figure S 6-4 Temporal profile of K-complexes and Slow-Waves

The temporal profiles of slow-oscillations detected in NREM2 (here referred as K-complexes, gray curve) and in NREM3 (here referred as slow-waves, black curve) are superimposed. Slow-oscillations were aligned to their down-state (for time and voltage). Shaded areas denote the standard error of the mean across slow-oscillations (N=1,079 and 2,644 for K-complexes and slow-waves respectively). Note the characteristic asymmetric profile of K-complexes compared to Slow-Waves.

	Wake	NREM	Not Heard
Performance (%)	46.80 (3.26)	24.44 (3.12)	22.14 (1.79)
U-test p-value	0.00	0.9	0.12

Table S 6-1 Performance in the post-nap questionnaire on stories heard during wakefulness (right), NREM sleep (NREM2 and NREM3, middle) compared to unheard stories (right). Numbers show the average accuracy across participants (N=24, 24 and 16 resp., standard error of the mean is indicated in the brackets). The bottom line shows the corresponding p-values of a Mann-Whitney U-test comparing the performance to the theoretical chance level (25%).

Chapter 3: Learning during sleep

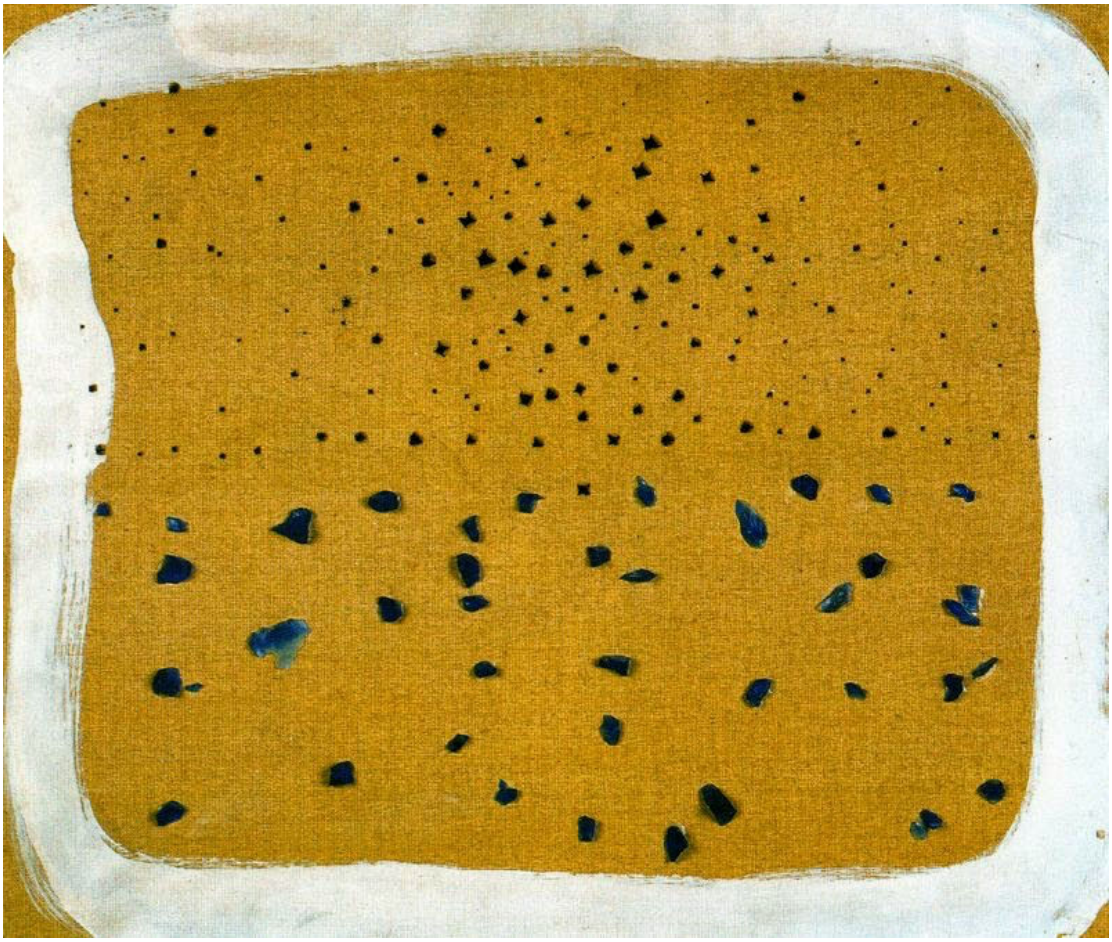

Concetto Spaziale
Lucio Fontana (1954)

Note on contributions:

Study 7: Sid Kouider and I designed the experiment. I collected and analyzed the data.

Study 8: Sid Kouider, Daniel Pressnitzer, Trevor Agus and I designed the experiment. I collected and analyzed the data.

Study 9: Sid Kouider and I designed the experiment. I collected and analyzed the data.

Study 7:
Implicit memory for words heard during sleep

Thomas Andrillon[1, 2] and Sid Kouider[1]

[1] *Brain and Consciousness Group,*
École Normale Supérieure
Paris, France

[2] *École Doctorale Cerveau Cognition Comportement,*
Université Pierre et Marie Curie
Paris, France

Summary

When we fall asleep, our awareness of the surrounding world fades. Yet, the sleeping brain is far from being dormant and recent research unraveled the preservation of complex sensory processing during sleep. In wakefulness, such processes usually lead to the formation of long-term memory traces, being it implicit or explicit. We examined here the consequences upon awakening of the processing of sensory information at a high level of representation during sleep. Participants were presented with words and pseudo-words during wake and sleep, which they were instructed to classify through left and right hand responses. An analysis of the electroencephalographic (EEG) signal revealed the preservation of lateralized motor activations in response to sounds, suggesting that stimuli were correctly categorized during sleep. Yet, upon awakening, participants did not explicitly remember words processed during sleep and failed to distinguish them from new words (old/new recognition test). However, both behavioral and EEG data indicate the presence of an implicit memory trace for words presented during sleep. In addition, the underlying neural signature of such implicit memories markedly differed from the explicit memories formed during wakefulness, in line with dual-process accounts of two independent systems for explicit and implicit memories. Thus, our results suggest that new memories can be formed in the absence of awareness and provide a novel approach to explore the neural implementation of explicit and implicit mnesic traces.

Introduction

Sleepers are not disconnected from their environment during sleep. On the contrary, the sleeping brain can encode sensory information (Issa and Wang, 2008; Y. Nir et al., 2013), recognize salient or familiar sounds such as a person's own name (Perrin et al., 1999), process sounds in their context and detect the violation of simple rules (oddball paradigm; (Czisch et al., 2009; Ruby et al., 2008; Strauss et al., 2015). Sleepers can even process sensory information at a high-level of representation such as the semantic level (Bastuji et al., 2002; Brualla et al., 1998; Ibanez et al., 2006). We recently showed that the sleeping brain could even build upon sensory processes and use semantic information to make decisions (Kouider et al., 2014). But can such processes trigger long-term memory? Indeed, when we are awake, experience constantly imprints on the brain. From pure noise (Andrillon et al., 2015a) to more complex types of sensory inputs such as words (Pulvermüller et al., 2001), processing a given piece of information, even passively, leads to the formation of a new memory trace or the strengthening of an existing one (Kolb and Whishaw, 1998).

Exploring the sleeping brain's ability to learn has been a long-lasting scientific quest (Emmons and Simon, 1956) but positive results are scarce. Until recently, only some forms of learning independent from hippocampal structures had been evidenced (Hennevin et al., 1995; Ikeda and Morotomi, 1996; Maho and Bloch, 1992). This contrasts with the abundance of results showing the crucial role of sleep in promoting memory consolidation (Rasch and Born, 2013) as well as studies showing how external stimulations can act upon this consolidation (Oudiette and Paller, 2013). To explain this discrepancy, the main theories on the role of sleep in memory consolidation have proposed that consolidation mechanisms would directly or indirectly prevent the formation of new memories (Diekelmann and Born, 2010; Hasselmo, 1999; Tononi and Cirelli, 2014). It has been proposed that memory systems (such as hippocampal structures) get disconnected from sensory circuits so as to prevent external input from interfering with the consolidation process (Rasch and Born, 2013). Alternatively, changes in neuromodulation occurring during sleep could impair synaptic plasticity itself and therefore the encoding of new memories (Hennevin et al., 2007; Tononi and Cirelli, 2014). Yet, recent studies have shown that even hippocampal-dependent forms of learning were possible during sleep (Arzi et al., 2012; de Lavilléon et al., 2015), putting the opposition between memory consolidation and formation into question.

To investigate brain's ability to form memory traces during sleep, we relied on the classical old/new paradigm. For more than a century (Ebbinghaus, 1885), this approach has been used to probe recognition memory, i.e. the ability to recognize elements previously encountered. Recognition is a form of long-term and declarative memory relying on the medio-temporal lobe, which includes the hippocampus (Eichenbaum et al., 2007; Squire et al., 2007). Accordingly, participants with bilateral lesions in these areas show strong deficits in recognition memory (Reed and Squire, 1997). More precisely, the ability to recognize a previously encountered item is thought to benefit from two separate systems: an explicit episodic memory (i.e. 'remembering') and an implicit sense of familiarity (i.e. 'knowing') (Tulving, 1985). However, it is unclear whether these two types of information are implemented through independent neural circuits (Aggleton and Brown, 2006; Manns et al., 2003; Squire et al., 2007). Part of the difficulty in disentangling these two forms of memory stems from the difficulty to separate them at the behavioral level (Malmberg, 2008). Indeed, both implicit and explicit memories contribute to item recognition. One potential solution consists in contrasting neural

correlates of recollection as a function of whether participants are aware or unaware of learning a specific content (Rosenthal et al., 2010). Sleep, in this regard, represents a unique tool to explore the formation of memories in the absence of awareness.

Here we investigated the formation of memory traces for words heard during Non-Rapid Eye-Movement (NREM) sleep. We used a paradigm in which participants were exposed to words and pseudo-words (phonologically valid but meaningless words) during wakefulness and sleep (Kouider et al., 2014). To maximize the probability that participants processed acoustic information during sleep, we asked participants to perform a task on these stimuli while falling asleep. Subjects were instructed to indicate, each time a stimulus was played, whether it was a real or an invented word (lexical decision task). The task-set and stimuli presentation were held constant throughout the experiment so that participants could automatize the task while being awake and pursue it after falling asleep. Importantly, novel, unpracticed items were presented exclusively during sleep (i.e., words which were not presented during the wake session), allowing to confirm interpretations in terms of lexico-semantic processing rather that stimulus-response mapping (Abrams and Greenwald, 2000). In a previous article, we have shown the maintenance of EEG indexes of motor lateralization after stimuli onset and in accordance with the expected side of response, showing that participants continue to classify stimuli while asleep (Kouider et al., 2014). A lexical decision task was used to prompt participants to process items at a high level of representation, as processing depth is known to influence recognition memory (Craik and Tulving, 1975). Upon awakening, participants recognized items presented during wakefulness with high accuracy. However, despite having categorized the novel items while sleeping, participants did not explicitly remember these words. We rather unraveled the presence of implicit mnesic traces for words heard during sleep by relying on more-in-depth analyses of behavioral and EEG data. Interestingly, the EEG correlates of memory for words presented during sleep markedly differed from those of the words presented in wakefulness, which were explicitly recognized. These results reveal not only that sleepers can form new memories while sleeping but also pinpoint critical differences in the neural implementation of explicit and implicit memories.

Material and Methods

Participants

Twenty-two (22) right-handed French speakers (16 females, age ranging from 20 to 28 years) without history of neurological or sleep disorders and with self-reported normal hearing participated in this study. Subjects had been selected based on their responses to the Epworth Sleepiness Scale (ESS) in order to target individuals who could fall asleep in a noisy, unfamiliar environment. Recruited participants had high but non-abnormal EES scores (11.95 ± 0.62, mean ± SEM, standard error of the mean). The day of the recordings, participants were moderately sleep deprived (30% less than their usual sleep time) and asked to avoid all exciting substances. This protocol has been approved by the local ethical committee (Conseil d'évaluation éthique pour les recherches en santé, Paris, France).

Stimuli

The auditory material consisted of 108 pairs of words and pseudo-words selected from the Lexique database (New et al., 2004). These 216 items were divided in three lists of 72 stimuli matched for their frequency, duration and consonant-vowel structures (half CVC monosyllabic and half CV-CV disyllabic). Pseudo-words did not violate the pronunciation rules of the French language. Words were uttered by a male native French speaker and digitized at 44,100 Hz. The attribution of the three lists to either the wake period, the sleep period or the new list in the old/new recognition task was counterbalanced across participants. Stimuli were presented at about 50dB through loud speakers using the Psychtoolbox extension (Brainard, 1997) for Matlab (MathWorks Inc. Natick, MA, USA).

Experimental Procedure

Participants first performed a lexical decision task on the spoken words presented every 9 seconds (nap session). Participants were instructed to indicate whether the spoken words existed in the French lexicon or not using response-handles placed in their left and right hands. The mapping between stimulus category (real or invented word) and the associated response side (left or right) was counterbalanced across participants. Participants initially performed this task for about 10 minutes with the instruction to remain awake and responsive. All the items of the wake list were played once during this initial part to ensure that all items of the wake list were processed at least once under optimal conditions. Participants were then placed in a reclining chair, in a dark, electrically and acoustically shielded cabin. They were asked to keep their eyelids closed. Participants were authorized to fall asleep but were instructed to keep responding to auditory stimuli as long as they were awake, and to resume responding in case of an awakening.

Subjects' vigilance state was assessed online using polysomnographic and behavioral data (see below). A novel list of words and pseudo-words was presented to participants when they entered the NREM2 stages (i.e. after the first spontaneous K-complex or sleep

spindle). The sleep list was played in NREM2 and NREM3 stages. However, only 11 participants entered the NREM3 stage. Participants were switched back to the wake list whenever they showed signs of arousal. This online sleep scoring was confirmed offline using standard guidelines (Iber et al., 2007). Trials associated with arousals (button presses or increase in low-amplitude fast rhythms such as alpha oscillations or oscillations above 16Hz for more than 3 seconds and stable for at least 10 seconds) and micro-arousals (less than 3 seconds) were carefully marked and corresponding items were discarded from further analyses. Indeed, our goal was here to analyze the presence of mnesic traces to words processed during sleep and while sleep was preserved. After offline confirmation of the sleep scoring, 4 participants could not be included in the sleep analyses (Figure 7-1b) due to a low number of trials scored as sleep. One additional participant had less than 20 novel words presented during sleep and was discarded from the memory test analyses. Overall, the 17 participants included in these analyses (Fig. 2-5) heard each item of the wake list 4.8 ± 0.3 times on average and each item of the sleep list 2.1 ± 0.2 times on average.

Upon awakening, after the nap session, participants were allowed a few minutes to dissipate sleep inertia and then underwent a memory test. Words (but not the pseudo-words) previously presented during the nap session were played once to participants (same voice, volume and experimental set-up) along with novel items (new list) and in random order. Participants were first asked to indicate whether they remembered having heard the word during the nap session ('old' or 'new'). They were then asked to indicate their confidence in their 'old' vs. 'new' response by using a scale going from 1 ('I am not sure at all') to 7 ('I am perfectly sure'). Responses were provided with a keyboard and without time pressure. Participants were instructed to keep their eyes closed and to remain still during the presentation of the words in order to minimize movement-related artifacts in the EEG signal. The memory-test was self-paced.

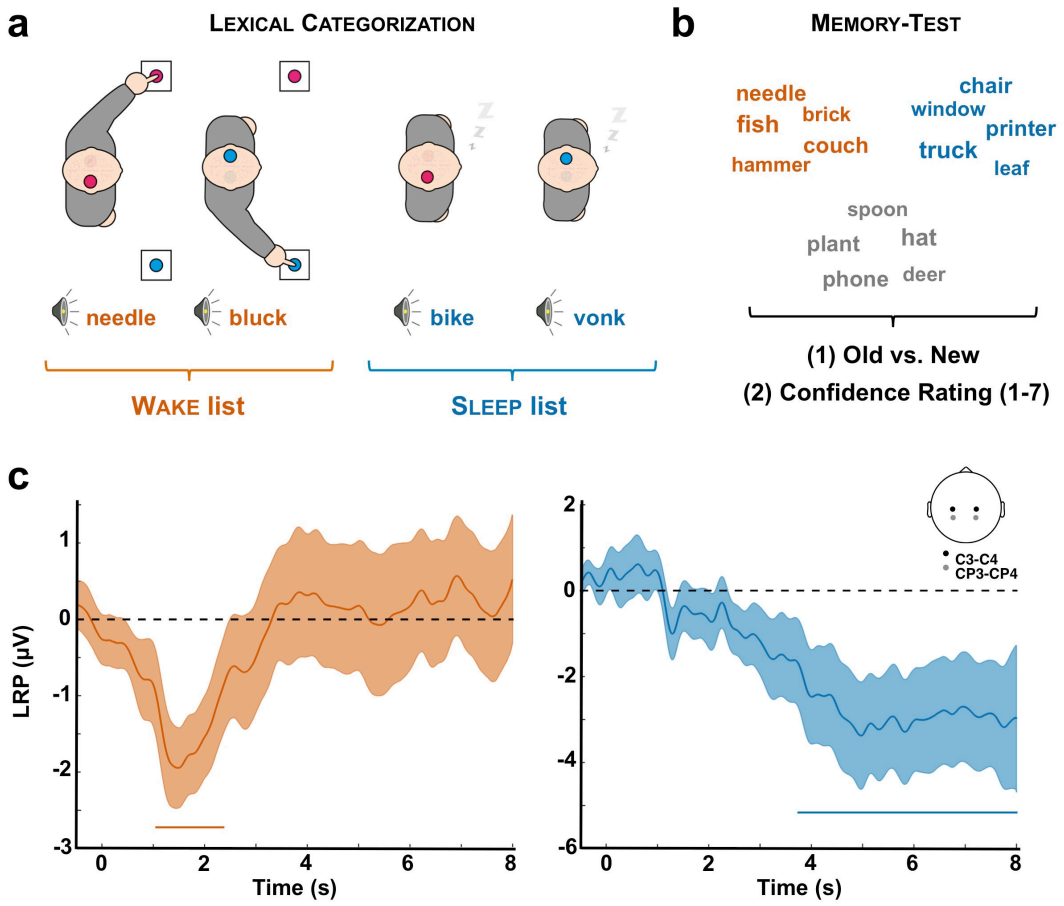

Figure 7-1 Experimental procedure and evidences for complex information processing during sleep

(a) Lexical categorization task: participants (N=22) were asked to classify spoken words and pseudo-words while falling asleep (daytime nap). Each category (word or pseudo-word) was associated to a response side (left or right). Once asleep (see Methods for criterion) and unknown to participants, novel words and pseudo-words were presented to participants (sleep list). Importantly, the initial set of stimuli (wake list) was played again to participants whenever they awoke in order to present the elements of the sleep list during sleep only. (b) Memory test: upon awakening, participants (N=17) underwent a memory test during which the words presented during the nap session (red: wake list; blue: sleep list) were played along new words (gray: new list). For each word, participants were asked to indicate whether they remembered hearing the word during the nap session (old vs. new recognition test). They were then instructed to estimate their confidence in their old vs. new response using a scale from 1 (not sure at all) to 7 (absolutely sure). (c) Lateralized Readiness Potentials (LRPs): during the nap session, we computed LRPs during wake (red, left) and sleep (blue, right) to determine whether participants performed the lexical categorization task even when unresponsive. The LRP was computed over right and left central electrodes (see inset and Methods) and averaged across participants. Shaded areas denote the standard error of the mean across participants (N=18). Horizontal bars show the significant clusters ($p_{cluster}<0.05$). The LRP determines whether neural activity is lateralized in respect to the expected side of response. A LRP was preserved, albeit delayed, from wakefulness to sleep.

Behavioral analyses

Using participants' responses recorded in the memory-test, we computed the average percentage of 'old' and 'new' responses for the different lists (1st order responses, Figure 7-2a) as well as the average confidence rating of these 'old' and 'new' responses (2nd order responses, Figure 7-2b) across participants. Confidence ratings were normalized by subtracting the average rating computed across all trials for a given participant in order to compensate for biases in the way participants scaled their own confidence. For the 1st order response, we also computed a sensitivity index: the d' (Macmillan, 2005). The d' provides an unbiased estimate of participants' ability to discriminate two conditions (here old words (wake or sleep list) vs. new ones). The d' was computed as follows:

$$d' = z(Hit) - z(FA)$$

where z(x) corresponds to the z-score for proportion x; Hit corresponds to the proportion of correct responses for the words heard during the nap session (either wake or sleep list) and FA (False Alarms) corresponds to the proportions of incorrect responses for the novel words.

To assess participants' performance on the 1st and 2nd order responses, we also computed Receiver Operating Characteristic (ROC) curves (Figure 7-2d, (Macmillan, 2005)). Type-I ROC curves were computed for each participant using the 1st order responses. For each confidence level (from 1 to 7), we computed the average proportion of hits ('old' response when an old item was presented) and of false alarms ('old' response when a novel item was presented). Figure 7-2d (left) shows the type-I ROC curve averaged across participants. Type-II ROC curves were computed for each participants using 2nd order responses (Fleming et al., 2010; Macmillan, 2005). Each confidence level was analyzed in turn (from 1 to 7): for the confidence level *n*, 2nd order hits correspond to trials in which participants scored their confidence higher or equal to *n* while being correct whereas false alarms correspond to trials in which participants scored their confidence higher or equal to *n* while being incorrect. For each confidence level, we computed the average proportions of 2nd order hits and false alarms to build the type-II ROC curves. Figure 7-2d (right) shows the type-II ROC curve averaged across participants.

We also extracted the area under the curves (AUC) for the type-I and type-II ROC curves for each participant using the 'polyarea' function in Matlab. AUC were compared with the AUC under the bisector line (0.5). Indeed, a type-I or type-II ROC curve overlapping the bisector line characterizes at-chance 1st or 2nd order performance, respectively. Leftward deviations from the bisector line characterize above-chance performance and rightward deviations below-chance performance. One participant did not have any 2nd order false alarm. Its AUC was thus put to 1 (perfect performance). Excluding this participant did not change the outcome of the statistical analyses performed on type-II ROC curves.

EEG recordings

Participants were equipped for polysomnographic recordings (electroencephalography (EEG), electromyography (EMG) and electrooculography (EOG)) using a 65-channels EEG cap and additional sensors placed on participants' skin (Electrical Geodesic Inc.).

Data were acquired at 250 Hz and EEG derivations were referenced online to Cz. EOG were extracted by using electrodes placed close to the right and left canthi and referenced to the opposite mastoids. Three EMG derivations were recorded: on the chin and on the right and left abductor pollicis brevis (thumb flexor muscle) to record EMG activity associated to hand responses. EEG, EMG and EOG data were continuously recorded in both the nap and the ensuing memory-test.

Lateralized Readiness Potentials (LRPs)

The EEG data acquired during the nap had been previously analyzed. Details can be found in (Kouider et al., 2014). Briefly, continuous EEG data were re-referenced to the average mastoids and high-pass filtered above 0.1 Hz (two-pass Butterworth filter at the 5th order). After a first epoching on large temporal windows centered on stimuli onset ([-16, 16]s), EEG data were low-pass filtered below 30 Hz (two-pass Butterworth filter at the 5th order), epoched from -2 to 8s and corrected for baseline activity ([-2, 0]s). Trials passing an absolute threshold of 250 μV were rejected from further analyses. LRP were computed by subtracting the EEG signal over the right (electrodes 50 and 46 in the EGI HCGSN-64 v1 net, equivalent to C4 and CP4 in the 10/20 montage) and left (electrodes 20 and 26 in the EGI HCGSN-64 v1 net, equivalent to C3 and CP3 in the 10/20 montage) electrodes:

$$LRP = \frac{(C3/CP3_{right-hand} - C3/CP3_{left-hand}) + (C4/CP4_{left-hand} - C4/CP4_{right-hand})}{2}$$

LRP quantifies the lateralization of brain activity toward the expected side of response (Smulders et al., 2012). Since novel words were presented during sleep, and since the decision to prepare for the right or left responses was based on stimulus category, the observation of an LRP also implies that auditory information was processed at a high (i.e., lexico-semantic) level of representation.

Event-Related Potentials (ERPs)

Upon awakening, participants underwent a memory-test during which EEG data were recorded along participants' behavioral responses. We computed ERPs time-locked to stimuli onset for the three lists (wake, sleep and novel words). EEG data were re-referenced to the averaged mastoids and high-pass filtered above 0.1 Hz (two-pass Butterworth filter at the 5th order). The EEG signal was then epoched on temporal windows time-locked to stimulus onset ([-4, 4] s) and low-pass filtered below 30 Hz (two-pass Butterworth filter at the 5th order). Next, EEG data were epoched from -0.2 to 1.5 s around stimulus onset and corrected for baseline activity ([-0.2 0] s). Finally, EEG data were de-noised using the joint joint decorrelation approach by optimizing the repeatability across trials (de Cheveigné and Parra, 2014). Briefly, a principal component analysis (PCA) was applied to the average ERP computed across all trials and for a given participant (i.e. regardless of the stimulus list). Components were sorted according to their participation to the average ERP. The first 10 components, characterized by the strongest mean effect relative to overall variability, were used as a bias filter on the single-trial EEG data. EEG data were then averaged for all the trials of a given list and for each participant. Figure 7-3 shows the corresponding ERP traces averaged across participants.

Differences were observed when comparing the wake and new lists ('P3' and 'Late Negativity' effects) and the sleep and new lists ('Early Negativity' effect).

Decoding

For each participant and EEG sensor, we extracted the signal averaged over the 'P3' cluster (wake vs. new comparison) for each and every trial. The cluster was defined as a [0.73, 0.86] ms window post-stimulus onset on parieto-occipital electrodes (electrodes showing the P3 effect: $p<0.05$ when comparing the wake and new lists across participants). A leave-one-out approach was performed at the subject-level. For all subjects but one, the cluster data were z-scored for each channel and trials, and aggregated across participants. The corresponding values (training set) were then used to fit a linear regression classifier that was then applied to the remaining participant (test set) in order to predict trials' category (wake or new). This procedure was iterated until all subjects had been included in the test set. The predictions were compared to the actual categories and a d' was computed for each participant (Figure 7-4). The same procedure was applied to the sleep vs. new cluster (Figure 7-3, [0.49, 0.63] ms post-stimulus onset over centro-parietal electrodes).

Time-frequency decomposition

We computed the time-frequency decomposition of the EEG signal in response to sounds. To do so, a Fast Fourier Transform (FFT) was applied to the EEG signal on band-passed de-noised stimulus-locked data ([0.1, 40] Hz, [-2, 2] s) using a window of 800ms. The average power was computed across all trials (Figure 7-5 top) or across all trials for a given list (Figure 7-5 bottom) and expressed as the log ratio of the power at a given time and frequency over the power average over the baseline for the corresponding frequency. We later focused on the alpha band ([8, 12] Hz) by averaging the power within the corresponding frequency range.

Statistics

Parametric statistics were used here (Student t-tests to compare conditions or a condition with chance-level, ANOVA for analyses of variance). To correct for multiple comparisons in time-plots and time-frequency-plots, we used a principled approach called 'cluster permutation' (Maris and Oostenveld, 2007). Each cluster was constituted by the samples (in one dimension (time) or two dimensions (time and frequency)) that consecutively passed a specified threshold (for time-plots: $p<0.1$; for time-frequency-plots: $p<0.01$). It has been shown that the rate of type-I errors (false positives) was immune to the choice of this cluster-defining threshold (Maris and Oostenveld, 2007). The cluster statistics were chosen as the sum of the t-values of all the samples within the cluster. Then, we compared the cluster statistics of each cluster with the maximum cluster statistics of 1000 random permutations (Monte-Carlo method). From this comparison, we obtained a Monte-Carlo p-value: the cluster p-value ($p_{cluster}$). When examining the presence of mnesic traces in the sleep lists, we obtained several null results. To check the informativeness of these null results, we computed Bayes Factors

given the effect observed in wakefulness (Dienes, 2014). Bayes factors allowed assessing whether a null result is in favor of the null hypothesis or reflects data's lack of sensitivity. The larger the Bayes Factor, the more the data is in favor of the null hypothesis.

Results

In a recent publication, we have shown that sleepers can maintain complex and flexible processing of sensory information during NREM sleep (Kouider et al., 2014). Such feat was not accompanied by any explicit memory, contrasting with what happens when we are awake. Here we investigated the presence of implicit mnesic traces for words heard during sleep by relying on more-in-depth analyses of behavioral and EEG data.

Memory traces for words heard while awake

We first checked whether the list category (wake, sleep or new) and the list itself (i.e. which list was defined as the wake, sleep or new list for a given participant) had an effect on correctness (1st order response) and confidence rating (2nd order response). Using ANOVAs, we observed, for both correctness and confidence, an effect of the list category ($F(2)=80.5$ and $F(2)=5.67$, $p=4.10^{-15}$ and $p=0.007$ resp.) but not of the list itself ($F(2)=2.39$ and $F(2)=0.03$, $p=0.10$ and $p=0.97$ resp.). There was no significant interaction ($F(4)=0.39$ and $F(4)=0.60$, $p=0.82$ and $p=0.66$ resp.).

Words presented during wakefulness were explicitly recognized as 'old' words with a high degree of accuracy (83 ± 4%, Figure 7-2a). Such performance led to a high d' index when contrasting these wake items with novel ones (t-test comparing with 0, $t(16)=6.62$, $p=6.10^{-6}$). For the wake list still, participants attributed high levels of confidence when they were correctly recognizing an item (6.2 ± 0.17 over 7) and low levels of confidence when missing to identify an item previously heard (3.7 ± 0.40 over 7, see Figure 7-2b for normalized values). Such pattern of results led to type-I and type-II ROC curves clearly distinct from the bisector line for the wake list. Accordingly, the wake list AUCs were highly significant when compared to bisector's AUC (t-test: $t(16)=11.2$, $p=6.10^{-9}$ and $t(16)=10.5$, $p=1.10^{-8}$ for the type-I and type-II ROC curves resp.). The type-I ROC curve in particular had an asymmetric shape that is typical of strong and explicit memory traces (Squire et al., 2007). Overall, participants were unsurprisingly able to accurately and confidently discriminate items heard while awake from new ones.

These behavioral effects were accompanied by differences in the ERP between the wake and new lists (Figure 7-3). Namely, a positivity over occipito-parietal electrodes was observed around 700 ms when comparing the wake and new lists across participant (cluster on Pz: [0.72, 0.86] s, $p_{cluster}=0.026$) in accordance with previously published results (Kayser et al., 2007; Rugg et al., 1998; Voss and Paller, 2007). This difference is termed the 'P3 effect' in the literature. Another negativity, maximal over parietal electrodes, was also observed later in time (cluster on Pz: [1.17, 1.40] s, $p_{cluster}=0.003$) and is termed 'late negativity' in the literature (Kayser et al., 2007).

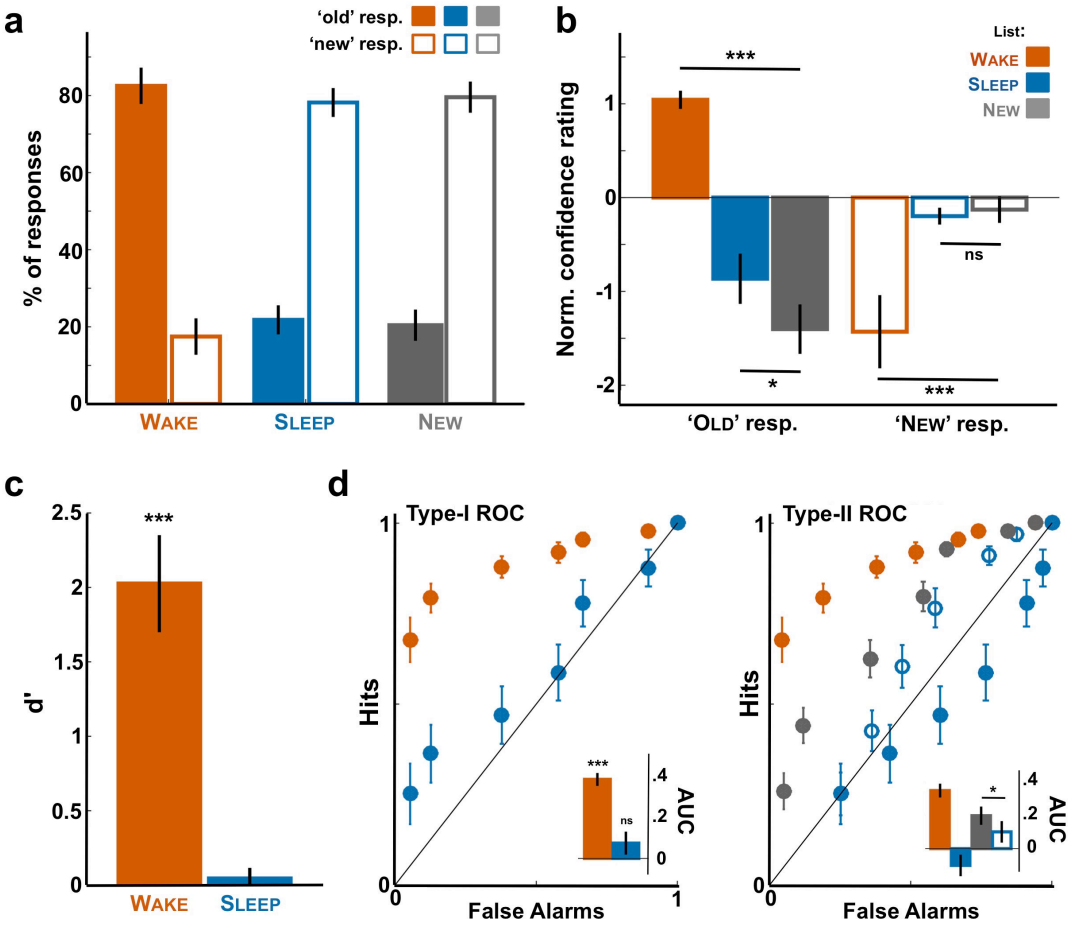

Figure 7-2 First and second-order responses in the recognition test

Behavioral results for the memory test. (a) Proportion of 'old' and 'new' responses for the wake (red), sleep (blue) and new (gray) lists (1st order responses). Proportions are averaged across participants (N=17) after excluding items heard around arousals or micro-arousals for the sleep list. Note that participants responded to sleep items as if they were new. (b) Confidence rating associated to the old and new responses for the wake, sleep and new lists (2nd order responses averaged across participants). Ratings were normalized by subtracting for each participant the average confidence rating. Note the increase in confidence for sleep items in comparison to new items when participants categorized them as old. (c) Sensitivity index d' averaged across participants for the old vs. new discrimination and computed for the wake and sleep lists separately. As in panel a, the null d' reveals participants failure to distinguish sleep and new items in their 1st order responses. (d) Type-I and type-II ROC (Receiver Operating Characteristic) curves computed for the 1st order (old vs. new, left) or 2nd order (confidence rating, right) responses. Inset shows the area under the curves (AUC) computed for the different ROC curves and averaged across participants (0.5: area under the bisector line). In all subpanels, error-bars denote the standard error of the mean across participant. Stars atop bars denote the significance levels when comparing with 0 (t-tests across participants; ***: $p<0.005$, **: $p<0.01$, *: $p<0.05$, ns: $p>0.05$). Stars between bars show the paired comparison between bars.

Implicit memory traces for words heard during sleep in the absence of explicit recognition

What about sleep? First of all, and as previously reported (Kouider et al., 2014), participants did not explicitly recognize the items presented during NREM sleep despite having processed them at a high-level of representation (Figure 7-1c). Indeed, the pattern of 'old/new' responses was strikingly similar to the new list (Figure 7-2a) leading to null d' (t-test comparison to 0: $t(16)=0.73$, $p=0.25$). To determine whether this null result was informative and not reflecting data insensitiveness, we computed the Bayes Factor associated to the sleep effect (on d') when considering the effect on the wake list. A Bayes Factor superior to 1000 indicates very strong evidence for the null hypothesis (Kass and Raftery, 1995). In line with the null d' for the sleep list, the type-I ROC curve for sleep items does not show a significant deviation from the bisector line (Figure 7-2d, left; t-test comparison to 0.5: $t(16)=1.53$, $p=0.14$; Bayes factor>1000).

However, when examining second-order responses we observed that the sleep list did not lead this time to identical responses as for the new list (Figure 7-2b). Indeed, participants were more confident when responding that a sleep item had been previously presented compared to a genuinely novel word (paired t-test: $t(15)=2.3$, $p=0.036$). This difference suggests the presence of an implicit mnesic trace for words heard during sleep, positively impacting confidence. However, despite this slight increase in performance, participants showed rather low confidence in determining that an item from the sleep list was old, which results in a trend for a below-chance type-II ROC curve (AUC=0.40 ± 0.058, t-test comparing with 0.5: $t(16)=-1.8$, $p=0.089$). When considering type-II ROC curves, the sleep and new lists drastically differ (the former is below the bisector line, the later above). This is due to the way these curves are computed and the fact that an 'old' response is considered as being correct for the sleep list and 'incorrect' for the new list. However, when re-computing the ROC curves while considering the 'old' response as being incorrect for the sleep list (i.e. when taking the point of view of the participants who did not have any explicit recollection of the sleep items), the sleep (unfilled blue dots) and new type-II ROC curves still differ, with the sleep list showing a smaller AUC (paired t-test comparing AUCs: $t(16)=-2.36$, $p=0.031$). Overall, 2nd order performance revealed the presence of an implicit memory trace, albeit weak, for sleep items in the absence of explicit recognition.

EEG evidence for implicit memory traces for words heard during sleep

Differences between the sleep list and the novel list were also observed when examining the corresponding ERPs (Figure 7-3). A centro-parietal negativity ('early negativity') was observed when comparing the sleep and novel lists (cluster on Pz: [0.48, 0.62] s, $p=0.006$; on Cz: [0.49 0.63]s, $p=0.044$), suggesting that the two lists were not processed identically. On the other hand, the P3 and the Late Negativity effects were not observed when comparing the sleep list with the new list, suggesting that the sleep list was not processed as the wake list. Interestingly, the negativity observed for the sleep lists overlapped spatially and temporally with the P3 positivity.

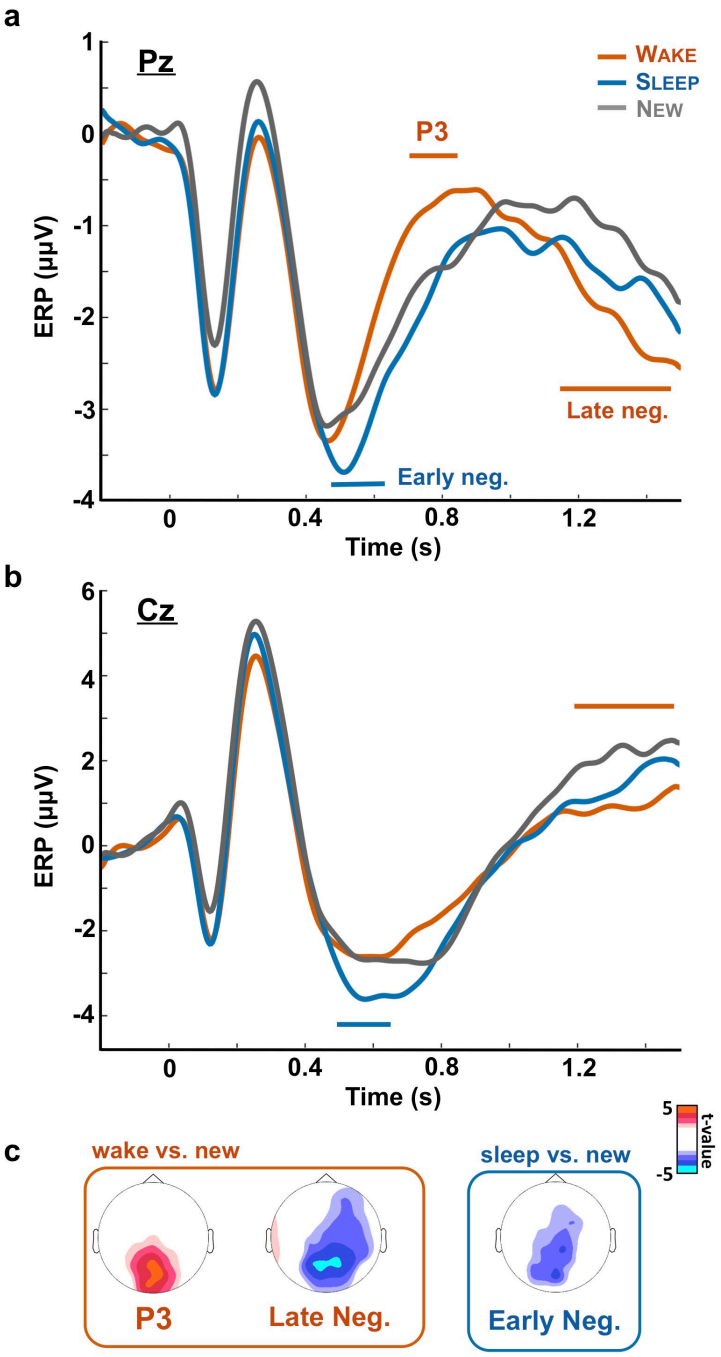

Figure 7-3 Event-Related Potentials to wake, sleep and new words

The EEG signal time-locked to sound onset was averaged across participants (N=17) for the three lists separately (red: wake; blue: sleep; gray: new lists). Panel a shows the event-related potentials (ERPs) for electrode Pz and panel b for electrode Cz. Horizontal bars show the significant clusters for the comparison between the wake list (red bars) or the sleep list (blue bars) and the new list ($p_{cluster}<0.05$). The scalp topographies corresponding to the different clusters are shown on panel c (t-values computed by comparing the signal averaged over the cluster time-window between the wake (or sleep) and new list, non significant t-values (p-value>0.05) were set to 0). Note the classical posterior positivity when comparing wake (explicitly remembered) and new items ('P3') as well as the 'late negativity'. For sleep items, an opposite negativity ('early negativity') was observed in lieu of a positivity and despite the absence of explicit recognition.

We further checked whether the differences observed in the ERP waveforms could allow us to predict stimuli category. To do so, we extracted the average voltage over the P3 cluster and the 'early negativity'. For each participant, we trained and tested a classifier using a leave-one-out approach (see Methods) to predict stimuli category based on the EEG signal. Figure 7-4 shows that such procedure led to above-chance levels discrimination for the wake vs. new lists discrimination when using the P3 cluster ($t(16)=5.21$, $p=8.10^{-5}$) but not for the sleep vs. new list contrast ($t(16)=1.16$, $p=0.26$, Bayes factor>1000), in accordance with the absence of P3 effect for the sleep list. However, when using the EEG data computed over the negative cluster associated to the sleep list, we could predict the stimuli category better than chance when comparing the sleep and the new lists ($t(16)=3.44$, $p=0.003$) and when comparing the wake vs. new lists ($t(16)=2.15$, $p=0.04$), reflecting the overlap between the P3 and negative clusters.

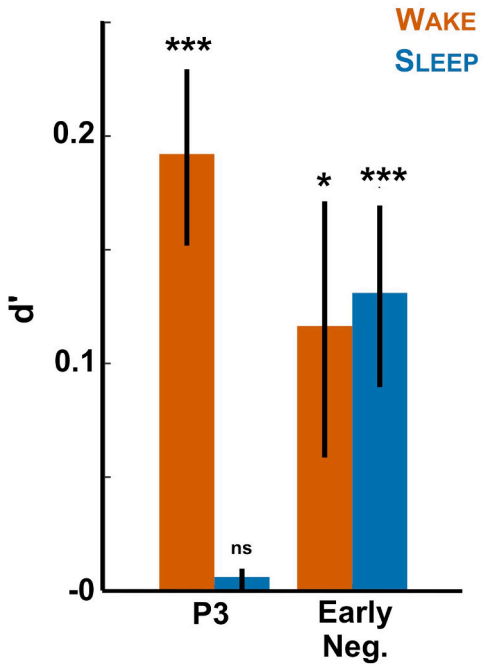

Figure 7-4 Decoding stimulus category with the EEG signal

The EEG amplitude over the clusters observed in Figure 7-3 ('P3': [0.73, 0.86] s over parieto-occipital electrodes; 'Early Neg.': [0.49, 0.62] s over centro-parietal electrodes) was retrieved on a single-trial basis for all participants. A leave-one-out approach was applied at the subject-level to fit a logistic regression (see Methods), which was then used to predict stimulus category (sleep vs. new or wake vs. new). The sensitivity index d' of this prediction was computed for each participant and each contrast and averaged across participants. The red bar shows therefore the sensitivity of using the EEG data to predict whether a wake item was previously heard and the blue bars the sensitivity in predicting the sleep items. Stars atop bars show the significance level of the t-test testing for the null hypothesis (***: $p<0.005$, **: $p<0.001$, *: $p<0.05$, ns: $p>0.05$). Note that the P3 cluster allows classifying only wake items while the negative sleep vs. new cluster could differentiate both wake and sleep items from new ones.

Finally, we examined the time-frequency decomposition of the EEG signal in response to the items of the different lists (Figure 7-5). When pooling all words from all lists, it

appears that stimulus presentation modulates the EEG signal in 3 distinct frequency bands. Stimulus onset was followed by a synchronization within the theta band (i.e. increase in power for the [4, 8]Hz band) and a desynchronisation (decrease in power) within the alpha ([8, 12]Hz) and beta band (>16Hz). Interestingly, variation in the theta and alpha power has been associated with changes in recollection performance (Klimesch, 1999; Klimesch et al., 1997). We did not observe any difference between lists within the theta band. However, the new list elicited stronger alpha desynchronisation over occipital regions compared to the wake list ($p_{cluster}$=0.02, Figure 7-5 bottom) in accordance with previous findings (Klimesch et al., 1997). Importantly, a similar and even stronger effect was observed when contrasting the wake and sleep lists ($p_{cluster}$=0.009). Once again, the brain response to the sleep and new lists show that despite equivalent 1st order responses, the sleep items were not processed as novel words.

Overall, both behavioral and EEG data reveal the presence of implicit mnesic traces for words heard during sleep. However, the opposite effects observed in the ERP between the wake and sleep lists suggest that the memory traces associated to wake and sleep items may qualitatively differ.

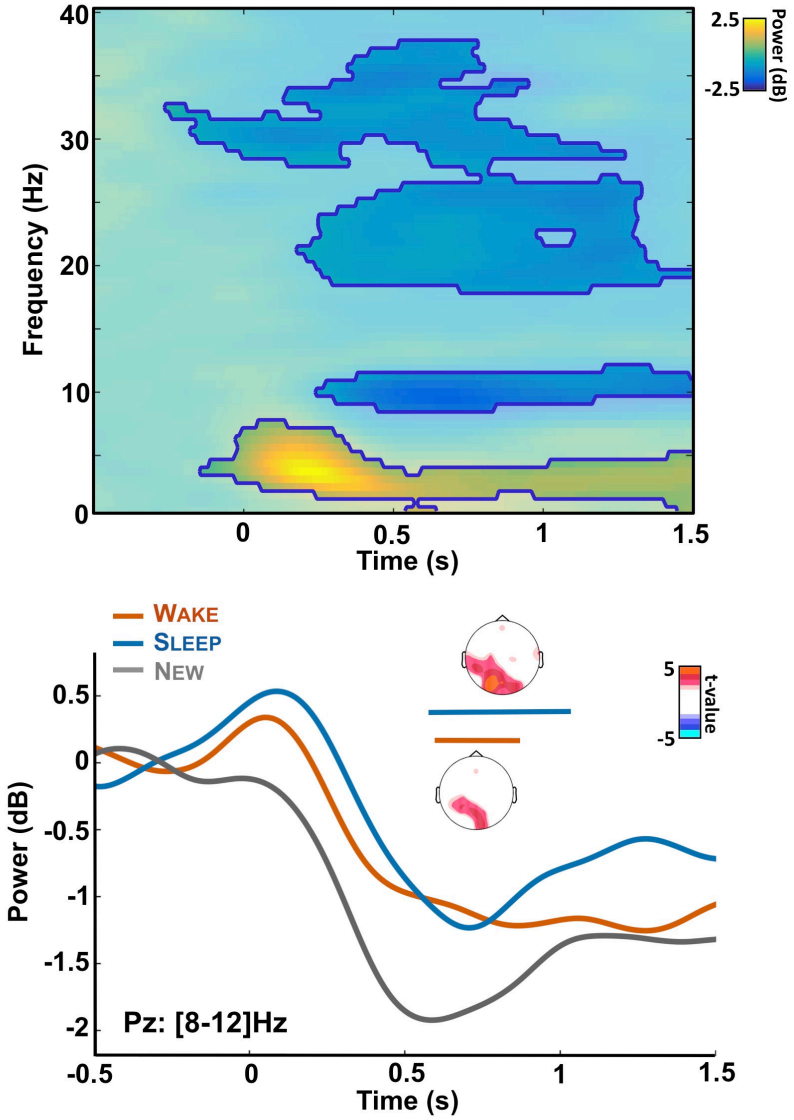

Figure 7-5 Alpha de-synchronization during memory recognition

Top: Time-frequency decomposition of the EEG signal recorded at electrode Pz and for all trials. Power is expressed as a log ration of the baseline activity and was averaged across participants (N=17). The mask and contours show the significant clusters ($p_{cluster}<0.05$). After stimuli onset, clear modulations of the power can be observed in the theta ([3-8] Hz), alpha ([8-12] Hz) and beta (>20 Hz) bands. Bottom: Power modulation for the alpha band ([8-12] Hz) over electrode Pz for the different lists of stimuli (red: wake, blue: sleep, gray: new list). Horizontal bars show the significant cluster when comparing the wake and new lists (red: $p_{cluster}=0.02$) or the sleep and new lists (blue: $p_{cluster}=0.009$) across participants. Insets show the corresponding topographies for these clusters: power was averaged on the clusters' time-window and t-values were computed by comparing the corresponding power for the wake (or sleep) list and the new one. Non-significant t-values ($p>0.05$, uncorrected) were set to 0.

Discussion

Memory for words heard during sleep

Until recently, scientific efforts to understand whether humans can learn while sleeping had remained largely inconclusive due to the paucity of positive results and doubts raised by methodological flaws (Bruce et al., 1970; Webb, 1990; Wood, JM, 1990). At first sight, our results are consistent with previous studies showing no memory for the words presented during sleep (Cox et al., 2014; Emmons and Simon, 1956; Wood et al., 1992). Indeed, while words presented during wakefulness elicited close-to-perfect explicit recognition (Figure 7-2) and classical ERP signatures of recollection (Figure 7-3, P3 effect), items presented during sleep seemed to be processed as new items when considering these two markers (Figure 7-2 and Figure 7-4).

However, a more detailed investigation of both behavioral and EEG data revealed differences between the sleep and new lists. Sleep items that were declared as previously encountered elicited higher confidence judgments than sleep items judged as 'old' (Figure 7-2b). This difference in confidence estimation between the wake and sleep lists was confirmed when analyzing the type-II ROC curves (Figure 7-2d). Analyzing brain responses to the sleep and new lists confirmed that these two lists were not processed identically (Figure 7-3), with sleep items eliciting a large centro-parietal negativity around 500ms. When extracting the EEG signal over the corresponding cluster, a classifier could separate novel from sleep items with above chance-performance (Figure 7-4), which participants themselves could not do. Differences between the sleep and new lists could also be evidenced when examining the stimulus-related alpha desynchronisation. The EEG signal contains therefore information about the fact that sleep items had been previously heard but participants did not use this information to perform the old/new task.

Nature of the memory traces formed in sleep

Although behavioral and EEG data indicate that words presented during sleep left a trace in participants' brain, such traces seem quite different from the explicit memory formed during wakefulness. Indeed, wake items were explicitly recognized (high 1st and 2nd order performance, Figure 7-2). On the contrary, sleep items did not lead to above chance 1st order performance. The memory effect was restricted, at the behavioral level, to 2nd order-responses. An improvement of 2nd order responses with at-chance 1st order responses can be interpreted as the manifestation of an unconscious (i.e. implicit) memory trace (Jachs et al., 2015; Rosenthal et al., 2010; Scott et al., 2014; Tulving, 1985).

In fact, the patterns of results observed on confidence rating (increased confidence for sleep items correctly categorized as old compared to new one but lower confidence ratings compared to sleep items incorrectly categorized as new, see Figure 7-2b) could be interpreted as a conflict between the absence of explicit memory for sleep items and the presence of implicit mnesic traces. Under such conditions, when the implicit memory trace is weak or absent, participants would tend to process sleep items as new with a rather high degree of confidence. On the contrary, when the implicit trace is stronger, participants would declare such items as old but with a rather low degree of confidence due to the lack of explicit recognition. Nonetheless, these items would elicit higher

confidence ratings compared to incorrectly classified new items for which no implicit memory trace exists.

Thus, our results could fit with the classical distinction between 'knowing' (explicit recollection) and 'remembering' (implicit recognition) (Tulving, 1985). According to this view, the explicit recollection and familiarity both contribute to recognition but recruit different memory systems (Rugg et al., 1998; Vilberg and Rugg, 2008; Voss and Paller, 2007). However, disentangling the contribution of explicit and implicit memory at the behavioral level and in their neural signature is very complex (Malmberg, 2008; Rotello et al., 2004; Voss and Paller, 2007). Here we can take advantage of the fact that participants were in a state of minimal, if not absent, consciousness during learning. As a consequence and contrary to many studies in which the explicit/implicit nature of a stimulus is manipulated by processing depth (e.g. (Rugg et al., 1998)), we can here better isolate the neural activity underlying implicit memory. Interestingly, many studies showed quantitative rather than qualitative changes between the neural correlates of implicit and explicit memory (Allan et al., 1998). Here, on the contary, sleep items elicited a centro-parietal negativity that appeared as the opposite of the classical signature of explicit recollection (P3 effect, Figure 7-3).

We further checked that this centro-parietal negativity depended on the stimuli and not subjects' response by focusing on sleep and new items both categorized as 'new' by participants. In such case, behavioral responses were identical for the two conditions (Figure 7-2a-b). Nevertheless, a similar cluster was observed over Pz ([0.48, 0.62] s, $p_{cluster}$=0.01), suggesting that the centro-parietal negativity depends on prior exposure and not on participants' choice.

Alternatively, it has been proposed that the difference between explicit and implicit memory could stem from a difference in memory strength rather than different neural sources (Squire et al., 2007). However, such view would predict a similar, albeit weaker, effect for the sleep list in lieu of the observed opposite effects. While both familiarity and recollection could be encoded in similar structures within the medio-temporal lobe (Squire et al., 2007), our results suggest that they can be dissociated under certain conditions.

Learning or consolidating during sleep?

Sleep has often been seen as a state promoting memory consolidation to the detriment of memory encoding (Hasselmo, 1999; Hennevin et al., 2007; Tononi and Cirelli, 2014). It has been proposed that the low-level of acetylcholine in NREM sleep as well as the relative disconnection of the sleepers from its environment would impair the formation of new memories. However, recent research showed that the consolidation of memory during sleep does not necessarily preclude any form of hippocampus-dependent sleep-learning. Accordingly, animals and humans can be conditioned during sleep (Arzi et al., 2014, 2012; de Lavilléon et al., 2015; Hennevin et al., 2007, 1995). One key element potentially explaining the success of these studies consists in their ability to bypass sensory isolation by providing either olfactive information (Arzi et al., 2012), which does not transit by thalamic relays (Jones, 2007), or by using intracranial stimulations (de Lavilléon et al., 2015). Here, we similarly ensure that the stimuli were processed at a high-level of representation by checking the preservation of task-related motor preparation indexes (Figure 7-1c) that can be observed if and only if the novel information is

correctly processed (Kouider et al., 2014). It is also important to note that we studied mostly light stages of NREM sleep (nap studies). It is possible that light NREM is a stage more favorable to the processing of external information and the formation of memory in opposition to deeper stages of sleep in which sensory isolation and changes in neuromodulation are more pronounced (Genzel et al., 2014). According to this view, the formation of memory during sleep is possible but is a highly constrained phenomenon with little effect at the behavioral level.

Study 8:
Perceptual learning of acoustic noise generates memory-evoked potentials

Published in **Current Biology**
November 2, 2015

Thomas Andrillon[1-3], Sid Kouider[1,2], Trevor Agus[2,4,5] & Daniel Pressnitzer[2,4]

[1] *Laboratoire de Sciences Cognitives et Psycholinguistique (UMR8554, ENS, EHESS, CNRS) Paris, France*

[2] *Département d'Études Cognitives, École Normale Supérieure – PSL Research University Paris, France*

[3] *École Doctorale Cerveau Cognition Comportement, Université Pierre et Marie Curie Paris, France*

[4] *Laboratoire des Systèmes Perceptifs, CNRS UMR 8248 Paris, France*

[5] *Sonic Arts Research Centre, School of Creative Arts, Queen's University Belfast Belfast, UK*

Summary

Experience continuously imprints on the brain, at all stages of life. The traces it leaves behind can produce perceptual learning (Gilbert et al., 2001), which drives adaptive behavior to previously encountered stimuli. Recently, it has been shown that even random noise, a type of sound devoid of acoustic structure, can trigger fast and robust perceptual learning after repeated exposure (Agus et al., 2010). Here, combining psychophysics, electroencephalography (EEG), and modeling, we show that the perceptual learning of noise is associated with evoked potentials, without any salient physical discontinuity or obvious acoustic landmark in the sound. Rather, the potentials appeared whenever a memory trace was observed behaviorally. Such memory-evoked potentials were characterized by early latencies and auditory topographies, consistent with a sensory origin. Furthermore, they were generated even on conditions of diverted attention. The EEG waveforms could be modeled as standard evoked responses to auditory events (N1-P2, (Picton, 2011)), triggered by idiosyncratic perceptual features acquired through learning. Thus, we argue that the learning of noise is accompanied by the rapid formation of sharp neural selectivity to arbitrary and complex acoustic patterns, within sensory regions. Such a mechanism bridges the gap between the short-term and longer-term plasticity observed in the learning of noise (Agus et al., 2010; Guttman, 1963; Kumar et al., 2014; Luo et al., 2013). It could also be key to the processing of natural sounds within auditory cortices (Mizrahi et al., 2014), suggesting that the neural code for sound source identification will be shaped by experience as well as by acoustics.

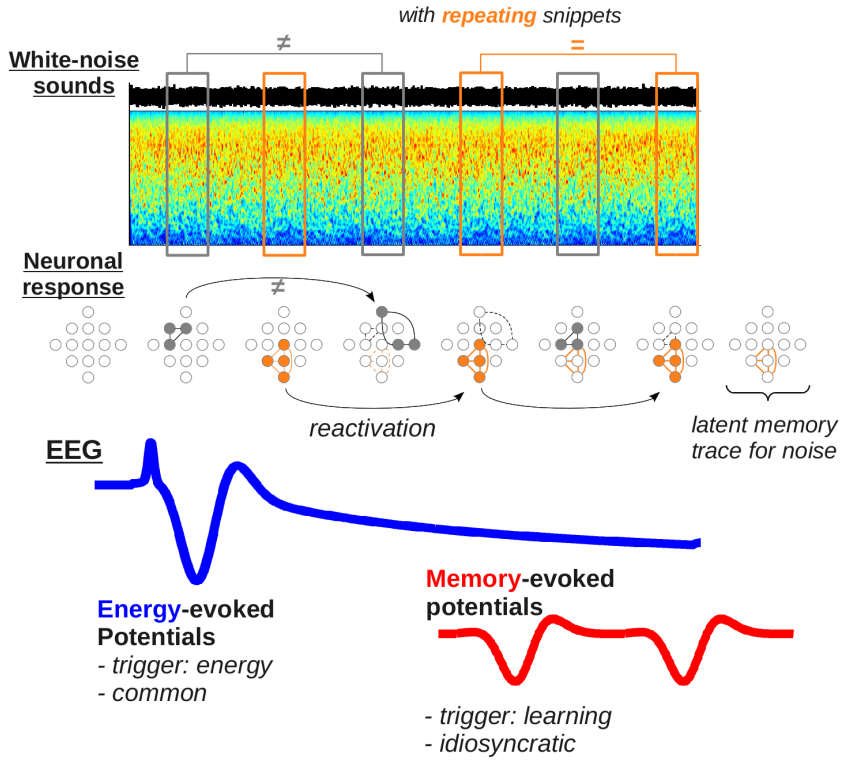

Graphic summary

Results

We used an experimental paradigm where listeners learnt exemplars of acoustic noise (Agus et al., 2010; Kumar et al., 2014; Luo et al., 2013). Although noise is not representative of natural sounds, it is a unique tool to probe auditory (Agus et al., 2010) or even visual (Gold et al., 2014; O'Toole and Kersten, 1992) perceptual learning. First, noise lacks semantic content, thus revealing pure perceptual learning. Also, there is normally no prior exposure to a specific noise exemplar. Finally, noise exemplars can contain tens of thousands of random samples, with no sample-to-sample predictability, pushing any learning mechanism to the extreme.

The surprising ability of listeners to learn meaningless, random patterns is also relevant to the long-standing debate about the nature of experience-dependent changes in the brain: are such changes distributed or local (Gilbert et al., 2001; Thorpe, 2011)? A distributed code posits subtle changes in a whole population of neurons, with the functional benefits appearing only at the population level. For audition, perceptual learning has indeed been observed through distributed changes in "tonotopic" frequency maps, using pure tones (Fritz et al., 2003; Schreiner and Polley, 2014). As noise has a flat spectrum on average, a distributed code could not rely on tonotopy, but it could possibly recruit more complex timbre maps (Elliott et al., 2013; McDermott et al., 2013). In contrast, a local code posits dramatic changes at the single-neuron or small-network level, with small neural populations expressing the full benefit of learning (Bathellier et al., 2012; Mizrahi et al., 2014). For noise, such a localized code could apply, if repeated exposure to a random pattern created a form of ultra-selective response (Klampfl and Maass, 2013; Masquelier et al., 2008).

Recently, Luo et al. (Luo et al., 2013) applied magnetoencephalography (MEG) to the noise-learning paradigm. They found that noise learning induced stable phase patterns in brain neural responses, as measured by inter-trial phase coherence (ITPC) in the 3-8 Hz theta range. Those results were interpreted as a distributed and holistic learning process (Giraud and Poeppel, 2012b; Luo and Poeppel, 2007). Strikingly, there was no effect of perceptual learning on event-related potentials (ERPs), which further advocated against a local process: if listeners learnt isolated perceptual events within the noise, those should be accompanied by ERPs (Gutschalk et al., 2008). However, the local account may be reprieved with an additional hypothesis. If learnt features were local but idiosyncratic, and thus activated at random times across listeners for the same noise (Agus et al., 2010; Kaernbach, 1993, 1992), then the associated ERPs would be impossible to observe on average, while ITPC would remain high. We devised a variant of the noise-learning paradigm to test this hypothesis.

Behavioral measures of perceptual learning: diffuse and compact conditions.

For half of the experiment (Figure 8-1A left), a standard noise-learning paradigm was used (Agus et al., 2010; Luo et al., 2013). Participants were instructed to discriminate trials containing continuous white noise (N) from trials made of the seamless concatenation of three copies of a 0.5s-long white-noise snippet (repeated noise, RN).

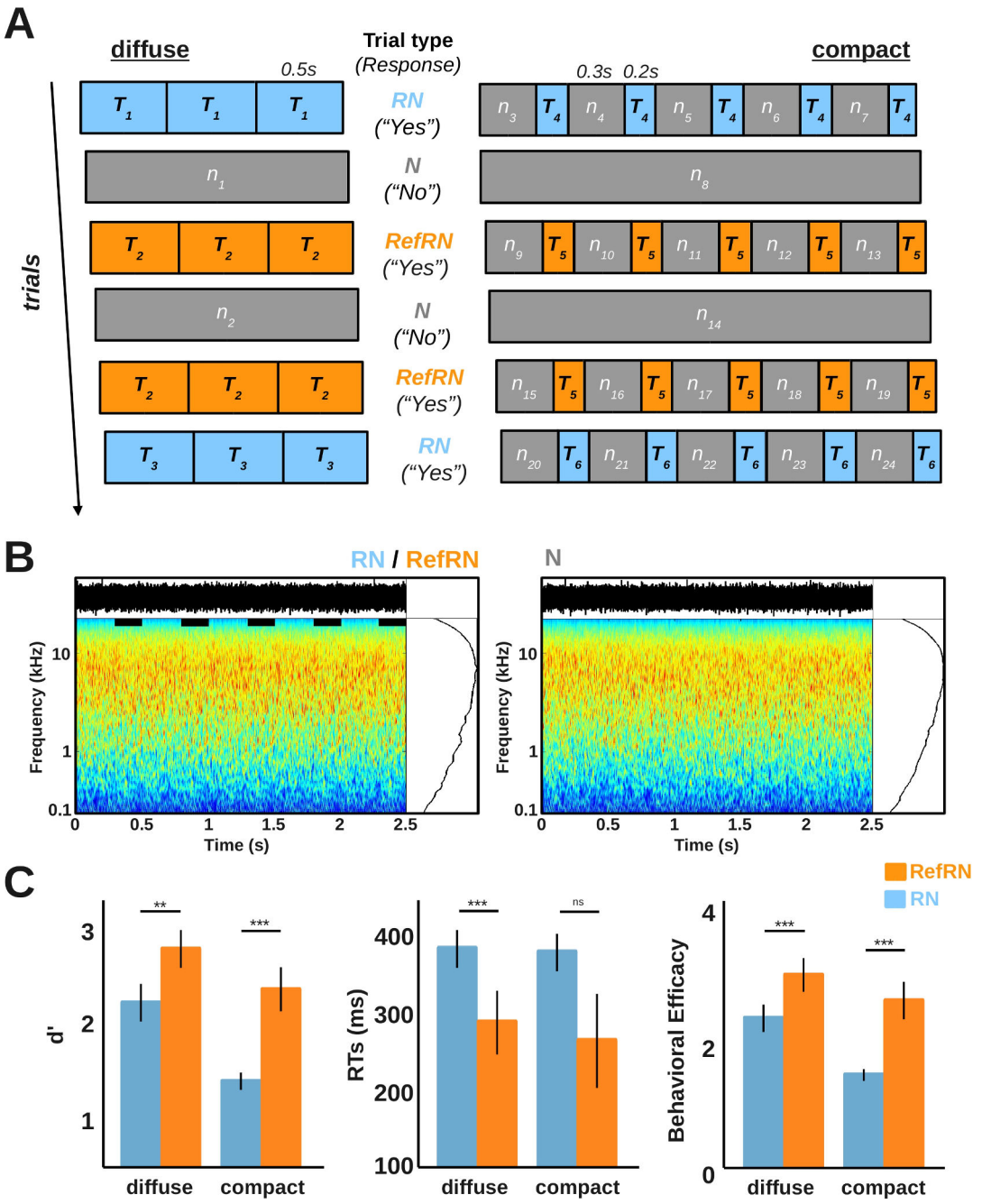

Figure 8-1 Experimental procedure and behavioral results

A: Stimuli and experimental design for Experiment 1. In the "diffuse" condition (left), participants had to discriminate between no-repeat trials, made of 1.5s of running white-noise (N), and with-repeats trials, made by concatenating, without any discontinuity, three identical 0.5-s long snippets of noise. For repeated noise trials (RN), a new snippet of noise was drawn for each trial. For reference repeated noise trials (RefRN), the exact same noise snippet re-occurred not only within a trial, but also across trials (illustrated here with target snippet T2). In the "compact" conditions, the task was the same but repeated snippets were shorter (0.2s) and concatenated, without any discontinuity, with 0.3s running white-noise fillers. Compact trials lasted 2.5s and included 5, 0.5s-long partially-repeating epochs (Supp. Procedures). B: Typical output of a peripheral auditory model (Spectro-Temporal Excitation Pattern, [39], see Supp. Methods for details) for repeated (RN/RefRN) and unrepeated (N) stimuli. The compact condition was used for the simulations. There are no obvious landmarks for the repeated stimuli in the waveform (top), average excitation pattern (right), nor spectro-temporal excitation pattern

(main panel). C: Behavioral performance in Experiment 1, averaged over n=42 blocks. Three measures were computed: sensitivity d', reaction times (RTs) and behavioral efficacy combining d' and RTs (Supp. Procedures). Error-bars denote standard errors of the mean (SEM) across blocks. Stars indicate the significance level for the RefRN vs RN comparisons (paired u-test, ns: $p>0.05$, *$p<0.05$, **$p<0.01$, ***$p<0.005$). RTs were faster for RefRN in the compact but not diffuse condition (paired u-test: $p=0.21$). A better performance (higher d' and behavioral efficacy, faster RTs) for RefRN compared to RN summarizes the amount of perceptual learning.

Without participants' knowledge, a third type of trial was introduced: one particular instance of repeated noise (reference repeated noise, RefRN) re-occurred, identically, over 16 trials throughout a block. A higher repetition-detection performance for RefRN relative to RN indicates perceptual learning (Agus et al., 2010). For the other half of the experiment, a change was introduced in the structure of trials containing repetitions: a shorter 0.2s-long white-noise snippet was repeated but seamlessly concatenated, between repetitions, to 0.3s fresh noises (Figure 8-1A, right). Thus, the temporal window over which repetition detection and perceptual learning could occur was restricted to 0.2s. This would induce less temporal variability in putative local EEG markers. We use the terms "diffuse" for fully repeating noise (Agus et al., 2010; Luo et al., 2013) and "compact" for partially repeating noise (Berti et al., 2000; Kaernbach, 2004).

Behavioral measures showed clear evidence of perceptual learning in both conditions (Figure 8-1C). First, signal-detection analysis (Macmillan, 2005) showed a better d' sensitivity for RefRN compared to RN. This difference between RefRN and RN was absent at the beginning of blocks, that is, before learning of RefRN could occur (Figure S 8-1A). Reaction times (RTs) were faster for RefRN than RN in the diffuse condition, and a higher accuracy was associated with faster responses for RefRN in both diffuse and compact conditions (Figure S 8-1B). This suggests that both d' and RTs indexed perceptual learning. We combined d' and RTs in a "behavioral efficacy" index (BE, Supp. Procedures). The compact condition led to lower BEs (Friedman test, $p<0.001$), showing that this condition was more difficult overall. However, the amount of learning, as measured by the BE difference between RefRN and RN, was the same across conditions (paired u-test, $p=0.46$).

Electrophysiological markers of learning

EEG was recorded while participants performed the task and analyses were restricted to the sensors most responsive to auditory stimuli (Supp. Procedures). Following (Luo et al., 2013), we investigated three possible neural markers of learning: ITPC (Figure 8-2A-B), EEG power (Figure 8-2C), and ERPs (Figure 8-2D).

For the diffuse condition (Figure 8-2, left, see legend for statistical tests), we observed higher ITPC for RefRNs in a [0.5, 5]Hz range. When averaging ITPC in this frequency range, only RefRN showed an increase compared to the N baseline. Further averaging ITPC over the whole stimulus duration (Figure 8-2B inset) confirmed that the effect was restricted to RefRN. Applying the same analyses to power responses did not reveal any significant difference across conditions. Finally, we estimated ERPs time-locked to stimuli onsets. We did not observe any difference across stimulus types. So far, results for ITPC, power, and ERPs fully replicate the MEG findings of (Luo et al., 2013).

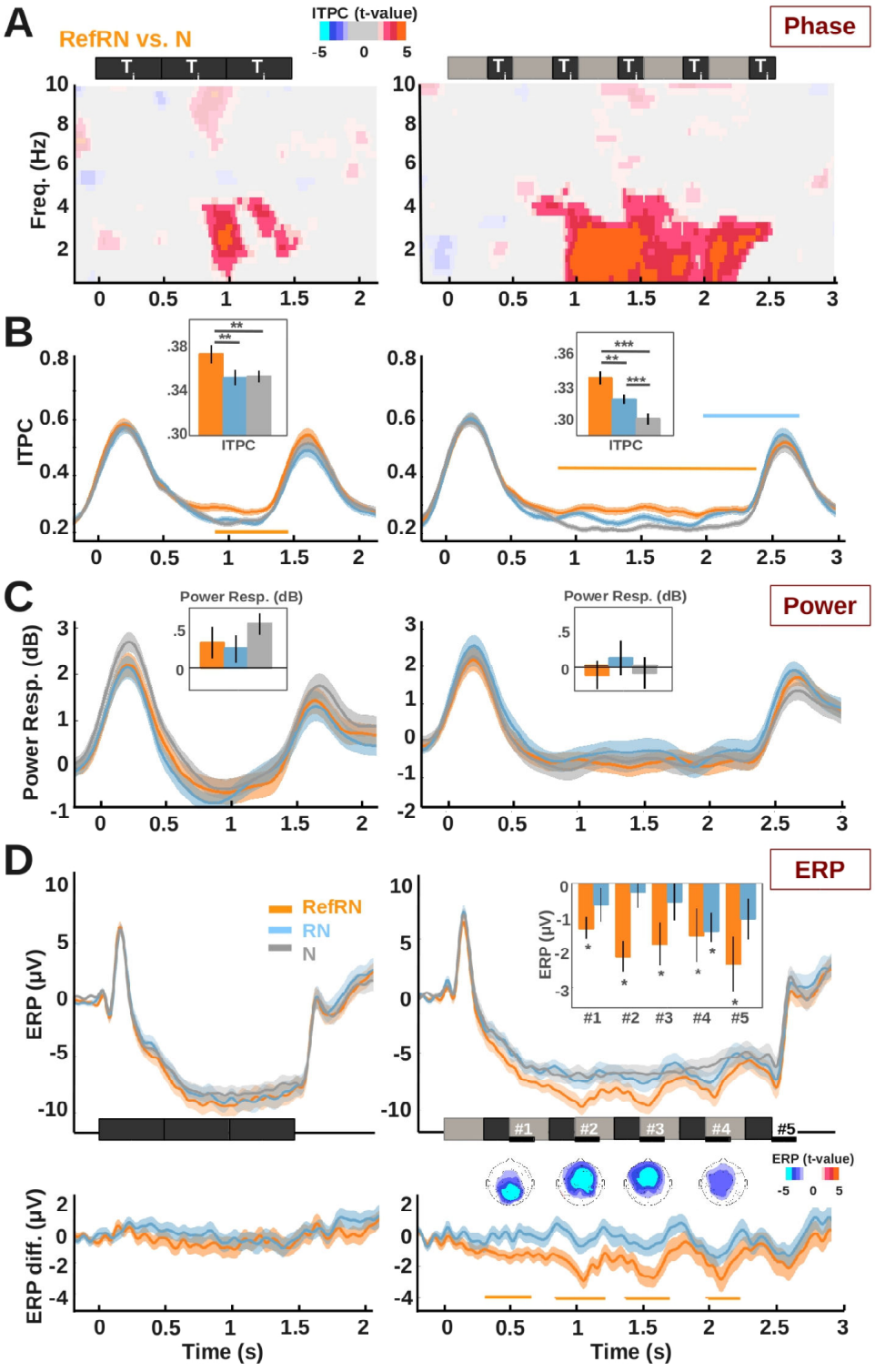

Figure 8-2 Electrophysiological Markers

Diffuse and compact conditions (Experiment 1) are presented on the left and right columns, respectively. A: Time-frequency distribution of the increase of inter-trial phase coherency (ITPC) for RefRN compared to N trials (t-values from uncorrected paired t-tests across 42 blocks). The transparency mask shows clusters surviving a Monte-Carlo permutation test (Monte-Carlo p-value <0.05). Here and below results are averages for the 10 most responsive auditory electrodes (Figure S 8-3A). B. Average ITPC in the 0.5Hz to 5Hz region of interest, for RefRN (orange), RN (blue) and N (gray). Horizontal colored lines show significant clusters for diffuse (RefRN vs.

N: [800, 1400]ms, Monte-Carlo p-value<0.005) and compact (RefRN vs. N: [800, 2400]ms, Monte-Carlo p-value<0.0001; RN vs. N: [2000, 2700]ms, Monte-Carlo p-value<0.0001) conditions. Insets show the mean ITPC further averaged over stimulus duration. Stars indicate the significance level of paired comparisons between conditions (paired t-tests, ns: p>0.05, *p<0.05, **p<0.01, ***p<0.005). C: Power response in the 0.5Hz to 5Hz region of interest, averaged across blocks. Insets show the mean power further averaged over stimulus duration. No significant difference could be observed between trial types. D: Evoked related potentials (ERPs, top) and difference waves (RefRN or RN minus N, bottom). No statistical difference was observed between trial types for the diffuse condition. For the compact condition, averaging ERPs after repeated snippets (inset) revealed larger negativities for RefRN and RN compared to N (paired t-tests, *p<0.05). Difference waves also showed significant clusters (Monte-Carlo p-value<0.05, with topographies of t-values also plotted). Note that the first cluster for the RefRN vs. N comparisons start right after the first target onset. Error-bars on insets and shaded areas around curves indicate standard errors of the mean (SEM) computed across blocks.

For the compact condition (Figure 8-2, right), the same analyses were performed. Again, there was an increase in ITPC for RefRN compared to N. Averaging ITPC over the low-frequency range revealed a significant cluster for RefRN compared to N, and here, also for RN compared to N. As the noise snippets for RN were different from one trial to the next, this shows that across-trial phase patterns cannot be specific to a noise snippet. The power analysis did not reveal any difference across stimulus types. Finally, and crucially, there were clear modulations of the ERPs. Averaging ERPs after each repetition revealed consistent negative potentials for RefRN and RN (Figure 8-2D inset). Remarkably, within the RefRN trials, ERPs were observed for each presentation of the repeated snippet, including the very first one (before any within-trial repetition). Therefore, such ERPs cannot be markers of within-trial repetition only. We also observed significant ERPs for RN trials, but only after several within-trial presentations of the repeated snippet.

In summary, ERPs were observed in response to a noise snippet if and only if the same snippet had been heard before, within (RN) or across (RefRN) trials. The appearance of ERPs was extremely rapid, as they developed within five presentations of a novel noise snippet in RN trials. Such time-locked ERPs occurred without any discontinuities in sounds' amplitude or any other short-term statistics. To illustrate this point, we ran the stimuli through a peripheral auditory model (Figure 8-1). The simulation showed that there were no obvious landmarks in RN/RefRN, at least not of the kind known to produce auditory ERPs before learning (Picton, 2011). To stress that the "events" producing the event-related potentials were related to past experience, we term such responses "memory-evoked potentials" (MEPs).

Memory-evoked potentials are sensory correlates of behavioral performance

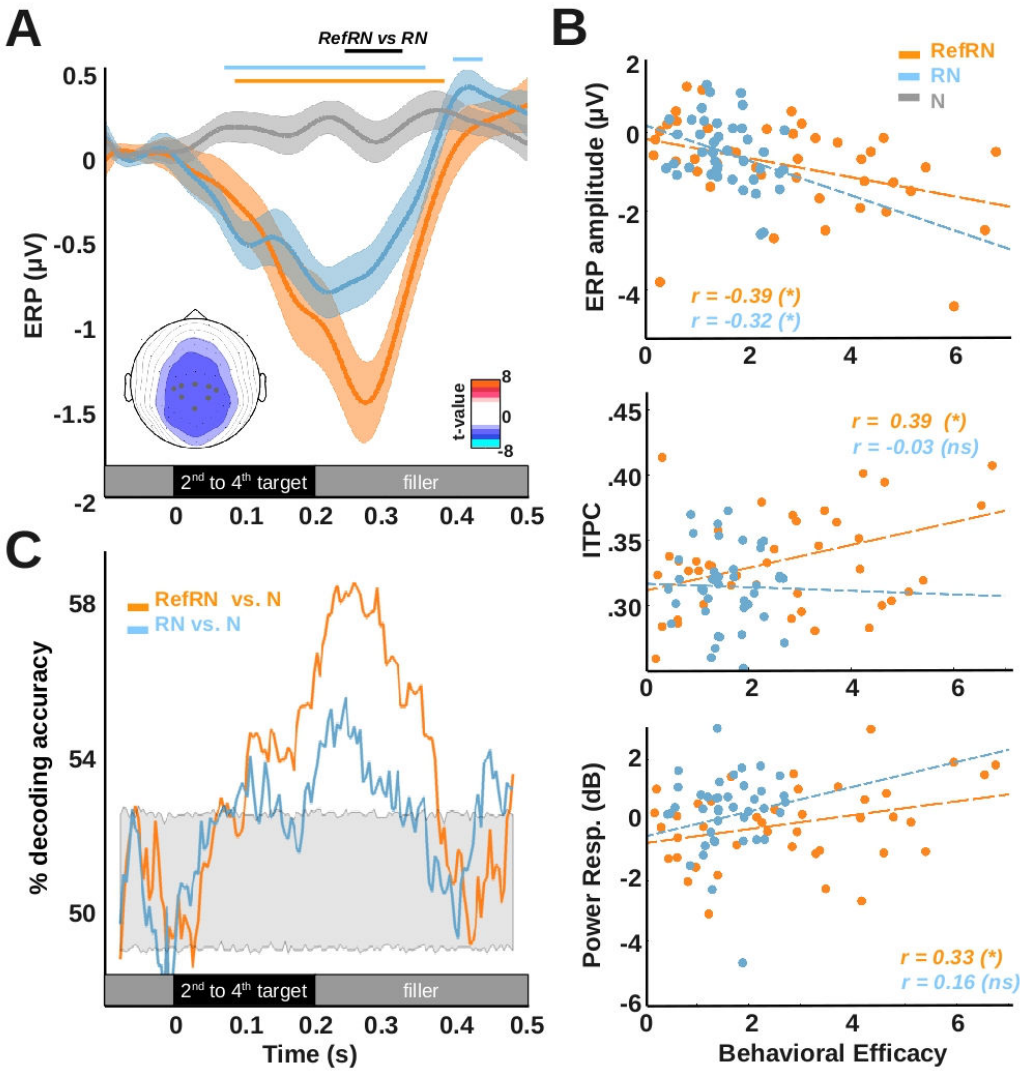

Figure 8-3 Correlation of neural markers to behavioral performance for the compact condition

A: ERPs were averaged across repetition epochs ([-100, 500]ms window from target onset, 2nd to 4th within-trial target occurrences). Horizontal lines indicate significant clusters when comparing RefRN with N (orange, [128, 364]ms), RN with N (blue, negative: [72, 328]ms, positive: [388, 472]ms) and RefRN with RN (black, [244, 316]ms) trials (Monte-Carlo p-values<0.05). Shaded areas indicate standard errors of the mean (SEM) across blocks. The inset shows the topographical map of the differences between RefRN and N expressed as t-values (paired t-tests on averaged ERP amplitude extracted over a [100, 400]ms window, n=42 blocks). Non-significant t-values (p>0.05/65, Bonferroni correction) were set to white. B: Correlation of Behavioral Efficacy with ERP amplitude (top), phase coherence (ITPC, middle) and EEG power (bottom) for RefRN (orange) and RN (blue) trials. Pearson's correlation coefficients (r) were computed for RefRN and RN conditions separately and displayed on scatter plots along their statistical significance level (ns: p>0.05, *p<0.05, **p<0.01, ***p<0.005). Orange and blue dashed lines show the linear fit estimated for RefRN and RN conditions respectively. C: Experimental conditions (RefRN vs. N (orange), RN vs. N (blue), Supp. Procedures) were decoded, at the single-trial level, using a logistic regression on the ERPs displayed in A. Gray area denotes the chance level obtained through permutations of trial types (n=1000). Decoding values above this gray area are higher than 95% of random values.

To further characterize MEPs, we averaged responses time-locked to the repeated noise snippets for the compact condition (Figure 8-3A). Both RefRN and RN induced clear MEPs with a latency of about 100ms. The MEPs' topography was very similar to the N1 topography (Figure S 8-3A), but their broad, mostly negative waveform differed from a standard N1-P2 complex (Picton, 2011). However, such topography and waveform are consistent with a superposition of time-jittered N1-P2 complexes (see Model). The MEPs were larger for RefRN compared to RN. Nonetheless, after amplitude normalization, the waveforms and topographies became identical (Figure S 8-3C). This suggests a common origin: for RN, MEPs could indicate the emergence of a mnesic trace towards the end of the trial, while for RefRN, the same mnesic trace would be re-activated from the very first snippet presentation, and then reinforced by subsequent presentations.

If this unified account were correct, MEPs should always correlate with behavioral performance. This is exactly what was found: amplitude correlated with BE for both RefRN and RN (Figure 8-3B). We further tested whether MEPs could differentiate between stimuli on a trial-by-trial basis, using a logistic regression on the MEPs amplitude (Figure 8-3C). We obtained significant decoding as early as 100ms post-presentation, supporting a sensory interpretation. The decoding accuracy was modest, but note that all sounds in this analysis were statistically exactly the same: a single epoch of white noise. Still, MEPs carried information about past experience, on a trial-by-trial basis.

Learning noise without paying attention

So far, listeners were instructed to detect noise-repetitions, so at least part of the MEPs could have been caused by attentional modulation. We tested this hypothesis in a supplemental experiment (Figure S 8-2). Listeners were not asked to detect repetitions, but, rather, had to perform a distracting auditory task (detection of amplitude modulations) (Luo et al., 2013). In addition, RN or RefRN sequences were embedded in 8min of continuous running noise: there was no amplitude-onset cue to signal that a new "learnable" sequence had begun, thus removing endogenous and exogenous attentional cues. Still, clear MEPs were observed, remarkably similar to those of the main experiment (Figure S 8-3B).

A simple model of memory-evoked responses

A possible interpretation for the MEPs is that they were triggered by acoustic events within the noise, which only became perceptually salient after learning. We implemented this idea in a simple quantitative model (Figure 8-4A). Whenever a snippet of noise had been heard before, we injected an ERP in the EEG waveform, with a canonical shape (N1-P2, (Picton, 2011)) and random onset time for each "listener" and noise. This was intended as an idealized version of one-shot learning: whenever the same noise would be heard again by the same listener, an ERP was invariably triggered and its onset time would remain exactly the same. But, a different noise or listener would result in an ERP with a different, random onset time.

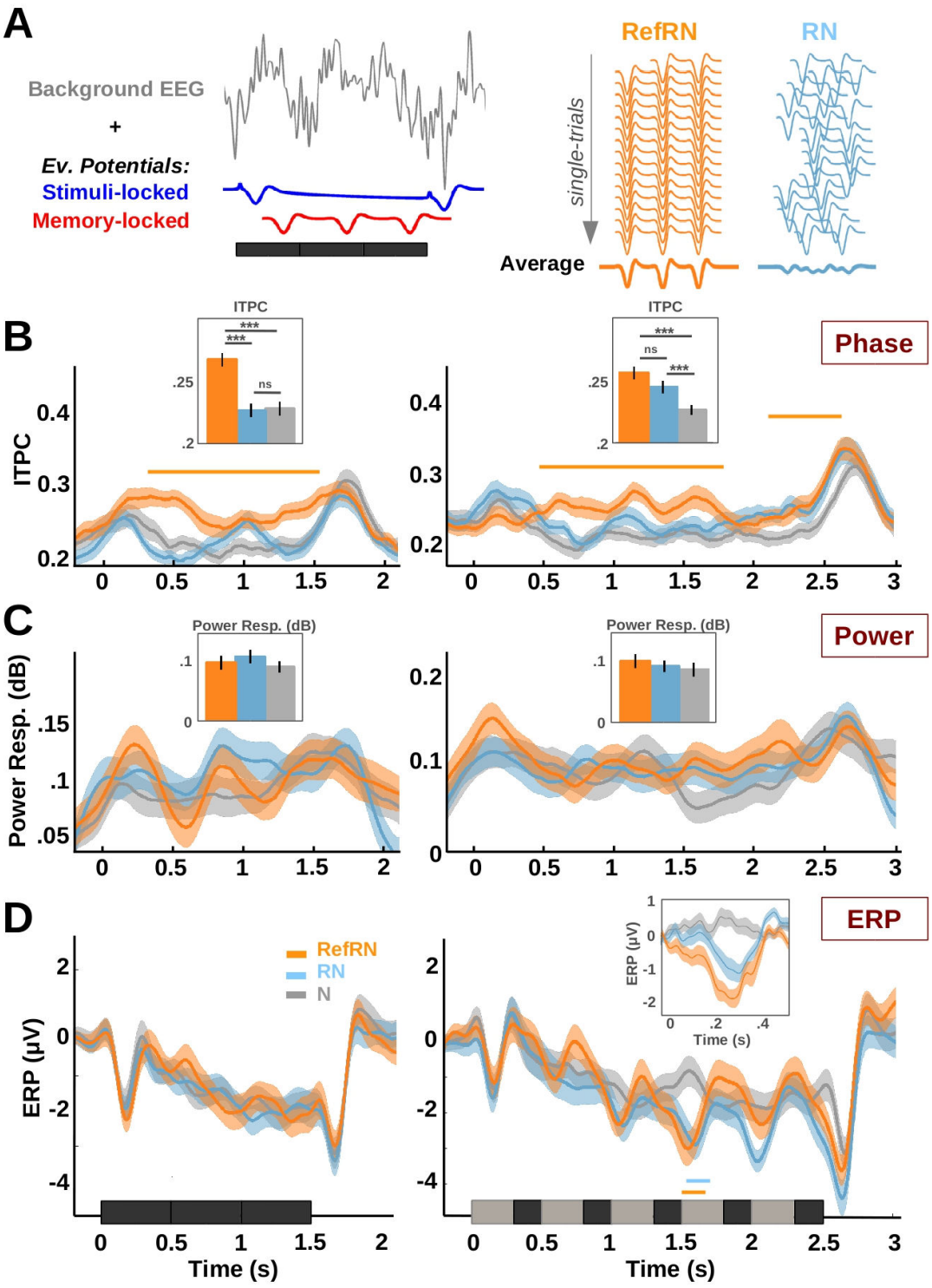

Figure 8-4 Model simulations

A: Illustration of the model's architecture. Background EEG was first synthesized (gray curve, Supp. Procedures) and evoked potentials were added at the onsets and offsets of acoustic energy (stimulus-locked, dark blue). If a noise snippet had been heard before, an additional ERP was added (memory-locked, red), with a random onset time. The onset time was then fixed for subsequent presentations of the same noise snippet. The illustration for the diffuse condition (right) shows that, by construction, RefRNs were associated with perfectly synchronous potentials throughout a block, as they contained the same noise snippets across trials, whereas an RN trial contained only two potentials (after the first repetition epoch of each trial) with time-

jitter across trials. 42 blocks were simulated with a Signal-to-Noise Ratio matching the empirical dataset (see Supp. Procedures and Figure S 8-4). B-D: Analyses of the simulated data, format as Figure 8-2. Inset of panel D shows the target-locked ERPs as in Figure 8-3A. Colored lines denote significant clusters for the RefRN vs. RN (orange) and RN vs. N (blue) comparisons (Monte-Carlo p-values<0.05, n=42 simulated blocks). In the insets, stars indicate the significance level (paired t-tests, ns: p>0.05, *p<0.05, **p<0.01, ***p<0.005).

As a result, for RN, the evoked activity was shifted across trials and shifted across blocks, whereas for RefRN, the evoked activity was fixed across trials and shifted across blocks. We analyzed the simulated data (Supp. Procedures) in the same way as the EEG recordings. The model replicated all of the main findings (Figure 8-4B-D). In particular, no ERPs were observed in the diffuse condition, as the memory-locked N1-P2 averaged out across blocks, due to the 500-ms onset-time jitter. Time-locked ERPs similar to MEPs were observed only for the compact condition, as the 200-ms onset-time jitter was too short for N1-P2 components to fully overlap and cancel out. The peculiar shape of the MEPs itself was reproduced by the additive model (Figure 8-4D inset).

Discussion

We used acoustic noise to probe the neural bases of auditory perceptual learning. Our results outline a simple mechanistic account of how initially nondescript, random sounds may acquire perceptual uniqueness. Through exposure, with or without focused attention, rapid plasticity creates sensory selectivity to subtle acoustic details within a specific noise pattern. Such details are localized in time, idiosyncratic, and only become salient after perceptual learning.

This account clarifies the puzzling issue of what is learnt within a noise. Repeated noise is introspectively reported as containing short "rasping, clanking" perceptual events (Julesz, 1963; Kaernbach, 1993). Behavioral data already suggested that those events differed across listeners for the same noise (Agus et al., 2010; Kaernbach, 1993, 1992), and thus could not be unambiguously traced back to acoustic landmarks. Our EEG data support this idea. Noise does contain short-term variations, which could be reflected by cortical activations (Barker et al., 2012; Steinmann and Gutschalk, 2012). However, if evoked potentials were due to a passive transmission of acoustic landmarks, all repeated snippets should have been equally signaled. Instead, we found that evoked potentials developed over time, correlated closely with behavior and were consistent with idiosyncratic perceptual learning.

These memory-evoked potentials were interpreted as the superposition of standard N1-P2 complexes. The N1-P2 complex has been associated to perceptual changes within constant-amplitude stimuli (Krumbholz et al., 2003), and it can be modulated by repeated exposure (Ross et al., 2013; Tremblay et al., 2014). Here, we demonstrated not only a modulation of N1-P2 on a much faster time scale, but also, the appearance of such an ERP where there was none before learning. As the planum temporale is one of the cortical sources of the N1-P2 complex (Näätänen and Picton, 1987), our results also advocates for a role of this secondary auditory structure in rapid plasticity and sensory memory. This is consistent with fMRI results using a noise-learning paradigm (Kumar et al., 2014) or, more classically, with mismatch-negativity studies (Berti et al., 2000; Näätänen et al., 2005).

Computationally, the learning of discriminant patterns within noise could be achieved through established plasticity mechanisms such as spike-time dependent plasticity (STDP). In STDP models, repeated exposure to random afferent patterns almost inevitably leads to pattern-specific selectivity, at the single-neuron (Masquelier et al., 2008) or small-network level (Klampfl and Maass, 2013). Experimentally, however, we recorded ERPs on scalp electrodes, which must involve relatively broad neural networks. So, was the code local or global? A possibility is that the scalp potentials were the outcome of a cascade of neural events, initially triggered by a sparse mnesic trace (Hromádka et al., 2008) and then amplified by perceptual awareness (Dehaene et al., 2006). Indeed, perceptual awareness of a target tone embedded within a stochastic masker is associated with an N1-like ERP (Gutschalk et al., 2008). So, even if our experimental measure was at the network level, we argue that altogether the data and model argue for a highly local neural code for experience-dependent changes induced by the perceptual learning of noise.

Functionally, sharp neural selectivity to past sensory experiences would help the auditory system distinguish previously heard sounds from truly novel ones. More generally, it could aid learning about frequently encountered natural sounds. In this respect, the

search for generic timbre dimensions useful for the identification of sound sources has proven surprisingly elusive (Agus et al., 2010; Leaver and Rauschecker, 2010; Patil et al., 2012). The present results suggest that this may be because source identification is shaped as much by idiosyncratic experience as by acoustic properties.

Experimental procedure

A brief description of experimental procedures can be found in the Results section. A complete description can be found in the Supplemental Experimental Procedures.

Supplemental Information

Participants

Fourteen (n=14) naive volunteers participated in Experiment 1 (age: 18-30 years, 10 females), and thirteen (n=13) different naive listeners participated in Experiment 2 (age: 18-26 years, 10 females). In Experiment 2, one subject was discarded due to a large proportion of artifacts in the EEG signal (see below). All participants had self-reported normal hearing. They sat with eyes closed, and were asked to report within-trial repetitions of a noise snippet (Experiment 1, see below) or amplitude-modulated sections within running noise (Experiment 2, see below). They responded through response buttons placed in their right and left hands (Experiment 1) or with a single response button (Experiment 2). The experimental protocols were approved by the local ethical committee (Conseil d'Evaluation Ethique pour les Recherches en Santé, University Paris Descartes, Paris, France).

Psychophysics

We used variants of the "noise-memory" paradigm, introduced by Agus et al. (Agus et al., 2010).

Experiment 1 (main experiment): Participants were asked to discriminate between sequences of continuously running white noise and sequences that contained seamless concatenations of the same, frozen noise snippet. There were three types of stimuli: (1) continuous running Noise (N) that contained no reoccurring patterns within or across trials, (2) Repeated Noises (RN) for which snippets of frozen noise were repeated within trials but not across trials and (3) Reference Repeated Noise (RefRN) for which fragments of frozen noise were repeated within and across trials. Noises were generated as sequences of normally distributed random numbers at a sample-rate of 44.1 kHz and a 16-bit amplitude resolution. Repeated snippets were seamlessly concatenated: noise snippets could be truncated or concatenated without introducing acoustical discontinuities because white noise (uniquely) lacks sample-to-sample correlations. Sounds were presented with Matlab (MathWorks Inc. Natick, MA, USA), using the Psychophysics Toolbox extensions (Brainard, 1997) and were played through headphones (Sennheiser HD 380 250 linear 2, Omega (Lexicon) sound-card) at 60dBA. There were two parts in the experiment, which differed only in terms of the details of the stimulus structure.

Diffuse condition: In half of the experiment, we used noise stimuli similar to those of previous studies (Agus et al., 2010; Agus and Pressnitzer, 2013; Luo et al., 2013). N stimuli consisted of 1.5s of randomly generated white-noise (n1 and n2 in Figure 8-1A, left). Snippets of noise lasting 0.5s were generated in the same manner (targets T1, T2 and T3 in Figure 8-1A, left), each presented 3 times in a continuous sequence, with no intervening silences, to form the RN and RefRN conditions. The RN and RefRN conditions differed only in that the same 0.5s noise target was used for all RefRN trials within a block (n=16) while a different target was generated and concatenated for each RN trial (n=16). The proportion of trials with and without within-trial repetitions were matched within a block: there were 32 N trials, 16 RN trials, and 16 RefRN trials. A temporal jitter of 2-3s was imposed between stimulus presentations to give participants

enough time to respond to the stimuli. Participants were asked to indicate the presence or absence of repetitions through lateralized hand responses (left vs. right). For each individual, the hand used to signify repetitions remained constant throughout the whole experiment, but which hand was used was counterbalanced across subjects. Each participant performed three (n=3) blocks with diffuse stimuli. Therefore, the participants were presented 3 RefRN each to learn. These RefRNs were different for all participants.

Compact condition: In the other half of Experiment 1, the types of condition (RefRN, RN and N) remained the same, but the stimuli's structure was changed to constrain the time window over which repetition detection and perceptual learning could occur: only 0.2s of white noise (target epochs) was repeated within each 0.5s time window. In between repetitions, 0.3s of ever-changing white-noise fillers were concatenated (see Figure 8-1A, right). The advantage of this structure is that the repetition epoch is still 0.5s, thus keeping the task relatively constant relative to the diffuse condition from the subject's point of view. However, repetitions were harder to detect for this compact structure as only two-fifths of each epoch were actually repeated. Based on pilot experiments (not shown) aimed at matching the difficulty of the tasks, the number of repetitions was increased from 3 to 5 for the compact stimuli, so the duration of all stimuli was increased from 1.5s to 2.5s. The other parameters (number of trials per condition and the number of blocks) were the same as for the diffuse stimuli.

Experiment 2 (diverted attention): In Experiment 1, listeners were instructed to detect repetitions within noise. This could have encouraged them to pay more attention to the repeated stimuli compared to the unrepeated ones. In addition, over the course of the experiment, listeners could have learnt the temporal structure of trials and rhythmically modulated their attention accordingly. Thus, at least part of the MEPs could have been caused by attentional modulation of ongoing EEG activity, and not by memory per se. We tested this hypothesis in Experiment 2 by minimizing the attentional focus on target noise snippets. The repeated noise snippets had the same temporal structure as the RN or RefRN trials of the "compact" condition (Figure S 8-2A). However, they were now embedded within a continuous running noise, at random times, rather than presented in isolation. Thirteen new naive listeners were recruited, who had never been exposed to repeated noise, and who were not told about the presence of repeated noise in the experiment. Instead of a repetition-detection task, listeners were now instructed to report short bursts of amplitude-modulation (AmN) occurring randomly in the continuous noise. Such a distracting task minimized endogenous attention to RN or RefRN sequences. In addition, and unlike any previous variation of the noise-memory paradigm, there was not even a sound-onset cue to signal that a new "learnable" sequence had begun, thus removing endogenous and exogenous attentional cues altogether. RefRN and RN stimuli were not played over successive trials separated by silence, but were rather embedded in continuous running white noise, to obtain a constant-amplitude stimulus for 8mn (except for AmN sequences, see below). Finally, as RefRN, RN, and AmN were separated by a random time-jitter of 4 s to 7.5 s, listeners could hardly anticipate the occurrence of any of these specific events.

AmN were constructed by multiplying 0.5s of the running white noise background with a 40-Hz sinusoid at a modulation depth of 20%. AmN sequences represented a clear perceptual change and were easy to detect. The AmN sequences never occurred simultaneously to RN or RefRN sequences. Each participant performed 9 blocks containing one RefRN repeated 24 times and 24 different RN. In addition, there were 24 AmN per block. Each block lasted about 8 minutes. Participants were allowed a break between blocks and at mid-block. They were asked to remain with eye-lids closed during

the presentation of sounds. Stimuli were played through headphones (Bayer DT 770 Pro, AudioFire Echo sound card) using the Psychophysics Toolbox (Brainard, 1997).

Peripheral auditory model

We ran the compact repeated stimuli (RN/RefRN) and non-repeated stimuli (N) through a peripheral auditory model. We used a standard Spectro-Temporal Excitation Pattern approach (STEP, [39]). First, the sounds were passed through a bandpass filter simulating outer and middle-ear pre-emphasis, transforming the flat-spectrum white noise into a broad bandpass spectrum. Cochlear frequency analysis was simulated by a bank of linear gammatone filters (N=128 filters). Temporal integration was applied on each filter output by applying half-wave rectification and a 100-Hz lowpass 2nd-order Butterworth filter. Finally, square-root compression was applied to the smoothed signals.

Behavioral data analysis

Experiment 1 (main experiment): Participants' performance was computed across experimental blocks (n=14 participants, 3 blocks diffuse and 3 blocks compact per participant, so 42 blocks total per condition). We computed the sensitivity index d' (Macmillan, 2005) for RefRN and RN independently to quantify the repetition-detection performance (see Equations 1 and 2):

(1) $$d'_{RefRN} = z\left(Hit_{RefRN}\right) - z\left(FA_N\right)$$

(2) $$d'_{RN} = z\left(Hit_{RN}\right) - z\left(FA_N\right)$$

where z(x) corresponds to the z-score for proportion x; HitRefRN corresponds to the proportion of correct responses for RefRN trials,; HitRN corresponds to the proportion of correct responses for RN trials; FAN corresponds to the proportion of incorrect responses for N trials.

Extreme performances (100%/0%) were adjusted to the equivalent of half of a single correct/incorrect response (Macmillan, 2005) to avoid infinite d' values. As a result, perfect performance on RefRN (or RN) led to a d' of 4.31 instead of $+\infty$ (see Figure S 8-1B).

We first extracted reaction times (RTs) as the time lapse between stimulus offset and participant's response for Figure S 8-1A and Figure 8-1C. This allowed comparison between diffuse and compact conditions, which did not have the same duration. There was a negative correlation between d' and RT for RefRN trials (see Figure S 8-1B, Spearman's correlation: diffuse: rho=-0.31, $p<0.05$; compact: rho=-0.40, $p<0.01$; n=42 blocks). Importantly, participants with close-to-perfect d' performance on RefRN (for certain blocks) still showed a sizable reduction in RTs (Figure S 8-1B) compared to N and RN conditions. Given this effect on both correctness (d') and rapidity (RTs), we decided to combine d' and RTs into a single value called "behavioral efficacy". Similar to the Inverse Efficiency Score (IES (Townsend and Ashby, 1978)), our behavioral efficacy was defined as follows:

$$BE_{RefRN} = d'_{RefRN} \times \left(\frac{RT_N}{RT_{RefRN}} \right) \quad (3)$$

$$BE_{RN} = d'_{RN} \times \left(\frac{RT_N}{RT_{RN}} \right) \quad (4)$$

Intuitively, Behavioral efficacy is increased for high d', and if the RTs to the stimulus of interest were faster than the N baseline. Because efficacy requires positive RT values for the N / (Ref)RN ratio, we computed RTs to the onset of the stimuli for this analysis. Behavioral efficacy led to larger effects for RefRN compared to RN than d' alone, particularly in the diffuse case (Figure 8-1C).

Finally, we also checked that differences in performance between RefRN and RN were truly due to perceptual learning of the RefRN, as by chance some RefRN may be particularly easy for the repetition-detection task. Differences between RefRN and RN in correctness and RTs emerged during a block (hence after learning) rather than being present at the beginning of the block (Figure S 8-1A). Statistical testing confirmed that no significant difference was present at the beginning of the block (3 first RN and RefRN trials, $p>0.2$, u-test), but there was a significant improvement in performance by the end (3 last RN and RefRN trials) in the compact case (diffuse: $p=0.05$, compact: $p<0.05$, u-test) and in RT in the diffuse case ($p<0.005$, u-test).

Experiment 2 (diverted attention): participants were asked to detect AmN sounds. We computed the proportions of button presses within a [0, 1.5]s window following the onset of 0.5s-long AmN sequences. In addition we checked whether erroneous button presses would be associated with RefRN or RN sequences in a [0, 3]s window around RefRN or RN onsets. On average, 98% of AmN were correctly detected (SEM: 4%, N=12 participants). Only 0.3 and 0.4 % of RefRN and RN sounds were associated with button presses respectively (SEM: 0.1% and 0.2 %), showing that repeated noise snippets were not confounded with AmN.

EEG analysis for Experiment 1 (main experiment)

EEG recordings and pre-processing

We used high-density electroencephalography (Electrical Geodesic Inc. system, n=65 gel-electrodes referenced to Cz) to record neural activity while listeners performed the behavioral task. Impedances of scalp electrodes were kept below 15kΩ. Data were acquired at a sampling rate of 250 Hz. Continuous data were re-referenced off-line to the averaged mastoids for further analysis. EEG data was preprocessed and analyzed with Matlab (MathWorks Inc. Natick, MA, USA) using a combination of SPM8 (Functional Imaging Laboratory, Univ. College London, London, UK), EEGlab (Delorme and Makeig, 2004) and Fieldtrip (Oostenveld et al., 2011) toolboxes.

EEG data were high-pass filtered (at 0.1 Hz for Figure 8-2 analysis, at 1 Hz for target-locked ERP (Figure 8-3) analysis in order to filter-out stimulus-locked slow potentials

observed in Figure 8-2, see also below) prior to epoching and low-pass filtered at 30 Hz on large epochs ([-10, 10]s around stimulus onset) with two-pass 5th-order Butterworth filters. A notch filter was also applied to reduce line-noise (50 Hz). Data were then epoched from -1 to 5s around sound onset and baseline-corrected ([-500, 0]ms).

Electrode Selection

Electrodes used in Evoked Related Potentials (ERPs) and time-frequency analyses (see Figure 8-2, Figure 8-3, Figure S 8-2 and Figure S 8-3) were selected based on the amplitude of the N1 potential measured at stimulus onset, which corresponds to a transition from silence to white noise (Experiment 1, Figure S 8-3A). We selected the 10 channels (out of 65) showing the most reliable responses to stimulus onset without taking experimental conditions into considerations (t-values computed across participants and all trials: n=14 participants, n=329 to 384 trials per participant). The topography of t-values and the corresponding channels are shown in Figure S 8-3A and correspond to a classical centro-parietal cluster of electrodes (Picton, 2011). All analyses (Experiments 1 and 2) were performed for these auditory electrodes. Spurious trials for which the EEG signal passed an absolute threshold of 150μV on at least one of the selected electrodes were discarded from further analysis.

ERP analysis

Data were also de-noised using joint decorrelation (de Cheveigné and Parra, 2014) by means of the optimization of repeatability across trials. Joint decorrelation was applied, for compact and diffuse conditions separately, using the average ERPs over all trials (RefRN, RN and N trials) as a bias filter for a given participant. The components were sorted according to the power of their means over the total power. Thus, the first components (we selected here the first 10) were characterized by the strongest mean effect relative to overall variability. Data were then averaged by condition (RefRN, RN and N trials separately) and across blocks (n=42) for correct trials only. Statistical differences were assessed between RefRN (or RN) and N conditions using cluster/permutation statistics calculated between blocks on paired t-tests (see below). Significant clusters (Monte-Carlo p-value<0.05) are shown on time-plots as colored lines. ERPs for RefRN and RN in the compact case showed a sequence of negative potentials after each target. We thus further extracted the mean differences between RefRN vs. N and RN vs. N on 200ms windows right after each target (marked with black lines on Figure 8-2D). The corresponding bar graphs showing this post-target effect are displayed on Figure 8-2D inset and statistical differences were assessed trough paired t-tests across blocks (n=42, *: $p<0.05$, **: $p<0.01$, ***: $p<0.005$). We then computed ERPs time-locked to repeated targets and hence during noise presentation. To do so, the EEG signal for all trials was averaged on [-100, 500]ms windows (baseline: [-100, 0]ms) around the central targets' onsets (2nd to 4th target) to avoid onset/offset effects (see Figure 8-2D). Here, the EEG signal was high-passed above 1Hz instead of 0.1Hz prior to epoching to get rid of the slow sustained auditory potentials. Only the 2nd to 4th targets were used here to avoid contaminations from evoked potentials locked to sounds onset and offset.

ERPs curves were smoothed over time (Gaussian kernel) for visual display only (not for statistical analysis, the values prior to smoothing were used) in Figure 8-2, Figure 8-3, Figure 8-4, Figure S 8-2 and Figure S 8-3 with a temporal window of 40 ms for stimulus-locked ERPs and 20 ms for target-locked ERPs.

Time-frequency analysis

We also examined whether the presence of repetitions translated into an increase in Inter-Trial Phase Coherency (ITPC) and Power Response in the time-frequency domain. To do so, the EEG signal was processed as previously described for ERPs but not de-noised through the Joint Decorrelation algorithm. All trials were included (correct and incorrect responses) for the time-frequency analysis. Indeed, ITPC critically depends on the number of trials n (see Equation 7) and focusing on correct trials would have introduced confounds between conditions due to mere differences in the numbers of correct trials across conditions. The EEG signal for a given electrode was decomposed in the time-frequency domain using a Fast Fourier Transform (FFT) on 800 ms windows (with an FFT padding ratio of 4 and on [0, 10]Hz range). The decomposed signal can be expressed with a complex representation, where A(t,f) is the power of the EEG signal and φ(t,f) the phase of the signal s(t,f) at a given time (t) and frequency (f):

$$s_{t,f} = A_{t,f}\left(e^{i?_{t,f}}\right) \tag{5}$$

Power response was computed by averaging across trials the absolute amplitude (At,f, see Equation 6) of the time-frequency decomposition at each time and frequency for a given block and stimulus condition. Power response was expressed as the natural logarithm of power over a baseline computed on a [-1000, -250] ms window.

$$\mathrm{PowerResp}_{t,f} = \log\left(\frac{mean\left(A_{t,f}\right)}{mean\left(A_{baseline,f}\right)}\right) \tag{6}$$

The phase φt,f was similarly extracted at each time sample and frequency. It can be represented as a vector of length (modulus) 1 and angle (argument) φ on a trigonometric circle. ITPC describes how the phase of the EEG signal is reproducible across trials for a given condition (RefRN, RN or N) and at a given sample and a given frequency. ITPC was defined as the average vector length of phase vectors for a given frequency and sample across n trials. In practice, ITPC was computed using Euler's formula:

$$ITPC_{t,f} = \sqrt{(\frac{1}{n}(\sum^{n}\cos(\varphi_{t,f}))^2 + \frac{1}{n}(\sum^{n}\sin(\varphi_{t,f}))^2)} \tag{7}$$

When the signal is perfectly coherent across trials (i.e. same phase across trials whatever the phase value), ITPC equals 1. On the contrary, uniformly distributed phases across trials result in a close-to-zero ITPC for large n. ITPC is therefore restricted to the interval [0, 1]. ITPC was estimated per block for each experimental conditions separately. The number of trials used to estimate ITPC was equalized across trial types for a given block: the condition with the smallest number of trials in a given block was chosen as the reference and the same number of trials were randomly picked for the other, more numerous conditions. Figure 8-2A shows differences (t-value of the difference computed with paired t-tests) in ITPC between RefRN and N conditions for diffuse (left) and compact (right) stimuli across blocks (n=42). Statistical differences were controlled for multiple comparison using a cluster/permutation approach in the time-frequency domain (cluster threshold: $p<0.1$, Monte-Carlo p-value <0.05, n=1000 permutations). In both compact and diffuse conditions, a significant cluster emerged in the low-frequency range

([0.5, 5] Hz). We then focused on this frequency range to extract ITPC and EEG power (Figure 8-2B-C and Figure 8-4B-C). We computed the average ITPC and Power Response on a [0.5, 5]Hz interval across blocks (n=42, see Figure 8-2B) to examine its temporal dynamics. As for the ERP analysis, statistical differences were assessed when comparing ITPC computed on RefRN (or RN) versus N using cluster/permutation statistics (cluster p-value threshold: 0.05, Monte-Carlo p-value: 0.05, n=1000 permutations). Finally, ITPC (Figure 8-2B) and power response (Figure 8-2C) were extracted over the entire stimulus presentation window (diffuse: [0, 1500]ms; compact: [0, 2500]ms) so as to quantify overall differences between conditions (Figure 8-2B and Figure 8-2C, inset). Statistical differences were determined by the means of paired t-tests (n=42 blocks).

Correlation between EEG and behavioral data

We then examined whether the ITPC, EEG power or ERPs in response to repeated patterns in noise could account for the variance in behavioral performance more precisely than simply reflecting trial types. To do so, we looked into the correlation between these markers and behavioral performance within trial types. This analysis was restricted to the compact stimulus structure, as it led to stronger correlates for both phase and evoked potentials (see Figure 8-2). First, we extracted the ITPC per block for RefRN and RN separately ([0.5, 5]Hz on a [0, 2500]ms window for all trials and electrodes selected on N1 amplitude) and correlated it with the behavioral efficacy score (see Equations 3 and 4 and Figure 8-2). Correlation between these two variables were determined across blocks (n=42) using Pearson's method. Similarly, to explore the correlation between evoked potentials and behavioral efficacy, we extracted the amplitude of target-locked ERPs (Figure 8-3A) on a [100, 400]ms window.

We then examined whether the EEG signal could differentiate between conditions at the single-trial level. For this purpose, we applied a logistic regression to the ERP amplitude over time. This method was not applied to ITPC since it cannot be estimated at the single-trial level. In practice, for the same subset of electrodes, the mean voltage amplitude was extracted for each trial from the target-locked ERP (Figure 8-3A, averaged on the 2nd to 4th target and over auditory electrodes) on 50 ms windows from -50 to 450ms after target onset. This voltage was z-scored for each block separately across all conditions and trials and pooled across blocks. We then performed a logistic regression by contrasting trials with repeated noise snippets (RefRN or RN) against trials without repetition (N). The numbers of items per category were counter-balanced. The logistic regression coefficients were used to decode the trial category. To assess the reliability of this decoding, we computed for each time point the mean accuracy of our prediction when compared to the actual trial category. The chance level was determined using the same methodology: 1000 permutations were performed on trial categories and for each permutation and time-point, the corresponding accuracy was estimated. Shaded areas in Figure 8-3C shows the range of decoding values corresponding to 90% of these permutations. Therefore, all values above the shaded area are higher than 95% of random values (non-parametric equivalent to a one-tail p-value <0.05).

EEG analysis for Experiment 2 (diverted attention)

EEG recordings, pre-processing and electrode selection

We used the same system and routine to record EEG (500Hz sampling rate instead of 250Hz). Data pre-processing consisted of a high-pass filter above 0.2Hz and a low-pass filter below 7Hz (two-pass 5th-order Butterworth filters). The low-pass filter cut-off frequency was set at a low value to filter out the alpha rhythm ([8, 11]Hz). Indeed, since participants kept their eyes closed for minutes, the amount of alpha rhythm was high in some participants. A notch filter was also applied to reduce line-noise (50 Hz). Data were then epoched on a [-1, 3.5]s window around RefRN and RN onsets. Electrodes used in ERPs analysis were the same as in Experiment 1 to keep the parameters of our analysis as close as possible. However, comparing with Figure 8-3A, the topography of the evoked activity associated to RefRN and RN trials was slightly more frontal (Figure S 8-2C and Figure S 8-3B). Spurious trials passing an absolute threshold of 150μV on broadband filtered data ([0.2, 30]Hz) and on at least one of the selected electrodes were discarded from further analysis.

ERP analysis

Data were here not de-noised using joint decorrelation (de Cheveigné and Parra, 2014). Indeed, de-noising aims at optimizing the repeatability across trials of the activity time-locked to a particular event. Here, we precisely wanted to investigate whether there was indeed any repeatable activity in the EEG signal associated with snippets embedded in the background noise. To avoid unnecessary confounds, joint decorrelation was therefore not applied. EEG was thus simply averaged by condition (RefRN and RN trials separately) and across blocks (n=101 in 12 participants) on a [-100, 500]ms window around target onsets and after correcting for baseline activity ([-100, 0]ms). Blocks with at least 20 trials (after artifact rejection and out of 24, see above) per conditions were kept for this ERP analysis, leading to the rejection of 16 blocks. One participant (out of 13) was discarded from all EEG analysis since the number of rejected trials was above this threshold in all blocks. Slow drifts were corrected by means of a linear de-trending over 240ms window (de Cheveigné and Parra, 2014). Here we used all targets (1st to 5th). Indeed, targets were embedded in continuous white-noise and unlike Experiment 1, there were no evoked potentials before and after the train of targets (sound onset and offset potentials). All targets could be therefore included in this ERP analysis. Note that the high-pass filter cut-off was here lower (0.2Hz vs. 1Hz) for the same reason (no sustained potentials during targets presentation in Experiment 2).

Statistical differences were assessed between RefRN (or RN) trials and baseline using cluster/permutation statistics calculated between blocks on paired t-tests. Significant clusters (Monte-Carlo p-value<0.05) are shown on time-plots as colored lines (Figure S 8-2B, Figure S 8-3B). For Figure S 8-2B and Figure S 8-3B, ERPs curves were smoothed over time (Gaussian kernel) for display purposes only (for statistical analysis, the values prior to smoothing were used) with a temporal window of 20 ms, as in Figure 8-3. Scalp topographies in Figure S 8-2C and Figure S 8-3B, were obtained by extracting the t-values of paired t-tests (RefRN vs. baseline or RN vs. baseline, across blocks) on a [200, 300]ms post-target onset window in Figure S 8-3B and on 100ms windows centered around the peak of the ERP for the corresponding target and condition in Figure S 8-2C. The center of the time-window used in the topographies of Figure S 8-2C are displayed on each topography. Non-significant t-values (p>0.05, uncorrected) were set to 0.

In order to compare MEPs obtained in RefRN and RN trials in both experiment, we computed the corresponding temporal profiles and scalp topographies (computed as in Figure 8-3A and Figure S 8-3B for experiment 1 and 2 respectively). We then normalized the amplitude of the MEPs across electrodes for scalp topographies (z-score across

sensors for each participant separately) and across time for temporal profiles (MEP normalized by the average amplitude on a [200, 300]ms window and baseline corrected between [-100, 0]ms). The corresponding normalized MEPs are shown in Figure S 8-3C. No significant difference were found between the RefRN and RN temporal profiles and topographical maps for both experiments.

Overall, in this Experiment 2, clear ERPs were observed, which were remarkably similar to the ERPs obtained when listeners actively performed the repetition task, both in temporal profile and topography. Strikingly, significant ERPs were observed right from the first noise target presentation within RefRN sequences (Figure S 8-2B). Such an ERP therefore occurred without any amplitude discontinuity in the noise, at a totally unpredictable time for the listener, and without having to be actively reported. Even though the distracting task does not imply that listeners were not paying attention to other, task-irrelevant parts the noise, this could not explain the ERPs: without learning, the repeated sequences and their first epochs were rigorously impossible to locate. Therefore, the evoked-potential could not have been causally and solely induced by attentional modulation.

Simulation

We hypothesized that, once learnt, noise snippets would be processed in such way that they would trigger evoked potentials, the so-called Memory-Evoked Potentials (MEPs). In our hypothesis, MEPs would account for all neural correlates of perceptual learning described earlier (ERPs and ITPC). We tested the validity of this statement with simulated data reproducing the experimental conditions of Experiment 1. In our simple model, when a snippet of noise is repeated, rapid neural plasticity would introduce a selectivity for a given pattern within it. This pattern in noise would thereafter elicit auditory potentials. Here we chose a N1-P2 complex as the evoked potential (see Discussion). In order to examine whether such evoked potentials could account for both our ERP and ITCP results, we implemented this simple model using synthetic EEG data.

Background EEG activity was synthesized in order to mimic human EEG spectrum at rest (adapted from (Yeung et al., 2007)). In short, more than 200 sinusoids were summed with frequencies ranging from 0 to 30Hz and amplitude matching a power profile similar to human EEG (see gray curve in Figure 8-4A). This background EEG was then perturbed by the presentation of noise stimuli following the compact and diffuse stimulus structures (16 N, 16 RefRN and 16 RN per simulation run, equivalent to an experimental block). Our model being an additive model, we simply added evoked potentials to the background EEG. First, stimulus-locked potentials were added for all stimuli (RefRN, RN and N). These potentials were composed of canonical P1-N1-P2 complexes (see Equation 8) injected at stimulus onset and offset along with a sustained potential (SustPot, see Equation 9) in between, in order to mimic EEG response to sounds (see Figure 8-2D). They were modeled as follows:

$$P1/N1/P2 = \frac{\exp\left(-a\left(x - t_{P1}\right)^2\right)}{b} - \exp\left(-c\left(x - t_{N1}\right)^2\right) + \frac{\exp\left(-d\left(x - t_{P2}\right)^2\right)}{e} \quad (8)$$

where x $\in$ [0, 500]ms, tP1=50ms, tN1=180ms, tP2=200ms, a=10000, b=5, c=200, d=106, e=1.8.

$$SustPot_{x\in[0.2,t1max]s} = \frac{1}{\log(x+t1)}$$

$$SustPot_{x\in[t1max,t2max]s} = \frac{a}{1+\exp\left(-b\left(x-t2\right)\right)} + SustPot_{t1max} \quad (9)$$

where t2max=1500ms, t1max=400ms, t1=1400ms, t2=200ms, a=1.4, b=30 for the diffuse case; t2max=2500ms, t1max=400ms, t1=1400ms, t2=200ms, a=1.4, b=30 for the compact case.

The resultant is plotted in blue in Figure 8-4A (diffuse case). Second, memory-locked potentials were injected for RefRN and RN trials for each repeated target after its first presentation (case of a perfect observer and learner). For RN, this corresponds to the second target of every trial, for RefRN to the second target of the first trial within a given simulation run. These MEPs were modeled as a N1-P2 complex:

$$N1/P2 = \exp\left(-c\left(x-t_{N1}\right)^2\right) + \frac{\exp\left(-d\left(x-t_{P2}\right)^2\right)}{e} \quad (10)$$

where x ∈ [0, 500]ms, tN1=180ms, tP2=200ms, c=200, d=106, e=1.8.

The resultant is plotted in red in Figure 8-4A for three repetitions of a learnt target. Importantly, for a given target, the onset of the N1/P2 complex was randomly chosen (uniform distribution) over the entire length of the target (0.2s for compact, 0.5s for diffuse conditions) with respect to target onset. However, this timing was held constant for a particular target as illustrated in Figure 8-4A (right). As a consequence, MEPs were injected at a fixed interval (0.5s) during a given noise containing repeated snippets. In addition, the timing of these MEPs would differ from trial to trial in the RN type but not for RefRN trials within a simulation run (block). Finally, in the diffuse case and across blocks, MEP-onsets would spread over half a second (length of a repeated target) while they would be constrained to 200ms windows in the compact case.

Once our synthetic data set had been simulated (42 simulation runs equivalent to experimental blocks in Experiment 1), we performed the exact same analysis as described above for ERPs, Power Response and IPTC analysis to the exception that here only one EEG channel was synthesized. Statistical analyses were also kept identical. Results are shown in Figure 8-4. Note that by considering an ideal observer and learner, our model did not feature any randomness except from ongoing background EEG and onset of MEPs. In particular, our model did not implement imperfect performance in repetition-detection and learning. Yet, all experimental results were replicated. One aspect of the model, replicating the data but perhaps less intuitively obvious, is the lack of effect in average power responses (Figure 8-2C), combined with a significant correlation between power and BE (Figure 8-3B). In an additive model, memory-evoked potentials should be reflected in EEG power. Manipulating the Signal-to-Noise Ratio in our model confirmed significant effects in power, but at a higher signal-to-noise ratio than the one extracted from our empirical data set.

Indeed, the relative amplitude of the N1/P2 complex compared to the amplitude of the background EEG signal (Signal-to-Noise Ratio, SNR) appeared to substantially influence the emergence of phase coherence, power response or ERPs associated to RefRN and RN (see Figure S 8-4). For our simulated data set as analyzed in Figure 8-4, we tried to remain as close as possible to our EEG recordings. To do so we chose the SNR of the

simulated data set that matched as closely as possible the SNR of our empirical data set. To estimate our empirical SNR, we extracted the magnitude of the difference between RefRN and N conditions in the target-locked ERPs (Figure 8-3A). More precisely, we extracted the t-value of the difference between RefRN and N target-locked ERPs (compact stimuli, ERPs averaged over a [100, 400]ms window) in our EEG data set by means of a paired t-test across blocks. Then, we estimated the SNR of simulated data sets (42 simulation runs per data set) at different SNR levels (20 iterations per SNR level, SNR from 0.1 (low) to 2 (high)). For each simulated data set, the magnitude of the ERP effect was estimated similarly to the EEG data as explained above. Figure S 8-4A (right) shows the t-values computed at the different SNR levels (orange curve) as well as the empirical t-value (blue dashed line). A SNR of 1.8 (black vertical line of Figure S 8-4) appeared to match the empirical SNR best and was used in Figure 8-4.

Following the same principle, we also examined the influence of the SNR on ITPC and power response effects in our simulation. To do so, we computed the effect sizes of the differences between RefRN vs. N (orange), RN vs. N (blue) and RefRN vs. RN (green) conditions in the ITPC, ERPs and power response analysis at different SNR (Figure S 8-1, 42 simulation runs per iteration, 20 iterations per SNR level). For ERPs, we replicated the operations described in the previous paragraph (in the diffuse case, the ERP amplitude was extracted on a [500, 1500]ms window after stimulus onset). For ITPC and Power Response, we extracted the averaged ITPC/Power Response for low frequencies ([0.5, 5]Hz) and over the entire stimulus presentation window (diffuse: [0, 1500]ms, compact: [0, 2500]ms) for each block and trial type. We then computed the t-values corresponding to the comparisons (paired t-tests across 42 simulation runs) between RefRN vs. N, RN vs. N and RefRN vs. RN conditions for each SNR (20 t-values for each SNR level). Effects in EEG power emerged at high SNR (SNR>3, $p<0.05$) in accordance with the additive nature of our model.

Statistics

Non-parametric statistics were used (Wilcoxon rank-test (u-test) to compare conditions, Friedman test for analyses of variance, and Spearman's method for correlations) when data were not normally distributed; parametric statistics were used otherwise (Student t-test to compare conditions, ANOVAs for analyses of variance, Pearson's method for correlations). Normality was checked by means of a Kolmogorov-Smirnov test.

To correct for multiple comparisons, we used a cluster-permutation statistics approach (Maris and Oostenveld, 2007). This approach aims at dealing with the issue of multiple comparisons in a principled manner. Each cluster was constituted by the samples (in a 1D (time-plots) or 2D (time-frequency) space) that consecutively passed a specified threshold (here, $p<0.05$ except for Figure 8-2A time-frequency cluster/permutation: $p<0.1$). The cluster statistics were chosen as the sum of the t-values of all the samples within the cluster. Then, we compared the cluster statistics of each cluster with the maximum cluster statistics of 1000 random permutations. We displayed on the Figure 8-2 to Figure 8-4 (colored lines on time-plots, unmasked sample on time-frequency plots) the significant clusters that passed a threshold Monte-Carlo p-value of 0.05.

Supplemental Figures

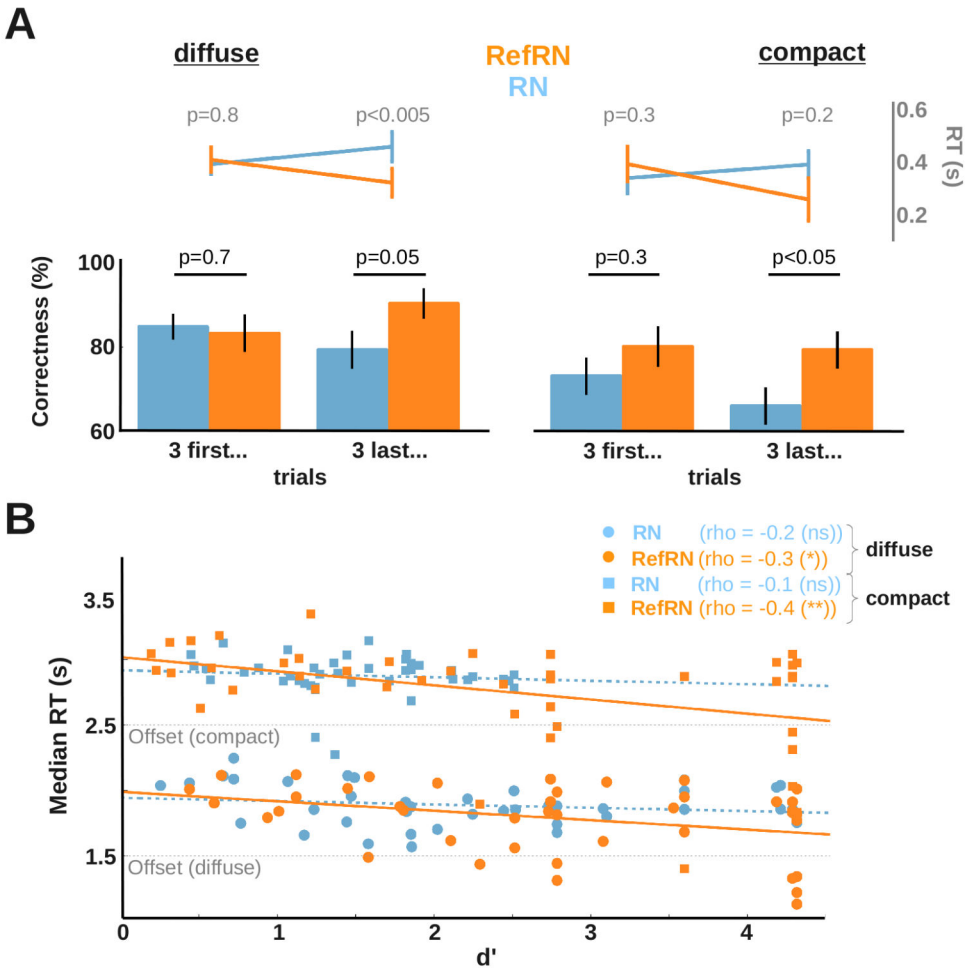

Figure S 8-1 Further behavioral characteristics of perceptual learning

A: Percent correct (bottom) and reaction times (RTs, top) in repetition detection for both stimulus conditions (left: diffuse, right: compact structures), computed at the beginning (first 3 trials) and end (last 3 trials) of each block (n=42). Bars denote standard errors of the mean (SEM) across blocks. The p-values for the comparison between RefRN and RN are paired u-tests. RTs were computed from stimulus offset, to better compare compact and diffuse conditions that had different stimulus durations The difference between RN and RefRN only arises at the end of the block, after learning. B: Correlation between median reaction times (RTs) and d' computed across blocks (n=42 for compact (squares) and diffuse stimuli (circles)). Here, RTs were computed from stimuli onset. Stimuli offsets are shown with black dotted lines (diffuse: 1.5s, compact: 2.5s). Correlation was assessed by means of the Spearman's rank correlation method for RefRN (orange) and RN (blue) and for each condition separately. Corresponding Spearman's rho and significance levels (ns: $p>0.05$, *: $p<0.05$; **: $p<0.01$) are displayed. Note the negative correlation between median RT and performances, for RefRN only.

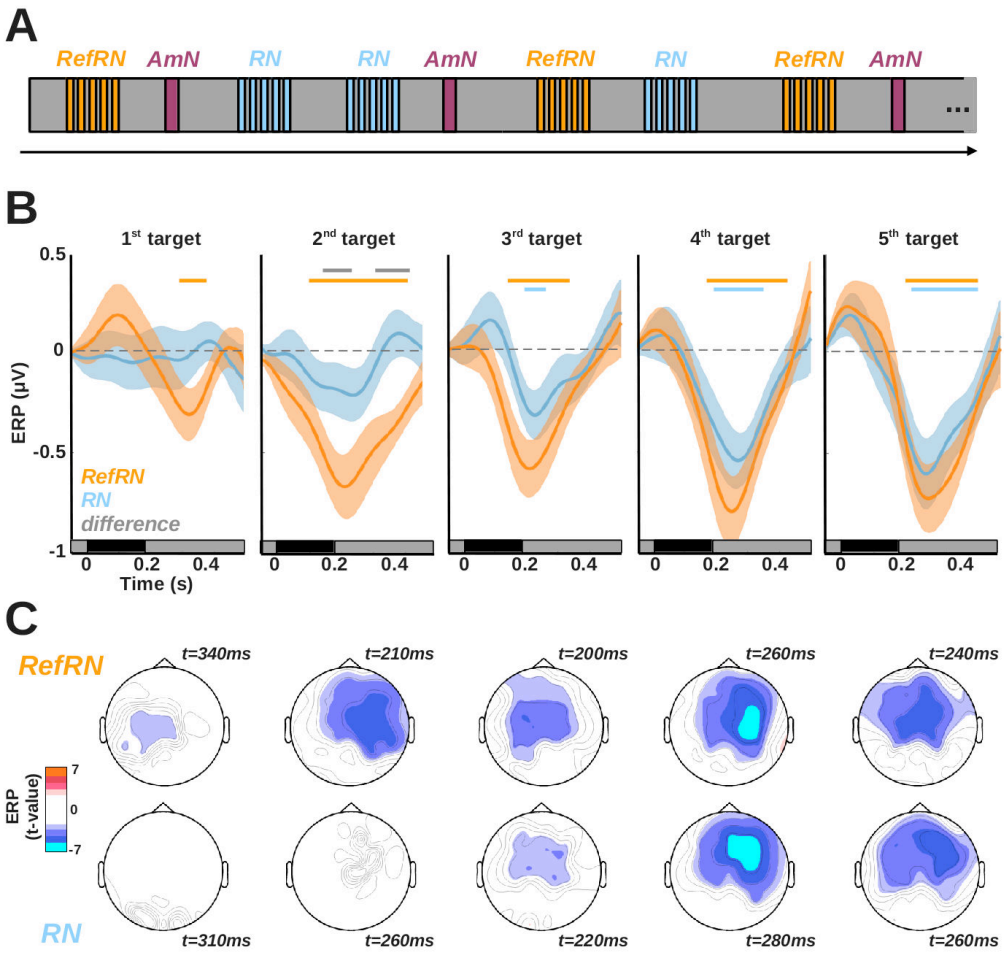

Figure S 8-2 Evoked potentials with diverted attention and continuous stimulation

A: Stimuli and experimental design for the experiment with diverted attention. Here, RefRN and RN sequences (same structure as "compact" stimuli in the main experiment) were embedded at random times within a continuous running white noise, with no discontinuity in either amplitude or short-term statistics. Participants were not informed about RefRN nor RN. Rather, they were instructed to detect short bursts of amplitude modulation imposed on the running noise (AmN, modulation frequency: 40Hz, depth: 20%, duration: 0.5s). B: ERP time-courses (top) computed for each target position (1st to 5th) for RefRN and RN trials (n=101 blocks in 12 participants). Shaded areas around curves indicate standard errors of the mean (SEM) across blocks (n=101). Colored lines indicate significant clusters when comparing RefRN (orange) and RN (blue) with baseline (0), or RefRN with RN (gray) (Monte-Carlo p-value<0.05, cluster-permutation). C: Topographical maps of the differences between RefRN (or RN) and baseline (0) were expressed as t-values (paired t-tests, 100ms windows centered around the negative peak of the ERP as computed above, the center of the window is detailed for each map). Non-significant t-values (p>0.05, uncorrected) were set to white.

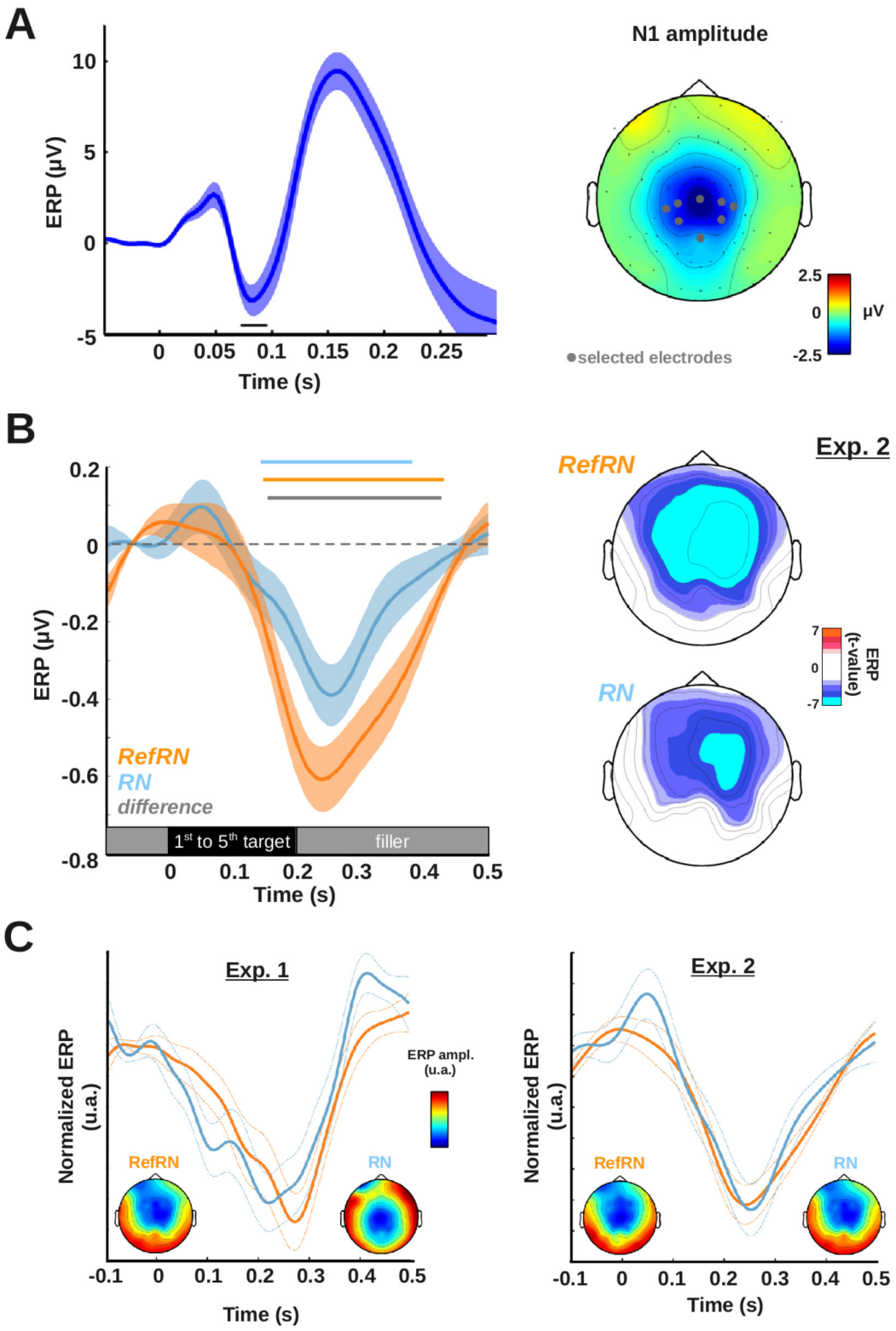

Figure S 8-3: Further characteristics of memory-evoked potentials and comparison with standard auditory evoked-potentials

A: Auditory Evoked Potentials (AEPs, left) locked on stimulus onset and computed across subjects (n=14) for all trials in the main experiment. A clear N1 is observed at around 90ms. The black vertical line shows the time window used to extract N1 amplitude (72-96ms). The time curve was smoothed using a Gaussian kernel of 40ms for display purposes only. Right: Topography of N1 amplitude. A large centro-parietal negativity is observed, typical of auditory

responses. Gray circles show the electrodes with the most consistent N1 (10 lowest t-values computed with two-sided t-tests comparing the ERP amplitude between [72, 96]ms and a [-50, 0]ms baseline across participants). Those electrodes were defined as auditory channels and used for the analyses of Figure 8-2, Figure 8-3, Figure S 8-2, Figure S 8-3. B: In the diverted attention experiment, ERPs (left) were averaged across repetitions ([-100, 500]ms window, 1st to 5th within-trial target occurrences) and blocks (n=101 blocks in 12 participants, see Supp. Procedures). Note the similarity with Figure 8-3. Colored lines indicate significant clusters when comparing RefRN (orange) and RN (blue) with baseline (0), or RefRN with RN (gray) (Monte-Carlo p-value<0.05, cluster-permutation). Right: Topographical maps of the differences between RefRN (or RN) and baseline (0) expressed as t-values (paired t-tests on averaged ERP amplitude extracted over a [200, 300]ms window). Non-significant t-values (p>0.05, uncorrected) were set to white. C: The amplitude of MEP was normalized for each condition and experiment independently. After normalization, the time-course and scalp topographies of MEPs were identical (no significant difference) for RefRN and RN, suggesting identical underlying neural mechanisms. Shaded-areas (A-B) and dashed lines (C) show standard errors of the mean (SEM) across blocks (B-C, n=101) or participants (A, n=14).

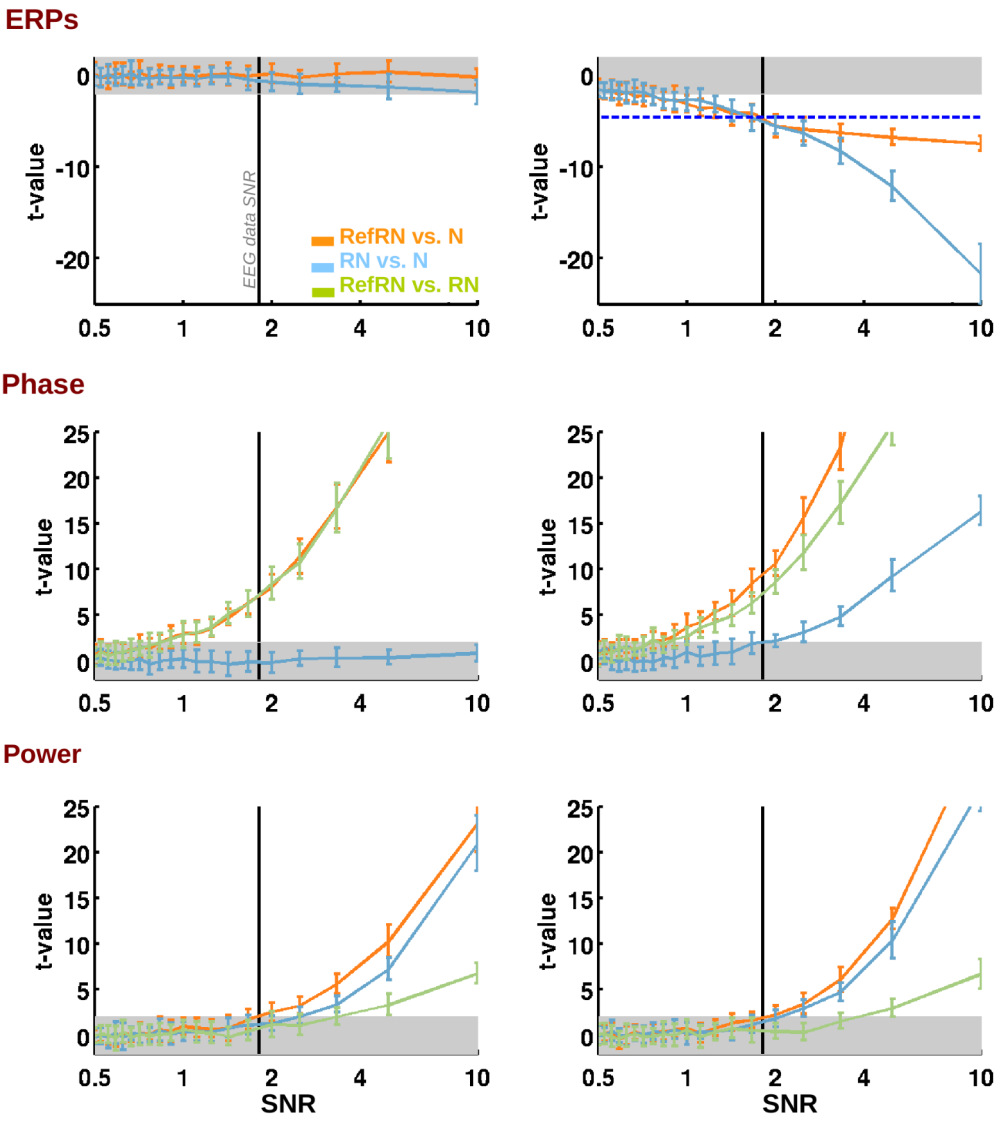

Figure S 8-4 Effect sizes for ERP, ITPC and Power Response in simulated data at different signal-to-noise ratios

Effect sizes were computed on simulated data, as described in the Supp. Procedures, but for different levels of signal-to-noise ratio (SNR, n=20 iterations for each SNR). The left column shows the results for the diffuse condition and the right column for the compact condition. The t-values were computed by means of a paired t-test across simulated runs (n=42 for each iteration) between RefRN and N conditions (orange), RN and N (blue) and RefRN and RN (green). The gray shaded areas show the non-significant interval of t-values (p>0.05, n=42 simulation runs). The black vertical solid line shows the SNR used in Figure 8-4 corresponding to the ERP effect size extracted from our empirical data (blue dashed line on top right panel). Note the absence of ERP effect in the diffuse case even for large SNR. ITPC effects were significant at lower SNR rate than Power Response effects (e.g. for SNR=1.8, significant effect for ITPC but not power, see also Figure 8-4). Error-bars denote the standard-error of the mean (SEM) computed across 20 simulated iterations for each SNR level.

Study 9:
Formation and suppression of novel acoustic memories in human sleep

Andrillon, Thomas[1-2]; Pressnitzer, Daniel[3]; Léger, Damien[4] & Kouider, Sid[1]

[1] *Brain and Consciousness Group, École Normale Supérieure Paris, France*

[2] *École Doctorale Cerveau Cognition Comportement, Université Pierre et Marie Curie Paris, France*

[3] *Laboratoire des Systèmes Perceptifs, École Normale Supérieure Paris, France*

[4] *Centre du Sommeil et de la Vigilance, Université Paris Descartes, Hôtel Dieu, Paris, France*

Summary

There is extensive evidence that sleep promotes the consolidation of existing memories. Yet, whether new memory representations can be formed during sleep remains unclear. Here, to track the formation of novel memories during human sleep, we used electroencephalographic (EEG) markers of perceptual learning for acoustic noise. In REM-sleep and light NREM-sleep, repeated exposure to novel noises led to EEG markers of perceptual learning. In addition, the learning occurring in REM-sleep, and especially tonic REM-sleep, led to subsequent performance improvements in wakefulness. In deep NREM-sleep, the effects of repeated exposure were strikingly different: EEG indexes of learning observed in lighter NREM stages were absent and subsequent perceptual learning in wakefulness was specifically impaired for those sounds heard during NREM-sleep. This suppressive effect was associated with slow-waves. Overall, new memory traces can be either formed or suppressed depending on sleep stage, suggesting an interplay between synaptic potentiation and down-scaling during sleep.

Introduction

Humans typically spend a third of their time sleeping (Kleitman, 1987). Taking advantage of this apparent idle time to learn new information has turned from an ancient fantasy (Huxley, 1932) to a scientific quest (Bruce et al., 1970). An abundant literature has already demonstrated the importance of sleep in the consolidation of existing memories (Diekelmann and Born, 2010; P Peigneux et al., 2001; Rasch and Born, 2013; Walker and Stickgold, 2006). However, the learning of novel information during sleep has proven difficult to establish, even when such information would be easily learnt during wakefulness (Bruce et al., 1970; Emmons and Simon, 1956; Wood et al., 1992). Indeed, successful demonstrations tended to be restricted to hippocampal-independent forms of learning, such as fear- or delay-conditioning (Beh and Barratt, 1965; Fifer et al., 2010; Ikeda and Morotomi, 1996; Maho and Hennevin, 2002), which are rudimentary enough to be implemented by basic neural networks (Carew and Sahley, 1986). Attempts to probe more complex forms of sleep-learning, e.g. situations requiring hippocampal structures, have often led to null results (Hennevin et al., 2007; Simon and Emmons, 1956; Wood et al., 1992).

A common interpretation is that the difficulty to learn novel information during sleep is due to a blockade of sensory information at the thalamic level (McCormick and Bal, 1994). Learning, as a consequence, would be prevented by the unavailability of sensory information in structures fed by thalamic relays. Indeed, the few notable exceptions having demonstrated hippocampus-dependent (Arzi et al., 2014, 2012)earning in sleep have bypassed thalamic relays. These studies relied either on olfactive information that does not transit through the thalamus (Arzi et al., 2014, 2012), or on endogenously generated activations (de Lavilléon et al., 2015), or on direct stimulations of hippocampal cells (Maho and Bloch, 1992).

However, while sensory information can be indeed blocked at the thalamic level in Non-Rapid Eye-Movement (NREM) sleep, this blockade seems restricted to the co-occurrence of sleep-spindles or periods of neuronal silencing (Schabus et al., 2012). In fact, sensory encoding in primary cortices turns out to be remarkably preserved during NREM and REM-sleep (Issa and Wang, 2008; Y. Nir et al., 2013). From a functional perspective, many aspects of sensory processing remain conserved in the sleeping brain: sounds deviating from standards can be detected (Sculthorpe et al., 2009; Strauss et al., 2015) and even higher-level information such as the semantic meaning of words can be extracted (Brualla et al., 1998; Ibanez et al., 2006). Recently, we found that not only can sensory information be processed up to the semantic level, but also that this information can be routed to non-sensory areas dealing with motor preparation (Kouider et al., 2014).

If sensory information can reach the cortex and if it can be successfully processed at various levels of representation during sleep, why is this information not remembered? One potential explanation could be that memory systems are mainly engaged in consolidation of existing memories, and thus decoupled from the thalamocortical loops conveying external information (Diekelmann and Born, 2010). Beside the impairment of memory at the systemic level, it has also been hypothesized that sleep, and especially NREM-sleep, was unfavorable to learning at the synaptic level (Tononi and Cirelli, 2014). Specifically, the decrease of Acetylcholine (ACh) during NREM-sleep would impair synaptic plasticity (Pawlak, 2010; Seol et al., 2007). One crucial prediction of this hypothesis is that low-level of ACh would prevent learning in NREM-sleep, even when the processing of sensory information is preserved. In REM-sleep, which is characterized

by higher levels of ACh (Jones, 2005), learning may be possible whenever sensory disconnection can be overcome.

To address all of these open questions, we investigated the perceptual learning of acoustic noise (Agus et al., 2010) during different sleep stages. The learning of noise is a challenging task: participants have to detect seamlessly embedded repeating patterns within fully random sounds (Figure 9-1). Nevertheless, during wakefulness, performance increases with exposure to a particular pattern, reflecting a powerful form of perceptual learning (Agus et al., 2010; Agus and Pressnitzer, 2013). The paradigm has several useful characteristics for the present purposes. First, the noise patterns to be learnt are guaranteed to have never been heard before, thus targeting the formation of novel memories rather than consolidation. Second, this form of learning is unsupervised and was observed even in the absence of directed attention (Andrillon et al., 2015a; Luo et al., 2013), so it has a chance to appear during sleep. Third, EEG markers of learning, closely correlated to behavior, have been found during wakefulness (Andrillon et al., 2015a), so learning can be assessed during sleep. Finally, and importantly, this form of complex learning reflects hippocampal-dependent memory, as it recruits a network including hippocampal structures together with sensory cortices (Kumar et al., 2014).

By using the EEG markers during sleep, we show that sleepers learn novel noises in light NREM sleep and REM sleep. Moreover, the noises learnt during REM-sleep were better discriminated upon subsequent wakefulness. Strikingly, we show that the exact same exposure during deep NREM sleep had opposite effects: upon subsequent awakening, the noises heard during NREM sleep were considerably more difficult to learn than novel noises. We could track the plasticity processes to specific sleep events: the positive effect of learning during REM-sleep was driven by phases of tonic REM-sleep (i.e. without Rapid Eye-Movements), while the negative effect of NREM-sleep was driven by the amount of slow-waves. These results are consistent with the notion that REM-sleep and lighter stages of NREM-sleep are accompanied by synaptic potentiation, while deep NREM sleep causes synaptic down-scaling.

Results

The noise-memory paradigm

In this study we used a variant of the noise-memory paradigm (Agus et al., 2010). Our protocol was divided in three separate phases (Figure 9-1). In the "wake-learning" phase, participants (N = 20) were asked to discriminate acoustic white noise (N stimuli) from white noise with embedded repeated patterns, those patterns being simply "frozen" snippets of white noise (RefRN and RN stimuli). Each participant was exposed to 5 different targets that repeated within trials and also reoccurred across trials (RefRN targets), along targets that only repeated within trials (RN targets). A higher target-detection performance for RefRN (within and across-trials repetitions) relative to RN (within-trial repetitions only) indicates perceptual learning (Agus et al., 2010; Agus and Pressnitzer, 2013; Andrillon et al., 2015a). In the "sleep-learning" phase, participants were authorized to sleep. When sleeping, they were exposed to similarly structured albeit longer stimuli (see Methods).

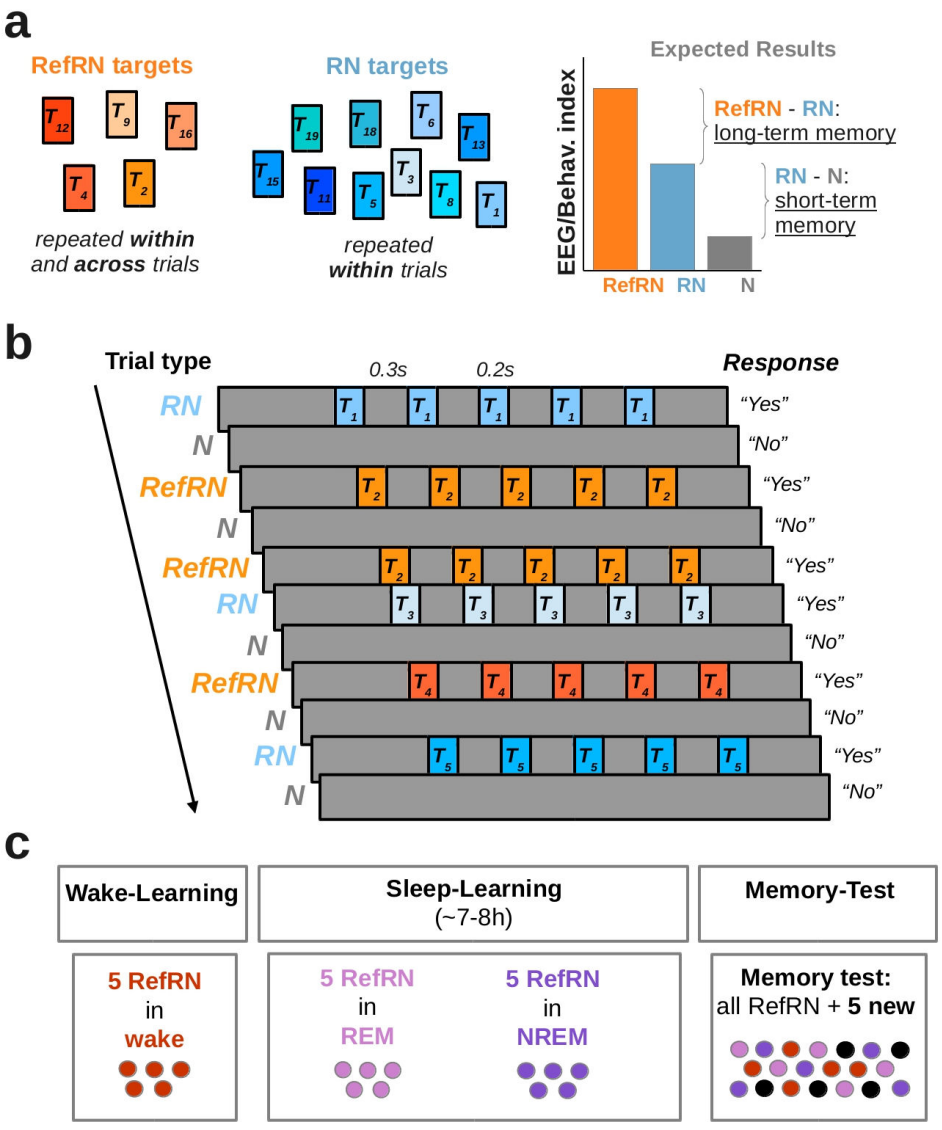

Figure 9-1 Noise memory paradigm in wake and sleep

(a-b) Stimuli and expected results. Participants (N = 20) were instructed to discriminate between trials made of running white noise (N) and trials that contained a repeated pattern, made by the seamless concatenation of short (0.2s) noise segments (targets) interleaved with 0.3s fresh white-noise fillers. Most targets were presented in one trial and one trial only (RN: within-trial repetition). Unknown to listeners, a small number of targets was recurrently presented across trials (RefRN, within and across-trial repetition). RefRN and RN had identical structure. They differed only regarding to the amount of exposure to the target. Participants' ability to discriminate RN from N trials evidences short-term memory for the novel repeated target. A better discrimination for RefRN compared to RN trials additionally indicates longer-term memory processes (panel a, right). In panel b, the left column shows an example of successive trial conditions and the right column shows expected responses. "YES" and "NO" responses were balanced across a block. (c) Full-night recordings. Each recording session started with a "wake-learning" phase, during which participants were instructed to remain awake and discriminate between trials with or without a repeating pattern. 5 unique, randomly generated RefRN were used in the "wake-learning" phase for each participant. The "sleep-learning" phase started during the night. Participants were laying in a bed while being continuously exposed to white-noise stimuli. They were instructed to continue performing the discrimination when awake but were allowed to sleep. Different sets of unique RefRN targets were used depending on participants' vigilance states (wake, Non-Rapid Eye-Movement (NREM) and REM sleep). The vigilance state was determined online by the experimenter. NREM and REM stimuli were constructed identically as in the "wake-learning" phase, except for their duration (6s instead of 3.5s, see Methods). Finally, participants were tested upon awakening ("Memory-Test") on all RefRN targets heard during the wake-learning and sleep-learning phases, along with 5 novel RefRN. Each RefRN target was played in a separate block along new RN and N trials.

Importantly, different sets of RefRN targets were selected depending on the participant's sleep stages: 5 different RefRN targets were used for NREM sleep, and another 5 different RefRN targets were used for REM sleep. Finally, upon awakening after their full-night sleep, participants underwent a "memory-test" during which they were presented with all types of RefRN targets: the 5 targets heard during wake, the 5 targets heard during NREM-sleep, and the 5 targets heard during REM-sleep. We also included 5 novel RefRN targets in the memory test, to establish the baseline for perceptual learning during the block.

This paradigm allowed us examining two intertwined questions: (i) Are participants able to detect the repetition of a given noise snippet (RN vs. N contrast) even during sleep? (ii) Is recurrent exposure facilitating such detection (RefRN vs. RN contrast)? The first contrast quantifies short-term memory processes (within-trial, time-scale of a few seconds) while the second contrast probes longer-term memory processes (across-trials, time-scale of minutes or hours; Figure 9-1a). The RefRN vs. N contrast reflects the joint effects of all memory processes.

Behavioral and EEG evidence for perceptual learning in wakefulness

We first focused on the "wake-learning" phase. Behaviorally, participants reliably detected the presence of repeated noise targets in both the RefRN and the RN conditions as revealed by the sensitivity index d' (Macmillan, 2005). Importantly, RefRN were associated with an increased sensitivity (d') and decreased reaction-times (RTs) compared to RN trials, despite identical acoustical structures (Figure 9-2a).

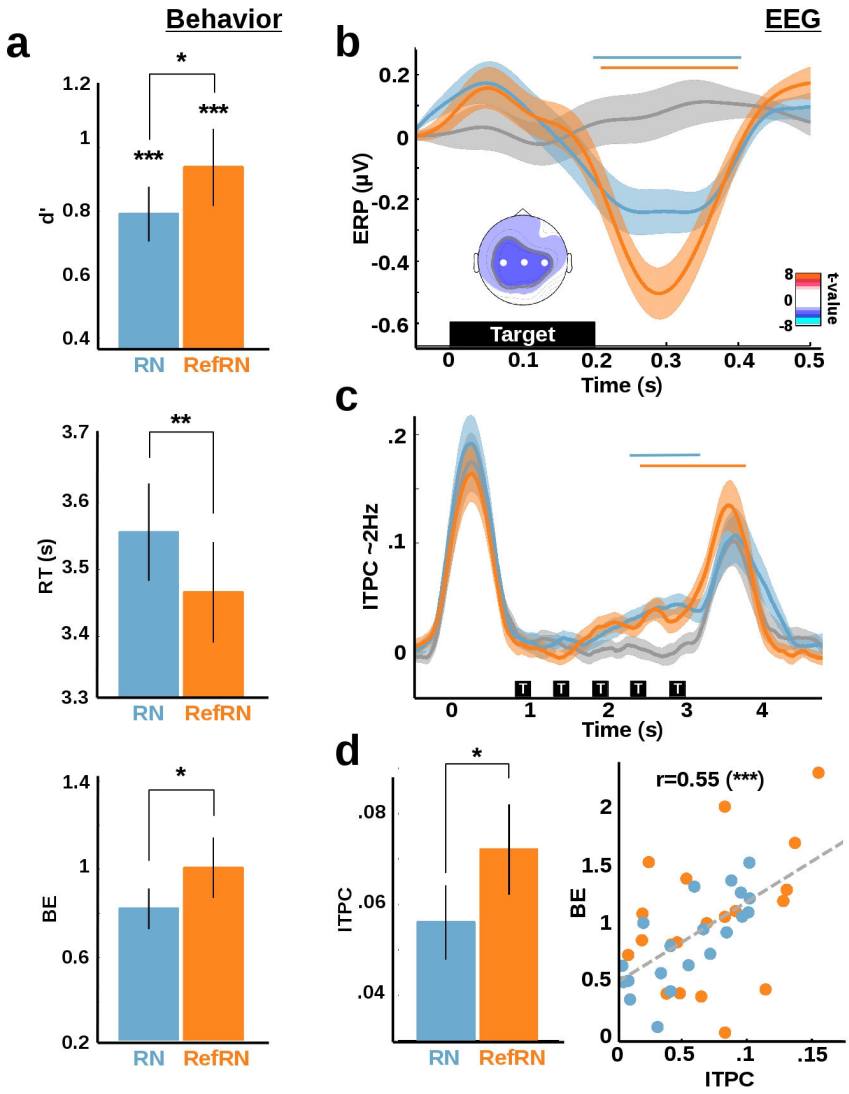

Figure 9-2 Behavioral and electrophysiological indexes of perceptual learning in wakefulness

(a) Behavioral indexes of memory for noise. Participants could discriminate RN and RefRN from noise as indicated by the positive sensitivity (d', top). In addition, performance was better for RefRN compared to RN: d' was increased while reaction times (RTs, middle) was decreased for RefRN. We combined these two variables into a Behavioral Efficiency (BE, bottom) index. Error-bars show the SEM across participants (N = 20). Statistical significance was assessed by means of paired t-tests (d', BE) or u-tests (RT) across participants. Stars atop bars refer to the comparison between the corresponding condition (RefRN or RN) and 0 (d') while stars between bars refer to the RefRN vs. RN comparison (here and below: $p < 0.005$: ***; $p < 0.01$: **; $p < 0.05$: *). (b) Target-locked Event-Related Potentials (ERPs). Averaged EEG activity time-locked to the position of targets onset for RefRN (orange), RN (blue) and N (gray) trials during the "wake-learning" phase. Despite the absence of any obvious discontinuity in the acoustic signal, clear evoked-potentials were observed for RefRN and RN targets compared to the N baseline. Shaded areas denote the SEM across participants (N = 20). Horizontal bars show significant cluster for the RefRN vs. N (orange) and RN vs. N (blue) comparisons ($p_{cluster}<0.005$). The inset shows the scalp topographies of t-values corresponding to the RefRN vs. N cluster. White dots show the central electrodes used in panels b-d. (c) Stimulus-locked Inter-Trial Phase Coherence (ITPC). An increase in ITPC around the target presentation rate ([1.5, 3.5] Hz) was observed for RefRN and RN trials compared to N, mostly toward the end of the stimulus presentation window trials (horizontal bars: significant clusters as in panel b, $p_{cluster}<0.05$). As in panel b, shaded areas denote SEM across participants. (d) Averaging ITPC over significant clusters (left;

orange: RefRN vs. RN; blue: RN vs. N) revealed higher ITPC values for RefRN values compared to RN (one-tailed paired t-test). ITPC was correlated with BE (right, Pearson's correlation coefficients displayed on the correlation plot). Error-bars denote the SEM across participants.

We combined these two variables into a Behavioral Efficiency (BE, see Methods) index (Andrillon et al., 2015a). Overall, behavioral results in the wake-learning phase confirm clear perceptual learning for repeated white-noise snippets.

EEG responses to repeated targets confirmed previous findings (Andrillon et al., 2015a). We observed event-related potentials (ERPs) locked to the to repeated noise snippets (Figure 9-2b, RefRN vs. RN cluster: [200, 400] ms post-target, RN vs. N: [200, 410] ms, $p_{cluster}<0.005$). These ERPs arose within ongoing noise, in the absence of any obvious acoustic landmark (Figure S 9-1), but they still resembled standard event-related auditory evoked potentials (AEPs; Figure S 9-4a; (Picton, 2011)). As the event triggering the potential emerges through learning, we term them Memory-Evoked Potentials (MEPs; (Andrillon et al., 2015a)). Learning and the MEPs also translated into an increase in Inter-Trial Phase Coherency (ITPC; (Luo et al., 2013)). The ITPC increase was observed around the target presentation rate (2Hz, Figure S 9-2a) and was maximal in central electrodes (Figure S 9-2b). Focusing on this ITPC region of interest ([1.5, 3.5] Hz), we observed an increase in ITPC for RefRN and RN compared to N trials (Figure 9-2c, RN vs. N: [2.2, 3.1] s post stimulus-onset, RefRN vs. N cluster: [2.3, 3.8] s, both $p_{clusters}<0.05$). Averaging ITPC over the clusters showed greater values for RefRN compared to RN (Figure 9-2d, one-tailed paired t-test: $p < 0.05$). In addition, ITPC correlated well with the behavioral index of learning BE (Figure 9-2d, Pearson's correlation coefficient: $r = 0.55$, $p < 0.001$).

Modulation of sleep rhythms by repeated exposure to noise patterns

When the noise patterns are presented during sleep, a first question is whether sleepers maintain the ability to discriminate between the different stimulus types. As they were not providing behavioral responses during sleep, we relied on the analysis of brain responses and EEG markers of learning.

We first investigated whether stimulus-locked responses differed across conditions. As depicted in Figure 9-3, sound onsets produced evoked potentials typical of the sleep stage investigated. In NREM2 and NREM3 stages, sound onsets were followed by evoked K-complexes and sleep spindles, the hallmarks of NREM-sleep (Loomis et al., 1938, 1935). As these components were evoked by sound onsets relative to silence, and thus before any target presentation, equivalent responses were observed across all stimulus conditions. In contrast, towards the end of the stimulus presentation window, we observed condition-specific modulations. In NREM2, RefRN trials were characterized by a decrease in power for slow-waves (< 5 Hz) and sleep-spindles ([11, 16] Hz) (Figure 9-3b). These modulations were not accompanied by signs of awakening (increase within the α ([8, 10] Hz) or β ([20, 40] Hz) ranges). This could be interpreted as a condition-dependent and network-specific modulation of sleep depth.

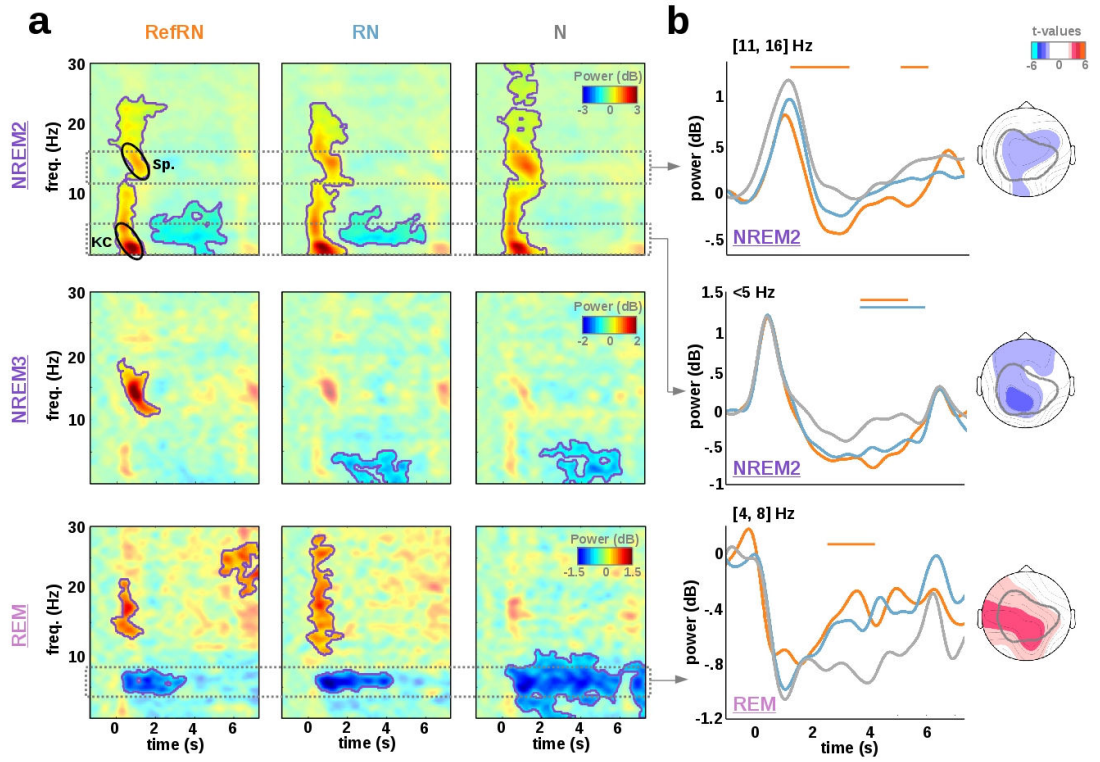

Figure 9-3 Brain responses to acoustic noise during sleep

(a) Time-frequency decomposition of the EEG signal recorded on Cz in response to RefRN (left), RN (middle) and N (right) trials in NREM2 (top), NREM3 (middle) and REM (bottom) sleep stages. Power is time-locked to stimulus onsets, averaged across participants (N = 20) and expressed in dB compared to a pre-stimulus baseline (SI). Magenta contours correspond to significant modulations compared to baseline activity (cluster-permutation, $p_{cluster}<0.05$). (b) Average activity in time-frequency bands typically associated to NREM (δ-power, < 5 Hz (corresponding to evoked KC: K-complexes,); σ-power, [11, 16] Hz (corresponding to Sp.: sleep-spindles)) and REM rhythms (θ: [4, 8] Hz). The power-responses were averaged over these frequency bands for NREM2 (top: σ, middle: δ) and REM-sleep (bottom: θ). Between-conditions differences are illustrated with horizontal bars (cluster-permutation test, pcluster<0.05, orange: RefRN vs. N, blue: RN vs. N). NREM2 was characterized by a decrease in σ and δ power, REM by an increase in θ power. The scalp distribution of the t-values of the RefRN vs. N comparison when averaging the power in the corresponding frequency band and over a [0.8, 5.5] s window are displayed on the side. The gray contour shows the scalp distribution of the MEPs observed in wakefulness (Figure 9-2b). Note the overlap between the scalp distributions of the effects observed in sleep.

Supporting this interpretation is the central scalp distribution of the effect (Figure 9-3b), which differs from the typical distribution of slow-wave and sleep-spindle power (Figure S 9-4c). Linear regressions (Figure S 9-3) across RefRN, RN and N showed that the effect was condition specific, with a gradual decrease (RefRN < RN < N) of sleep-spindles ($\beta = 0.38$, $p < 0.05$) and slow-waves power ($\beta = 0.24$, $p = 0.056$). In NREM3, all of these effects vanished. In particular, linear regressions in NREM3 were not significant. Comparisons between the two sleep states lead to significant differences between the two models (χ-test, $p < 0.001$). Thus, repeated exposure to a noise snippet seemed to locally lighten sleep in NREM2, but had no obvious effect on sleep markers in NREM3.

In REM-sleep, sounds robustly modulated the EEG signal within the θ band ([4, 8] Hz), which is characteristic of REM sleep ((Buzsáki, 2006), see also Figure S 9-4). When comparing RefRN with N, we observed an increase in θ power ([2.45, 4.15] s, $p_{cluster} < 0.01$). Again, this effect was maximal at central electrodes (Figure 9-3b). However, compared to NREM2, the direction of the effect was reversed: θ power increased when the target RefRN was presented, whereas sleep-spindles and slow waves power decreased in NREM2. Still, the results show again a local modulation of sleep rhythms by repeated exposure to a noise snippet during REM sleep.

EEG markers of perceptual memory during sleep

In addition to the modulation of sleep rhythms, we investigated whether repeated exposure to noise snippets during sleep was accompanied by learning-specific MEPs, as in wakefulness. We averaged EEG responses to RefRN, RN and N stimuli, time-locked to target onsets (see Methods; Figure 9-4). Again, we compared the different sleep stages. In NREM2, RefRN trials elicited evoked-potentials similar to wake MEPs, with a similar central negative deflection ([305, 405] ms, $p_{cluster} < 0.05$). In NREM3, evoked-potentials associated to the repetition of noise snippets were also observed albeit only marginally significantly (RefRN vs. N cluster: [130, 300] ms, $p_{cluster} = 0.052$). In addition, the evoked activity in NREM3 no longer resembled MEPs: the negative deflection observed in wake and NREM2, interpreted as an auditory N1 ((Andrillon et al., 2015a), was replaced by a positive deflection with a central scalp distribution (Figure 9-4, middle). Interestingly, such changes mirror the established transformations observed in AEPs from wake to NREM-sleep ((Picton, 2011), Figure S 9-4a).

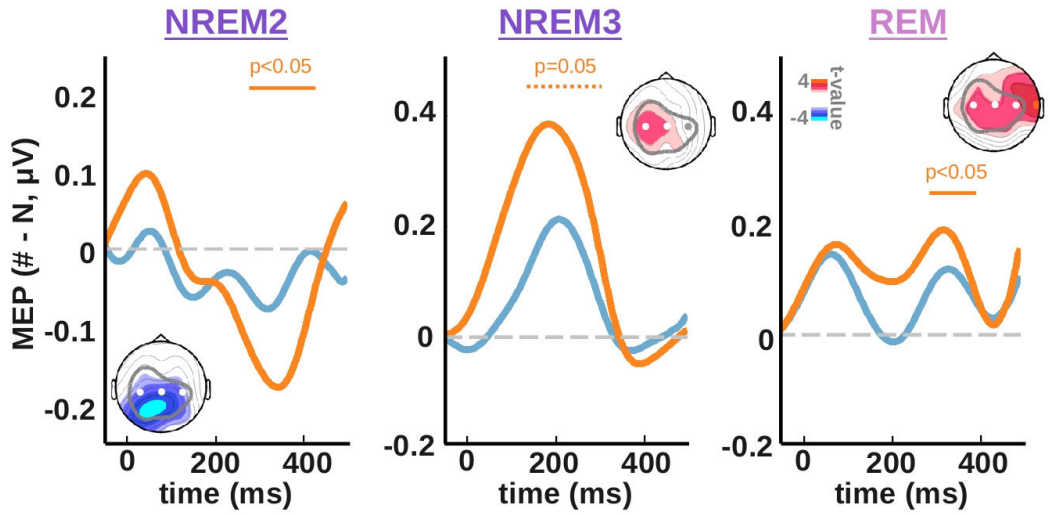

Figure 9-4 Evoked-activity to repeated noise snippets during sleep

Target-locked Event-Related Potentials (ERPs) in NREM2 (left), NREM3 (middle) and REM (right) stages of sleep for RefRN (orange) or RN (blue) trials compared to N trials. Central electrodes were used (circles on scalp topographies). Note the resemblance between the NREM2 ERPs and the MEPs observed in wakefulness (Figure 9-2b). Horizontal bars show significant clusters (pcluster<0.05; the NREM3 positive cluster was marginally significant: pcluster = 0.052) for the RefRN vs. N difference (orange; no RN vs. N difference). Insets: scalp distribution of t-values (RefRN vs. N, paired t-tests) over temporal windows corresponding to the abovementioned clusters. The gray contour shows the scalp distribution of the MEPs observed in wakefulness (Figure 9-2b).

In REM, RefRN trials differed from N trials ([280, 390] ms, pcluster < 0.05). The temporal shape of the evoked potential was different from typical MEPs (Figure 9-4, right). Again, this temporal profile was consistent with the established transformations of auditory potentials from wake to REM-sleep, with a decrease of N1 amplitude in favor of P1 and P2 potentials ((Atienza et al., 2001); Figure S 9-4a).

Overall, the sleeping brain was able to discriminate RefRN trials from N trials in light NREM2 and REM sleep. This shows that complex memory processes, such as those needed to distinguish one particular noise snippets from all others, were to some extent preserved. However, the associated EEG activity (target-locked ERPs) was qualitatively different across sleep stages.

Opposite effects upon awakening of exposure during NREM and REM sleep

Do the EEG markers of exposure during sleep translate into perceptual learning upon awakening? To answer this question, we examined, during the memory-test, whether behavioral performance for those sounds heard during sleep was affected. We computed BE separately for the 4 different lists of RefRN targets: wake, NREM, REM or new RefRN. We focused on the RefRN vs. RN contrast ($BE_{RefRN} – BE_{RN}$) as this is the more stringent index of longer-term perceptual learning. An issue we encountered was that new RefRN could be learnt rapidly during wakefulness, especially as participants were now trained. So, previously-heard RefRNs may be learnt as well, even if past exposure had no effect. Ideally, analyzing the very first trial would minimize the issue, but this is not statistically robust. We restricted our analysis to the first 3 trials out of 8 (Methods, Figure 9-5a left). Thus, participants showed significantly higher initial performance for those RefRNs heard during wakefulness (paired t-test: $p < 0.01$) as well as those heard during REM sleep ($p < 0.01$), compared to RN. As expected before learning, there was no initial advantage for new RefRN ($p = 0.12$), but the modest trend suggested that perceptual learning might have already started. This limitation might explain the marginally significant differences between the wake or REM lists and the new list (BE RefRN – RN: wake vs. new: $p = 0.09$, REM vs new: $p = 0.07$, one-tailed t-test).

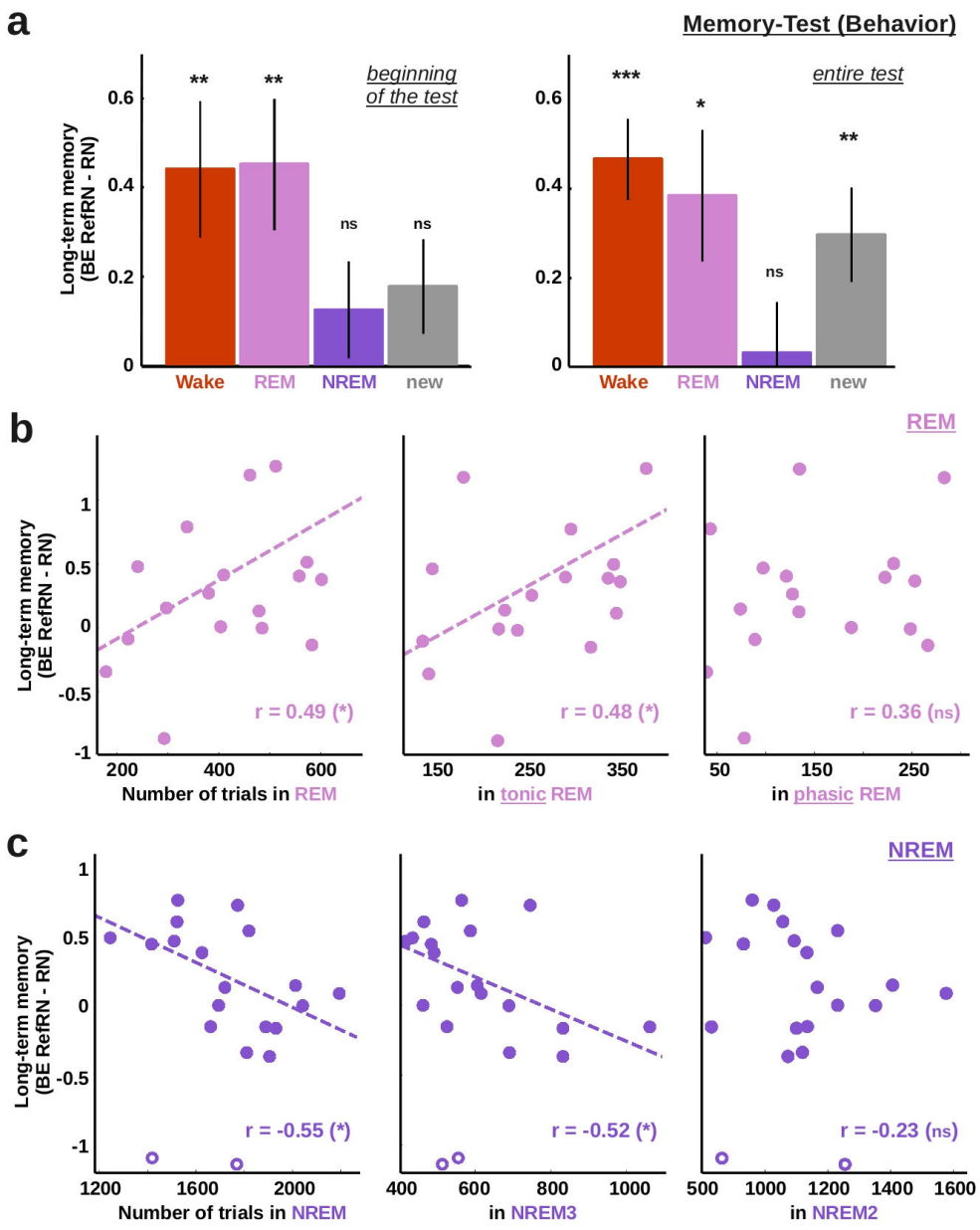

Figure 9-5 Impact of prior exposure on behavioral performance upon awakening

(a) Behavioral efficacy indexes of long-term memory (RefRN - RN) computed for the beginning (left, 3 first trials) or the entire (right) "Memory-Test" blocks. BE was computed separately for the RefRN heard during wakefulness, REM, NREM or for the novel RefRN introduced in the "memory-test". Error-bars denote the SEM across participants (N = 20) and stars atop bars indicate the results of the statistical tests (t-tests against 0, $p < 0.005$: ***; $p < 0.01$: **; $p < 0.05$: *, ns: $p \geq 0.05$). Performance is better for RefRN sounds heard during wake and REM sleep at the beginning of "Memory-Test" blocks. For the whole test analysis, all conditions improve as participants could learn even new RefRNs during the block, with the notable exception of RefRN sounds heard during NREM sleep: those were not learnt even after the whole test. (b) Correlation between the REM sleep long-term memory index (BERefRN - BERN) and the number of trials played in REM-sleep (left), tonic REM sleep (middle) and phasic REM sleep (right) across participants. (c) Correlation between the NREM sleep long-term memory index and the number of trials played in NREM sleep (NREM2+NREM3, left), NREM3 (middle) and NREM2 (right) across participants. For panels b and c, Pearson's correlation coefficients are displayed on each correlation plot ($p < 0.05$: *, ns: $p \geq 0.05$). Open circles (panel c, N = 2 over 20) were considered as outliers (SI) and were not included in the computation of the correlation

coefficients. Dotted lines show the linear fit for pairs of variables with significant correlation. Note the opposite patterns between NREM and REM sleep.

For those RefRN heard during NREM-sleep, there was no trace of improvement due to prior exposure ($p = 0.57$). We further computed a Bayes factor, a non-parametric method for testing the plausibility of the null hypothesis (Dienes, 2014; Kass and Raftery, 1995). We found a Bayes factor of 8.1, which is taken as substantial evidence for the null hypothesis. This null effect, strikingly, was further strengthened when analyzing behavioral data over the entire memory test, with a large Bayes Factor of 34.07. This is remarkable, as over the entire test, performance increased for all conditions including the novel RefRNs, which were learnt from scratch (Figure 9-5a, right). Of all lists of RefRNs, only the NREM3 list did not show any advantage over RN over the whole memory test (all differences NREM3 with other list $p < 0.05$). This pattern of results was conserved even when discarding RefRNs from the NREM and REM lists that have been presented around micro-awakenings (see SI; Figure S 9-5). This suggest a strong suppressive effect of exposure during NREM3: not only sounds heard during this sleep phase were not learnt during sleep, but they were also harder to learn upon awakening compared to sounds that were statistically identical but never heard before.

We further tested how finer sleep characteristics of REM and NREM sleep impacted behavioral performance upon awakening (Figure 9-5b-c). For the REM list and across subjects, we found a positive correlation between the increase in performance and the number of trials played in REM sleep (Pearson $r = 0.49$, $p < 0.05$). For the NREM list, and across subjects, there was a negative correlation between performance and the number of trials played in NREM sleep (Pearson $r = -0.55$, $p < 0.05$). A stepwise regression analysis comparing the influence of NREM stages (NREM 1-3) showed that only the number of trials played in deep-sleep (NREM3) was predictive of the performance upon awakening ($\beta = -0.50$, $p < 0.05$). A similar analysis in REM-sleep comparing the respective influence of tonic and phasic REM-sleep (tREM and pREM respectively) indicated that only the number of tREM trials was predictive of the increase in performance upon awakening ($\beta = 0.48$, $p < 0.05$).

We replicated this highly specific pattern of results when considering an EEG marker of learning (Figure 9-6a-b). The EEG learning index (RefRN – RN difference in ITPC) was positively correlated with the proportion of tonic REM trials in REM sleep ($r = 0.51$, $p<0.05$), while it was negatively correlated with the proportion of NREM3 trials in NREM sleep ($r = -0.53$, $p < 0.05$). Thus, upon awakening, both behavioral performance and brain activity demonstrate an opposite effect of sound exposure during REM and NREM sleep.

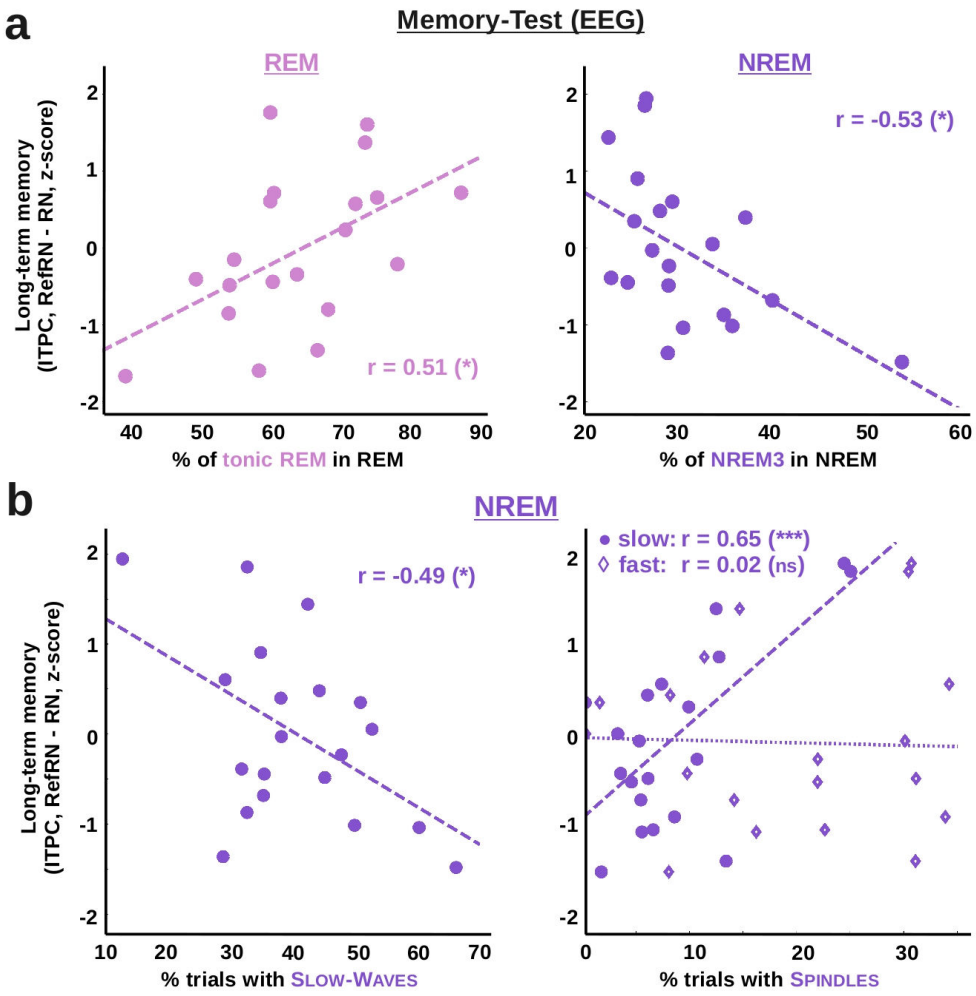

Figure 9-6 Impact of prior exposure and sleep rhythms on phase coherence upon awakening

EEG index (Inter-Trial Phase Coherence, ITPC) quantifying long-term memory (ITPCRefRN – ITPCRN) for RefRN sounds heard during REM and NREM sleep, computed over the whole "Memory-Test" blocks. (a) Left: Correlation between the magnitude of the REM sleep EEG index (z-scored across participants) and the proportion of trials in tonic REM sleep (left). Right: Correlation between the magnitude of the NREM sleep EEG index and the proportion of NREM3 trials within NREM sleep. As for the behavioral index (Figure 9-5b-c), there was a positive correlation between REM sleep learning and the prevalence of tonic REM sleep, and a negative correlation between NREM sleep learning and the prevalence of NREM3 sleep. (b) Correlation between the magnitude of the EEG index (z-scored across participants) for the RefRN heard in NREM and the proportion of trials containing slow-waves (left) or sleep-spindles (right; circles: slow spindles; diamonds: fast spindles). Note the negative correlation between the EEG learning index and the proportion of trials associated to slow-waves on one hand and the positive correlation with the proportion of trials associated with slow spindles on the other hand. Pearson's correlation coefficients are displayed on each correlation plot ($p < 0.005$: ***; $p < 0.01$: **; $p < 0.05$: *, ns: $p \geq 0.05$) and dotted lines show the linear fit between the pairs of variables.

Slow waves dynamically suppress memories in deep NREM sleep

Even within NREM sleep, exposure seemed to have opposite effects depending on sleep stage. EEG markers suggested learning in NREM2 (Figure 9-4). However, behavioral

(Figure 9-5c) and EEG (Figure 9-6a) indexes of learning suggested a suppression during NREM3. More precisely, there was a negative correlation between the EEG index of learning upon awakening and the percentage of trials containing slow waves overnight (Figure 9-6b; $r = -0.49$, $p < 0.05$). When mapping the correlation onto scalp sensors, the effect was maximal both at frontal electrodes, where slow waves are most prevalent, and at central electrodes, where the effect of learning was observed in wakefulness (Figure S 9-6).

A hypothesis consistent with all of those observations would be that the suppressive effect of NREM3 exposure was mediated by slow oscillations, which increase in density from NREM2 to NREM3. This was tested by tracking the amount of learning over the course of the night, using EEG markers of learning. First, ITPC was compared with the overall power in the δ band (< 5 Hz), a good proxy for slow waves density. We found a clear negative correlation between δ power and ITPC for RefRN trials (Figure 9-7, $r = -0.1$, $p < 0.005$) but, crucially, not for RN trials ($r = -0.03$, $p = 0.3$). The link between slow waves and EEG markers was thus specific to longer-term memory processes.

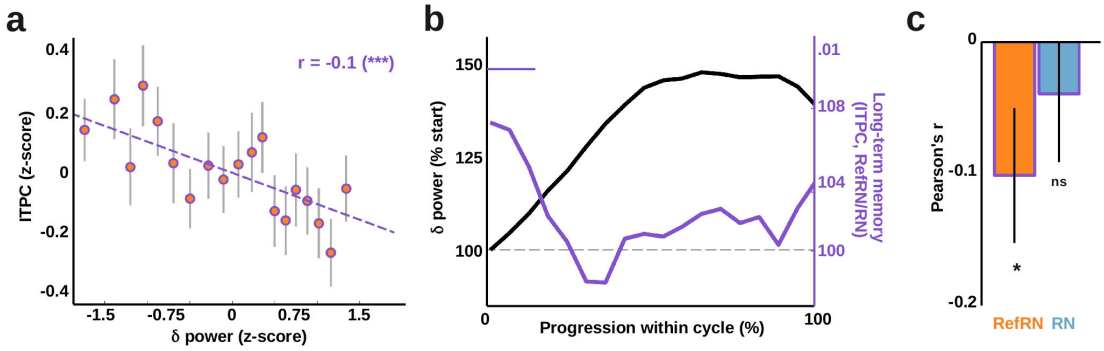

Figure 9-7 The learning index is dynamically correlated with slow-wave power in NREM sleep

(a) Correlation between ITPC values computed for RefRN trials (z-scored per sleep-cycle, see SI) and δ (< 5 Hz) power (N = 76 cycles in 18 participants). Data were binned for illustrative purpose. The Pearson's correlation coefficient is displayed on the graph (***: $p < 0.005$) as well as the regression line between the two variables, both estimated on un-binned data. (b) Evolution of long-term memory index (ITPC, RefRN over RN ratio computed on fixed windows) and δ-power within sleep cycles. Cycle-durations were normalized to average cycles with different durations and the position within a cycle is expressed as a percentage of total duration. δ-power was normalized by the value at the beginning of each cycle (100%). Note that, at the beginning of sleep cycles (typically light NREM), there was evidence for perceptual learning (RefRN>RN, pcluster<0.05), which is consistent with Figure 9-3 and Figure 9-4. This advantage disappeared with the increase in δ-power and the deepening of NREM-sleep, which consistent with Figure 9-5 and Figure 9-6. (c) Pearson's correlations coefficients between ITPC and δ-power for RefRN (orange) and RN (blue) computed and averaged across sleep-cycles (n = 76 cycles). Pearson's coefficients were significantly negative for RefRN (one-tailed t-test, $p < 0.05$) but not RN trials.

Sleep being structured into cycles characterized by a gradual descent from light to deep NREM-sleep, we examined whether the negative correlation between ITPC and δ power over the entire night was also maintained within individual sleep cycles. To do so, we normalized the sleep cycles' durations (see Methods, N = 76 cycles in 18 participants) and examined the time course of δ power and ITPC. A clear increase in δ power was visible within the cycle progression, corresponding to the transition from lighter stages of

NREM to NREM3 (Figure 9-7b). At the beginning of the cycles, higher ITPC were observed for RefRN compared to RN (ratio RefRN/RN > 100%, $p_{cluster} < 0.05$). This is suggestive of learning in light NREM sleep, as previously shown by other analyses (Figure 9-3 and Figure 9-4). Later in the sleep cycle, the advantage for RefRN decreased and was eventually cancelled out, closely mirroring an increase in δ power and slow waves density (Figure S 9-7). Moreover, the negative correlation between ITPC and δ power was observed within-cycles for RefRN but not for RN trials (Figure 9-7c). This is strong evidence of a dynamic involvement of slow oscillations in the suppressive effects of exposure during NREM3 sleep.

Slow spindles mediate learning in light NREM sleep

Which mechanism could subserve the facilitating effects on learning during light NREM sleep (NREM2)? We discovered a strong and positive correlation between the percentage of trials containing slow frontal spindles and the amount of EEG markers of learning upon awakening (ITPC RefRN – RN; $r = 0.65$, $p < 0.005$, Figure 9-6b, right). Importantly, there was no correlation when considering fast centro-parietal spindles ($r = 0.02$, $p=0.9$). In addition, although slow spindles are maximal at frontal electrodes, the correlation between learning and spindles incidence was maximal at central electrodes, overlapping again with the effects of learning observed in wakefulness and NREM2 (Figure S 9-6). Slow-spindles could therefore play a role in potentiating learning during NREM-sleep.

Tonic REM sleep favors perceptual learning

When examining the effect of sleep exposure on perceptual learning upon awakening, REM sleep had a positive impact (Figure 9-5). This positive effect of REM sleep significantly correlated with the amount of time spent in tonic REM sleep but not in phasic REM sleep (Figure 9-6). To further explore this potential dissociation, we computed the size of the effect observed overnight in the θ band (Figure 9-3) and the magnitude of evoked potentials (Figure 9-4), for all trials in REM sleep, then split for trials in tonic REM (tREM) or phasic REM (pREM).

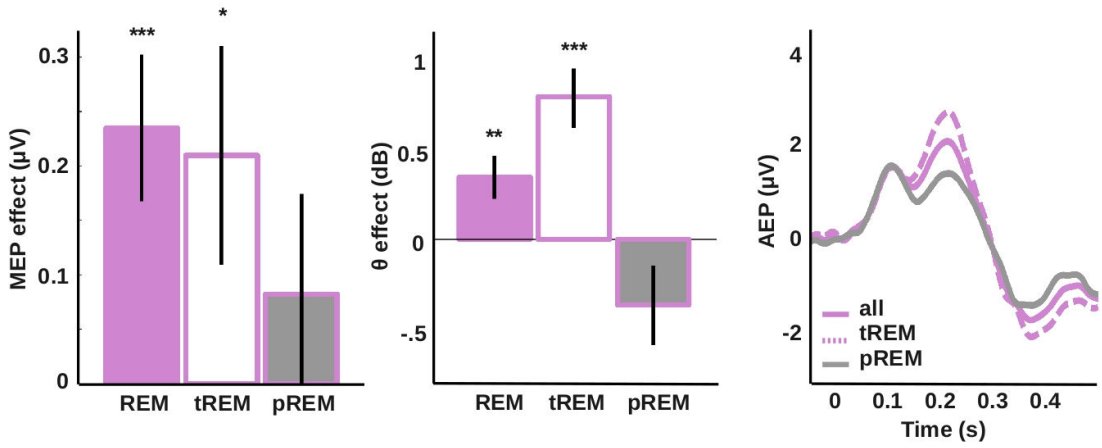

Figure 9-8 Tonic REM sleep is more favorable to learning than phasic REM sleep

Left: Magnitude of the ERPs illustrated in Figure 9-4 (RefRN vs. N cluster in REM-sleep) computed for all trials in REM sleep and trials in tonic (tREM) or phasic REM-sleep (pREM, see Methods). Middle: Similar analysis for the θ-band effect observed in REM sleep (Figure 9-3). Error-bars denote the SEM across participants (N = 20) and stars atop bars indicate the results of the statistical tests (t-tests against 0, $p < 0.005$: ***, $p < 0.01$: **, $p < 0.05$: *, ns: $p \geq 0.05$). Note the preservation of the effects observed for all trials in tREM but not pREM. Right: Auditory-evoked potentials computed at stimulus-onset (and irrespective of experimental conditions) for all REM-sleep trials, tREM and pREM-sleep trials. Note the enhancement of the P2 component in tREM-sleep, which is reminiscent of the increased P2 component associated to RefRN trials in Figure 9-4.

Figure 9-8 shows that effects were equivalent or greater in tREM compared to REM but disappeared in pREM. Interestingly, tREM and pREM could not be differentiated based on overall θ power ([4, 8] Hz, t-test $p = 0.20$). However, there were marked differences in the auditory potentials associated to sound-onset (i.e. irrespective of stimulus-type): tREM was characterized by an enhancement of the P2 auditory potential compared to pREM (Figure 9-8, right), similar to the potential that was increased in MEPs by the presence of RefRN targets (Figure 9-4). Considered altogether, these results suggest a profound functional difference between tREM and pREM, at least for auditory processing. This is consistent with previous demonstrations of an increased sensitivity to sensory information in tREM compared to pREM (Sallinen et al., 1996).

Discussion

We developed a paradigm that tracked the formation and long-term maintenance of new perceptual memories across vigilance states. Our results revealed a sharp distinction between REM and deep NREM sleep. Presentation of acoustic stimuli during REM induced learning, while presentation of the same stimuli during deep NREM induced a suppressive effect. Both learning and suppression transferred to subsequent wakefulness, behaviorally and for EEG markers. A more detailed examination of EEG markers during the night further specified the vigilance states that favored or, in contrast, suppressed learning. The suppressive effect was primarily driven by periods of deep, slow-wave NREM3 sleep, whereas lighter, NREM2 sleep allowed for some perceptual learning. For REM-sleep, perceptual learning was primarily driven by tonic REM.

The learning of novel perceptual information is possible in light NREM sleep

NREM-sleep is classically characterized by high-arousal thresholds (Rechtschaffen et al., 1966) and sleepers' unresponsiveness to external stimulations. Does such unresponsiveness imply unconnectedness (Sanders et al., 2012)? The notion of a thalamic gating (McCormick and Bal, 1994) has been challenged by numerous studies showing faithful encoding of information (Issa and Wang, 2008; Y. Nir et al., 2013) or complex information processing in NREM-sleep (Bastuji, 1999; Bastuji et al., 2002; Campbell, 2000; Hennevin et al., 2007). Interestingly, however, the large-scale integration of information remains largely reduced compared to wakefulness (Casali et al., 2013; Massimini et al., 2005) so NREM sleep has been argued to prevent synchronous processing across distributed brain regions (Tononi and Massimini, 2008). But even large-scale integration may be preserved, at least to a certain extent: we recently showed that, when subjects fall asleep while performing a complex task linking auditory signals to semantic categories and motor preparation, distributed processes can be continued in NREM2 sleep (Kouider et al., 2014). Here, we extended these findings by providing the first compelling evidence for the learning of complex and novel sensory information during NREM2 sleep (i.e. light NREM-sleep). In NREM2, we observed evoked potentials for recurrently presented noise snippets (Figure 9-4) as well as an increase in phase coherence across trials (Figure 9-7), demonstrating sleepers' ability to form new representations for initially nondescript noises. Such a form of learning involves a network of brain regions comprising secondary auditory cortices and the hippocampus (Kumar et al., 2014), suggesting that rather extensive networks can be recruited and coordinated in NREM-sleep, despite the loss of awareness and responsiveness. The resemblance between NREM2 evoked potentials and classical N1-P2 complexes (Andrillon et al., 2015a) further advocates the involvement of a distributed network, since the N1-P2 complexes are thought to be generated in primary and secondary auditory cortices (Picton, 2011).

Such a preservation of complex information processing could be supported by local modulations of sleep-depth, a phenomenon called local sleep. Indeed, it has been shown that sleep is not a monolithic phenomenon but that different brain regions can show different activity patterns (Nir et al., 2011; Peter-Derex et al., 2015). In particular, some brain regions can recover wake-like activity in the absence of awakening at the scalp level (Nobili et al., 2012). Interestingly, in NREM2, auditory "events" in the form of

recurrently presented noises were accompanied by the presence of evoked potentials resembling wake responses (Figure 9-4). This contrast with the evoked-potentials observed in NREM3 and classical auditory evoked potentials reported for NREM sleep (Figure S 9-4a). Thus, the presence of wake-like activity in NREM2 could be interpreted as the recovery of some local wake-like processing in the context of global NREM sleep (no increase in α or γ power on scalp recordings). The association of these wake-like potentials with a region-specific decrease in the magnitude of NREM-sleep oscillations (δ and σ power; Figure 9-3) further strengthens this interpretation. Overall, our data argue that sleep-depth may be flexibly modulated depending on sensory input, to allow for the timely recovery of wake-like information processing and learning.

In NREM sleep, memories are formed or suppressed depending on sleep depth

An unexpected finding was that exposure to novel information in deep phases of NREM sleep not only failed to improve participants' performance upon awakening, but rather, impaired their ability to learn this exact same information when awake again (Figure 9-5a). Furthermore, during the night, learning observed in light NREM2 was suppressed in deep NREM3 (Figure 9-7). This suggests a highly specific suppressive influence of deep NREM sleep on learning. Such a contrast between light and deep NREM-sleep is consistent with a qualitative distinction between these two sleep stages in relation to neural plasticity (Genzel et al., 2014). In this view, light NREM-sleep favors synaptic potentiation, while deep NREM-sleep promotes synaptic down-scaling.

Could sleep rhythms such as slow oscillations and sleep spindles fully account for this light vs. deep NREM dissociation? In our study, frontal sleep spindles were positively correlated with the positive learning effect (Figure 9-6b and S6). Along this line, numerous studies have demonstrated the link between sleep spindles and memory consolidation (Diekelmann and Born, 2010). In addition, *in vitro* studies showed that neuronal activations mimicking sleep spindles could induce Long-Term Potentiation (LTP) and hence synaptic plasticity (Rosanova, 2005). We also found that slow-waves were negatively correlated with memory formation (Figure 9-6b and Figure 9-7). This is consistent with the idea that slow waves could trigger Long-Term Depression (LTD) (Czarnecki et al., 2007). However, sleep spindles are typically nested within slower oscillations, which argue against diametrically opposed roles (Mölle and Born, 2011; Staresina et al., 2015). In addition, both rhythms are present in light and deep NREM sleep and therefore cannot fully explain the differential impact of these sleep stages on learning.

We thus propose that a contextual change from light to deep NREM-sleep explains the observed differences. Indeed, it has been recently shown that sleep rhythms such as sleep spindles and slow-oscillations undergo transformations from light to deep NREM-sleep (Siclari et al., 2014a). In particular, slow-oscillations decrease in amplitude, slope, spatial expanse, but increase in density (Figure S 9-7). Two types of synchronization processes have been proposed to account for these changes. In light NREM sleep subcortico-cortical processes, potentially stimulus-driven, would occur (type-I slow-waves, corresponding approximately to K-complexes), leading to high-amplitude, steep and widespread slow-waves. These type-I waves could be associated to activations of the arousal system, restoring some ability to process sensory information and to form new memory traces. In deep NREM sleep however, slow waves (type-II) would arise from

local cortico-cortical synchronization processes independently from external stimulations or arousal. The type-II waves could in turn favor synaptic downscaling, leading to the deep-NREM suppressive effect we observed. We therefore verified whether the EEG learning index computed overnight ($ITPC_{RefRN}$ / $ITPC_{RN}$) correlated with several slow-waves parameters (density, slope, number of negative peaks and spatial expanse, Figure S 9-7). Interestingly, the suppression effect was paralleled with the emergence of more numerous but more local, and putatively cortico-cortical, slow-waves.

In REM-sleep, tonic episodes promote the learning of novel information

In REM-sleep, evoked-potentials were observed when novel information was presented several times (RN & RefRN; Figure 9-4). The presence of such evoked-potentials, in the absence of any salient feature within the acoustic signal, already indicates in itself that complex auditory processing and learning are possible in REM sleep. REM-sleep exposure also improved performance upon awakening, confirming this view (Figure 9-5 and Figure 9-6). Although the evoked potentials observed in REM sleep displayed a different shape to wake responses (Figure 9-2b), they were comparable to the typical auditory-evoked potentials observed in REM sleep (Figure S 9-4a), with a disappearance of the N1 component but a preservation of the P2 component (Picton, 2011). Recurrent exposure (RefRN) enhanced specifically the P2 potential, as is the case for perceptual learning in wakefulness (Tremblay et al., 2014). We also observed an increase in θ power for learnt trials (RefRN) in REM-sleep (Figure 9-3), which is reminiscent of the enhancement of θ oscillations during the encoding of new memories (Rutishauser et al., 2010). It is therefore possible that perceptual learning in REM sleep recruits similar neural mechanisms as during wakefulness.

Our results are consistent with previous research showing that sensory processing(Atienza and Cantero, 2001; Sallinen et al., 1996; Sculthorpe et al., 2009) and the learning of new associations (Arzi et al., 2012; Hennevin et al., 2007, 1995) are possible during REM sleep. However, such results seem at odd with the relatively low incorporation of external stimulations to the dream scenery (Nir and Tononi, 2010). To reconcile these observations, it is worth noting that, here, the effects on ERPs and θ oscillations were observed in tREM but not pREM phases (Figure 9-8). This result is in line with previous findings of increased sensitivity to sensory information in tREM compared to pREM (Sallinen et al., 1996). Interestingly, dream reports seem more vivid in pREM (Berger and Oswald, 1962) although this relationship has been debated (Molinari and Foulkes, 1969). It is therefore possible that, in pREM, the brain is more isolated from sensory inputs (Wehrle et al., 2007) due to the processing of endogenously generated sensory information (i.e. dream contents; (Andrillon et al., 2015b; De Carli et al., 2015)). On the contrary, tREM would be more permeable to external sensory information. Thus, in REM sleep, the bottleneck limiting learning would be the sleepers' connectedness to their environment. Finally, it is particularly interesting to note the difference between pREM and tREM in the learning-induced P2 component (Figure 9-4) or even the standard auditory P2 (Figure 9-8). The magnitude of the P2 component could be used as a proxy to quantify sensory permeability during REM-sleep.

A unified view of the role of sleep in memory

From a mechanistic point of view, we yet have to explain why REM sleep or light NREM sleep favor learning while deep NREM sleep suppresses the possibility of subsequent learning. What could account for such a dramatic reversal of function across phases of sleep? Drastic changes in the level of neuromodulators across sleep phases (McCarley, 2007; Siegel, 2004) could be responsible for such a reversal. In particular, Acetylcholine (ACh) drops in slow-waves sleep compared to both wakefulness and REM sleep (Jones, 2005; Marrosu et al., 1995). Such a drop could affect the brain's ability to learn since ACh can control the polarity of Spike-Timing Dependent Plasticity (STDP; (Pawlak, 2010; Seol et al., 2007)). Interestingly, modeling showed that synthetic neuronal networks endowed with STDP could learn and almost inevitably learned recurrent random inputs (Klampfl and Maass, 2013; Masquelier et al., 2008). An ACh-dependent modification of the STDP rule could therefore tentatively account for our results. Under higher levels of ACh (wake, REM-sleep, light NREM-sleep), learning occurs through the potentiation of the specific synapses recruited by the recurrent acoustic signal (Klampfl and Maass, 2013). Under low-levels of ACh (deep NREM-sleep), the same synapses would, on the contrary, be down-scaled, so not only would learning not occur, but the subsequent re-activation of the network upon wakefulness would be suppressed and future learning would be more difficult. We do not suggest any functional role for this suppressive effect; rather, it seems an inevitable byproduct of the synaptic down-scaling needed for homeostatic purposes (Tononi and Cirelli, 2014).

Finally, although we investigated the formation of new memories during sleep rather than the consolidation of existing ones, our work is still relevant for the vast literature on memory consolidation. Indeed, both acquisition and consolidation may rely on similar synaptic plasticity mechanisms (Diekelmann and Born, 2010; Tononi and Cirelli, 2014). We provide here a comprehensive and unified model of the role of sleep in memory, in which (i) content-specific consolidation occurs in light NREM-sleep and REM-sleep through phasic and global events such as type-I slow-waves (approximately K-complexes) and sleep-spindles (Diekelmann and Born, 2010) ,(ii) general down-scaling of synaptic weights would take place in deep NREM-sleep, enabling synaptic renormalization (Tononi and Cirelli, 2014). Such synaptic pruning could be mediated by local slow-waves trains (Nere et al., 2013) under conditions of low ACh levels (Tononi and Cirelli, 2014). Our model can also account for the possibility to improve a given memory by playing, overnight, a sound paired to the information learnt during wakefulness (Targeted Memory Reactivation, TMR; (Oudiette and Paller, 2013)). Phasic events would play again a central role in allowing the consolidation of the re-activated information by organizing hippocampo-cortical communications (Diekelmann and Born, 2010). Such view implies that TMR would be more efficient in NREM2 than NREM3. Accordingly, Oudiette et al. reported that TMR efficiency was negatively correlated with δ power (Oudiette et al., 2013). We conclude that our results and interpretations are consistent with a large body of previous experimental data, and provide a simple but comprehensive framework on the role of sleep in memory.

Experimental Procedure

Participants

20 right-handed subjects (11 females, age 20-31) with no history of neurological or sleep disorders participated to this study, which had been approved by the local ethics committee (Comité de Protection des Personnes, Ile-de-France I, Paris, France). Sleep habits matched the general population standards (SI).

Noise-memory paradigm

We used a variant (Andrillon et al., 2015a) of the noise-memory paradigm (Agus et al., 2010). In this paradigm (Figure 9-1), participants were instructed to discriminate between 2 types of acoustic noise: fresh white-noise stimuli deprived of any repeating sequence (N: noise, no repetition) and white-noise stimuli in which a sequence (target) is repeated within a trial (RN: repeated-noise, within-trial repetition). Unknown of participants, some targets were randomly selected to be recurrently presented throughout the experiment (RefRN: reference repeated-noise, within and across trials repetitions).

Protocol Outline

On the day of recordings (Figure 9-1c), participants were first familiarized with acoustic noise with or without repeating patterns. Then, participants underwent a "wake-learning" phase during which they were asked to discriminate stimuli with or without repetitions while remaining awake. They were then put to bed while being exposed to structurally identical but longer stimuli ("sleep-learning" phase, see below for stimuli details). After the night and upon awakening, participants were tested on previously heard stimuli ("memory-test") along novel ones. Participants were instructed to remain awake and to respond to stimuli during the wake-learning and memory-test phases while keeping eyes-closed. In the sleep-learning phase, they were allowed to sleep but were instructed to keep responding to the stimuli as long as they remained awake.

Stimuli

Acoustic stimuli were generated as random sequences of normally distributed values. The outcome is called white noise and is characterized by a flat spectrum, constant envelope amplitude and no sample-to-sample predictability (Figure S 9-1). In the "wake-learning" phase, N stimuli were made of 3.5s of fresh white-noise without any repeating pattern within and across trials (Figure 9-1b). RN stimuli included a 0.2s white-noise target that was copied identically 5 times within the trial. The target was interleaved with fresh white-noise fillers to keep the same duration as for N trials (3.5s). Repeated targets were randomly generated for each participant and used only once for RN trials. Targets were spaced every 0.5s (presentation frequency: 2Hz) starting from 0.8s after stimulus onset. RefRN stimuli were identical to RN stimuli in their structure but the repeating target was chosen among a set of arbitrarily selected targets (Figure 9-1a, N = 5 per participants). A fourth type of stimuli (Reference Noise, RefN) was introduced to balance the number of

trials with and without repeating patterns. In these trials, there was no within-trial repetition of a target. However, we injected the RefRN targets every 0.5s. These trials were not included in further analysis. Participants were not told about the presence of RefRN trials.

In the "sleep-learning" phase, similarly structured stimuli were used. However, different sets of RefRN targets were played in NREM (N = 5) and REM (N = 5) sleep according to an online assessment of vigilance states. In addition, the number of within-trial repetition was increased (from 5 to 10) in NREM and REM-sleep (duration: 6s instead of 3.5s in wakefulness). Whenever participants showed signs of awakening during the night, the wake set of RefRNs were played. NREM targets were presented after NREM2 onset, therefore in NREM2 and NREM3 stages predominantly.

Finally, in the "memory-test" phase, participants were tested on all RefRN targets presented in the wake and sleep-test along 5 new RefRN. Each RefRN was tested in a separate 5-minutes block along freshly generated RN and N trials. There were 8 presentations of each stimulus conditions. Block-order was randomized. The number of within-trial repetition was set to 5 as in the "wake-learning" phase.

Electrophysiological recordings

Electroencephalographic (EEG, 10-20 montage), electrooculographic (EOG), electromyograhpic (EMG) and electrocardiographic (ECG) data were continuously recorded along video monitoring (SI). Participants were constantly monitored during both wake and sleep. During the sleep-test, a given set of RefRN (wake, NREM or REM) was selected according to participant's vigilance state.

Sleep assessment and sleep rhythms detection

Vigilance states were assessed online using standard guidelines (Iber et al., 2007) by an experienced scorer (TA) and confirmed off-line by two scorers (TA, and DL) blind to experimental conditions (see Table S 9-1 for a summary). The spectral profiles of sleep stages were in accordance with the literature (Figure S 9-4b-c). In NREM-sleep slow-waves and sleep-spindles were detected using algorithms detailed elsewhere (Andrillon et al., 2011; Nir et al., 2011). Spatial distributions of average densities are shown in Figure S 9-6.

Behavioral data and analysis

Participants were instructed to indicate the presence or absence of repetitions through handles placed in their right and left hand (response mapping counterbalanced across participants). For each stimulus, we recorded participants' response (if any) as well as reaction times (RTs). Leaning on previously published results (Andrillon et al., 2015a), we computed participants' sensitivity d' (Macmillan, 2005) when discriminating RefRN from N trials or RN from N trials. RTs and d' can be combined in a Behavioral Efficiency (BE) index, used here to titrate the amount of learning (SI). The RefRN vs. RN contrast

focuses on long-term memory (across-trial) while the RN vs. N trials targets short-term memory (within-trial; Figure 9-1a).

EEG preprocessing and analysis

EEG data were epoched around stimuli onsets and bandpass-filtered (stimulus-locked Event-Related Potentials (ERPs): [0.1, 40] Hz, target-locked ERPs: [1, 40] Hz). Notch filtering at 50Hz was applied to reduce line noise. Spurious trials were discarded. Time-frequency decomposition of the EEG signal was estimated to extract both power (absolute power or modulation over baseline activity) and inter-trial phase coherency (ITPC) in response to a given stimulus category. Complete details are provided in SI. Based on previous studies (Andrillon et al., 2015a; Luo et al., 2013), we used ITPC in RefRN and RN trials to estimate the amount of learning in absence of behavior. Target-locked ERPs were also used to assess perceptual learning. Unless stated otherwise, analyses were performed on central electrodes (Cz, C3, C4), which correspond to the strongest auditory responses.

Supplemental Experimental Procedures

Subjects and Sleep Study

20 right-handed subjects (11 females, age 20-31 years) with no history of neurological or sleep disorders participated to this study. They filled in questionnaires about their sleep habits and had an interview with a sleep specialist prior to recordings. They were also monitored for 7-10 days prior to the recording session through actigraphy and sleep diaries to ensure stable sleep/wake rhythms. The day of the recordings, participants were familiarized with the stimuli used in our protocol (white-noise acoustic stimuli). They were equipped for polysomnographic recordings and performed an initial test-phase while remaining awake ("wake-learning" phase: 41 ± 1 minutes, mean ± standard error of the mean (SEM) across participants) consisting in the detection of repetitions in the acoustic noise (see below). They were then put to bed and asked to perform the same task as long as they were awake. Stimuli were continuously presented over the whole night ("sleep-learning" phase: 494 ± 20 minutes). Finally, upon spontaneous awakening, participants underwent a "memory-test" without being explicitly told so; i.e., they continued detecting repetitions within noise trials (89 ± 2 minutes). Polysomnographic equipments were removed at the end of the memory-test. This protocol had been approved by our local ethics committee (Comité de Protection des Personnes Île-de-France I, Université Paris-Decartes, Paris, France).

Stimuli and noise-memory paradigm

We used a variant of the noise-memory paradigm (Agus et al., 2010), which had been optimized for Electroencephalographic (EEG) recordings (Andrillon et al., 2015a). Each recording session was separated in 3 different phases (Figure 9-1c). In the initial "wake-learning" phase, participants were instructed to discriminate: (i) noise stimuli (N, duration: 3.5s), i.e. acoustic stimuli made of ever-changing white-noise, (ii) repeated-noise (RN) stimuli in which a 0.2s white-noise target was presented 5 times to listeners (Figure 9-1b). In RN trials, the noise targets were interleaved with ever-changing white-noise fillers to keep stimulus duration similar to N trials (3.5s). The first target was presented 0.8s after stimulus onset and targets were presented every 0.5s. Both target and fillers being made of white-noise (no sample-to-sample predictability), such concatenation is seamless as illustrated in Figure S 9-1 (no change in sound envelope for example). Repeated noise targets differed from one trial to the other. In this condition, we therefore introduced a repetition of the same piece of acoustic information within but not across trials (Figure 9-1b). A different set of RN targets was presented to each participant (Figure 9-1a). Unknown to participants, another set of repeated targets (N = 5 for each participant) were randomly selected to be recurrently presented across the entire "wake-learning" phase. Such trials were termed Reference Repeated-Noise (RefRN) stimuli and correspond to the presentation of the same targets both within and across trials. Classically (Agus et al., 2010; Agus and Pressnitzer, 2013; Andrillon et al., 2015a; Luo et al., 2013), RefRN trials are associated with improved repetition-detection performance compared to RN trials. From the perspective of participants, RefRN and RN trials differed only through prior exposure. Thus, the difference in performance between RefRN and RN trials can be used to titrate long-term perceptual learning

(Figure 9-1a, right). In addition, the ability to differentiate RN trials from N trials may also involve the rapid formation of memory to noise (Andrillon et al., 2015; Figure 9-1a, right). Lastly, a fourth type of stimuli (Reference Noise, RefN) was introduced to balance the number of trials with and without repeating patterns. In these trials, there was no within-trial repetition of a target but the RefRN targets were introduced every 0.5s. These RefN trials were not further analyzed.

Response-handles were attached to participants' hands who were instructed to indicate the presence of a repeating pattern by pressing the right or left handle (the 'response-side / stimulus-condition' mapping was counterbalanced across subjects). Response-side (first button press after stimulus onset) and reaction times (RTs) were recorded for further analysis. Participants were instructed to remain awake and to respond to stimuli during the whole "wake-learning" phase while keeping eyes-closed. Stimuli were played every 5.5 to 7.5 s (jitter: uniform distribution) with a break every 64 trials.

In the "sleep-learning" phase, similar stimuli were used. N and RN trials were freshly generated for each N or RN trial. However, different sets of RefRN targets were played in periods of wakefulness (same as the "wake-learning" phase), NREM- (N = 5) and REM-sleep (N = 5) according to an online assessment of vigilance states (Figure 9-1c). In practice, when participants were awake, only the RefRN containing the wake targets were played (wake RefRN). In NREM-sleep (NREM2 and 3) the NREM set of RefRN was played to participants. And in REM-sleep, the REM set was used. Each time participants awoke, the RefRN set was set back to wake RefRN targets. In addition, for this sleep-learning phase, the duration of stimuli was increased (6 s instead of 3.5 s in wakefulness) in order to double (10 vs. 5) the number of within-trial repetitions in RefRN and RN trials. Yet, the general structure (0.2s-long targets separated by 0.3s-long white-noise fillers) was conserved. Participants were instructed to respond to stimuli as long as they would remain awake and to resume responding in case of an awakening. They were remembered to do so by the experimenter, in case of prolonged awakening without responses. Stimuli were played every 6.5 to 9.5 s in wake and every 9 to 12 s in sleep (jitter: uniform distribution).

Finally, in the "memory-test" phase, participants were tested on all RefRN targets presented in the "wake-learning" and "sleep-learning" phases (N = 5 wake, NREM and REM RefRN targets per participant) along 5 new RefRN targets. Task instructions remained the same (detection of repetitions in noise) and participants were not informed of the presence of previously presented noises. Each RefRN was tested in a separate 5-minutes block along freshly generated RN and N trials. The order of presentations of wake, NREM, REM and new RefRN was randomized. Stimuli were played every 5.5 to 7.5 s. Participants were instructed to remain awake and to respond to stimuli in the entire "memory-test". However, in some cases, participants failed to indicate the presence or absence of repetitions. "Memory-test" blocks with more than 20% trials without responses were excluded from our analysis (17 out of 400 blocks in 20 participants).

All stimuli were randomly generated to create acoustic white-noise (sampled at 44100 Hz). Each stimulus is therefore made of thousands of normally distributed numbers. White-noise stimuli have a flat spectrum on average, constant amplitude envelope and are deprived of short-term regularities (no sample-to-sample predictability) or salient features making the detection of any pattern very difficult (Figure S 9-1). In addition, since stimuli were randomly generated, prior exposure can be precisely controlled since the probability, for each participant, to have encountered the exact same noise-segments before the experiment is close to 0. The white-noise learning paradigms provide

therefore a unique opportunity to investigate the learning of novel sensory information. Stimuli were presented to participants using the PyschToolbox extension (Brainard, 1997) for Matlab (Mathworks Inc., Natick, MA, USA) and were played through a loud-speaker (soundcard: Echo Indigo, Echo Digital Sound Corp., Santa Barbara, CA, USA) placed near the bed and at 50dB to ensure comfortable listening conditions while minimally disturbing sleep.

Contrasts of interest and expected results

As thoroughly discussed recently (Andrillon et al., 2015a), the noise-memory paradigm allows exploring the rapid formation of memory to noise at different time-scales. The fact that listeners could discriminate between RN trials and N trials demonstrates their ability to detect the re-occurrence of a nondescript noise segment embedded in running noise after only few presentations (max: 5 in the "wake-learning" phase) and despite the statistical similarity between targets and fillers. Therefore the RN vs. N contrast reveals the formation of a form of short-term memory to noise (Figure 9-1a, right). On the contrary, RefRN and RN stimuli have identical structures (Figure 9-1b). They only differ through participants' prior exposure. Improvement in repetition-detection performance for RefRN compared to RN trials can only be explained by the formation of long-term memory to noise (time-scales of minutes or hours; Figure 9-1a, right). Such long-term learning of acoustic noise has been confirmed by several studies (Agus et al., 2010; Agus and Pressnitzer, 2013; Andrillon et al., 2015a; Luo et al., 2013). Importantly, Agus and colleagues showed that such learning was preserved after 2 weeks of time (Agus et al., 2010). Finally, the RefRN vs. N contrast focuses on the cumulative effect of short- and long-term memory. Overall, when focusing on EEG or behavioral indexes of repetition-detection, we expect the pattern of results described in Figure 9-1a (right): a difference in both the RN vs. N contrast (short-term memory) and RefRN vs. RN contrast (long-term memory) when the brain is in a state favorable to learning.

Electrophysiological recordings

Participants were equipped for polysomnographic recordings according to the ASSM guidelines. We continuously recorded electroencephalographic (EEG, N = 19 derivations, 10-20 montage), electroocculographic (EOG, N = 2 derivations, placed above and under the right and left canthus resp.), electromyograhpic (EMG, 1 derivation on the chin and 2 derivations on right and left abductor pollicis brevis (thumb flexor muscle) in order to record muscle activity associated to hand-responses), electrocardiographic (ECG, N = 1 derivation) data in parallel with video monitoring. To ensure the reliability of data collection through hours of recordings, AgCl electrodes were attached to participants' scalp using an adhesive past (EC2, Natus Neurology Inc., Middleton, WI, USA) amplified through a B1IP or B2IP MEDATEC amplifier (Medical Data Technology SPRL, Bruxelles, Belgique). This technique, while minimizing electrodes displacement, limits the number of channels that can be recorded. EEG electrodes were re-referenced to the averaged mastoids offline and EOG electrodes were referenced to the opposite mastoids. EEG, ECG and EMG data were recorded at a 200Hz sampling-rate. Impedances of scalp electrodes were generally below 5kΩ. An external channel was used to synchronize EEG data with stimuli presentation times.

Participants were constantly monitored during both wake and sleep. As explained above, during the "sleep-learning" phase, a given set of RefRN (wake, NREM or REM) was selected according to participant's vigilance state. To do so, the vigilance state was assessed online using standard guidelines (Iber et al., 2007) by an experienced scorer (TA) and confirmed offline by two scorers (TA, and DL) blind to experimental conditions (see below and Table S 9-1).

Behavioral indexes of perceptual learning

To behaviorally assess listeners' ability to detect the presence of repeating noise segments, we computed their sensitivity to the presence of these repetitions by means of a d' index (Macmillan, 2005). The d' index has the advantage to take into consideration participants' biases for one response (presence of repetitions) or the other (absence), facilitating the averaging across participants. Thus, a significant deviation from 0 indicates participants' ability to reliably discriminate the two conditions of interest at the group level. d' indexes were computed for RefRN and RN conditions independently and for each participant (see Equations 1 and 2):

(1) $$d'_{\mathrm{Re}\,fRN} = z(Hit_{\mathrm{Re}\,fRN}) - z(FA_N)$$

(2) $$d'_{RN} = z(Hit_{RN}) - z(FA_N)$$

where z(x) corresponds to the z-score for proportion x, Hit_{RefRN} corresponds to the proportion of correct responses for RefRN trials, Hit_{RN} corresponds to the proportion of correct responses for RN trials, FA_N corresponds to the proportion of incorrect responses for N trials. Extreme performances (100%/0%) were adjusted to the equivalent of half of a single correct/incorrect response (Macmillan, 2005) to avoid infinite d' values. As previously shown, RefRN trials were associated to higher d' indexes compared to RN trials (Figure 9-2a, top).

Reaction times (RTs) captured also the formation of memory traces to noise. Typically, RefRN trials lead to faster responses, often anticipating the end of the stimulus presentation window (< 3.5 s; Figure 9-1a, middle). We therefore combined the improvement in response accuracy and rapidity using the Behavioral Efficiency (BE) index, which we recently developed in a similar experimental context (Andrillon et al., 2015a). Inspired by the Inverse Efficiency Score (Townsend and Ashby, 1978), BE was defined as follows:

(3) $$BE_{\mathrm{Re}\,fRN} = d'_{\mathrm{Re}\,fRN} \times \left(\frac{RT_N}{RT_{\mathrm{Re}\,fRN}} \right)$$

(4) $$BE_{RN} = d'_{RN} \times \left(\frac{RT_N}{RT_{RN}} \right)$$

where RTs for RefRN and RN trials were computed from stimuli onsets. Intuitively, BE is increased for high d', and if the RTs to the stimulus of interest were faster than the N baseline. BE was higher for RefRN trials compared to RN trials (Figure 9-2a, bottom).

Behavioral data were analyzed in the "wake-learning" (Figure 9-2a) and "memory-test" (Figure 9-5) phases but not in the "sleep-learning" phases due to the absence of behavioral response during sleep. Trials without responses were not included in behavioral analyses. In the "sleep-learning" phase, RefRN targets were presented according to participants' vigilance state. However, in the course of the night, some of these RefRN have been presented around micro-awakenings, as assessed by a double offline scoring (N = 38 over 100 RefRN targets in NREM-sleep and 18 over 100 in REM-sleep). However, the isolated presentation of NREM targets during wake can hardly explain the suppressive effects observed for NREM targets. Nevertheless, to avoid this confound and to make sure that the positive effect for REM targets could not be due to these awakenings, BE was computed when excluding all NREM or REM RefRN heard during wakefulness (Figure S 9-5), which led to identical results as in Figure 9-5.

Polysomnographic data preprocessing

Polysomnographic data were analyzed using a combination of SPM (Functional Imaging Laboratory, Univ. College London, London, UK), FieldTrip (Oostenveld et al., 2011) and EEGlab (Delorme and Makeig, 2004) toolboxes running on Matlab (Mathworks Inc., Natick, MA, USA).

Offline sleep scoring: EEG, EOG, EMG and ECG data were preprocessed according to established guidelines. EEG data was high-pass filtered above 0.1 Hz and then low-pass filtered below 30 Hz (5^{th} order two-pass Butterworth filters). EMG data were band-pass filtered between [60, 80] Hz (5^{th} two-pass Butterworth filter). In addition, EEG, EOG, EMG and ECG were notch-filtered around 50Hz to reduce line-noise. Fz, C3, C4, Pz EEG derivations were used to score sleep along ECG and chin EMG derivations. As described above, vigilance states were assessed online using standard guidelines (Iber et al., 2007) by an experienced scorer (TA) and confirmed offline on 20s-long windows by two scorers (TA and DL) blind to experimental conditions. Tonic and phasic periods of REM-sleep were scored offline, using the presence of Rapid-Eye Movements (REMs) on EOG derivations as a criterion for phasic REM-sleep (pREM). 20s-long windows in REM-sleep without any REM but presenting otherwise the markers of REM-sleep (near-absent chin EMG tonus, absence of alpha oscillations or NREM sleep graphoelements such as K-complexes and sleep-spindles, presence of saw-tooth waves and theta oscillations) were considered as tonic REM-sleep (tREM). Table S 9-1 gives a summary of this scoring across participants.

Sleep cycles identification: Sleep cycles were individualized using participants' hypnograms (97 cycles in 18 participants, 5.6 ± 0.2 per participant, mean ± SEM). Sleep cycles having different durations (86 ± 3.6 minutes), we normalized cycles' length to be able to average variables of interest across cycles (N = 18 bins). The progression within the cycles was therefore expressed in percentage of the total duration (Figure 9-7 and Figure S 9-7). 76 cycles in 18 participants were eventually included in the analysis, the others not having enough RefRN or RN trials (at lest 20 trials per condition and per bin, see below). Two participants were not included in the sleep-cycle analysis due to the difficulty of clearly identifying sleep-cycles.

Sleep rhythms detection: Slow-waves and sleep-spindles were detected in NREM sleep using algorithms that have been presented in details elsewhere (Andrillon et al., 2011; Nir et al., 2011). Scalp distributions of the densities of detected events are shown in Figure S 9-6. For each slow-wave we extracted its onset, peak-to-peak amplitude (amplitude), down-to-up state slope (slope), number of negative peaks and spatial expanse (i.e. for a given channel of reference, here Cz, and for each slow-wave, the proportion of channels showing also a slow-wave in a 100 ms window centered on the reference slow-wave's starting point). For each spindle, we computed its frequency by extracting the peak in power (estimated through a Fast-Fourier Transform, FFT) within a [11, 16] Hz window. Spindles with a frequency below 13 Hz were declared slow-spindles and spindles with a frequency above 13 Hz, fast-spindles (Andrillon et al., 2011). It is worth noting that the slow-wave detection well replicated recent findings on the changes in slow-waves properties from light to deep NREM (Siclari et al., 2014; Figure S 9-7) while the spindle detection replicated the known frontal distribution of slow-spindles and centro-parietal distribution of fast-spindles (De Gennaro and Ferrara, 2003). In particular, the density of slow waves and the number of negative peaks robustly increased during sleep cycles ($r = 0.95$ and 0.88 resp., $p < 0.001$) while their slope or spatial expanse decreased ($r = -0.89$ and -0.95 resp., $p < 0.001$). In parallel, we computed the EEG learning index ($ITPC_{RefRN}$ / $ITPC_{RN}$, Figure S 9-7). The learning index negatively correlated with slow waves density (Pearson correlation: $r = -0.67$, $p < 0.005$) and the number of negative peaks ($r = -0.61$, $p < 0.01$), which is concordant with the correlation with δ-power (Figure 9-7). Importantly, the learning index was positively correlated to the slow-waves slope ($r = 0.55$, $p < 0.05$) and spatial expanse, ($r = 0.65$, $p < 0.005$).

In order to compute the percentage of trials associated with slow-waves, fast and slow sleep spindles (Figure 9-6b), we examined, for each trial in NREM2 and 3 stages, whether a slow-wave or fast or slow sleep-spindle was detected during the presentation of the stimulus. Each time we used an electrode of reference (green dot in Figure S 9-6) that corresponds to the electrode with the highest density for the corresponding graphoelement (slow-waves and slow spindles: Fz; fast spindles: Pz).

EEG preprocessing: EEG data was first high-pass filtered above 0.1 Hz (5^{th} order two-pass Butterworth filter) and then epoched on large temporal windows ([-14, 14] s) around stimulus onsets. EEG data was then low-pass filtered below 20 Hz (5^{th} order two-pass Butterworth filter) and a notch-filter at 50 Hz was also applied to reduce line-noise. A second epoching on shorter windows was performed ([-2, 7] s). Data was corrected for baseline activity after each epoching by subtracting pre-stimulus activity for each EEG derivation. Minimal artifact rejection was applied here: trials for which the maximal absolute value of the EEG signal in at least one of the central electrodes (C3, C4, Cz) was higher than a given threshold were excluded from our analyses. Brain dynamics drastically changing from wake to sleep, the thresholds differed across vigilance states (wake and REM: 80 μV, NREM2-3: 150 μV). In this study, we focused mainly on central electrodes (C3, C4 and Cz in the 10-20 montage) since these electrodes showed the largest responses to noise (Picton, 2011) and noise-repetition (Andrillon et al., 2015a). All analyses were performed on these electrodes except when stated otherwise.

Electrophysiological (EEG) indexes of perceptual learning

Event-Related Potentials (ERPs) analyses: We focused on either stimulus-locked (Figure S 9-4) or target-locked (Figure 9-2, Figure 9-4) ERPs. Stimulus-locked ERPs show EEG potentials triggered by the transition from silence to noise irrespective of experimental conditions. Indeed, we here focused on the Late Auditory Evoked Potentials (AEPs, (Picton, 2011)) occurring within the first 500 ms following stimulus onset and therefore before any presentation of a RefRN or RN target (starting at 800 ms). As classically observed, these AEPs present stereotypical and state-dependent profiles (Picton, 2011).

We also computed target-locked ERPs. For target-locked ERPs, the EEG signal was high-pass filtered above 1Hz instead of 0.1Hz to get rid of slow-drifts. These ERPs had the particularity to be computed within the stimulus presentation window. White-noise being deprived of significant fluctuations in acoustic energy of salient perceptual landmarks that usually trigger ERPs (e.g. silence-to-noise transition in the case of AEPs), any deviation from the N condition for RefRN and RN trials can be interpreted as an indication that the brain had detected the presence of the repeated noise segment. We termed the ERPs associated to repeated targets Memory-Evoked Potentials (MEPs) to emphasize the fact that they parallel perceptual learning (Andrillon et al., 2015a). Comparing AEPs and MEPs can provide means to explore the neural mechanisms underlying MEPs and in particular whether they share common generators. Target-locked ERPs were first averaged from the 2nd to last target (wake trials: 4 targets per trial; sleep trials: 9) for each trial and then averaged across trials for each participant and condition.

Time-Frequency analyses: Time-frequency decompositions were performed using the EEGlab toolbox (Delorme and Makeig, 2004) on the EEG data epoched around stimulus onsets (Figure 9-3). We employed the wavelet method. For a given scalp sensor, we obtained the decomposed signal ($s_{t,f}$) for each time point (t) and frequency (f) in its complex representation:

(5) $$s_{t,f} = A_{t,f} e^{i\varphi_{t,f}}$$

where A(t,f) is the power of the EEG signal and φ(t,f) its phase at given time and frequency.

Power response for each condition and vigilance state was computed by averaging across the corresponding trials the absolute amplitude (Figure 9-3). Power response was normalized by pre-stimulus-onset activity and expressed on a log-scale:

(6) $$Power_{t,f} = \log\left(\frac{mean(A_{t,f})}{mean(A_{baseline,f})}\right)$$

Inter-trial phase coherency (ITPC) was also computed using wavelets. We focused on a frequency band ([1.5, 3.5] Hz) around stimulus presentation (2 Hz) based on previous studies (Andrillon et al., 2015a; Luo et al., 2013) and the "wake-learning" phase (see Figure S 9-2). ITPC describes how the phase of the EEG signal is reproducible across trials for a given condition and participant. Thus, high ITPC values across participants indicate that each participant exhibited a reproducible phase for the corresponding time

and frequency (for a given condition), even if the particular phase differed between participants. To compute ITPC, we extracted the phase of the signal for each time and frequency ($\varphi_{t,f}$) and averaged it across trials (*n*) using Euler's formula:

$$(7) \qquad ITPC_{t,f} = \sqrt{(\frac{1}{n}(\sum_{n}\cos(\varphi_{t,f}))^2 + \frac{1}{n}(\sum_{n}\sin(\varphi_{t,f}))^2)}$$

The presence of ERPs and the increase in ITPC are tightly linked: ERPs (and MEPs) lead to higher ITPC values since they have a reproducible shape across trials. We recently showed that the increase in ITPC associated to noise-learning could be explained by the presence of MEPs (Andrillon et al., 2015a). However, ITPC has several advantages compared to ERPs: (i) it allows targeting a certain frequency range (Figure S 9-2); (ii) contrary to ERPs, it is not affected by high-amplitude physiological events (such as slow-waves) or artifacts; (iii) it can capture non-time locked activity (see Andrillon et al., 2015 for a comparison between ERPs and ITPC in the context of the noise-memory paradigm). We therefore focused on ITPC rather than ERPs to compute an EEG index of perceptual learning (Figure 9-5, Figure 9-6 and Figure 9-7).

Such EEG index was particularly useful during sleep where behavioral responses are abolished, preventing the computation of any behavioral index of learning. To make sure that ITPC captured the variation in behavioral performance across participants and represented a good proxy for behavioral performance, we verified that our EEG (ITPC) and behavioral (BE) indexes correlated with each other ('wake-learning" phase, Figure 9-2d). For Figure 9-5 and Figure 9-6, we computed ITPC on identical time and frequency windows for RefRN and RN trials so as to better compare these conditions (ITPC was averaged on [1, 3.8] s and [1.5, 3.5] Hz windows over central electrodes which is in line the clusters observed in Figure S 9-2). In Figure 9-7 and Figure S 9-7, we targeted a narrower frequency range around 2Hz for ITPC ([1.5, 2.5] Hz), which was made possible by the increase in stimuli duration during sleep (time window: [0.8, 5.5]).

Lastly, as can be noted in the Equation 7, ITPC depends on the number *n* of trials on which it is computed. We kept this number identical across conditions: for each participant and experimental phase, the condition with the smallest number of trials was chosen as the reference and trials were randomly picked for the other, more numerous conditions. During the night, ITPC was computed by dividing all sleep-cycles into fixed windows of 20 stimuli presentations (either RefRN and RN). This was done by cycle to avoid averaging data from different cycles. These fixed windows were slid trial-by-trial. Thus, if a cycle contained *n* RefRN trials, we obtained *n-19* ITPC values that were then binned in 18 bins for each cycle (Figure 9-7b). ITCP and slow-wave power were computed on Cz only for Figure 9-7.

To obtain the power spectra displayed in Figure S 9-4, we used a Fast-Fourier Transform (FFT) and extracted the power for all trials altogether (and not per condition). We then averaged it in time across the entire epoch ([-2, 7] s).

Statistics

Parametric statistics were used (Student t-tests to compare pairs of variables, Pearson's method for correlations) when variables were normally distributed (Kolmogorov-Smirnov test). Otherwise, we used non-parametric statistics (Wilcoxon rank-test (u-test) to compare conditions and Spearman's method for correlations) when data were not normally distributed. For Figure 9-5c, two data points were excluded from the correlation analysis since considered as outliers (the corresponding ITPC values ($ITPC_{RefRN}$ - $ITPC_{RN}$) were outside the mean ± 2 standard-deviations range).

Statistics used for time and time-frequency plots were corrected for multiple comparisons by means of a cluster-permutation approach (Maris and Oostenveld, 2007). The rational is the following: each cluster was constituted by the samples (in a 1D (time-plots) or 2D (time-frequency) space) that consecutively passed a specific threshold (here, $p < 0.05$ except for Figure 9-7b where $p < 0.01$). The cluster statistics were chosen as the sum of the t-values of all the samples within the cluster. Then, we compared the cluster statistics of each cluster with the maximum cluster statistics of 1000 random permutations and obtained a non-parametric p-value ($p_{cluster}$). Significant clusters are displayed as horizontal bars or contours on plots, $p_{cluster}$ are reported in the main text and figures' legends.

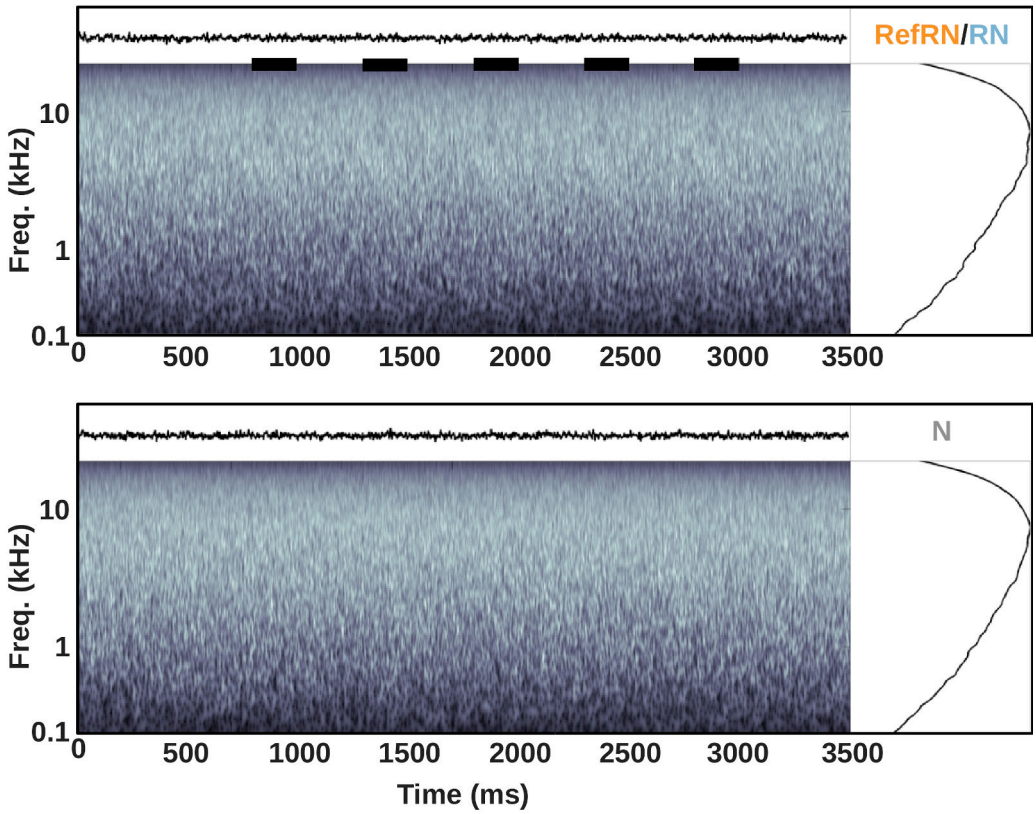

Figure S 9-1 Modeled cochlear representation of RefRN/RN and N stimuli

Output of a peripheral auditory model (Spectro-Temporal Excitation Pattern, (Moore, 2003)) for noise exemplars either presenting repeated segments (RN/RefRN, top) or not (N, bottom). The model simulates the cochlear filter, providing an estimate of the information transmitted to the central nervous system. In the RefRN/RN condition, the positions of repeated segments are indicated with black horizontal bars.

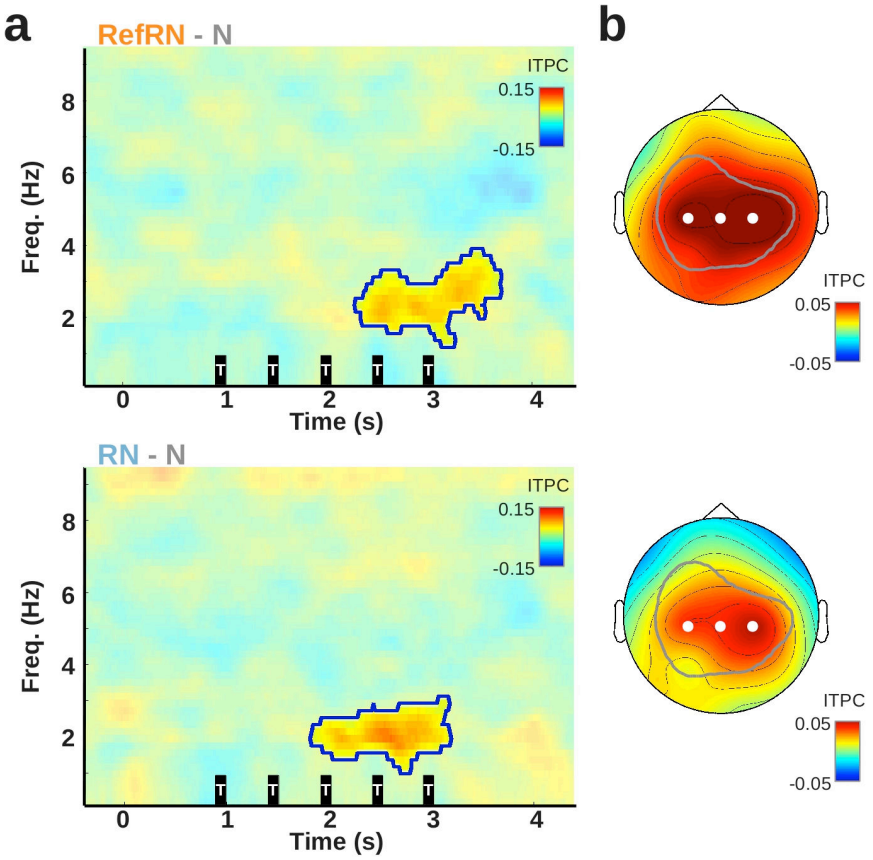

Figure S 9-2 Noise-repetitions are associated with an increase in Inter-Trial Phase Coherency (ITPC)

(a) Time-frequency decomposition of the difference in ITPC between RefRN (top) or RN (bottom) and N trials. ITPC was computed over central electrodes (C3, C4, Cz: white circles in panel b) and averaged across participants (N = 20) for the "wake-learning" phase (participants awake and responsive). Purple contours show clusters surviving a Monte-Carlo permutation test (pcluster < 0.05). (b) Scalp topographies of ITPC values for the RefRN (top) and RN (bottom) conditions when averaged over the corresponding clusters in panel a. Gray circles show, for comparison, the distribution of the RefRN vs. N effect observed in evoked-potentials (Memory-Evoked Potentials, MEP, see Figure 9-2b).

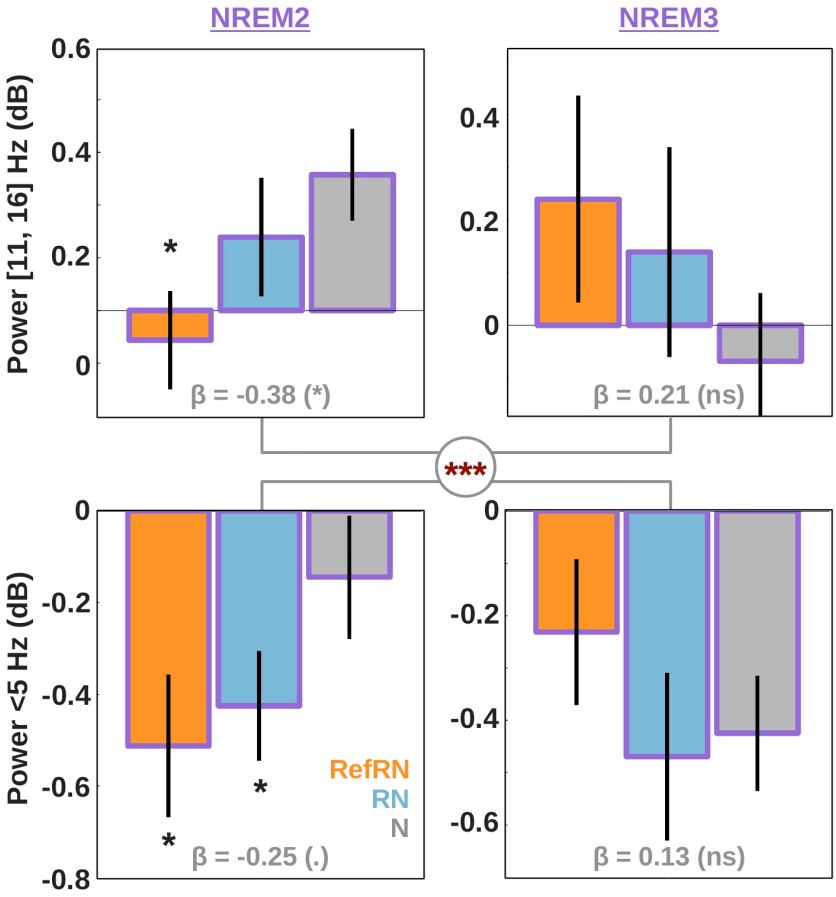

Figure S 9-3 Condition-dependent modulations of sleep-depth observed in NREM2 disappear in NREM3

(a) Power increase within the δ (< 5 Hz) and σ bands ([11, 16] Hz) for the RefRN, RN and N conditions. The power responses were computed on a [1, 5.5] s window locked to stimulus onsets (see Figure 9-3) and average across participants (N = 20) for NREM2 and NREM3 trials separately. Error-bars indicate the standard error of the mean (SEM) across participants. A linear model was fitted for all subpanels (RefRN / RN / N) and the regression coefficients (β) are displayed for each sleep stage and frequency band. Stars atop bars indicate the significance level for the RefRN vs. N or RN vs. N comparisons (paired t-tests, no star: $p > 0.05$, (*): $p < 0.05$) while stars aside β indicate the significance level of the linear regression (ns: $p>0.05$, (.): $p < 0.1$, (*): $p < 0.05$). Finally, we compared the linear models estimated for NREM2 and NREM3 stages for each frequency band separately. Highly significant p-values (***: $p < 0.001$) suggest a complete disappearance of the effects observed in NREM2 with the transition to NREM3 rather than a mere decrease in effects' magnitude.

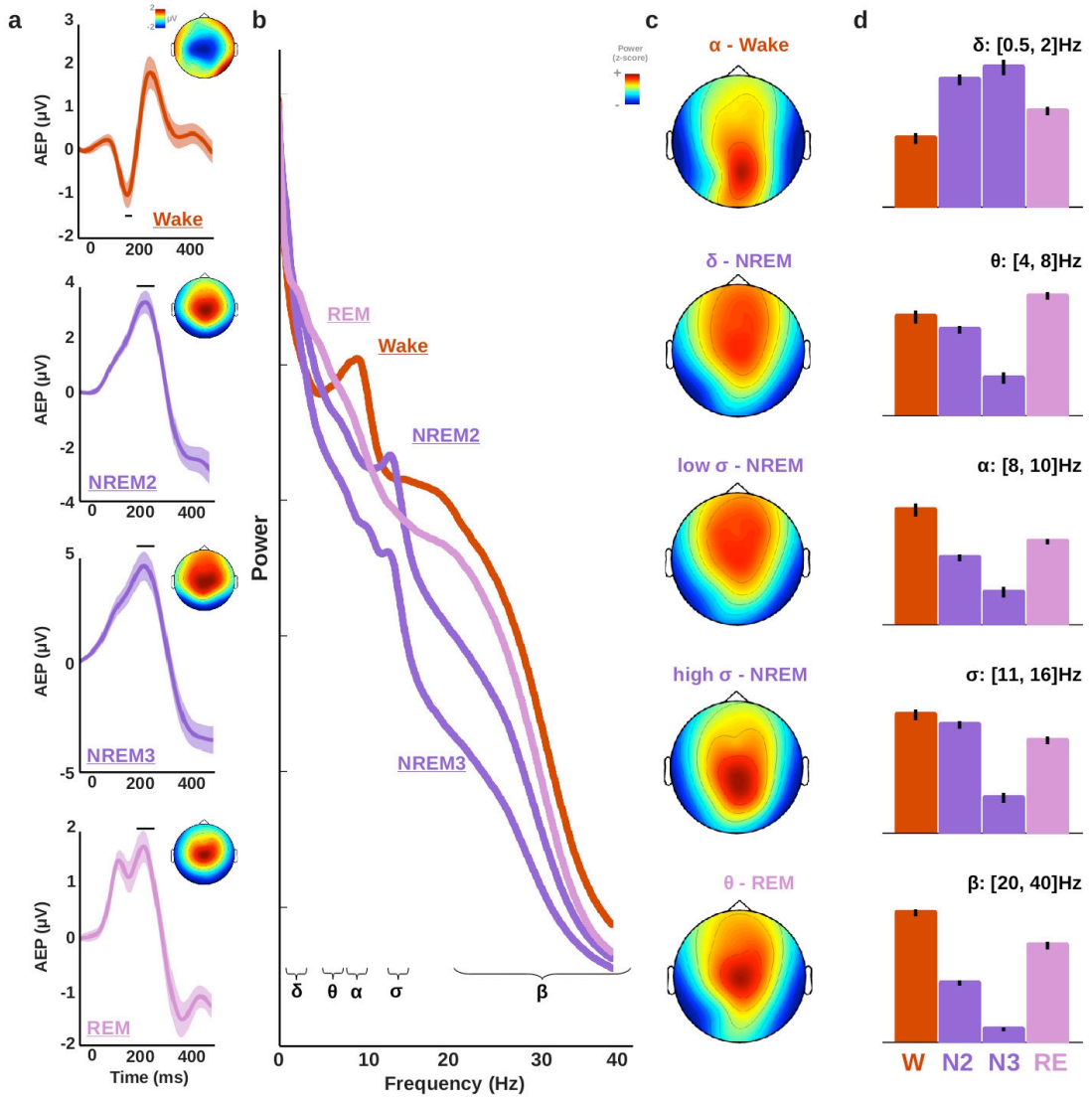

Figure S 9-4 Differences in Auditory-Evoked Potentials (AEPs) and spectral profiles across sleep stages

(a) Electroencephalographic (EEG) signal time-locked to stimuli onset and averaged across participants (N = 20) for the "sleep-learning" phase. Stimuli were collapsed across experimental conditions. Curves show the Event-Related Potentials (ERPs) associated to the silence-to-noise transition across participants. Note the canonical evoked potentials (Auditory-Evoked Potentials, AEPs, Picton, 2011). These AEPs differed between vigilance states. 1st row: Wake AEP with typical N1 and P2 components; 2nd row: NREM2 AEP with the N1 component replaced by a high-amplitude positive component; 3rd row: NREM3 AEP similar as NREM2; 4th row: REM AEP characterized by the disappearance of the N1 component bringing the preserved P1 and P2 components out. Shaded areas around curves indicate the standard error of the mean (SEM) computed across participants. Insets show the scalp topographies of the component marked with a black horizontal bars. Note that given the time-window considered, these AEPs only reflect the silence-to-noise transition since the window ends before the presentation of repeated targets. (b) Power spectra computed across participants for the "sleep-learning" phase using a Fast-Fourier Transform (FFT). Power was normalized and expressed in decibels (dB). Note several deviations from the 1/f trend. These increases in certain frequency bands depend on the vigilance state: wake was characterized by an increase within the α band ([8, 10] Hz) and β band ([20, 40] Hz), NREM sleep by an increase within the δ band (< 5 Hz) and σ band ([11, 16] Hz) and REM-sleep

by an increase within the θ band ([4, 8] Hz). (c) Scalp distributions of the power in different frequency bands for the appropriate vigilance state (wake: α, β; NREM: δ, σ; REM: θ). Power was z-scored across sensors in order to stress the differences in the spatial distribution of these brain rhythms. (d) Power averaged across the abovementioned frequency bands and for each vigilance state for electrode Cz. As classically observed, the transition from wake to NREM2 is characterized by the disappearance of α and β rhythms replaced by an increase in δ and σ bands corresponding to the apparition and multiplication of NREM-sleep hallmarks that are slow-waves and sleep-spindles. Transition to REM-sleep is characterized by the partial recovery of α and β rhythms as well as the emergence of strong θ oscillations. Thus the vigilance states here investigated correspond to drastically different brain states.

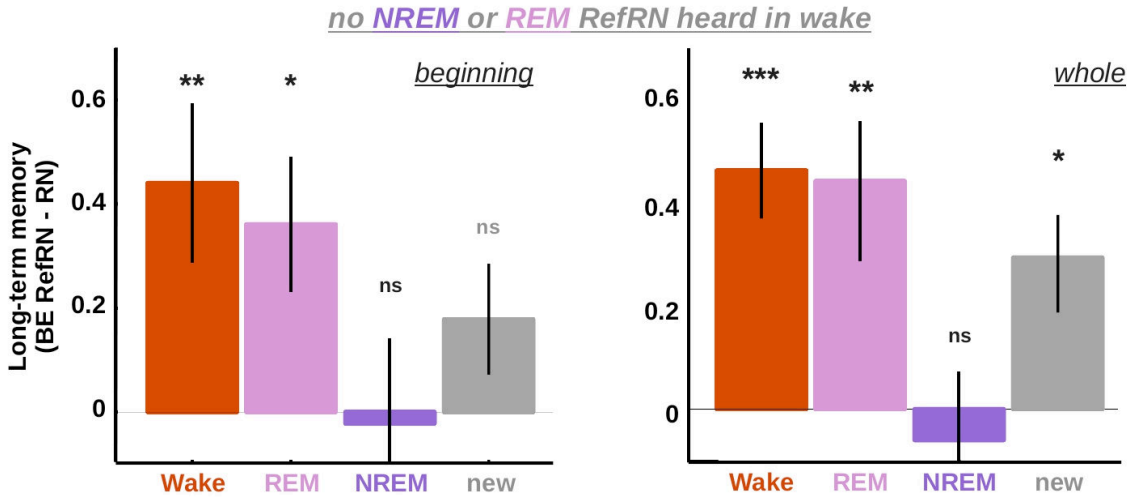

Figure S 9-5 The positive effect of REM-sleep and negative effect of NREM-sleep in the "memory-test" is conserved when excluding sleep RefRN trials heard around (micro-)awakenings

Figure 9-4a shows the RefRN vs. RN contrast on the behavioral efficiency (BE) index computed in the "memory-test" that participants underwent upon awakening. In particular, we showed in Figure 9-4a an increase in performance for RefRN items heard in REM-sleep. To check that this effect is not due to the few RefRN targets that were presented around (micro-)awakenings, the very same analysis was performed, this time excluding these items (see SI). BE was computed separately for RefRN heard during wakefulness, REM, NREM or new RefRN. Error-bars denote the SEM across participants (N = 20) and stars atop bars indicate the results of the statistical tests (t-tests against 0, $p < 0.005$: ***; $p < 0.01$: **; $p < 0.05$: *, ns: $p \geq 0.05$). Note that the exact same pattern of results was observed as in Figure 9-4a ruling out the possibility that our effect is driven by such RefRN targets.

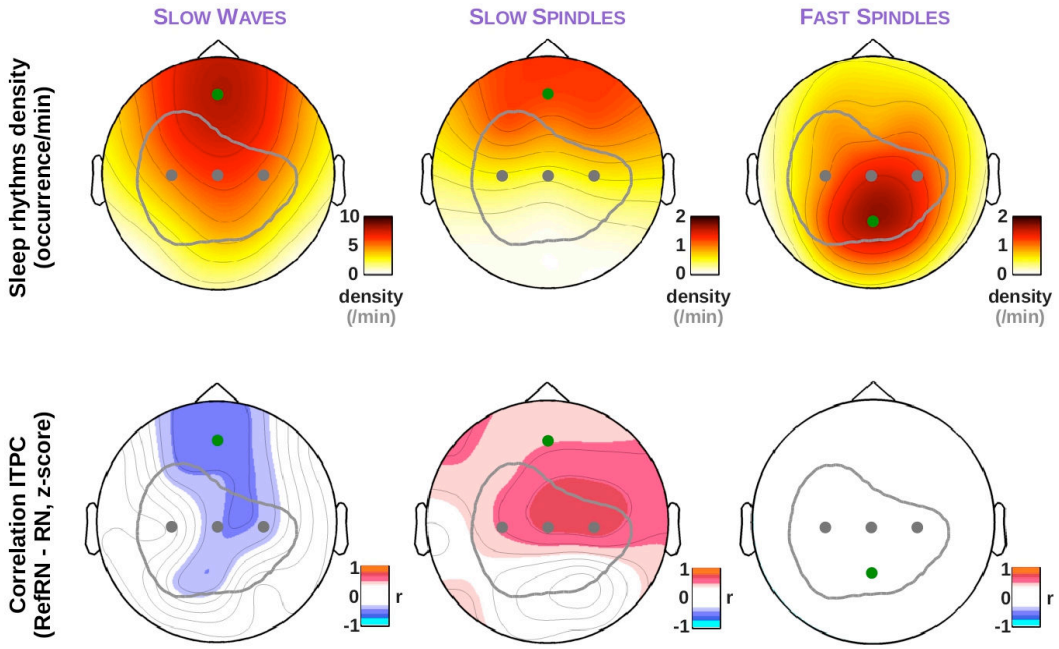

Figure S 9-6 Correlations between slow-waves, fast and slow spindles overnight and the EEG learning index upon awakening

1st row: scalp distribution of slow-waves (left), slow-spindles (spindle frequency: [11, 13] Hz, middle) and fast-spindles (spindle frequency: [13, 16] Hz, right) densities as detected using dedicated algorithms (see SI for details). Note the typical frontal predominance of slow-waves and slow spindles and the centro-parietal predominance of fast spindles. Green dots show the electrodes with the highest densities: Fz for slow-waves and slow spindles, Pz for fast spindles. 2nd row: scalp distribution of Pearon's correlation coefficients computed between the EEG learning index (ITPCRefRN - ITPCRN) and slow-waves (left), slow-spindles (middle) and fast spindles (right) densities (across participants). Non-significant ($p>0.05$, uncorrected) coefficients were set to 0. Note that the EEG learning index was positively correlated with the density of slow-waves and negatively correlated with frontal spindles over regions known to be involved in noise-learning during wakefulness (gray circles showing the distribution of the RefRN vs. N effect observed in evoked-potentials in wakefulness, Figure 9-2b). Importantly these distributions were not centered on the peak of the scalp distribution for the corresponding sleep rhythms. There was no significant correlation between fast spindles and the EEG learning index (all $p > 0.05$).

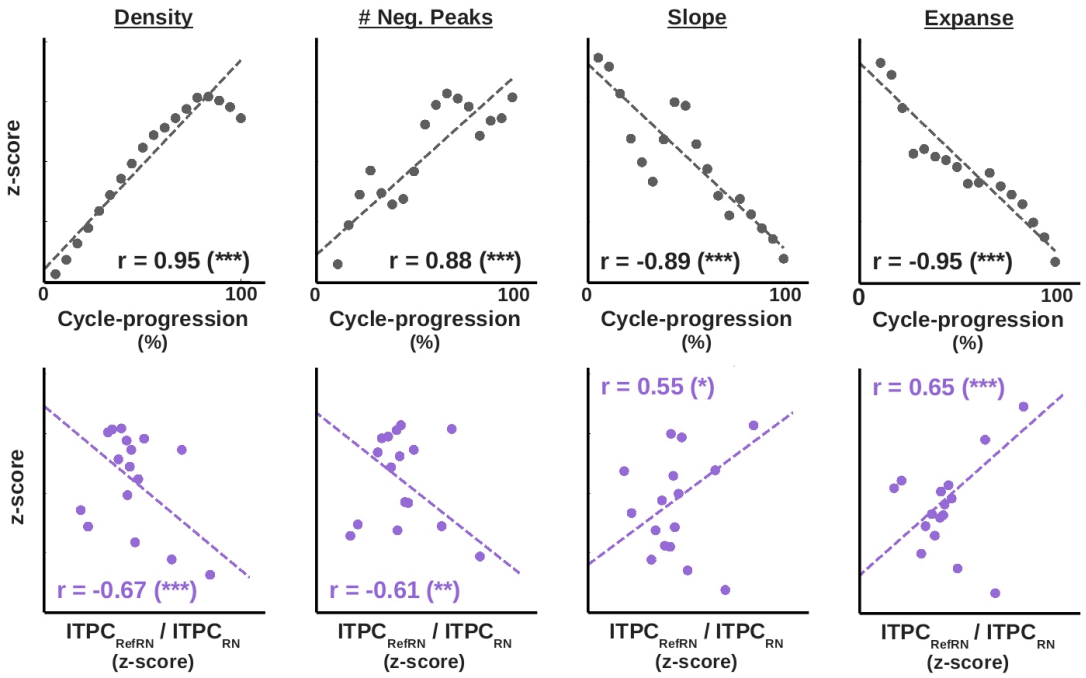

Figure S 9-7 Slow-waves characteristic are modified from light to deep NREM-sleep

1st row: Evolution along sleep cycles of some properties of the slow-waves detected in NREM sleep (NREM2-3, N = 76 in 18 participants, see SI). Seep cycles were binned in order to normalize their length. Progression within the cycles is expressed in percentage (see also Figure 9-7). While density and the number of negative peaks increased within cycles, the slope and spatial expanse (i.e. proportion of sensors affected by a given slow-waves, see SI) decreased. 2nd row: Correlations between the slow-waves parameters and the EEG learning index (ITPCRefRN / ITPCRN) computed as in Figure 9-7b. The learning index was negatively correlated with slow-waves' density and the number of negative peaks but positively correlated with slow-waves slope or spatial expanse. Thus, the suppressive effect observed in deep NREM-sleep corresponds to the appearance of more numerous but also more local slow-waves (type-II slow-waves, Siclari et al., 2014). Pearson's correlation coefficients were computed between each slow-waves parameter and cycle-progression (top) or ITPC (bottom) and are displayed on each graph. Dotted lines show linear regressions between the pairs of variable. Stars indicate the significance level of the correlation coefficients (*: $p < 0.05$, **: $p < 0.01$, ***: $p < 0.005$).

	Wake	**NREM**			**REM**		***total***
		NREM1	***NREM2***	***NREM3***	***tREM***	***pREM***	
duration	220	50.1	200	110	49.2	29.8	659
(min.)	(9.4)	(4.7)	(8.4)	(6.8)	(3.3)	(3.4)	(8.7)
%	33	7.5	30	16	7.4	4.4	
	(1.31)	(0.73)	(1.18)	(0.90)	(0.52)	(0.49)	

Table S 9-1 Results of the sleep scoring

Sleep was scored as wakefulness, NREM (Non-Rapid-Eye Movement) sleep stage 1 (NREM1), NREM-sleep stage 2 (NREM2), NREM-sleep stage 3 (NREM3), tonic REM-sleep (tREM) and phasic REM-sleep (pREM) according to established guidelines (Iber et al., 2007). Numbers refer here to the average across participants (N = 20). Numbers in brackets refer to the standard error of the mean computed across participants. The "wake-learning" and "memory-test" phases were here included (entire recording session), which explain the extent of the wake periods.

General Discussion

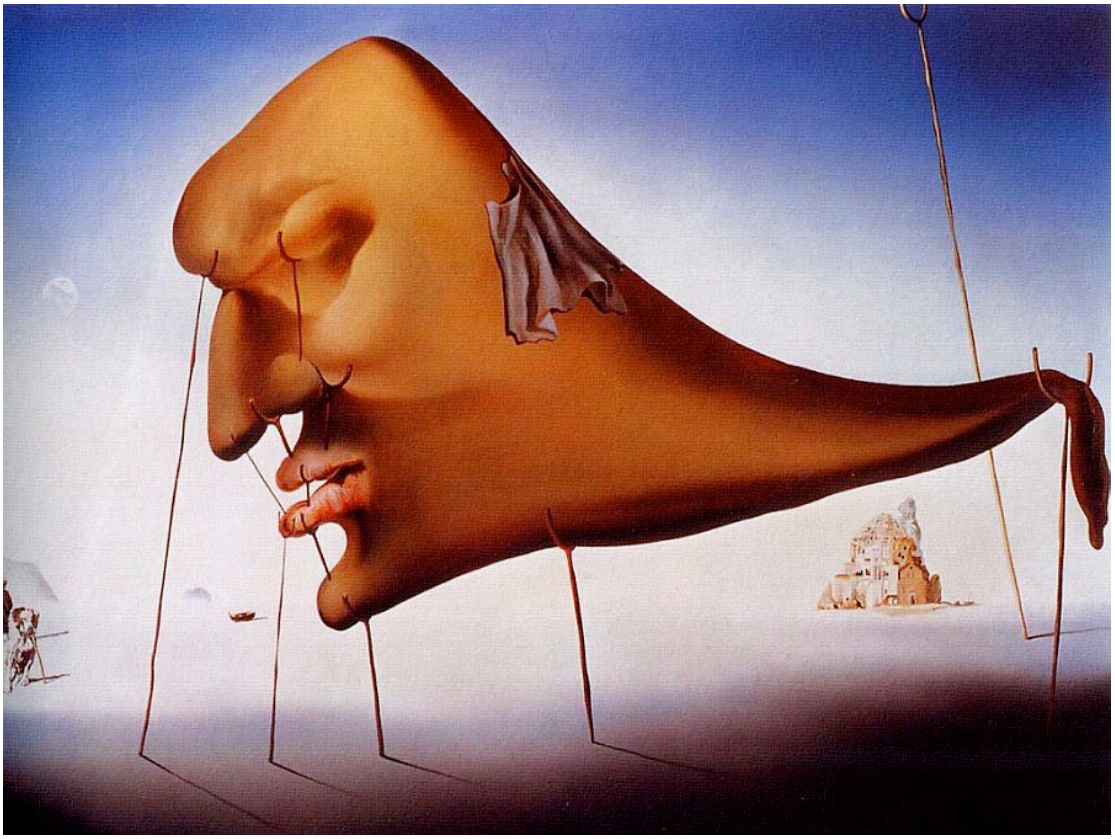

Le Sommeil
Salvador Dali (1937)

During my doctoral work, I have attempted to study sleep from physiology to cognition and from single-units recordings to whole-brain activity. I have used sleep as an experimental tool to manipulate consciousness but also focused on sleep in itself. Despite the variety of approaches developed, all the studies presented here emphasize the importance of considering sleep as a dynamic process. Local aspects of sleep in time and space are to be investigated in order to understand sleep's mechanisms and functions. Thus, sleep and wake, rather than being two mutually exclusive states, are better represented as a gradient whose balance is self-regulated.

Here, I will discuss the functional implications of sleep's local aspects illustrated in Studies 1 to 3. I will present wake and sleep as a continuum rather than immiscible states. A direct consequence is that intrusions of sleep rhythms in the awake brain will affect behavior. Conversely, intrusions of wake activity in the sleeping brain could allow for the recovery of wake-like processing.

And indeed, I presented in Studies 4 to 6 how the sleeping brain can complexly process external information, as when awake. But the sleeping brain is not completely pervasive to external output either. I will thus discuss the potential mechanisms allowing the coupling or decoupling of the sleeping brain with its environment.

Finally, in Studies 7 to 9, I investigated whether the sleeping brain could learn new information while sleeping. While possible, such learning contrasts with the rapidity and automaticity of mnesic processes occurring when we are awake. I will discuss the different theoretical proposals that could explain this contrast and propose a synthetic account of the role of sleep in memory and plasticity.

Local sleep and its functional consequences

Slow-waves: the hallmark of NREM sleep or neuronal fatigue?

Slow-waves are an iconic EEG pattern. Among the first brain rhythms to be identified (Loomis et al., 1935), only a few years after the invention of the EEG (Berger, 1929), they are the largest non-pathological neural events that can be recorded on the scalp, with peak-to-peak amplitudes exceeding 100µV. The mechanisms underlying these waves have been extensively investigated in the past, notably in the laboratory of Mircea Steriade (Mircea Steriade, 2003). Slow-waves are the resultant of neurons' bi-stable membrane potential ((Steriade et al., 2001), Figure 10-1) and are characterized by a down-state (or OFF period corresponding to the silencing of neuronal assemblies) followed by an up-state (during which units recover wake-like activation levels). These down and up-states typically alternate every second in deep NREM sleep when slow-waves trains are continuous (a form of sleep often referred as Slow-Wave Sleep (SWS)).

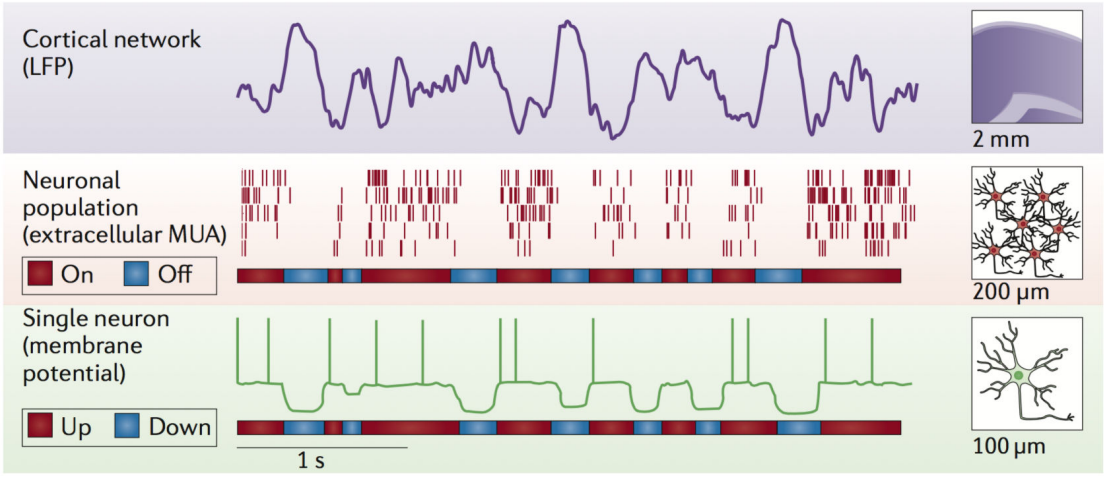

Figure 10-1 Slow-waves, from single neurons to cortical networks

At the network level, slow-waves are characterized by positive and negative peaks alternating every second or so. This 1Hz oscillation translates into ON and OFF states at the neuronal population level, during which vast neuronal assemblies are silenced (OFF states) or get activated (ON states) in synchrony. These ON and OFF states (also referred as UP and DOWN sates) are clearly visible at the level of the single neuron. Neurons' membrane potentials oscillate indeed between two values. The UP period allows the emission of action potentials while the DOWN state represent a period of hyperpolarization in which no action potential can be initiated. From (Vyazovskiy and Harris, 2013).

I will not dive here into the details of the generation of slow-oscillations (see (Mircea Steriade, 2003)). Briefly, slow-waves are thought to be the result of a modification of the excitation/inhibition balance in cortical networks. The activations of neurons is accompanied by the build-up of slow adaptative currents, which would ultimately force the neurons in an hyperpolarized silent state (Compte et al., 2003). This bistable dynamic seems to be established by changes in the level of critical neuromodulators such as Acetylcholine (Riekkinen et al., 1991). The emergence of slow-waves would be therefore due to a global change in brain chemistry, which could explain why the brain falls in NREM sleep as a whole.

However, recent research has tempered the relationship between NREM sleep and slow-waves. Indeed, slow-waves have been found in other states than NREM sleep: in wakefulness after prolonged sleep deprivation (Vyazovskiy et al., 2011) and recently in the superficial layers of primary cortices in REM sleep (Funk et al., 2016). Although the mechanisms underlying the presence of slow-waves outside NREM sleep are currently unknown, these findings reveal that slow-waves cannot be seen as a signature of NREM sleep, and are not uniquely triggered by the changes in neuromodulation occurring at NREM sleep onset. Rather slow-waves might be seen as a marker of neuronal fatigue. According to the 'excitable model' and as presented above, down-states are triggered following the build-up of hyperpolarizing conductances. Down-states can therefore be seen as a consequence of the up-states. It is therefore possible that prolonged periods of sustained activity (i.e. wakefulness) would also affect the excitation/inhibition balance at the cell level and increase the probability that an OFF state would occur (Vyazovskiy and Harris, 2013). According to this view, neuronal bi-stability could be achieved through both systemic changes and local changes in the excitation-inhibition balance. Slow-waves can therefore be seen as a use-dependent process (Tononi and Cirelli, 2014).

Numerous experimental studies are concordant with the view that slow-waves are modulated in a use-dependent fashion. First, slow-wave activity (SWA) has often been taken as a proxy for homeostatic pressure (Borbely and Achermann, 1999): the more an individual has been awake, the larger the SWA. Reversely the more an individual has been asleep, the lesser the SWA and the shorter are the OFF periods (Riedner et al., 2007; V. V. Vyazovskiy et al., 2009). Second, the time spent awake is not the only predictor of SWA. Rather, SWA depends on prior activity in a use-dependent fashion and can be locally modulated (which provides a powerful control for effects related to the circadian cycle and time spent awake). Huber and colleagues showed, in a seminal study, that cerebral regions involved in a motor learning task will express larger amounts of SWA than regions that were not involved in the extensive practice of the task (Huber et al., 2004)[6]. A mirror-study has shown that the immobilization of an arm led to a reduction of SWA in the corresponding somatosensory areas (Huber et al., 2006). These activity-dependent modulations of slow-waves could again be interpreted within the framework of the 'excitable model', with a use-dependent modification of the excitation/inhibition balance at the single-unit level during the wake period (Vyazovskiy and Harris, 2013).

From local to global or from global to local?

This link between prior activity and the occurrence of slow-waves could explain the emergence of slow-waves during wakefulness as well as the fact that the modulation of SWA can be local. But a paradox remains: slow-waves appear to be more global in early NREM sleep and more local in later NREM sleep (Siclari et al., 2014a). If SWA builds upon previous wakefulness, the reverse should be observed. Sleep onset should be characterized by the apparition first of local slow-waves becoming more and more global. However, when recording sleep onset, the first slow-waves to be seen are usually the largest. An interaction between the homeostatic and circadian processes (see

[6] Importantly, this regional increase in SWA was predictive of the performance gain upon awakening, which links slow-waves not only to the prior period of wakefulness but to the restoration or improvement in the ensuing period of wakefulness.

Introduction, (Borbély, 1982)) could explain this complex pattern. Local slow-waves would occur after prolonged wakefulness due to the homeostatic pressure (see Introduction). But we usually go to bed before reaching such a state of sleep deprivation. We typically fall asleep at a given time of the day in accordance with our circadian rhythms. At sleep onset, the circadian process would thus introduce a global change in the chemistry of the brain, favoring the apparition of large and global slow-waves. Then, these slow-waves will get more and more local with the dissipation of the homeostatic pressure.

Local slow-waves and information processing

During slow-waves, neurons go silent for an instant. Such hyperpolarized state logically affects brain's internal computations. In a very important study, Vlad Vyazovskiy and colleagues showed that the occurrence of local slow-waves impairs the behavior in a task-dependent fashion (Vyazovskiy et al., 2011). The generalization of such down-states is likely to prevent any complex processing of information in NREM sleep (see p325-326). Reversely, the fact that slow-waves can be local could provide periods in which some brain regions are not affected by slow-oscillations (Nobili et al., 2012), allowing them to recover wake-like processing abilities. Of course, since we used scalp EEG recordings, we cannot directly test this hypothesis in our data since (i) slow-waves recorded on the scalp are likely to be global events (Study 1, (Nir et al., 2011)), (ii) scalp EEG recordings are not precise enough for us to know whether a given brain region is not affected by a slow-wave. However, we observed in independent datasets (Studies 5 and 9) that the processing of external information was paralleled by a local decrease in slow-wave or spindle power. Importantly, the timing of these modulations corresponded to the timing of the EEG indexes of information processing and the scalp distribution overlapped with the areas involved in these sensory processes. It is therefore possible that this local lightening of sleep depth, in time and space, traduces a form of local sleep allowing sensory processes to be completed.

However, we face here again a paradox. As we said earlier, slow-waves tend to be more global at sleep onset and more local afterwards (Siclari et al., 2014a). Yet, we found in Studies 5 and 9 that indexes of responsiveness to the environment were stronger at the beginning of NREM sleep cycle and disappeared with slow-waves becoming more numerous but more local. First of all, it should be reminded that in light NREM sleep, although slow-waves comprise mostly K-complexes which are global but discrete events, the vast majority of light NREM sleep is deprived of slow-waves (>80% by definition (Iber et al., 2007)). We showed in Study 5 that the integrated processing of information was possible only when such slow-waves were absent. Second, the apparition of local slow-waves in deep NREM sleep does not mean that sleep is lighter. On the contrary, in deep NREM sleep, slow-waves are more numerous, appear in trains, SWA is higher but slow-waves tend to be more local (Siclari et al., 2014a). This spatial fragmentation of slow-waves could be due to the breakdown of cortico-cortical connectivity taking place in NREM sleep (Massimini et al., 2005). This loss of connectivity would similarly impair the processing of information in brain regions not showing slow-waves. Thus, the relationship between local sleep and information processing is complex and a difference should be drawn between 'systemic' local sleep (that could stem from a loss of connectivity within the brain) and induced local sleep (that could traduce a stimulus-driven local awakening allowing information processing).

The case of sleep spindles

Sleep spindles, a waxing-and-waving oscillations between 11 and 16 Hz and lasting for 0.5 to 2 s on average, is also a distinctive feature of NREM sleep (De Gennaro and Ferrara, 2003). As slow-waves, sleep spindles were thought to be rather global events. Indeed, sleep spindles are a thalamo-cortical oscillation whose pacemaker is in the thalamus (Mircea Steriade, 2003). Thalamic nuclei having widespread projections to the cortex, sleep spindles were thought to appear synchronously over the entire neocortex. In Study 2, we showed that this was not necessarily the case (Andrillon et al., 2011). As slow-waves, sleep spindles can be local. As slow-waves (Massimini et al., 2004), sleep spindles travel, potentially reflecting the traveling of spindle oscillations within the thalamus (Andrillon et al., 2011). We argued in Study 2 that sleep spindles actually reveal thalamo-cortical connectivity and how the various thalamic nuclei project to the cortex.

Thus, contrary to slow-oscillations, the spatial expanse of sleep spindles does not reflect different synchronization processes at the cortical level. Rather, local aspects of sleep spindles recorded in cortical areas (spatial expanse, frequency) could reflect the activity of the thalamic nuclei projecting to them (Andrillon et al., 2011). The predominance of slow spindles in frontal areas could be therefore due to (i) the fact that anterior thalamic nuclei project predominantly in frontal areas (Jones, 2007), and to (ii) the fact that anterior thalamic nuclei have a slightly hyperpolarized membrane potential that would affect spindle frequency (McCormick and Bal, 1997; Mircea Steriade, 2003). Likewise, different generators at the thalamic level could explain the presence of local and global spindles. Indeed, thalamic relay cells can be divided in core and matrix cells, i.e., cells projecting rather focally on a given cortical regions or cells projecting broadly respectively (Jones, 2007). Thus, the differential involvement of core and matrix cells could give rise to local or global spindles.

The fact that sleep spindles properties seem to mostly reflect the activity of the underlying thalamic generator rather than properties of the cortical regions in which it is expressed is of importance when considering the function of sleep spindles. Depending on which thalamic nuclei and which cell type is involved in the generation of a spindle, the spindle oscillation could target a focal or broader cortical network. The ability to target and produce spindles locally advocate for their role in the active consolidation and transfer of memories form the hippocampal storage to the neo-cortex (Diekelmann and Born, 2010), which was harder to conceive with global spindles. Accordingly, we found that spindles correlated with the learning of new information during sleep (Study 9), which resonate with the many studies showing a correlation between memory consolidation this time and sleep spindles (Rasch and Born, 2013). Such potential involvement in both memory formation and consolidation could point toward a more general involvement of sleep spindles in synaptic plasticity, as demonstrated in vitro (Rosanova, 2005).

On the other hand, the fact that sleep spindles are mainly local events temper the notion that spindles serve to isolate sleepers from their environment (McCormick and Bal, 1994; Schabus et al., 2012; Yamadori, 1971) (see (De Gennaro and Ferrara, 2003) for a critical review). While global spindles could indeed block sensory information at the thalamic level (Schabus et al., 2012), more local spindles could allow a partial relay of the incoming sensory information. Consistent with this idea, we observed in Study 6 that sleep spindles

moderately affected our ability to reconstruct auditory inputs from brain activity. This result is not surprising when considering how little cortical units' firing rate is affected by the occurrence of sleep spindles (Contreras and Steriade, 1996; Peyrache et al., 2011) (in Study 2, we observed rather a phase-locking of neuronal discharges to the spindle phase (Andrillon et al., 2011; Peyrache et al., 2011)). A recent study from Yuval Nir's group showed that even when a spindle was detected within the primary auditory cortex, the encoding of external information was preserved (Sela et al., 2016). Thus, contrary to slow-waves, sleep spindles, local or global, could have in the end little effect on sensory processing.

Gating sensory information during sleep

Breaching the thalamic gate

The fact that sleepers get disconnected from their environment is perhaps the most striking consequence of sleep. Stimuli that would generally trigger a behavioral response leave the sleeper absolutely still and somewhat vulnerable. 'How' and 'why' such disconnection occurs has been on the spotlight of sleep research for decades. In the 90s, McCormick and Bal proposed the so-called 'Thalamic Gating Hypothesis' (McCormick and Bal, 1994). Their proposal was both straightforward and elegant: first, most of sensory input are relayed through the thalamus before reaching the cortex (Jones, 2007); second, NREM sleep is characterized by a modification in the activity of cortico-thalamic loops (Mircea Steriade, 2003); thus, the thalamus could gate external input in NREM sleep. Such pivotal role of the thalamus could have also explained the loss of consciousness associated with NREM sleep since the contemporary 'Dynamic Core Hypothesis' (Tononi and Edelman, 1998) attributed a central role to thalamo-cortical loops in the emergence of consciousness.

Investigation of the brain response to external inputs during sleep have proved to be inconclusive for a long time: many studies reported reduced responses to external stimuli during sleep, while many other showed their preservation (see (Hennevin et al., 2007) for a review). But a recent set of well-controlled studies reported a faithful encoding of auditory information (compared to wakefulness) during NREM and REM sleep (Issa and Wang, 2008; Y. Nir et al., 2013; Sela et al., 2016), although with some potential distortions (Issa and Wang, 2011). The investigation of cerebral responses to sounds at the whole-brain level helped clarifying the scope and limits of thalamic gating. Indeed, fMRI and EEG data showed that sensory information can be encoded and processed passed the thalamus (Atienza et al., 2001; Bastuji, 1999; Hennevin et al., 2007; Portas et al., 2000). Nonetheless, external input could be effectively blocked at the thalamic level whenever they co-occur with sleep spindles or down-states of slow-oscillations (Schabus et al., 2012; Yamadori, 1971) although these results may conflict with single-cell recordings (Sela et al., 2016). Overall, empirical evidence indicates that the thalamic gating can be breached during sleep.

An interesting question is whether sensory disconnection can be modulated. It is quite common to experience exceptionally light sleep before an important and stressing event (professional meeting, travel). This deterioration of sleep quality can lead to objective or subjective[7] sleep insomnia (Attarian, 2004). Interestingly, this can be accompanied by a decrease in delta power (i.e. SWA, (Dijk, 2010)) and the presence of alpha ([8-11]Hz) or beta (>20Hz) oscillations superimposed with slow-waves (alpha-delta sleep, (Hauri and Hawkins, 1973)). Such pattern of activity is called 'hyperarousal' (Perlis et al., 1997; Riemann et al., 2010). Although the associated mechanisms are unknown, it can be interpreted as a failure of the brain to stop endogenous and exogenous processing. Such abnormal maintenance of brain excitability could explain the increased level of alpha and beta rhythms. It could also explain the subjective feeling of not having slept. Interestingly, a direct prediction of the hyperarousal model is that the processing of

[7] Also called sleep state misperception or paradoxical insomnia, subjective insomnia refers to the feeling of not having slept in contradiction with objective sleep assessment such as polysomnographic or actigraphic recordings (Attarian, 2004).

external information should be facilitated during sleep in these individuals. Accordingly, when recording participants during the full-night paradigm presented in this manuscript, I observed that some participants were able to overtly respond (i.e. press the response buttons) even in NREM2 without showing other signs of arousal in the polysomnographic recordings. Interestingly, these participants reported episodes of subjective insomnia[8]. The small number of such cases does not allow drawing any definite conclusion but this angle may be further investigated in the future. The coupling of ERP indices of responsiveness with the extraction of brain signal's complexity (as in Study 5) would indicate whether increased processing abilities are associated with increased complexity and perhaps even awareness of the stimuli being presented. More generally, it would be of great interest to explore the inter-individual differences in the ability to process external information (or on the contrary to isolate from it) during sleep.

Such a modulation of sleepers' connectedness is what we eventually tried to achieve when using our induction paradigm (see Studies 4-7,9). Indeed, in these studies, participants initiated the task (that we wanted to investigate in sleep) while being awake. The reason was two-fold. First, we aimed at bypassing the pre-frontal de-activation taking place in sleep so that participants only had to continue the task initiated in wakefulness (while their cognitive abilities were optimal) rather than to initiate the task while being already asleep (Kouider et al., 2014). Second and more importantly here, we wanted to prime participants to pay attention to external stimuli. Task instructions stressing the fact that stimuli would be played during sleep and that participants were expected to respond to them whenever possible, our assumption was that the experimental setting would increase the probability that sleepers would process the acoustic stimuli (Wood, JM, 1990). Although our data argue in favor of this hypothesis, it remains to be further tested.

Neuronal bi-stability impairs information processing

In the previous section, we have seen that the thalamic gating of sensory information could be breached during sleep. Yet, we are usually not aware of what happens in our surrounding environment when we sleep. How is such sensory isolation performed if sensory information does reach the cortex? An alternative hypothesis posits the existence of a cortical gating rather than a thalamic gating. Such hypothesis is based on the TMS/EEG studies developed by Marcello Massimini and colleagues (Massimini et al., 2009a, 2009b). In these studies, volunteers were stimulated through TMS pulses. Such pulses transiently perturb brain activity and this perturbation is recorded through the EEG. The idea here is that the imposed electrical activity will percolate in the brain following the brain effective connectivity at the moment of the stimulation. TMS pulses can therefore reveal how information can propagate in a given state. Interestingly, the use of a massive and non-physiological perturbation such as a TMS pulse can better unravel the 'open tracks' present in the brain than a sensory stimulation that will be constrained by its modality (i.e. auditory stimulation will say little on the connectivity within the visual system).

[8] These participants were not included in the final analyses. The recording session had to be terminated, participants complaining that auditory stimulations prevented them from sleeping.

These TMS/EEG studies evidenced a breakdown of functional connectivity after sleep onset (Massimini et al., 2009b, 2005). More precisely, stimulation initiated in a given brain area tended to stay within this area, which contrasts with the long-range propagations observed in wakefulness. This can be interpreted as a reduced cortico-cortical connectivity. How does this relate to the processing of sensory information? As the TMS pulses, it is likely that sensory information will have a reduced ability to propagate within the cortex during NREM sleep. Thus, even if sensory information can breach the thalamic gate and reach the primary sensory cortices, it will tend to stay there, preventing the further processing of information. This could explain why sleepers are not aware of sensory information during sleep, in fact, why they are not conscious at all (Tononi and Massimini, 2008).

What is the mechanisms preventing the cortical cross-talk in NREM sleep? As others before, I will argue that slow-waves are mainly responsible for this breakdown of cortical connectivity (Massimini et al., 2012). Indeed, as discussed earlier, slow-waves entail OFF periods during which vast neuronal assemblies are silenced. Such periodic (or transient) silencing would stop any computation that would have been in progress, preventing the integrated processing of information in time and space, just as TMS pulses are limited in their propagation in time and space. Accordingly, we found in Study 5 that, when down-states were absent, acoustic information could be processed up to the decision level, that is to say, across a distributed set of brain regions and on a temporal window of few seconds. These processes were stopped by the occurrence of down-states. Similarly, the group of Marcello Massimini has recently found that slow-waves break deterministic processes (that is to say causal relationship between computational processes), a phenomenon that would again prevent the integration of information (Pigorini et al., 2015).

Interestingly, down-states are often evoked by external stimulation and were thus often seen as a mechanisms protecting the sleeper from external stimulations (Bastien et al., 2000; Wauquier et al., 1995). In Study 5, we analyzed more in depth the dynamic of brain responses to sounds and its consequences on the further processing of information. In NREM sleep, we observed that sound onset was followed by an initial positive potential in the EEG (P200), often interpreted as a marker of local stimulus-dependent excitability (Laurino et al., 2014). And indeed, this P200 correlated positively with markers of responsiveness when down-states were absent. Interestingly, this correlation was reversed when down-states followed the P200. One interpretation is that the P200 can trigger down-states in a certain proportion of trials. Indeed, it has been shown that down-states are preceded by a transient excitation (Menicucci et al., 2013). According to this idea, in NREM sleep, the brain offers a bistable mode whereby the stimulus-evoked excitation is followed or not by a down-state. The down-state (when elicited) will in turn gate sensory processes. It is worth pointing that contrary to the P200, the down-state (or N550) is not modality-dependent but originate mostly in frontal cortices (Colrain et al., 1999; Laurino et al., 2014; Riedner et al., 2007). Thus, the P200 would not only trigger an associated suppressive mechanism, but this suppressive mechanisms will occur in frontal areas, which will efficiently prevent awakening and awareness of the stimulation. Indeed, frontal areas are known to play a central role in the broadcasting of information within the cortex (Dehaene, 2014; Dehaene et al., 2006).

But what determines whether a down-state will be evoked by the stimulus? Just as spontaneous bi-stability, this evoked bi-stability will be under the control of the homeostatic and circadian processes (Borbély, 1982; Vyazovskiy and Harris, 2013). Accordingly, we found a reduced ability to process information from light to deep

NREM sleep, but a recovery of these processing abilities toward the end of the sleep cycles, when sleep depth and homeostatic pressure lighten (Study 5). Thus, NREM sleep can be seen as a state where sensory stimulation will induce a competition between excitation and inhibition and where the completion of sensory processes will depend toward which side the balance topples. The preservation of processing abilities in light NREM sleep would also make sense in the light of the reduced sleep inertia associated to this state in case of an awakening (Tassi and Muzet, 2000). Such reduced sleep inertia would allow the individual to appropriately react to a potentially relevant stimulus, contrary to deeper stages of NREM sleep.

But this interpretation of evoked oscillations as a protective mechanisms from external stimulation seems to contradict not only previous findings (Destexhe et al., 2007; Halasz, 2005) but also the results of Study 6, in which we found that information processing and attention allocation were enhanced after K-complexes (after a transient suppression). I will argue though that the results of Study 5 (showing a suppression of sensory processes when K-complexes are evoked) and Study 6 (in which the processing of information seem enhanced after K-complexes) can be interpreted within the same framework. Indeed, I have focused so far on experimental settings in which acoustic stimuli were played in isolation and argued that processing of stimuli is blocked whenever a down-state is elicited. In Study 6, the stimulation was continuous. Interestingly, down-states are usually followed by up-states, which may represent, according to Alain Destexhe and colleagues (Destexhe et al., 2007), 'fragments' of wakefulness within sleep. In the case of continuous stimulation, acoustic information is therefore presented to the sleeper during such up-states, potentially enabling the processing of information. And indeed, Manuel Schabus and colleagues showed that the sleeping brain was more sensitive to sensory information in the up-state of slow-oscillations (Schabus et al., 2012).

These considerations can actually lead to an ecological model of how the brain regulates the monitoring of its surrounding environment during sleep. Indeed, the brain faces a dilemma when asleep: how to benefit from the restorative consequences of slow-wave sleep without being forced in a state of unresponsiveness when a potential threat materializes. Peter Halász sees K-complexes as a central element in this regulation of sleep in face of external perturbations (Halász, 2016). Accordingly, I here argue that K-complexes could help solving this issue in an optimal way. Thus, in the case of isolated perturbations, a K-complex would shut down the processing of these perturbing inputs in order to preserve sleep (see above). But the suppression is followed by an up-state, which will allow processing acoustic information, in case the initial sound (which elicited the K-complex is the first place) is followed by another sound. Indeed, relevant stimuli (like a predator approaching or someone calling) are not expected to happen in isolation. On the contrary, stimuli worth being processed would happen in succession. For these potentially interesting stimuli, the sleepers would actually put themselves in the position of processing them.

Dreams gate sensory information in REM sleep?

In REM sleep, the brain is also disconnected from its environment. Thus, despite the associated recovery of consciousness and a brain activity close to wakefulness (Yuval Nir et al., 2013), external stimuli are rarely incorporated to the flow of conscious thoughts that constitute our dreams (Nir and Tononi, 2010). Responsiveness to external stimuli is

abolished and arousal thresholds are high (Ermis et al., 2010). So, if REM sleep resembles so much wakefulness, how is sensory disconnection achieved? The exact mechanisms are yet unknown but few recent studies can help proposing potential mechanisms.

In a recent study (Funk et al., 2016), Funk and colleagues recorded LFP within the superficial layers of primary sensory cortices and, surprisingly, observed that slow-waves occur not only in NREM sleep but also in REM sleep in these layers specifically. This discovery (despite decades of physiological investigation of sleep) is both surprising and of high interest for sensory disconnection. Indeed, the superficial layers of the primary cortices represent the main point of entry of sensory information after the thalamic relay (Jones, 2007). Therefore, these slow-waves could perturb the transmission of sensory information to the neo-cortex, establishing an early cortical gating. In parallel, since REM sleep is characterized by a recovery of cortico-cortical connectivity (as evidenced by TMS/EEG studies, (Massimini et al., 2010)), the integration of information within the isolated cortex could explain the occurrence of conscious thoughts (dreams) isolated from the external world (see Introduction).

However, these slow-waves cannot fully explain the sensory disconnection. First, their impact on the encoding of incoming stimuli by primary cortices is unknown as well as the underlying mechanisms (do they entail periods of neuronal silencing?). Second, several studies showed that external inputs do actually reach the cortex during REM sleep (Edeline et al., 2001; Y. Nir et al., 2013; Peña et al., 1999) and that some ability to process sensory information is preserved (Bastuji, 1999; Hennevin et al., 2007). The cortex in REM sleep is therefore not completely disconnected from its environment. Accordingly, we showed in Studies 5 and 9 that sensory information could be processed and learnt in REM sleep. But, if sensory information reaches the cortex during REM sleep and if cortical activity favors the integrated processing of information, why are we not aware of these external stimulations?

The results obtained in Study 5 could shed a new light on this question. We indeed found that EEG markers of response preparation (and thus of the completion of the stimulus processing) negatively correlated with the complexity of the brain signal (as estimated through the Lempel-Ziv algorithm (Schartner et al., 2015; Ziv and Lempel, 1977)). This is the opposite of what we found in wakefulness and even NREM sleep. Interestingly, complexity has been proposed as a proxy for measuring levels of consciousness. Using complexity, different teams have been able to track the modulation of consciousness levels during sleep and anesthesia and in patients with disorders of consciousness (Abásolo et al., 2015; Casali et al., 2013; Sarasso et al., 2015; Schartner et al., 2015). The fact that complexity negatively correlates with the ability to process external information in REM sleep could mean that the consciousness level antagonizes with sensory processing in REM sleep specifically. A potential mechanism could be a competition for brain computing resources between the endogenously generated contents (i.e. dreams) and the exogenous information (i.e. stimuli). The inability to process information in REM sleep would therefore stem from a form of 'informational gating'.

Such a competition has been proposed by Yuval Nir and Giulio Tononi who argue that REM sleep would be characterized by the dominance of top-down over bottom-up signaling, which would isolate sleepers and conscious contents from external inputs (Nir and Tononi, 2010). However, direct evidence for the dominance of top-down information in REM sleep is still missing. But the presence of slow-waves in primary cortices could participate to the attenuation of bottom-up perturbations (Funk et al.,

2016). In Study 5, we further showed that higher complexity (and perhaps higher consciousness levels) means less connectedness to the environment. Such view would explain the preserved encoding and basic information processing in REM sleep in the absence of integration to the dream scenery. It could also explain why the processing of external information is paradoxically more limited in REM sleep compared to light NREM sleep (Study 5). Overall, sensory disconnection could be achieved by two complementary mechanisms in REM sleep: (i) a low-level but partial gating of sensory information within primary cortices, (ii) a high-level cornering of computational resources by endogenous dream contents.

In Study 9, we have also found differences in the processing of information between tonic and phasic REM sleep. Namely, the occurrence of eye-movements in REM sleep (phasic REM sleep) was accompanied by a reduced ability to process external information. This result is in line with previous findings showing an attenuation of responses to external sounds in phasic REM sleep (Wehrle et al., 2007), higher arousal thresholds (Ermis et al., 2010) and less processing abilities (Sallinen et al., 1996). Interestingly, Funk and colleagues reported an increase in the REM slow-waves in phasic REM sleep (at least in the visual cortex) (Funk et al., 2016). In parallel, we found in Study 3 that eye-movements in REM sleep were accompanied by epochs of visual-like activity in high-order visuo-mnesic areas (medio-temporal lobe) usually involved in visual awareness (Andrillon et al., 2015b). It is therefore possible that phasic REM sleep is characterized by an increase in the two gating mechanisms described above: (i) an increase in slow-waves which would gate sensory information at an early stage of processing, (ii) an increase in the generation of endogenous contents which would monopolize high-order areas[9].

Dreams as a hallucination of reality?

I will conclude on this section with the strange case of RSBD patients (REM Ssleep Behavior Disorder, (Mahowald and Schenck, 2000)). These patients suffer from an absence of the paralysis of skeletal muscles that normally take place in REM sleep. As a consequence, these patients enact their dreams while they sleep, with dramatic consequences for themselves or the people they sleep with. Interestingly, these patients use elements of their environment and incorporate them in their motor actions while being in the same time so intensely immerged in their dream that they can hurt others or themselves. For example, while dreaming of a fight, a RBD patient can use elements of his[10] bedroom to attack or defend himself. And yet, when they awake, they typically ask who or what caused such a mess in their bedroom.

In all appearances trifling, this kind of observations suggests that elements of the external world are actually integrated in the dream scenery. However, these elements are not integrated as such but in a hallucinated form (a well-known friend can become a foe, a harmless night-table object a weapon and so on). Assuming that, apart form the lack of

[9] However, such mechanisms do not necessarily imply that high-order contents are generated in a top-down fashion. Indeed PGO waves emitted by the brainstem are known to trigger eye-movements in REM sleep (Mouret et al., 1963), and endogenous contents gating the processing of external information could well be orchestrated by the brainstem as proposed by Allan Hobson (Hobson, 1990).
[10] The vast majority of these RSBD patients are males.

muscular paralysis, RSBD patients exhibit normal sleep, this observation could help re-thinking the isolation from the external world occurring REM sleep. It is possible that external information is actually incorporated in the dream scenery during REM sleep but in a transformed way preventing the ability to process this information for what it is. It also possible that the decoupling from the environment is specific to sensory systems (in order to prevent external inputs from interfering with memory consolidation for example) but do not affect motor output and the sensory close-loops that are recruited during the production and control of movements.

Thus, external information in REM sleep could be processed at two levels: (i) at a low-level of representation involving non-conscious information processing (for example grasping or locomotion movements involving the cerebellum (for RSDB patients), sensory encoding and basic auditory processing involving primary and secondary cortices (in the sleepers we recorded)), (ii) at a high-level of representation in which the object is however represented as something else. REM sleep could therefore be seen as a state in which the brain is actually connected to its environment but processes it in a hallucinated way.

Dream as a hallucination of reality

Painting from Salvador Dali entitled '*Dream, Caused by the Flight of a Bee (Around a Pomegranate, a Second Before Waking Up)*' (1944). Dali reproduced a dream of his wife, Dala, which he thought was caused by the sound of a bee's flight. Modern science tends to dismiss such view by saying that external information is not incorporated in the dream scenery. Perhaps however such external stimuli are not integrated as such in our dreams but in an unpredictable way, such as a bee being transformed in a roaring tiger. Under such circumstances, we would ignore that an external stimuli would have been integrated in the dream.

Sleep, memory and plasticity

Remembering past events is crucial in our lives and it is thus not surprising if memory has been intensely studied in neuroscience. Memory can be divided in three distinct processes: (i) encoding (i.e. the formation of a new memory within the brain), (ii) consolidation (i.e. the strengthening and re-organization of mnesic traces) and (iii) retrieval (i.e. the access to a stored memory) (see (Eichenbaum, 2008)). In theory, only encoding and retrieval are necessary for memory. But the brain is not a simple memory system (when considering long-term memory). On the contrary, the number of items that can be learnt in the course of a life is incredibly large. This implies efficient encoding processes, which were modestly illustrated in Study 8. Despite the plethora of memory stored in our brains, we can still retrieve a particular trace rapidly and without apparent effort. As famously depicted by Marcel Proust[11], the memory just appears to our mind. Consolidation is key to conceive a system that can both efficiently encode and retrieve memory. Trough the strengthening of memories and their reorganization, consolidation can facilitate recollection ("There must be time for the processes of organization and assimilation (of memory) to take place" (Burnham, 1903)). I will discuss here mostly the involvement of sleep in the consolidation process, but I will also review experimental data showing that encoding and retrieval can also occur during sleep.

The role of sleep in memory

Since the antiquity, a link between sleep and memory consolidation has been suspected. For instance, the roman rhetorician Quintilian stated in the first century A.D.:

"[it] is a curious fact, of which the reason is not obvious, that the interval of a single night will greatly increase the strength of the memory…
Whatever the cause, things which could not be recalled on the spot are easily coordinated the next day, and time itself, which is generally accounted one of the causes of forgetfulness, actually serves to strengthen the memory."

Hermann Ebbinghaus, the pioneer of the scientific study of memory accordingly observed that forgetting was reduced after sleep compared to wakefulness. Sleep can therefore be seen as a 'time that serves to strengthen memory' contrary to the waking life that rather prompts us to forget; a fact that has been illustrated by Jenkins and Dallenbach who showed that recall (of learnt syllables) decreased with time spent awake, but stabilized when participants slept (Jenkins and Dallenbach, 1924). These observations have fueled countless investigations of the link between sleep and memory. The 1,358 references of the Rasch and Born review on the topic illustrate this intense focus (Rasch

[11] "No sooner had the warm liquid mixed with the crumbs touched my palate than a shudder ran through me and I stopped, intent upon the extraordinary thing that was happening to me. An exquisite pleasure had invaded my senses, **something isolated, detached, with no suggestion of its origin**. And at once the vicissitudes of life had become indifferent to me, its disasters innocuous, its brevity illusory – this new sensation having had on me the effect which love has of filling me with a precious essence; or rather this essence was not in me it was me. ... Whence did it come? What did it mean? How could I seize and apprehend it? ... **And suddenly the memory revealed itself.**" Marcel Proust, *In the search of lost time* (1906-1922)

and Born, 2013). But the mechanisms behind the protective effect of sleep are still debated.

One element that could explain the lack of consensus on the consolidation mechanisms at play during sleep is the variety of processes assembled in the term 'memory'. Indeed, memory is classically divided into declarative and non-declarative memory (Eichenbaum, 2008). The former is associated with awareness and relies heavily on the medio-temporal lobe (MTL), a set of brain structures comprising the hippocampus. The latter encompasses heterogeneous memory system, such as motor skills or certain forms of conditioning, and are implemented in various brain systems that do not depend on the MTL. Does sleep affect these different types of memory in the same way? Are consolidation mechanisms dependent on the dedicated memory systems? On the other hand, sleep is also a diverse process (see Introduction). Do REM and NREM sleep act upon memory in the same way? The richness of sleep and of memory may explain the diversity of ideas on the role of sleep in memory. However, recent research has polarized mostly on two proposals: the active consolidation hypothesis (Diekelmann and Born, 2010) and the synaptic homeostasis hypothesis (Tononi and Cirelli, 2006). I will here provide a synthesis of these views, often presented as conflicting.

Sleep and the preservation from interference

One of the first accounts attempting to explain the protective role of sleep in memory focused on interference. In his seminal series of experiment on himself, Hermann Ebbinghaus showed that time was associated with a decrease in the number of items of a list he could recall (Ebbinghaus, 1885). John McGeoch later hypothesized that the more time passes, the more one experiences new situations and memorizes new things that will ultimately interfere with the maintenance or retrieval of previously stored memories (McGeoch, 1932). According to this idea, we forget not because of a natural decay of memories but because of the very fact that our brains are ceaseless learners. Sleep therefore has been initially seen as sheltering memory for the interference occurring during wakefulness, preventing the "obliteration of the old by the new" (Jenkins and Dallenbach, 1924). In this view, the role of sleep is purely passive. Such view could be related to Jeremy Siegel's proposal to consider sleep as an adaptive form of rest (Siegel, 2009), whereby sleep would represent a state in which animals save energy and prevent a ceaseless encoding of new memories. But accumulating evidence argue for an active role of sleep in memory consolidation (Ellenbogen et al., 2006b; Stickgold and Walker, 2005). For example, Ellebogen and colleagues demonstrated that sleep protected memories pro-actively (Ellenbogen et al., 2006a). The fact that sleep protects memories against *future* interferences argues against a purely passive role.

Nevertheless, the notion of sleep protecting from interference can be reprieved when considering that sleep enables the consolidation of memories. Indeed, consolidation can be harmed by interference. As said above, consolidation is usually thought to entail two components: the strengthening of mnesic traces and their re-organization (Dudai, 2004). The strengthening of mnesic traces is thought to rely on the replay of learnt information. Memories are stored in the brain through synaptic connections (Kandel, 2000). Synaptic strength (i.e. how reliable is the link between two neurons) increases with use (Mayford et al., 2012). Therefore, the re-activation of a given trace will consequently strengthen the trace. However, if other processes such as the processing of external information co-

occur with the re-activation of a given memory, the consolidation process may be perturbed and the memory de-stabilized (see (Ellenbogen et al., 2006b)). Similarly, if sensory processing interferes with the re-organization of memory (for example, the transfer of long-term memories from the hippocampal to the neo-cortical storage), consolidation can be impaired.

Therefore, it has been proposed that sleep would represent the ideal situation to consolidate existing memories. Indeed, the sleeping brain being isolated from the external world (to a certain extent), consolidation processes would be more efficient during sleep (Mednick et al., 2011). Such 'opportunistic' view of the role of sleep in memory consolidation could explain the stabilization of memory over the sleep period, however it denies any specificity in the role of sleep in memory. Rather, sleep would represent a context more favorable to memory consolidation. Contradicting this view however, many studies have stressed the importance of sleep stages and sleep rhythms in the consolidation of memory (see (Ellenbogen et al., 2006b) for a brief overview), which argue in favor of the existence of consolidation mechanisms specific to sleep. SWA activity in particular has been linked with memory improvement. Are sleep rhythms participating to the consolidation of memory in a specific way?

Active replay…

When rats run in a maze, some cells in the hippocampus fire in a precise order for a given trajectory. These cells are called 'place cells'. A place cell fires whenever the rat is in a particular portion of space (Moser, 2014). Thus, the firing pattern of place cells can retrace the path taken by the rat. Interestingly, place cells can orderly fire even when the rat is not moving. Such events are called replay. These replays often occur during sharp wave-ripples (SPW-R[12]: (Vanderwolf, 1969)) in a temporally condensed fashion. Wilson and McNaughton showed in 1994 that replay also occurs during sleep (Wilson and McNaughton, 1994). In addition such replay depends on wake experience (Skaggs and McNaughton, 1996): a particularly important track would have greater chance to be replayed in sleep. Finally, the suppression of these replays impaired later performance (Girardeau et al., 2009). These results provided support to the notion that sleep promotes consolidation through the active replay of memory traces. But, as said above, replay also occurs during wake. So what is special about replays occurring during sleep?

SPW-R in sleep are nested with sleep rhythms: slow-waves and sleep spindles (Staresina et al., 2015). This observation is the basis of the active consolidation (or 'synaptic embossing') hypothesis (Diekelmann and Born, 2010; Ribeiro, 2004) (see Figure 10-2). According to this hypothesis, sleep oscillations would represent a temporal window during which mnesic traces are replayed in the hippocampus and transferred to the cortex for long-term storage. And indeed, coordinated replay in the neo-cortex and hippocampus has been observed in link with slow-oscillations (Daoyun Ji and Wilson, 2007). The consolidation mechanism would here be specific to sleep and more precisely

[12] Sharp-wave ripples (SPW-R) refer to a transient hippocampal rhythm occurring in both awake rest and sleep. It has been observed in both rodents and humans. SPW-R accompany the replay of place cells and are therefore thought to be involved in memory consolidation and retrieval. See (Buzsáki, 2015) for a review.

NREM sleep since slow-waves and spindles are not normally seen in other vigilance states.

The importance for memory of the re-activation of place cells in sleep has been recently illustrated by the group of Karim Benchenane (de Lavilléon et al., 2015). They showed that pairing the firing of a given place cell with a rewarding electrical pulse modified behavior upon awakening, with the animal moving preferentially to the spatial area coded by the place cell conditioned in sleep. Thus, sleep represents a period in which neuroplastic changes can occur either in terms of memory consolidation or formation. Such proposal is all the more elegant since it also provides a mechanism preventing interference during the consolidation and transfer of memory. As we have seen earlier, external information could be blocked during spindles (Dang-Vu et al., 2010; Schabus et al., 2012) although recordings at the cellular level temper this view (Sela et al., 2016).

Replays have also been evidenced, albeit more rarely, in REM sleep (e.g. (Louie and Wilson, 2001)), which is concordant with the smaller impact of REM sleep deprivation on memory consolidation compared to NREM sleep. However, PGO waves, which are a signature of REM sleep (see Introduction), have been linked to experience-dependent neuroplastic changes occurring in REM sleep (Hobson, 2009). Accordingly, PGO waves have larger amplitude or increase in frequency after learning (Datta, 2000; Sanford et al., 2001). It has thus been proposed that PGO waves would play a role in the consolidation of existing memories. First, PGO waves could help isolating the sleeper from the surrounding environment by decoupling the brain from peripheral external input (Hobson, 2009). Our results in Studies 3 and 9 are concordant with this view since we showed that (i) eye-movements (that are typically generated by PGO waves) are associated with sensory-like activations which could represent a form of replay (Andrillon et al., 2015b), (ii) processing of external information was observed in tonic REM sleep (where PGO waves are less frequent) but not in phasic REM sleep. In addition, despite the smaller amount of evidence showing replay in sleep, genes intervening in synaptic plasticity are more expressed in REM sleep (Ribeiro et al., 2002) and neuromodulators promoting synaptic potentiation such as Acetylcholine have secretion levels close to wakefulness in REM sleep (Jones, 2005; Pawlak, 2010; Seol et al., 2007). Overall, while studies typically emphasize the role of SWS in active consolidation, REM sleep could also participate to the consolidation of existing memories.

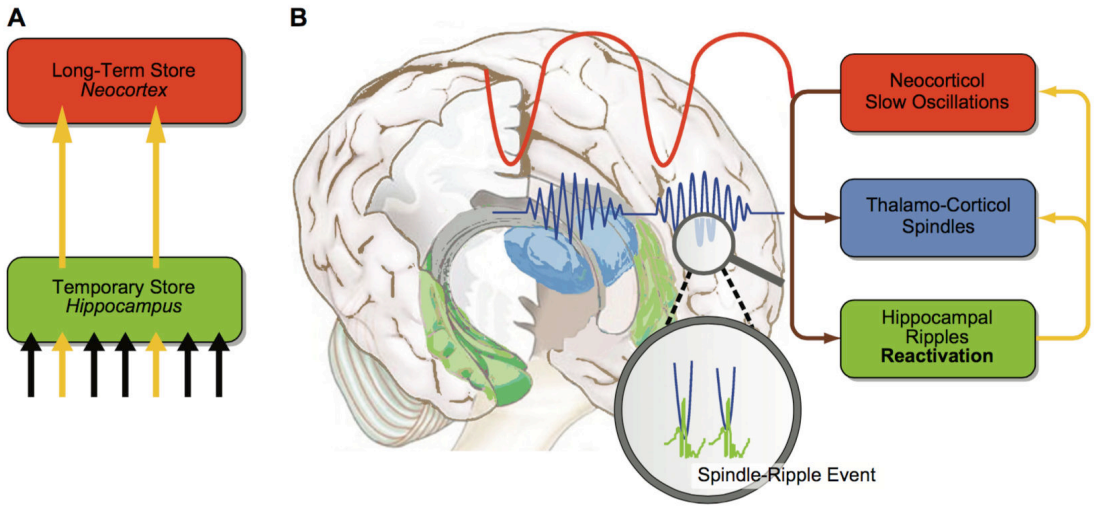

Figure 10-2 The active consolidation hypothesis

A: During Slow-Wave Sleep, memories stored in the hippocampus are re-activated which allows their strengthening and transfer to the long-term neo-cortical store. B: Replay of learnt memories occur during sharp-wave ripples. These ripples are themselves nested in spindle oscillations generated in the thalamus and spindles often occur on the up-states of neo-cortical slow-oscillations. Thus NREM sleep rhythms organize the condensed replay of information within the hippocampus and its potential transfer toward the neo-cortex. From (Rasch and Born, 2013).

However, criticisms have been raised regarding the occurrence of active consolidation through replay during sleep. First of all, replay occurs in wakefulness and suppression of SPW-R during rest also impairs memory (Ego-Stengel and Wilson, 2010) putting the specificity of such mechanisms into question. To this regard, a study following on the work of Girardeau and colleagues (on the impairment of memory with SPW-R suppression), but now targeting sleep spindles, could help understanding whether the nesting of SPW-R during sleep spindle is important for memory consolidation. Critics have also pointed the fact that these studies focused mostly on the murine model and spatial memory. Similar replay in Humans have not yet been evidenced (that is to say, the replay of neuronal assemblies in a condensed manner during SPW-R). Replay has been observed through MEG and fMRI data (see (Rasch and Born, 2013) for a review) but the temporal resolution of these techniques necessarily points out to a different kind of replay. And the different temporal scale of these 'human' replays would imply different mechanisms. Indeed, non-condensed memories cannot be replayed during SPW-R, which typically last for about 100ms. These replays might reveal other consolidation mechanisms than the ones observed for the consolidation of spatial memories in rodents.

In addition, while the active consolidation hypothesis provides an elegant framework for the consolidation of spatial memory, it is unclear how such mechanisms would generalize to other types of memory. Indeed, if the consolidation of a given trajectory in a maze could benefit for the replay of this trajectory while sleeping, what about the consolidation of memories that are not temporally encoded such as a the memory of a face, a visual scene? Finally, the active consolidation hypothesis supposes the reversal of the cortico-hippocampal dialogue from the hippocampus to the cortex compared to wakefulness where encoding is predominant (and information flows from the cortex to the hippocampus) (Hasselmo, 1999; Rasch and Born, 2007). However such reversal remains to be convincingly shown (see (Tononi et al., 2006; Tononi and Cirelli, 2014)).

… or general down-scaling?

Another model, the Synaptic Homeostasis Hypothesis (Tononi and Cirelli, 2012, 2006), proposes a seemingly opposed view on the role of plasticity in sleep-dependent memory consolidation. According to such view, sleep is a state in which the formation and consolidation of memories is *less* likely to happen (see Figure 10-3). Rather, Cirelli and Tononi argue that synaptic down-scaling take place during sleep, and that sleep promotes forgetting rather than learning. Indeed, when awake the sleeping brain constantly learn which represents a challenge for the neural system in the long run since: (i) synapses are costly to create and maintain, (ii) the brain is a finite system and synapses cannot be created indefinitely, (iii) a ceaseless increase in synapses and synaptic strength would diminish the neural signal-to-noise ratio and therefore the quality of stored memories.

Jorge Luis Borges vividly described the burden of memorizing without being able to forget[13]:

"He was, let us not forget, almost incapable of general, platonic ideas. It was not only difficult for him to understand that the generic term dog embraced so many unlike specimens of differing sizes and different forms; he was disturbed by the fact that a dog at three-fourteen (seen in profile) should have the same name as the dog at three-fifteen (seen from the front)."

"My memory, sir, is like a garbage disposal."

As for the active consolidation hypothesis, synaptic homeostasis has been backed by numerous studies (see (Tononi and Cirelli, 2014)). At the synaptic level, AMPAR receptor, which are particularly involved in synaptic potentiation, decrease during NREM sleep compared to wakefulness (Vyazovskiy et al., 2008). The reduction observed in SWA throughout a night could be a direct consequence of synaptic down-scaling (Vyazovskiy et al., 2008). With less synaptic contacts overall, slow-waves would turn smaller (Olcese et al., 2010). Gene expression seems also to be in favor of synaptic depression during NREM sleep since gene coding for proteins involved in synaptic potentiation are more expressed in wakefulness and REM sleep (Cirelli, 2009; Ribeiro et al., 2002). Finally, there is also evidence that sleep affect the brain at the structural level (Bellesi et al., 2015). Importantly, in adolescent mice, the number of dendritic spines reduces after sleep which correspond to a suppression of the number of synaptic contacts after sleep (Maret et al., 2011).

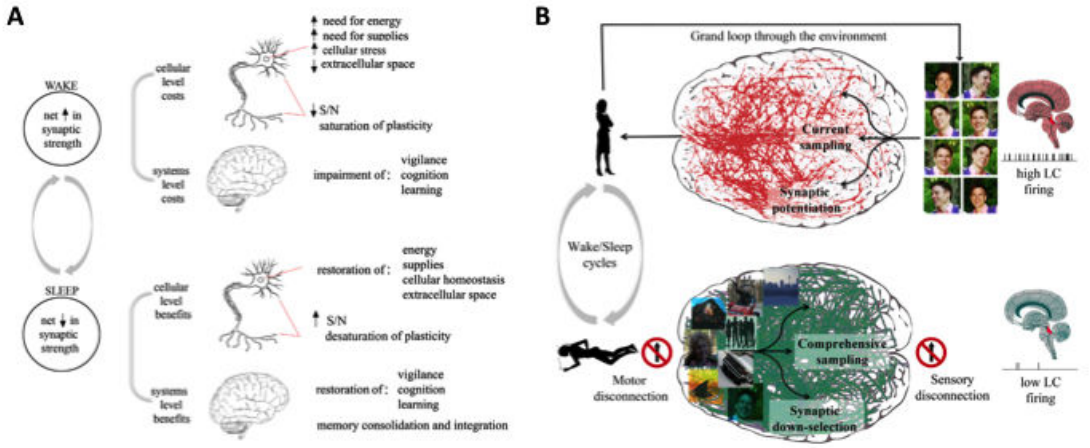

Figure 10-3 The synaptic homeostasis hypothesis

A: During wakefulness, there is a net increase in synaptic strength due to the constant interaction with the environment. As a result, the costs associated to the maintenance and formation of synaptic contacts increase. During sleep, a homeostatic regulation of synaptic weights would allow a net decrease in synaptic strength and avoid the escalation of metabolic costs. B: According to this hypothesis, sleep would also be an ideal state for the normalization of synaptic weights. Indeed, during wakefulness, brain activity is determined by the interaction with the environment and the sampling of memories is therefore biased by the environmental context. During sleep on the other hand, sensory disconnection is achieved through reduced noradrenergic activity, allowing a comprehensive sampling of memories (old and new) and therefore an unbiased normalization of synaptic weights. Adapted from (Tononi and Cirelli, 2014).

[13] Jorge Luis Borges, *Funes the memorious* (1942)

What are the mechanisms of synaptic depression and why does it paradoxically lead to memory consolidation? Tononi and Cirelli proposed a central role of slow-waves and changes in neuromodulation in the general down-scaling of synaptic weights. Indeed, NREM sleep is characterized by low levels of acetylcholine and both NREM and REM sleep show reduced noradrenergic activations (Jones, 2005; Siegel, 2004). Interestingly, acetylcholine and noradrenaline are known to be involved in synaptic plasticity (Rasmusson, 2000; Sara, 2009). Low levels of acetylcholine in particular have been shown to reverse the polarity of STDP (spike-time dependent plasticity) from long-term potentiation to long-term depression (Pawlak, 2010; Seol et al., 2007). The role of slow-waves would consist in randomly but exhaustively re-activate neural assemblies (during up-states), what Tononi and Cirelli call a comprehensive sampling of stored memories (Figure 10-3). The replay would be here general rather than targeting specific memories (for example recent, emotional or rewarding memories (Perogamvros and Schwartz, 2013)). In addition, the re-activation would lead here to a general decrease of the synaptic weights: the Hebbian rule (Hebb, 1949) being transformed from "what fire together, bind together" to "what fire together, unbind".

What would be the consequence of such synaptic normalization? According to modeling studies (Hashmi et al., 2013; Nere et al., 2013), the leveling of synaptic weights would erase weak memories and decrease the strength of the strong ones (without erasing them completely). At the level of the system however, such overall decrease in synaptic weight increases the signal-to-noise ratio associated to the surviving memories. Thus, synaptic homeostasis could both satisfy energy saving principles and the role of sleep in memory consolidation. However, direct evidence showing the suppression of memories during sleep are lacking. In Study 9, we show nonetheless that SWS is associated to the suppression of new memories formed in light NREM sleep and that this suppression is tightly linked to the amount of slow-waves in support of the synaptic homeostasis hypothesis.

The role of sleep in forgetting is not only limited to NREM sleep and to the synaptic homeostasis hypothesis. Crick and Mitchison (Crick and Mitchinson, 1983) and Walker (Walker, 2009) proposed that sleep was important to erase useless component of a memory. For example, after burning myself with a hot pan, the memory that hot pans hurt could be seen as quite useful and worth storing in the long term. However, remembering the context in which I got burnt (where, which pan…) is less useful. According to these authors, REM sleep could therefore help the erasure of parasite memories or of emotional components of memory. The later argument is supported by a reduced amygdala activation during recollection of emotional memories after REM sleep (Sterpenich et al., 2007; van der Helm et al., 2011). But other studies found the reverse pattern (see (Rasch and Born, 2013) for a review) leaving this potential role of REM sleep unsettled.

Sleep and memory: a synthesis

When summarizing the active consolidation and the synaptic homeostasis hypotheses, it seems that the former posits the consolidation of memory through selective replay and the latter the opposite, a general down-scaling of memories' strength. At first so, it seems that if one is proven right, the other must be wrong. Nevertheless, both hypotheses are

supported by compelling empirical data (Diekelmann and Born, 2010; Rasch and Born, 2013; Tononi and Cirelli, 2014, 2012).

Recently, Lisa Genzel and colleagues proposed a synthesis of the two hypotheses (Genzel et al., 2014) (see Figure 10-4). Their analysis mostly relies on the observation that evidence for active consolidation and synaptic homeostasis often come from different experimental settings. Indeed, it appears that scientists studying active consolidation mostly focused on light sleep, while the upholders of synaptic homeostasis have examined the consequence of entire nights (including therefore light and deep NREM sleep). Genzel and colleagues argue that such differences in the experimental approach could explain diametrically opposed conclusions. Namely, according to these authors, synaptic potentiation and depression could both occur in NREM sleep but at a different time. Potentiation would take place in light NREM sleep, mediated by global events such as K-complexes. On the other hand, in deep NREM sleep (also referred as Slow-Wave Sleep), cortical activity would be dominated by local slow-waves that would trigger synaptic depression.

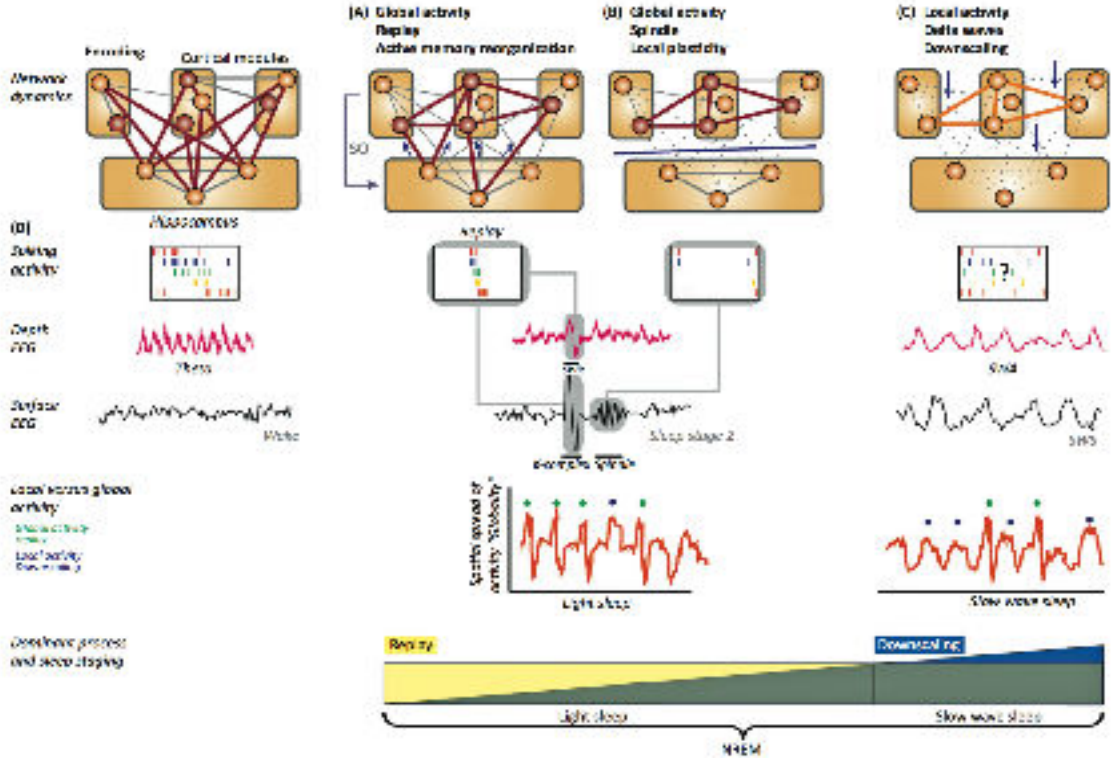

Figure 10-4 A synthesis of active consolidation and synaptic homeostasis

During wakefulness, memories are encoded in a hippocampo-cortical network. In light NREM sleep (A), phasic global events predominate that would organize the hippocampal replay of learnt information and its consolidation. Sleep spindles would isolate the neo-cortex from the hippocampus and trigger local cortical plastic processes (B). As a consequence, memories will become more and more dependent of cortical networks and less and less dependent of the hippocampus. In deep NREM sleep (C), local slow-waves are preponderant and organize the local down-scaling of synaptic weights. Strongest memories are conserved. These memories are to be found mostly in the cortical storage while the hippocampus storage is freed for future learning. From (Genzel et al., 2014).

This framework is of high interest since it proposes an elegant synthesis of the two main hypotheses on the role of sleep in memory. It is backed by experimental data (see (Genzel et al., 2014)). A comparable proposal has been modeled by the group of Sidarta Ribeiro (Blanco et al., 2015), where they show that alternation of synaptic downscaling during SWS and synaptic potentiation at the transition between SWS and REM sleep (i.e. in light sleep) maximize the effect of synaptic embossing. Another study (Perrett et al., 2001) showed that both synaptic depression and potentiation occur during 1Hz electric stimulation of cortical neurons. However, the authors observed that depression offset potentiation when stimulations are regular (i.e. like slow-wave trains in SWS) but potentiation dominates when they are transient (i.e. like in light NREM sleep).

To this date, however direct evidence showing synaptic potentiation in light NREM sleep and depression in deep NREM sleep is missing. We believe that the results obtained in Study 9 go in this direction (although the technique used here, EEG, do not allow to directly link our results with mechanisms at the cellular level). Indeed, when presenting human volunteers with recurring white-noise snippets, fast and automatic learning processes occur (Agus et al., 2010; Andrillon et al., 2015a; Luo et al., 2013) that are thought to rely on neuroplastic phenomena like STDP (Klampfl and Maass, 2013; Masquelier et al., 2008). The presentation of recurring white-noise snippets can therefore be used to probe synaptic plasticity within the human brain (Study 8).

We used this approach in a full-night experiment (Study 9) and observed that NREM sleep had, overall, a suppressive effect of memory, contrary to REM sleep and wakefulness. Indeed, after exposure in REM sleep and wakefulness, detection of recurring white-noise snippets was facilitated. Strikingly, participants' performance was worst for sounds heard in NREM sleep than for novel sounds. Behavioral data collected upon awakening were supported by electrophysiological indexes of learning, showing that perceptual learning was possible in REM sleep but was suppressed in deep NREM sleep. However, learning was observed in light NREM sleep. The suppression of memories for noise in deep NREM sleep was tightly associated with the occurrence of continuous (deep NREM sleep) but more local slow-waves. On the contrary, sleep spindles (which are more frequent in light NREM sleep and which are often associated to K-complexes) correlated positively with perceptual learning. Overall, our results support the notion of interplay between synaptic potentiation and down-scaling in NREM sleep depending on sleep depth.

But what could explain such reversal? We propose in Study 9 that a contextual change could account for the reversal of neuroplastic processes form light to deep NREM sleep (rather than a change of the associated mechanisms). Indeed, the learning of noise was not only observed in light NREM sleep and wakefulness but also in REM sleep. Contrary to slow-wave sleep, REM sleep is characterized by levels of acetylcholine that are close to wakefulness (Jones, 2005), which is known to favor synaptic potentiation (Pawlak, 2010; Seol et al., 2007). A change in the level of neuro-modulators could also impact the synchronization processes at play during NREM sleep with more global events occurring in light NREM sleep and rather local slow-waves in deep NREM sleep, as recently proposed (Siclari et al., 2014a).

Thus, we argue that a change in the level of acetylcholine could explain the different outcome observed in deep NREM sleep on the one hand and light NREM and REM sleep on the other hand. In light NREM sleep, the levels of acetylcholine could be high enough to allow for synaptic potentiation. In addition, global slow-oscillations that are the hallmark of light NREM sleep (such as K-complexes) are thought to involve arousal-

promoting structures (Siclari et al., 2014a), among which are cholinergic structures (Schwartz and Roth, 2008). Global slow-oscillations could therefore provide windows within NREM sleep during which synaptic potentiation can take place. Similarly, sleep spindles have been found to trigger synaptic potentiation in vitro depending on the phase of slow-oscillations (Rosanova, 2005). Thus, the nesting of hippocampal replays through global oscillations could enable the consolidation of replayed information (or the learning of new information when presented at that time) even if the context (NREM sleep) is globally unfavorable to synaptic potentiation.

In deep NREM sleep however, the level of acetylcholine being at its lowest, the polarity of synaptic plasticity would be reversed. In addition, slow-waves would be mostly local and would not recruit arousal-promoting structures anymore (Siclari et al., 2014a). The re-activation of neural networks would therefore lead to synaptic down-scaling rather than up-scaling. This is in line with our findings, since we observed that memories formed in light NREM sleep were suppressed with increasing sleep depth, in close association with the emergence of more numerous but more local slow-waves (Study 9).

While the consolidation in light NREM sleep would target replayed memories stored in the hippocampus (and therefore supposes a form of selection of the information to be consolidated like newly formed memories), the stochastic nature of local slow-waves in deep NREM sleep would allow the comprehensive sampling of all memories stored in the cortical storage as proposed by Tononi and Cirelli. The reason why we observed a suppression of memory to noise would be therefore a side-effect of these down-scaling mechanisms: since we imposed (through acoustic stimulations) the (re)-activation of a given network (corresponding to the sound played) in deep NREM sleep, the corresponding network was down-selected.

Of course, other neurotransmitters would act in synergy with the Acetylcholine (Pawlak, 2010). Noradrenaline for example has a key role in the orientation of attention, sensory processing and synaptic plasticity (Berridge and Waterhouse, 2003; Sara, 2009). However, noradrenaline, considered in isolation, could not account for our pattern of results since it reaches its lowest level during REM-sleep (a state in which learning is possible as shown in Study 9). Yet, noradrenaline could facilitate learning during sleep by favoring sensory processing and could explain why stimulations during light NREM-sleep have a greater impact on memory than in REM-sleep (Arzi et al., 2012).

The synthesis presented here is very close to the framework proposed by Genzel and colleagues (Genzel et al., 2014). However, these authors toned down the role of sleep spindles in the active consolidation of memories. And indeed, direct evidence is missing showing and a causal involvement of sleep spindles in the strengthening and transfer of replayed memories. However, numerous correlations have been found between memory consolidation and sleep spindles (see (Diekelmann and Born, 2010; Rasch and Born, 2013) for reviews and Study 9). Sleep spindles were also shown to trigger synaptic potentiation *in vitro* (Rosanova, 2005). True, sleep spindles have a relatively moderate impact on cortical units' firing rate (Andrillon et al., 2011; Contreras and Steriade, 1996; Peyrache et al., 2011) but cortical units' appeared to be phase-locked to spindles oscillations (Andrillon et al., 2011; Peyrache et al., 2011) which could organize the transfer of relevant information form the hippocampus to the neo-cortex.

Manipulating memory during sleep

Recently, more and more studies investigated whether external stimulation (acoustic or electric) could act upon the consolidation processes occurring during sleep. For example, Ngo and colleagues showed that the entrainment of slow-oscillations had a positive impact on subsequent performance in a memory task (Ngo et al., 2013). In parallel, Delphine Oudiette and Ken Paller proposed the Targeted Memory Reactivation (TMR) approach, which consists in pairing a memory with a neutral sound during encoding in wakefulness and to replay the associated sound during NREM sleep (Oudiette and Paller, 2013). The idea is that the paired sound will increase the probability that the associated memory gets re-activated during sleep and thus consolidated. The aim is here to influence the brain in consolidating a given memory, through external stimulutions.

Supporting the TMR, a new study showed that playing a sound right after the cued stimulus cancels the effect of TMR (Schreiner et al., 2015). This could be interpreted as a disruption, through the presentation of an additional stimulus, of the replay. Interestingly, Oudiette and colleagues found a negative correlation between delta power and the impact of TMR, which is concordant with the idea that active consolidation would be predominant in lighter stages of NREM sleep (Oudiette et al., 2013). Given the framework presented above, it can also be expected that TMR would be the most efficient when associated to slow-oscillations, as shown recently (Batterink et al., 2016). However, according to our model, TMR would be diminished if not reversed in deep NREM sleep, a prediction that could be easily tested and controlled for in future experiments. Thus, the synthesis proposed above for sleep's role in memory and plasticity could also apply to these intervening approaches.

Concluding remarks

I hope that throughout this manuscript I will have done the richness of sleep justice. As sleep is a many-faced phenomenon, it can be examined at various levels: from the physiology of simple neurons to more philosophical considerations. After having dedicated these past few years to studying sleep, I am still impressed by the profusion of things we know and things we still ignore. Indeed, as recent research has proven, there is still much to understand about sleep. First, the question of its function is still debated. Second, the mechanisms involved in the well-known restorative effects of sleep have generated often-conflicting models. Third, even at the physiological level and despite decades of careful investigation of sleep's physiology, new discoveries can be made, such as the recent discovery of slow-waves in REM sleep.

In the course of my doctoral research, I mostly focused on the main observable effect of sleep: the associated loss of responsiveness. Leaning on the work of our predecessors, we confirmed that the sleeping brain is only partially disconnected from its environment and that some monitoring of external information can be achieved while we sleep. Strikingly, we showed that sleepers could complete tasks that should necessitate being awake, as one might have thought at first. To understand how such complex processing of external input are possible, we explored the mechanisms allowing the sleeping brain to pay attention to its environment or, on the contrary, isolate from it. We propose a model in which sleep is self-regulated: perturbations can be counter-balanced by a stimulus-evoked suppression of sensory information in order to preserve sleep.

In this doctoral work, I also investigated whether sleepers could benefit from the time spent asleep. Indeed, modern societies often see sleep as an idle time that one could try to benefit from. Using the time spent asleep to learn new information has been an old human fantasy[14], as well as a scientific quest. We showed that sleep and memory share a complex relationship and that opposite effects can be observed depending on sleep stages. Importantly, we corroborated the notion that sleep is important to strengthen existing memories, but also to forget. Along this line, I believe that this work can provide useful insights for the growing interest in sleep optimization. Companies and products are being launched which aim at improving sleep quality or memory consolidation. These endeavors are often based on the assumption that the mechanisms by which we benefit from sleep are well established. As it appears, they are not and care must be taken when trying to manipulate sleep, in order to prevent harmful consequences.

Finally, I hope that this research will prove useful and pave the way for further efforts in 'unlock[ing] the mystery of the three pounds of matter that sits between our ears'[15]. The exploration of inter-individual differences (pathological or not) in the way sleeping brains process external information could prove of high interest, both for fundamental and clinical research. I also hope that the experimental tools and studies developed here will participate to the broader investigation of consciousness and the understanding of how brain activity constrains our perception of the world. Since in the end, awake or asleep, we are nothing but our brains.

---

[14] I have been countlessly reminded of Aldous Huxley's *'Brave New World'* (1932) over the past three years, which I unfortunately did not have the chance to read yet.

[15] Barack Obama, President of the United States of America, April 3rd 2013.

Annexes

Annex A: General-audience article written for the Conversation[16] and dealing with Study 4. The article was republished in several newspaper or websites such as the Washington Post[17].

Annex B: General-audience article. French version of Annex A, written for the French edition of the Conversation.

Annex C: General-audience article written for the French edition of the Conversation and dealing with Study 3.

[16] www.theconversation.com

[17] www.washingtonpost.com/posteverything/wp/2014/09/17/your-brain-actually-makes-decisions-while-you-sleep/

Annex A:
Brains can make decisions while we sleep – here they are in action

Thomas Andrillon & Sid Kouider
The Conversation, September 17 2014

Doing the shopping, kind of. Pedro Simoes

The idea that during sleep our minds shut down from the outside world is ancient and one that is still deeply anchored in our view of sleep today, despite some everyday life experiences and recent scientific discoveries that would tend to prove our brains don't completely switch off from our environment.

On the contrary, our brains can keep the gate slightly open. For example, we wake up more easily when we hear our own name or a particularly salient sound such as an alarm clock or a fire alarm compared to equally loud but less relevant sounds.

In research published in Current Biology we went one step further to show that complex stimuli can not only be processed while we sleep but that this information can be used to make decisions, similarly as when we're awake.

Our approach was simple: we built on knowledge about how the brain quickly automates complex chores. Driving a car, for example, requires integrating a lot of information at the same time, making rapid decisions and putting them into action through complex motor sequences. And you can drive all the way to home without remembering anything, as we do when we say we're on automatic pilot.

When we're asleep, the brain regions critical for paying attention to or implementing instructions are deactivated, of course, which makes it impossible to start performing a task. But we wanted to see whether any processes continued in the brain after sleep onset if participants in an experiment were given an automatised task just before.

To do this, we carried out experiments in which we got participants to categorise spoken words that were separated into two categories: words that referred to animals or objects, for example "cat" or "hat" in a first experiment; then real words like "hammer" versus pseudo-words (words that can be pronounced but are found nowhere in the dictionary) like "fabu" in a second one.

Participants were asked to indicate the category of the word that they heard by pressing a left or right button. Once the task became more automatic, we asked them to continue to respond to the words but they were also allowed to fall asleep. Since they were lying down in a dark room, most of them fell asleep while words were being played.

At the same time we monitored their state of vigilance thanks to EEG electrodes placed on their head. Once they were asleep, and without disturbing the flow of words they were hearing, we gave our participants new items from the same categories. The idea here was to force them to extract the meaning of the word (in the first experiment) or to check whether a word was part of the lexicon (in the second experiment) in order to be able to respond.

Of course, when asleep, participants stopped pressing buttons. So in order to check whether their brains were still responding to the words, we looked at the activity in the motor areas of the brain. Planning to press a button on your left involves your right hemisphere and vice-versa. By looking at the lateralisation of brain activity in motor areas, it is possible to see whether someone is preparing a response and toward which side. Applying this method to our sleepers allowed us to show that even during sleep, their brains continued to routinely prepare for right and left responses according to the meaning of the words they were hearing.

Even more interesting, at the end of the experiment and after they woke up, participants had no memory of the words they heard during their sleep though they recalled the words heard while they were awake very well. So not only did they process complex information while being completely asleep, but they did it unconsciously. Our work sheds new light about the brain's ability to process information while asleep but also while being unconscious.

This study is just the beginning. Important questions have yet to be answered. If we are able to prepare for actions during sleep, why is it that we do not perform them? What kind of processing can or cannot be achieved by the sleeping brain? Can sentences or series of sentences be processed? What happens when we dream? Would these sounds be incorporated into the dream scenery?

But most importantly, our work revives that age-old fantasy of learning during our sleep. It is well known that sleep is important to consolidate previously learned information or that some basic form of learning like conditioning can take place while we are asleep. But can more complex forms of learning take place and what would be the cost in terms of what sacrifices the brain would make to do this?

Sleep is important for the brain and total sleep deprivation leads to death after about two to four weeks. Indeed, it should be borne in mind that sleep is a crucial phenomenon and universal to all animals. We proved here that sleep is not an all-or-none state, not that forcing our brain to learn and do things during the night would be ultimately beneficial in the long run.

Annex B:
Pendant que nous dormons, notre cerveau travaille

Thomas Andrillon & Sid Kouider
The Conversation France, September 20 2015

Endormis, nous accomplissions des tâches de façon inconsciente. Vera Kratochvil/Pixabay

Une intuition répandue veut que le cerveau soit comme isolé pendant le sommeil et perde de sa sensibilité au monde extérieur. Cependant, tant nos expériences de la vie quotidienne que de récentes découvertes scientifiques mettent en difficulté cette idée. Comment expliquer par exemple que nous puissions nous réveiller plus facilement en entendant notre prénom ou un autre bruit particulièrement significatif comme une alarme de réveil ou une alarme incendie, si le cerveau dormant n'est pas sensible à cette information et capable de la reconnaître comme importante ?

Dans une étude parue l'an dernier dans la revue Current Biology, nous avons entrepris d'aller plus loin dans la mise en évidence de traitements sophistiqués effectués par le cerveau pendant le sommeil. Nous avons pu montrer que non seulement une information auditive complexe pouvait être traitée par le cerveau, mais que cette information pouvait être utilisée pour prendre une décision, à l'instar de l'éveil.

Notre approche se base sur les connaissances acquises quant à la capacité du cerveau à automatiser des tâches complexes. Conduire une voiture par exemple requiert l'intégration de multiples informations sensorielles, des prises de décisions rapides ainsi que leur mise en œuvre via la production de mouvements synchrones. Pourtant, il arrive que l'on conduise jusqu'à chez soi sans même s'en rendre compte !

Lorsque nous dormons, certaines régions du cerveau logées dans le cortex préfrontal et qui ont un rôle central dans l'orientation de l'attention ou la compréhension des consignes sont désactivées, rendant impossible le démarrage d'une tâche. Nous nous

sommes concentrés sur la possibilité qu'une tâche déjà commencée et automatisée au réveil puisse être poursuivie pendant le sommeil.

Classer des mots

Pour cela, nous avons conduit deux expériences dans lesquelles des volontaires devaient écouter et catégoriser des mots. Dans la première expérience, il fallait discriminer des noms d'objets (par exemple, « chapeau ») de noms d'animaux (« chat »). Dans la seconde, des vrais mots (« marteau ») par rapport à des mots inventés (« flipu »). Les participants devaient indiquer la catégorie du mot en pressant un bouton à droite ou à gauche. Une fois l'exercice automatisé, nous avons demandé aux participants de le poursuivre, mais cette fois-ci en leur permettant de s'endormir. Confortablement allongés dans une pièce obscure, la plupart d'entre eux se sont assoupis en écoutant les mots.

Dans le même temps, l'état de vigilance des participants a fait l'objet d'un suivi grâce à des capteurs électroencéphalographiques placés sur leur tête. Une fois endormit, et sans modifier le rythme de l'expérience, nous avons transmis aux participants une liste de mots inédits, mais appartenant toujours aux mêmes catégories. L'idée était ici de pousser les participants à accéder à la catégorie sémantique ou lexicale des mots pour pouvoir répondre.

Endormis, les participants ne répondaient plus. Afin de vérifier que le cerveau continuait, lui, à réagir aux mots, nous avons examiné l'activité cérébrale dans les aires motrices situées dans chaque hémisphère au sommet du crâne. En effet, prendre la décision d'appuyer à gauche implique l'aire motrice droite et inversement. En quantifiant la latéralisation de l'activité cérébrale dans les aires motrices, il est donc possible de savoir si une personne prépare une réponse et laquelle. Appliquant cette méthode aux dormeurs, nous avons pu montrer que même pendant le sommeil, le cerveau continue à préparer des réponses en fonction des instructions données à l'éveil et de la catégorie des mots.

À la fin de l'expérience, les participants étaient réveillés et devaient effectuer un exercice de mémoire. De façon tout à fait étonnante, alors que des mots entendus à l'éveil étaient reconnus, les participants n'avaient aucun souvenir des mots entendus pendant le sommeil. Ainsi, non seulement ces participants ont pu classer ces mots, mais ils l'ont fait de manière « inconsciente ».

Depuis la publication de cette étude, nous avons poursuivi nos efforts dans cette direction et confirmé nos premiers résultats. Mais de nombreuses questions restent encore à élucider. Pourquoi les participants endormis n'appuyaient-ils pas sur le bouton si leur cerveau préparait des réponses ? Quels types de traitement peuvent ou ne peuvent pas être effectués pendant le sommeil ? Des phrases entières peuvent-elles être traitées ? Qu'arrive-t-il quand nous rêvons ? Peut-on incorporer des éléments étrangers dans les rêves ?

Apprendre en dormant

Ces travaux ravivent également le vieux rêve (ou la crainte ancienne) que l'on puisse un jour apprendre ou faire apprendre pendant le sommeil. Les scientifiques ont déjà

démontré le lien entre le sommeil et la consolidation des souvenirs créés pendant la journée. Des formes simples d'apprentissage par conditionnement ont également été mises en lumière lorsque l'on est endormi. Plus récemment, des études chez l'homme et l'animal ont réussi à implanter dans le cerveau des associations, des mémoires nouvelles pendant le sommeil (associer l'odeur de cigarette à un son déplaisant chez des fumeurs par exemple). Des formes plus complexes d'apprentissage seraient-elles possibles ?

Si le sommeil est un phénomène universel c'est parce qu'il est essentiel à notre survie. Nous avons montré dans notre étude que le sommeil n'était pas un état de « tout ou rien ». Mais l'activité cérébrale a un coût : faire en sorte que le dormeur effectue des opérations pendant son sommeil pourrait ne pas être sans conséquence sur le long terme.

Annex C:
Les mouvements oculaires pendant le sommeil : une fenêtre sur les rêves ?

Thomas Andrillon
The Conversation France, September 20 2015

What happens behind the eyelids when we sleep?

Une nuit tranquille. Dans la pièce voisine, une personne dort, équipée de capteurs. Le corps est immobile. L'enregistrement indique un tonus musculaire faible, une respiration profonde, un pouls lent. Pourtant, depuis quelques minutes, l'activité cérébrale du dormeur a changé. Alors que de grandes ondes lentes étaient auparavant visibles sur l'écran de contrôle de l'électroencéphalogramme, le cerveau montre désormais une activité proche de l'éveil. Soudain, le pouls et la respiration s'accélèrent. Derrière les paupières closes du dormeur, on peut voir ses yeux bouger. Réveillées à cet instant, les personnes rapportent en général le souvenir d'un rêve, des images, des émotions. Un cerveau éveillé dans un corps endormi, tel est le sommeil paradoxal.

Ce sommeil, différent du sommeil dit « lent » où les rêves se font rares, se reconnaît à ces mouvements oculaires rapides qui l'accompagnent, d'où son nom en anglais : sommeil REM (Rapid Eye-Movement). Depuis 80 ans et l'invention des premières techniques d'enregistrement cérébral, ces mouvements oculaires pendant le sommeil ont suscité bien des questions : sont-ils en rapport avec la scène rêvée ?

À l'éveil, nos yeux bougent sans cesse pour appréhender les alentours. L'œil a en effet ses limites : seul le centre de la rétine permet une vision nette et en couleurs. Les mouvements oculaires permettent de déplacer ce centre dans le champ visuel et d'explorer au mieux notre environnement. Entre chaque mouvement, donc entre chaque image ainsi formée sur la rétine, l'information visuelle, floue et peu informative, est inhibée. Ainsi, la vision est une série de captures d'images plus qu'un flux continu. Mais

alors, pourquoi observe-t-on ces mouvements oculaires pendant le sommeil, lorsque les yeux sont clos et qu'il n'y a rien à voir ?

L'étoffe des rêves

Les mouvements oculaires exploreraient-ils une scène rêvée ? Construite par le cerveau mais tout aussi visuelle que notre vie éveillée ? Une telle proposition a d'importantes implications. Non seulement elle contredit l'hypothèse souvent avancée que les rêves ne sont qu'une (re)construction faite au réveil, mais elle précise « l'étoffe dont sont faits les rêves ». Bien que séduisante, cette hypothèse, dite du balayage (scanning hypothesis) a longtemps été controversée.

Il y a en effet d'autres explications possibles. Notamment, ces mouvements oculaires pourraient traduire un changement physiologique sans rapport avec le contenu des rêves. De la même façon que les hommes connaissent des érections (elles se produisent pendant 80 % du temps de sommeil paradoxal) sans pour autant que cela soit toujours en relation avec un contenu onirique érotique. Par ailleurs, n'oublions pas que les aveugles de naissance ou encore des animaux sans vision comme les taupes produisent de tels mouvements oculaires.

Depuis quelques années pourtant, la piste du balayage semble étayée par l'observation clinique. Lorsque la paralysie du sommeil paradoxal est abolie (cela arrive aux personnes affectées par le syndrome dit du trouble du comportement en sommeil paradoxal ou TCSP), les mouvements effectués par ces dormeurs concordent avec les mouvements oculaires ainsi qu'avec le récit du rêve. Ainsi, si l'on parvenait à lever la paralysie musculaire liée au sommeil paradoxal, il est possible que nous nous agiterions comme des pantins dans nos lits. Mais sommes-nous de simples poupées de chiffon dans notre sommeil ou des marionnettes sensibles ?

Réponse neuronale

Dans une étude récente publiée dans la revue Nature Communications, nous avons tenté d'explorer cette question en examinant l'activité cérébrale associée à ces mouvements oculaires pendant l'éveil et le sommeil. Pour cela, nous avons analysé des enregistrements de neurones uniques et de populations de neurones chez des individus humains atteints d'épilepsie et temporairement implantés d'électrodes intracrâniennes, dans le cadre de leur traitement.

Nous avons comparé les réponses des neurones aux mouvements oculaires effectués pendant l'éveil et le sommeil paradoxal. Ces réponses ont également été comparées aux réponses associées à la présentation d'images sans mouvement oculaire. En effet, les régions cérébrales prises en compte (amygdale, hippocampe…) ont un rôle central dans la reconnaissance des objets et l'exploration visuelle.

Il apparaît que les mouvements oculaires ont des effets similaires, à l'éveil comme pendant le sommeil, sur l'organisation de l'activité de ces aires visuelles et mnésiques. À l'échelle individuelle, certains neurones réduisent leur activité juste avant les mouvements oculaires et l'augmentent juste après : cela constituerait la base du traitement séquentiel

de l'information visuelle. De plus, la hiérarchie cérébrale semble être conservée de l'éveil au sommeil : les neurones les plus sélectifs (permettant la reconnaissance d'images très spécifiques comme la Tour Eiffel, par rapport à des neurones moins sélectifs s'activant pour les bâtiments en général) sont ceux qui s'activent le plus tardivement.

À l'échelle des populations de neurones, les oscillations électriques dans la bande de fréquences autour de 4-8 Hertz (dites oscillations thêta) notamment impliquées dans l'exploration visuelle et la mémoire, sont comme remises à zéro suite aux mouvements oculaires. À l'éveil comme pendant le sommeil.

Enfin, non seulement l'organisation de l'activité cérébrale pendant les mouvements oculaires est conservée de l'éveil au sommeil, mais elle est similaire à celle associée à la visualisation d'images sans mouvement oculaire. En revanche, cette activité ne se retrouve pas à l'éveil lorsque des mouvements oculaires sont réalisés dans l'obscurité. Que nous dormions ou que nous explorions notre environnement, tout se passe comme si les mouvements oculaires conservaient la même fonction.

Il semble que les mêmes processus cérébraux sous-tendant la vision se reproduisent pendant le sommeil. Les mouvements oculaires pourraient donc ouvrir une fenêtre sur les rêves : ils indiqueraient, certes de façon imparfaite, quand des images sont visualisées. Des neuro-scientifiques sont déjà parvenus à décoder des éléments de rêve via l'imagerie cérébrale. Ici, les séquences de mouvements oculaires pourraient être utilisées pour détecter la survenue de cauchemars récurrents et réveiller le dormeur à temps. Les applications concrètent d'une telle découverte sont bien sûr encore lointaines. Reste le plaisir d'en savoir un peu plus sur la nature des rêves.

References

Abásolo, D., Simons, S., Morgado da Silva, R., Tononi, G., Vyazovskiy, V.V., 2015. Lempel-Ziv complexity of cortical activity during sleep and waking in rats. J. Neurophysiol. 113, 2742–2752. doi:10.1152/jn.00575.2014

Abe, T., Ogawa, K., Nittono, H., Hori, T., 2004. Lack of presaccadic positivity before rapid eye movements in human REM sleep. Neuroreport 15, 735–738. doi:10.1097/01.wnr.0000111330.04354.43

Abrams, R.L., Greenwald, A.G., 2000. Parts outweigh the whole (word) in unconscious analysis of meaning. Psychol. Sci. 11, 118–124.

Achermann, P., Borbely, A.A., 1998. Temporal evolution of coherence and power in the human sleep electroencephalogram. J Sleep Res 7 Suppl 1, 36–41.

Aeschbach, D., Cutler, A.J., Ronda, J.M., 2008. A role for non-rapid-eye-movement sleep homeostasis in perceptual learning. J Neurosci 28, 2766–72. doi:10.1523/JNEUROSCI.5548-07.2008

Aggleton, J.P., Brown, M.W., 2006. Interleaving brain systems for episodic and recognition memory. Trends Cogn. Sci. 10, 455–463. doi:10.1016/j.tics.2006.08.003

Agus, T.R., Pressnitzer, D., 2013. The detection of repetitions in noise before and after perceptual learning. J. Acoust. Soc. Am. 134, 464. doi:10.1121/1.4807641

Agus, T.R., Thorpe, S.J., Pressnitzer, D., 2010. Rapid Formation of Robust Auditory Memories: Insights from Noise. Neuron 66, 610–618. doi:10.1016/j.neuron.2010.04.014

Akkal, D., Dum, R.P., Strick, P.L., 2007. Supplementary motor area and presupplementary motor area: targets of basal ganglia and cerebellar output. J Neurosci 27, 10659–73. doi:10.1523/JNEUROSCI.3134-07.2007

Albouy, G., Sterpenich, V., Balteau, E., Vandewalle, G., Desseilles, M., Dang-Vu, T., Darsaud, A., Ruby, P., Luppi, P.H., Degueldre, C., Peigneux, P., Luxen, A., Maquet, P., 2008. Both the hippocampus and striatum are involved in consolidation of motor sequence memory. Neuron 58, 261–72. doi:10.1016/j.neuron.2008.02.008

Alhola, P., Polo-Kantola, P., 2007. Sleep deprivation: Impact on cognitive performance. Neuropsychiatr. Dis. Treat. 3, 553–567.

Allan, K., Wilding, E.L., Rugg, M.D., 1998. Electrophysiological evidence for dissociable processes contributing to recollection. Acta Psychol. (Amst.) 98, 231–252.

Amaral, D.G., Price, J.L., Pitkanen, A., Carmichael, S.T., 1992. Anatomical organization of the primate amygdala, in: Aggleton, J.P. (Ed.), The Amygdala: Neurobiological Aspects of Emotion, Memory, and Mental Dysfunction. Wiley-Liss, New York, pp. 1–66.

Amzica, F., Steriade, M., 1998. Cellular substrates and laminar profile of sleep K-complex. Neuroscience 82, 671–86. doi:S0306452297003199 [pii]

Amzica, F., Steriade, M., 1996. Progressive cortical synchronization of ponto-geniculo-occipital potentials during rapid eye movement sleep. Neuroscience 72, 309–314.

Amzica, F., Steriade, M., 1995. Disconnection of intracortical synaptic linkages disrupts synchronization of a slow oscillation. J Neurosci 15, 4658–77.

Anderer, P., Klosch, G., Gruber, G., Trenker, E., Pascual-Marqui, R.D., Zeitlhofer, J., Barbanoj, M.J., Rappelsberger, P., Saletu, B., 2001. Low-resolution brain electromagnetic tomography revealed simultaneously active frontal and parietal sleep spindle sources in the human cortex. Neuroscience 103, 581–92.

Andersen, P., Andersson, S., 1968. Physiological Basis of the Alpha Rhythm. Meridith, New York.

Andrillon, T., Kouider, S., Agus, T.R., Pressnitzer, D., 2015a. Perceptual Learning of Acoustic Noise Generates Memory-Evoked Potentials. Curr. Biol. 25. doi:10.1016/j.cub.2015.09.027

Andrillon, T., Nir, Y., Cirelli, C., Tononi, G., Fried, I., 2015b. Single-neuron activity and eye movements during human REM sleep and awake vision. Nat. Commun. 6, 7884. doi:10.1038/ncomms8884

Andrillon, T., Nir, Y., Staba, R.J., Ferrarelli, F., Cirelli, C., Tononi, G., Fried, I., 2011. Sleep Spindles in Humans: Insights from Intracranial EEG and Unit Recordings. J. Neurosci. 31, 17821–17834. doi:10.1523/Jneurosci.2604-11.2011

Aristotle, 350AD. On Sleep and Sleeplessness.

Arnulf, I., 2011. The "scanning hypothesis" of rapid eye movements during REM sleep: a review of the evidence. Arch. Ital. Biol. 149, 367–382.

Arzi, A., Holtzman, Y., Samnon, P., Eshel, N., Harel, E., Sobel, N., 2014. Olfactory Aversive Conditioning during Sleep Reduces Cigarette-Smoking Behavior. J. Neurosci. 34, 15382–15393. doi:10.1523/JNEUROSCI.2291-14.2014

Arzi, A., Shedlesky, L., Ben-Shaul, M., Nasser, K., Oksenberg, A., Hairston, I.S., Sobel, N., 2012. Humans can learn new information during sleep. Nat. Neurosci. 15, 1460–1465. doi:10.1038/nn.3193

Aserinsky, E., Kleitman, N., 1953. Regularly occurring periods of eye motility, and concomitant phenomena, during sleep. Science 118, 273–4.

Atienza, M., Cantero, J.L., 2001. Complex sound processing during human REM sleep by recovering information from long-term memory as revealed by the mismatch negativity (MMN). Brain Res. 901, 151–160.

Atienza, M., Cantero, J.L., Escera, C., 2001. Auditory information processing during human sleep as revealed by event-related brain potentials. Clin. Neurophysiol. 112, 2031–2045. doi:10.1016/S1388-2457(01)00650-2

Attarian, H.P. (Ed.), 2004. Clinical handbook of insomnia, Current clinical neurology. Humana, Totowa, N.J.

Baars, B.J., 1988. A cognitive theory of consciousness. Cambridge University Press, Cambridge [England] ; New York.

Bahill, A.T., Clark, M.R., Stark, L., 1975. The main sequence, a tool for studying human eye movements. Math. Biosci. 24, 191–204. doi:10.1016/0025-5564(75)90075-9

Baloh, R.W., Sills, A.W., Kumley, W.E., Honrubia, V., 1975. Quantitative measurement of saccade amplitude, duration, and velocity. Neurology 25, 1065–1070.

Bal, T., von Krosigk, M., McCormick, D.A., 1995. Synaptic and membrane mechanisms underlying synchronized oscillations in the ferret lateral geniculate nucleus in vitro. J Physiol 483 (Pt 3), 641–63.

Bareham, C.A., Manly, T., Pustovaya, O.V., Scott, S.K., Bekinschtein, T.A., 2014. Losing the left side of the world: rightward shift in human spatial attention with sleep onset. Sci. Rep. 4, 5092. doi:10.1038/srep05092

Barker, D., Plack, C.J., Hall, D.A., 2012. Reexamining the Evidence for a Pitch-Sensitive Region: A Human fMRI Study Using Iterated Ripple Noise. Cereb. Cortex 22, 745–753. doi:10.1093/cercor/bhr065

Barr, D.B., Barr, J.R., Weerasekera, G., Wamsley, J., Kalb, S.R., Sjodin, A., Schier, J.G., Rentz, E.D., Lewis, L., Rubin, C., Needham, L.L., Jones, R.L., Sampson, E.J., 2007.

Identification and quantification of diethylene glycol in pharmaceuticals implicated in poisoning epidemics: an historical laboratory perspective. J Anal Toxicol 31, 295–303.

Bassetti, C., Vella, S., Donati, F., Wielepp, P., Weder, B., 2000. SPECT during sleepwalking. Lancet 356, 484–5. doi:10.1016/S0140-6736(00)02561-7

Bastien, C.H., Crowley, K.E., Colrain, I.M., 2002. Evoked potential components unique to non-REM sleep: relationship to evoked K-complexes and vertex sharp waves. Int J Psychophysiol 46, 257–74. doi:S0167876002001174 [pii]

Bastien, C.H., Ladouceur, C., Campbell, K.B., 2000. EEG characteristics prior to and following the evoked K-Complex. Can. J. Exp. Psychol. Rev. Can. Psychol. Expérimentale 54, 255–265.

Bastuji, H., 1999. Evoked potentials as a tool for the investigation of human sleep. Sleep Med. Rev. 3, 23–45. doi:10.1016/S1087-0792(99)90012-6

Bastuji, H., Perrin, F., Garcia-Larrea, L., 2002. Semantic analysis of auditory input during sleep: studies with event related potentials. Int J Psychophysiol 46, 243–55.

Bathellier, B., Ushakova, L., Rumpel, S., 2012. Discrete Neocortical Dynamics Predict Behavioral Categorization of Sounds. Neuron 76, 435–449. doi:10.1016/j.neuron.2012.07.008

Batterink, L.J., Creery, J.D., Paller, K.A., 2016. Phase of Spontaneous Slow Oscillations during Sleep Influences Memory-Related Processing of Auditory Cues. J. Neurosci. 36, 1401–1409. doi:10.1523/JNEUROSCI.3175-15.2016

Becker, W., Fuchs, A.F., 1969. Further properties of the human saccadic system: eye movements and correction saccades with and without visual fixation points. Vision Res. 9, 1247–1258.

Beh, H.C., Barratt, P.E., 1965. Discrimination and Conditioning during Sleep as Indicated by the Electroencephalogram. Science 147, 1470–1.

Bellesi, M., de Vivo, L., Tononi, G., Cirelli, C., 2015. Effects of sleep and wake on astrocytes: clues from molecular and ultrastructural studies. BMC Biol. 13. doi:10.1186/s12915-015-0176-7

Benington, J.H., Heller, H.C., 1995. Restoration of brain energy metabolism as the function of sleep. Prog. Neurobiol. 45, 347–360.

Benjamini, Y., Yekutieli, D., 2011. The control of the false discovery rate in multiple testing under dependency. Ann. Stat. 29, 1165–1188.

Berchicci, M., Stella, A., Pitzalis, S., Spinelli, D., Di Russo, F., 2012. Spatio-temporal mapping of motor preparation for self-paced saccades. Biol Psychol 90, 10–7. doi:10.1016/j.biopsycho.2012.02.014

Berger, H., 1929. On the electroencephalogram in man. Arch. Psychiatr. Nervenkr. 87, 527–543.

Berger, R.J., Oswald, I., 1962. Eye movements during active and passive dreams. Science 137, 601.

Bernardi, G., Siclari, F., Yu, X., Zennig, C., Bellesi, M., Ricciardi, E., Cirelli, C., Ghilardi, M.F., Pietrini, P., Tononi, G., 2015. Neural and Behavioral Correlates of Extended Training during Sleep Deprivation in Humans: Evidence for Local, Task-Specific Effects. J. Neurosci. 35, 4487–4500. doi:10.1523/JNEUROSCI.4567-14.2015

Berridge, C.W., Waterhouse, B.D., 2003. The locus coeruleus-noradrenergic system: modulation of behavioral state and state-dependent cognitive processes. Brain Res Brain Res Rev 42, 33–84.

Berti, S., Schröger, E., Mecklinger, A., 2000. Attentive and pre-attentive periodicity analysis in auditory memory: an event-related brain potential study. Neuroreport 11, 1883–1887.

Blanco, W., Pereira, C.M., Cota, V.R., Souza, A.C., Rennó-Costa, C., Santos, S., Dias, G., Guerreiro, A.M.G., Tort, A.B.L., Neto, A.D., Ribeiro, S., 2015. Synaptic Homeostasis and Restructuring across the Sleep-Wake Cycle. PLOS Comput. Biol. 11, e1004241. doi:10.1371/journal.pcbi.1004241

Bonjean, M., Baker, T., Lemieux, M., Timofeev, I., Sejnowski, T., Bazhenov, M., 2011. Corticothalamic feedback controls sleep spindle duration in vivo. J Neurosci 31, 9124–34. doi:10.1523/JNEUROSCI.0077-11.2011

Borbély, A.A., 1982. A two process model of sleep regulation. Hum. Neurobiol. 1, 195–204.

Borbely, A.A., Achermann, P., 1999. Sleep homeostasis and models of sleep regulation. J Biol Rhythms 14, 557–68.

Boulanger, M., Galiana, H.L., Guitton, D., 2012. Human eye-head gaze shifts preserve their accuracy and spatiotemporal trajectory profiles despite long-duration torque perturbations that assist or oppose head motion. J. Neurophysiol. 108, 39–56. doi:10.1152/jn.01092.2011

Brainard, D.H., 1997. The Psychophysics Toolbox. Spat. Vis. 10, 433–436.

Braun, A.R., Balkin, T.J., Wesenten, N.J., Carson, R.E., Varga, M., Baldwin, P., Selbie, S., Belenky, G., Herscovitch, P., 1997. Regional cerebral blood flow throughout the sleep-wake cycle. An H2(15)O PET study. Brain 120 (Pt 7), 1173–97.

Bremmer, F., Kubischik, M., Hoffmann, K.P., Krekelberg, B., 2009. Neural dynamics of saccadic suppression. J Neurosci 29, 12374–83. doi:10.1523/JNEUROSCI.2908-09.2009

Brooks, D.C., 1968a. Waves associated with eye movement in the awake and sleeping cat. Electroencephalogr Clin Neurophysiol 24, 532–41.

Brooks, D.C., 1968b. Localization and characteristics of the cortical waves associated with eye movement in the cat. Exp Neurol 22, 603–13.

Brooks, D.C., Bizzi, E., 1963. Brain Stem Electrical Activity during Deep Sleep. Arch. Ital. Biol. 101, 648–65.

Brualla, J., Romero, M.F., Serrano, M., Valdizan, J.R., 1998. Auditory event-related potentials to semantic priming during sleep. Electroenc Clin Neurophysiol 108, 283–90.

Bruce, D.J., Evans, C.R., Fenwick, P.B.C., Spencer, V., 1970. Effect of Presenting Novel Verbal Material during Slow-wave Sleep. Nature 225, 873–874. doi:10.1038/225873a0

Bruck, D., Ball, M., Thomas, I., Rouillard, V., 2009. How does the pitch and pattern of a signal affect auditory arousal thresholds? J. Sleep Res. 18, 196–203. doi:10.1111/j.1365-2869.2008.00710.x

Burnham, W.H., 1903. Retroactive Amnesia: Illustrative Cases and a Tentative Explanation. Am. J. Psychol. 14, 118. doi:10.2307/1412310

Burr, D., Morrone, M.C., 2005. Eye movements: building a stable world from glance to glance. Curr Biol 15, R839–40. doi:10.1016/j.cub.2005.10.003

Buzsáki, G., 2015. Hippocampal sharp wave-ripple: A cognitive biomarker for episodic memory and planning: HIPPOCAMPAL SHARP WAVE-RIPPLE. Hippocampus 25, 1073–1188. doi:10.1002/hipo.22488

Buzsáki, G., 2006. Rhythms of the brain. Oxford University Press, Oxford ; New York.

Buzsaki, G., 1998. Memory consolidation during sleep: a neurophysiological perspective. J Sleep Res 7 Suppl 1, 17–23.

Buzsáki, G., Logothetis, N., Singer, W., 2013. Scaling Brain Size, Keeping Timing: Evolutionary Preservation of Brain Rhythms. Neuron 80, 751–764. doi:10.1016/j.neuron.2013.10.002

Caderas, M., Niedermeyer, E., Uematsu, S., Long, D.M., Nastalski, J., 1982. Sleep spindles recorded from deep cerebral structures in man. Clin Electroencephalogr 13, 216–25.

Campbell, I.G., 2009. EEG recording and analysis for sleep research. Curr Protoc Neurosci Chapter 10, Unit10 2. doi:10.1002/0471142301.ns1002s49

Campbell, K.B., 2000. Information processing during sleep onset and sleep. Can. J. Exp. Psychol. Rev. Can. Psychol. Expérimentale 54, 209–229.

Cantero, J.L., Atienza, M., Salas, R.M., 2002. Human alpha oscillations in wakefulness, drowsiness period, and REM sleep: different electroencephalographic phenomena within the alpha band. Neurophysiol. Clin. Clin. Neurophysiol. 32, 54–71.

Caporale, N., Dan, Y., 2008. Spike timing-dependent plasticity: a Hebbian learning rule. Annu Rev Neurosci 31, 25–46. doi:10.1146/annurev.neuro.31.060407.125639

Cappe, C., Morel, A., Barone, P., Rouiller, E.M., 2009. The thalamocortical projection systems in primate: an anatomical support for multisensory and sensorimotor interplay. Cereb Cortex 19, 2025–37. doi:10.1093/cercor/bhn228

Carew, T.J., Sahley, C.L., 1986. Invertebrate Learning and Memory: From Behavior to Molecules. Annu. Rev. Neurosci. 9, 435–487. doi:10.1146/annurev.ne.09.030186.002251

Carpenter, R.H.S., 1988. Movements of the eyes. Pion, London.

Carskadon, M.A., Dement, W.C., 2011. Monitoring and staging human sleep, in: Kryger, M.H., Roth, T., Dement, W.C. (Eds.), Principles and Practice of Sleep Medicine. Elsevier Saunders, St-Louis, pp. 16–26.

Casali, A.G., Gosseries, O., Rosanova, M., Boly, M., Sarasso, S., Casali, K.R., Casarotto, S., Bruno, M.-A., Laureys, S., Tononi, G., Massimini, M., 2013. A Theoretically Based Index of Consciousness Independent of Sensory Processing and Behavior. Sci. Transl. Med. 5, 198ra105–198ra105. doi:10.1126/scitranslmed.3006294

Cash, S.S., Halgren, E., Dehghani, N., Rossetti, A.O., Thesen, T., Wang, C., Devinsky, O., Kuzniecky, R., Doyle, W., Madsen, J.R., Bromfield, E., Eross, L., Halasz, P., Karmos, G., Csercsa, R., Wittner, L., Ulbert, I., 2009. The human K-complex represents an isolated cortical down-state. Science 324, 1084–7. doi:10.1126/science.1169626

Cavada, C., Company, T., Tejedor, J., Cruz-Rizzolo, R.J., Reinoso-Suarez, F., 2000. The anatomical connections of the macaque monkey orbitofrontal cortex. A review. Cereb Cortex 10, 220–42.

Chase, M.H., Morales, F.R., 2005. Control of motoneurons during sleep, in: Principles and Practice of Sleep Medicine,. Saunders, New-York, pp. 154–168.

Chauvette, S., Volgushev, M., Timofeev, I., 2010. Origin of Active States in Local Neocortical Networks during Slow Sleep Oscillation. Cereb Cortex. doi:10.1093/cercor/bhq009

Chelazzi, L., Miller, E.K., Duncan, J., Desimone, R., 2001. Responses of neurons in macaque area V4 during memory-guided visual search. Cereb. Cortex N. Y. N 1991 11, 761–772.

Chennu, S., Bekinschtein, T.A., 2012. Arousal modulates auditory attention and awareness: insights from sleep, sedation, and disorders of consciousness. Front. Psychol. 3, 65. doi:10.3389/fpsyg.2012.00065

Chennu, S., Finoia, P., Kamau, E., Allanson, J., Williams, G.B., Monti, M.M., Noreika, V., Arnatkeviciute, A., Canales-Johnson, A., Olivares, F., Cabezas-Soto, D., Menon, D.K., Pickard, J.D., Owen, A.M., Bekinschtein, T.A., 2014. Spectral Signatures of Reorganised Brain Networks in Disorders of Consciousness. PLoS Comput. Biol. 10, e1003887. doi:10.1371/journal.pcbi.1003887

Cherry, E.C., 1953. Some Experiments on the Recognition of Speech, with One and with Two Ears. J. Acoust. Soc. Am. 25, 975. doi:10.1121/1.1907229

Chrobak, J.J., Buzsaki, G., 1996. High-frequency oscillations in the output networks of the hippocampal-entorhinal axis of the freely behaving rat. J Neurosci 16, 3056–66.

Cirelli, C., 2009. The genetic and molecular regulation of sleep: from fruit flies to humans. Nat. Rev. Neurosci. 10, 549–560. doi:10.1038/nrn2683

Cirelli, C., Tononi, G., 2008. Is sleep essential? PLoS Biol. 6, e216. doi:10.1371/journal.pbio.0060216

Clemens, Z., Molle, M., Eross, L., Barsi, P., Halasz, P., Born, J., 2007. Temporal coupling of parahippocampal ripples, sleep spindles and slow oscillations in humans. Brain 130, 2868–78. doi:10.1093/brain/awm146

Clemens, Z., Molle, M., Eross, L., Jakus, R., Rasonyi, G., Halasz, P., Born, J., 2010. Fine-tuned coupling between human parahippocampal ripples and sleep spindles. Eur J Neurosci. doi:10.1111/j.1460-9568.2010.07505.x

Coles, M.G., 1989. Modern mind-brain reading: psychophysiology, physiology, and cognition. Psychophysiology 26, 251–269.

Colrain, I.M., 2005. The K-complex: a 7-decade history. Sleep 28, 255–73.

Colrain, I.M., Webster, K.E., Hirst, G., 1999. The N550 component of the evoked K-complex: a modality non-specific response? J Sleep Res 8, 273–80.

Compte, A., Sanchez-Vives, M.V., McCormick, D.A., Wang, X.-J., 2003. Cellular and network mechanisms of slow oscillatory activity (<1 Hz) and wave propagations in a cortical network model. J. Neurophysiol. 89, 2707–2725. doi:10.1152/jn.00845.2002

Contreras, D., Destexhe, A., Sejnowski, T.J., Steriade, M., 1996. Control of spatiotemporal coherence of a thalamic oscillation by corticothalamic feedback. Science 274, 771–4.

Contreras, D., Destexhe, A., Steriade, M., 1997a. Spindle oscillations during cortical spreading depression in naturally sleeping cats. Neuroscience 77, 933–6. doi:S0306452296005738 [pii]

Contreras, D., Destexhe, A., Steriade, M., 1997b. Intracellular and computational characterization of the intracortical inhibitory control of synchronized thalamic inputs in vivo. J Neurophysiol 78, 335–50.

Contreras, D., Steriade, M., 1996. Spindle oscillation in cats: the role of corticothalamic feedback in a thalamically generated rhythm. J Physiol 490 (Pt 1), 159–79.

Cowey, A., Stoerig, P., 2004. Stimulus cueing in blindsight. Prog. Brain Res. 144, 261–277. doi:10.1016/S0079-6123(03)14418-4

Cox, R., Korjoukov, I., de Boer, M., Talamini, L.M., 2014. Sound Asleep: Processing and Retention of Slow Oscillation Phase-Targeted Stimuli. PLoS ONE 9, e101567. doi:10.1371/journal.pone.0101567

Craik, F.I.M., Tulving, E., 1975. Depth of processing and the retention of words in episodic memory. J. Exp. Psychol. Gen. 104, 268–294. doi:10.1037/0096-3445.104.3.268

Crick, F., Mitchinson, G., 1983. The function of dream sleep. Nature 304, 111–114.

Crick, F.C. Koch, C., 2000. The Neural Correlate of Consciousness. MIT Press, Cambridge.

Csercsa, R., Dombovari, B., Fabo, D., Wittner, L., Eross, L., Entz, L., Solyom, A., Rasonyi, G., Szucs, A., Kelemen, A., Jakus, R., Juhos, V., Grand, L., Magony, A., Halasz, P., Freund, T.F., Magloczky, Z., Cash, S.S., Papp, L., Karmos, G., Halgren, E., Ulbert, I., 2010. Laminar analysis of slow wave activity in humans. Brain 133, 2814–29. doi:10.1093/brain/awq169

Czarnecki, A., Birtoli, B., Ulrich, D., 2007. Cellular mechanisms of burst firing-mediated long-term depression in rat neocortical pyramidal cells: Firing modes and synaptic plasticity. J. Physiol. 578, 471–479. doi:10.1113/jphysiol.2006.123588

Czisch, M., Wehrle, R., Stiegler, A., Peters, H., Andrade, K., Holsboer, F., Sämann, P.G., 2009. Acoustic Oddball during NREM Sleep: A Combined EEG/fMRI Study. PLoS ONE 4, e6749. doi:10.1371/journal.pone.0006749

Dagnino, N., Loeb, C., Massazza, G., Sacco, G., 1969. Hypnic physiological myoclonias in man: an EEG-EMG study in normals and neurological patients. Eur. Neurol. 2, 47–58.

Dang-Vu, T.T., Desseilles, M., Laureys, S., Degueldre, C., Perrin, F., Phillips, C., Maquet, P., Peigneux, P., 2005. Cerebral correlates of delta waves during non-REM sleep revisited. NeuroImage 28, 14–21.

Dang-Vu, T.T., McKinney, S.M., Buxton, O.M., Solet, J.M., Ellenbogen, J.M., 2010. Spontaneous brain rhythms predict sleep stability in the face of noise. Curr. Biol. 20, R626–R627. doi:10.1016/j.cub.2010.06.032

Datta, S., 2000. Avoidance task training potentiates phasic pontine-wave density in the rat: A mechanism for sleep-dependent plasticity. J. Neurosci. Off. J. Soc. Neurosci. 20, 8607–8613.

De Carli, F., Proserpio, P., Morrone, E., Sartori, I., Ferrara, M., Gibbs, S.A., De Gennaro, L., Lo Russo, G., Nobili, L., 2015. Activation of the motor cortex during phasic rapid eye movement sleep. Ann. Neurol. n/a–n/a. doi:10.1002/ana.24556

de Cheveigné, A., Parra, L.C., 2014. Joint decorrelation, a versatile tool for multichannel data analysis. NeuroImage 98, 487–505. doi:10.1016/j.neuroimage.2014.05.068

de Curtis, M., Avanzini, G., 2001. Interictal spikes in focal epileptogenesis. Prog Neurobiol 63, 541–67.

De Gennaro, L., Ferrara, M., 2003. Sleep spindles: an overview. Sleep Med Rev 7, 423–40.

De Gennaro, L., Ferrara, M., Bertini, M., 2000. The spontaneous K-complex during stage 2 sleep: is it the "forerunner" of delta waves? Neurosci. Lett. 291, 41–43.

De Gennaro, L., Ferrara, M., Curcio, G., Bertini, M., 2001. Visual search performance across 40 h of continuous wakefulness: Measures of speed and accuracy and relation with oculomotor performance. Physiol. Behav. 74, 197–204.

Dehaene, S., 2014. Consciousness and the brain: deciphering how the brain codes our thoughts. Viking Adult, New York, New York.

Dehaene, S., Changeux, J.-P., Naccache, L., Sackur, J., Sergent, C., 2006. Conscious, preconscious, and subliminal processing: a testable taxonomy. Trends Cogn. Sci. 10, 204–211. doi:10.1016/j.tics.2006.03.007

Dehaene, S., Naccache, L., Le Clec, H.G., Koechlin, E., Mueller, M., Dehaene-Lambertz, G., van de Moortele, P.F., Le Bihan, D., 1998. Imaging unconscious semantic priming. Nature 395, 597–600.

Dehghani, N., Cash, S.S., Chen, C.C., Hagler, D.J., Huang, M., Dale, A.M., Halgren, E., 2010a. Divergent cortical generators of MEG and EEG during human sleep spindles suggested by distributed source modeling. PLoS One 5, e11454. doi:10.1371/journal.pone.0011454

Dehghani, N., Peyrache, A., Destexhe, A., 2010b. Dynamics of excitation and inhibition, and local interactions, during slow wave sleep oscillations in rat prefrontal cortex, in: Neuroscience, S. for (Ed.), . Presented at the Annual Meeting - Society for Neuroscience.

de Lavilléon, G., Lacroix, M.M., Rondi-Reig, L., Benchenane, K., 2015. Explicit memory creation during sleep demonstrates a causal role of place cells in navigation. Nat. Neurosci. 18, 493–495. doi:10.1038/nn.3970

Delorme, A., Makeig, S., 2004. EEGLAB: an open source toolbox for analysis of single-trial EEG dynamics including independent component analysis. J. Neurosci. Methods 134, 9–21. doi:10.1016/j.jneumeth.2003.10.009

Dement, W., Kleitman, N., 1957. The relation of eye movements during sleep to dream activity: an objective method for the study of dreaming. J Exp Psychol 53, 339–46.

Dement, W., Wolpert, E.A., 1958. The relation of eye movements, body motility, and external stimuli to dream content. J. Exp. Psychol. 55, 543–553.

Dennett, D.C., 1991. Consciousness Explained. Boston: Little, Brown.

Dennett, D.C., 1976. Are Dreams Experiences? Philos. Rev. 85, 151. doi:10.2307/2183728

Destexhe, A., Contreras, D., Steriade, M., 1999. Spatiotemporal analysis of local field potentials and unit discharges in cat cerebral cortex during natural wake and sleep states. J Neurosci 19, 4595–608.

Destexhe, A., Contreras, D., Steriade, M., 1998. Mechanisms underlying the synchronizing action of corticothalamic feedback through inhibition of thalamic relay cells. J Neurophysiol 79, 999–1016.

Destexhe, A., Hughes, S.W., Rudolph, M., Crunelli, V., 2007. Are corticothalamic "up" states fragments of wakefulness? Trends Neurosci. 30, 334–342. doi:10.1016/j.tins.2007.04.006

Destexhe, A., Sejnowski, T.J., 2002. The initiation of bursts in thalamic neurons and the cortical control of thalamic sensitivity. Philos Trans R Soc Lond B Biol Sci 357, 1649–57. doi:10.1098/rstb.2002.1154

Destexhe, A., Sejnowski, T.J., 2001. Thalamocortical assemblies : how ion channels, single neurons and large-scale networks organize sleep oscillations. Oxford University Press, Oxford.

Diekelmann, S., Born, J., 2010. The memory function of sleep. Nat Rev Neurosci 11, 114–26.

Dienes, Z., 2014. Using Bayes to get the most out of non-significant results. Front. Psychol. 5. doi:10.3389/fpsyg.2014.00781

Dijk, D.-J., 2010. Slow-wave sleep deficiency and enhancement: Implications for insomnia and its management. World J. Biol. Psychiatry 11, 22–28. doi:10.3109/15622971003637645

Dijk, D.J., Beersma, D.G., Daan, S., 1987. EEG power density during nap sleep: reflection of an hourglass measuring the duration of prior wakefulness. J. Biol. Rhythms 2, 207–219.

Ding, N., Simon, J.Z., 2012a. Neural coding of continuous speech in auditory cortex during monaural and dichotic listening. J. Neurophysiol. 107, 78–89. doi:10.1152/jn.00297.2011

Ding, N., Simon, J.Z., 2012b. Emergence of neural encoding of auditory objects while listening to competing speakers. Proc. Natl. Acad. Sci. 109, 11854–11859. doi:10.1073/pnas.1205381109

Dinner, D.S., Lüders, H.O., 2001. Epilepsy and sleep: physiological and clinical relationships. Academic Press, San Diego, CA.

Dodge, R., 1905. The Illusion of Clear Vision during Eye Movement. Psychol. Bull. 2, 193–199.

Doelling, K.B., Arnal, L.H., Ghitza, O., Poeppel, D., 2014. Acoustic landmarks drive delta–theta oscillations to enable speech comprehension by facilitating perceptual parsing. NeuroImage 85, 761–768. doi:10.1016/j.neuroimage.2013.06.035

Doran, S.M., Van Dongen, H.P., Dinges, D.F., 2001. Sustained attention performance during sleep deprivation: evidence of state instability. Arch. Ital. Biol. 139, 253–267.

Dorran, D., Lawlor, R., 2003. An efficient audio time-scale modification algorithm for use in a subband implementation. Presented at the International Conference on Digital Audio Effects, London, England.

Dudai, Y., 2004. The Neurobiology of Consolidations, Or, How Stable is the Engram? Annu. Rev. Psychol. 55, 51–86. doi:10.1146/annurev.psych.55.090902.142050

Duhamel, J.R., Colby, C.L., Goldberg, M.E., 1992. The Updating of the Representation of Visual Space in Parietal Cortex by Intended Eye-Movements. Science 255, 90–92.

Durmer, J.S., Dinges, D.F., 2005. Neurocognitive consequences of sleep deprivation. Semin. Neurol. 25, 117–129. doi:10.1055/s-2005-867080

Ebbinghaus, H., 1885. Memory: A Contribution to Experimental Psychology. Teachers College, Columbia University.

Edeline, J.M., Dutrieux, G., Manunta, Y., Hennevin, E., 2001. Diversity of receptive field changes in auditory cortex during natural sleep. Eur. J. Neurosci. 14, 1865–1880.

Ego-Stengel, V., Wilson, M.A., 2010. Disruption of ripple-associated hippocampal activity during rest impairs spatial learning in the rat. Hippocampus 20, 1–10. doi:10.1002/hipo.20707

Eichenbaum, H., 2008. Learning & memory, 1st ed. ed. W. W. Norton & Co, New York.

Eichenbaum, H., Yonelinas, A.P., Ranganath, C., 2007. The Medial Temporal Lobe and Recognition Memory. Annu. Rev. Neurosci. 30, 123–152. doi:10.1146/annurev.neuro.30.051606.094328

Eimer, M., Schlaghecken, F., 1998. Effects of masked stimuli on motor activation: behavioral and electrophysiological evidence. J. Exp. Psychol. Hum. Percept. Perform. 24, 1737–1747.

Ellenbogen, J.M., Hulbert, J.C., Stickgold, R., Dinges, D.F., Thompson-Schill, S.L., 2006a. Interfering with theories of sleep and memory: sleep, declarative memory, and associative interference. Curr. Biol. CB 16, 1290–1294. doi:10.1016/j.cub.2006.05.024

Ellenbogen, J.M., Payne, J.D., Stickgold, R., 2006b. The role of sleep in declarative memory consolidation: passive, permissive, active or none? Curr. Opin. Neurobiol. 16, 716–722. doi:10.1016/j.conb.2006.10.006

Elliott, T.M., Hamilton, L.S., Theunissen, F.E., 2013. Acoustic structure of the five perceptual dimensions of timbre in orchestral instrument tones. J. Acoust. Soc. Am. 133, 389–404. doi:10.1121/1.4770244

Emmons, W.H., Simon, C.W., 1956. The Non-Recall of Material Presented during Sleep. Am. J. Psychol. 69, 76. doi:10.2307/1418117

Ermentrout, G.B., Kleinfeld, D., 2001. Traveling electrical waves in cortex: insights from phase dynamics and speculation on a computational role. Neuron 29, 33–44. doi:S0896-6273(01)00178-7 [pii]

Ermis, U., Krakow, K., Voss, U., 2010. Arousal thresholds during human tonic and phasic REM sleep. J. Sleep Res. 19, 400–406. doi:10.1111/j.1365-2869.2010.00831.x

Esser, S.K., Huber, R., Massimini, M., Peterson, M.J., Ferrarelli, F., Tononi, G., 2006. A direct demonstration of cortical LTP in humans: a combined TMS/EEG study. Brain Res Bull 69, 86–94. doi:10.1016/j.brainresbull.2005.11.003

Evarts, E.V., 1964. Temporal Patterns of Discharge of Pyramidal Tract Neurons during Sleep and Waking in the Monkey. J Neurophysiol 27, 152–71.

Farber, J., Marks, G.A., Roffwarg, H.P., 1980. Rapid eye movement sleep PGO-type waves are present in the dorsal pons of the albino rat. Science 209, 615–7.

Ferrarelli, F., Huber, R., Peterson, M.J., Massimini, M., Murphy, M., Riedner, B.A., Watson, A., Bria, P., Tononi, G., 2007. Reduced sleep spindle activity in schizophrenia patients. Am J Psychiatry 164, 483–92. doi:10.1176/appi.ajp.164.3.483

Ferrarelli, F., Peterson, M.J., Sarasso, S., Riedner, B.A., Murphy, M.J., Benca, R.M., Bria, P., Kalin, N.H., Tononi, G., 2010. Thalamic dysfunction in schizophrenia suggested by whole-night deficits in slow and fast spindles. Am J Psychiatry 167, 1339–48. doi:10.1176/appi.ajp.2010.09121731

Fifer, W.P., Byrd, D.L., Kaku, M., Eigsti, I.-M., Isler, J.R., Grose-Fifer, J., Tarullo, A.R., Balsam, P.D., 2010. Newborn infants learn during sleep. Proc. Natl. Acad. Sci. 107, 10320–10323. doi:10.1073/pnas.1005061107

Finelli, L.A., Borbely, A.A., Achermann, P., 2001. Functional topography of the human nonREM sleep electroencephalogram. Eur J Neurosci 13, 2282–90. doi:ejn1597 [pii]

Fischer, S., Drosopoulos, S., Tsen, J., Born, J., 2006. Implicit Learning–Explicit Knowing: A Role for Sleep in Memory System Interaction. J. Cogn. Neurosci. 18, 311–319. doi:10.1162/jocn.2006.18.3.311

Fleming, S.M., Weil, R.S., Nagy, Z., Dolan, R.J., Rees, G., 2010. Relating Introspective Accuracy to Individual Differences in Brain Structure. Science 329, 1541–1543. doi:10.1126/science.1191883

Ford, A., White, C.T., Lichtenstein, M., 1959. Analysis of eye movements during free search. J. Opt. Soc. Am. 49, 287–292.

Formby, D., 1967. Maternal recognition of infant's cry. Dev Med Child Neurol 9, 293–8.

Frank, M.G., Cantera, R., 2014. Sleep, clocks, and synaptic plasticity. Trends Neurosci. 37, 491–501. doi:10.1016/j.tins.2014.06.005

Fried, I., Wilson, C.L., Maidment, N.T., Engel, J., Behnke, E., Fields, T.A., MacDonald, K.A., Morrow, J.W., Ackerson, L., 1999a. Cerebral microdialysis combined with single-neuron and electroencephalographic recording in neurosurgical patients. Technical note. J Neurosurg 91, 697–705. doi:10.3171/jns.1999.91.4.0697

Fried, I., Wilson, C., Maidment, N., Engel, J., Behnke, E., Fields, T., MacDonald, K., Morrow, J. and Ackerson, L, 1999b. Cerebral microdialysis combined with single neuron and electroencephalographic recording in neurosurgical patients. J Neurosurg 91, 697–705.

Friedman, L., Bergmann, B.M., Rechtschaffen, A., 1979. Effects of sleep deprivation on sleepiness, sleep intensity, and subsequent sleep in the rat. Sleep 1, 369–391.

Fries, C.C., 1952. The structure of english: an introduction to the construction of english sentences. Harcourt, Brace & World, inc., New York.

Fritz, J.B., Elhilali, M., David, S.V., Shamma, S.A., 2007. Auditory attention—focusing the searchlight on sound. Curr. Opin. Neurobiol. 17, 437–455. doi:10.1016/j.conb.2007.07.011

Fritz, J., Shamma, S., Elhilali, M., Klein, D., 2003. Rapid task-related plasticity of spectrotemporal receptive fields in primary auditory cortex. Nat. Neurosci. 6, 1216–1223. doi:10.1038/nn1141

Funk, C.M., Honjoh, S., Rodriguez, A.V., Cirelli, C., Tononi, G., 2016. Local Slow Waves in Superficial Layers of Primary Cortical Areas during REM Sleep. Curr. Biol. doi:10.1016/j.cub.2015.11.062

Gallant, J.L., Connor, C.E., Van Essen, D.C., 1998. Neural activity in areas V1, V2 and V4 during free viewing of natural scenes compared to controlled viewing. Neuroreport 9, 2153–2158.

Genzel, L., Kroes, M.C.W., Dresler, M., Battaglia, F.P., 2014. Light sleep versus slow wave sleep in memory consolidation: a question of global versus local processes? Trends Neurosci. 37, 10–19. doi:10.1016/j.tins.2013.10.002

Gevers, W., Deliens, G., Hoffmann, S., Notebaert, W., Peigneux, P., 2015. Sleep deprivation selectively disrupts top-down adaptation to cognitive conflict in the Stroop test. J. Sleep Res. 24, 666–672. doi:10.1111/jsr.12320

Gibbs, F.A., 1950. Atlas of Electroencephalography. Addison-Wesley, Massachussets.

Gilbert, C.D., Sigman, M., Crist, R.E., 2001. The neural basis of perceptual learning. Neuron 31, 681–697.

Girardeau, G., Benchenane, K., Wiener, S.I., Buzsáki, G., Zugaro, M.B., 2009. Selective suppression of hippocampal ripples impairs spatial memory. Nat. Neurosci. 12, 1222–1223. doi:10.1038/nn.2384

Giraud, A.-L., Poeppel, D., 2012a. Cortical oscillations and speech processing: emerging computational principles and operations. Nat. Neurosci. 15, 511–517. doi:10.1038/nn.3063

Giraud, A.-L., Poeppel, D., 2012b. Cortical oscillations and speech processing: emerging computational principles and operations. Nat. Neurosci. 15, 511–517. doi:10.1038/nn.3063

Gold, J.M., Aizenman, A., Bond, S.M., Sekuler, R., 2014. Memory and incidental learning for visual frozen noise sequences. Vision Res. 99, 19–36. doi:10.1016/j.visres.2013.09.005

Golshani, P., Liu, X.B., Jones, E.G., 2001. Differences in quantal amplitude reflect GluR4-subunit number at corticothalamic synapses on two populations of thalamic neurons. Proc Natl Acad Sci U A 98, 4172–7. doi:10.1073/pnas.061013698

Gottselig, J.M., Bassetti, C.L., Achermann, P., 2002. Power and coherence of sleep spindle frequency activity following hemispheric stroke. Brain 125, 373–83.

Goupil, L., Bekinschtein, T.A., 2012. Cognitive processing during the transition to sleep. Arch. Ital. Biol. 150, 140–154.

Gucer, G., Viernstein, L.J., 1979. Intracranial pressure in the normal monkey while awake and asleep. J Neurosurg 51, 206–10. doi:10.3171/jns.1979.51.2.0206

Guillery, R.W., Harting, J.K., 2003. Structure and connections of the thalamic reticular nucleus: Advancing views over half a century. J Comp Neurol 463, 360–71. doi:10.1002/cne.10738

Gujar, N., McDonald, S.A., Nishida, M., Walker, M.P., 2011. A Role for REM Sleep in Recalibrating the Sensitivity of the Human Brain to Specific Emotions. Cereb. Cortex 21, 115–123. doi:10.1093/cercor/bhq064

Gutschalk, A., Micheyl, C., Oxenham, A.J., 2008. Neural correlates of auditory perceptual awareness under informational masking. PLoS Biol. 6, e138. doi:10.1371/journal.pbio.0060138

Guttman, N., 1963. Lower Limits of Auditory Periodicity Analysis. J. Acoust. Soc. Am. 35, 610. doi:10.1121/1.1918551

Haggard, P., 2005. Conscious intention and motor cognition. Trends Cogn. Sci. 9, 290–295. doi:10.1016/j.tics.2005.04.012

Hagmann, P., Cammoun, L., Gigandet, X., Meuli, R., Honey, C.J., Wedeen, V.J., Sporns, O., 2008. Mapping the structural core of human cerebral cortex. PLoS Biol 6, e159. doi:10.1371/journal.pbio.0060159

Hahne, A., Jescheniak, J.D., 2001. What's left if the Jabberwock gets the semantics? An ERP investigation into semantic and syntactic processes during auditory sentence comprehension. Cogn. Brain Res. 11, 199–212. doi:10.1016/S0926-6410(00)00071-9

Hahn, T.T., Sakmann, B., Mehta, M.R., 2007. Differential responses of hippocampal subfields to cortical up-down states. Proc Natl Acad Sci U A 104, 5169–74. doi:10.1073/pnas.0700222104

Halassa, M.M., Siegle, J.H., Ritt, J.T., Ting, J.T., Feng, G., Moore, C.I., 2011. Selective optical drive of thalamic reticular nucleus generates thalamic bursts and cortical spindles. Nat Neurosci 14, 1118–20. doi:10.1038/nn.2880

Halász, P., 2016. The K-complex as a special reactive sleep slow wave – A theoretical update. Sleep Med. Rev. 29, 34–40. doi:10.1016/j.smrv.2015.09.004

Halasz, P., 2005. K-complex, a reactive EEG graphoelement of NREM sleep: an old chap in a new garment. Sleep Med Rev 9, 391–412.

Halász, P., Bódizs, R., Parrino, L., Terzano, M., 2014. Two features of sleep slow waves: homeostatic and reactive aspects – from long term to instant sleep homeostasis. Sleep Med. 15, 1184–1195. doi:10.1016/j.sleep.2014.06.006

Halász, P., Terzano, M., Parrino, L., Bódizs, R., 2004. The nature of arousal in sleep. J. Sleep Res. 13, 1–23.

Hamker, F.H., Zirnsak, M., Ziesche, A., Lappe, M., 2011. Computational models of spatial updating in peri-saccadic perception. Philos Trans R Soc Lond B Biol Sci 366, 554–71. doi:10.1098/rstb.2010.0229

Hanes, D.P., Thompson, K.G., Schall, J.D., 1995. Relationship of presaccadic activity in frontal eye field and supplementary eye field to saccade initiation in macaque: Poisson spike train analysis. Exp. Brain Res. 103, 85–96.

Harrison, Y., Horne, J.A., 2000. Sleep loss and temporal memory. Q. J. Exp. Psychol. A 53, 271–279. doi:10.1080/713755870

Harrison, Y., Horne, J.A., 1999. One Night of Sleep Loss Impairs Innovative Thinking and Flexible Decision Making. Organ. Behav. Hum. Decis. Process. 78, 128–145. doi:10.1006/obhd.1999.2827

Hashmi, A., Nere, A.T., Tononi, G., 2013. Sleep-dependent synaptic down-selection (II): single-neuron level benefits for matching, selectivity, and specificity. Sleep Chronobiol. 4, 148. doi:10.3389/fneur.2013.00148

Hasselmo, M.E., 1999. Neuromodulation: acetylcholine and memory consolidation. Trends Cogn Sci 3, 351–359.

Haufe, S., Meinecke, F., Görgen, K., Dähne, S., Haynes, J.-D., Blankertz, B., Bießmann, F., 2014. On the interpretation of weight vectors of linear models in multivariate neuroimaging. NeuroImage 87, 96–110. doi:10.1016/j.neuroimage.2013.10.067

Hauri, P., Hawkins, D.R., 1973. Alpha-delta sleep. Electroencephalogr. Clin. Neurophysiol. 34, 233–237. doi:10.1016/0013-4694(73)90250-2

Hebb, D.O., 1949. The organization of behavior: a neuropsychological theory. L. Erlbaum Associates.

Henderson, J.M., 2003. Human gaze control during real-world scene perception. Trends Cogn Sci 7, 498–504.

Hennevin, E., Hars, B., Maho, C., Bloch, V., 1995. Processing of learned information in paradoxical sleep: relevance for memory. Behav Brain Res 69, 125–35.

Hennevin, E., Huetz, C., Edeline, J.M., 2007. Neural representations during sleep: from sensory processing to memory traces. Neurobiol Learn Mem 87, 416–40.

Himanen, S.L., Virkkala, J., Huhtala, H., Hasan, J., 2002. Spindle frequencies in sleep EEG show U-shape within first four NREM sleep episodes. J Sleep Res 11, 35–42.

Hobson, J.A., 2009. REM sleep and dreaming: towards a theory of protoconsciousness. Nat Rev Neurosci. doi:10.1038/nrn2716

Hobson, J.A., 2005. Sleep is of the brain, by the brain and for the brain. Nature 437, 1254–6. doi:10.1038/nature04283

Hobson, J.A., 1990. The dreaming brain. Penguin, Harmondsworth.

Hobson, J.A., Pace-Schott, E.F., 2002. The cognitive neuroscience of sleep: neuronal systems, consciousness and learning. Nat Rev Neurosci 3, 679–93. doi:10.1038/nrn915

Hori, T., Hayashi, M., Morikawa, T., 1994. Topographical EEG changes and the hypnagogic experience., in: Ogilvie, R.D., Harsh, J.R. (Eds.), Sleep Onset: Normal and Abnormal Processes. American Psychological Association, Washington, pp. 237–253.

Hromádka, T., DeWeese, M.R., Zador, A.M., 2008. Sparse Representation of Sounds in the Unanesthetized Auditory Cortex. PLoS Biol. 6, e16. doi:10.1371/journal.pbio.0060016

Huber, R., Ghilardi, M.F., Massimini, M., Ferrarelli, F., Riedner, B.A., Peterson, M.J., Tononi, G., 2006. Arm immobilization causes cortical plastic changes and locally decreases sleep slow wave activity. Nat Neurosci 9, 1169–76. doi:10.1038/nn1758

Huber, R., Ghilardi, M.F., Massimini, M., Tononi, G., 2004. Local sleep and learning. Nature 430, 78–81. doi:10.1038/nature02663

Hung, C.-S., Sarasso, S., Ferrarelli, F., Riedner, B., Ghilardi, M.F., Cirelli, C., Tononi, G., 2013. Local experience-dependent changes in the wake EEG after prolonged wakefulness. Sleep 36, 59–72. doi:10.5665/sleep.2302

Huxley, A., 1932. Brave new world, 1st Perennial Classics ed. ed. Perennial Classics, New York.

Ibanez, A., Lopez, V., Cornejo, C., 2006. ERPs and contextual semantic discrimination: degrees of congruence in wakefulness and sleep. Brain Lang 98, 264–75.

Ibbotson, M., Krekelberg, B., 2011. Visual perception and saccadic eye movements. Curr. Opin. Neurobiol. 21, 553–558. doi:10.1016/j.conb.2011.05.012

Iber, C., Ancoli-Israel, S., Chesson, A., Quan, S., 2007. The AASM Manual for the Scoring of Sleep and Associated Events: Rules, Terminology and Technical Specifications.

Ikeda, K., Morotomi, T., 1996. Classical conditioning during human NREM sleep and response transfer to wakefulness. Sleep 19, 72–74.

Ioannides, A.A., 2004. MEG Tomography of Human Cortex and Brainstem Activity in Waking and REM Sleep Saccades. Cereb. Cortex 14, 56–72. doi:10.1093/cercor/bhg091

Isomura, Y., Sirota, A., Ozen, S., Montgomery, S., Mizuseki, K., Henze, D.A., Buzsaki, G., 2006. Integration and segregation of activity in entorhinal-hippocampal subregions by neocortical slow oscillations. Neuron 52, 871–82. doi:10.1016/j.neuron.2006.10.023

Issa, E.B., Wang, X., 2011. Altered Neural Responses to Sounds in Primate Primary Auditory Cortex during Slow-Wave Sleep. J. Neurosci. 31, 2965–2973. doi:10.1523/JNEUROSCI.4920-10.2011

Issa, E.B., Wang, X., 2008. Sensory responses during sleep in primate primary and secondary auditory cortex. J Neurosci 28, 14467–80.

Ito, J., Maldonado, P., Singer, W., Grün, S., 2011. Saccade-related modulations of neuronal excitability support synchrony of visually elicited spikes. Cereb. Cortex N. Y. N 1991 21, 2482–2497. doi:10.1093/cercor/bhr020

Iwasaki, M., Kellinghaus, C., Alexopoulos, A.V., Burgess, R.C., Kumar, A.N., Han, Y.H., Lüders, H.O., Leigh, R.J., 2005. Effects of eyelid closure, blinks, and eye movements on the electroencephalogram. Clin. Neurophysiol. Off. J. Int. Fed. Clin. Neurophysiol. 116, 878–885. doi:10.1016/j.clinph.2004.11.001

Jachs, B., Blanco, M.J., Grantham-Hill, S., Soto, D., 2015. On the independence of visual awareness and metacognition: a signal detection theoretic analysis. J. Exp. Psychol. Hum. Percept. Perform. 41, 269–276. doi:10.1037/xhp0000026

Jacobs, L., Feldman, M., Bender, M.B., 1972. Are the eye movements of dreaming sleep related to the visual images of the dreams? Psychophysiology 9, 393–401.

Jagadeesh, B., Chelazzi, L., Mishkin, M., Desimone, R., 2001. Learning increases stimulus salience in anterior inferior temporal cortex of the macaque. J. Neurophysiol. 86, 290–303.

Jagla, F., Jergelová, M., Riecanský, I., 2007. Saccadic eye movement related potentials. Physiol. Res. Acad. Sci. Bohemoslov. 56, 707–713.

Jankel, W.R., Niedermeyer, E., 1985. Sleep spindles. J Clin Neurophysiol 2, 1–35.

Jeannerod, M., Sakai, K., 1970. Occipital and geniculate potentials related to eye movements in the unanaesthetized cat. Brain Res. 19, 361–377.

Jenkins, J.G., Dallenbach, K.M., 1924. Obliviscence during Sleep and Waking. Am. J. Psychol. 35, 605. doi:10.2307/1414040

Ji, D., Wilson, M.A., 2007. Coordinated memory replay in the visual cortex and hippocampus during sleep. Nat Neurosci 10, 100–7. doi:10.1038/nn1825

Ji, D., Wilson, M.A., 2007. Coordinated memory replay in the visual cortex and hippocampus during sleep. Nat. Neurosci. 10, 100–107. doi:10.1038/nn1825

Jobert, M., Poiseau, E., Jahnig, P., Schulz, H., Kubicki, S., 1992. Topographical analysis of sleep spindle activity. Neuropsychobiology 26, 210–7.

Jones, B.E., 2005. From waking to sleeping: neuronal and chemical substrates. Trends Pharmacol. Sci. 26, 578–586. doi:10.1016/j.tips.2005.09.009

Jones, E.G., 2009. Synchrony in the interconnected circuitry of the thalamus and cerebral cortex. Ann N Acad Sci 1157, 10–23. doi:10.1111/j.1749-6632.2009.04534.x

Jones, E.G., 2007. The thalamus, 2nd ed. Cambridge University Press, Cambridge, UK ; New York.

Jones, E.G., 2002. Thalamic circuitry and thalamocortical synchrony. Philos Trans R Soc Lond B Biol Sci 357, 1659–73. doi:10.1098/rstb.2002.1168

Jones, L.M., Fontanini, A., Sadacca, B.F., Miller, P., Katz, D.B., 2007. Natural stimuli evoke dynamic sequences of states in sensory cortical ensembles. Proc Natl Acad Sci U A 104, 18772–7. doi:10.1073/pnas.0705546104

Jouvet, M., 1992. Le sommeil et le rêve. Odile Jacob, Paris.

Jouvet, M., 1965. Paradoxical Sleep--a Study of Its Nature and Mechanisms. Prog Brain Res 18, 20–62.

Jouvet, M., Michel, F.C., 1959. L'activite electrique du rhinencephale au cours dusommeil chez le chat. CR Soc Biol 101–105.

Joyce, C.A., Gorodnitsky, I.F., King, J.W., Kutas, M., 2002. Tracking eye fixations with electroocular and electroencephalographic recordings. Psychophysiology 39, 607–618. doi:10.1017.S0048577202394113

Julesz, B., 1963. Auditory Memory. J. Acoust. Soc. Am. 35, 1895. doi:10.1121/1.2142719

Jutras, M.J., Fries, P., Buffalo, E.A., 2013. Oscillatory activity in the monkey hippocampus during visual exploration and memory formation. Proc. Natl. Acad. Sci. U. S. A. 110, 13144–13149. doi:10.1073/pnas.1302351110

Kaernbach, C., 2004. The memory of noise. Exp. Psychol. 51, 240–248.

Kaernbach, C., 1993. Temporal and spectral basis of the features perceived in repeated noise. J. Acoust. Soc. Am. 94, 91–97.

Kaernbach, C., 1992. On the consistency of tapping to repeated noise. J. Acoust. Soc. Am. 92, 788–793.

Kandel, E.R., 2000. The Molecular Biology of Memory Storage: A Dialog between Genes and Synapses.

Kass, R.E., Raftery, A.E., 1995. Bayes Factors. J. Am. Stat. Assoc. 90, 773–795. doi:10.1080/01621459.1995.10476572

Kayama, Y., Riso, R.R., Bartlett, J.R., Doty, R.W., 1979. Luxotonic Responses of Units in Macaque Striate Cortex. J. Neurophysiol. 42, 1495–1517.

Kayser, J., Tenke, C.E., Gates, N.A., Bruder, G.E., 2007. Reference-independent ERP old/new effects of auditory and visual word recognition memory: Joint extraction of stimulus- and response-locked neuronal generator patterns. Psychophysiology 44, 949–967. doi:10.1111/j.1469-8986.2007.00562.x

Khazipov, R., Sirota, A., Leinekugel, X., Holmes, G.L., Ben-Ari, Y., Buzsaki, G., 2004. Early motor activity drives spindle bursts in the developing somatosensory cortex. Nature 432, 758–61. doi:10.1038/nature03132

Killian, N.J., Jutras, M.J., Buffalo, E.A., 2012. A map of visual space in the primate entorhinal cortex. Nature 491, 761–764. doi:10.1038/nature11587

Kim, U., Bal, T., McCormick, D.A., 1995. Spindle waves are propagating synchronized oscillations in the ferret LGNd in vitro. J Neurophysiol 74, 1301–23.

King, J.-R., Sitt, J.D., Faugeras, F., Rohaut, B., El Karoui, I., Cohen, L., Naccache, L., Dehaene, S., 2013. Information Sharing in the Brain Indexes Consciousness in Noncommunicative Patients. Curr. Biol. 23, 1914–1919. doi:10.1016/j.cub.2013.07.075

Klampfl, S., Maass, W., 2013. Emergence of Dynamic Memory Traces in Cortical Microcircuit Models through STDP. J. Neurosci. 33, 11515–11529. doi:10.1523/JNEUROSCI.5044-12.2013

Kleiser, R., Seitz, F.J., Krekelberg, B., 2004. Neural correlates of saccadic suppression in humans. Curr. Biol. 14, 386–390. doi:10.1016/j.cub.2004.02.036

Kleitman, N., 1987. Sleep and wakefulness. University of Chicago Press, Chicago.

Klimesch, W., 1999. EEG alpha and theta oscillations reflect cognitive and memory performance: a review and analysis. Brain Res. Brain Res. Rev. 29, 169–195.

Klimesch, W., Doppelmayr, M., Schimke, H., Ripper, B., 1997. Theta synchronization and alpha desynchronization in a memory task. Psychophysiology 34, 169–176.

Klimesch, W., Doppelmayr, M., Schwaiger, J., Auinger, P., Winkler, T., 1999. "Paradoxical" alpha synchronization in a memory task. Brain Res. Cogn. Brain Res. 7, 493–501.

Koch, C., Tsuchiya, N., 2007. Attention and consciousness: two distinct brain processes. Trends Cogn. Sci. 11, 16–22. doi:10.1016/j.tics.2006.10.012

Kohlschütter, E., 1862. Messungen der Festigkeit des Schlafes. Kreysing.

Kolb, B., Whishaw, I.Q., 1998. Brain plasticity and behavior. Annu. Rev. Psychol. 49, 43–64. doi:10.1146/annurev.psych.49.1.43

Kothe, C.A., Makeig, S., 2013. BCILAB: a platform for brain-computer interface development. J. Neural Eng. 10, 056014. doi:10.1088/1741-2560/10/5/056014

Kouider, S., Andrillon, T., Barbosa, L.S., Goupil, L., Bekinschtein, T.A., 2014. Inducing Task-Relevant Responses to Speech in the Sleeping Brain. Curr. Biol. 24, 2208–2214. doi:10.1016/j.cub.2014.08.016

Kouider, S., de Gardelle, V., Sackur, J., Dupoux, E., 2010. How rich is consciousness? The partial awareness hypothesis. Trends Cogn Sci 14, 301–7.

Kouider, S., Dehaene, S., 2007. Levels of processing during non-conscious perception: a critical review of visual masking. Philos Trans R Soc Lond B Biol Sci 362, 857–75. doi:10.1098/rstb.2007.2093

Kouider, S., Dupoux, E., 2005. Subliminal speech priming. Psychol Sci 16, 617–25. doi:10.1111/j.1467-9280.2005.01584.x

Kovach, C.K., Tsuchiya, N., Kawasaki, H., Oya, H., Howard, M.A., Adolphs, R., 2011. Manifestation of ocular-muscle EMG contamination in human intracranial recordings. NeuroImage 54, 213–233. doi:10.1016/j.neuroimage.2010.08.002

Kramis, R., Vanderwolf, C.H., Bland, B.H., 1975. Two types of hippocampal rhythmical slow activity in both the rabbit and the rat: relations to behavior and effects of atropine, diethyl ether, urethane, and pentobarbital. Exp. Neurol. 49, 58–85.

Kristiansen, K., Courtois, G., 1949. Rhythmic electrical activity from isolated cerebral cortex. Electroencephalogr Clin Neurophysiol 1, 265–72.

Krueger, J.M., Rector, D.M., Roy, S., Van Dongen, H.P., Belenky, G., Panksepp, J., 2008. Sleep as a fundamental property of neuronal assemblies. Nat Rev Neurosci 9, 910–9. doi:10.1038/nrn2521

Krumbholz, K., Patterson, R.D., Seither-Preisler, A., Lammertmann, C., Lütkenhöner, B., 2003. Neuromagnetic evidence for a pitch processing center in Heschl's gyrus. Cereb. Cortex N. Y. N 1991 13, 765–772.

Kumar, S., Bonnici, H.M., Teki, S., Agus, T.R., Pressnitzer, D., Maguire, E.A., Griffiths, T.D., 2014. Representations of specific acoustic patterns in the auditory cortex and hippocampus. Proc. R. Soc. B Biol. Sci. 281, 20141000–20141000. doi:10.1098/rspb.2014.1000

Kutas, M., Donchin, E., 1980. Preparation to respond as manifested by movement-related brain potentials. Brain Res. 202, 95–115.

LaBerge, S., 2000. Lucid dreaming: Evidence and methodology. Behav. Brain Sci. 23, 962.

Lam, Y.W., Sherman, S.M., 2011. Functional organization of the thalamic input to the thalamic reticular nucleus. J Neurosci 31, 6791–9. doi:10.1523/JNEUROSCI.3073-10.2011

Landry, M., Appourchaux, K., Raz, A., 2014. Elucidating unconscious processing with instrumental hypnosis. Front. Psychol. 5. doi:10.3389/fpsyg.2014.00785

Landsness, E.C., Crupi, D., Hulse, B.K., Peterson, M.J., Huber, R., Ansari, H., Coen, M., Cirelli, C., Benca, R.M., Ghilardi, M.F., Tononi, G., 2009. Sleep-dependent improvement in visuomotor learning: a causal role for slow waves. Sleep 32, 1273–84.

Laureys, S., 2005. The neural correlate of (un)awareness: lessons from the vegetative state. Trends Cogn. Sci. 9, 556–559. doi:10.1016/j.tics.2005.10.010

Laurino, M., Menicucci, D., Piarulli, A., Mastorci, F., Bedini, R., Allegrini, P., Gemignani, A., 2014. Disentangling different functional roles of evoked K-complex components: Mapping the sleeping brain while quenching sensory processing. NeuroImage 86, 433–445. doi:10.1016/j.neuroimage.2013.10.030

Leaver, A.M., Rauschecker, J.P., 2010. Cortical representation of natural complex sounds: effects of acoustic features and auditory object category. J. Neurosci. Off. J. Soc. Neurosci. 30, 7604–7612. doi:10.1523/JNEUROSCI.0296-10.2010

Leclair-Visonneau, L., Oudiette, D., Gaymard, B., Leu-Semenescu, S., Arnulf, I., 2010. Do the eyes scan dream images during rapid eye movement sleep? Evidence from the rapid eye movement sleep behaviour disorder model. Brain 133, 1737–46. doi:10.1093/brain/awq110

Lee, A.K., Wilson, M.A., 2002. Memory of sequential experience in the hippocampus during slow wave sleep. Neuron 36, 1183–94. doi:S0896627302010966 [pii]

Lehmann, D., 1971. Multichannel Topography of Human Alpha Eeg Fields. Electroencephalogr. Clin. Neurophysiol. 31, 439–&.

Leigh, R.J., 2003. Using saccades as a research tool in the clinical neurosciences. Brain 127, 460–477. doi:10.1093/brain/awh035

Leuthold, H., 2003a. Programming of expected and unexpected movements: effects on the onset of the lateralized readiness potential. Acta Psychol. (Amst.) 114, 83–100.

Leuthold, H., 2003b. Programming of expected and unexpected movements: effects on the onset of the lateralized readiness potential. Acta Psychol. (Amst.) 114, 83–100.

Le Van Quyen, M., Bragin, A., Staba, R., Crepon, B., Wilson, C.L., Engel, J., Jr., 2008. Cell type-specific firing during ripple oscillations in the hippocampal formation of humans. J Neurosci 28, 6104–10. doi:10.1523/JNEUROSCI.0437-08.2008

Le Van Quyen, M., Staba, R., Bragin, A., Dickson, C., Valderrama, M., Fried, I., Engel, J., 2010. Large-scale microelectrode recordings of high-frequency gamma oscillations in human cortex during sleep. J Neurosci 30, 7770–82. doi:10.1523/JNEUROSCI.5049-09.2010

Lim, A.S., Lozano, A.M., Moro, E., Hamani, C., Hutchison, W.D., Dostrovsky, J.O., Lang, A.E., Wennberg, R.A., Murray, B.J., 2007. Characterization of REM-sleep associated ponto-geniculo-occipital waves in the human pons. Sleep 30, 823–827.

Loomis, A.L., Harvey, E.N., Hobart, G., 1935. Potential Rhythms of the Cerebral Cortex during Sleep. Science 81, 597–598. doi:10.1126/science.81.2111.597

Loomis, A.L., Harvey, E.N., Hobart, G.A., 1938. DISTRIBUTION OF DISTURBANCE-PATTERNS IN THE HUMAN ELECTROENCEPHALOGRAM, WITH SPECIAL REFERENCE TO SLEEP. J. Neurophysiol. 1, 413–430.

Louie, K., Wilson, M.A., 2001. Temporally structured replay of awake hippocampal ensemble activity during rapid eye movement sleep. Neuron 29, 145–156.

Luo, H., Poeppel, D., 2007. Phase patterns of neuronal responses reliably discriminate speech in human auditory cortex. Neuron 54, 1001–1010. doi:10.1016/j.neuron.2007.06.004

Luo, H., Tian, X., Song, K., Zhou, K., Poeppel, D., 2013. Neural Response Phase Tracks How Listeners Learn New Acoustic Representations. Curr. Biol. 23, 968–974. doi:10.1016/j.cub.2013.04.031

Luthi, A., McCormick, D.A., 1998. Periodicity of thalamic synchronized oscillations: the role of Ca2+-mediated upregulation of Ih. Neuron 20, 553–63.

Macmillan, N.A., 2005. Detection theory: a user's guide, 2nd ed. ed. Lawrence Erlbaum Associates, Mahwah, N.J.

Magnin, M., Rey, M., Bastuji, H., Guillemant, P., Mauguiere, F., Garcia-Larrea, L., 2010. Thalamic deactivation at sleep onset precedes that of the cerebral cortex in humans. Proc. Natl. Acad. Sci. 107, 3829–3833. doi:10.1073/pnas.0909710107

Maho, C., Bloch, V., 1992. Responses of hippocampal cells can be conditioned during paradoxical sleep. Brain Res. 581, 115–122.

Maho, C., Hennevin, E., 2002. Appetitive conditioning-induced plasticity is expressed during paradoxical sleep in the medial geniculate, but not in the lateral amygdala. Behav. Neurosci. 116, 807–823. doi:10.1037/0735-7044.116.5.807

Mahowald, M., Schenck, C., 2000. REM sleep parasomnias, in: Kryger, M., Roth, T., Dement, W.C. (Eds.), Principles and Practices of Sleep Medicine. W. B. Saunders, Philadelphia, pp. 724–741.

Mahowald, M.W., Schenck, C.H., 2005. Insights from studying human sleep disorders. Nature 437, 1279–85. doi:10.1038/nature04287

Mak-McCully, R.A., Rosen, B.Q., Rolland, M., Régis, J., Bartolomei, F., Rey, M., Chauvel, P., Cash, S.S., Halgren, E., 2015. Distribution, Amplitude, Incidence, Co-Occurrence, and

Propagation of Human K-Complexes in Focal Transcortical Recordings(1,2,3). eNeuro 2. doi:10.1523/ENEURO.0028-15.2015

Malmberg, K.J., 2008. Recognition memory: A review of the critical findings and an integrated theory for relating them. Cognit. Psychol. 57, 335–384. doi:10.1016/j.cogpsych.2008.02.004

Malow, B.A., Carney, P.R., Kushwaha, R., Bowes, R.J., 1999. Hippocampal sleep spindles revisited: physiologic or epileptic activity? Clin Neurophysiol 110, 687–93.

Manns, J.R., Hopkins, R.O., Reed, J.M., Kitchener, E.G., Squire, L.R., 2003. Recognition Memory and the Human Hippocampus. Neuron 37, 171–180. doi:10.1016/S0896-6273(02)01147-9

Maquet, P., 2000. Functional neuroimaging of normal human sleep by positron emission tomography. J Sleep Res 9, 207–31. doi:jsr214 [pii]

Maquet, P., 1995. Sleep function(s) and cerebral metabolism. Behav Brain Res 69, 75–83.

Maret, S., Faraguna, U., Nelson, A.B., Cirelli, C., Tononi, G., 2011. Sleep and waking modulate spine turnover in the adolescent mouse cortex. Nat. Neurosci. 14, 1418–1420. doi:10.1038/nn.2934

Marg, E., 1951. Development of electro-oculography; standing potential of the eye in registration of eye movement. AMA Arch. Ophthalmol. 45, 169–185.

Marini, G., Macchi, G., Mancia, M., 1992. Potentiation of electroencephalographic spindles by ibotenate microinjections into nucleus reticularis thalami of cats. Neuroscience 51, 759–62.

Maris, E., Oostenveld, R., 2007. Nonparametric statistical testing of EEG- and MEG-data. J. Neurosci. Methods 164, 177–190. doi:10.1016/j.jneumeth.2007.03.024

Marrosu, F., Portas, C., Mascia, M.S., Casu, M.A., Fà, M., Giagheddu, M., Imperato, A., Gessa, G.L., 1995. Microdialysis measurement of cortical and hippocampal acetylcholine release during sleep-wake cycle in freely moving cats. Brain Res. 671, 329–332.

Marshall, L., Helgadóttir, H., Mölle, M., Born, J., 2006. Boosting slow oscillations during sleep potentiates memory. Nature 444, 610–613. doi:10.1038/nature05278

Masaki, H., Wild-Wall, N., Sangals, J., Sommer, W., 2004. The functional locus of the lateralized readiness potential. Psychophysiology 41, 220–230. doi:10.1111/j.1469-8986.2004.00150.x

Masquelier, T., Guyonneau, R., Thorpe, S.J., 2008. Spike Timing Dependent Plasticity Finds the Start of Repeating Patterns in Continuous Spike Trains. PLoS ONE 3, e1377. doi:10.1371/journal.pone.0001377

Massimini, M., Boly, M., Casali, A., Rosanova, M., Tononi, G., 2009a. A perturbational approach for evaluating the brain's capacity for consciousness. Prog Brain Res 177, 201–14. doi:10.1016/S0079-6123(09)17714-2

Massimini, M., Ferrarelli, F., Huber, R., Esser, S.K., Singh, H., Tononi, G., 2005. Breakdown of cortical effective connectivity during sleep. Science 309, 2228–2232. doi:10.1126/science.1117256

Massimini, M., Ferrarelli, F., Murphy, M.J., Huber, R., Riedner, B.A., Casarotto, S., Tononi, G., 2010. Cortical reactivity and effective connectivity during REM sleep in humans. Cogn. Neurosci. 1, 176–183. doi:10.1080/17588921003731578

Massimini, M., Ferrarelli, F., Sarasso, S., Tononi, G., 2012. Cortical mechanisms of loss of consciousness: insight from TMS/EEG studies. Arch. Ital. Biol. 150, 44–55.

Massimini, M., Huber, R., Ferrarelli, F., Hill, S., Tononi, G., 2004. The sleep slow oscillation as a traveling wave. J. Neurosci. Off. J. Soc. Neurosci. 24, 6862–6870. doi:10.1523/JNEUROSCI.1318-04.2004

Massimini, M., Tononi, G., Huber, R., 2009b. Slow waves, synaptic plasticity and information processing: insights from transcranial magnetic stimulation and high-density EEG experiments. Eur J Neurosci 29, 1761–70. doi:10.1111/j.1460-9568.2009.06720.x

Mayers, A.G., Baldwin, D.S., 2005. Antidepressants and their effect on sleep. Hum. Psychopharmacol. 20, 533–559. doi:10.1002/hup.726

Mayford, M., Siegelbaum, S.A., Kandel, E.R., 2012. Synapses and Memory Storage. Cold Spring Harb. Perspect. Biol. 4, a005751–a005751. doi:10.1101/cshperspect.a005751

Mazza, S., Perchet, C., Frot, M., Michael, G.A., Magnin, M., Garcia-Larrea, L., Bastuji, H., 2014. Asleep but aware? Brain Cogn. 87, 7–15. doi:10.1016/j.bandc.2014.02.007

McCarley, R.W., 2007. Neurobiology of REM and NREM sleep. Sleep Med. 8, 302–30. doi:10.1016/j.sleep.2007.03.005

Mccarley, R.W., Winkelman, J.W., Duffy, F.H., 1983. Human Cerebral Potentials Associated with Rem-Sleep Rapid Eye-Movements - Links to Pgo Waves and Waking Potentials. Brain Res. 274, 359–364.

McCormick, D.A., Bal, T., 1997. Sleep and arousal: thalamocortical mechanisms. Annu Rev Neurosci 20, 185–215. doi:10.1146/annurev.neuro.20.1.185

McCormick, D.A., Bal, T., 1994. Sensory gating mechanisms of the thalamus. Curr Opin Neurobiol 4, 550–6.

McCormick, D.A., Pape, H.C., 1990. Properties of a hyperpolarization-activated cation current and its role in rhythmic oscillation in thalamic relay neurones. J Physiol 431, 291–318.

McDermott, J.H., Schemitsch, M., Simoncelli, E.P., 2013. Summary statistics in auditory perception. Nat. Neurosci. 16, 493–498. doi:10.1038/nn.3347

McDonald, A.J., 1998. Cortical pathways to the mammalian amygdala. Prog Neurobiol 55, 257–332. doi:S0301-0082(98)00003-3 [pii]

McGeoch, J.A., 1932. Forgetting and the law of disuse. Psychol. Rev. 39, 352–370. doi:10.1037/h0069819

Mednick, S.C., Cai, D.J., Shuman, T., Anagnostaras, S., Wixted, J.T., 2011. An opportunistic theory of cellular and systems consolidation. Trends Neurosci. 34, 504–514. doi:10.1016/j.tins.2011.06.003

Menicucci, D., Piarulli, A., Allegrini, P., Laurino, M., Mastorci, F., Sebastiani, L., Bedini, R., Gemignani, A., 2013. Fragments of wake-like activity frame down-states of sleep slow oscillations in humans: New vistas for studying homeostatic processes during sleep. Int. J. Psychophysiol. 89, 151–157. doi:10.1016/j.ijpsycho.2013.01.014

Mesgarani, N., Chang, E.F., 2012. Selective cortical representation of attended speaker in multi-talker speech perception. Nature 485, 233–236. doi:10.1038/nature11020

Mesgarani, N., David, S.V., Fritz, J.B., Shamma, S.A., 2009. Influence of context and behavior on stimulus reconstruction from neural activity in primary auditory cortex. J. Neurophysiol. 102, 3329–3339. doi:10.1152/jn.91128.2008

Miyauchi, S., Misaki, M., Kan, S., Fukunaga, T., Koike, T., 2009. Human brain activity time-locked to rapid eye movements during REM sleep. Exp Brain Res 192, 657–67. doi:10.1007/s00221-008-1579-2

Miyauchi, S., Takino, R., Fukuda, H., Torii, S., 1987. Electrophysiological evidence for dreaming: human cerebral potentials associated with rapid eye movement during REM sleep. Electroencephalogr Clin Neurophysiol 66, 383–90.

Mizrahi, A., Shalev, A., Nelken, I., 2014. Single neuron and population coding of natural sounds in auditory cortex. Curr. Opin. Neurobiol. 24, 103–110. doi:10.1016/j.conb.2013.09.007

Mohajerani, M.H., McVea, D.A., Fingas, M., Murphy, T.H., 2010. Mirrored bilateral slow-wave cortical activity within local circuits revealed by fast bihemispheric voltage-sensitive dye imaging in anesthetized and awake mice. J Neurosci 30, 3745–51. doi:10.1523/JNEUROSCI.6437-09.2010

Molinari, S., Foulkes, D., 1969. Tonic and phasic events during sleep: psychological correlates and implications. Percept. Mot. Skills 29, 343–368. doi:10.2466/pms.1969.29.2.343

Mölle, M., Born, J., 2011. Slow oscillations orchestrating fast oscillations and memory consolidation. Prog. Brain Res. 193, 93–110. doi:10.1016/B978-0-444-53839-0.00007-7

Molle, M., Marshall, L., Gais, S., Born, J., 2002. Grouping of spindle activity during slow oscillations in human non-rapid eye movement sleep. J Neurosci 22, 10941–7.

Molle, M., Yeshenko, O., Marshall, L., Sara, S.J., Born, J., 2006. Hippocampal sharp wave-ripples linked to slow oscillations in rat slow-wave sleep. J Neurophysiol 96, 62–70. doi:10.1152/jn.00014.2006

Morison, R.S., Bassett, D.I., 1945. Electrical activity of the thalamus and basal ganglia in decorticated cats. J Neurophysiol 8, 309–314.

Mormann, F., Kornblith, S., Quiroga, R.Q., Kraskov, A., Cerf, M., Fried, I., Koch, C., 2008. Latency and selectivity of single neurons indicate hierarchical processing in the human medial temporal lobe. J Neurosci 28, 8865–72. doi:10.1523/JNEUROSCI.1640-08.2008

Moser, M.-B., 2014. Grid Cells, Place Cells and Memory.

Mouret, J., Jeannerod, M., Jouvet, M., 1963. [Electrical activity of the visual system during the paradoxical phase of sleep in the cat.]. J Physiol Paris 55, 305–6.

Mudrik, L., Faivre, N., Koch, C., 2014. Information integration without awareness. Trends Cogn. Sci. 18, 488–496. doi:10.1016/j.tics.2014.04.009

Mukhametov, L.M., Supin, A.Y., Polyakova, I.G., 1977. Interhemispheric asymmetry of the electroencephalographic sleep patterns in dolphins. Brain Res 134, 581–4. doi:0006-8993(77)90835-6 [pii]

Murphy, M., Riedner, B.A., Huber, R., Massimini, M., Ferrarelli, F., Tononi, G., 2009. Source modeling sleep slow waves. Proc Natl Acad Sci U A 106, 1608–13. doi:10.1073/pnas.0807933106

Muzur, A., Pace-Schott, E.F., Hobson, J.A., 2002. The prefrontal cortex in sleep. Trends Cogn. Sci. 6, 475–481.

Näätänen, R., Jacobsen, T., Winkler, I., 2005. Memory-based or afferent processes in mismatch negativity (MMN): a review of the evidence. Psychophysiology 42, 25–32. doi:10.1111/j.1469-8986.2005.00256.x

Näätänen, R., Picton, T., 1987. The N1 Wave of the Human Electric and Magnetic Response to Sound: A Review and an Analysis of the Component Structure. Psychophysiology 24, 375–425. doi:10.1111/j.1469-8986.1987.tb00311.x

Nakabayashi, T., Uchida, S., Maehara, T., Hirai, N., Nakamura, M., Arakaki, H., Shimisu, H., Okubo, Y., 2001. Absence of sleep spindles in human medial and basal temporal lobes. Psychiatry Clin Neurosci 55, 57–65.

Nakamura, K., Colby, C.L., 2000. Visual, saccade-related, and cognitive activation of single neurons in monkey extrastriate area V3A. J. Neurophysiol. 84, 677–692.

Nakamura, M., Uchida, S., Maehara, T., Kawai, K., Hirai, N., Nakabayashi, T., Arakaki, H., Okubo, Y., Nishikawa, T., Shimizu, H., 2003. Sleep spindles in human prefrontal cortex: an electrocorticographic study. Neurosci Res 45, 419–27.

Nere, A.T., Hashmi, A., Cirelli, C., Tononi, G., 2013. Sleep-dependent synaptic down-selection (I): modeling the benefits of sleep on memory consolidation and integration. Sleep Chronobiol. 4, 143. doi:10.3389/fneur.2013.00143

New, B., Pallier, C., Brysbaert, M., Ferrand, L., 2004. Lexique 2: a new French lexical database. Behav. Res. Methods Instrum. Comput. J. Psychon. Soc. Inc 36, 516–524.

Ngo, H.-V.V., Martinetz, T., Born, J., Mölle, M., 2013. Auditory Closed-Loop Stimulation of the Sleep Slow Oscillation Enhances Memory. Neuron 78, 545–553. doi:10.1016/j.neuron.2013.03.006

Nir, Y., Le Van Quyen, M., Tononi, G., Staba, R., 2014. , in: Kreiman, G., Cerf, M., Rutishauser, U., Fried, I. (Eds.), Single Unit Studies of the Human Brain. MIT Press.

Nir, Y., Massimini, M., Boly, M., Tononi, G., 2013. Sleep and Consciousness, in: Cavanna, A.E., Nani, A., Blumenfeld, H., Laureys, S. (Eds.), Neuroimaging of Consciousness. Springer Berlin Heidelberg, Berlin, Heidelberg, pp. 133–182.

Nir, Y., Mukamel, R., Dinstein, I., Privman, E., Harel, M., Fisch, L., Gelbard-Sagiv, H., Kipervasser, S., Andelman, F., Neufeld, M.Y., Kramer, U., Arieli, A., Fried, I., Malach, R., 2008. Interhemispheric correlations of slow spontaneous neuronal fluctuations revealed in human sensory cortex. Nat Neurosci 11, 1100–8.

Nir, Y., Staba, R., Andrillon, T., Vyazovskiy, V.V., Cirelli, C., Fried, I., Tononi, G., 2011. Regional slow waves and spindles in human sleep. Neuron 70, 153–69. doi:10.1016/j.neuron.2011.02.043

Nir, Y., Tononi, G., 2010. Dreaming and the brain: from phenomenology to neurophysiology. Trends Cogn Sci 14, 88–100.

Nir, Y., Vyazovskiy, V.V., Cirelli, C., Banks, M.I., Tononi, G., 2013. Auditory Responses and Stimulus-Specific Adaptation in Rat Auditory Cortex are Preserved Across NREM and REM Sleep. Cereb. Cortex. doi:10.1093/cercor/bht328

Nishida, M., Walker, M.P., 2007. Daytime naps, motor memory consolidation and regionally specific sleep spindles. PLoS One 2, e341. doi:10.1371/journal.pone.0000341

Nobili, L., De Gennaro, L., Proserpio, P., Moroni, F., Sarasso, S., Pigorini, A., De Carli, F., Ferrara, M., 2012. Local aspects of sleep, in: Progress in Brain Research. Elsevier, pp. 219–232.

Nobili, L., Ferrara, M., Moroni, F., De Gennaro, L., Russo, G.L., Campus, C., Cardinale, F., De Carli, F., 2011. Dissociated wake-like and sleep-like electro-cortical activity during sleep. NeuroImage 58, 612–619. doi:10.1016/j.neuroimage.2011.06.032

Noda, H., Adey, W.R., 1970. Firing of neuron pairs in cat association cortex during sleep and wakefulness. J Neurophysiol 33, 672–84.

Nordby, H., Hugdahl, K., Stickgold, R., Bronnick, K.S., Hobson, J.A., 1996. Event-related potentials (ERPs) to deviant auditory stimuli during sleep and waking. Neuroreport 7, 1082–6.

Nunez, A., Curro Dossi, R., Contreras, D., Steriade, M., 1992. Intracellular evidence for incompatibility between spindle and delta oscillations in thalamocortical neurons of cat. Neuroscience 48, 75–85.

Obin, N., 2011. MeLos: Analysis and Modelling of Speech Prosody and Speaking Style. Université Pierre et Marie Curie - Paris VI.

Ogilvie, R.D., 2001. The process of falling asleep. Sleep Med. Rev. 5, 247–270. doi:10.1053/smrv.2001.0145

Olcese, U., Esser, S.K., Tononi, G., 2010. Sleep and synaptic renormalization: a computational study. J. Neurophysiol. 104, 3476–3493. doi:10.1152/jn.00593.2010

Oostenveld, R., Fries, P., Maris, E., Schoffelen, J.-M., 2011. FieldTrip: Open source software for advanced analysis of MEG, EEG, and invasive electrophysiological data. Comput. Intell. Neurosci. 2011, 156869. doi:10.1155/2011/156869

Orzeł-Gryglewska, J., 2010. Consequences of sleep deprivation. Int. J. Occup. Med. Environ. Health 23. doi:10.2478/v10001-010-0004-9

O'Sullivan, J.A., Power, A.J., Mesgarani, N., Rajaram, S., Foxe, J.J., Shinn-Cunningham, B.G., Slaney, M., Shamma, S.A., Lalor, E.C., 2014. Attentional Selection in a Cocktail Party Environment Can Be Decoded from Single-Trial EEG. Cereb. Cortex. doi:10.1093/cercor/bht355

Oswald, I., Taylor, A.M., Treisman, M., 1960. Discriminative responses to stimulation during human sleep. Brain 83, 440–53.

O'Toole, A.J., Kersten, D.J., 1992. Learning to see random-dot stereograms. Perception 21, 227–243.

Oudiette, D., Antony, J.W., Creery, J.D., Paller, K.A., 2013. The Role of Memory Reactivation during Wakefulness and Sleep in Determining Which Memories Endure. J. Neurosci. 33, 6672–6678. doi:10.1523/JNEUROSCI.5497-12.2013

Oudiette, D., Constantinescu, I., Leclair-Visonneau, L., Vidailhet, M., Schwartz, S., Arnulf, I., 2011. Evidence for the re-enactment of a recently learned behavior during sleepwalking. PloS One 6, e18056. doi:10.1371/journal.pone.0018056

Oudiette, D., Paller, K.A., 2013. Upgrading the sleeping brain with targeted memory reactivation. Trends Cogn. Sci. 17, 142–149. doi:10.1016/j.tics.2013.01.006

Pare, D., Collins, D.R., Pelletier, J.G., 2002. Amygdala oscillations and the consolidation of emotional memories. Trends Cogn Sci 6, 306–314.

Pare, D., Steriade, M., Deschenes, M., Oakson, G., 1987. Physiological characteristics of anterior thalamic nuclei, a group devoid of inputs from reticular thalamic nucleus. J Neurophysiol 57, 1669–85.

Pasley, B.N., David, S.V., Mesgarani, N., Flinker, A., Shamma, S.A., Crone, N.E., Knight, R.T., Chang, E.F., 2012. Reconstructing Speech from Human Auditory Cortex. PLoS Biol. 10, e1001251. doi:10.1371/journal.pbio.1001251

Patil, K., Pressnitzer, D., Shamma, S., Elhilali, M., 2012. Music in our ears: the biological bases of musical timbre perception. PLoS Comput. Biol. 8, e1002759. doi:10.1371/journal.pcbi.1002759

Pawlak, V., 2010. Timing is not everything: neuromodulation opens the STDP gate. Front. Synaptic Neurosci. 2. doi:10.3389/fnsyn.2010.00146

Peigneux, P., Laureys, S., Delbeuck, X., Maquet, P., 2001. Sleeping brain, learning brain. The role of sleep for memory systems. Neuroreport 12, A111–124.

Peigneux, P., Laureys, S., Fuchs, S., Delbeuck, X., Degueldre, C., Aerts, J., Delfiore, G., Luxen, A., Maquet, P., 2001. Generation of rapid eye movements during paradoxical sleep in humans. Neuroimage 14, 701–8. doi:10.1006/nimg.2001.0874

Peña, J.L., Pérez-Perera, L., Bouvier, M., Velluti, R.A., 1999. Sleep and wakefulness modulation of the neuronal firing in the auditory cortex of the guinea pig. Brain Res. 816, 463–470.

Perlis, M.L., Giles, D.E., Mendelson, W.B., Bootzin, R.R., Wyatt, J.K., 1997. Psychophysiological insomnia: the behavioural model and a neurocognitive perspective. J. Sleep Res. 6, 179–188.

Perogamvros, L., Schwartz, S., 2013. Sleep and Emotional Functions, in: Meerlo, P., Benca, R.M., Abel, T. (Eds.), Sleep, Neuronal Plasticity and Brain Function. Springer Berlin Heidelberg, Berlin, Heidelberg, pp. 411–431.

Perrett, S.P., Dudek, S.M., Eagleman, D., Montague, P.R., Friedlander, M.J., 2001. LTD induction in adult visual cortex: role of stimulus timing and inhibition. J. Neurosci. Off. J. Soc. Neurosci. 21, 2308–2319.

Perrin, F., Garcia-Larrea, L., Mauguiere, F., Bastuji, H., 1999. A differential brain response to the subject's own name persists during sleep. Clin Neurophysiol 110, 2153–64.

Peter-Derex, L., Magnin, M., Bastuji, H., 2015. Heterogeneity of arousals in human sleep: A stereo-electroencephalographic study. NeuroImage. doi:10.1016/j.neuroimage.2015.07.057

Peyrache, A., Battaglia, F.P., Destexhe, A., 2011. Inhibition recruitment in prefrontal cortex during sleep spindles and gating of hippocampal inputs. Proc. Natl. Acad. Sci. 108, 17207–17212. doi:10.1073/pnas.1103612108

Picton, T.W., 2011. Late Auditory Potentials: Changing the Things Which Are, in: Human Auditory Evoked Potentials. Plural Pub., pp. 335–398.

Picton, T.W., 2010. Human auditory evoked potentials. Plural Pub, San Diego.

Pigorini, A., Sarasso, S., Proserpio, P., Szymanski, C., Arnulfo, G., Casarotto, S., Fecchio, M., Rosanova, M., Mariotti, M., Lo Russo, G., Palva, J.M., Nobili, L., Massimini, M., 2015. Bistability breaks-off deterministic responses to intracortical stimulation during non-REM sleep. NeuroImage 112, 105–113. doi:10.1016/j.neuroimage.2015.02.056

Plöchl, M., Ossandón, J.P., König, P., 2012. Combining EEG and eye tracking: identification, characterization, and correction of eye movement artifacts in electroencephalographic data. Front. Hum. Neurosci. 6. doi:10.3389/fnhum.2012.00278

Portas, C.M., Krakow, K., Allen, P., Josephs, O., Armony, J.L., Frith, C.D., 2000. Auditory processing across the sleep-wake cycle: simultaneous EEG and fMRI monitoring in humans. Neuron 28, 991–999.

Praamstra, P., Boutsen, L., Humphreys, G.W., 2005. Frontoparietal control of spatial attention and motor intention in human EEG. J. Neurophysiol. 94, 764–774. doi:10.1152/jn.01052.2004

Pulvermüller, F., Kujala, T., Shtyrov, Y., Simola, J., Tiitinen, H., Alku, P., Alho, K., Martinkauppi, S., Ilmoniemi, R.J., Näätänen, R., 2001. Memory Traces for Words as Revealed by the Mismatch Negativity. NeuroImage 14, 607–616. doi:10.1006/nimg.2001.0864

Purpura, K.P., Kalik, S.F., Schiff, N.D., 2003. Analysis of perisaccadic field potentials in the occipitotemporal pathway during active vision. J. Neurophysiol. 90, 3455–3478. doi:10.1152/jn.00011.2003

Quian Quiroga, R., Nadasdy, Z., Ben-Shaul, Y., 2004. Unsupervised spike sorting with wavelets and superparamagnetic clustering. Neural Comput. 16, 1661–1687.

Quiroga, R.Q., Nadasdy, Z., Ben-Shaul, Y., 2004. Unsupervised spike detection and sorting with wavelets and superparamagnetic clustering. Neural Comput 16, 1661–87. doi:10.1162/089976604774201631

Quiroga, R.Q., Reddy, L., Kreiman, G., Koch, C., Fried, I., 2005. Invariant visual representation by single neurons in the human brain. Nature 435, 1102–1107. doi:10.1038/Nature03687

Rajkai, C., Lakatos, P., Chen, C.-M., Pincze, Z., Karmos, G., Schroeder, C.E., 2008. Transient Cortical Excitation at the Onset of Visual Fixation. Cereb. Cortex 18, 200–209. doi:10.1093/cercor/bhm046

Rasch, B., Born, J., 2013. About Sleep's Role in Memory. Physiol. Rev. 93, 681–766. doi:10.1152/physrev.00032.2012

Rasch, B., Born, J., 2007. Maintaining memories by reactivation. Curr. Opin. Neurobiol. 17, 698–703. doi:10.1016/j.conb.2007.11.007

Rasmusson, D.D., 2000. The role of acetylcholine in cortical synaptic plasticity. Behav. Brain Res. 115, 205–218.

Rattenborg, N.., Amlaner, C.., Lima, S.., 2000. Behavioral, neurophysiological and evolutionary perspectives on unihemispheric sleep. Neurosci. Biobehav. Rev. 24, 817–842. doi:10.1016/S0149-7634(00)00039-7

Rattenborg, N.C., Amlaner, C.J., Lima, S.L., 2001. Unilateral eye closure and interhemispheric EEG asymmetry during sleep in the pigeon (Columba livia). Brain Behav Evol 58, 323–32. doi:bbe58323 [pii]

Rechtschaffen, A., Hauri, P., Zeitlin, M., 1966. Auditory Awakening Thresholds in REM and NREM Sleep Stages. Percept. Mot. Skills 22, 927–942. doi:10.2466/pms.1966.22.3.927

Reed, J.M., Squire, L.R., 1997. Impaired recognition memory in patients with lesions limited to the hippocampal formation. Behav. Neurosci. 111, 667–675. doi:10.1037/0735-7044.111.4.667

Rees, G., Kreiman, G., Koch, C., 2002. Neural correlates of consciousness in humans. Nat Rev Neurosci 3, 261–70. doi:10.1038/nrn783

Reppas, J.B., Usrey, W.M., Reid, R.C., 2002. Saccadic eye movements modulate visual responses in the lateral geniculate nucleus. Neuron 35, 961–974.

Ribeiro, S., 2004. Reverberation, storage, and postsynaptic propagation of memories during sleep. Learn. Mem. 11, 686–696. doi:10.1101/lm.75604

Ribeiro, S., Mello, C.V., Velho, T., Gardner, T.J., Jarvis, E.D., Pavlides, C., 2002. Induction of hippocampal long-term potentiation during waking leads to increased extrahippocampal zif-268 expression during ensuing rapid-eye-movement sleep. J. Neurosci. Off. J. Soc. Neurosci. 22, 10914–10923.

Riedner, B.A., Vyazovskiy, V.V., Huber, R., Massimini, M., Esser, S., Murphy, M., Tononi, G., 2007. Sleep homeostasis and cortical synchronization: III. A high-density EEG study of sleep slow waves in humans. Sleep 30, 1643–57.

Riekkinen, P., Buzsaki, G., Riekkinen, P., Soininen, H., Partanen, J., 1991. The cholinergic system and EEG slow waves. Electroencephalogr. Clin. Neurophysiol. 78, 89–96. doi:10.1016/0013-4694(91)90107-F

Riemann, D., Spiegelhalder, K., Feige, B., Voderholzer, U., Berger, M., Perlis, M., Nissen, C., 2010. The hyperarousal model of insomnia: a review of the concept and its evidence. Sleep Med. Rev. 14, 19–31. doi:10.1016/j.smrv.2009.04.002

Ringo, J.L., Sobotka, S., Diltz, M.D., Bunce, C.M., 1994. Eye movements modulate activity in hippocampal, parahippocampal, and inferotemporal neurons. J.Neurophysiol. 71, 1285–1288.

Robertson, E.M., 2009. From Creation to Consolidation: A Novel Framework for Memory Processing. PLoS Biol. 7, e1000019. doi:10.1371/journal.pbio.1000019

Robinson, D.A., 1963. A METHOD OF MEASURING EYE MOVEMENT USING A SCLERAL SEARCH COIL IN A MAGNETIC FIELD. IEEE Trans. Biomed. Eng. 10, 137–145.

Roebel, A., 2010. A shape-invariant phase vocoder for speech transformation, in: Digital Audio Effects (DAFx). pp. 1–1.

Roffwarg, H.P., Dement, W.C., Muzio, J.N., Fisher, C., 1962. Dream imagery: relationship to rapid eye movements of sleep. Arch Gen Psychiatry 7, 235–58.

Rosanova, M., 2005. Pattern-Specific Associative Long-Term Potentiation Induced by a Sleep Spindle-Related Spike Train. J. Neurosci. 25, 9398–9405. doi:10.1523/JNEUROSCI.2149-05.2005

Rosenthal, C.R., Kennard, C., Soto, D., 2010. Visuospatial Sequence Learning without Seeing. PLoS ONE 5, e11906. doi:10.1371/journal.pone.0011906

Ross, B., Jamali, S., Tremblay, K.L., 2013. Plasticity in neuromagnetic cortical responses suggests enhanced auditory object representation. BMC Neurosci. 14, 151. doi:10.1186/1471-2202-14-151

Rotello, C.M., Macmillan, N.A., Reeder, J.A., 2004. Sum-Difference Theory of Remembering and Knowing: A Two-Dimensional Signal-Detection Model. Psychol. Rev. 111, 588–616. doi:10.1037/0033-295X.111.3.588

Rubio-Garrido, P., Perez-de-Manzo, F., Porrero, C., Galazo, M.J., Clasca, F., 2009. Thalamic input to distal apical dendrites in neocortical layer 1 is massive and highly convergent. Cereb Cortex 19, 2380–95. doi:10.1093/cercor/bhn259

Ruby, P., Caclin, A., Boulet, S., Delpuech, C., Morlet, D., 2008. Odd Sound Processing in the Sleeping Brain. J. Cogn. Neurosci. 20, 296–311. doi:10.1162/jocn.2008.20023

Rugg, M.D., Mark, R.E., Walla, P., Schloerscheidt, A.M., Birch, C.S., Allan, K., 1998. Dissociation of the neural correlates of implicit and explicit memory. Nature 392, 595–598. doi:10.1038/33396

Rutishauser, U., Ross, I.B., Mamelak, A.N., Schuman, E.M., 2010. Human memory strength is predicted by theta-frequency phase-locking of single neurons. Nature 464, 903–907. doi:10.1038/nature08860

Sallinen, M., Kaartinen, J., Lyytinen, H., 1996. Processing of auditory stimuli during tonic and phasic periods of REM sleep as revealed by event-related brain potentials. J. Sleep Res. 5, 220–228. doi:10.1111/j.1365-2869.1996.00220.x

Sanchez-Vives, M.V., Mattia, M., Compte, A., Perez-Zabalza, M., Winograd, M., Descalzo, V.F., Reig, R., 2010. Inhibitory Modulation of Cortical Up States. J. Neurophysiol. 104, 1314–1324. doi:10.1152/jn.00178.2010

Sanchez-Vives, M.V., McCormick, D.A., 2000. Cellular and network mechanisms of rhythmic recurrent activity in neocortex. Nat Neurosci 3, 1027–34. doi:10.1038/79848

Sanders, R.D., Tononi, G., Laureys, S., Sleigh, J., 2012. Unresponsiveness not equal Unconsciousness. Anesthesiology.

Sanford, L.D., Silvestri, A.J., Ross, R.J., Morrison, A.R., 2001. Influence of fear conditioning on elicited ponto-geniculo-occipital waves and rapid eye movement sleep. Arch. Ital. Biol. 139, 169–183.

Sara, S.J., 2009. The locus coeruleus and noradrenergic modulation of cognition. Nat Rev Neurosci 10, 211–23.

Sarasso, S., Boly, M., Napolitani, M., Gosseries, O., Charland-Verville, V., Casarotto, S., Rosanova, M., Casali, A.G., Brichant, J.-F., Boveroux, P., Rex, S., Tononi, G., Laureys, S., Massimini, M., 2015. Consciousness and Complexity during Unresponsiveness Induced by Propofol, Xenon, and Ketamine. Curr. Biol. 25, 3099–3105. doi:10.1016/j.cub.2015.10.014

Sarasso, S., Proserpio, P., Pigorini, A., Moroni, F., Ferrara, M., De Gennaro, L., De Carli, F., Lo Russo, G., Massimini, M., Nobili, L., 2014. Hippocampal sleep spindles preceding neocortical sleep onset in humans. NeuroImage 86, 425–432. doi:10.1016/j.neuroimage.2013.10.031

Schabus, M., Dang-Vu, T.T., Albouy, G., Balteau, E., Boly, M., Carrier, J., Darsaud, A., Degueldre, C., Desseilles, M., Gais, S., Phillips, C., Rauchs, G., Schnakers, C., Sterpenich, V., Vandewalle, G., Luxen, A., Maquet, P., 2007. Hemodynamic cerebral correlates of sleep spindles during human non-rapid eye movement sleep. Proc Natl Acad Sci U A 104, 13164–9. doi:10.1073/pnas.0703084104

Schabus, M., Dang-Vu, T.T., Heib, D.P.J., Boly, M., Desseilles, M., Vandewalle, G., Schmidt, C., Albouy, G., Darsaud, A., Gais, S., Degueldre, C., Balteau, E., Phillips, C., Luxen, A., Maquet, P., 2012. The Fate of Incoming Stimuli during NREM Sleep is Determined by Spindles and the Phase of the Slow Oscillation. Front. Neurol. 3. doi:10.3389/fneur.2012.00040

Schabus, M., Gruber, G., Parapatics, S., Sauter, C., Klosch, G., Anderer, P., Klimesch, W., Saletu, B., Zeitlhofer, J., 2004. Sleep spindles and their significance for declarative memory consolidation. Sleep 27, 1479–85.

Schartner, M., Seth, A., Noirhomme, Q., Boly, M., Bruno, M.-A., Laureys, S., Barrett, A., 2015. Complexity of Multi-Dimensional Spontaneous EEG Decreases during Propofol Induced General Anaesthesia. PLOS ONE 10, e0133532. doi:10.1371/journal.pone.0133532

Schenck, C.H., Arnulf, I., Mahowald, M.W., 2007. Sleep and sex: what can go wrong? A review of the literature on sleep related disorders and abnormal sexual behaviors and experiences. Sleep 30, 683–702.

Schenck, C.H., Bundlie, S.R., Ettinger, M.G., Mahowald, M.W., 1986. Chronic behavioral disorders of human REM sleep: a new category of parasomnia. Sleep 9, 293–308.

Schreiner, C.E., Polley, D.B., 2014. Auditory map plasticity: diversity in causes and consequences. Curr. Opin. Neurobiol. 24, 143–156. doi:10.1016/j.conb.2013.11.009

Schreiner, T., Lehmann, M., Rasch, B., 2015. Auditory feedback blocks memory benefits of cueing during sleep. Nat. Commun. 6, 8729. doi:10.1038/ncomms9729

Schwartz, J., Roth, T., 2008. Neurophysiology of Sleep and Wakefulness: Basic Science and Clinical Implications. Curr. Neuropharmacol. 6, 367–378. doi:10.2174/157015908787386050

Scott, R.B., Dienes, Z., Barrett, A.B., Bor, D., Seth, A.K., 2014. Blind insight: metacognitive discrimination despite chance task performance. Psychol. Sci. 25, 2199–2208. doi:10.1177/0956797614553944

Sculthorpe, L.D., Ouellet, D.R., Campbell, K.B., 2009. MMN elicitation during natural sleep to violations of an auditory pattern. Brain Res 1290, 52–62.

Sela, Y., Vyazovskiy, V.V., Cirelli, C., Tononi, G., Nir, Y., 2016. Responses in Rat Core Auditory Cortex are Preserved during Sleep Spindle Oscillations. Sleep.

Seol, G.H., Ziburkus, J., Huang, S., Song, L., Kim, I.T., Takamiya, K., Huganir, R.L., Lee, H.-K., Kirkwood, A., 2007. Neuromodulators Control the Polarity of Spike-Timing-Dependent Synaptic Plasticity. Neuron 55, 919–929. doi:10.1016/j.neuron.2007.08.013

Siapas, A.G., Lubenov, E.V., Wilson, M.A., 2005. Prefrontal phase locking to hippocampal theta oscillations. Neuron 46, 141–51. doi:10.1016/j.neuron.2005.02.028

Siclari, F., Bernardi, G., Riedner, B.A., LaRocque, J.J., Benca, R.M., Tononi, G., 2014a. Two Distinct Synchronization Processes in the Transition to Sleep: A High-Density Electroencephalographic Study. SLEEP. doi:10.5665/sleep.4070

Siclari, F., LaRocque, J.J., Bernardi, G., Postle, B.R., Tononi, G., 2014b. The neural correlates of consciousness in sleep: a no-task, within-state paradigm. bioRxiv. doi:10.1101/012443

Siclari, F., Larocque, J.J., Postle, B.R., Tononi, G., 2013. Assessing sleep consciousness within subjects using a serial awakening paradigm. Front. Psychol. 4, 542. doi:10.3389/fpsyg.2013.00542

Siegel, J.M., 2009. Sleep viewed as a state of adaptive inactivity. Nat Rev Neurosci 10, 747–53. doi:10.1038/nrn2697

Siegel, J.M., 2004. The neurotransmitters of sleep. J. Clin. Psychiatry 65 Suppl 16, 4–7.

Simon, C.W., Emmons, W.H., 1956. Responses to material presented during various levels of sleep. J. Exp. Psychol. 51, 89–97. doi:10.1037/h0043637

Sirota, A., Buzsaki, G., 2005. Interaction between neocortical and hippocampal networks via slow oscillations. Thalamus Relat Syst 3, 245–259. doi:10.1017/S1472928807000258

Sirota, A., Csicsvari, J., Buhl, D., Buzsaki, G., 2003. Communication between neocortex and hippocampus during sleep in rodents. Proc Natl Acad Sci U A 100, 2065–9. doi:10.1073/pnas.0437938100

Skaggs, W.E., McNaughton, B.L., 1996. Replay of neuronal firing sequences in rat hippocampus during sleep following spatial experience. Science 271, 1870–1873.

Smulders, F.T., Miller, J.O., Luck, S.J., Kappenman, E., 2012. The lateralized readiness potential. Oxf. Handb. Event-Relat. Potential Compon. 209–229.

Sobotka, S., Nowicka, A., Ringo, J.L., 1997. Activity linked to externally cued saccades in single units recorded from hippocampal, parahippocampal, and inferotemporal areas of macaques. J. Neurophysiol. 78, 2156–2163.

Sprenger, A., Lappe-Osthege, M., Talamo, S., Gais, S., Kimmig, H., Helmchen, C., 2010. Eye movements during REM sleep and imagination of visual scenes. Neuroreport 21, 45–49. doi:10.1097/Wnr.0b013e32833370b2

Squire, L.R., 2009. Encyclopedia of neuroscience. Academic Elsevier, [London].

Squire, L.R., Wixted, J.T., Clark, R.E., 2007. Recognition memory and the medial temporal lobe: a new perspective. Nat. Rev. Neurosci. 8, 872–883. doi:10.1038/nrn2154

Staba, R.J., Wilson, C.L., Bragin, A., Jhung, D., Fried, I., Engel, J., Jr., 2004. High-frequency oscillations recorded in human medial temporal lobe during sleep. Ann Neurol 56, 108–15. doi:10.1002/ana.20164

Staresina, B.P., Bergmann, T.O., Bonnefond, M., van der Meij, R., Jensen, O., Deuker, L., Elger, C.E., Axmacher, N., Fell, J., 2015. Hierarchical nesting of slow oscillations, spindles and ripples in the human hippocampus during sleep. Nat. Neurosci. 18, 1679–1686. doi:10.1038/nn.4119

Steinmann, I., Gutschalk, A., 2012. Sustained BOLD and theta activity in auditory cortex are related to slow stimulus fluctuations rather than to pitch. J. Neurophysiol. 107, 3458–3467. doi:10.1152/jn.01105.2011

Steriade, M., 2005. Sleep, epilepsy and thalamic reticular inhibitory neurons. Trends Neurosci 28, 317–24. doi:10.1016/j.tins.2005.03.007

Steriade, M., 2003. Neuronal Substrates of Sleep and Epilepsy, 1st ed. Cambridge University Press, Cambridge, UK.

Steriade, M., 2003. The corticothalamic system in sleep. Front Biosci 8, d878–99.

Steriade, M., 2000. Corticothalamic resonance, states of vigilance and mentation. Neuroscience 101, 243–76.

Steriade, M., Amzica, F., 1998. Coalescence of sleep rhythms and their chronology in corticothalamic networks. Sleep Res Online 1, 1–10.

Steriade, M., Contreras, D., Curro Dossi, R., Nunez, A., 1993a. The slow (< 1 Hz) oscillation in reticular thalamic and thalamocortical neurons: scenario of sleep rhythm generation in interacting thalamic and neocortical networks. J Neurosci 13, 3284–99.

Steriade, M., Deschenes, M., Oakson, G., 1974. Inhibitory processes and interneuronal apparatus in motor cortex during sleep and waking. I. Background firing and responsiveness of pyramidal tract neurons and interneurons. J Neurophysiol 37, 1065–92.

Steriade, M., Domich, L., Oakson, G., Deschenes, M., 1987. The deafferented reticular thalamic nucleus generates spindle rhythmicity. J Neurophysiol 57, 260–73.

Steriade, M., Nunez, A., Amzica, F., 1993b. Intracellular analysis of relations between the slow (< 1 Hz) neocortical oscillation and other sleep rhythms of the electroencephalogram. J Neurosci 13, 3266–83.

Steriade, M., Nunez, A., Amzica, F., 1993c. A novel slow (< 1 Hz) oscillation of neocortical neurons in vivo: depolarizing and hyperpolarizing components. J Neurosci 13, 3252–65.

Steriade, M., Paré, D., Datta, S., Oakson, G., Curró Dossi, R., 1990. Different cellular types in mesopontine cholinergic nuclei related to ponto-geniculo-occipital waves. J. Neurosci. Off. J. Soc. Neurosci. 10, 2560–2579.

Steriade, M., Parent, A., Hada, J., 1984. Thalamic projections of nucleus reticularis thalami of cat: a study using retrograde transport of horseradish peroxidase and fluorescent tracers. J Comp Neurol 229, 531–47. doi:10.1002/cne.902290407

Steriade, M., Timofeev, I., 2003. Neuronal plasticity in thalamocortical networks during sleep and waking oscillations. Neuron 37, 563–76.

Steriade, M., Timofeev, I., Grenier, F., 2001. Natural waking and sleep states: a view from inside neocortical neurons. J Neurophysiol 85, 1969–85.

Sterpenich, V., Albouy, G., Boly, M., Vandewalle, G., Darsaud, A., Balteau, E., Dang-Vu, T.T., Desseilles, M., D'Argembeau, A., Gais, S., Rauchs, G., Schabus, M., Degueldre, C., Luxen, A., Collette, F., Maquet, P., 2007. Sleep-related hippocampo-cortical interplay during emotional memory recollection. PLoS Biol. 5, e282. doi:10.1371/journal.pbio.0050282

Stickgold, R., Walker, M.P., 2007. Sleep-dependent memory consolidation and reconsolidation. Sleep Med 8, 331–43. doi:10.1016/j.sleep.2007.03.011

Stickgold, R., Walker, M.P., 2005. Memory consolidation and reconsolidation: what is the role of sleep? Trends Neurosci. 28, 408–415. doi:10.1016/j.tins.2005.06.004

Straube, A., Büttner, U. (Eds.), 2007. Neuro-ophthalmology: neuronal control of eye moments, Developments in ophthalmology. Karger, Basel [Switzerland] ; New York.

Strauss, M., Sitt, J.D., King, J.-R., Elbaz, M., Azizi, L., Buiatti, M., Naccache, L., van Wassenhove, V., Dehaene, S., 2015. Disruption of hierarchical predictive coding during sleep. Proc. Natl. Acad. Sci. 112, E1353–E1362. doi:10.1073/pnas.1501026112

Takahashi, K., Atsumi, Y., 1997. Precise measurement of individual rapid eye movements in REM sleep of humans. Sleep 20, 743–52.

Tanaka, H., Hayashi, M., Hori, T., 1997. Topographical characteristics and principal component structure of the hypnagogic EEG. Sleep 20, 523–534.

Tassi, P., Muzet, A., 2000. Sleep inertia. Sleep Med. Rev. 4, 341–353. doi:10.1053/smrv.2000.0098

Terzaghi, M., Sartori, I., Tassi, L., Didato, G., Rustioni, V., LoRusso, G., Manni, R., Nobili, L., 2009. Evidence of dissociated arousal states during NREM parasomnia from an intracerebral neurophysiological study. Sleep 32, 409–12.

Terzano, M.G., Mancia, D., Salati, M.R., Costani, G., Decembrino, A., Parrino, L., 1985. The cyclic alternating pattern as a physiologic component of normal NREM sleep. Sleep 8, 137–145.

Thorpe, S.J., 2011. Grandmother Cells and Distributed Representations., in: Visual Population Codes-Toward a Common Multivariate Framework for Cell Recording and Functional Imaging. Nikolaus Kriegeskorte, Gabriel Kreiman, pp. 23–51.

Thorpe, S.J., Fabre-Thorpe, M., 2001. Neuroscience. Seeking categories in the brain. Science 291, 260–263.

Timofeev, I., Grenier, F., Steriade, M., 2001. Disfacilitation and active inhibition in the neocortex during the natural sleep-wake cycle: an intracellular study. Proc Natl Acad Sci U A 98, 1924–9. doi:10.1073/pnas.041430398

Tollner, T., Rangelov, D., Muller, H.J., 2012a. How the speed of motor-response decisions, but not focal-attentional selection, differs as a function of task set and target prevalence. Proc. Natl. Acad. Sci. 109, E1990–E1999. doi:10.1073/pnas.1206382109

Tollner, T., Rangelov, D., Muller, H.J., 2012b. How the speed of motor-response decisions, but not focal-attentional selection, differs as a function of task set and target prevalence. Proc. Natl. Acad. Sci. 109, E1990–E1999. doi:10.1073/pnas.1206382109

Tononi, G., 2012. Phi: a voyage from the brain to the soul, 1st ed. ed. Pantheon, New York.

Tononi, G., Cirelli, C., 2014. Sleep and the Price of Plasticity: From Synaptic and Cellular Homeostasis to Memory Consolidation and Integration. Neuron 81, 12–34. doi:10.1016/j.neuron.2013.12.025

Tononi, G., Cirelli, C., 2012. Time to Be SHY? Some Comments on Sleep and Synaptic Homeostasis. Neural Plast. 2012, 1–12. doi:10.1155/2012/415250

Tononi, G., Cirelli, C., 2006. Sleep function and synaptic homeostasis. Sleep Med. Rev. 10, 49–62. doi:10.1016/j.smrv.2005.05.002

Tononi, G., Edelman, G.M., 1998. Consciousness and complexity. Science 282, 1846–51.

Tononi, G., Koch, C., 2015. Consciousness: here, there and everywhere? Philos. Trans. R. Soc. B Biol. Sci. 370, 20140167–20140167. doi:10.1098/rstb.2014.0167

Tononi, G., Massimini, M., 2008. Why does consciousness fade in early sleep? Ann. N. Y. Acad. Sci. 1129, 330–334. doi:10.1196/annals.1417.024

Tononi, G., Massimini, M., Riedner, B.A., 2006. Sleepy dialogues between cortex and hippocampus: who talks to whom? Neuron 52, 748–9. doi:10.1016/j.neuron.2006.11.014

Townsend, J.T., Ashby, F.G., 1978. Methods of modeling capacity in simple processing systems., in: Cognitive Theory. Erlbaum Associates, Hillsdale, NJ, pp. 200–239.

Tremblay, K.L., Ross, B., Inoue, K., McClannahan, K., Collet, G., 2014. Is the auditory evoked P2 response a biomarker of learning? Front. Syst. Neurosci. 8. doi:10.3389/fnsys.2014.00028

Tulving, E., 1985. Memory and consciousness. Can. Psychol. Can. 26, 1–12. doi:10.1037/h0080017

Uematsu, M., Matsuzaki, N., Brown, E.C., Kojima, K., Asano, E., 2013. Human occipital cortices differentially exert saccadic suppression: Intracranial recording in children. NeuroImage 83, 224–236. doi:10.1016/j.neuroimage.2013.06.046

van der Helm, E., Yao, J., Dutt, S., Rao, V., Saletin, J.M., Walker, M.P., 2011. REM Sleep Depotentiates Amygdala Activity to Previous Emotional Experiences. Curr. Biol. 21, 2029–2032. doi:10.1016/j.cub.2011.10.052

Vanderwolf, C.., 1969. Hippocampal electrical activity and voluntary movement in the rat. Electroencephalogr. Clin. Neurophysiol. 26, 407–418. doi:10.1016/0013-4694(69)90092-3

VanRullen, R., Koch, C., 2003. Is perception discrete or continuous? Trends Cogn Sci 7, 207–213.

Varghese, L., Bharadwaj, H.M., Shinn-Cunningham, B.G., 2015. Evidence against attentional state modulating scalp-recorded auditory brainstem steady-state responses. Brain Res. 1626, 146–164. doi:10.1016/j.brainres.2015.06.038

Vilberg, K.L., Rugg, M.D., 2008. Memory retrieval and the parietal cortex: a review of evidence from a dual-process perspective. Neuropsychologia 46, 1787–1799. doi:10.1016/j.neuropsychologia.2008.01.004

Volgushev, M., Chauvette, S., Mukovski, M., Timofeev, I., 2006. Precise long-range synchronization of activity and silence in neocortical neurons during slow-wave oscillations [corrected]. J Neurosci 26, 5665–72. doi:10.1523/JNEUROSCI.0279-06.2006

von Krosigk, M., Bal, T., McCormick, D.A., 1993. Cellular mechanisms of a synchronized oscillation in the thalamus. Science 261, 361–4.

Vorberg, D., Mattler, U., Heinecke, A., Schmidt, T., Schwarzbach, J., 2003. Different time courses for visual perception and action priming. Proc. Natl. Acad. Sci. U. S. A. 100, 6275–6280. doi:10.1073/pnas.0931489100

Voss, J.L., Paller, K.A., 2007. Neural correlates of conceptual implicit memory and their contamination of putative neural correlates of explicit memory. Learn. Mem. Cold Spring Harb. N 14, 259–267. doi:10.1101/lm.529807

Vyazovskiy, Faraguna, U., Cirelli, C., Tononi, G., 2009. Triggering slow waves during NREM sleep in the rat by intracortical electrical stimulation: effects of sleep/wake history and background activity. J. Neurophysiol. 101, 1921–1931. doi:10.1152/jn.91157.2008

Vyazovskiy, V., Borbely, A.A., Tobler, I., 2000. Unilateral vibrissae stimulation during waking induces interhemispheric EEG asymmetry during subsequent sleep in the rat. J Sleep Res 9, 367–71.

Vyazovskiy, V.V., Cirelli, C., Pfister-Genskow, M., Faraguna, U., Tononi, G., 2008. Molecular and electrophysiological evidence for net synaptic potentiation in wake and depression in sleep. Nat. Neurosci. 11, 200–208. doi:10.1038/nn2035

Vyazovskiy, V.V., Harris, K.D., 2013. Sleep and the single neuron: the role of global slow oscillations in individual cell rest. Nat. Rev. Neurosci. 14, 443–451. doi:10.1038/nrn3494

Vyazovskiy, V.V., Olcese, U., Hanlon, E.C., Nir, Y., Cirelli, C., Tononi, G., 2011. Local sleep in awake rats. Nature 472, 443–7. doi:10.1038/nature10009

Vyazovskiy, V.V., Olcese, U., Lazimy, Y.M., Faraguna, U., Esser, S.K., Williams, J.C., Cirelli, C., Tononi, G., 2009. Cortical firing and sleep homeostasis. Neuron 63, 865–78.

Walker, M.P., 2009. The role of sleep in cognition and emotion. Ann. N. Y. Acad. Sci. 1156, 168–197. doi:10.1111/j.1749-6632.2009.04416.x

Walker, M.P., Stickgold, R., 2006. Sleep, Memory, and Plasticity. Annu. Rev. Psychol. 57, 139–166. doi:10.1146/annurev.psych.56.091103.070307

Wang, H.X., Freeman, J., Merriam, E.P., Hasson, U., Heeger, D.J., 2012. Temporal eye movement strategies during naturalistic viewing. J. Vis. 12, 16–16. doi:10.1167/12.1.16

Watrous, A.J., Fried, I., Ekstrom, A.D., 2011. Behavioral correlates of human hippocampal delta and theta oscillations during navigation. J. Neurophysiol. 105, 1747–1755. doi:10.1152/jn.00921.2010

Wauquier, null, Aloe, null, Declerck, null, 1995. K-complexes: are they signs of arousal or sleep protective? J. Sleep Res. 4, 138–143.

Webb, W.B., 1990. Letters to the Editor. Psychol. Sci. 1, 329–329. doi:10.1111/j.1467-9280.1990.tb00229.x

Wehrle, R., Kaufmann, C., Wetter, T.C., Holsboer, F., Auer, D.P., Pollmächer, T., Czisch, M., 2007. Functional microstates within human REM sleep: first evidence from fMRI of a thalamocortical network specific for phasic REM periods: Thalamocortical network in phasic REM sleep. Eur. J. Neurosci. 25, 863–871. doi:10.1111/j.1460-9568.2007.05314.x

Wei, H.G., Riel, E., Czeisler, C.A., Dijk, D.J., 1999. Attenuated amplitude of circadian and sleep-dependent modulation of electroencephalographic sleep spindle characteristics in elderly human subjects. Neurosci Lett 260, 29–32.

Weiskrantz, L., 1990. Blindsight. Oxford University Press.

Werth, E., Achermann, P., Borbely, A.A., 1997. Fronto-occipital EEG power gradients in human sleep. J Sleep Res 6, 102–12.

Westermann, J., Lange, T., Textor, J., Born, J., 2015. System Consolidation During Sleep – A Common Principle Underlying Psychological and Immunological Memory Formation. Trends Neurosci. 38, 585–597. doi:10.1016/j.tins.2015.07.007

Wierzynski, C.M., Lubenov, E.V., Gu, M., Siapas, A.G., 2009. State-dependent spike-timing relationships between hippocampal and prefrontal circuits during sleep. Neuron 61, 587–596. doi:10.1016/j.neuron.2009.01.011

Wilson, M.A., McNaughton, B.L., 1994. Reactivation of hippocampal ensemble memories during sleep. Science 265, 676–679.

Wimmer, null, Hoffmann, null, Bonato, null, Moffitt, null, 1992. The effects of sleep deprivation on divergent thinking and attention processes. J. Sleep Res. 1, 223–230.

Wolansky, T., Clement, E.A., Peters, S.R., Palczak, M.A., Dickson, C.T., 2006. Hippocampal slow oscillation: a novel EEG state and its coordination with ongoing neocortical activity. J. Neurosci. Off. J. Soc. Neurosci. 26, 6213–6229. doi:10.1523/JNEUROSCI.5594-05.2006

Wood, JM, 1990. Implicit and explicit memory for verbal stimuli presented during sleep. The University of Arizona.

Wood, J.M., Bootzin, R.R., Kihlstrom, J.F., Schacter, D.L., 1992. Implicit and Explicit Memory for Verbal Information Presented During Sleep. Psychol. Sci. 3, 236–239. doi:10.1111/j.1467-9280.1992.tb00035.x

Wurtz, R.H., 2008. Neuronal mechanisms of visual stability. Vis. Res 48, 2070–89. doi:10.1016/j.visres.2008.03.021

Wurtz, R.H., Joiner, W.M., Berman, R.A., 2011. Neuronal mechanisms for visual stability: progress and problems. Philos Trans R Soc Lond B Biol Sci 366, 492–503. doi:10.1098/rstb.2010.0186

Wyler, A.R., Ojemann, G.A., Ward, A.A., 1982. Neurons in human epileptic cortex: correlation between unit and EEG activity. Ann. Neurol. 11, 301–308. doi:10.1002/ana.410110311

Xiang, J., Simon, J., Elhilali, M., 2010. Competing Streams at the Cocktail Party: Exploring the Mechanisms of Attention and Temporal Integration. J. Neurosci. 30, 12084–12093. doi:10.1523/JNEUROSCI.0827-10.2010

Xie, L., Kang, H., Xu, Q., Chen, M.J., Liao, Y., Thiyagarajan, M., O'Donnell, J., Christensen, D.J., Nicholson, C., Iliff, J.J., Takano, T., Deane, R., Nedergaard, M., 2013. Sleep drives metabolite clearance from the adult brain. Science 342, 373–377. doi:10.1126/science.1241224

Yamadori, A., 1971. Role of the spindles in the onset of sleep. Kobe J. Med. Sci. 17, 97–111.

Yee, R.D., Schiller, V.L., Lim, V., Baloh, F.G., Baloh, R.W., Honrubia, V., 1985. Velocities of vertical saccades with different eye movement recording methods. Invest. Ophthalmol. Vis. Sci. 26, 938–944.

Yeung, N., Bogacz, R., Holroyd, C.B., Nieuwenhuis, S., Cohen, J.D., 2007. Theta phase resetting and the error-related negativity. Psychophysiology 44. doi:10.1111/j.1469-8986.2006.00482.x

Young, L.R., Sheena, D., 1975. Survey of eye movement recording methods. Behav. Res. Methods Instrum. 7, 397–429. doi:10.3758/BF03201553

Zepelin, H., Siegel, J.M., Tobler, I., 1994. Mammalian Sleep, in: Kryger, M.H., Roth, T., Dement, W.C. (Eds.), Principles and Practice of Sleep Medicine. Saunders, London, pp. 91–100.

Zhang, D., Snyder, A.Z., Shimony, J.S., Fox, M.D., Raichle, M.E., 2009. Noninvasive functional and structural connectivity mapping of the human thalamocortical system. Cereb Cortex 20, 1187–94. doi:10.1093/cercor/bhp182

Zikopoulos, B., Barbas, H., 2007. Parallel driving and modulatory pathways link the prefrontal cortex and thalamus. PLoS One 2, e848. doi:10.1371/journal.pone.0000848

Zion Golumbic, E.M., Ding, N., Bickel, S., Lakatos, P., Schevon, C.A., McKhann, G.M., Goodman, R.R., Emerson, R., Mehta, A.D., Simon, J.Z., Poeppel, D., Schroeder, C.E., 2013. Mechanisms underlying selective neuronal tracking of attended speech at a "cocktail party." Neuron 77, 980–991. doi:10.1016/j.neuron.2012.12.037

Ziv, J., Lempel, A., 1977. A universal algorithm for sequential data compression. IEEE Trans. Inf. Theory 23, 337–343. doi:10.1109/TIT.1977.1055714

Zygierewicz, J., Blinowska, K.J., Durka, P.J., Szelenberger, W., Niemcewicz, S., Androsiuk, W., 1999. High resolution study of sleep spindles. Clin Neurophysiol 110, 2136–47.

Résumé

Tous les soirs, nous nous endormons; tous les matins, nous nous réveillons. De ce qui advient entre temps nous gardons peu de souvenirs. Les personnes qui nous entourent pourraient nous dire que nous avons bougé, parlé, ri ou crié, que les émotions les plus vives ont pris le contrôle de notre corps sans pour autant avoir laissé le moindre souvenir. Ou encore, les personnes qui nous entourent ont pu bouger, parler, rire ou crier sans que nous nous en rendîmes compte le moins du monde. Ou au contraire, nous pouvons émerger de la plus fantastique des aventures dans un lit pourtant bien calme, bercé par le calme tic-tac de l'horloge. Il semble que le sommeil opère une dissociation complète entre ce qui arrive dans notre environnement immédiat et dans notre esprit, sans pour autant que la chose éveille en nous la moindre alarme. À tout moment qui plus est, nous pouvons nous réveiller et reprendre conscience de notre environnement de façon quasi instantanée. Curieusement, il semble que certains sons aient une plus grande facilité à nous réveiller que d'autres. Sommes-nous donc complètement déconnectés de notre environnement quand nous dormons ?

Mots-Clés

Sommeil - Cognition - Perception - Apprentissage - Mémoire - Physiologie

Abstract

Every night we fall asleep and every morning we wake up. From what happens in the meantime, little is remembered. Others may say that we have moved, talked, laughed or cried, that the strongest and most vivid emotions took control of our body without leaving the faintest memory behind. Or others may have moved, talked, laughed or cried without our slightest notice. On the contrary, we can emerge from the most fantastic adventure in a quiet bed, cradled by a peaceable ticking clock. Without causing us much alarm, it seems that sleep entails a dissociation between what happens in our environment and within our mind. Yet, at any moment, we can wake up and immediately regain consciousness of the surrounding world. Interestingly, it seems that certain sounds are more likely to awake us than others. Thus, are we completely disconnected from our environment when we sleep?

Keywords

Sleep - Cognition - Perception - Learning - Memory - Physiology

Numero national de thèse :
xxxx xxxxxxxx